

Coordinated Transit Response Planning and Operations Support Tools for Mitigating Impacts of All-Hazard Emergency Events

PREPARED BY

**Hubert Ley, Joshua Auld, Ömer Verbas,
Randy Weimer, Shon Driscoll**
Argonne National Laboratory,
University of Chicago

**Kouros Mohammadian, Nima Golshani,
Ehsan Rahim, Ramin Shabanpour**
University of Illinois at Chicago

**Zongzhi Li, Yongdoo Lee, Yunseung Noh,
Lu Wang, Ji Zhang**
Illinois Institute of Technology

Josianne Bechara, Angela Fontes
University of Chicago

Vadim Sokolov, Tuan Le
George Mason University

Kuilin Zhang, Qinjie Lyu
Michigan Technological University

James Garner
Pace Suburban Bus



COVER PHOTO

Courtesy of Argonne National Laboratory

DISCLAIMER

This document is disseminated under the sponsorship of the U.S. Department of Transportation in the interest of information exchange. The United States Government assumes no liability for its contents or use thereof. The United States Government does not endorse products or manufacturers. Trade or manufacturers' names appear herein solely because they are considered essential to the objective of this report. The opinions and/or recommendations expressed herein do not necessarily reflect those of the U.S. Department of Transportation.

Coordinated Transit Response Planning and Operations Support Tools for Mitigating Impacts of All-Hazard Emergency Events

SEPTEMBER 2022

FTA Report No. 0229

PREPARED BY

Hubert Ley

Director, Transportation Research and Analysis Computing Center
Argonne National Laboratory & University of Chicago, 9700 S Cass Ave, Lemont, IL 60439

Joshua Auld, Ömer Verbas, Randy Weimer, Shon Driscoll

Engineering Systems Division
Argonne National Laboratory & University of Chicago, 9700 S Cass Ave, Lemont, IL 60439

Kouros Mohammadian, Nima Golshani, Ehsan Rahimi, Ramin Shabanpour

Department of Civil and Materials Engineering
University of Illinois at Chicago, 842 Taylor St, Chicago IL, 60608

Zongzhi Li, Yongdoo Lee, Yunseung Noh, Lu Wang, Ji Zhang

Department of Civil and Architectural Engineering
Illinois Institute of Technology, 3201 S Dearborn St, Chicago, IL 60616

Zongzhi Li, Yongdoo Lee, Yunseung Noh, Lu Wang, Ji Zhang

Department of Civil and Architectural Engineering
Illinois Institute of Technology, 3201 S Dearborn St, Chicago, IL 60616

Josianne Bechara, Angela Fontes

National Opinion Research Center, University of Chicago, 1155 E 60th St, Chicago, IL 60637

Vadim Sokolov, Tuan Le

Volgenau School of Engineering
George Mason University, 4400 University Dr, Fairfax, VA 22030

Kuilin Zhang, Qinjie Lyu

Department of Civil and Environmental Engineering
Michigan Technological University, Houghton Dr, MI 49931

James Garner

Pace Suburban Bus, Arlington Heights, IL

SPONSORED BY

Federal Transit Administration
Office of Research, Demonstration, and Innovation
U.S. Department of Transportation
1200 New Jersey Avenue, SE
Washington, DC 20590

AVAILABLE ONLINE

<https://www.transit.dot.gov/about/research-innovation>

Metric Conversion Table

SYMBOL	WHEN YOU KNOW	MULTIPLY BY	TO FIND	SYMBOL
LENGTH				
in	inches	25.4	millimeters	mm
ft	feet	0.305	meters	m
yd	yards	0.914	meters	m
mi	miles	1.61	kilometers	km
VOLUME				
fl oz	fluid ounces	29.57	milliliters	mL
gal	gallons	3.785	liters	L
ft³	cubic feet	0.028	cubic meters	m ³
yd³	cubic yards	0.765	cubic meters	m ³
NOTE: volumes greater than 1000 L shall be shown in m ³				
MASS				
oz	ounces	28.35	grams	g
lb	pounds	0.454	kilograms	kg
T	short tons (2000 lb)	0.907	megagrams (or "metric ton")	Mg (or "t")
TEMPERATURE (exact degrees)				
°F	Fahrenheit	5 (F-32)/9 or (F-32)/1.8	Celsius	°C

REPORT DOCUMENTATION PAGE

Form Approved
OMB No. 0704-0188

The public reporting burden for this collection of information is estimated to average 1 hour per response, including the time for reviewing instructions, searching existing data sources, gathering and maintaining the data needed, and completing and reviewing the collection of information. Send comments regarding this burden estimate or any other aspect of this collection of information, including suggestions for reducing the burden, to Department of Defense, Washington Headquarters Services, Directorate for Information Operations and Reports (0704-0188), 1215 Jefferson Davis Highway, Suite 1204, Arlington, VA 22202-4302. Respondents should be aware that notwithstanding any other provision of law, no person shall be subject to any penalty for failing to comply with a collection of information if it does not display a currently valid OMB control number.

1. REPORT DATE September 2022		2. REPORT TYPE Final		3. DATES COVERED July 2015–December 2019	
4. TITLE AND SUBTITLE Coordinated Transit Response Planning and Operations Support Tools for Mitigating Impacts of All-Hazard Emergency Events				5a. CONTRACT NUMBER FP062899-01-PR	
6. AUTHOR(S) Hubert Ley, Joshua Auld, Ömer Verbas, Randy Weimer, Shon Driscoll (Argonne National Laboratory); Kourou Mohammadian, Nima Golshani, Ehsan Rahim, Ramin Shabanpour (Univ of Illinois at Chicago); Zongzhi Li, Yongdoo Lee, Yunseung Noh, Lu Wang, Ji Zhang (Illinois Inst of Technology); Josianne Bechara, Angela Fontes (Univ of Chicago); Vadim Sokolov, Tuan Le (George Mason Univ); Kuilin Zhang, Qinjie Lyu (Michigan Technological Univ), James Garner (Pace Suburban Bus)				5b. GRANT NUMBER FTA-2013-005-TRI	
				5c. PROGRAM ELEMENT NUMBER	
				5d. PROGRAM NUMBER	
				5e. TASK NUMBER	
				5f. WORK UNIT NUMBER	
				7. PERFORMING ORGANIZATION NAME(S) AND ADDRESS(ES) Argonne National Laboratory, University of Chicago, 9700 S Cass Ave, Lemont, IL 60439 Univ of Illinois at Chicago, 842 Taylor St, Chicago IL 60608 Illinois Inst of Technology, 3201 S Dearborn St, Chicago, IL 60616 Univ of Chicago, 1155 E 60th St, Chicago, IL 60637 George Mason Univ, 4400 University Dr, Fairfax, VA 22030 Michigan Technological Univ, Houghton Dr, MI 49931 Pace Suburban Bus, Arlington Heights, IL	
9. SPONSORING/MONITORING AGENCY NAME(S) AND ADDRESS(ES) U.S. Department of Transportation Federal Transit Administration Office of Research, Demonstration and Innovation 1200 New Jersey Avenue, SE, Washington, DC 20590				10. SPONSOR/MONITOR'S ACRONYM(S) FTA	
				11. SPONSOR/MONITOR'S REPORT NUMBER(S)	
12. DISTRIBUTION/AVAILABILITY STATEMENT Available from: National Technical Information Service (NTIS), Springfield, VA 22161; (703) 605-6000, Fax (703) 605-6900, email orders@ntis.gov ; Distribution Code TRI-30					
13. SUPPLEMENTARY NOTES [www.transit.dot.gov/research-innovation/fta-reports-and-publications] [https://www.transit.dot.gov/about/research-innovation] [https://doi.org/10.21949/1527642] Suggested citation: Federal Transit Administration. Coordinated Transit Response Planning and Operations Support Tools for Mitigating Impacts of All-Hazard Emergency Events. Washington, D.C.: United States Department of Transportation, 2022. https://doi.org/10.21949/1527642 .					
14. ABSTRACT This report summarizes current computer simulation capabilities and the availability of near-real-time data sources allowing for a novel approach of analyzing and determining optimized responses during disruptions of complex multi-agency transit system. The authors integrated a number of technologies and data sources to detect disruptive transit system performance issues, analyze the impact on overall system-wide performance, and statistically apply the likely traveler choices and responses. The analysis of unaffected transit resources and the provision of temporary resources are then analyzed and optimized to minimize overall impact of the initiating event.					
15. SUBJECT TERMS Innovative Safety, Resiliency, and All-Hazards Emergency Response and Recovery (SRER), transit response planning, transit operations support tools, POLARIS					
16. SECURITY CLASSIFICATION OF:			17. LIMITATION OF ABSTRACT Unlimited	18. NUMBER OF PAGES 353	19a. NAME OF RESPONSIBLE PERSON
a. REPORT Unclassified	b. ABSTRACT Unclassified	c. THIS PAGE Unclassified			19b. TELEPHONE NUMBER

TABLE OF CONTENTS

1	Executive Summary
3	Section 1. Context and Project Overview
16	Section 2. Tools, Data Sources, and Computing Resources
45	Section 3. Stated-Preference Intercept Survey of Transit-Rider Response to Service Disruptions
74	Section 4. Time-Dependent Intermodal A* Algorithm: Methodology and Implementation on Large-Scale Network
91	Section 5. Bayesian Forecast of Transit Demand
146	Section 6. Integer Programming Model for Bus Vehicle Routing Problem for Emergency Response
161	Section 7. Passenger Behavior in Response to Unplanned Transit Disruption
185	Section 8. Analysis of Evacuation Destination and Departure Time Choices for No-Notice Emergency Events
203	Section 9. All-Hazard Emergency Events for Transit Response Case Studies
259	Section 10. Review of Hazards Classification, Detection, Communication, and Mitigation Methods and Technologies
301	Section 11. Implementation of Emergency Response Technologies
323	References

LIST OF FIGURES

22	Figure 2-1 Screenshot of POLARIS Network Editor displaying CMA network used in POLARIS
24	Figure 2-2 Illustration of fidelity of POLARIS network
29	Figure 2-3 Density of transit network at various scales in Chicago metropolitan area
30	Figure 2-4 Example of real-time data for buses servicing Route 208 on Pace network
35	Figure 2-5 Screenshot of visualization showing load on simulated transit vehicles in northern part of Chicago metropolitan region
37	Figure 2-6 Illustration of scenario configuration in vicinity of Jefferson Park showing simulation methodology for transit disruptions in specific area (actual bus stops and rail stations)
38	Figure 2-7 Jefferson Park scenario—affected area on normal day
39	Figure 2-8 Jefferson Park scenario—onset of disruption of transit

40	Figure 2-9 Jefferson Park scenario—short-term demand analysis
41	Figure 2-10 Jefferson Park scenario—initial transit agency response and short-term demand estimation
41	Figure 2-11 Jefferson Park scenario—passenger response to transit disruption
42	Figure 2-12 Jefferson Park scenario—optimization of resource allocation
43	Figure 2-13 Jefferson Park scenario—feedback cycle over successive rolling horizon time intervals
44	Figure 2-14 Jefferson Park scenario—aggregate short-term demand forecasting
52	Figure 3-1 Trip-based information using Google Maps API
53	Figure 3-2 Question on TNC and taxi travel experiences
54	Figure 3-3 Transit trip disruption response example question
57	Figure 3-4 Chicago transit system and survey sample locations
61	Figure 3-5 Comparison of survey household and person characteristics to CMAP transit riders
62	Figure 3-6 Distribution of activity types at origin and destination of each trip
63	Figure 3-7 Departure time distribution in sample
63	Figure 3-8 Cumulative distributions of trip distance and travel time by mode
64	Figure 3-9 Cumulative distribution of access and egress distances by mode
68	Figure 3-10 Transit mode share by transit wait time and transit IVTT
69	Figure 3-11 Share of TNC and auto drive/passenger by TNC cost (US\$)
70	Figure 3-12 Mode share by activity type with auto and without auto access
71	Figure 3-13 Mode share by activity start flexibility with auto and without auto access
79	Figure 4-1 Multimodal network representation
82	Figure 4-2 Pseudo-code for Time-Dependent Intermodal A* (TDIMA*) algorithm
85	Figure 4-3 Subroutine for evaluating transit neighbor link
86	Figure 4-4 Subroutine for evaluating non-transit neighbor link
88	Figure 4-5 Online-routing results from Google API and RTA Trip Planner
89	Figure 4-6 Comparison of TDIMA* results to online routers
94	Figure 5-1 General form of routing matrix for three-stop problem
94	Figure 5-2 Relationship between variables d , c , and data A , dh
97	Figure 5-3 Distribution of average hourly APC ON and OFF (October 2016)
98	Figure 5-4 Distribution of total hourly APC ON and OFF (25 = 1:00 am, 26 = 2:00 pm, October 2016)

99	Figure 5-5 Distribution of total hourly APC ON and OFF (25 = 1:00 am, 26 = 2:00 pm, October 2016)
100	Figure 5-6 Distribution of total APC ON per weekdays (October 2016)
102	Figure 5-7 Total APC ON per day of week
102	Figure 5-8 Average APC ON per day of week
103	Figure 5-9 Total APC ON per each month
103	Figure 5-10 Average APC ON per each month
103	Figure 5-11 Total APC ON per day of the year (2015)
107	Figure 5-12 Stan program modeling linear regression with unknown coefficients
108	Figure 5-13 OD pair zones 98 and 124 – MCMC solution and Kalman-Filter solution vs. simulated true demand over 365 days
109	Figure 5-14 OD pair zones 98 and 124 – MCMC solution vs. simulated true demand over 365 days
110	Figure 5-15 OD pair zones 98 and 124 – MCMC solution vs. simulated true demand over 365 days
111	Figure 5-16 OD pair zones 98 and 124 – MCMC solution vs. true demand over 365 days
112	Figure 5-17 Day 362 – Distribution of estimated demand between OD zone pairs 86 and 315; 1 and 39 look similar to Normal
112	Figure 5-18 Day 362 – Distribution of estimated demand between OD zone pairs 86 and 315; 1 and 39 look similar to Normal
113	Figure 5-19 OD pair zones 98 and 124 – MCMC solution (red) vs true demand when $\epsilon_1 \sim U(0,0.05)$
113	Figure 5-20 OD pair zones 98 and 124 – MCMC solution (red) vs true demand (black) when $\epsilon_1 \sim U(0,0.02)$
119	Figure 5-21 Snapshot of counts and flows on Fox News network at time $t = 1$ (9:05:30 February 23, 2015)
120	Figure 5-22 Network schematic and notation for flows at time t
126	Figure 5-23 Sample network with eight bus stops
129	Figure 5-24 Distributions of first four components of true demand d
130	Figure 5-25 Distributions of first four components of true demand d
132	Figure 5-26 Geographical heat map of automatic passenger counters for boarding PACE buses per day of week in October 2016

133	Figure 5-27 Geographical heat map of automatic passenger counters for alighting from PACE buses per day of week in October 2016
134	Figure 5-28 Geographical heat map of automatic passenger counters for boarding PACE buses per day of week in 2015
135	Figure 5-29 Geographical heat map of automatic passenger counters for alighting from PACE Buses per day of week in 2015
136	Figure 5-30 Geographical heat map of automatic passenger counters for boarding PACE buses per month in October 2015
137	Figure 5-31 Geographical heat map of automatic passenger counters for alighting from PACE buses per month in October 2015
138	Figure 5-32 Aggregated automatic passenger counter values for boarding buses on Route 769 per each day of week (Tuesday and Thursday service only)
139	Figure 5-33 Aggregated automatic passenger counter values for boarding buses on Route 714 per each day of week
140	Figure 5-34 Mean automatic passenger counter values for boarding buses on Route 769 per each day of week (Tuesday and Thursday service only)
141	Figure 5-35 Mean automatic passenger counter values for boarding buses on Route 714 per each day of week
147	Figure 6-1 Concepts of route, pattern, trip
147	Figure 6-2 Illustration of sub-request
157	Figure 6-3 Solution procedure
157	Figure 6-4 Illustration of input and output files
159	Figure 6-5 Pace 626 line
164	Figure 7-1 Gathering transit trip information using Google Maps API
165	Figure 7-2 Example of experience questions regarding TNC and taxi
166	Figure 7-3 Example of SP question regarding disruption scenario
171	Figure 7-4 Activity types in origin and destination of intercepted trip
172	Figure 7-5 Departure time in data
172	Figure 7-6 Number of transfers during trip
173	Figure 7-7 Travel distance
173	Figure 7-8 Travel time
174	Figure 7-9 Travel distance between origin and initial transit stop
174	Figure 7-10 Travel distance between last transit stop and destination
175	Figure 7-11 General opinions toward public transit
176	Figure 7-12 Willingness to wait for transit system to be restored

176	Figure 7-13 Respondent trust to various sources of information
177	Figure 7-14 Respondent first level alternatives
177	Figure 7-15 Alternative modes in case of modal shift
179	Figure 7-16 Restricted DT model for first level (performing or canceling trip)
180	Figure 7-17 Restricted DT model for second level (changing destination of trip)
183	Figure 7-18 Importance of variables used in first-level DT model
184	Figure 7-19 Importance of variables used in second-level DT model
184	Figure 7-20 Importance of variables used in third-level DT model
192	Figure 8-1 Destination choice distribution
192	Figure 8-2 Evacuation destination type and tour formation
193	Figure 8-3 Total distances for each destination type
193	Figure 8-4 Evacuation departure time distribution
194	Figure 8-5 Distribution of departure times across destination choices
203	Figure 9-1 Map of Chicago metropolitan area
204	Figure 9-2 Residents across Chicago
205	Figure 9-3 Households where English is only spoken language
206	Figure 9-4 Households where English is poorly spoken
207	Figure 9-5 Aggregate retiree income
208	Figure 9-6 Residents age 18 and under
209	Figure 9-7 Residents age 65 and older
213	Figure 9-8 PACE bus stops
214	Figure 9-9 Number of terrorist activities targeting educational institutions in world (1970–2020)
214	Figure 9-10 Locations of educational units in Chicago Public School District
215	Figure 9-11 Major hospitals in Chicago
216	Figure 9-12 Major malls and plazas in Chicago
217	Figure 9-13 PACE bus route 270 area map
218	Figure 9-14 PACE bus route 270 area map
222	Figure 9-15 PACE bus route 270 area map
224	Figure 9-16 Des Plaines River watershed area
225	Figure 9-17 Flooding in 1986
227	Figure 9-18 Streams of concern of Des Plaines River

228	Figure 9-19 Primary road system and overtopping map along Des Plaines River watershed
228	Figure 9-20 Map of risk of flooding
229	Figure 9-21 Historical flooding event map in Des Plaines area
230	Figure 9-22 Contour map in Des Plaines area
230	Figure 9-23 Case study area
231	Figure 9-24 Historical flooding event map
231	Figure 9-25 Transit routes in study area
232	Figure 9-26 Monthly precipitation distribution in Des Plaines area
233	Figure 9-27 Average monthly gauge heights in Des Plaines area
233	Figure 9-28 Des Plaines River gauge height changes, 2018
234	Figure 9-29 Categories of FEMA flood stages for Des Plaines River
235	Figure 9-30 Des Plaines River flooding record, September 13, 2008
235	Figure 9-31 Des Plaines River flooding record, April 18, 2014
236	Figure 9-32 Changes in Des Plaines River flood stages after flooding event
236	Figure 9-33 Des Plaines River flood stages
237	Figure 9-34 Des Plaines River moderate flood stage
238	Figure 9-35 Des Plaines River major flood stage
240	Figure 9-36 CTA Blue Line Station at Cumberland and Rosemont
241	Figure 9-37 Two major hospitals in case study area
243	Figure 9-38 BNSF route map
244	Figure 9-39 Hazmat example
245	Figure 9-40 Hazardous materials signs
248	Figure 9-41 Metra BNSF line and Cass Avenue rail-highway crossing intersection
252	Figure 9-42 Alternative PACE bus routes
253	Figure 9-43 Hazmat failure location
255	Figure 9-44 Initial clearance
256	Figure 9-45 Hazmat emergency affected area in Phase 3
258	Figure 9-46 Hazmat emergency affected area in Phase 4
259	Figure 10-1 Typical hazard classifications
274	Figure 10-2 Classification of fire detection technologies
277	Figure 10-3 Classification of hazardous material detection technologies
286	Figure 10-4 Hazard impacts assessment process

288	Figure 10-5 Conflict points at an intersection
288	Figure 10-6 Conflict point reduction strategy
289	Figure 10-7 Contraflow Alternative 1
290	Figure 10-8 Contraflow Alternative 2
296	Figure 10-9 Evacuation plan feedback process
302	Figure 11-1 Signal timing prioritization
307	Figure 11-2 Factors affecting efficient transit resource use
312	Figure 11-3 Design elements for use of contraflow
313	Figure 11-4 Conflict points at an intersection
313	Figure 11-5 Lane-based routing strategy
321	Figure 11-6 Role of EOC for coordination of emergency management

LIST OF TABLES

23	Table 2-1 Major POLARIS Network Tables for Chicago Model
65	Table 3-1 Duration of In-Transit Activity in Sample
66	Table 3-2 Average Characteristics by Selected Mode When Transit Delayed vs Canceled
67	Table 3-3 Standard Deviation of Characteristics by Selected Mode When Transit Delayed vs Canceled
114	Table 5-1 OD Pair Zones 98 and 124 – 365-day Average MSE and MAPE for Four Cases of Prior Likelihood
114	Table 5-2 365-day Average MSE and MAPE of Every OD Pair for Four Cases of Prior Likelihood
159	Table 6-1: Settings of Experiment
160	Table 6-2 Settings of Test Scenarios
160	Table 6-3 Result of Test Scenarios
169	Table 7-1 Household Demographic Characteristics
170	Table 7-2 Individual Demographic Characteristics
175	Table 7-3 Duration of In-Transit Activity in Sample
179	Table 7-4 Example of Two-Class Coincidence Matrix for Classification Problem
181	Table 7-5 Variables Used in DT Models
181	Table 7-6 Performance Measurements for First-Level (Performing Trip) DT Model
182	Table 7-7 Performance Measurements for Second-Level (Changing Destination) DT Model

182	Table 7-8 Performance Measurements for Third-Level (Mode Choice) DT Model
190	Table 8-1 Summary of Studies on Evacuation Departure Time and Destination Choice
195	Table 8-2 Summary Statistics of Key Variables
199	Table 8-3 Estimation Results of Joint Destination and Departure Time Choice Model
212	Table 9-1 Bomb Stand-off Distances
219	Table 9-2 Transit Services Expected to be Affected
222	Table 9-3 Transit Services Expected to be Affected
232	Table 9-4 PACE Bus Information, Northwest Division Garage
232	Table 9-5 Precipitation in Des Plaines Area
234	Table 9-6 Description of FEMA Flood Stages
238	Table 9-7 Metra UP-NW Passengers at Des Plaines Station
239	Table 9-8 Flooding Event by Flooding Stage and Countermeasures in Des Plaines Area
241	Table 9-9 CTA Blue Line Demand, Rosemont and O’Hare International Airport
242	Table 9-10 Power Outage Scenario and Countermeasures by Hour
245	Table 9-11 Hazmat Accident Consequence Levels
246	Table 9-12 Hazard Distances Used in NRHM Routing Guidelines
247	Table 9-13 Estimated Unit Values for Damage to Structures
247	Table 9-14 Estimated Unit Values for Damages to Environment
249	Table 9-15 Census Data, Village of Westmont, IL
250	Table 9-16 BNSF Station-Level Ridership, AM
251	Table 9-17 BNSF Station-Level Ridership, PM
252	Table 9-18 PACE Bus Supply
253	Table 9-19 Historical Data on Wind Speed in Illinois
254	Table 9-20 Alternative Transit Options
256	Table 9-21 Affected Transit Pattern in Phase 3
257	Table 9-22 Affected Transit Pattern in Phase 4
258	Table 9-23 Summary of Four-Phase Hazmat Emergency Response Process
260	Table 10-1 Flood Categories
261	Table 10-2 Saffir-Simpson Wind Scale for Hurricane Hazard Measurement
262	Table 10-3 Enhanced Fujita Scale for Tornado Hazard Measurement

264	Table 10-4 Richter Scale for Earthquake Hazard Measurement
265	Table 10-5 INES Scale for Nuclear Hazard Measurement
271	Table 10-6 Summary of Hazard Impact and System Resilience Levels
272	Table 10-7 Classification of Hazard Detection Technologies
273	Table 10-8 Advantages and Disadvantages of Flooding Detection Technologies
278	Table 10-9 Characteristics of Active Monitoring Detection
278	Table 10-10 Advantages and Disadvantages of Hazardous Material Detection Technologies
280	Table 10-11 Advantages and Disadvantages of Nuclear Material Detectors
285	Table 10-12 Summary of Communication Technologies and Characteristics
303	Table 11-1 Signal Preemption Technology Features
305	Table 11-2 Strategies of Active Transit Signal Priority

Abstract

This report summarizes current computer simulation capabilities and the availability of near-real-time data sources allowing for a novel approach of analyzing and determining optimized responses during disruptions of complex multi-agency transit system. The authors integrated a number of technologies and data sources to detect disruptive transit system performance issues, analyze the impact on overall system-wide performance, and statistically apply the likely traveler choices and responses. The analysis of unaffected transit resources and the provision of temporary resources are then analyzed and optimized to minimize overall impact of the initiating event.

Executive Summary

This project was led by a team at the University of Chicago. The principal investigator was Dr. Hubert Ley, Director of the Transportation Research and Analysis Computing Center at Argonne, holding a joint appointment with the University of Chicago initially through the Computing Institute (CI) and then later through the Consortium for Advanced Science and Engineering (CASE). His work includes the development of tools to capture and analyze the massive static and dynamic data, develop storage strategies, develop the underlying databases for efficient access and relational consistency, develop features in the POLARIS network editor to import and edit the transit schedules for all local transit agencies, and perform spatial analysis to automatically match the various spatial entities (stops, stations, transit links, road networks, rail lines, walk ways) for cross-reference and to create a consistent simulation network from the various data sources. His work also included the provision of computing resources, e.g., designing, configuring, and operating the data servers to accommodate reliable and redundant data capture from real-time sources. He also developed a number of prototype implementations of the planned software development to guide the more complex development in high performance implementation for POLARIS. This includes the development of initial transit routing algorithms based on the data derived from GTFS and stored in SQL databases to ensure that this approach was feasible as well as the development of parallelization methods for the microsimulation of vehicular traffic.

The software development for POLARIS was otherwise led by Dr. Joshua Auld, leading a team of developers in Argonne's Transportation Research Systems Modeling and Control Group, which is part of the Energy Systems division at Argonne. His primary work included the design and development of the agent-based activity model as well as the development of the transit intercept survey. He also worked closely with UIC on the implementation of algorithms and software applications that use the survey's results in POLARIS to modify traveler choice in a statistically accurate manner when encountering transit disruptions. His team worked under joint appointments with the University of Chicago as well. Dr. Ömer Verbas was responsible for the development of the transit simulation capabilities in POLARIS and developed the complex routing algorithms and the interaction of transit vehicles with vehicles on regular network links. Randy Weimer and Shon Driscoll worked on software implementations and updates, hardware compatibility, and platform independence of POLARIS.

The transit intercept survey was performed by a team at the National Opinion Research Center under the direction of Josianne Bechara and Angela Fontes. The group developed the survey to ensure that it was statistically corrected for bias,

in close collaboration with Dr. Auld and Dr. Ley, who developed the web-based survey logic and user interface. NORC deployed personnel to 100 transit stops and station in the region, with each survey location being operated for 4 hours.

The work on implementing the survey results into the activity-based travel model was led by Kouros Mohammadian, Professor and Department Head of the Civil and Materials Engineering department at the University of Illinois at Chicago. The primary developer and implementer of the algorithms, methodologies, and software implementations was Dr. Nima Golshani, supported by Ehsan Rahimi and Ramin Shabanpour. The team worked closely with Dr. Auld to implement the logic in POLARIS.

A team of researchers at the Illinois Institute of Technology performed background research on emergency evacuation and response strategies, determined data sources, developed case studies, and supported Dr. Ley's development of the POLARIS network editor with detailed verification of network coding and strategies. The team was led by Dr Zongzhi Li, Director of Transportation Engineering and Infrastructure Engineering and Management at the Armour College of Engineering. His team included Yongdoo Lee, Yunseung Noh, Lu Wang, and Ji Zhang.

The work on the Bayesian short term demand forecasting model was led by Dr. Vadim Sokolov, a former team member of Dr. Ley's group at TRACC, who is now Professor for Systems Engineering and Operations Research at George Mason University. He holds a Ph.D. in Mathematics, and worked closely with Tuan Le to analyze the fare card data and automatic passenger counter data made available by Pace (data that could be captured and made available in real time in the future but that is currently made available with delay after being processed and download in the operator's facilities). Another former team member at TRACC, Dr. Kuilin Zhang, is now a professor at Michigan Technological University in the Department of Civil and Environmental Engineering. He has a strong background in transportation systems modeling and developed the optimization methodologies for determining the best use of transit vehicles under system constraints.

The work performed under this project would not have been possible without relying on extensive knowledge of hands-on transit operations, such as the typical constraints operators are under, background knowledge about procedures and operation of transit agencies, availability of the various data sources, vetting of methodologies and assumptions about operational capabilities, and providing deep insight into the needs of the transit agencies. James Garner of PACE was instrumental in supporting the team with in-depth knowledge on these issues.

Details of the research work conducted can be found in the report.

Section 1

Context and Project Overview¹

The Chicago metropolitan area is one of the largest and most dense concentrations of people, industry, and commerce in the U.S. As a transportation hub, the region must be prepared to quickly recover from natural and man-made hazards. At the same time, transportation networks are a critical resource in disaster management and recovery operations. Transit systems are needed for the (1) evacuation of exposed populations, (2) transport of injured persons, (3) movement of emergency personnel and first responders, and (4) delivery of needed supplies.

As witnessed in recent natural disasters, the lack of evacuation planning and coordination among transit systems can be catastrophic. Hurricane Katrina underscored the need to plan for efficient mass evacuation procedures for non-drivers and to design systems capable of prioritizing the transit needs of the most vulnerable populations before, during, and after disaster events.

The Chicago metropolitan area is an ideal test bed for new emergency planning and response tools and strategies. A regional plan (GO TO 2040) has emphasized emergency preparedness as a key goal; the regional transit systems are interlinked and coordinated better in Chicago than in many other metro regions. The research team has extensive experience with transit-specific planning for emergencies. A team partner on this project, Pace Suburban Bus Service, was also the test agency for the Federal Transit Administration (FTA)-funded Transit Operations Decision Support System (TODSS). The project team was also responsible for developing the interactive Regional Transportation Simulation Tool for Evacuation Planning (RTSTEP) for the City of Chicago under the Regional Catastrophic Preparedness Grant Program funded by the Federal Emergency Management Agency (FEMA) in 2011.

The Chicago area is vulnerable to many categories of hazards, including flooding, tornadoes, blizzards, and man-made emergencies, and the large geography of the region exposes residents to a variety of these hazards. The region benefits from a large, integrated, multimodal transportation system. This project leverages that transportation system to best help the region be ready for, respond to, and recover from emergency situations associated with the many hazards.

In emergency situations, even those with access to vehicles may be unable to evacuate if there is not adequate planning and coordination among transit and emergency response systems. During Hurricane Rita in 2005, evacuation routes along the roads leading away from the Texas coastline experienced traffic jams that were 100 miles long. Many drivers were forced to turn around and head

¹ Authored by Hubert Ley, University of Chicago, Argonne.

back toward the storm, opting to wait out the weather in their homes rather than be completely exposed on the clogged roadways (Blumenthal, 2005). This is one of the reasons that integrated modeling and simulation tools were deployed and further developed, including population synthesis, behavioral models based on survey and statistical data, and a full traffic simulation of all transportation modes.

This research investigated methods, techniques, technologies, and practices that can help emergency responders improve the efficiency of the decision-making process for detecting, analyzing, and responding to emergencies, service disruptions, and catastrophic failures associated with multimodal transportation systems and recovering system services in an effective manner using available transit assets.

The project assessed a variety of technologies and strategies, including those dedicated to locating persons and resources, improving communications, assessing the operability of transit systems, and re-deploying resources. Examples of these technologies and strategies include TODSS, automated vehicle location systems, improved sensor and detector networks, communication network technologies and protocols, both those between agencies and transportation/transit assets and those with the public (such as STARCOM21), variable messaging sign (VMS) networks, public alert broadcasts, e-mail or short message service (SMS) notifications, transit signal prioritization, and others. The project also assesses the value of pre-planning for emergency operations, including developing alternate transit routes/schedules, using bus, bus rapid transit (BRT), and train assets for transit vehicle bridging, and other strategies that can be developed with such a decision support tool.

The team also conducted an extensive survey that informed them about how individuals react to a variety of hazards (stated preference survey). This information was used to develop computational models of how the Chicago area operates under a number of emergency conditions and behavioral data-driven assumptions. The project team then developed computational models that evaluate the most viable technologies and strategies in relation to various hazards to which they might respond. In addition, these models were integrated as a new Emergency Planning Module in the existing open source Planning and Operations Language for Agent-Based Regional Integrated Simulations (POLARIS) modeling system in use for the Chicago area. Given the far-reaching and unpredictable effects of emergency events, such a system greatly augments planning for and executing time efficient hazardous situations management.

POLARIS is an open source transportation planning tool that simulates the transportation system in large metropolitan regions. It was created through funding provided by the Federal Highway Administration (FHWA) Office of Planning. It is distinguished from other similar tools by its faster-than-real-time

speed of operation and its ability to account for the choices and behaviors of a large population of individuals and their behavior while traveling, in an integrated simulation. These qualities make it an ideal foundation for examining how an all-hazards emergency might play out in the real world and providing meaningful operational metrics.

Objectives

The Chicago metropolitan area is one of the largest markets for public transportation in the U.S. Millions of people are safely transported each day on a system that constantly faces natural and man-made hazards. The project developed and showcased innovative technology for supporting emergency planning, response, and recovery that can be useful for transit agencies throughout the country. The project significantly advances FTA's objectives for improving the ability of transit agencies to plan for, operate in, and recover from emergency situations.

The project advances numerous FTA objectives that seek to enhance the operations of public transit agencies. The main product deliverable—the evacuation behavior and emergency response simulation capabilities in the POLARIS framework—is a toolbox of emergency planning scenario evaluation models customized for public transportation. By developing the capabilities using the existing open source POLARIS technology, the project was able to deliver the final product in a timely and cost-efficient manner. The system represents a significant technical accomplishment; in particular, its demonstration of integrating real-time data feeds with transportation modeling software represents an emerging technique that will continue to gain value as monitoring technologies and the quality of data sources advance.

In emergency situations, communication is always a primary concern. This project synthesizes information from multiple data sources to allow for more efficient decision-making and communication in emergency situations. Numerous steps were built into the work plan to ensure the general effectiveness of the resulting technology, including the continued participation of the transit operators in the project, demonstrations of the technology, and use of the best available data for the simulations and decision-making tools.

The transit project partners, Pace Suburban Bus Service and Metra Rail, provide multimodal transit services via fixed-route buses, special-route bus services, commuter rails, and vanpools to millions of people across the region. This project demonstrates how to use those multiple modes to improve upon an efficient public transportation system in an emergency situation with an increase in reliability, ability to function in an emergency, and speed of recovery. The team significantly advanced current technology that until now could not consider the resources, benefits, and challenges of all these modes in one

simulation. It allows for replication by other transit agencies that offer one or more of these modes of transportation.

The suburban bus agency, Pace, deploys one of the largest networks of fixed-route bus services, paratransit, special-route, and vanpool services in the region. The partner rail agency, Metra, operates the nation's second-largest commuter rail system. Operating in a large, complex region, the combination of Pace and Metra was ideal for testing a model for national use that accommodates several modes of commuter transit. This project built on existing resources, such as the Pace-initiated TODSS system and the base POLARIS model, as well as on previous work in regional emergency evacuation planning, such as RTSTEP.

The team leading the project had extensive experience, as outlined later in this report and comprised nationally-recognized transportation planners, engineers, project evaluators, and computer simulation experts. A multidisciplinary research team composed of the University of Chicago (UC), the University of Illinois at Chicago (UIC), Illinois Institute of Technology (IIT), Michigan Technological University (MTU), George Mason University (GMU), and the National Opinion Research Center (NORC) worked closely with local transit operators, including Pace, the Chicago Transit Authority (CTA), Metra, and the Illinois Department of Transportation (IDOT). These research entities have collectively participated in multiple efforts to model transportation systems under emergency conditions and previously developed tools that can support operators and policy-makers. This collaboration ensured the development of an operational support technology in addition to employable techniques and strategies that were vetted through analytical case studies. The technologies developed focus on hazardous event management needs in the Chicago metropolitan area, but due to the flexibility of the software and generality of the investigated strategies, they should also be widely applicable to other communities served by a transit system.

The methods, procedures, techniques, and strategies for hazard impacts mitigation investigated will integrate transit assets into the core of developing countermeasures that are effective with respect to efficiency, response time, and cost that may be employed in case of various emergency situations. Involving Pace, Metra, and IDOT throughout the project helped to expand the knowledge and understanding of coordinated transit responses to emergency scenarios, pre-planning for and responding in real-time to hazardous situations, and identify areas for its potential improvements for broader applications. Further, the identified needs for emergency response planning improvements and products from the research project offer opportunities for researchers to explore scientific solutions to further advance such efforts.

Challenges

The project addressed a number of issues and delivered new capabilities of high interest for local and national transit operators. The project conducted a technological review of hazard and emergency response capabilities but also learned about the many constraints under which transit agencies have to operate, including operational issues such as operating from many different and only loosely integrated dispatch centers, a strong focus on operational efficiency, a general lack of coordination between transit agencies when it comes to transit disruptions, and the difficulty of managing large operations in the region. These findings do not intend to criticize the transit agencies; the underlying issue is that a strong focus on resilience and emergency response naturally conflicts with an efficient day-to-day operation that is responsive to the ever-changing needs of a dense urban population. As a result, many otherwise logical response strategies are not feasible given their impact on day-to-day operations. Thus, the project concentrated on demonstrating the impact of a disruption on multiple agencies and a response optimization that may be based on strategies that may or may not be realistic at this time. It is obvious that simulations can only work in conjunction with actual emergency responders and their wealth of experience.

Many transit operators use one or more command centers that contain a number of tools that target efficient daily operation but may not contain technologies that are designed to aid in planning for and responding to all hazards emergencies. This work attempted to implement such a capability, although the complexity of the approach is still a major limitation for practical implementation. The expanded POLARIS toolbox provides analysis of data already collected by transit agencies and provides new decision-making capabilities to transit command centers. However, there are clearly limitations when using real-time data sources that are currently available. The improved collection and provisioning of real-time data over readily-available communication networks would be of great benefit if collected with better spatial and relational accuracy. For example, automatic passenger counter data and fare card data would be of much higher value for determining the current state of the transit network if the data were clearly correlated to specific transit stops and routes. The underlying problem is that the data a currently collected for a specific purpose, and secondary uses are difficult or impossible to correlate with other data sources.

A key benefit of using a predictive computer model is that it allows local authorities to explore the possible effects of a number of different hazards and responses for which there may be little or no experience in-house. Creating and testing an array of emergency plans for a variety of hazards allows transit agencies to train more adequately and prepare their responders in advance of a true emergency. This project was tested on emergency scenarios in the Chicago

metropolitan area, which encounters a wide variety of natural and man-made hazards. The tool can significantly enhance emergency planning capabilities for transit operators. A major challenge was the lack of scalability of some components of the models, which made integration difficult and led to results that are too highly aggregated for evaluating localized effects.

Local operators acquire a large amount of information about ridership patterns and the operational status of their assets; however, there may be a gap in the level of depth with which they understand the composition and travel behavior of the communities they serve. Although the modeling techniques used in this project have generally the potential to provide them with this information, the lack of resources to make use of this wealth of data is a great challenge.

Task Overview

The project resulted in the development of capabilities that can be used by transit agencies and emergency responders and resulted in a demonstration of a decision support tool for planning and operations management purposes. The project included research, development, and synthesis, followed by a capability demonstration and review by an independent third party.

The research and deployment plan was structured as follows:

- *Review of Existing Methods, Techniques, and Technologies for All Hazards Emergency Management* – The first task of this project involved a review of potential hazards ranging from emergencies and service disruptions to catastrophic failures that might disrupt a transportation system and technologies or response strategies that may aid in reducing the adverse impacts of such hazards. The aim of this phase was to develop a set of hazards, methods, technologies, and response strategies that could be further evaluated in subsequent tasks. This task also provided a baseline understanding of how institutional policies and decision processes are oriented toward responding to potentially catastrophic situations. This was used as the benchmark for how agencies are inclined to potentially revise their policies after incorporating the results from simulations. This task also involved the review of data sources and the collection of new data regarding individual behavior under emergency scenarios including individual responses to emergency management interventions.
- *Development of Computational Models for Evacuation Demand and Emergency Responses* – Design and development proceeded with creating an Emergency Planning Module within the POLARIS simulation framework capable of modeling the selected hazards and the responses to the hazards using the transit system and further evaluating the efficiency of the candidate technologies and response strategies. Updates to the POLARIS simulation system included the addition of a Transit Module to support

the use of transit assets for non-transit all hazards emergency responses. The POLARIS system was updated to account for individual behavior of the evacuation demand under emergency scenarios and the interactions of individuals with the transit system used for emergency responses. Finally, new visual paradigms and prototype implementations were developed to visualize results of emergency impacts before and after implementing emergency response strategies.

- *Development, Calibration, and Validation of Baseline Model* – The transit network details for the Chicago metropolitan area were added to update the current POLARIS model for its function to a decision support tool. The updated model was tested for functionality and was calibrated and validated using properly-balanced field data to produce the baseline Chicago POLARIS model for conducting the case studies pertaining to hazardous events analysis and emergency management. Critical evaluation of the baseline model were conducted through cross comparisons of results generated from it.
- *Investigation and Development of Operational Capabilities for Regional Simulation* – The properly-calibrated baseline model was further refined to incorporate real-time sources of data on network performance from a variety of sensors, probes, and other detection and surveillance equipment. This includes the various Google Transit Feeds (both static and dynamic) and the Chicago Train and Bus Tracker data. A review of the data sources was performed to determine suitability and applicability for this task. The potential for incorporating the sources into an operational version of the simulation was evaluated. Ultimately, it was found that the quality and reliability of the available real-time data sources were limited, for a number of reasons. For example, the reliable cross-identification of vehicle trace data and payment records was limited by insufficient coding within the data sources, making it difficult to associate specific automated passenger counters with bus stops, reconcile payment records with exact stops, or match static and dynamic GTFS trip data reliably. An important outcome from this study is that the spatial and temporal resolution of a real-time data source is more limited than it appears in available documentation; thus, a higher level of aggregation of such data had to be employed, with a corresponding loss of precision.
- *Design and Conduct of Case Studies* – The metrics for the evaluation were identified and defined, including reliability, speed of access, and efficiency of operation. Case studies for implementing the baseline model were designed in coordination with the various stakeholders involved. Three categories of hazards—Emergencies, Service Disruptions, and Catastrophic Failures—and a combination of two or three of the situations that occur simultaneously or in close proximity were the subject of the simulation and analysis. The scenarios were chosen with varying degree of probability of occurrence as well as spatial locations. The primary scenario was chosen

to be an event at Jefferson Park so all Chicago area transit operators were affected. The simulations included CTA buses and trains, Metra trains, and Pace buses as well as a dense and highly-urbanized population. The various cases of hazardous events were analyzed considering the use of transit assets in the response and recovery phases of the emergency management process. The baseline model was applied to evaluate transit and vehicular delays and the resulting congestion as well as safety impacts of alternative hazards management strategies and to develop effective countermeasures for the Chicago metropolitan area.

- *Demonstration and Evaluation of Project Results* – This analysis revolved around the successful demonstration of emergency response technologies and strategies recommended as a result of the case studies. Results from the scenarios were shared with stakeholders.

Project Partners

The UC Computation Institute was the primary project contractor. Work was performed by staff members of the Institute who hold joint appointments with Argonne National Laboratory as well as by subcontractors from other universities listed below. Argonne National Laboratory is owned by the Federal government and is operated by the University of Chicago through a limited liability corporation, UChicago Argonne, LLC. Joint appointments at both Argonne and the Computation Institute at the University of Chicago provide a mechanism to tap into a broad range of expertise than would be otherwise available to nationally-significant research projects.

Argonne and the University of Chicago work closely with international university and industry partners, being involved in hundreds of partnerships and cooperative research relationships. The University of Chicago and Argonne have numerous contracts with the universities involved with this project and could easily subcontract the work described in the statement of work.

Argonne's Transportation Research and Analysis Computing Center (TRACC) was part of the Energy Systems Division at Argonne (now part of the nuclear Engineering Division) and is one of the national user facilities within the national laboratory system providing dedicated computing resources and expertise exclusively to the transportation research field. The work was performed primarily by staff members of the Computation Institute at the University of Chicago affiliated with Argonne's TRACC facility through joint appointments. Additional work was performed by the following partners in this project.

- The IIT Department of Civil, Architectural and Environmental Engineering was a subcontractor working primarily on the implementation of emergency technology models, model calibration and validation, and case studies.

- The UIC Department of Civil and Environmental Engineering was a subcontractor working primarily on the travel demand model specifically as it applies to emergencies as well as the necessary data acquisition through surveys.
- The MTU Department of Civil and Environmental Engineering was a subcontractor working primarily on network model calibration and validation, as well as case studies.
- The UIC Urban Transportation Center served as the independent evaluator, as required by the project. This is a different department of UIC and was not involved in the work performed by the other department mentioned above.
- GMU became a subcontractor due to one of the key researchers taking a position there. This work focused on real-time data sources and the estimation of short-term demand driven by real-time data sources.
- NORC was subcontracted to perform an extensive survey of transit riders across the region and intercepted several thousand travelers at 100 distinct transit stops and stations to invite them to participate in an online survey used to create models for transit rider behavior during transit system disruptions.

Two major transit agencies in the Chicago metropolitan area also partnered on this project. Pace operates fixed-route, special event route, paratransit, and vanpool services in northeastern Illinois, most of which are in the inner- and outer-ring suburbs around Chicago, with some paratransit and commuting services in Chicago itself. Metra operates the commuter rail network in northeastern Illinois.

All team members had rich experience in transportation planning, traffic management, and systems engineering. The formation of this particular team maximized the collective benefits of experience, expertise, and accomplishments of individual team members and effectively integrated these qualities for the thorough execution of the research program.

Key Research Personnel

Dr. Hubert Ley is Director of the Transportation Research and Analysis Computing Center (TRACC) of Argonne National Laboratory (operated by UChicago Argonne LLC). He holds a joint appointment with the Computation Institute at the UC. He received his doctorate in Mechanical Engineering in 1994 from the prestigious RWTH Aachen University, Aachen, Germany, where he specialized in Nuclear Engineering, with a focus on the subject of simulating fission product transport in graphite fuel elements for high-temperature, gas-cooled reactors. While finishing his thesis in 1991, he visited Argonne as a visiting scholar and was hired to work on nuclear fuel simulations in Argonne's

Fuels and Engineering Division. At Argonne, he worked extensively on reactor accident simulations, image processing, visualizations, sensor data acquisition, and digital data processing. From 1996 to 2001, he was the key developer of the International Nuclear Safety Center (INSC) network, a communications and collaboration project established by Congress and the Clinton Administration to enhance remote collaboration between the United States and various countries of the former Soviet Union on nuclear safety research and technology. Subsequently, from 2001 to 2006, he worked with the International Atomic Energy Agency on behalf of the U.S. Department of Energy on establishing the collaboration framework for the Asian Nuclear Safety Network (ANSN). In late 2006, he became one of the initial team members forming the Transportation Research and Analysis Computing Center at Argonne under a large congressional SAFETEALU grant (2006 to 2012, Sponsor: Dawn Tucker-Thomas, RITA) with the goal of technology transfer from the national laboratory complex to the transportation research community.

TRACC's supercomputers, as acquired over the past years, are now the largest computing resource provided by the U.S. Department of Transportation (USDOT) to the research community. Dr. Ley was primarily responsible for developing advanced transportation simulation systems for supercomputers based on the USDOT TRANSIMS code. He developed complex transportation systems models (e.g., for Chicago), developed extensive training materials on the use of this software on supercomputers, taught dozens of training classes on the subject to the U.S. user community, and developed and supported a large number of projects using the shared supercomputers at TRACC for dozens of TRANSIMS users and user groups. He is still heavily involved in software design and development, focusing on visualization software as well as productivity software such as graphical user interfaces, adaptive run time environments, highly-structured network editing solutions, and similar technologies that are an essential part of dealing with the ever-increasing complexity of current transportation simulations. He became Director of TRACC in 2010 and has been responsible for several multi-million-dollar projects for USDOT, the Federal Emergency Management Agency (FEMA), the City of Chicago, and IDOT. Under his leadership, TRACC has implemented key software and simulation projects for emergency preparedness, such as the Regional Transportation Simulation Tool for Evacuation Planning (RTSTEP) software developed under the Regional Catastrophic Preparedness Grant Program for the City of Chicago in 2010 and 2011. The development of the POLARIS framework, under an interagency agreement with the FHWA Office of Planning (Sponsor: Brian Gardner) is one of the more recent milestones in fusing the needs of the planning community with the needs of the emergency response community to leverage tool development with funding from both sources to address common and overlapping challenges. POLARIS is currently being developed and refined and served as the basis for the project's toolbox.

As the Director of TRACC, Dr. Ley has also helped to establish a sizable capability in other technical areas, such as by helping USDOT's Turner Fairbank Highway Research Laboratory (TFHRC) to transition from experimental hydraulics to computational fluid dynamics and multi-physics codes (Sponsor: Kornel Kerényi) and by providing technical support and computing capabilities to the National Highway Traffic Safety Administration (NHTSA) Office of Crashworthiness (Sponsor: Stephen Summers). Other current projects involve evacuation planning for U.S. Department of Defense sites, an urban planning project, and analysis of transit response capabilities for FEMA Region 5 in Chicago. During his involvement with TRACC at Argonne, he built a diverse team of scientists and built extensive relationships with both local and remote universities and research organizations, positioning TRACC as an excellent source for performing complex and challenging transportation systems simulations.

Dr. Joshua Auld is a Staff Scientist at Argonne's TRACC and holds joint appointments with both the Computation Institute at UC and UIC. His primary research area is in travel-demand modeling, traveler behavior, travel surveying, and activity-based microsimulation modeling. He completed his doctoral studies at the UI and was a National Science Foundation Integrative Graduate Education and Research Traineeship (IGERT) fellow in a multidisciplinary research group focusing on the information technology aspects of transportation. His research has led to 16 journal publications, 17 peer-reviewed conference presentations, and 3 book chapters as well as a number of other presentations and technical reports and 2 guest editorials. He serves on the Committee on Travel Demand Forecasting and the Special Committee for Travel Forecasting Resources on the Transportation Research Board (TRB) of the National Research Council and was a recipient of the Ryuichi Kitamura Paper Award from TRB.

Dr. Vadim Sokolov was a Computational Transportation Engineer at TRACC in Argonne's ES Division and moved to GMU at the time the project started. His areas of expertise include mathematical/statistical modeling and scientific computing, optimization, discrete choice models, and regression analysis. He joined Argonne in 2008 after receiving a Ph.D. in computational mathematics from Northern Illinois University. At Argonne, he worked on developing models of transportation systems and was a member of the team that developed the RTSTEP, work sponsored by the U.S. Department of Homeland Security. Currently, he is a member of the team that works on developing the next-generation transportation systems planning tool, which is sponsored by FHWA. He has a joint appointment with the UC Computation Institute.

Dr. P. S. Sriraj is Director of Metropolitan Transportation Support Initiative and Research Assistant Professor at the Urban Transportation Center (UTC) at UIC. He served as Senior Associate at UTC from 2005–10, and his research

areas are public transportation systems, sustainability and transportation, and visualization of transportation. Other relevant topics are stakeholder analysis techniques, transportation asset management, and transportation equity. He has published numerous technical papers and reports, including over 20 refereed journal papers, and serves on TRB's Committee on Socio-economic Factors in Transportation and Environmental Justice. He is also paper review-chair of TRB's Committee on Environmental Justice and serves as the Research Needs Coordinator for both committees. He was a recipient of the Outstanding Paper Award from TRB and has been honored for his teaching by the Dean of Armour College of Engineering at IIT in Chicago.

Dr. Abolfazl (Kouros) Mohammadian is a Professor of Transportation Systems at UIC. He has over 20 years' experience in transportation planning and travel behavior research and has authored over 200 scholarly publications in scientific journals, conference proceedings, book chapters, and project reports. His research has covered various areas of transportation planning including travel behavior analysis, modeling of activity and travel patterns, freight transportation, travel survey, land-use, urban energy, and development of state-of-the-art travel demand models for implementation in practice. He is well-known for his computational analysis of transportation system as well as his advanced freight and passenger microsimulation models. He chairs the TRB subcommittees on Behavioral Processes and New Technologies and also serves on several other TRB committees, including Transportation Demand Forecasting, Traveler Behavior and Values, Telecommunications and Travel Behavior, Travel Survey Methods, Statistical Methodology in Transportation Research, and the Taskforce on Moving activity-based approach to practice. He received the 2007 Charley Wootan award, the 2008 Fred Burggraf award, and the 2011 Ryuichi Kitamura award from TRB in recognition of his contributions to transportation research.

Dr. Zongzhi Li is an Associate Professor at IIT. He received a BE from Chang'an University in Xi'an, China and MSCE, MSIE, and PhD degrees (December 2003) from Purdue University in West Lafayette, Indiana. He currently coordinates the IIT Transportation Engineering Program and the Infrastructure Engineering and Management Program and serves as Director of the IIT Transportation Engineering Laboratory and the IIT Center for Work Zone Safety and Mobility (renamed as IIT Sustainable Transportation and Infrastructure Research Center). He is a Senior Research Fellow of the Reason Foundation, secretary of the TRB Committee on Transportation Asset Management, member of TRB Committee on Trucking Industry Research, member of the Task Force on Logistics of Disaster Response and Business Continuity, and member of the Special Task Force on Data for Decisions and Performance Measures. He also serves on the American Railway Engineering and Maintenance-of-Way Association (AREMA) Committee on Education and Training and is a member of editorial board of

American Society of Civil Engineers (ASCE) *Journal of Infrastructure Systems*. His areas of expertise are in multimodal transportation infrastructure and dynamic traffic network mobility, safety, security and emergency evacuation, and energy consumption/vehicle emission performance modeling; transportation asset management addressing issues of system component interdependency, integration, risk and uncertainty, and sustainability; and transportation network economics. Since 2004, he has conducted a vast amount of research at IIT totaling over \$4.5 million. His research team has had close research collaboration with Argonne National Laboratory and is one of the major partners of the U.S. Region 5 University Transportation Center sponsored by USDOT. In particular, he led the development of the Chicago TRANSIMS model and the National Highway Work Zone Safety Audit Guidelines, both funded by FHWA, and participated in the development of Chicago RTSTEP tool led by Argonne's TRACC Center. He has published extensively, authoring three books with a fourth book in preparation, three book chapters, and over 40 refereed journal and conference publications. He has filed one US patent (U.S. Patent No.: 8109690, 2011) and has received numerous awards, including the ASCE Arthur M. Wellington Prize (2011), the IIT Sigma Xi Award for Excellence (2011), the Charley V. Wootan Award of the U.S. Council of University Transportation Centers (2000), and the International Road Federation Fellowship Award (1998).

Dr. Kuilin Zhang is an Assistant Professor in the Department of Civil and Environmental Engineering at MTU. His research interests focus on multimodal transportation network modeling and traffic simulation, transportation planning, travel demand analysis, rail-based intermodal freight systems, and Intelligent Transportation Systems. He has published over 30 peer-reviewed papers in international journals and conference proceedings as well as technical reports on traveler behavior, dynamic traffic assignment, congestion pricing, BRT, rail-based intermodal freight systems, and integrated passenger transportation corridor management. He is a member of the TRB standing committees on Transportation Network Modeling (ADB30) and Freight Transportation Planning and Logistics (AT015). He has worked on various national and international projects, such as the Strategic Highway Research Program (SHRP 2 C04) and the National Cooperative Highway Research Program (NCHRP 08-57) funded by TRB and the REORIENT project for seamless inter-modal freight transport funded by the European Commission. He has been a key developer of an FHWA-funded intelligent transportation network planning and evaluation tool, DYNASMART-P, led the evacuation network modeling task in RTSTEP, and conducted a dynamic network assignment and traffic simulation task for developing a planning and operations language for agent-based regional integrated simulation (POLARIS). Currently, he is a Co-PI for investigating the impact of high-speed passenger trains on freight train efficiency in shared railway corridors, sponsored by USDOT.

Section 2

Tools, Data Sources, and Computing Resources²

POLARIS, the most essential component extended as part of this project to address extremely detailed transit capabilities, is a fully-integrated transportation system simulation tool that uses an agent-based model of travelers, activities, road networks, transit schedules, land use information, zoning information, Census data, and travel activity surveys, its major components. It is also a dynamic application that simulates the competing actions and intent of all the various agents over time. The term “agent” applies not only to travelers but also to vehicles, traffic signals, and many other elements that are part of the overall model. In an agent-based model, each agent interacts appropriately with other agents on an as-needed basis; for example, agents in close proximity may act to coordinate their driving to share road space and avoid collisions. Agents may also coordinate their activities across a distance; for example, family relationships are an important factor in understanding emerging travel behaviors. In general, travel of family members is coordinated within a complex activity model so that ride sharing and the planning of coordinated pickups can be realistically simulated.

Overview of POLARIS Concept

The above description lays out a fundamental capability of the application—it analyses a synthetic population of travelers across the region and builds a realistic set of daily activities for all individuals who create the need for transportation between those activities. This is a very important approach, because travel is rarely a primary activity but usually results from a need to move between primary daily activities. The data for creating the population come largely from Census data, although it is synthetically reconstructed to match spatial and socioeconomic aggregate data. In other words, the synthetic population is fairly realistic with regards to their choice of home location, work location, and the locations needed to complete daily activities (shopping, school, hospital visits, etc.). With regard to transit, travel survey data can be used to create a subgroup of travelers who organize their lifestyle around access to a transit system, even considering socioeconomic parameters and employment data. These travelers would choose to live and work at locations that are reasonably close to transit stops and hubs, including commuters who use a park-and-ride concept to get to their places of work.

Generally, the choice of whether to use transit or other forms of transportation is not primarily driven by travel time considerations. Socioeconomic factors play a large role and vary from area to area. Accessibility to cars in dense

² Authored by Hubert Ley, University of Chicago, Argonne.

urban areas plays a large role but also is a personal choice when it comes to using park-and-ride options to commute to the inner city. For example, for the purpose of finding the shortest path in the network from place A to place B, a traveler would not necessarily compare transit options vs. driving. This behavior may change during transit outages or major disturbances and may deviate temporarily from a normal choice travelers make. For the purpose of establishing a baseline model, the choice of transit vs. driving was taken from activity surveys, which created a very reasonable ridership model.

The above paragraphs can constitute a normal-day demand model. The term “demand” is used to describe the need for travel based on a thorough understanding of the population to move around to perform their varying coordinated activities. The term is used throughout this document, so it is important to understand it conceptually. This is distinctly different from the concept of supply, which is described in more detail in the following paragraphs. Demand describes the need for movement to do things, and the term “supply” is used to describe the network resources available to the travelers to do so.

Supply is largely the road network, which is represented as a graph, simply a network of streets between intersections but including a number of more complex arrangements, such as ramps onto freeways, walkways that cannot be used by cars, bus stops along the road network, traffic signals that may be dumb or intelligent, and everything else that puts serious constraints on the movement of travelers. For example, individual buses and trains have capacity constraints, and all vehicles have speed limitations, which are also highly controlled on individual streets on the network.

The complex task of assigning demand (travelers and their travel needs) to supply (the road network with vehicles and transit options) creates a complex competition for resources. All cars will have to keep speed-dependent distances from each other, change between lanes, and obey signals and signs and will encounter events all the time (triggering a sensor, reaching waypoints, and so on). In the past, traffic models would iterate between finding paths for each traveler based on congestion on each individual road segment and the development of this congestion based on their choice of path under the constraint of road capacities. Such models were largely static and were not responsive to sudden changes and disruptions. Specifically, these models were aggregated into time intervals throughout the days rather than progressing through time with the possibility of simulating events and changes to the network.

The implementation as an agent-based system in POLARIS turns that logic around. Rather than assigning a route through the road and transit network to a traveler and then sending him on his way to see what happens when he encounters other vehicles, the agent is scheduled to make these decisions

himself in a continuous manner while traveling to his destinations. For example, a person planning to leave home at 8:00 am to arrive at work at 8:30 will be scheduled to determine his best route shortly before departure (this would be like a high-level plan not yet based on actual network performance but rather a general knowledge of conditions on a normal days). The agent executes a call into the POLARIS router, which could be compared to a Google Maps search. Other travelers have been on the way for hours and have started creating congestion already, so the traveler is advised to use a route based on current congestion levels. Once he leaves for his trips, he will stick to this schedule but will potentially experience delays that are emerging for a wide variety of reasons. If the additional delay becomes pressing enough, he will make another call into the POLARIS router and find a better alternative that he may or may not follow.

The above description uses the fact that people make routing decisions not only based on the current congestion on the network but also based on travel time reliability experienced in the past. Historical knowledge is thus considered in the routing algorithm when it comes to high-level evaluation of possible paths through the network. Also, trips may vary with regard to their time points. For example, when driving to work, the departure time is flexible while the traveler aims for a specific arrival time (plus some spare time, probably). When leaving work, this logic may turn around. If the person leaves from work to pick up a child at daycare, arrival time at the daycare center may be the primary concern. In other cases, such as shopping, neither end of the trip needs to meet a particular criteria other than making the trip convenient.

This logic also extends into a much larger picture. Although we are not generally thinking about this, the decision where we live and where we work and what travel we encounter in between will cause us to choose home and work locations based on travel. These decisions are often non-optimal or not even rational, but they need to be considered as a part of the important feedback from the assignment process back to the population and activity model.

To summarize, the interplay of the demand model (travelers and their travel needs to accommodate their activities) and the supply model (street network topology and constraints, transit options) and the emerging behavior of drivers leads to a solution that resembles a real-world road network, its performance, and the movement of travelers. One major challenge is to model the behavior of individuals that is less than optimal (or not even rational). How do you address people that drive around for personal enjoyment? How do deal with people who hesitate to change their route because they are not familiar with the area? The short answer is that each traveler is an agent and may make decisions differently based on a number of criteria. Outcomes emerge from a set of parameters that can be individualized as necessary. For example, drivers could be assigned a preferred speed-dependent distance when driving behind other

cars, may exceed speed limits at different levels, or may change lanes more aggressively. The agent-based approach allows each agent to be constructed differently as long as they share the same basic feature. For example, an ambulance can be built on the model for a regular car but have additional logic and capabilities that are up to the programmer. Such ambulances could receive directions from a dispatcher, could trigger traffic signal priorities, and much more. POLARIS has been specifically designed to be extensible and build more complex agents based on the basic agents implemented in the base version.

As part of this project, a transit model was implemented that interacts with the road traffic in an integrated manner, using the same underlying agent-based approach. In this model, travelers determine the path through the transit network by evaluating all possible connections that could be made while minimizing travel time under constraints such as limiting or penalizing the number of transfers between routes. The model is closely integrated with the street network (as buses drive and interact with the traffic on the roads), includes walking modes as part of the transit routing, and implements more complex options such as park-and-ride. The transit stops and schedules were initially imported from Google's General Transit Feed Specification (GTFS) and are based on exact real schedules of all routes and transit runs. The transit model even has feedback with the population synthesis and activity models because the proximity to transit stops determines whether travelers may choose transit options or not.

Road Network

One of the more essential design criteria of POLARIS is the use of relational and geospatial databases to store much of the configuration information. As outlined in the previous section, the POLARIS model distinguishes between two major entities, the demand model and the supply model. To recap, the demand model describes the need for all travelers to move between their primary activities during the day, and the supply model describes the resources available to accommodate these movements, with knowledge about the time of day, emerging congestion, the ability to change constraints on the fly (e.g., remove or increase bus runs on certain routes, close streets, communicate events through overhead signs, and more).

The demand database is the output from extensive preprocessing, e.g., building the population, coordinating family activities, meeting socioeconomic parameters and matching them spatially, and more. In simple terms, the demand database provides input to POLARIS with regard to who wants to go from where to where at what time and how they are planning to accomplish this. This is certainly more complex than stated here, but for a conceptual understanding, the simplification is appropriate. It should be noted that all activities are performed at specific street addresses, and these locations have

been created in the supply database. One could think of them as individual addresses. In the demand database, their relationship to the street network is not significant, but their geospatial locations can be correlated with land use data, traffic analysis zones, Census zones, employment data, and many other data sources. Much of this is based on geospatial matching of these locations against polygons in GIS layers.

The supply database does not actually know anything about individual travelers. The information in the supply database is rather an extensive and consistent description of the underlying road network, with regard to regular vehicles and transit vehicles. The level of detail is quite amazing. For example, signal systems and stops can be created at each intersection where appropriate, and there will be individual turn lanes if necessary. There are also a number of other network constraints that are defined in the network database, such as speed limits on all roads, one-way designations, turn restrictions at intersections, phasing and timing of traffic signals, connectivity at intersections, use limitations on streets and lanes such as bus lanes and walkways, sensors in the road, location of bus stops, the entire bus and train schedule for the region, and so on.

The supply (or network) database, in all its complexity, is still reasonably small for modern computers to deal with. For example, the network database for the Chicago metropolitan area used in this project is approximately 1GB in size. Due to the use of database technology, the enormous level of detail can be reliably maintained and edited using a variety of standardized and custom tools (developed as part of this project). This provides a level of flexibility that makes work with the network manageable despite the large size.

There are several key features of a database approach that help with maintaining and editing a consistent network at this level of complexity, and although it would be prohibitive to explain these mechanisms in all their detail, the following items give a brief overview how they apply:

- *Atomic transactions* – There are a few modifications that a user may want to make that affect just a single entity. For example, if the user changes a speed limit on a particular street, the change will have no impact on the topology of the road network. But that changes dramatically when the user splits a link to introduce a new intersection. Instead of a single link, the new version of the database will have two. There will be new connectivity records and possibly signal records with new phasing and timing, and there may be turn restrictions. If the application, like a network editor, makes the slightest mistake in changing, deleting, and creating hundreds of records, the network could be easily broken and cease to provide travel in this area. Using a database means that the intermediate can never become permanent by accident, and consistency checks will be applied when committing the changes as a block. The consistency is enforced by the

database engine, not by the user application, so this mechanism protects the database integrity even when using a faulty application to edit the database.

- *Relational integrity* – This is closely related to the previous item. No record can be deleted if it is still needed (referenced) by any other entity in the network. For example, a street cannot be deleted if there is still a bus stop on that street or a traffic signal at the intersection. Again, this is a powerful mechanism to avoid damaging the topology of the network.
- *Relational tables* – Storing large data sets in database tables means that many entities can be stored in a single file. This avoids the problem with partial transmissions and inconsistent versions of data sets. Another advantage is that large datasets need never be fully loaded into valuable RAM in the application. A database provides very powerful mechanisms to load just the data needed for a specific purpose, and will be automatically very efficient with memory.
- *Spatial extensions* – Using a database with geospatial capabilities opens up a whole new world of relating records with each other. In a nutshell, rather than performing formulaic expressions (such as calculating the Euclidian distances between X and Y values of two stops), spatial queries operate on a much higher level and can use spatial indexes to speed up these operations enormously. For example, a spatial query can fetch all bus stops that are within a certain distance from a particular curved street. This is a one-line instruction that would require coding of hundreds of lines of custom code otherwise, and these queries are very fast if constructed properly. Another example would be to find all street addresses that fall within land use zones to assign land use information to these addresses.

The specific database implementation used for POLARIS is Sqlite3. Sqlite3 is not necessarily well known, but it is open source and is the most-used database in application development. The enormous user base assures that the application will be available forever and that the implementation is rock-solid and well-tested at all times.

To provide the geospatial capabilities, POLARIS uses the Spatialite extension library, a plug-in for Sqlite3. Spatialite has become a rock-solid implementation over the past years and is being widely used for major open source projects. This approach allows the use of powerful GIS applications, such as Quantum GIS, to directly access the network database for editing and data processing.

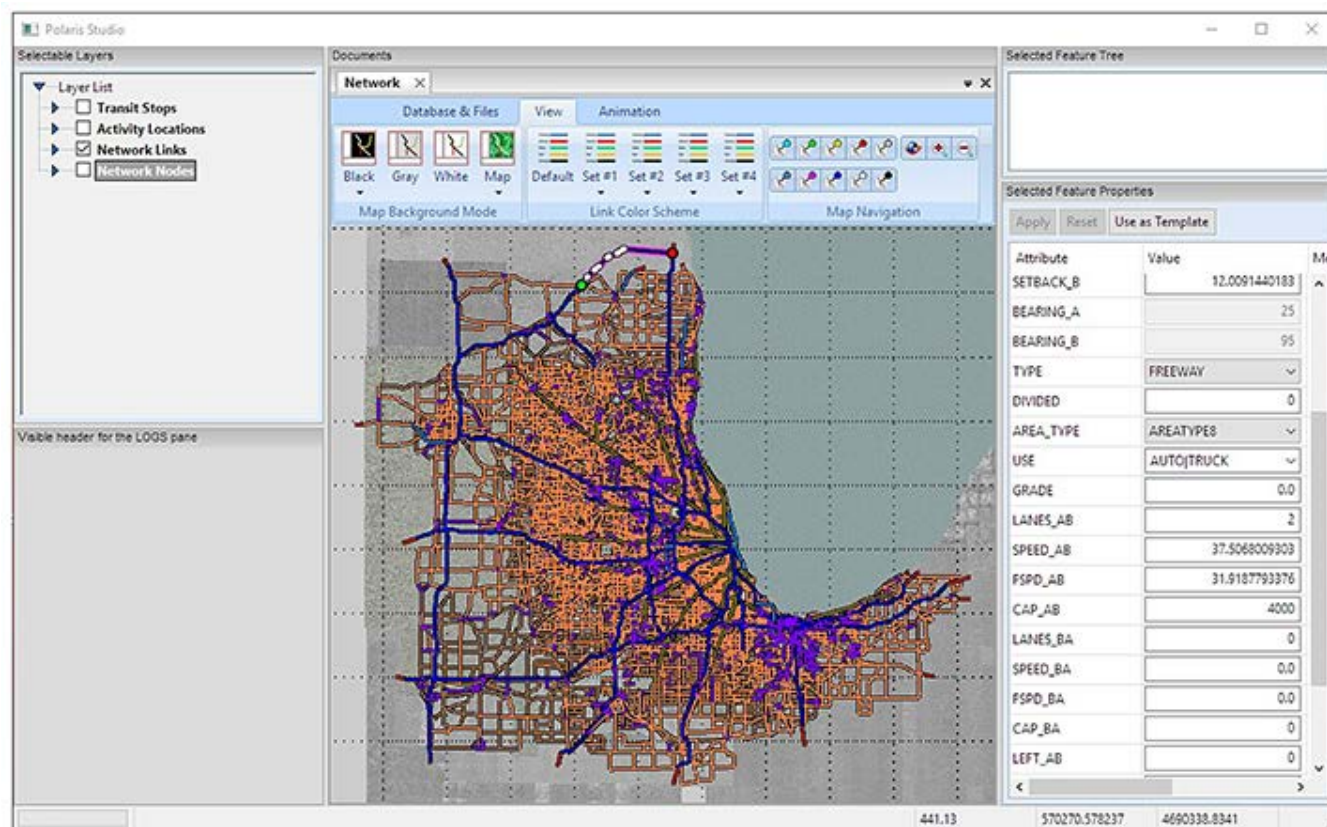


Figure 2-1 Screenshot of POLARIS Network Editor displaying CMA network used in POLARIS

The network editor for POLARIS has been developed over the past 10 years and was modified to accommodate this project. In particular, the ability to import GTFS feeds and matching them with the POLARIS street network is a new feature that enabled much of the flexibility needed for this project.

The network is quite sizable. Currently, the street network is represented with 32,000 street segments, most of which are bi-directional. Expressed in directional connectivity, the street consists of 57,000 street segments between intersections. Table 2-1 illustrates the various network elements.

Table 2-1 Major POLARIS Network Tables for Chicago Model

Network Component	Records	Description
Link Table	~57,000	These street links are the primary elements of the road network and provide fields for speed limits, capacities, vehicle types, link types, use codes, geometries, and more.
Node Table	~19,200	Nodes are intersections for all practical purposes. Each link starts and ends at one of these nodes, and other parameters such as traffic signal phasing and timing are also associated with these nodes.
Location Table	~171,000	Locations are the equivalent of street addresses where activities are performed by each individual. They are representative, and all 30 million daily trips in the Chicago metropolitan area start and end at these specific locations.
Connectivity Table	~129,000	Connectivity records describe the allowed movements at each intersection
Signal Table	~8,000	Table with an entry for every traffic signal system in the metropolitan area (equivalent to the number of intersections with traffic signals)
Transit Link Table	~38,000	Each transit link has been imported from GTFS for the region and represents a connection between a pair of transit stops
Transit Stops Table	~35,000	All transit stops being used on a specific day, also loaded from the GTFS of the three transit agencies in the region.
Transit Walk Links	~65,100	In addition to using transit vehicles between stops and stations, travelers must also be able to walk from their origins and destinations to the various stops and need to be able to use the walk network to make connections between stops when transferring between routes

The network was originally developed by the Chicago Metropolitan Agency for Planning and has been enhanced over the past 10 years to refine the Chicago Business District and to align roadways more precisely with satellite imagery. Although the Chicago Business District is now modeled with nearly all existing streets, most of the network is a planning network that covers only major arterials and some major streets in the outlying areas. This is still perfectly valid as long as there is a complete and accurate road network model where any of the transit vehicles in the area drive. The network has been edited so that all transit routes are now properly projecting onto the road network. The network, in its current state, provides all relevant details on 54,700 miles of roads (speed limits, signals, numbers of lanes, and more) and covers approximately 10,000 square miles at reasonable accuracy.

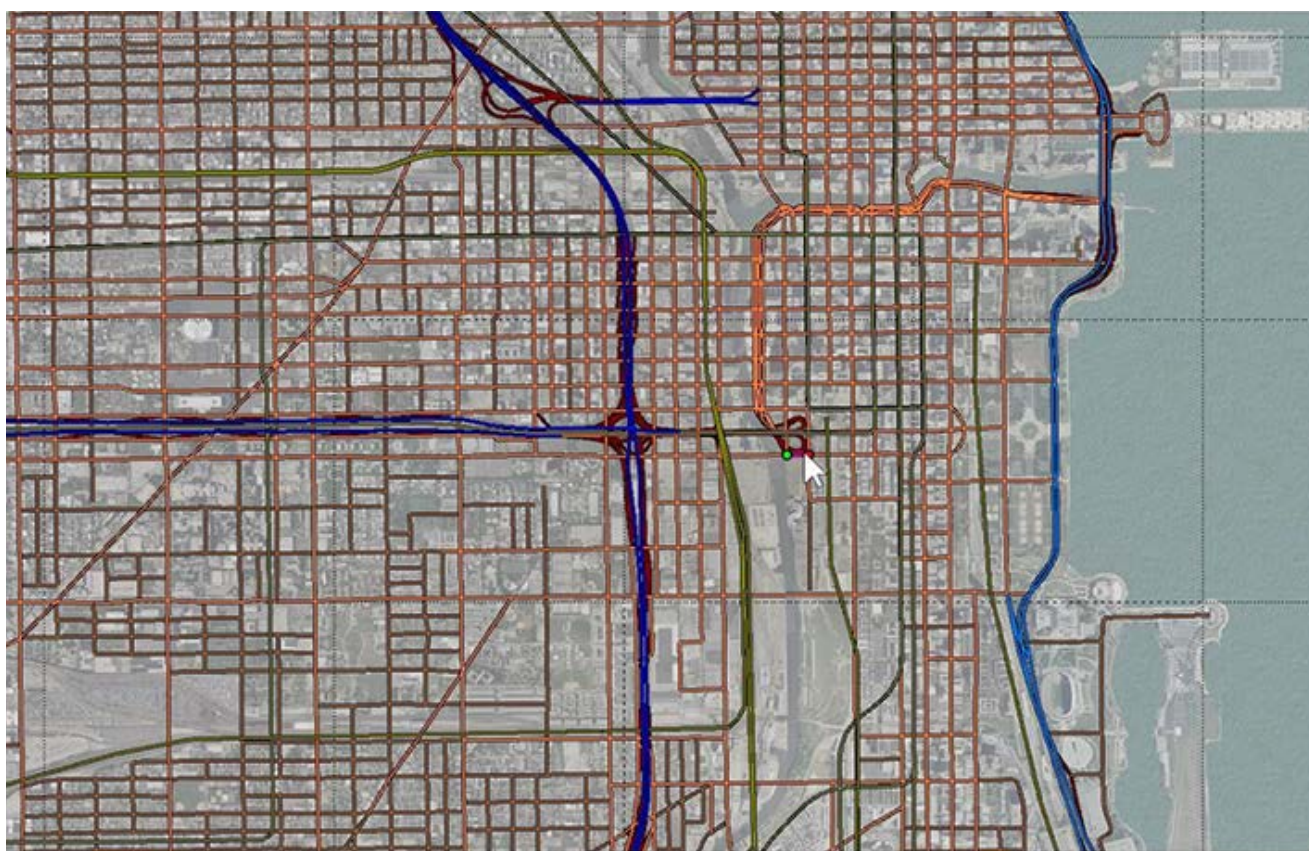


Figure 2-2 Illustration of fidelity of POLARIS network (shown for Chicago business district and surrounding areas)

Transit Network Sources

The transit network in POLARIS is based on GTFS feeds, the mechanism used by transit agencies to send their scheduling information to Google. The advantage of using these feeds is that the data are continuously prepared and submitted to Google on an ongoing basis, and basic qualifications ensure that the data feeds are reasonably accurate most of the time. The GTFS feeds are, in essence, compressed archives in .zip format that are placed on a specific web server owned by the transit agency, which are, in turn, regularly imported by Google to be used for their routing services. The static feeds contain all relevant schedule information as well as stop locations and other important metadata. Each feed file is fully self-contained.

The .zip archive contains entries describing all stop locations, scheduled trips, departure and arrival times at all stops, routes, route variations, daily schedules and exceptions, and more. These feed files are examined by our servers at least once per day and are captured and stored when their contents change. All

transit agencies, specifically Metra, Pace, and CTA, publish this information in respective web server locations, although the frequency of updates varies by agencies depending on their individual implementation of this service.

The acquisition of feed files from Metra started in October 2016, and there have been more than 300 newly-posted feed files since then. It is notable that Metra posts new versions of its GTFS feeds quite frequently on subsequent days. More commonly, though, their files are posted on a weekly schedule. This indicates that updates to their expected schedules are included on a rather frequent basis. The feeds from CTA and Pace are posted less frequently; the number of CTA posts since July 2016 is less than 60 at roughly 2–3 weeks intervals. Even with the CTA feed files, it occurs occasionally that a new feed file is posted on subsequent days, probably to fix errors in the data provided in the previous feed file. Pace has also posted about 60 feed files since April 2016 when this project started capturing these files; these feed files are updated every 2–4 weeks.

There were a few limitations to using this data that were not originally obvious, although some were not too serious.

The exact specifications contained in the data files are very concise, but only within each individual archive file. The files contain the locations of all reference transit stops in form of longitudes and latitudes and the exact arrival and departure times for every transit trip. But the next feed file may have updated information—for example, modified longitude and latitude entries for transit stops. These changes may be significant—for example, Pace making an effort to correct its stop locations over the past years, leading in some cases to significant movements of otherwise static objects (a few stops moving by several hundred meters, for example).

In interviews with the transit agencies, it also became clear that their preparation of GTFS feed files is not 100% automated and that some data errors make their way into these files. There are also a number of interpretations and assumptions that do not hold up under scrutiny. For example, GTFS feed files posted by Pace, according to requirements established by Google, have to be posted one week before the schedules go into effect. Based on that requirement, a feed file posted on a given day may not have any trips scheduled for the first day after posting and guarantees correctness only for six days after posting. One example of this issue is the April 1, 2017, posting of a GTFS feed file by Pace, which when queried, did not show any trips on April 1. This leads to a certain “fuzziness” of validity of entries over time, which has to be considered when using this data.

A closely-related issue is that any given GTFS feed file may contain the specifics of a trip scheduled in a few weeks. The internal structures to identify service calendars and calendar exceptions are very concise and will schedule trips with

specific trip IDs on a particular route for these future dates. Nevertheless, before this scheduled date is encountered, one or more new feed files are potentially posted by the transit agency. The trip identifiers used by these subsequent feed files may be consistent within each file but not across multiple files. This means that a particular trip appears to be identified by different IDs when using subsequent feeds, and there is uncertainty with regards to whether the new feed file is correct or whether the old feed file should be authoritative (mostly because feed files are posted by the agencies on their websites, and there is no indication on whether Google detects their presence and starts using this information).

This issue becomes a problem when dealing with dynamic GTFS feeds and correlating them properly to the static feeds (more about dynamic feeds is provided in a later section). The dynamic feeds, providing real-time transit vehicle locations and schedule adherence every 30 seconds throughout the day, are a powerful data source for examining delays and performance statistics, but IDs used in these dynamic files to identify specific trips may be inconsistent between two or more static GTFS files with which they should correspond, and there are additional issues because the dynamic feeds are typically provided not by the transit agencies themselves but rather by a third party. There is no information when the third party reads static GTFS feeds and bases its real-time feeds on those identifiers.

In summary, although the format of static GTFS files is very concise and is checked for quality, the effect of posting only a single file at a time removes the needed historical perspective on these feeds, and much of the changes over time need to be reconstructed as best as possible before the data can be used.

The servers used by the team capture these data as well as the dynamic GTFS feeds from Pace and CTA and reconstruct the historical procession of the feeds. This mechanism allows for a software library that can be used to extract all relevant transit data for a specific date from the overall set of source feeds, which is needed to populate the transit model within a POLARIS network. This is an important detail that should be clearly understood: the GTFS representation of transit data covers at the very least a time frame of a few weeks, whereas the representation in POLARIS must be for a specific day extracted from this superset of data. This is a common approach for large system simulations, especially when dealing with large regional models.

Transit Network in POLARIS

To import transit data from GTFS feeds, the first decision is to select a specific day for which to load data. This day should be chosen to be representative of a typical working day, such as a Wednesday not enveloped by holidays. It also

makes sense to consider seasonal variations, and the most representative transit operations typically were in the early fall of each year.

The tools developed as part of this project allow reading these data considering a multitude of GTFS feed files and automatically selecting the most recent list of transit stops, routes, trips, and individual schedules. The data also were merged from all feed files of all agencies before doing so to create a network representation that was as complete as possible.

Because transit stops may be defined differently in subsequent feed files (e.g., slight location or feature changes), only stops used by any of the day's trips were loaded. This was still a significant number—approximately 35,000 stops in the Chicago metropolitan area.

GTFS stops have well-defined identifiers used in the list of trips and the departure schedules to identify these locations and in which order they are traversed by transit vehicles. The stops are located at specific longitudes and latitudes, but their spatial relationship to the POLARIS network was not explicitly known. A special matching application was developed and is documented in great detail later. The matching application compared the location of transit stops with the roads in POLARIS and decided on their location along the street network based on spatial considerations and the succession of stops served on the many trips contained in the feeds. This correlation is important, because performance of buses on the road network may lead to delays, and travelers will have to find their path through both the transit and the street network with a combination of buses, trains, and walking.

For the purpose of finding a path through the network, all GTFS trips were evaluated to determine which pairs of stops are being served by each. The 350 routes in the Chicago area have around 2,300 different sequences of stops that are being served in succession. Each route has usually at least two sequences for the opposing travel directions, but there are many variations created by areas served only by a subset of trips, different start and end points, express buses and routes skipping otherwise successive stops, and so on. From the need for routing passengers through the network, any pair of stops that may be directly connected by at least one route was created as a transit link and supplemented with regard to all routes and arrival and departure schedules extracted from the GTFS feed for the stop. The process resulted in about 38,000 unique transit links. As noted, the exact succession of streets through which the vehicles pass between these stops was needed to determine interaction with other vehicles, but the transit link table is more abstract and does not care about the exact path of vehicles in between; describe are only the arrival and departure information that can be used to connect from one stop to any of its neighbors.

From a routing perspective, all travelers start their trips at street address or activity locations in the POLARIS concept. Thus, a transit trip always begins with a walk segment, although there may be driving involved for park-and-ride passengers. Walking is also required for most transfers between the many transit routes available to travelers. Specific stops, especially when serviced by different transit agencies, are rarely used by more than one route. Thus, a passenger must walk along the POLARIS street network to make connections. This is a much-improved alternative to having passengers move on straight lines between possible transfer stops, because it considers the topology of the underlying network. A simple example would be the location of two stops that are located on the two sides of a freeway. A person cannot freely walk across the traffic in this case and would have to use bridges or traffic signals at intersections to do so. The sometimes subtle differences caused by having to walk realistically across the street network to make connections greatly improves the predictive ability of POLARIS with regard to what transit routes a passenger will choose to serve his or her needs.

The supply model, meaning the network resources and transit schedules, is blind with regard to the population served. The population varies widely with socio-economic characteristics, employment opportunities, zoning, and land use; these are all properties of travelers in the POLARIS demand model that make use of the road network to move people around. But the existing scheduling of transit trips and the areas served by transit routes contain implicit knowledge of these important factors. Areas that have been determined to need a higher density of transit service will have that denser service schedule, and the travel times from stop to stop at different times of the day contain implicit traffic congestion information. The use of exact GTFS feeds in the traffic models is, therefore, a resource that is very valuable for understanding the interplay at a level that POLARIS deals with.

The transit system in Chicago is an extensive operation covering a very large area. Pace covers the largest transit operation by area in the U.S., although not in passenger volume. Commuter rail operations provide transportation to many of the outlying areas and is especially important for effective movement of large numbers of park-and-ride passengers. In the region, transit travelers make approximately 2.7 million daily transit trips; the total number of trips, including regular vehicular traffic, is close to 30 million, with a population of about 9 million living in this area. Given the importance of transit operations and especially the congestion issues involved with moving large numbers of people in and out of the business district on a daily basis requires a reliable and resilient transit operation. Incidents may happen anywhere in the region but will likely have their largest impact in the business district or in the large surrounding suburban areas.

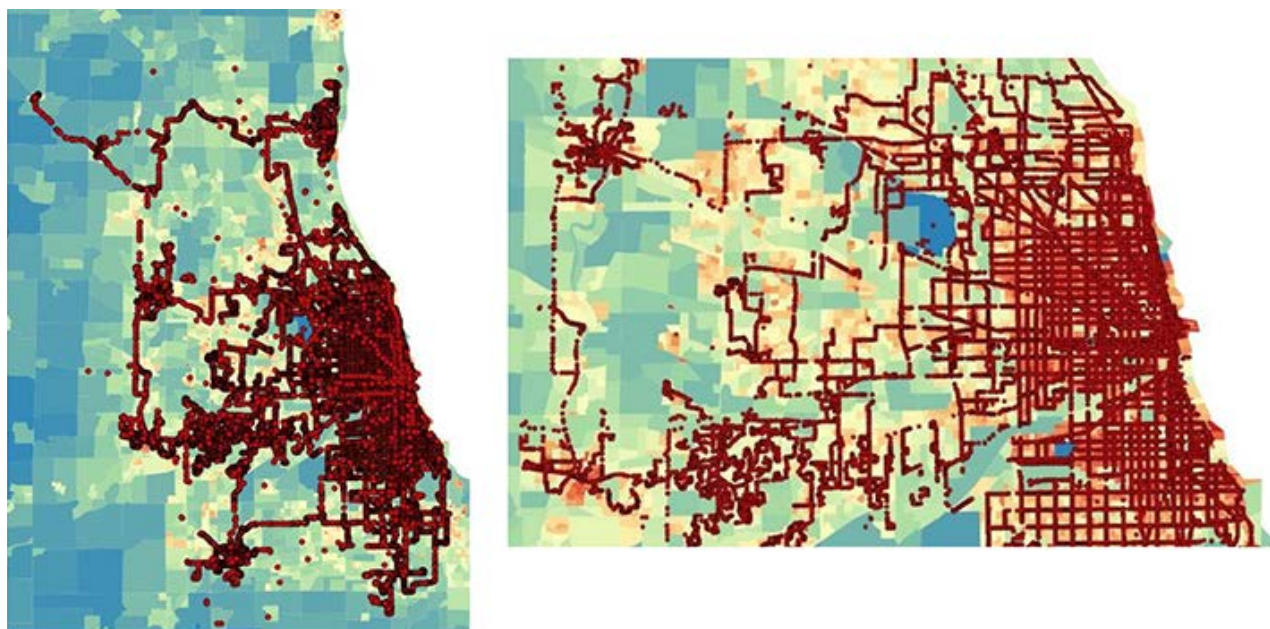


Figure 2-3 *Density of transit network at various scales in Chicago metropolitan area*

Real-Time Transit Feeds

The project team captured real-time data from the transit agencies, with the exception of Metra, where real-time data were not readily available and would be less significant in a transportation systems model due to the fact that rail schedules do not normally influence traffic on the road network and vice versa.

The real-time data are generally unfiltered, as shown in Figure 2-4, which shows the traces of buses serving Pace route 208. The data were filtered to show which data points fall into the vicinity of where this route operates, resulting in the green set of points. There are many reasons for these messy traces, because data are captured indiscriminately and buses may be en route to start servicing route 208 or may have ended servicing that route and are on the way to the next run. On some days, there may have been detours encountered, and there is the possibility that the trip being serviced by the bus was not properly coded to the vehicle, leading to data that should apply to a different route by error.

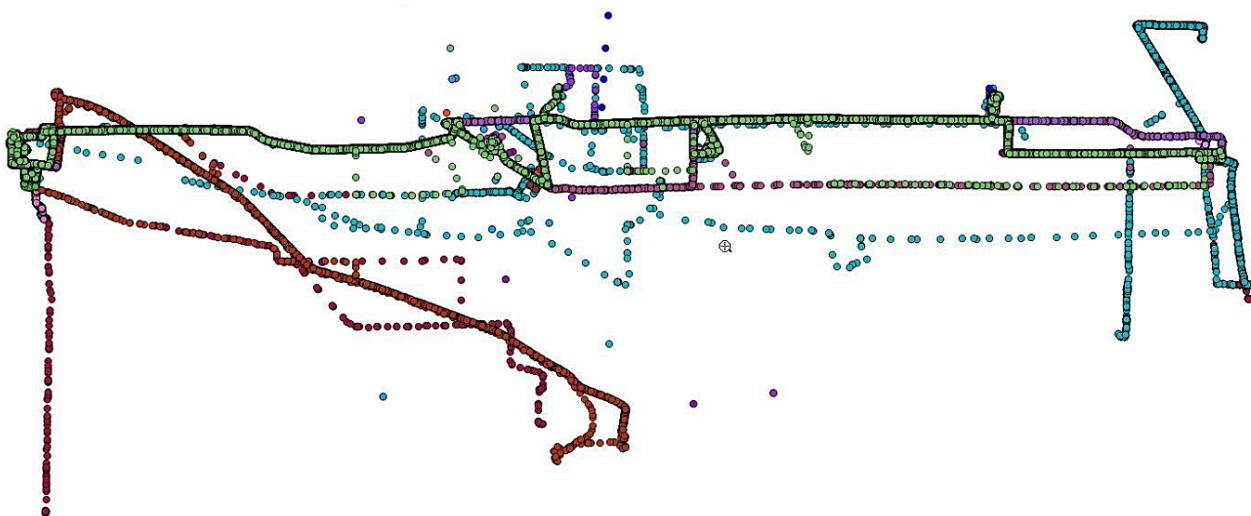


Figure 2-4 Example of real-time data for buses servicing Route 208 on Pace network

This route also exemplifies the challenges for capturing, processing, and referencing real-time data for bus routes. A typical route will make extra loops, returning to the main trunk after making a few stops. The buses may also drive in small and larger loops—for example, using ramps to enter expressways. Algorithms that filter the data points cannot rely on interpreting subsequent locations based on the time elapsed, because samples are usually taken only in 30-second intervals, which means that a bus may have traveled a significant distance since the last sample was taken.

Before discussing data quality issues and processing algorithms, a discussion on available data sources in the Chicago region is presented that includes the issues and methodologies for capturing these data for use with this project.

Real-time data comes from three sources. For Pace, the team had access to the real-time GTFS feed that Pace provides to Google for transmitting current transit states around the clock. For CTA trains (L-trains) and buses, two separate custom systems were accessed to extract the relevant data.

Pace Real-Time GTFS Feed

The real-time feed that Pace uses to transmit data to Google also was available to the project team. It comes out of a system operated by a Pace subcontractor and is not directly under the control of Pace planners or operators. The data are posted using protocol buffers, as a file format developed and maintained by Google to transmit data in a consistent format in an efficient, compressed, and easy manner, including error control and detection, and more. From a user perspective, it is a file posted on a specific web server and is updated on a

regular basis. For Pace, the file is re-posted with fresh data every 30 seconds. These files are reasonably small considering the amount of information contained in them. Each file provides the current location of every bus Pace operates as well as projected arrival and departure times for a series of upcoming stops for every trip currently being serviced. This description is very general, and there are issues that limit whether the data are current, what data may be missing for technical reasons, and so on. Similar to the static GTFS feeds, each file is self-contained, and data from a previously posted file are not needed to interpret the content of the next feed file. These feed files vary in size but hold data for hundreds of vehicles and trips currently operating on the network. Each file is usually a few hundred kilobytes and may contain data for 500 concurrent vehicles.

The files are being captured every 30 seconds, amounting to 120 files per hour or 2880 per day. The data take up a little less than 1 Gigabyte per day, which is not a problem with regard to storage capacity on modern computer systems but requires a significant amount of computing capacity for data extraction, data cleaning, data compression, and other data-related tasks. The raw data in the protocol buffer files are meant to support the display of current locations and the ability to display projected arrival and departure times within Google Maps. When being used for data mining, the context for these data points needs to be more closely established, bad data need to be identified and filtered out, and errors in the data stream need to be recovered from. The data points also need to be correlated to all the other data collected for the road network, including matching the data to the road networks used in the models.

As outlined earlier, each protocol buffer file is completely self-contained and can be used without the need for preceding data files. Each data file is timestamped with regard to the time it was created, which may be different from the time the file was downloaded. To not miss any data files, the download operations were oversampled, with a download every 25 seconds or so. As a first action, the time stamp was read for the only downloaded file, and the file was discarded if it was identical to the one previously downloaded. This avoided data duplication on the systems and ensured that no data files were missed due to timing issues.

The time stamp for each data file identifies the time at which the data file was assembled. The data contained in the file is a collection of GPS locations of all transit vehicles that may have been acquired recently but not at this exact time. First, the vehicle captures the GPS coordinates, then it transmits them by some wireless method to a central system, which eventually assembles the records and posts them as a collection of data points in the protocol buffer. The important thing is that the exact time stamp for each vehicle location is retained throughout the process and is part of that vehicle record in the protocol buffer. This leads to situations where a vehicle location may have occurred a few minutes before but no new records have been received by the central service.

Thus, the next protocol buffer contains a time stamp for the vehicle location that has not been updated in this feed file compared to the last feed file but because each capture time of a GPS location is known, this does not pose a data interpretation problem.

The project team may not use all data contained in the protocol buffer files. Of specific interest are performance data that can be extracted from these files. At a minimum are the following data fields extracted for each vehicle:

- Vehicle identifier
- Trip identifier for trip being serviced by this vehicle
- Time of when GPS location was captured at 1-second precision
- Longitude and latitude of vehicle at that time

In addition to vehicle positions, there are sizable trip data entries contained in these files as well. The trip data entries provide the following information on a per-vehicle basis (it should be noted that there may be more than one vehicle serving a trip at any given time, e.g., to increase capacity, so the trip data table is on a per vehicle basis):

- Route identifier
- Trip identifier
- Vehicle identifier
- Date on which trip was scheduled to depart
- Scheduled departure time on this date
- Time table for arrivals and departures at nearby stops (preceding and future)

These data entries provide the key for correlating the real-time data to the static GTFS feeds, although these matches are not always perfect. For example, the Trip ID may reference an older static GTFS feed depending on when and how the newest feed file was posted and downloaded by the various servers in the communication and processing framework. It should be noted that the above data are sufficient for Google Maps to provide identifying data to users on their website.

The actual bulk of the payload in a protocol buffer file is the time table of arrivals and departures at nearby stops. This is rarely a list of all stops serviced by the vehicle along its trip, and given that these data must be transmitted every 30 seconds, it makes little sense to transmit projections for the entire trip. However, the table is meant to be used in conjunction with the static GTFS feed, which has the schedule for all stops of this trip. This means that the projected arrival times in the real-time feed are meant to supplement the static schedule. For example, if a bus is known to be 10 minutes late at the next upcoming stop, it will also be assumed to be late at all later stops by that amount unless an

entry is found in the real-time data that resets projections for upcoming stops to their defaults.

The real-time feed is also meant to provide the means for a transit operator to provide information about unscheduled trips to Google. That means that a vehicle and trip found in the real-time feed that does not correlate to a statically scheduled trip may be an extra service being run by the agency, in which case the scheduled arrival and departure times in the dynamic stop list can be used by Google for routing passengers. This is where a few data consistency issues originate. For example, if a Trip ID is not found in a static GTFS feed, Google would not consider this to be a data quality issue but simply use the real-time data. If the same would be operating at the same time under a different Trip ID, it would not matter much for Google or transit passengers because duplicate routing options may not be something that passengers would notice. From a perspective of using these data for data mining purposes, such as extracting performance data, these data consistency issues become much more important.

Other data consistency issues have been identified in the static and real-time GTFS feeds. For example, a static GTFS file may schedule trip to depart at 25:34 on a specific date. This makes sense because this trip serves passengers of that day but happens to be scheduled to leave after midnight. The static GTFS feeds for the Chicago region occasionally schedule trips departing as late as 27:00 on any given day. Also, the arrival and departure time of trips originating before midnight may extend to the next day and are provided in 24-hour format beyond midnight. The real-time feeds do not use times beyond 23:59:59. From a perspective of time passing by second by second, that makes sense. But a trip scheduled for a specific date may be scheduled to leave at 01:34 am, making it difficult to understand whether this corresponds to the same day's schedule or the next day's schedule.

The real-time GTFS feeds have the arrival and departure time lists for each of the trip entries. This list is somewhat over-specified because there are six entries in the table:

- Sequence number of stop on trip
- Stop ID for stop
- Projected arrival time
- Projected arrival delay
- Projected departure time
- Projected departure delay

The real-time GTFS files for Pace do not provide all these values for every record. Typically, the departure time and departure delay are given but the arrival time and arrival delay are not. This is good enough in most cases, but

there are times when the entries also contain a record for the arrival time and arrival delay. In those cases, the Pace feed provides the information in two records rather than one (specific arrival and departure times and delays in the four data fields). Instead, the first record has the arrival time and delay, and the second record has the departure time and delay. To do this in two records, whatever software generates the data increases the sequence number for the second record and duplicates the stop identifier. This means that for all upcoming stops, the sequence number is increased by one and is incorrect according to the GTFS specifications published by Google. In some cases, record duplication occurs more often than once, forcing the sequence to be off by 2 or even 3. The feed data can be repaired using some external logic if the static feed is known. But the issue illustrates the complexities of providing a real-time data feed and the level of complexities to be understood when processing the data to extract meta information such as performance data.

CTA Real-Time Data Feeds

CTA operates its own services for real-time data service—the CTA Train Tracker and the CTA Bus Tracker. Both services provide access to location information in a custom format that is published by the agency. The data are very different for CTA trains, so the project team captured data for CTA trains and buses using separate mechanisms.

For CTA trains, the data were captured every 30 seconds. The resulting data file was organized by line (route), and within each line there is an entry for each run currently operating. Each run was identified by timestamp, longitude, and latitude, and the information contains other useful meta data such as the Stop ID, Stop name, arrival time of and at the next station, destination overhead display value, compass heading, and so on.

CTA Bus Tracker data are collected every 60 seconds, and each file covers hundreds of location records for CTA buses. Each entry consists of a number of data fields that can be used to extract performance data when examined over time:

- Route identifier
- Time stamp for when the data was collected
- Vehicle identifier
- Longitude and latitude
- Final destination of this trip
- Heading of vehicle
- Trip information

The records do not contain a reference to the static GTFS feed with regard to trips, so matching the vehicles with scheduled trips is a larger problem than with the other data source used for this project.

Data Analysis Tools, Case Configuration, Simulations, and Visualizations

The massive amount of data from this project, and especially the results from the simulations, were difficult to validate and debug. For this purpose, visualizations were developed that allow tracking down problems in the software and to illustrate the movements of transit vehicles throughout the simulation.

The datasets from POLARIS, using the individual transit passengers and their use of transit vehicles throughout the day, were aggregated into passenger counts on vehicles that can be compared with APC data from the transit agencies. The basis for these visualizations is an Open Source software application, Quantum GIS, which was chosen because of its compatibility with the POLARIS Network Editor and the network database maintained for this project.

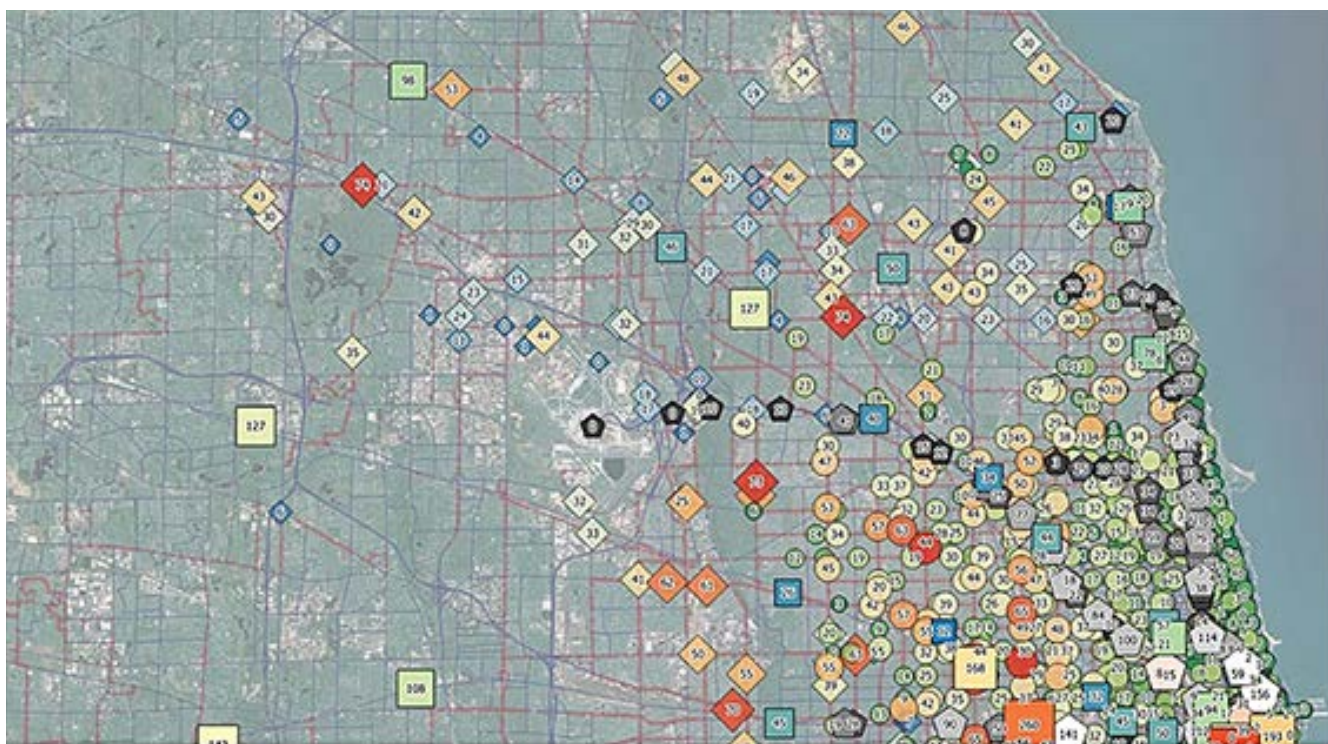


Figure 2-5 Screenshot of visualization showing load on simulated transit vehicles in northern part of Chicago metropolitan region

The scenarios analyzed had to be configured for POLARIS using both the POLARIS Network Editor and Quantum GIS. Within the network editor, an area can be selected dynamically to determine the streets and rail lines affected by the scenario. The software then disables traffic on these network links and determines the associated stops. An analysis of the routes using parts of the unavailable network is then performed to determine the segments of bus and rail routes that are artificially terminated in the vicinity of the closed area. Incoming route segments are considered to be serviceable, but outgoing segments are removed from the simulation.

This leads to a complex modification of the transit network in the vicinity of the transit disruption, specifically for the duration of the event. In the case of the Jefferson Park scenario, a significant number of trips is interrupted, and passengers are stranded at the location within the affected area (at the onset of the event) or in the surrounding area (if arriving after the onset of the event). It is realistic to assume that passengers arriving on buses will terminate their current trips and search for new available options using the transit router. This includes now-significant walking distances to stops not affected by the scenario. The still-available transit stops are located on a perimeter outside the affected area, and the software analyzes the existing routes to prevent them to terminate on streets that are affected. This leaves a significant number of bus stops available, most of which are not immediately suitable to re-enter the transit system in a meaningful way. For example, a rarely-served bus stop on a close-by street is useless for the purpose of continuing a trip in the immediate future.

In Figure 2-6, these issues become more obvious. As shown, in the center of the area is the Jefferson Park Transit Station, which is served by Pace, Bus, and Metra. The green stops along the road network (at a radius of about one mile in this scenario) are locations where current transit trips are immediately terminated. Passenger will have to leave the buses and continue their trips by walking along the streets to a suitable connecting stop or station. Some passengers may be able to stay on the buses as they use the road network to leave the area on non-scheduled paths, but that is not significant. Some passengers will change their travel plans, and others will use taxis or ride shares or other means of transportation. This particular configuration step deals with the changes to the transit system and resources and not with the demand.

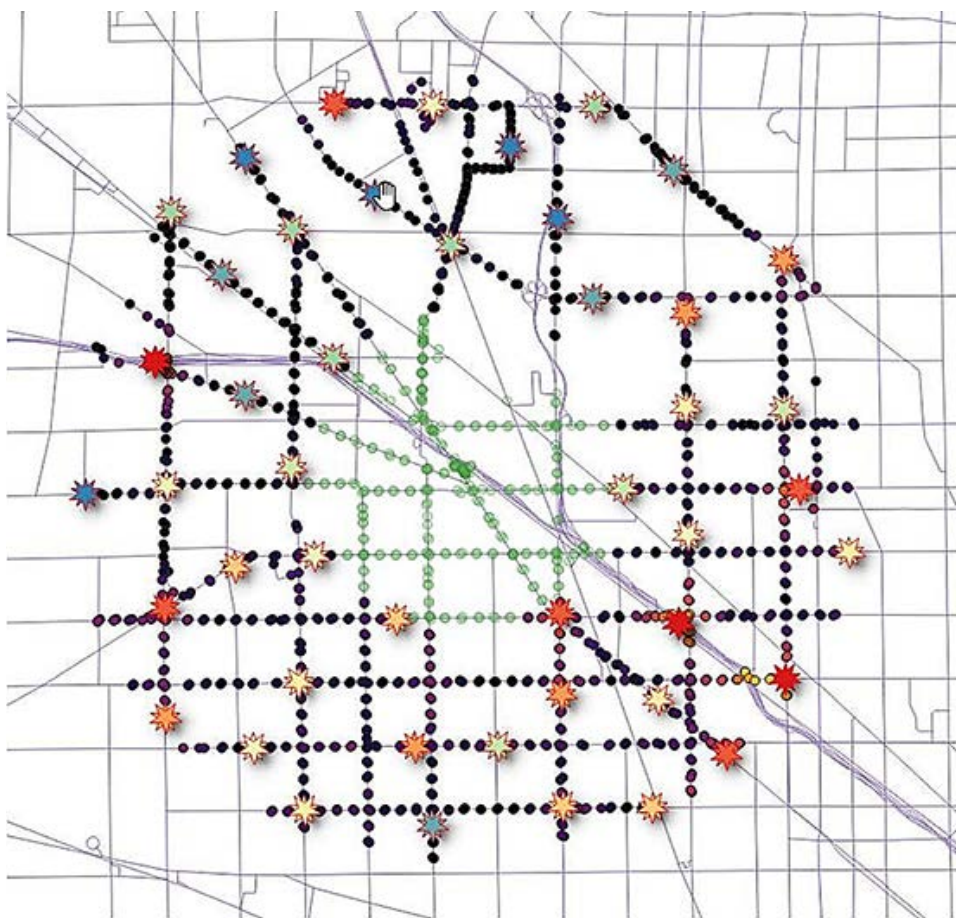


Figure 2-6 *Illustration of scenario configuration in vicinity of Jefferson Park showing simulation methodology for transit disruptions in specific area (actual bus stops and rail stations)*

To model an active emergency response by transit agencies, the problem needs to be configured with a number of suitable ad hoc point-to-point bus trips that move an optimum number of stranded passengers across the affected area. The constraint is the number of buses available to do so, but to find the optimum set of point-to-point trips across the area given the limited number of buses available, the software determines a soft criteria of “suitability” of stops in the perimeter to serve as start and end points for such ad hoc trips. To do so, each stop on the unaffected street network is evaluated for its proximity to a maximum number of routes. The top locations are shown in Figure 2-6, colored by their local attractiveness within a reasonable walking distance. As an optimum location within a certain distance from each stop within a cluster of stops is found, it is selected as a candidate for the origin and/or destination for an ad hoc trip. The algorithm selects the stops marked by stars in the figure, colored by their local attractiveness.

Ultimately, the number of these origins and destinations is too large to be served by ad hoc bus trips, but the software creates a larger number of candidate ad hoc routes on the fly anyway using an internal router within the network editor. This router uses only network segments that are still available despite the emergency, and routes paths randomly around the affected area. This may result in a set of 100 or more potential ad hoc point-to-point routes, which are candidates for optimization with the optimization model. They will be chosen based on constraints such as the number of buses available in the area or changes in passenger volume.

The process can be illustrated using a set of figures, which are part of a demonstration video that was prepared to illustrate the methodology to the operators and stakeholders in the area. The illustrations are more abstract than the above tools setting up the scenario but are more suitable to illustrate the algorithms and their individual steps.

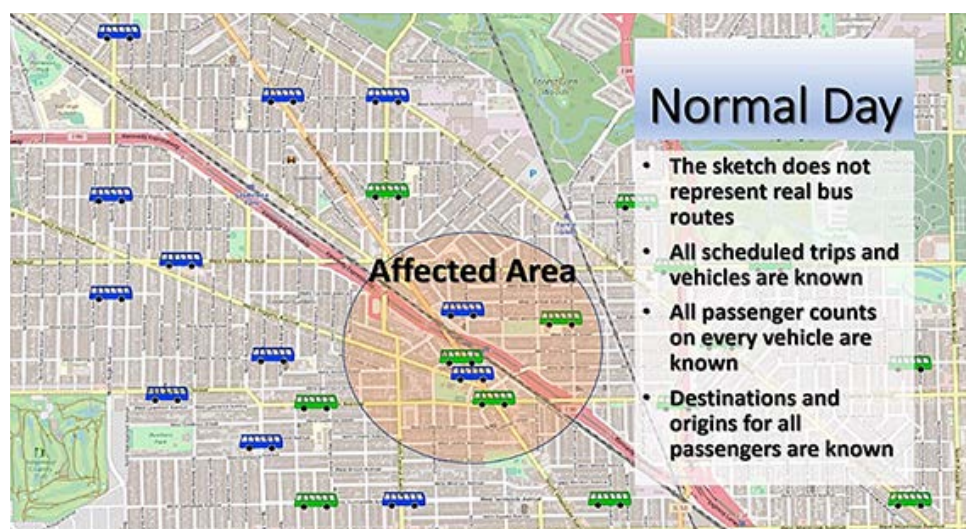


Figure 2-7 Jefferson Park scenario—affected area on normal day

At the onset of the scenario, the transit system is operating under normal day conditions. As simulation progresses forward in time (or as the incident develops in the real world), a specific area is affected and disrupts travelers in the vicinity of the event. Buses caught in the event are shown in red, although the schematic is not meant to provide a very real-world understanding of the details. From a simulation perspective, the red buses are caught up in the disruption and cease to operate. At this point, passengers are stranded at the next stop at which the vehicle would stop anyway; they accumulate on the street network and may start walking to alternative connection points, either informed by announcements by the transit agencies, but more likely doing so based on information gathered privately from cell phones and personal

communication. Although the immediate and total discontinuation of service in the area would happen more gradually in the real world and some buses will be able to continue their trips, the overall effect is a build-up of stranded travelers and others trying to leave the area.

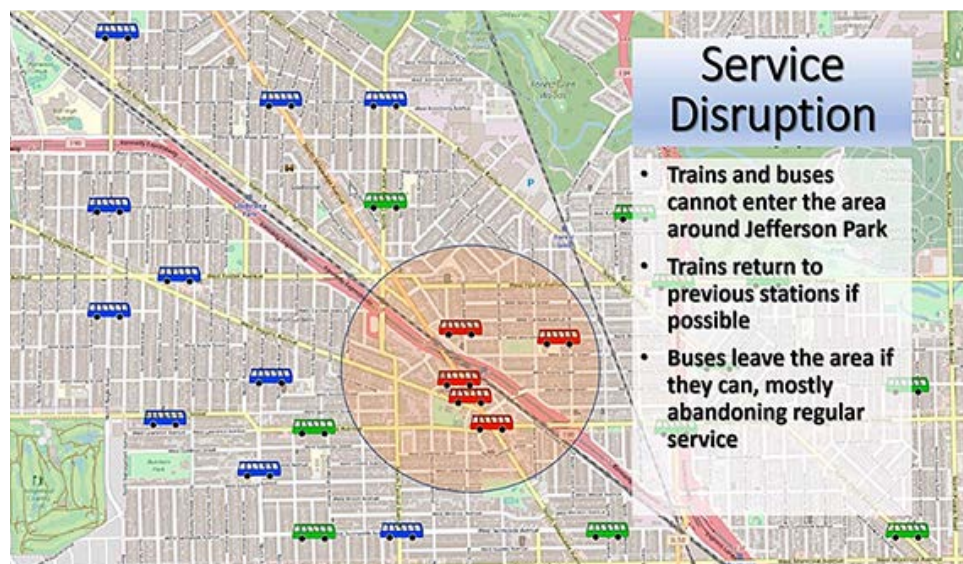


Figure 2-8 Jefferson Park scenario—onset of disruption of transit

At this point, operations are under the assumption that automatic passenger counters and fare card data could be available in real time to the transit operator dispatch centers and could be fed immediately to a rather fast-running short-term demand forecasting model (developed by GMU). The data are, in reality, collected overnight by downloading it from buses or accessing the fare card provider's databases. Thus, the automatic detection of short-term demand changes cannot yet be truly handled in real time, but the accumulation of stranded passengers in the transit system based on their location at the time of the disruption could be determined by observing the actual counts with normal data counts and the corresponding statistical analysis.

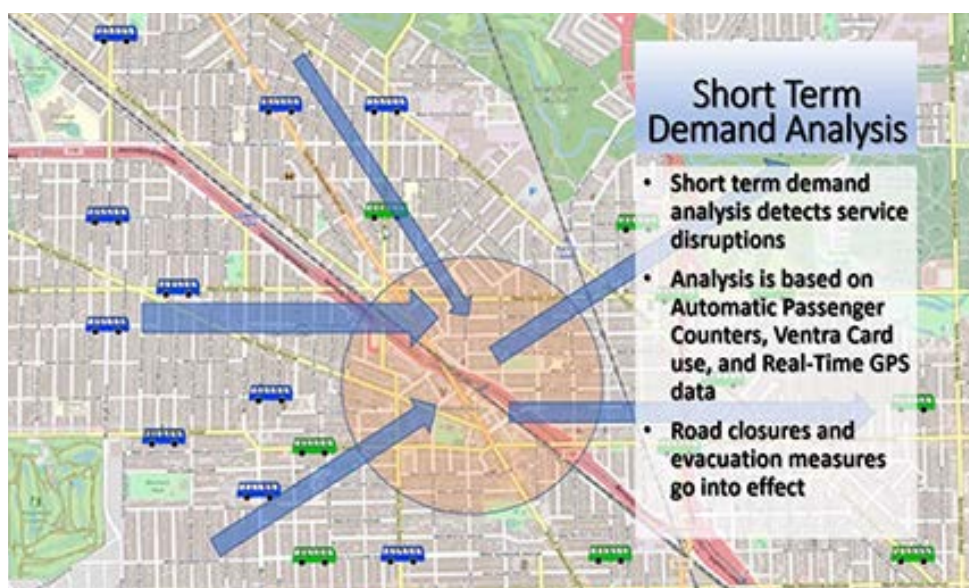


Figure 2-9 Jefferson Park scenario—short-term demand analysis

A point of caution—the original concept was using Bayesian statistics to determine the succession of changes in boardings and alightings at the stop by stop level throughout the region, but the total number of stops, routes, trips, and passengers throughout the day is too computationally-intensive to be achieved within a meaningful time. Thus, the process is based on aggregate statistics by travel analysis zone, which is too broad for fine-grained analysis at this time. By knowing the general location of incident in advance, the process can be limited to a smaller region, but it remains important to understand that the trips of travelers going through a central location such as Jefferson Park has ultimately large consequences for connectivity to far-away trip origins and destinations.

While the event unfolds and more and more people are stranded in the area, transit agencies will start organizing a response based on incomplete assessment of the scope but generally based on local observations by police and other officials. Traffic counters are not usually available in urban areas, but the short-term demand model would observe the change in passenger boardings and alightings, providing meaningful input to the transit agency responses. Coordination among the transit agencies may start at this time, and the most likely response would consist of assessing the availability of buses and drivers at the various depots and dispatchers identifying the stranded buses to determine if they can be used to support an active response. These actions would be imperfect but would take place. The problem is that the dispatchers would not know where to send the buses unless the accumulation of stranded passengers was easily observed or reported. Thus, the short-term demand model based on real-time knowledge of passenger location would be extremely helpful.

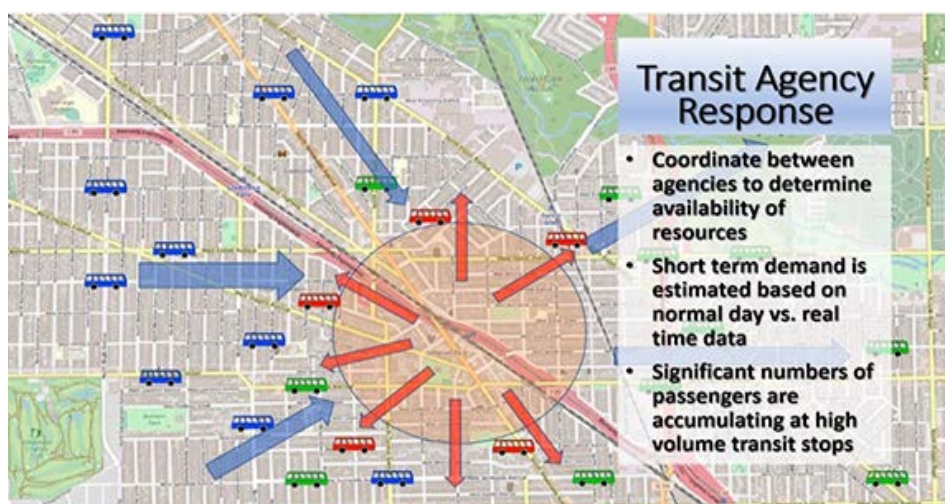


Figure 2-10 Jefferson Park scenario—initial transit agency response and short-term demand estimation

In project simulations, POLARIS was used as a real-world stand-in to determine the effects of evacuation strategies being deployed. The short-term demand model informs POLARIS of the scope of the disruption, and the process of determining remaining transit assets begins. This includes the determination of suitable point-to-point routes using the scarce remaining buses available to responders and the assessment of their potential routes on the perimeter of the incident.

At this point, it is expected that travelers will make their own decisions about how they will continue their trips. Some will wait for the system to become operational again, some will use alternate transportation, and some will depend on buses made available as part of the regions emergency response. Communication is a key component at this time, letting passengers know what their options are and selecting the optimum use of the remaining bus fleet in the area.

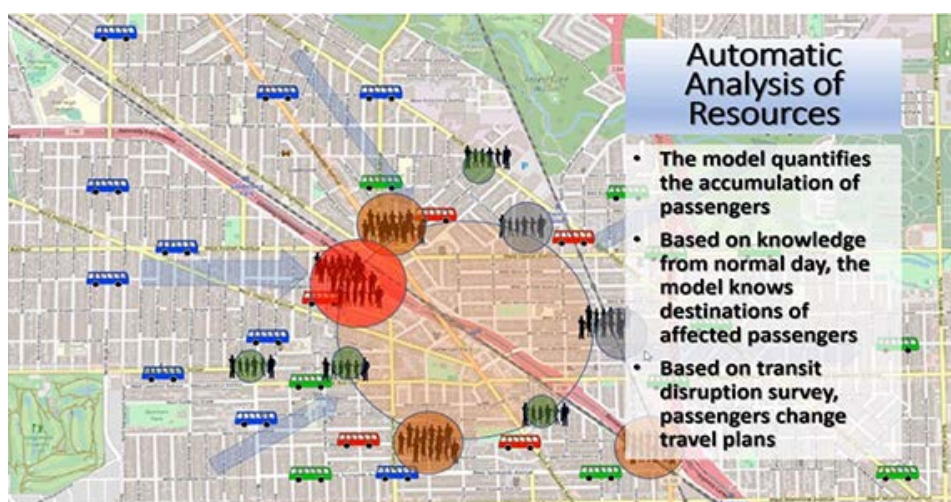


Figure 2-11 Jefferson Park scenario—passenger response to transit disruption

The emergency response, as chosen by the operators, will be hindered by a developing congestion on the road network. Depending on the cause of the incident, vehicular traffic may increase dramatically and may cause further difficulties with deploying the remaining fleet of buses. POLARIS has been modified to have the buses flow in the actual traffic on the roads, which is especially important on these ad hoc bus routes that are being evaluated and optimized.

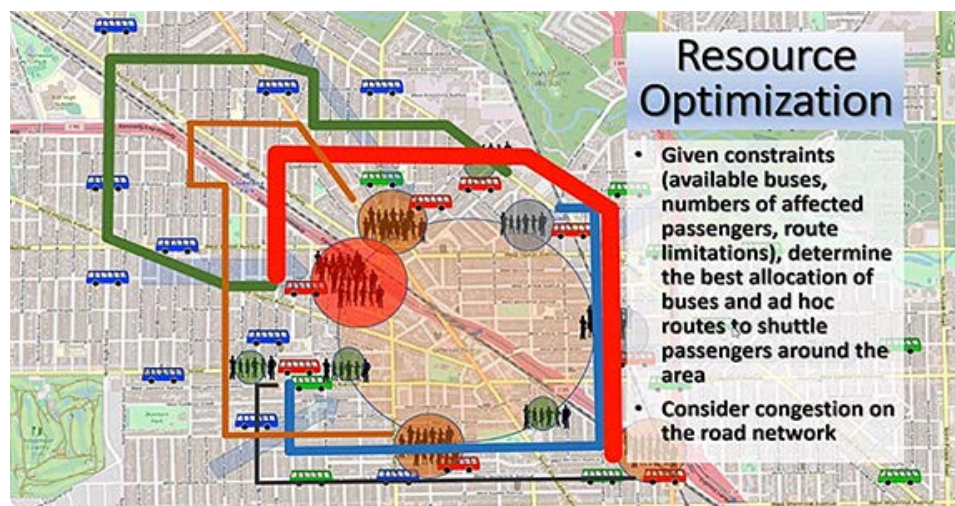


Figure 2-12 Jefferson Park scenario—optimization of resource allocation

In the simulated world, all these events happen in a fairly rigorous manner, whereas events unfold differently in the real world. The initial choice of ad hoc bus routes may have been inefficient or caused by statistical spikes, or the traveler's behaviors may have changed. The large survey undertaken by the project team that led to the underlying estimates on how people react to these disrupts was conducted at 100 different transit stops and stations, and although vetted to be statistically relevant, suffered from the fact that people react differently in real life than they would when asked about their likely responses in a survey.

Therefore, it was important to keep the feedback loop going over multiple time periods and on a rolling horizon. The movement of passengers as they use the ad hoc fleet of buses implicitly conveys information on how they would respond compared to the initial assumptions about the demand. At this point in the theoretically-optimized response, the lack of real-time data and the absence of an observable response of an actual population becomes very theoretical and may be significantly different from on-the-ground observations. The limited knowledge provided by this approach is better than the absence of knowledge altogether, but it demonstrates that the decisions of emergency responders cannot be meaningfully replaced by any fully automated system.

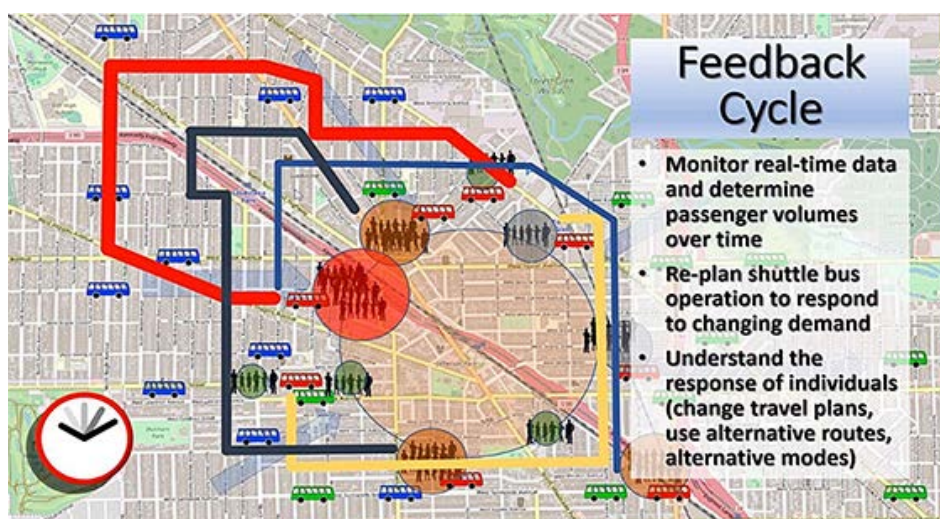


Figure 2-13 Jefferson Park scenario—feedback cycle over successive rolling horizon time intervals

After an initial time period, the active response may also be easier to control by human decision-making rather than automated tools. Eventually, on-the-ground observations and the ability of people to look out for themselves will diminish the need for an automated tool.

One frequent issue is the need for responders to deal with special-needs populations in such scenarios. The project team could not find meaningful data sources to integrate such a level of detail into the simulations. As noted, the use of models and simulations is limited under these circumstances and mostly serve as an aid for first responders to make better decisions.

The final figure in this series illustrates the regional effect of transit service disruptions. This is a particular problem when rail commuter routes are affected, as they tend to be significantly delayed when encountering service disruptions.

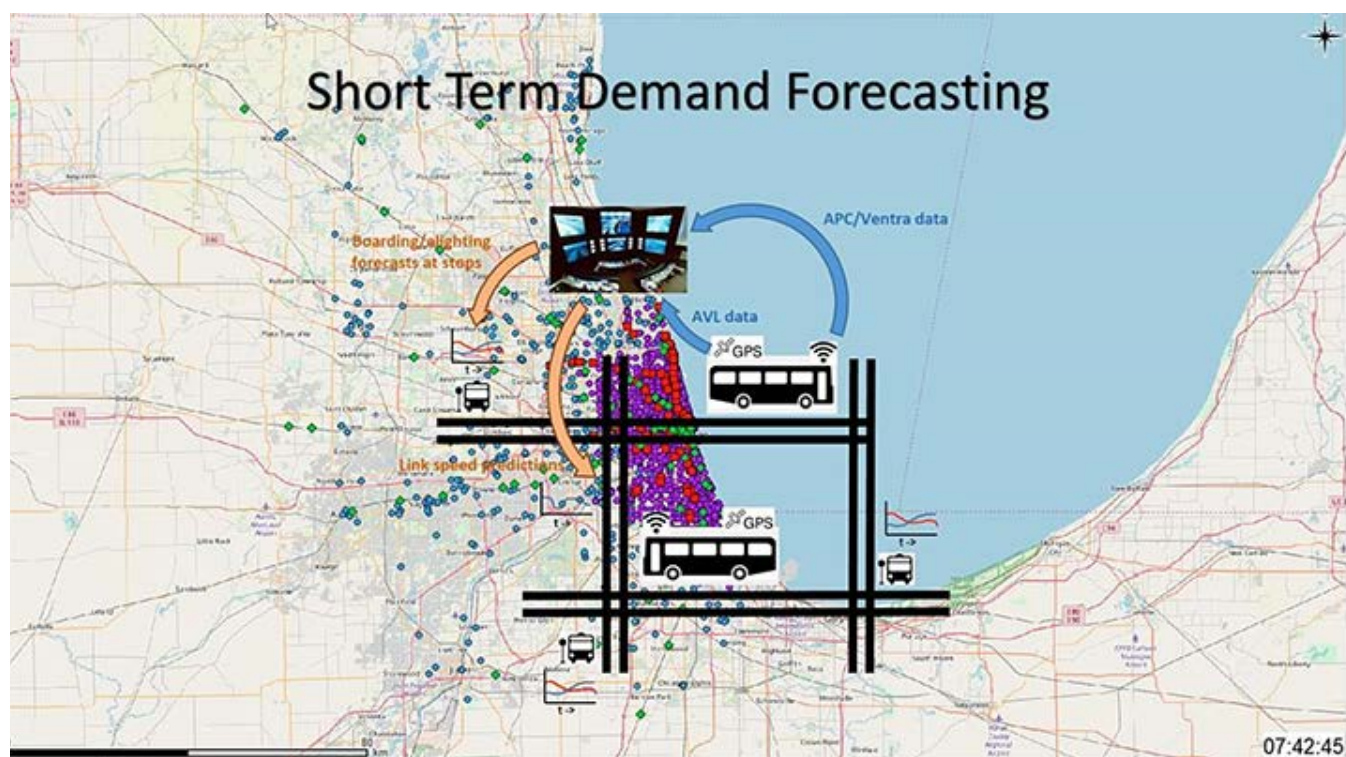


Figure 2-14 Jefferson Park scenario—aggregate short-term demand forecasting

Section 3

Stated-Preference Intercept Survey of Transit-Rider Response to Service Disruptions³

A web-based intercept survey was designed and implemented to capture the response of transit riders in the Chicago metropolitan area to a variety of service disruptions. Current transit riders were intercepted in the field from November 2017 through January 2018 according to a sampling plan based on local ridership information to gain a representative sample for analysis. Each participant completed a questionnaire regarding the intercepted trip and demographic and travel experience information. The survey included a series of stated-preference responses where the current trip was randomly disrupted and alternative travel modes were proposed with service characteristics randomly altered from a baseline scenario. This was designed to understand individual trade-offs between various mode alternatives and travel plan modification strategies under a variety of scenarios. Altogether, 659 transit riders gave responses to 2,626 different disruption scenarios. In general, a plurality of riders (49%) chooses to continue using transit, either waiting for service restoration or using agency-provided shuttle service, although at a decreasing rate as the travel delay increases. Fewer riders, approximately 15%, choose to alter their activity patterns altogether, and 26% would alter their travel to use either a taxi or an alternative Transportation Network Company (TNC). Having a more detailed understanding of the behavior of riders under various disruption scenarios should allow transit agencies to better prepare for service recovery and restoration after and during local disruptions.

Introduction

The Chicago metropolitan area is one of the largest and most dense concentrations of people, industry, and commerce in the U.S. The Chicago area is also vulnerable to many categories of hazards, including flooding, tornadoes, blizzards, and man-made emergencies. As a transportation hub, it is imperative that the region be prepared to recover quickly from these various hazards. Transportation networks are a critical resource in disaster management and recovery operations. A key component of understanding how transportation

³ Authored by Joshua Auld, Ömer Verbas, Hubert Ley, UC/Argonne; Nima Golshani, UIC; and Josianne Bechara, Angela Fontes, National Opinion Research Center. This work was performed under an FTA grant awarded to the University of Chicago in December 2016 (IL-26-7015-01 – Coordinated Transit Response Planning). The authors acknowledge Pace and Metra as representative stakeholders for Chicago's transit operators, providing much of their operating experience and rich data resources to the project. In addition, CTA generously provided access to its own data sources and supported the project team by providing access to its facilities for the survey and reviewing the survey design during the planning stage. Thanks are offered to IDOT for its input and to other municipal, local, regional, and national stakeholders for their willingness to participate.

authorities can best plan for and manage a transportation system to help the region be ready to respond and recover from emergency situations for many hazards lies in understanding traveler behavior. It is imperative to understand how travelers, specifically transit users, respond to emergencies to understand the requirements for any response and recovery effort.

Survey data were collected that focused on the regional transit network in the Chicago metropolitan area—Pace (suburban bus operator), Metra (commuter rail), and Chicago Transit Authority (CTA) (urban rail and bus operator). Passengers were intercepted at 100 separate stops/stations belonging to each of the three transit operators to direct travelers to a custom web-based online survey. The web-based survey captured background information on participant's general travel behavior and transit system usage, posed specific questions regarding their travel plans regarding the trip during which they were intercepted, and captured hypothetical behaviors and choices in response to a variety of possible emergency scenarios occurring along their travel route. This information was used to develop computational models simulating and evaluating how the Chicago area transit systems operate under a number of hazard conditions. The outcome of this research was used with a decision support tool that will allow for the development and evaluation of emergency response plans by transit operators based on an understanding of the responses of travelers to disruptions in their systems.

Literature Review

Two types of disruption in transit networks are generally discussed in the literature. The first group corresponds to the pre-planned disruptions that may occur due to pre-planned activities such as maintenance and labor strikes (Pnevmatikou et al., 2015; van Exel and Rietveld, 2009; Yap et al., 2018). This study focused on the second group, which deals with unplanned disruptions due to abnormal events such as severe weather conditions, accidents, or terrorist attacks. Generally, transit system restoration and managing the situation is performed by finding the best alternative for the out-of-service mode without considering any passenger behavioral responses to the disruption. Failing to account for passenger behavior and perceptions may lead to selecting a management strategy that is far from optimal (Currie and Muir, 2017); therefore, some studies started to collect data and estimate behavioral models for such events. A thorough review of recent literature regarding surveys of transit rider response to disruptions was recently conducted by Lin et al. (2016), where several limitations of existing research and data collection efforts into this topic were observed, the most significant being the lack of consideration for different disruption types and differentiation between pre-trip and en-route response. Some of these limitations were addressed in the implementation of a survey by the same authors (Lin et al., 2018) through the

use of a combined revealed preference and stated-preference design where the disruption type and characteristics could be varied.

One of the first studies focusing on people's behavioral response to transit disruption (Tsuchiya et al., 2007) designed a support system for passengers using a revealed preference (RP) dataset. The data were collected from all disruptions in the rail network over an 18-month period in Japan. The proposed system considers passenger perceptions towards information and recommended the optimal decision (e.g., change route, wait for service restoration) to them. Murray-Tuite et al. (2014) conducted an RP survey five months after a deadly transit accident in Washington, DC. and investigated its long-term effects on passenger behavior. Respondents were asked to indicate what changes they made to their transit trips (no change, change seating location, change mode, change both mode and seating location) after the accident; in total, 10% changed their mode of travel and 17% changed their seating location in the same train.

To avoid lack of variation in choice experiments, some researchers have conducted stated preference (SP) surveys in which respondents indicate their decisions when faced with hypothetical scenarios. For instance, Bachok (2008) conducted an SP survey from transit riders in Klang Valley, Malaysia to estimate mode choice behavior in the case of train derailment. In this study, respondents were asked to select among alternatives of other trains, shuttle bus, private vehicles, and wait for restoration of the rail system in case of hypothetical scenarios. Fukasawa et al. (2012) analyzed the mode shift in response to sudden transit disruption using a dataset from an SP survey. They found higher frequency of shifting to other trains in cases where adequate information about available alternatives was provided to the passengers compared to when no information was given. On the other hand, Bai and Kattan (2014) conducted an SP survey on light rail transit users in Calgary, Canada and found that the majority of respondents were willing to change their mode of travel if no information was provided about possible time to restoring the transit system.

Arguing that RP surveys are not able to capture a wide range of variations in choice scenarios (Lin et al., 2018) and SP surveys are not the exact representative of travel behavior (Rubin et al., 2007), some studies focus on combining the two methods. For instance, Teng and Liu (2015) used an RP survey to estimate the choice attributes of an SP survey to investigate passenger mode shift during a disruption in Shanghai's urban rail system. They found that more than half of the respondents would use the replacement shuttle bus instead of other travel modes. Lin et al. (2018) conducted a combined RP-SP survey in Toronto to investigate passenger mode behavior in the case of subway disruption. The RP section corresponds to respondents' last experience with such event, and the SP section presented hypothetical disruption scenarios in which respondents could select from a range of replacement modes or even

cancel their trip. They found that providing accurate and timely information could help passengers select the optimal replacement mode and route. This survey built on the work of Lin et al. (2018), by conducting an intercept survey of transit riders and then basing the hypothetical stated response scenarios on that trip representing a wide range of disruption types, which should provide for more accurate estimation of the sensitivities to changes in travel times and costs due to disruptions.

Regarding transit disruptions, there is also a great body of research on the supply side, i.e., transit disruption management. Cacchianai et al. (2014) present an overview for railway disturbance and disruption management. Another comprehensive review is provided in Ghaemi et al. (2017). Strategies to control randomness in transit operations date back to 1974 (Barnett, 1974). In this study, vehicle holding strategies are proposed to optimize the trade-off between the waiting times at stops/stations and the delay of riders already on board. The holding problem with real-time information is solved as a quadratic program in Eberlein et al. (2001). A more recent study revisits the holding problem, where the number of waiting passengers is not known beforehand (Bender et al., 2013). Deadheading (skipping stops) is another common strategy, and one of the studies on real-time deadheading is presented in Eberlein et al. (1998). Other real-time strategies include a combination of holding and short-turning (Shen and Wilson, 2001). Strategies beyond holding, deadheading, and short-turning involve modifications of existing lines and addition of new lines (Kiefer et al., 2016). Another method is bus bridging, where rail passengers are carried between metro stations via buses (Jin et al., 2014; Kepaptsoglou and Karlaftis, 2009). One very important aspect in transit disruption management is rescheduling of crews, which increases the complexity of the problem (Carosi et al., 2015; Malucelli and Tresoldi, 2019). Other studies focus on the vulnerability of the existing transit network (Candelieri et al., 2019; Xing et al., 2017). Finally, some studies incorporate passenger behavior explicitly (Cadaro et al., 2013), including information contagion (Hua and Ong, 2018). The efficient and successful application of many of these incident management strategies critically depends on accurate information regarding passenger behavior and response to the disruption and mitigation strategy. To this end, surveys of rider responses can be used to inform transit agencies and event managers with likely demand levels, mode shifts, etc., for a given strategy to allow for more optimal implementation.

Survey Design

To understand the response of transit riders to operational disruptions, an intercept-based survey of current Chicago-area transit riders was conducted. The survey was implemented in form of a web-based surveying platform accessible through a survey link and PIN distributed to respondents. It is similar in design to the survey of Lin et al. (2018), with the addition of using an

intercepted transit trip rather than a previous recalled trip as the basis for the stated-preference response portion of the survey. In fact, many respondents (~48%) completed the survey on the intercepted trip or on the same day after completing the trip. Over 67% of respondents completed the survey within two days of initial contact, so overall recall periods were short. Respondents were intercepted in the field at Pace bus, Metra train, and CTA bus and rail stations according to a sampling plan developed using daily ridership and boarding/alighting information from each service agency. Participants were screened in the field for suitability (over age 18, resident, on a transit trip), and if agreeing to participate were given a contact card with a unique PIN that identified the service, contact time, and contact stop for pre-populating the survey questionnaire. Respondents entering the survey link with the PIN were prompted to complete the details regarding the intercepted trip, including where they were coming from and going to preceding/following the transit trip. They were also asked about the locations of departure and/or arrival station(s), depending on where they were intercepted along the trip, and a variety of activity and travel characteristics regarding origin/destination (OD) activities, access/egress to transit, and experiences on the transit trip(s). The survey had four primary components, including:

- Person and household demographic information
- Intercepted transit trip characteristics including fares, times, ride quality, time use, etc.
- General transit and other travel mode experiences
- SP response questionnaires based on the intercepted transit trip

The personal and household demographic section collected standard household information designed to be compatible with the previously-collected Chicago Travel Tracker Household Travel Survey from 2008–2009 (CMAP, n.d.) to facilitate validation and weighting. This included most standard demographic questions regarding age, race, education, income, employment status, etc. for the person, as well as household type, housing unit, vehicle ownership, transit pass ownership, and number of children, students, employed adults, etc., for the household.

The web-based survey made extensive use of the Google Maps Application Programming Interface (API) to reliably collect location information (for the starting and ending transit stations and trip OD, display of transit routes, and to calculate experienced travel times and alternative mode information. The information was stored anonymously in the form of longitude and latitude only at the back-end of the survey instrument to comply with the conditions laid out to obtain authorization by the institutional review board at UC. Examples of the use of the API in the survey instrument are shown in Figure 3-1. In addition to the geographic information and the automatically-generated travel times, wait times, number of transfers, etc., the user also

provided information regarding the trip, including fare paid for the trip, whether a fare card was used, the number of members in the travel party, the access and egress modes, activities that were conducted at the origin point, and activity timing flexibilities. The flexibilities in terms of timing—i.e., whether the start time or duration could be changed or if there was significant pressure to complete the trip on the scheduled time—provided crucial context under which the travel was occurring*.

According to the PIN you entered, we handed you the survey invitation on 03/05/2018 at the "LaSalle Street" METRA station at approximately 8:00am.

Please indicate whether this station was:

The starting station of the transit portion of your trip

The end station of the transit portion of your trip

A transfer station where you switched between transit trips.

(a)

* Auld, J., Ley, H., Verbas, O., et al. (2020), A stated-preference intercept survey of transit-rider response to service disruptions, *Public Transportation* 12, 557–585, <https://doi.org/10.1007/s12469-020-00243-z>

Please enter the information for both the **START** and **END** stations/stops for your trip which went through the "Transfer Station" shown below, as indicated using the search boxes above the map: (examples: 'Naperville Metra', 'State and Lake - CTA Red')

NOTE: The START and END stations are the first and last transit stations you traveled through on this trip, regardless of the number of intermediate transfer stations.

Please enter the **START** station/stop for the intercepted trip

Please enter the **END** station/stop for the intercepted trip

Include terms like "CTA", "Metra", or "Pace" in your search as needed to improve results

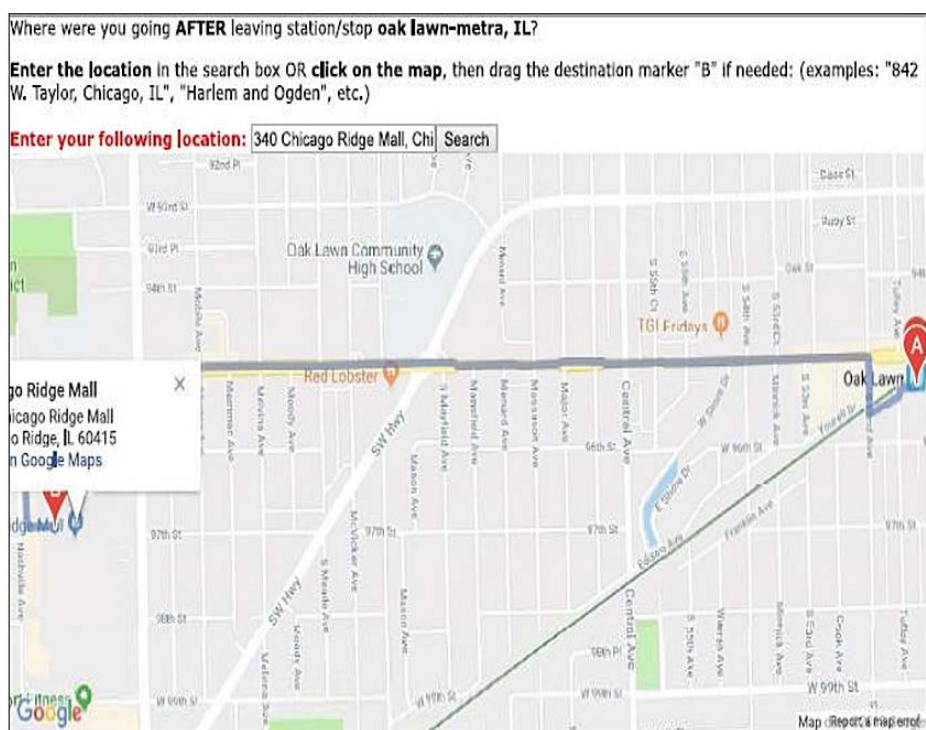
(b)

Where were you coming from **BEFORE** arriving at the starting station/stop: **uic - blue, IL?**

Enter the location in the search box OR **click on the map**, then drag the origin marker "A" if needed: (examples: "842 W Taylor, Chicago, IL", "Harlem and Ogden", etc.)

Enter your prior location:

(c)



(d)

Figure 3-1 Trip-based information using Google Maps API—(a) Identifying if contact point was start, end, or transfer point in trip; (b) collecting start and/or end transit stop; (c) origin location of trip; (d) final destination of trip (Map Data © 2018 Google)

An additional set of questions related to the traveler's transit experiences with both major transit services in the Chicago region as well as with other mobility services such as taxis, TNCs such as Uber and Lyft, the city bike-sharing system (Divvy), and car-sharing services (Car2Go, Zipcar). For each transportation alternative, users were prompted to respond how frequently it was used (when traveling in the Chicago region and when on travel), how long they had been using it, which service they used if multiple options existed, and, for the transit, taxi, and TNC options, how the time in the vehicle typically was used. An example of the experience questions regarding TNC and taxi is shown in Figure 3-2.

66. How frequently do you use Uber or Lyft-type ride-sharing services?	
	Frequency
While in the Chicago metro area	Once a year or less ▼
While traveling in other areas	Several times per month ▼
67. Which ridesharing/ridehailing service options do you use?	
<input checked="" type="checkbox"/> UberPool <input checked="" type="checkbox"/> UberX <input type="checkbox"/> UberBlack <input type="checkbox"/> LyftLine <input checked="" type="checkbox"/> Lyft <input type="checkbox"/> LyftLux <input type="checkbox"/> Via <input type="checkbox"/> Curb <input type="checkbox"/> Arro <input type="checkbox"/> Other _____	
68. How many years ago did you first start using ride-sharing/ride-hailing services?	
2 _____	
70. Please indicate how frequently you engage in the following activities while riding in a taxi or other ride-hailing vehicle:	
	Amount of time spent on activity
Reading a book/magazine/newspaper	All of my time ▼
Using a smartphone/tablet/laptop for entertainment (reading, videos, etc.)	Most of my time ▼
Talking on the phone	Some of my time ▼
Work related activities	Very little of my time ▼
School related activities	None ▼
Socializing or talking with others	_____ ▼
Relaxing (sleeping, resting, window gazing, doing nothing)	_____ ▼
Other	_____ ▼

Figure 3-2 Question on TNC and taxi travel experiences

Design of Stated Preference Scenarios

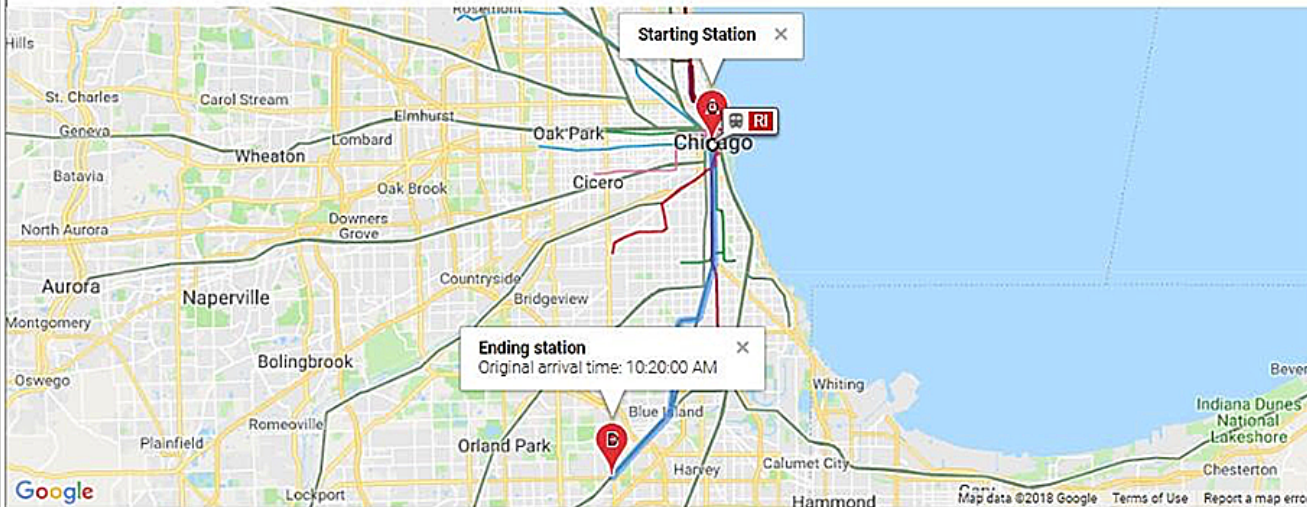
The trip characteristics collected, as shown in Figure 3-1, were used as the basis for a set of stated-preference questionnaires with randomly-altered modal characteristics set according to an experimental design (discussed in the next section). This information was used to construct the stated-preference disruption response questions. An example of the disruption response is shown in Figure 3-3, where the service was cancelled and a shuttle bus was provided.

The questionnaires where the service was delayed look similar, but the first option was renamed “Wait for service restoration” instead of “Shuttle bus,” and the descriptive paragraph similarly notes “Delayed” instead of “Canceled.”

After arriving at LaSalle Street you are informed by METRA that your planned trip to oak forest, IL has been cancelled, due to an incident along the service route.

METRA has agreed to make shuttle buses available to take passengers to oak forest, IL.

Trip characteristics for the service, as well as several other possible travel options are shown below. Please review the possible options and then select which action you would likely take in this scenario from the list shown.



Travel Option	Wait Time	Travel Time	Arrival Time	Cost	Select
Shuttle bus	37 min.	76 min.	11:22:25 AM	Same as usual trip	<input type="radio"/>
Ride-share company	5 min.	35 min.	10:10:27 AM	\$52	<input type="radio"/>
Taxi	4 min.	35 min.	10:09:08 AM	\$56	<input type="radio"/>
Pick up my vehicle and drive to destination	0 min.	59 min.	10:28:33 AM	\$15	<input checked="" type="radio"/>
Get a ride from family/friend	min.	35 min.	-	\$0	<input type="radio"/>
Change my destination	-	-	-	-	<input type="radio"/>
Cancel my travel plans	-	-	-	-	<input type="radio"/>

Figure 3-3 Transit trip disruption response example question (Map Data © 2018 Google)

The information displayed to the respondent pivoted off the exact transit and driving trip characteristics as determined by the Google Direction API router at the actual time of departure, so real-time traffic congestion, current transit schedule, etc., were accounted for when setting the scenario values. Each respondent was shown four randomly-generated choice situations, generated as described below.

The construction of the option table started with three known parameters—drive time T_{drive}^t , drive distance D_{drive} , and transit time $T_{transit}^t$, estimated using the Google router based on the currently-observed trip. There were six additional key parameters generated randomly in each choice scenario, including:

- S: status of original trip (cancelled or delayed)
- D: transit travel time delay (as a percentage of original trip)

- P : TNC surge pricing factor, as a % increase in base fare
- W_{taxi} : taxi waiting time, in minutes
- W_{tnc} : TNC waiting time, in minutes
- $W_{shuttle}$: Shuttle service waiting time, % of the delay D due to waiting for shuttle

In the current scenario generator, there was a 50% change of setting trip status S to “cancelled.” In this case, the traveler was informed that the shuttle service would be provided and $W_{shuttle}$ percent of D was assigned to shuttle waiting, while the remainder of the delay was due to slower/more circuitous shuttle service.

The delay parameter D was set using a random value r between three regimes:

$$\begin{aligned} &\in (0.15, 0.3) && | && r \leq 0.33 \\ D = &\{\in (0.5, 1.0) && | && 0.33 < r \leq 0.66 \\ &\in (1.5, 3.0) && | && r > 0.66 \end{aligned}$$

Similarly, the surge pricing parameter P was set as:

$$\begin{aligned} &\in (0.15, 0.25) && | && r \leq 0.33 \\ P = &\{\in (0.5, 1.5) && | && 0.33 < r \leq 0.66 \\ &\in (2.5, 4.0) && | && r > 0.66 \end{aligned}$$

The taxi wait time W_{taxi} was set as:

$$\begin{aligned} &r(5, 15) && | && r \leq 0.5 \\ W_{taxi} = &\{\in (30, 45) && | && r > 0.5 \end{aligned}$$

The TNC wait time W_{tnc} was set as a single regime, with lower range than taxi, as it was assumed that surge pricing would minimize increases in wait time for a vehicle. The value was set as:

$$W_{tnc} \in (3, 15)$$

Finally, the shuttle wait $W_{shuttle}$ is set randomly using r in two regimes, as:

$$\begin{aligned} &\in (0.25, 0.4) && | && r \leq 0.5 \\ W_{shuttle} = &\{\in (0.5, 0.75) && | && r > 0.5 \end{aligned}$$

The settings for all six parameters were chosen to give enough realistic variance in the attributes shown to the chooser without being too far outside of realistic values but have no direct meaning in and of themselves. The six parameters were then used to create the display values shown to the respondent, as seen in Figure 3-3. Note that two options—change destination and cancel trip—have no characteristics, while the “get a ride from family/friend” option simply used the drive time, with no additional cost. If this option was selected, however, the respondent was prompted to estimate what the wait time for the pickup would

be. The “pick up my vehicle” option was defined with the drive time along with an additional travel time to pick up the vehicle depending on its location, but was allowed only as an option if the traveler indicated that there was a vehicle available. The remainder of the display parameters were set as follows.

The wait times for a non-cancelled transit trip and a shuttle transit trip were calculated as:

$$T_{Wtransit} = D * T_{ttransit}$$

$$T_{Wshuttle} = W_{shuttle} * T_{Wtransit}$$

For shuttle trips, the new travel time became:

$$T_{tshuttle} = T_{Wtransit} + T_{ttransit} - T_{Wshuttle}$$

Thus, the shuttle and transit options (depending on which was shown) both used the same delay parameter, but the shuttle used a smaller fraction of the delay to the wait time, assuming that shuttles could be provided faster than service could be restored. The remainder of the delayed time was then added to the observed transit travel time to represent worse level of service for the shuttle bus compared to the regular route. This allowed exploration of trade-offs between rail and bus service and between wait time and in-vehicle time, depending on the differential impacts between shuttle and delayed service.

The wait times for the taxi and TNC modes were set as described above, and the carpool mode was entered directly by the user. The travel times for all auto-based modes were the same, T_{drive}^t , except for using the “pick up vehicle” option, as described above. The costs for taxi and TNC were set using the drive distance, D_{drive} , as follows, where cost is in dollars and distance is in miles, with the parameter values assigned using approximations based on local taxi and TNC rate information:

$$C_{taxi} = 3.25 + D_{drive} * 2.25$$

$$C_{tnc} = (1.75 + D_{drive} * 1.0) * P$$

The TNC price was set to be approximately half of the taxi cost, before surge pricing was applied. The randomly-applied scenarios represent a range of cases where sometimes service was restored quickly or slowly or replaced with alternate shuttle service which had high, moderate, or low performance characteristics, which compete against taxi and TNC modes that vary on wait time and cost. Overall, the scenarios should allow for reasonable estimates of behavior under limited transit disruptions, especially as they are grounded in observed trips and travel behavior.

It is important to note that the cost and time levels for the modal service parameters here were not set to be exactly what would be observed in any real-world scenario, but rather were designed to vary within reasonable bounds. This is crucial, as the

intended use of these survey data is to study how travelers value different service attributes and characteristics under different travel and disruption scenarios through behavioral choice model development. To study these various trade-offs, having this variance in the experimental design was critical.

Sampling Frame Design and Survey Administration

The survey was conducted at 100 stops, randomly selected based on ridership patterns and distributed among the service agencies. In total, 30 bus and 30 rail locations from CTA were selected, along with 20 Metra and 20 Pace locations. The Metra and Pace stops were oversampled due to lower ridership and more infrequent service to ensure adequate sample sizes for further analysis. A map of the Chicago transit system and the location of the intercept points is shown in Figure 3-4.

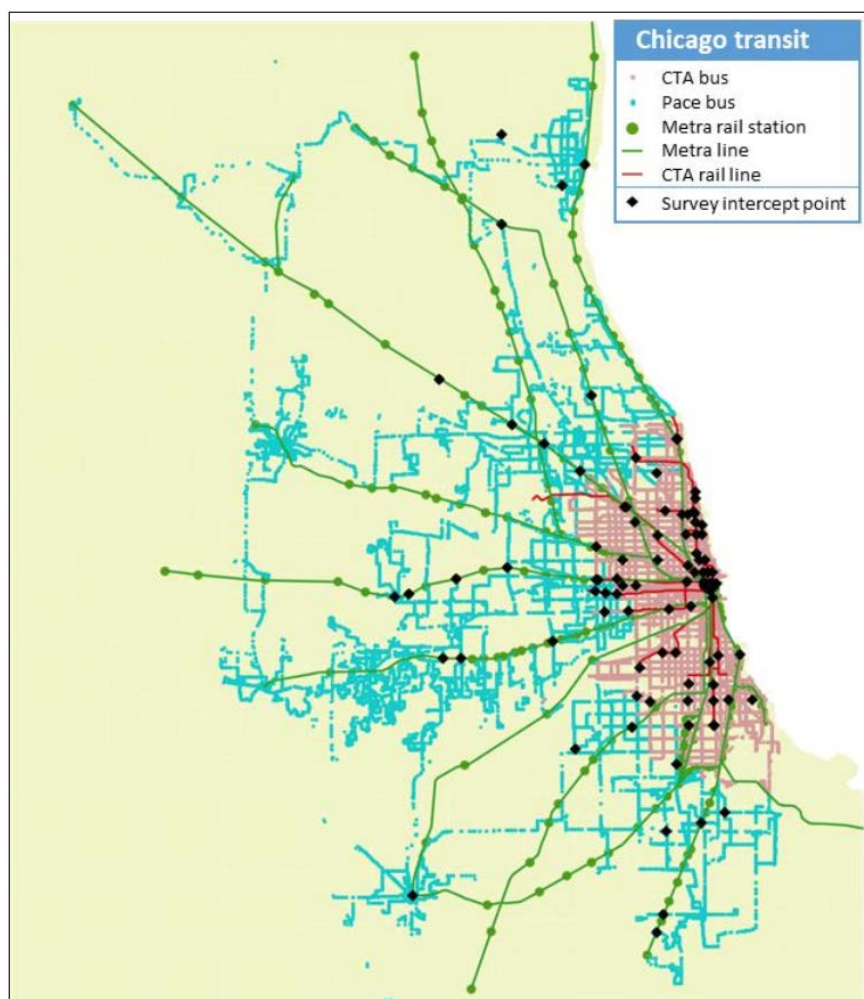


Figure 3-4 Chicago transit system and survey sample locations

Description of Sampling Frames and Stratification

Transit riders were recruited at each of the four major transit systems in the Chicago area—CTA L trains, CTA buses, Metra commuter trains, and Pace suburban bus stops. Stations and stops were sampled using a Probability Proportional to Size (PPS) sampling approach, with the size represented by the number of riders passing through each station. Based on this approach, a representative sample of stations was drawn from the universe of stations within each transit system.

Each transit system had uniquely organized station throughput data. Some systems provided only data for weekday ridership, and others provide only ridership by route, with only approximate information about boarding and alighting for each station. For this reason, along with statistical considerations, each transit system was considered a sampling stratum. This allowed for independent sampling from each of the transit system and removed the need to combine data from each of the systems into a single file for sampling. In general, sample frames were built based on the number of weekday boarders and alighters where the data allowed.

As noted, stations and stops were selected within each transit mode using PPS sampling. Each selected station/stop, also referred as a Primary Sampling Unit (PSU), was randomly assigned a weekday time block for data collection. These time blocks constituted six-hour blocks that spanned Monday through Friday of each week. PSUs were assigned time blocks between 7:00 am–1:00 pm or 1:00–7:00 pm.

A number of stations within most of the transit systems did not have enough throughput data to provide an adequate number of riders for recruitment. In addition, a few stations and routes fell outside the data collection region, namely McHenry and Kane counties. However, the total ridership for all four transit systems included riders from these low traffic and remote stations and routes. To compensate for the exclusion of these stations from selection, the stations that remained in the frame were treated as a sample, and the ridership of stations and routes that were not in the sample across all the stations that were eligible for selection were proportionally distributed. As the stations and stops were selected within each transit mode using PPS sampling, this meant that the size for each station or stop was derived from the “reweighted ridership” after the sub-sampling was implemented. Each transit mode presented its own sampling challenges based on data structure and/or distribution of ridership in the system.

Boarding and alighting data at each stop were available for CTA bus stops along with information related to direction and bus routes. Only stops with at least 400 total riders boarding and alighting the bus on an average weekday were considered for selection. This meant that 1,307 total stops, or about 10%

of all stops were considered. Given the distribution of ridership and eligibility of selection, no special treatment was necessary for any large stations. CTA L trains stations were sampled based on boarding data only, as alighting data were not available. As all stations had adequate throughput data for sampling, all 144 CTA L stations were eligible for selection. It is important to note that these data are station-based; no information was available on which direction boarders were going or which train line they were boarding for stations with multiple platforms or lines. For this reason, only boarders at the point(s) of entry for any selected station were recruited.

Metra stations were selected based on boarding and alighting in both directions at each given station. To be eligible for selection, stations needed to service at least 400 riders on an average weekday; this amounted to 156 of 238 stations. There were four stations with a large portion of total ridership, all of which were commuter destination stations near the loop—Union, Ogilvie, LaSalle, and Randolph. It was determined that these stations allowed for the sampling of riders with geographically-diverse originations and destinations, so all were included in the sample as certainty PSUs. The remaining Metra stations were sampled using PPS.

Pace was the only transit system that did not have loading and unloading station data; thus, sampling could not rely on that information. Instead, routes that were determined to have adequately large ridership (≥ 300 riders per weekday) were sampled based on overall ridership. With that, a single stop was then selected for that route based on a distribution of boarders and alighters for each route. This amounted to an extra sampling step for Pace.

Recruitment and Survey Administration

Transit commuters were recruited at Pace, Metra, and CTA transit stations within the Chicago metropolitan area based on the sampling strategy for the study from November 27, 2017, through January 21, 2018. Trained interviewers were positioned in or near stations depending on access rights granted by each transit authority to intercept respondents. Interviewers were instructed to select commuters entering or exiting the station, provide a short description of the study, and offer a tear-off sheet that contained all information necessary for completing the web survey. In addition, they provided pens as token incentives and explained that a \$5 Amazon electronic gift card would be offered when the participant completed the web survey. The entire interaction between the interviewer and the respondent lasted about three minutes. Interviewers used a tear-off notepad, where each sheet had an ID number on the top and lower portions. The bottom portion included instructions on how to log in to UC's online survey and additional project contact information. The invitation provided a PIN that the respondent would use to log in to the online survey. The use of a PIN prevented non-invited riders from participating to receive the

incentive. Interviewers saved the top portion of the sheet and mailed it back to management headquarters at the end of the field period. After recruiting at every station, interviewers were instructed to immediately input the number of tear-off sheets they successfully distributed at each station. Safety was an issue in several neighborhoods; for those areas, management dispatched multiple field interviewers at each station.

For Metra and Pace stations, transit commuter boarders and alighters were sampled in both directions to ensure that both were covered. For CTA buses, commuters were surveyed only on one side of the street at the exact stop. Aerial maps and a description of each stop were provided for interviewers to reference. For CTA trains, interviewers were instructed to stand just beyond the turnstiles to capture riders boarding and alighting multiple lines at each station. Bus stations proved to be the most difficult to work, as ridership was very low and six hours was a long time to stand and wait during the cold winter months. In contrast, train stations had high ridership and presented their own challenges to intercepting a large group of moving people who did not want to stop. Commuters using the Metra train stations and some CTA L suburb train stations were generally more open to being approached and were not as apprehensive as commuters on the inner-city CTA L, CTA bus, and Pace stations.

In preparation for the survey, 15,500 survey cards with tear-offs were printed, to be handed out to transit passengers at intercept points (~150 per station, with 250 per major transit hub). In total, 6,377 travelers were approached and given the tear-off portion of the survey form. Of those contacted, 892 followed up by logging in to the online survey, and 659 completed the full survey in an average time of 21.9 minutes, a 10.3% rate of completed survey entries. In total, 73.5% of participants fully submitted the survey. In a dry-run performed in advance of the actual survey, the team captured information on how much time users spent on individual pages of the questionnaire and addressed issues on several survey pages that appeared to be challenging for users. The team did not analyze the timing information during the actual survey, although the data likely contain interesting insights that may warrant further evaluation. For example, browser identification strings were captured, allowing distinguishing between mobile and other devices. Based on anecdotal observations, the return rate for Metra riders and users of CTA trains was substantially higher than for bus passengers, with suburban bus riders having a much lower turnout. Many train passengers started the survey shortly after being handed the forms using mobile devices, quite often finishing the survey from a stationary device later. The meta-data captured was not specifically relevant for the primary purpose of the survey but may provide interesting insights for other research topics.

Survey Results

The dataset included information on 659 individuals making 659 transit-based trips and included socio-demographic characteristics of households,

persons, vehicles, and detailed information on a random transit-based trip for all purposes as well as detailed information regarding respondent commute trips. Also collected was detailed information related to respondent perception toward transit systems and their opinions regarding other types of travel modes. The dataset consisted of 46% male and 54% female participants who lived in Chicago metropolitan area and included 72% full-time workers, 11% part-time workers, 3% unemployed, 3% retired, 9% students, and 2% other. Overall, 32% of participant households had an annual income below \$50k, 32% between \$50k and \$100k, and 36% more than \$100k per year. A full description of the sample with regards to household and individual demographic characteristics of the respondents compared against weighted estimates from the last regional household travel survey (CMAP, n.d.) for transit riders age 18 and over are presented in Figure 3-5.

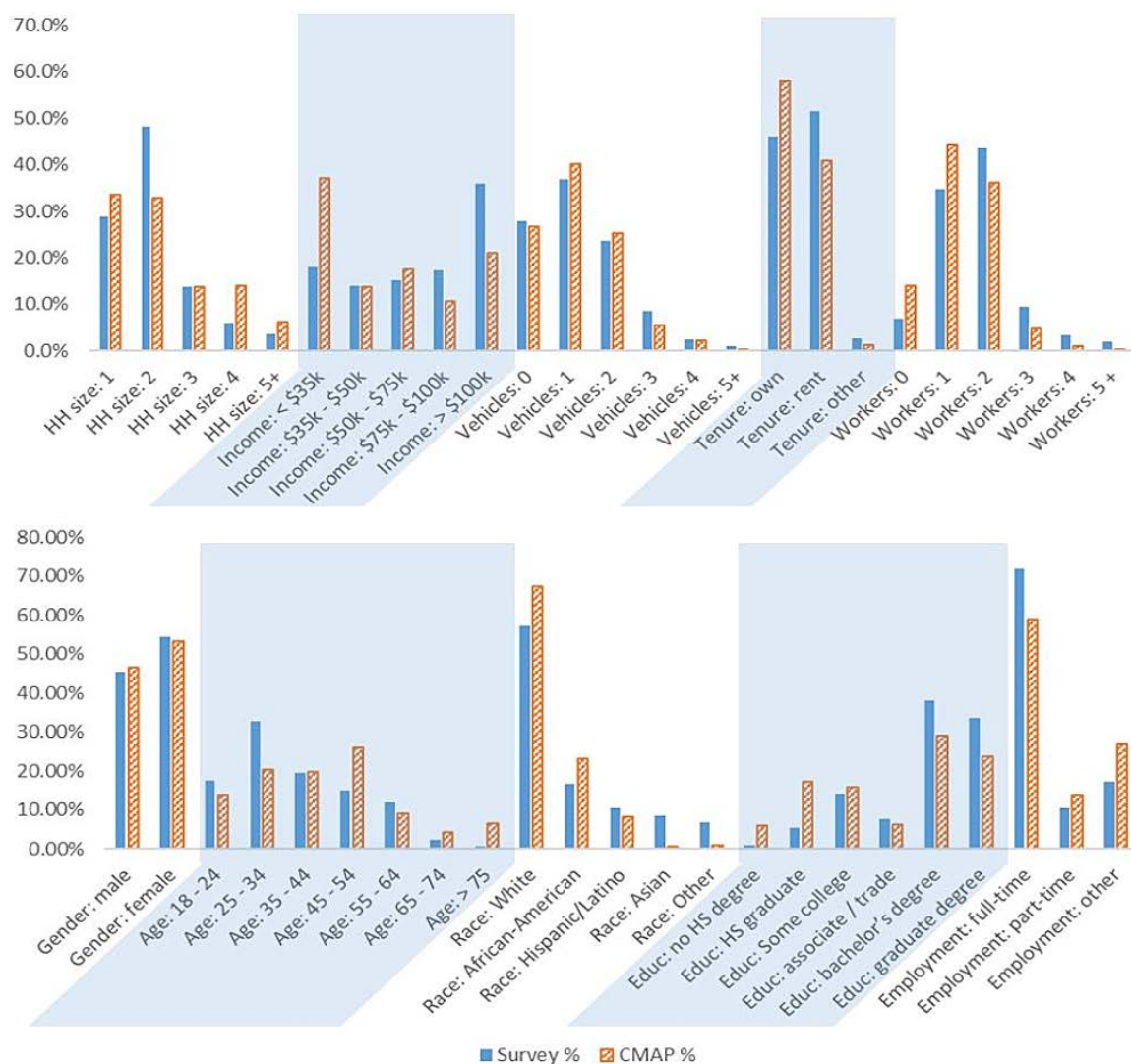


Figure 3-5 Comparison of survey household and person characteristics to CMAP transit riders

The survey gathered detailed trip attributes for a random trip chain on a typical day. Respondents were asked to provide full information about transit trip attributes and the corresponding access and egress trips. Of the 659 respondents, 350 were intercepted at CTA rail stops, 107 at CTA bus stops, 174 at Metra stops, and 28 using Pace. Approximately 68% were intercepted during their commute to work trips, 16% stated that they took the trip regularly but not for work, and the remainder stated that they did not make the intercepted trip regularly. Figure 3-6 presents the distribution of activity types at the origin and the destination of the intercepted trip.

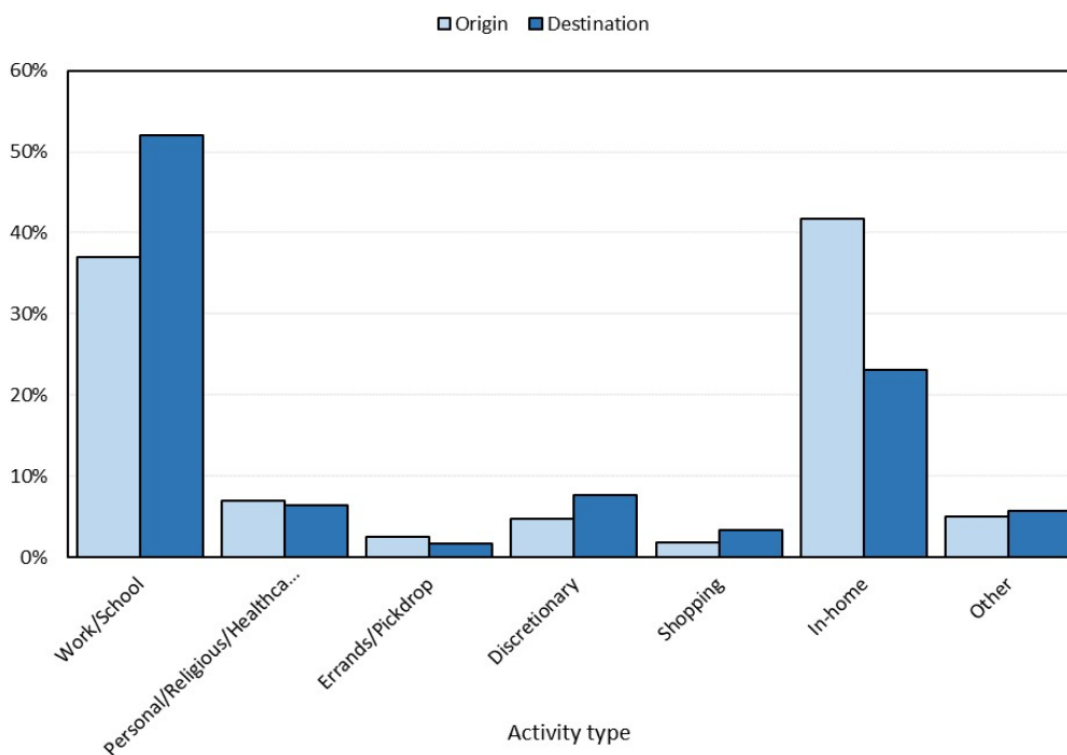


Figure 3-6 Distribution of activity types at origin and destination of each trip

In addition to respondent activity type at the origin and destination, the survey collected information regarding flexibility of these activities. Analysis of the dataset revealed that 20.64% and 28.55% of respondents had complete freedom about timing of departure from the origin and arrival at the destination, respectively. On the other hand, 33.69% had to leave the origin and 29.14% had to arrive to the destination at an inflexible time. Figure 3-7 presents the distribution of departure time in the sample.

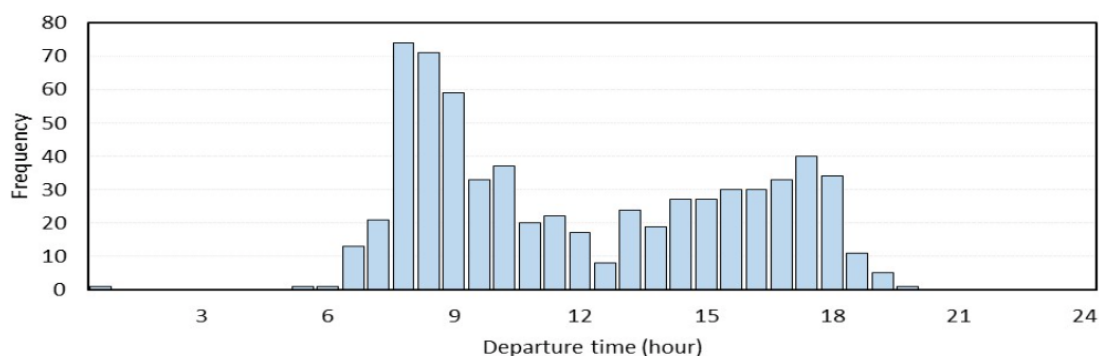


Figure 3-7 Departure time distribution in sample

The survey also collected other characteristics of the trip such as travel distance, travel time, number of transfers, and accompaniment. Figure 3-8 shows the distributions for travel distance and travel time in the sample. Suburban mode riders tended to have travel longer distances, and the bus mode riders tended to have longer travel times. Also observed was that the majority of trips, 67%, had no transfers and only 10.5% had more than one transfer. Moreover, 86% of respondents were traveling alone and 11% were traveling with friends and family; the remaining 3% were traveling with others such as co-workers.

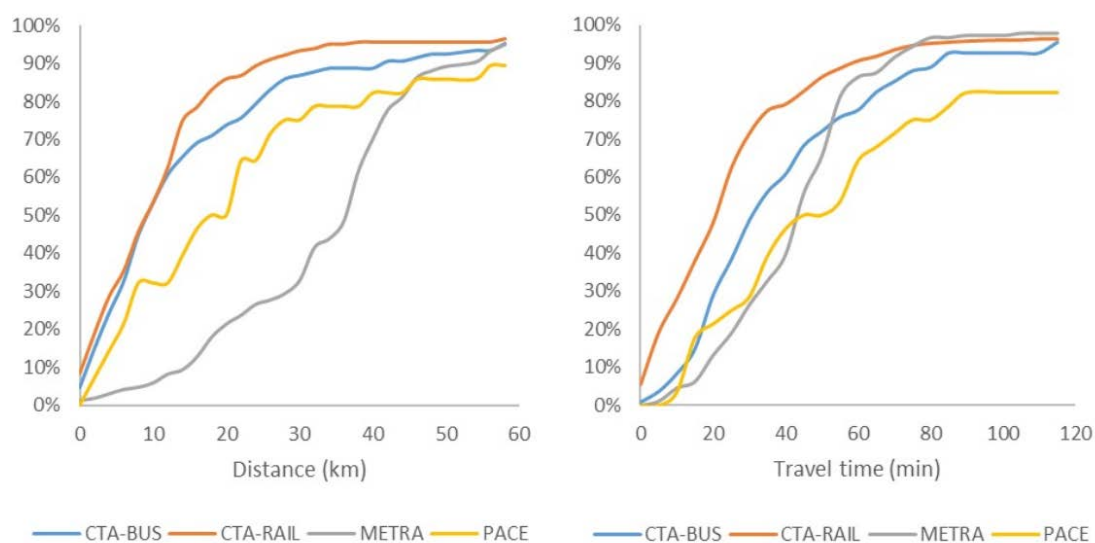


Figure 3-8 Cumulative distributions of trip distance and travel time by mode

Access and egress characteristics of the trip were also a key factor in the survey. The distribution of access and egress distance to the first/last station on the transit trip by transit mode are shown in Figure 3-9. The suburban modes tended to have much higher access distances compared to the urban modes as expected, with 75% of all CTA trips originating and terminating within 2 km of the start and end stop.

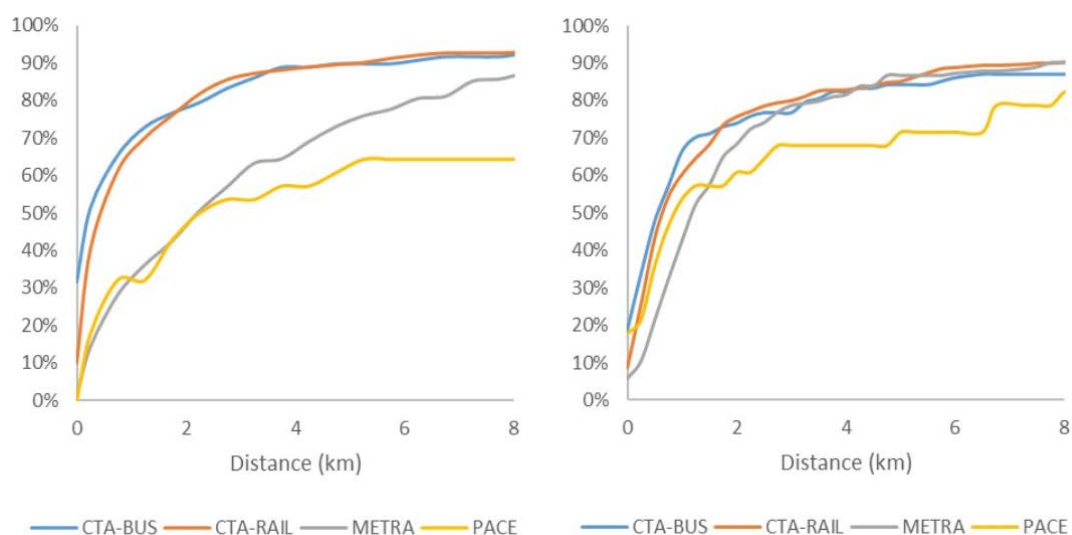


Figure 3-9 Cumulative distribution of (left) access and (right) egress distances by mode

A unique feature of the survey was the focus on the time-use behavior of transit riders during the intercepted trip. It was hypothesized that time use and the ability to use time productively during travel would be a critical driver of both baseline mode choice and choices made under the disrupted scenarios. Respondents were asked to answer questions about time spent on various activities during their trip to include this effect in later model development. Activities included reading, conducting work or school-related activities, using smartphones for entertainment, talking on the phone, socializing, and relaxing; Table 3-1 presents the distribution of in-transit activity duration in the sample. Based on the result of data analysis, using a smartphone for entertainment and relaxing were the most-conducted activities. A substantial number of travelers, however, spent at least some time on work- (14%) or school-related (6%) activities while traveling, indicating some productive use of in-vehicle time. Interestingly, time-use behavior did not vary significantly between the bus and rail modes. Preliminary modeling work using these data indicated the importance of time use to mode choice, although more work is needed to extend this to the disrupted travel context (Krueger et al., 2019).

Table 3-1 *Duration of In-Transit Activity in Sample*

Activity type	None	Very little of my time	Some of my time	Most of my time	All of my time
Reading	68.74%	6.22%	10.17%	10.77%	4.10%
Using smartphone for entertainment	20.03%	11.53%	23.52%	28.83%	16.08%
Talking on phone	83.92%	7.28%	6.53%	1.52%	0.76%
Work-related activity	79.21%	7.13%	9.86%	2.73%	1.06%
School-related activities	91.50%	2.58%	4.25%	1.21%	0.46%
Socializing or talking with others	81.18%	5.77%	7.44%	3.49%	2.12%
Relaxing/doing nothing)	44.31%	13.66%	25.19%	10.62%	6.22%
Other	93.17%	2.12%	3.03%	0.61%	1.06%

Preliminary Data Analysis

As the purpose of the survey was to understand how transit travelers respond to unexpected disruptions, a preliminary data analysis was conducted to explore the stated traveler responses to the random disruption scenarios. Responses and key mode option characteristics such as average wait time, travel time and cost, and the standard deviation of those values are shown in Tables 3-2 and 3-3. The responses and characteristics are differentiated based on whether the respondents had access to a private automobile and whether the trip was delayed or canceled and replaced by shuttle service. The main difference in the delayed vs. canceled trips was on whether additional travel time was included as part of the wait for transit to be restored (delayed) or in the transit in-vehicle travel time (canceled) provided by a less-efficient shuttle mode. These values are reported as Avg Trans. Wait and Avg Trans. IVTT in Table 3-2. The remaining characteristics were, on average, approximately similar between each scenario; however, substantial difference was observed when the characteristics were further distinguished by the selected mode.

Table 3-2 Average Characteristics by Selected Mode When Transit Delayed vs. Canceled

Selected Mode	Count	Avg Transp Wait (min)	Avg Transp IVTT (min)	Avg TNC Wait (min)	Avg TNC Cost (USD)	Avg Taxi Wait (min)	Avg Taxi Cost (USD)	Avg Auto Time (min)
No Auto Available								
Transit delayed	685	82.4	44.1	9.6	47.4	21.5	35.6	
Ask for ride	7.0%	108.9	54.9	9.9	67.1	21.1	48.3	
Wait for transit	46.6%	49.0	38.7	9.6	41.8	21.3	32.5	
Use taxi	9.9%	132.1	52.7	10.2	52.9	18.8	35.3	
Use TNC	20.0%	75.5	32.8	9.2	22.7	24.0	21.2	
Cancel trip	8.9%	179.7	74.0	9.9	109.2	21.7	68.3	
New destination	7.6%	102.2	51.2	9.6	48.0	20.5	42.8	
Transit canceled	730	36.3	93.4	9.4	48.0	21.8	37.5	
Ask for ride	8.4%	58.4	114.8	8.7	70.5	22.1	51.4	
Use shuttle	54.7%	59.5	118.4	9.5	49.5	14.7	35.7	
Use taxi	9.2%	29.3	90.4	8.9	23.9	21.7	22.8	
Use TNC	18.1%	58.4	114.8	8.7	70.5	22.1	51.4	
Cancel trip	6.7%	59.7	154.8	9.6	83.4	24.6	67.9	
New destination	3.0%	46.8	100.3	9.7	44.6	19.9	30.5	
Auto Available								
Transit delayed	480	77.9	42.2	9.6	58.4	21.4	42.7	52.7
Ask for ride	6.6%	128.8	52.4	10.2	77.3	21.0	55.8	52.8
Auto drive	8.9%	133.9	51.8	8.7	78.8	22.2	59.7	53.6
Wait for transit	47.2%	37.6	35.7	9.7	51.0	21.8	38.3	52.1
Use taxi	6.8%	111.1	41.3	10.2	61.0	16.7	31.9	50.1
Use TNC	13.9%	85.1	40.7	9.9	34.6	22.2	31.9	45.4
Cancel trip	10.1%	110.0	47.5	9.8	80.5	20.3	55.5	59.6
New destination	6.6%	141.7	62.5	8.6	78.3	22.9	52.8	64.8
Transit canceled	498	36.6	95.7	9.5	58.4	22.5	43.6	51.8
Ask for ride	5.9%	65.8	210.4	8.6	88.5	23.8	65.4	60.3
Ask for ride	12.8%	40.3	112.3	9.3	82.4	23.1	56.2	56.1
Use shuttle	46.9%	20.3	64.1	9.8	48.2	21.4	35.4	46.6
Use taxi	5.5%	88.2	129.7	9.5	83.8	18.4	52.3	64.7
Use TNC	12.6%	40.9	96.8	8.8	31.5	24.8	31.6	50.7
Cancel trip	12.3%	43.2	98.4	9.6	58.7	23.8	51.0	58.6
New destination	4.0%	67.4	185.4	10.0	106.2	26.6	70.8	57.8
Total	2586	51.1	66.1	9.5	48.5	21.7	36.8	47.9

Table 3-3 Standard Deviation of Characteristics by Selected Mode When Transit Delayed vs. Canceled

Selected Mode	Count	Std Dev Transp Wait (min)	Std Dev Transp IVTT (min)	Std Dev TNC Wait (min)	Std Dev TNC Cost (USD)	Std Dev Taxi Wait (min)	Std Dev Taxi Cost (USD)	Std Dev Auto Time (min)
No Auto Available								
Transit delayed	685	162.9	63.1	2.8	118.4	15.7	35.6	
Ask for ride	7.0%	88.4	55.1	2.8	108.8	16.2	48.3	
Wait for transit	46.6%	151.0	63.7	2.8	112.1	16.0	32.5	
Use taxi	9.9%	295.6	88.5	2.8	50.2	15.3	35.3	
Use TNC	20.0%	69.6	26.0	2.8	65.7	15.2	21.2	
Cancel trip	8.9%	197.7	78.9	2.8	251.1	15.7	68.3	
New destination	7.6%	99.4	63.5	3.0	55.9	15.3	42.8	
Transit canceled	730	110.5	186.2	2.8	87.5	15.5	37.5	
Ask for ride	8.4%	96.9	110.1	2.7	95.3	15.2	51.4	
Use shuttle	54.7%	130.5	143.0	2.9	81.7	15.5	37.3	
Use taxi	9.2%	104.9	237.6	2.8	62.5	14.0	35.7	
Use TNC	18.1%	53.3	262.6	2.8	54.3	15.8	22.8	
Cancel trip	6.7%	77.5	257.0	2.6	179.1	15.5	67.9	
New destination	3.0%	43.5	79.1	2.9	35.6	14.6	30.5	
Auto Available								
Transit delayed	480	118.1	40.5	2.9	72.9	15.7	42.7	52.7
Ask for ride	6.6%	93.3	27.2	2.7	50.0	15.9	55.8	52.8
Auto drive	8.9%	134.2	28.2	3.0	94.8	16.4	59.7	53.6
Wait for transit	47.2%	58.5	33.6	2.9	57.8	15.7	38.3	52.1
Use taxi	6.8%	167.5	46.5	2.8	129.7	15.3	31.9	50.1
Use TNC	13.9%	75.6	47.9	2.8	59.5	15.9	31.9	45.4
Cancel trip	10.1%	83.6	28.8	2.7	68.7	15.4	55.5	59.6
New destination	6.6%	284.7	77.3	2.7	87.8	15.5	52.8	64.8
Transit canceled	498	69.8	173.9	2.8	81.2	15.8	43.6	51.8
Ask for ride	5.9%	87.9	418.0	3.0	162.2	15.8	65.4	60.3
Auto drive	12.8%	37.9	58.1	2.8	74.6	15.7	56.2	56.1
Use shuttle	46.9%	32.9	119.5	2.9	69.2	16.0	35.4	46.6
Use taxi	5.5%	220.9	206.3	2.7	130.2	16.7	52.3	64.7
Use TNC	12.6%	48.3	186.4	2.7	41.3	15.6	31.6	50.7
Cancel trip	12.3%	44.7	82.6	2.7	51.0	15.2	51.0	58.6
New destination	4.0%	74.1	321.4	2.7	88.8	14.4	70.8	57.8
Total	2586	51.1	123.2	137.1	2.8	92.7	15.76	39.6

Overall, about 49% of travelers would stay with the transit service, either waiting for the service to be restored or taking the provided shuttle. The next-highest selected mode was the use of a TNC, at about 19%, when no auto was available or 13% when an auto was available. Users with access to a nearby car would choose to use that car in only 11% of cases. Finally, about 15% of travelers indicated they would alter their trip by either cancelling it or choosing a new destination. The selected modes had different characteristics, as expected, with cases in which auto modes are used having very high transit wait and/or transit in-vehicle travel times. This effect can be observed in Figure 3-10, which shows transit mode-share after disruption by both the transit wait time and transit in vehicle time. As shown, the transit share drops off as the wait time and travel time increase, to about 15–20% for the longest times.

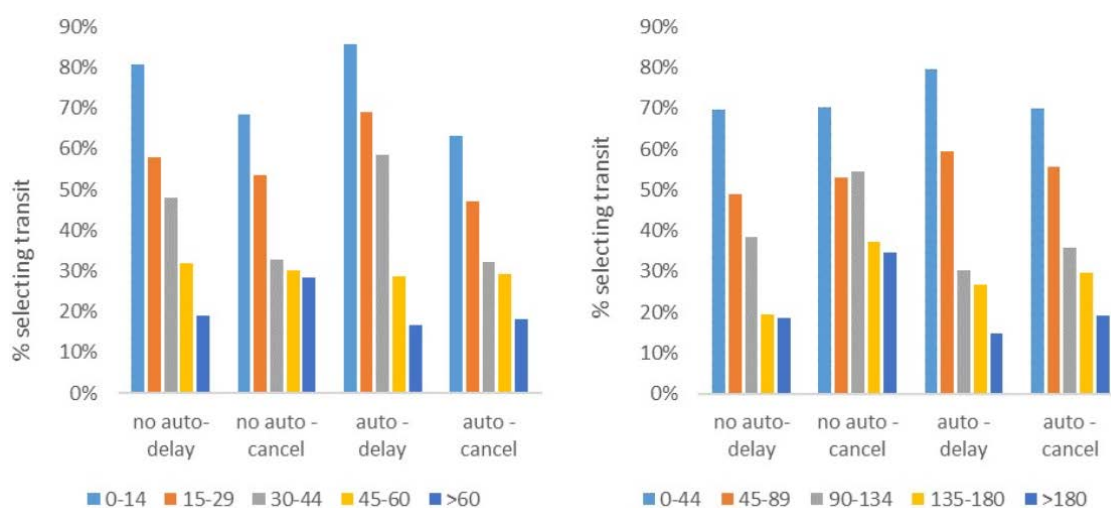


Figure 3-10 Transit mode share by (left) transit wait time and (right) transit IVTT

A similar effect can be observed for the other modes. For example, the TNC and the combined auto-drive and ask for ride mode shares are shown in Figure 3-11, respectively, for increasing TNC cost. As the cost increases, the TNC mode decreases from 27% of the sample to less than 5%, and the combined auto modes increase from 5% to almost 15% (when no auto is available) and 25–30% when an auto is available.

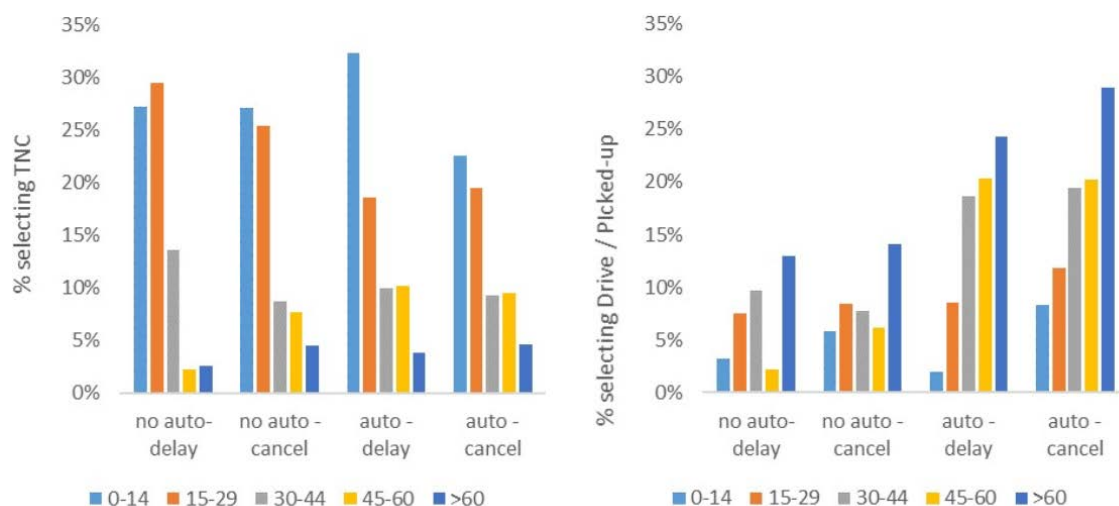


Figure 3-11 Share of (left) TNC and (right) auto drive/passenger by TNC cost (US\$)

The type of activity to which the transit rider is originally traveling also had a strong impact on the response decision. The distributions of the selected mode by activity type for scenarios with and without auto access are shown in Figure 3-12. Several key differences between the responses for each scenario can be seen. Interestingly, the availability of an auto to complete the trip did not seem to influence the overall rate at which transit was used, dropping the overall rate from 51% to 47%. However, the type of trips that stayed with the transit mode in each scenario was quite different. For those with auto access, shopping and work trip passengers stayed with transit at a higher rate than those without, likely reflecting the more competitive nature of transit travel for those already electing to take transit in spite of automobile access. Alternatively, although the majority of discretionary trips for travelers with no auto stayed with the transit mode, almost 20% of such trips were canceled when an auto was present. Errand trips also were substantially more likely to be re-planned when an auto was present, whereas many were canceled when no automobile was present.

A related factor that also influenced mode response is start time flexibility of the activity. This is often closely related to the activity type, although there is substantial variation within the activity categories.

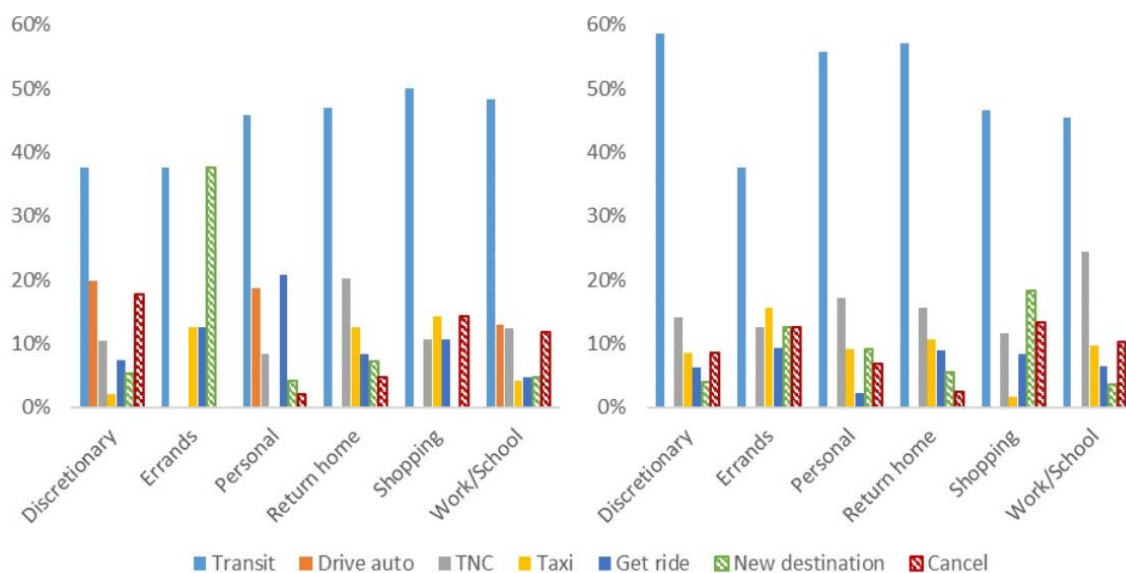


Figure 3-12 Mode share by activity type (left) with auto and (right) without auto access)

Figure 3-13 shows the choice distributions for response mode with and without auto access. As flexibility decreases, the likelihood of switching to the auto mode increases substantially when an auto is available. Interestingly the selection of TNC mode decreased as the selection of driving increased, opposite the effect observed for the case when no automobile is available. In both cases, there is a slight decrease of 4–7% in the use of the transit mode. Given the large number of factors driving mode choice behavior under disruption and the complex interactions between these factors, further multivariate analysis of the behavioral processes observed here are needed. Modeling and analysis studies of these data are ongoing, with several preliminary studies already completed that document variations in willingness to pay for various services under disruption (Saxena et al., 2019) as well as exploring in greater depth the use of time and multitasking behavior while traveling (Krueger et al., 2019).

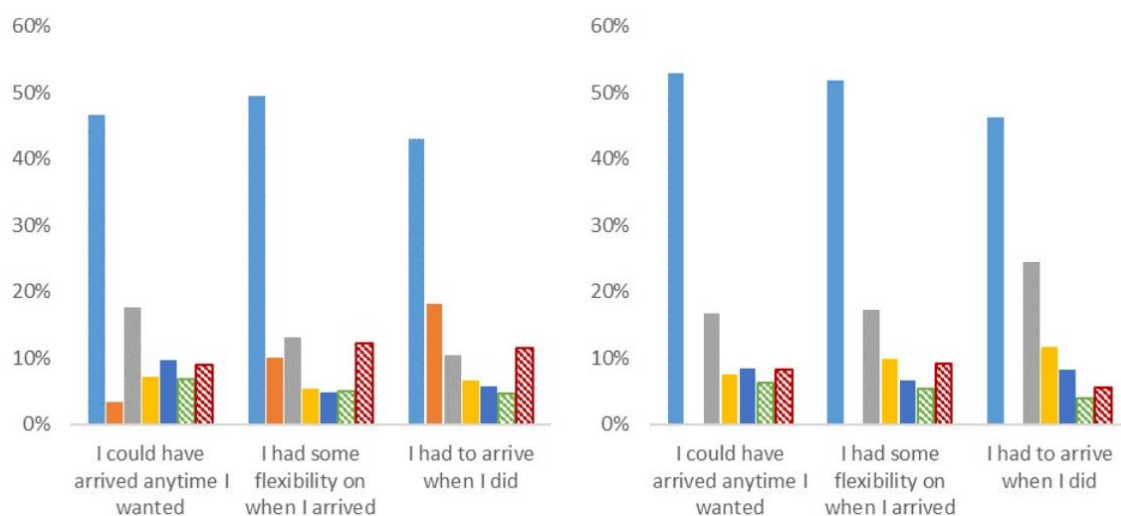


Figure 3-13 Mode share by activity start flexibility (left) with auto and (right) without auto access

Discussion

Key preliminary findings from the exploratory analysis of the survey data demonstrated how transit rider response to disruptions is influenced by many factors. These include type of service restoration provided (delayed until service is restored vs. providing shuttles to route around disruptions), characteristics of the service in terms of wait time and cost, presence of high-quality modal alternatives, and the individual's travel context. Travelers with access to an automobile at the point of learning about the service disruption had quite different response profiles than those that did not, with fewer travelers staying with transit service. Also, the context in which the travel is occurring, especially if it is to mandatory-type activities (i.e., work, school, business, etc.) and has low flexibility, strongly influences the response behavior.

The findings in this study were compared to those in other, similar surveys of transit rider response. According to Currie and Muir (2017), 68% of travelers used the shuttle buses, whereas in this study it was 54.7% and 46.9% depending on auto availability. The difference can be attributed to the fact that their study focused on rail service disruptions in Melbourne, Australia, where overall satisfaction with rail service is quite high. On the other hand, this study comprised urban bus and rail, suburban bus, and commuter rail, with overall satisfaction expected to vary. As a result, travelers are more likely to switch to other modes, change destination, or cancel their trip.

The study by Lin et al. (2018) found that subway and shuttle delays were significant and more impactful than in-vehicle time, indicating the higher burden to travelers of wait time than in-vehicle time, as observed in the

preliminary analysis above. Interestingly, no significant impact from information provision about service recovery time or shuttle service was found in that study. This could not be compared to the findings in this study, as information provision was not tested in the SP-design, but potential future versions of this study could test for such an effect. Similar distributions of disrupted mode choices were observed in the Lin et al. (2018) study as in this study, with the majority of riders staying with a transit mode (67% vs. 50%), with smaller shares for auto-based modes (16% vs. 36%) and trip cancellation (5% vs. 9%). It is important to note, however, that these results are both from SP surveys and, as such, are highly dependent on the choice attribute assumptions and not directly comparable. More important is the trend in key variables that can be studied through comparison with choice modeling results. Shares are mentioned here only to indicate similar trends.

Further analysis is needed to explore the relationships between all these factors, but preliminary findings demonstrate the presence of these effects, which can help transit agencies in planning appropriate transit alternatives under disruption scenarios. For example, shuttle service provided to commuter rail stations of the type operated by Metra, where many travelers are on the way to work or school and arrive with autos, would need less capacity than some services serving a more transit-dependent market, such as Pace. It is also clear from this study that with the growth in TNC deployment in the Chicago area, this would relieve some pressure from transit agencies to provide alternative service in areas where TNCs are prevalent and surge pricing is not too onerous. TNC providers especially seem to be filling a niche with transit riders without access to an automobile for completing mandatory, low-flexibility trips, with about 25% of such hypothetical riders in this situation choosing that mode. These findings provide impetus for further analysis through behavioral modeling and simulation for more specific scenarios of interest to transit agency operations managers and can help inform future response plans.

Conclusions

A web-based intercept survey was conducted that was designed and implemented to understand better the responses of transit riders in the Chicago metropolitan area to a variety of unplanned service disruptions. Transit riders on three primary Chicago-area bus and rail service providers (CTA, Metra, Pace) were intercepted in the field and asked to complete a web-based revealed preference and stated preference survey instrument regarding the intercepted trip. Area transit stops were sampled according to a sampling plan based on local ridership information to ensure a representative sample of transit riders for further analysis. Each participant completed a questionnaire regarding the intercepted trip and provided demographic and travel experience information. The respondents then answered a series of stated preference questionnaires where the current trip was randomly disrupted and alternative travel modes

were proposed with service characteristics based on a full factorial random design.

The transit disruption scenarios were designed to understand individual trade-offs between various mode alternatives and travel plan modification strategies under a variety of scenarios. Altogether, 659 transit riders gave responses to 2,626 different disruption scenarios. Overall, the survey sample matched well to the regional characteristics of transit users as observed in the previous household travel survey collected by the local metropolitan planning organization. In general, a plurality of riders (46%) chooses to continue using transit, either waiting for service restoration or using agency-provided shuttle service, although at a decreasing rate as the travel delay increased. Such information is potentially significant for transit agencies when understanding the level of service and transit resources to allocate to recovery of disrupted routes. Fewer riders, approximately 15%, choose to alter their activity patterns altogether, and 26% would alter their travel to use either a taxi or an alternative transportation network company service. A key finding is that transit riders respond more positively to shuttle service than to waiting for service restoration, even when the total travel time is the same.

Having a more detailed understanding of the behavior of riders under various disruption scenarios should allow transit agencies to better prepare for service recovery and restoration after and during local disruptions. Preliminary analysis of the responses observed during the hypothetical disruption scenarios demonstrate the need for more detailed multi-variate analysis of the response behavior of individual travelers. Such analyses can determine the importance that modal travel characteristics (e.g., wait, travel time, costs), individual demographics, and disruption scenario characteristics (i.e., delayed vs. canceled service, information provision, etc.) have on the decision-making of individuals. Such models have been estimated using the data collected through this survey, such as the research on commuter willingness to pay under disruptions (Saxena et al., 2019). These models can be used to improve forecasting for general disruption response including during service recovery efforts to better transit and make more effective use of transit assets. Additionally, other information collected during the survey effort, including traveler trip-specific and generalized time use in transit and other modes, attitudes towards transit and other modes, and experiences with new mobility as a service option can be used to help improve understanding of transit rider time use, time valuation, and mode choice behavior.

Time-Dependent Intermodal A* Algorithm: Methodology and Implementation on a Large-Scale Network⁴

This study proposed a Time-Dependent Intermodal A* (TDIMA*) algorithm. The algorithm works on a multimodal network with transit, walking, and vehicular network links and finds paths for the three major modes (transit, walking, driving) and any feasible combination thereof (e.g., park-and-ride). Turn penalties on the vehicular network and progressive transfer penalties on the transit network are considered for improved realism. Moreover, upper bounds to prevent excessive waiting and walking are introduced, as well as an upper bound on driving for the park-and-ride (PNR) mode. The algorithm is validated on the large-scale Chicago regional network using real-world trips against the Google Directions API and the Regional Transit Authority router.

Introduction

TNCs such as Uber and Lyft, car-sharing and bike-sharing companies, on-demand transit services, Connected and Autonomous Vehicle (CAV) technologies, and the increasing availability of real-time traffic and transit information give travelers the opportunity to evaluate their multiple routing options and make better-informed decisions. The advent of real-time control and management technologies and vehicle-to-vehicle (V2V) and vehicle-to-infrastructure (V2I) communication technologies provide opportunities to increase mobility, accessibility, throughput, and safety in the entire transportation network. These advancements call for a comprehensive modeling of the transportation system as an integrated multimodal network.

Most existing transportation network modeling literature focuses on the vehicular traffic network or the transit network. The full integration of the two major modes is usually limited to small hypothetical networks, which is not practical for large cities. At the large scale, the integration is performed in an ad hoc fashion, where separate models communicate with each other at designated outer iterations. The drawbacks of this approach are as follows:

- The interaction between the transit traffic and vehicular traffic cannot be modeled properly. For instance, transit buses share the street network with passenger cars and affect the performance characteristics of each other.

⁴ Authored by Ömer Verbas, Joshua Auld, and Hubert Ley, University of Chicago/Argonne, and Randy Weimer and Shon Driscoll, Argonne.

- The modeling of intermodal routing such as PNR, kiss-and-ride (KNR), taxi/TNC/CAV to transit, taxi/TNC/CAV after transit is limited.
- The modeling of en-route mode switching is limited.

As a result of all of the above, the integration of the transportation supply model with the Activity-Based Demand Models (ABM) is limited.

This study proposed a flexible intermodal routing algorithm that can provide time-dependent shortest paths for conventional modes such as passenger car and walk-to-transit, as well as any feasible intermodal combination such as PNR, KNR, taxi/TNC/CAV before/after transit, and so on.

Literature Review

Shortest path algorithms with label setting (Dijkstra, 1959) and label correcting (Ford, 1956; Bellman, 1958) algorithms date back to 1950s, where the link costs are static and deterministic. The first time-dependent algorithm was introduced by Cooke and Halsey in 1966 (Cooke and Halsey, 1966), whereas the first hybrid label setting/correcting algorithm was introduced by Glover et al. in 1985 (Glover, Klingman, and Phillips, 1985).

A series of large-scale implementations was introduced in Ziliaskopoulos and Mahmassani (1993), Ziliaskopoulos (1994), Ziliaskopoulos and Mahmassani (1996), and Ziliaskopoulos and Wardell (2000). A time-dependent large-scale implementation was presented in Ziliaskopoulos and Mahmassani (1993), whereas a static implementation with intersection movement penalties and prohibitions were introduced in Ziliaskopoulos and Wardell (1996). A multimodal, time-dependent algorithm with movement and transfer penalties was introduced in Ziliaskopoulos and Wardell (2000). In this study, every link carries multiple modes and services. At every node, time-dependent transfer costs are defined between every adjacent link/service pair (Ziliaskopoulos, 1994; Ziliaskopoulos and Wardell, 2000). Another approach to multimodal shortest path algorithm is the “divide-and-conquer” technique (Abdelghany and Mahmassani, 2001; Mahmassani and Abdelghany, 2002; Abdelghany, Mahmassani, and Abdelghany, 2007). In this approach, the network is divided into sub-networks for every mode, and transfer between the sub-networks is allowed only at certain nodes. First, non-dominated sub-paths are found within every mode’s sub-network (divide); then, these are combined to form non-dominated multimodal paths (conquer) (Abdelghany and Mahmassani, 2001; Mahmassani and Abdelghany, 2002; Abdelghany, Mahmassani, and Abdelghany, 2007).

In conventional shortest path algorithms, the output is a link-path incidence matrix with binary values: A link either belongs to a path (1) or not (0). In a transit network, a node can serve multiple routes that can take a traveler to

his destination. In this case, the binary condition is relaxed to be a probability between 0 and 1 to represent the likelihood of a certain link-route (service) pair being boarded. This phenomenon was first introduced by Chriqui and Robillard (1975). A decade later, Nguyen and Pallottino (1988), and Spies and Florian (1989) introduced solution algorithms to solve the common bus lines problem. The former introduced the term “hyperpath,” whereas the latter used the term “optimal strategy.” Later, capacity constraints were introduced into the transit shortest path algorithms (DeCea and Fernandez, 1993; Cominetti and Correa, 2001; Schmocker, Bell, and Kurauchi, 2008; Schmocker et al., 2011). Verbas (2014) and Verbas and Mahmassani (2015) introduced a transit hyperpath algorithm that is time-dependent on a frequency-based network with seat and standing capacities.

The initial transit hyperpath algorithms were frequency-based. In the more recent years, a schedule-based literature has emerged (Friedrich, Hofsaess, and Webeck, 2001). Some exceptions aside (Verbas, 2014; Verbas and Mahmassani, 2015), frequency-based algorithms are static, whereas schedule-based algorithms are time-dependent (Noh, 2013). Schedule-based algorithms incorporated capacity penalties, congestion pricing, and the differentiation between seated and standing passengers (Hamdouch and Lawphongpanich, 2008; Hamdouch and Lawphongpanich, 2020; Hamdouch et al., 2011; Noh, Hickman, and Khani, 2012). Most schedule-based algorithms require the temporal expansion of the network; however, Noh, Hickman, and Khani (2012) developed a schedule-based algorithm that does not require the said expansion.

Another branch of the shortest path algorithms deals with user heterogeneity (Lu, Mahmassani, and Zhou, 2008; Lu and Mahmassani, 2008; Lu and Mahmassani, 2009). In their seminal work, Lu and Mahmassani proposed a bi-criterion time-dependent shortest path algorithm where the different value of time (VOT) classes emerge naturally from a continuous distribution.

All algorithms introduced up to this point are tree-based algorithms, where the shortest path from (to) a single origin (destination) is found to (from) all destination (origin) nodes. In 1968, Hart et al. (1968) introduced the first A* algorithm that makes it possible to find an exact shortest path algorithm between any two nodes in a static network. In A* algorithms, the node label has two components—the actual cost from the origin to the node and the estimated (heuristic) remaining cost from the node to the destination. Usually, the estimated component is the Euclidean distance divided by the maximum allowed speed, which is a lower bound on the actual remaining cost to the destination (Hart, Nilsson, and Raphael, 1968). The authors proved admissibility of the algorithm as long as the estimated cost is never larger than the actual cost. A very low estimated cost guarantees an exact solution at the expense of a large number of node scans. At the extreme case, the estimated cost can be set to zero, which makes the algorithm identical to Dijkstra’s (1959) algorithm

that terminates when the destination node is reached. Conversely, the larger the estimated cost is, the faster the algorithm terminates. However, the code may return non-exact solutions if the admissibility condition is violated (Hart, Nilsson, and Raphael, 1968).

Chabini and Lan (2002) extended the A* algorithm to the time-dependent case. Zhao et al. (2008) showed that in the time-dependent case, a small enough estimated code is a necessary but not a sufficient condition for admissibility. First-in-first-out (FIFO) conditions must also be satisfied, which is not guaranteed in transit networks. In 1991, Bander and White (1991) introduced a transit A* algorithm called Interruptible A* (IA*), where a set of island nodes are pre-selected, which are favored by the algorithm for faster termination. In 2015, Khani, Hickman, and Noh (2015) introduced a Trip-Based A* (TBA*) algorithm for transit networks. The algorithm has two major contributions—1) once a node (stop) belonging to a transit is scanned, all the downstream nodes are scanned and potentially updated; however, unlike in the conventional shortest path algorithms, the predecessor node is set as the boarding node, not as the previous node, and 2) for the estimated component of the shortest path label, instead of using a Euclidean-based estimator, the authors use the resulting labels of a static, all-to-all label setting algorithm. In this estimation algorithm, no waiting or transfer times are considered. For the link costs, the minimum observed travel time throughout the time horizon from different trips on a given link is used. The authors suggest that these costs would serve as a lower bound on the actual costs, since any in-vehicle or walking time on a link would be greater than or equal to the chosen minimum. Moreover, there would be non-negative waiting times.

This study introduced a Time-Dependent Intermodal A* algorithm (TDIMA*), which extends on Khani et al.'s (2015) TBA* algorithm and makes the following contributions:

- The network representation is multimodal with three types of links—transit, vehicular traffic, and walking. Walking links are derived from the street network, and walking is not limited to designated transfer areas (no pre-defined hierarchy) but allowed along all local and arterial roads.
- The TDIMA* algorithm is multimodal and finds paths for passenger cars, walking, and walk-to-transit modes.
- The TDIMA* algorithm is intermodal and finds paths for PNR, KNR, and any other feasible combinations such as PNR, KNR, taxi/TNC/CAV before/after transit, and so on.
- Similar to the TBA* algorithm, the TDIMA* algorithm uses the results of a label-setting algorithm as estimated costs. However, instead of performing the label setting algorithm from every link to every link, we perform the algorithm from every traffic analysis zone (TAZ) to every link in order to reduce computational time.
- Unlike the TBA* algorithm, this algorithm does not follow a trip's further downstream stops.

- Unlike the TBA* algorithm, TDIMA* updates the link labels as opposed to node labels and thereby accounts for node switching penalties in an easier fashion.

Network Representation

As noted, the multimodal network used in the TDIMA* algorithm has three layers:

- Transit
- Walking
- Vehicular traffic

The transit network is constructed using GTFS. First, a “typical” weekday is chosen to detect the used service IDs from the “calendar” file. The same service IDs are also seen in the “trips” file. Using these, the transit trips in service on that day are detected. Although every trip $q \in Q$ is associated with a route, in most major cities the routes have variations called “patterns,” $p \in P$ (Furth and Day, 1985). Depending on the transit agency, patterns are properly and uniquely linked with a shape ID in an optional file. However, to guarantee consistency, the following method was used to identify patterns: Any unique sequence of stops/stations under a route is defined as a pattern. Thus, every transit trip exclusively belongs to one pattern $q \in Q_p$, and every pattern exclusively belongs to one route. The set Q_p is ordered by departure time. This is obtained from the “stop_times” file.

Generation of the nodes N is trivial—every used transit stop/station is a transit node. Similarly, any two consecutive node pair of a pattern form a transit link $i \in A$. After all the transit links are generated, an ordered set of links is generated for every pattern $i \in A_p$. Conversely, on every link, a set of patterns $p \in P_i$ is generated. Afterwards, the number s_{ip} is stored, which is the sequence number of link $i \in A_p$ along pattern $p \in P_i$. Finally, using the schedule information in the “stop_times” file, the arrival $a_{s_{ip}}^q$ and departure times $d_{s_{ip}}^q$ of a trip $q \in Q_p$ are associated with the sequence number s_{ip} .

The vehicular network can be obtained using any existing network data-source available to the modeler. In this study, the existing Chicago Regional network data designed for POLARIS, an integrated activity-based modeling and traffic simulation software, were used (Auld et al., 2016). The walking links are derived from the vehicular traffic network and are segmented into smaller links whenever a transit stop/station is nearby. In other words, the walking layer initially is a partially duplicate layer of the vehicular network, where the link types are arterial or local (no ramps, highway, or freeway links are allowed). Afterwards, transit nodes are projected onto these links to segment the walking links and provide connectivity between the transit and vehicular traffic layer. Figure 4-1 is an illustration of the network representation.

As shown, the walking links run parallel with the vehicular network and provide connectivity between the vehicular and transit network. Walking through a transit node without boarding a vehicle is allowed. Since the sum of the lengths of the two segmented walking links equals to the length of the corresponding vehicular link, this does not cause any detouring. In case of rail stations far away from any vehicular link, additional walking links are added.

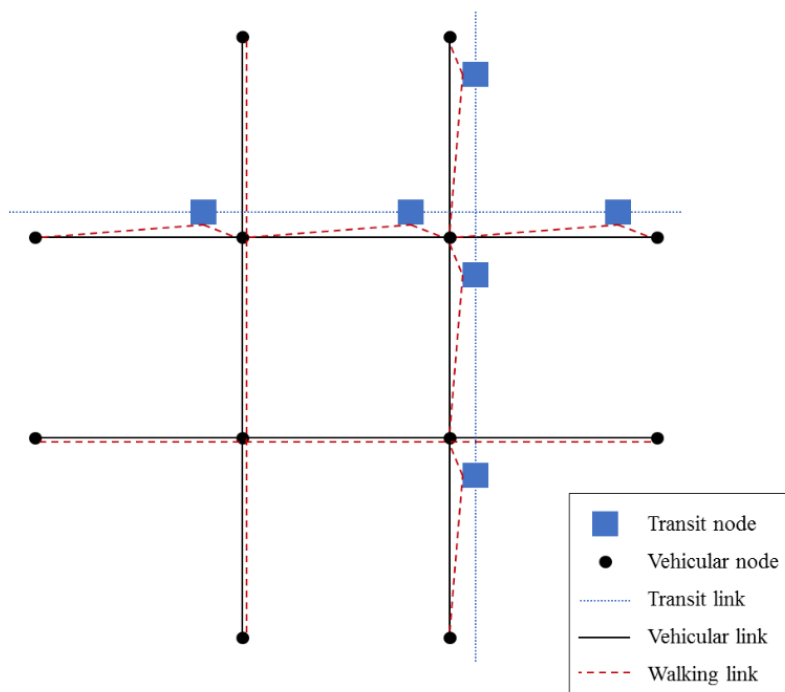


Figure 4-1 *Multimodal network representation*

Time-Dependent Intermodal A* Algorithm

The following notations are used throughout the rest of this section:

Sets

- N : Set of nodes
- A : Set of links
- O : Set of origin links; $O \subseteq A$
- D : Set of destination links; $D \subseteq A$
- A_{+i} : Set of successor links of link $i \in A$
- P : Set of patterns
- P_i : Set of patterns that pass-through link $i \in A$; $P_i \subseteq P$
- A_p : Ordered set of links that belong to pattern $p \in P$; links are ordered by their sequence traversal by the pattern
- Q : Set of trips

- Q_p : Ordered set of trips that belong to pattern $p \in P$; trips are ordered by departure time
- Ω : Set of scan-eligible links; $\Omega \subseteq A$

Parameters

- δ : Traveler's departure time from origin
- x : Base transfer penalty
- w_ω : Weight of time spent waiting
- w_κ : Weight of time spent walking
- w_λ : Weight of time spent in a transit vehicle
- w_μ : Weight of time spent in a traffic vehicle
- U^ω : Upper bound on individual waiting time
- U^κ : Upper bound on total walking time
- U^μ : Upper bound on total time in a traffic vehicle
- m_i : Type of link $i \in A$; $m_i \in \{\text{Transit, Vehicular, Walk}\}$
- l_i : Length of link $i \in A$
- v_κ : Walking speed
- $\tau_i(t)$: Time-dependent travel time on a vehicular link $i \in A$ at time t
- τ_i : Travel time on a walking link; $\tau_i = l_i/v_\kappa$
- $\psi_{ij}(t)$: Time-dependent switching delay from link $i \in A$ at time t to link $j \in A$
- s_{ip} : Sequence number of link $i \in A_p$ along pattern $p \in P_i$
- s : A generic sequence number
- α_{sqip} : Arrival time of trip $q \in Q_p$ at the upstream node of link $i \in A_p$; $p \in P_i$ and s_{ip} is the sequence number of link $i \in A_p$ along pattern $p \in P_i$
- d_{sqip} : Departure time of trip $q \in Q_p$ from the upstream node of link $i \in A_p$; $p \in P_i$ and s_{ip} is the sequence number of link $i \in A_p$ along pattern $p \in P_i$
- H_i : Estimated cost label from link $i \in A$ to destination

Decision Variables

- π_i : Selected predecessor link of link $i \in A$; $\pi_i \in A$
- φ_i : Selected trip on link $i \in A$; $\varphi_i \in Q_p$ and $p \in P_i$

Endogenous Variables

- G_i : Generalized cost label from origin to link $i \in A$
- F_i : Total cost label from origin to destination through link $i \in A$
- ρ_i : Total number of waiting occurrences from origin to link $i \in A$
- ω_i : Total waiting time from origin to link $i \in A$
- χ_i : Total transfer penalty from origin to link $i \in A$

κ_i : Total walking time from origin to link $i \in A$
 λ_i : Total in-transit-vehicle time from origin to link i
 $\in A$, μ_i : Total in-traffic-vehicle time from origin to link i
 $\in A$, α_i : Arrival time at the downstream node of link $i \in A$

Algorithm

It is important to emphasize that the transit portion of the TDIMA* algorithm is similar to Khani and Noh's (2015) TBA* algorithm except the downstream stops (links) of a trip are not followed. The presented algorithm is link-based. Any label such as the generalized cost G_i is associated with the downstream node of the link. In other words, G_i is the generalized cost of the path from the upstream node of the origin link to the downstream node of link $i \in A$.

This algorithm was developed under the framework of POLARIS, although it serves as a stand-alone tool as well. In POLARIS, a trip starts and terminates at designated activity locations as opposed to TAZs. Every activity location is projected on a walking link and a vehicular link. To prevent unnecessary U-turns or unrealistic walking back and forth, the reverse links are also associated with the given activity location. As a result, the algorithm query is from a set of origin links $i \in O$ (one or two elements) to a set of destination links $i \in D$ (one or two elements). If the selected mode is PNR/KNR, the mode of the origin links $m_i =$ Vehicular, and the mode of the destination links $m_i =$ Walking. If the selected mode is transit, the mode of the origin and destination links $m_i =$ Walking.

This algorithm uses several upper bounds and conditionals for improved computational performance and realism. All cost components such as waiting, walking, etc., are weighted. These weights w , and the walk-speed v_κ are traveler-dependent, which enables the modeling of traveler heterogeneity.

The version presented in the following pseudo-code is for walk-to-transit and drive-to-transit modes, e.g., PNR and KNR. Figure 4-2 presents the main algorithm. The labels G_i and F_i of every link $i \in A \setminus O$ are set to infinity. The label G_i of every origin link $i \in O$ is set based on the mode (walking or driving). It is the cost of traversing the link based on the weighted travel time of walking $w_\kappa \tau_i$ or weighted time-dependent travel time of driving $w_\mu \tau_i(\delta)$ at the departure time δ . Similarly, total walking time κ_i , total in-vehicle-traffic time μ_i , and the arrival time at the downstream node α_i are updated.


```

TDIMA*(O, D,  $\delta$ )

Initialization
 $\Omega = \{\}$  //the set of scan eligible links is set as empty
For every link  $i \in A \setminus O$ :
     $G_i = F_i = \infty$  //the non-origin link labels are set as infinity

For every origin link  $i \in O$ :

    If  $m_i = \text{Walk}$ : //if origin link is a walking link
         $G_i = w_\kappa \tau_i$  //generalized cost label is the weighted walking time
         $\kappa_i = \tau_i$  //total walking time is the link's walking time
         $\mu_i = 0$  //total in-traffic-vehicle time is zero
         $\alpha_i = \delta + \tau_i$  //arrival time is departure time plus link travel time

    Else: //if origin link is a traffic vehicle link
         $G_i = w_\mu \tau_i(\delta)$  //generalized cost label is the weighted time-dependent in-traffic-vehicle time
         $\kappa_i = 0$  //total walking time is zero
         $\mu_i = \tau_i(\delta)$  //total in-traffic-vehicle time is the time-dependent in-traffic-vehicle time
         $\alpha_i = \delta + \tau_i(\delta)$  //arrival time is departure time plus link travel time

     $\pi_i = \{\}$  //there is no predecessor to origin link
     $\varphi_i = \{\}$  //an origin link is never a transit link, hence there is no transit trip
     $F_i = G_i + H_i$  //total cost label is generalized cost label plus heuristic cost
     $\rho_i = \omega_i = \chi_i = \lambda_i = 0$  //all other labels are zero
     $\Omega = \Omega \cup \{i\}$  //the set of scan eligible links now includes i

Main
While  $\Omega \neq \{\}$ :
    Select  $i = \underset{j \in \Omega}{\text{argmin}}\{F_j\}$  //select the link from the set of scan eligible links with the minimum total cost

     $\Omega = \Omega \setminus \{i\}$  //remove the current link i from the set of scan eligible links

    If  $i \in D$ : //if we reached the destination terminate the algorithm
        Stop and report results!

    Else:
        For every  $j \in A_i^+$  where  $m_j = \text{Transit}$ : //scan and evaluate every successor transit link
            Call Evaluate_Transit_Neighbor(i,j)

        For every  $j \in A_i^+$  where  $m_j = \text{Walk}$ : //scan and evaluate every successor walking link
            Call Evaluate_Non_Transit_Neighbor(i,j)

        If  $m_i = \text{Vehicular}$ :
            For every  $j \in A_i^+$  where  $m_j = \text{Vehicular}$ : //scan and evaluate every successor vehicular link
                Call Evaluate_Non_Transit_Neighbor(i,j)

```

Figure 4-2 Pseudo-code for Time-Dependent Intermodal A* (TDIMA*) algorithm

H_i is the pre-calculated heuristic cost from the downstream node of a given link $i \in A$ to the destination links $i' \in D$. The algorithm selects the link with the least total cost $F_i = G_i + H_i$. If $H_i = 0$, the algorithm becomes a conventional label-setting algorithm (Dijkstra, 1959), where the link with the minimum cost from the origin is selected. Although this guarantees an exact solution, the algorithm would not be “guided” towards the destination; hence, a longer computational time. Hence, a heuristic cost H_i is used, and the algorithm picks the link with the minimum total cost F_i . F_i is the cost of a path from origin to destination that traverses link $i \in A$ (Hart et al., 1968). The cost G_i from origin to link $i \in A$ is exact, whereas the cost H_i from link $i \in A$ to destination is an estimate. The higher the estimate, the faster the code reaches the destination with a caveat: If it is inadmissibly high, the solution is not the least cost path. Still, the final cost at the destination link is $F_i = G_i$, where $H_i = 0$. This means that the final cost is the ‘exact’ cost of a sub-optimal path. Traditionally, H_i is the Euclidean distance divided by the maximum possible speed, which is an admissible lower bound (Hart et al., 1968). Similar to Khani, Hickman, and Noh (2015), the results of a static label setting algorithm for the estimated cost H_i is used. The travel times on the static network are the minimum observed travel time on a link. Waiting times, transfer or turn penalties are not included. Hence, the cost on a given link in this static network can never be higher than the cost of that link in the actual network, which makes the algorithm admissible (Khani, Hickman, and Noh, 2015). Instead of performing the label setting algorithm from every link to every link, performed is the algorithm from every traffic analysis zone (TAZ) to every link in order to reduce computational time.

Hence, H_i is the heuristic cost from link i 's zone to the destination link. However, the zonal aggregation is for the heuristic cost H_i calculation only. The TDIMA* algorithm calculates an exact cost G_i from an origin location to the link $i \in A$ in question until eventually that link is one of the (two) destination links $i \in D$. Back-tracking recursively from that link terminates in one of the origin links. Hence, the algorithm finds the least cost path between an origin-destination pair at a given departure time, where both the optimal origin and destination links are implicitly selected in the process.

Once the link $i = \text{argmin}\{F_j\}$ with the minimum total label is selected, the algorithm starts scanning the downstream links $j \in A+i$. If the downstream mode $m_j = \text{Transit}$, then *Evaluate_Transit_Neighbor(i,j)* is called (see Figure 4-3). If the downstream mode $m_j = \text{Walk}$, then *Evaluate_Non_Transit_Neighbor(i,j)* is called (see Figure 4-4). Finally, if both the current mode $m_i = \text{Vehicular}$ and $m_j = \text{Vehicular}$, then *Evaluate_Non_Transit_Neighbor(i,j)* is called again. The last two conditions are proper for PNR and KNR trips. No vehicle can be generated in the middle of the journey. However, this constraint is relaxed if the intermodal trip allows for taking a taxi or other services. The algorithm terminates ideally once a destination link $i \in D$ is reached, or unideally when Ω becomes empty, i.e., no path could be found between the two location pairs (O, D) at departure time δ .

In *Evaluate_Transit_Neighbor(i,j)* subroutine, the algorithm loops over all the patterns $p \in P_j$ that serve on the successor link $j \in A_{+i}$. For a given pattern $p \in P_j$, it loops over all the trips $q \in Q_p$ of that pattern. First, the sequence number s_{jp} of link $j \in A_p$ along pattern $p \in P_j$ is obtained. For simplicity, we call it s . By using s , the algorithm obtains the departure time d_s^q and calculates the waiting time $\omega' = d_s^q - \alpha_i$. If $\omega' < 0$, the trip is skipped. If ω' is larger than the traveler-specific upper bound U^ω , then all the trips departing later than q will exceed the upper bound. Hence, no further scanning of this pattern is required. In case trip q in question is the same as the arrival trip φ_i , then there is no waiting. Hence the candidate waiting count ρ' is the same as the waiting count ρ_i . The in-transit-vehicle travel time of the link is set to the difference between the arrival time a_s^{q+1} at the downstream node of link j and the current time α_i . Otherwise, the traveler is waiting to board, the waiting count $\rho' = \rho_i + 1$, and the in-transit-vehicle travel time μ' is the difference between the arrival time a_s^{q+1} at the downstream node of link j and the departure time d_s^q from the upstream node of link j .

The algorithm keeps track of the total number of transfers $\max\{0, \rho' - 1\}$ and progressively penalizes transfers using $\chi' = \max\{0, \rho' - 1\} x$. That is the first transfer is penalized by x , the second by $2x$, and so on. Hence, a trip with two transfers has a total transfer penalty of $3x$, whereas a trip with three transfers has a total transfer penalty of $6x$. Interested readers are referred to Verbas (2014 and Verbas and Mahmassani (2015) for details. The candidate label G' is the weighted sum of the waiting time ω' , in-transit-vehicle time μ' , the transfer penalty χ' , and the label G_i of the current link i . If $G' < G_j$ then link j should be traversed on trip $\varphi_j = q$ and be preceded by link $\pi_j = i$. The arrival time is set to $\alpha_j = a_s^{q+1}$. All the labels are updated as seen in Figure 4-3.

As seen in Figure 4-4, if the successor link j 's mode $m_j = \mathbf{Walk}$, then the algorithm first checks whether the potential cumulative walking time $\kappa_i + \tau_j$ is larger than the traveler-specific upper bound U^κ . If it is true, the algorithm skips that link. If not, the algorithm calculates the candidate label G' , the candidate arrival time α' , the candidate total walking time κ' and the candidate intrajourney-vehicle time μ' .

If the successor link j 's mode $m_j = \mathbf{Vehicular}$, the time-dependent travel time has two components: the time-dependent switching delay $\psi_{ij}(\alpha_i)$ at time α_i and the time-dependent link travel time $\tau_i(\alpha_i + \psi_{ij}(\alpha_i))$ at time $\alpha_i + \psi_{ij}(\alpha_i)$, i.e., after the turn movement is completed.

Similar to walking, the algorithm checks whether the cumulative driving time exceeds the upper bound U^μ on driving. This prevents the algorithm from excessive driving almost all the way up to the destination and then taking transit for just a few blocks. If the upper bound is not exceeded, the algorithm calculates the candidate label G' , the candidate arrival time α' , the candidate total walking time κ' and the candidate in-traffic-vehicle time μ' .

If $G' < G_j$ then link j should be preceded by link $\pi_j = i$. All the labels are updated as seen in Figure 4-4.

```

Evaluate_Transit_Neighbor(i,j)
For every pattern  $p \in P_j$ :
  For every trip  $q \in Q_p$ :
     $s = s_{jp}$  //get the sequence number of link j along pattern p
     $\omega' = d_s^q - \alpha_i$  //waiting time is departure time minus current time

    If  $\omega' < 0$ , go to next trip //if waiting time is negative skip that trip

    If  $\omega' > U^\omega$ , go to next pattern //if waiting time is higher than the upper bound skip that pattern

    If  $m_i = \text{Transit AND } q = \varphi_i$ : //if the candidate trip q equals to the arrival trip  $\varphi_i$ 
       $\omega' = 0$  //then there is no waiting
       $\rho' = \rho_i$  //candidate waiting count equals to the value of current link i
       $\mu' = a_{s+1}^q - \alpha_i$  //in-transit-vehicle time is arrival at the next stop minus current time
    Else:
       $\rho' = \rho_i + 1$  //then there is waiting and candidate waiting count is increased by one
       $\mu' = a_{s+1}^q - d_s^q$  //in-transit-vehicle time is arrival at the next stop minus departure time

     $\chi' = \max\{0, \rho' - 1\} \times$  //transfer penalty is base penalty times (waiting count minus one) or zero
     $G' = G_i + w_\omega \omega' + w_\mu \mu' + \chi'$  //candidate generalized cost is a weighted sum of previous link's cost,
    //waiting time, in-transit-vehicle time, and transfer penalty

    If  $G' < G_j$ : //if the candidate cost is less than the prevailing generalized cost label
       $G_j = G'$  //generalized cost label is set as the candidate cost label
       $F_j = G_j + H_j$  //total cost label is generalized cost label plus heuristic cost

       $\pi_j = i$  //predecessor link of j is set as i
       $\varphi_j = q$  //selected trip on link j is set as q
       $\alpha_j = a_{s+1}^q$  //arrival time at the downstream node is set as the arrival time of the trip q

       $\rho_j = \rho'$  //total number of waiting occurrences from origin is set as the candidate value
       $\omega_j = \omega_i + \omega'$  //total waiting time from origin is increased by  $\omega'$ 
       $\chi_j = \chi'$  //total transfer penalty from origin is set as the candidate value
       $\kappa_j = \kappa_i$  //total walking time from origin is set as the value of current link i
       $\lambda_j = \lambda_i + \lambda'$  //total in-transit-vehicle time from origin is increased by  $\lambda'$ 
       $\mu_j = \mu_i$  //total in-traffic-vehicle time from origin is set as the value of current link i

    If  $j \notin \Omega$ , then  $\Omega = \Omega \cup \{j\}$  //add link j to the set of scan eligible links if it is not already there

```

Figure 4-3 Subroutine for evaluating transit neighbor link

```

Evaluate_Non_Transit_Neighbor(i,j)

If  $m_j = \text{Walk}$ :

    If  $\kappa_i + \tau_j > U^k$ :
        Return //if the total walking time is larger than the upper bound return to main

     $G' = G_i + w_k \tau_j$  //candidate generalized cost is weighted walk time plus current link's cost
     $\alpha' = \alpha_i + \tau_j$  //candidate arrival time is increased by walking time
     $\kappa' = \kappa_i + \tau_j$  //candidate walking time is increased by walking time
     $\mu' = \mu_i$  //candidate in-traffic-vehicle time is set as the value of current link i

If  $m_i = \text{Vehicular}$ :

    If  $\mu_i + \psi_{ij}(\alpha_i) + \tau_j(\alpha_i + \psi_{ij}(\alpha_i)) > U^k$ :
        Return //if the weighted total in-traffic-vehicle time is larger than the upper bound return to main

     $G' = G_i + w_{\mu} \psi_{ij}(\alpha_i) + \tau_j(\alpha_i + \psi_{ij}(\alpha_i))$ 
        //candidate generalized cost is a weighted sum of previous link's cost,
        //time-dependent switching delay, and time-dependent in-traffic-vehicle time

     $\alpha' = \alpha_i + \psi_{ij}(\alpha_i) + \tau_j(\alpha_i + \psi_{ij}(\alpha_i))$ 
        //candidate arrival time is increased by the time-dependent switching delay,
        //and the time-dependent in-traffic-vehicle time

     $\kappa' = \kappa_i$  //candidate walking time is set as the value of current link i

     $\mu' = \mu_i + \psi_{ij}(\alpha_i) + \tau_j(\alpha_i + \psi_{ij}(\alpha_i))$ 
        //candidate walking time is increased by the time-dependent switching delay,
        //and the time-dependent in-traffic-vehicle time

If  $G' < G_j$  //if the candidate cost is less than the prevailing generalized cost label

     $G_j = G'$  //generalized cost label is set as the candidate cost label
     $F_j = G_j + H_j$  //total cost label is generalized cost label plus heuristic cost

     $\pi_j = i$  //predecessor link of j is set as i
     $\varphi_j = \{\}$  //there is no transit trip
     $\alpha_j = \alpha'$  //arrival time at the downstream node is set as the candidate arrival time

     $\rho_j = \rho_i$  //total number of waiting occurrences is set as the value of current link i
     $\omega_j = \omega_i$  //total waiting time from origin is set as the value of current link i
     $\chi_j = \chi_i$  //total transfer penalty from origin is set as the value of current link i
     $\kappa_j = \kappa'$  //total walking time from origin is set as candidate walking time
     $\lambda_j = \lambda_i$  //total in-transit-vehicle time from origin is set as the value of current link i

```

Figure 4-4 Subroutine for evaluating non-transit neighbor link

Validation Results

The Time-Dependent Intermodal A* algorithm implementation was verified against observed trips drawn from the Chicago Metropolitan Agency for Planning (CMAP) 2008 Travel Tracker survey. A multimodal Chicago regional network was generated using the existing POLARIS (Auld et al., 2016) vehicular network and the GTFS data for the three transit agencies—CTA (urban bus and rail), PACE (suburban bus), and Metra (commuter rail). The network properties are as follows:

- 54,028 nodes
 - 35,077 transit
 - 18,951 vehicular
- 217,119 links
 - 37,642 transit
 - 123,000 walking
 - 56,477 vehicular
- 173,236 activity locations
- 1,961 traffic analysis zones
- 344 transit routes
- 2,098 transit patterns
- 28,138 transit trips

The validation trips were drawn from the set of multimodal trips observed in the survey, i.e., a trip that involved transit at any point and at least one non-walking leg. This subset was further limited to multimodal trips where the access mode was PNR/KNR trips. Of a total set of 6,500 valid transit trips, 556 met this criterion and passed a set of data validity checks for use in the validation analysis. A subset of 180 randomly-selected trips was then routed from origin coordinate to destination coordinate at the specified departure time in three different routing engines:

- TDIMA* algorithm using PNR mode
- Google Directions API using transit mode, as it does not have PNR/KNR option
- Regional Transit Authority (RTA) trip planner using PNR mode, as it provides PNR directions

The reason for selecting 180 trips is due to the need to input trips manually into the RTA router. Results from the two online direction finders for a hypothetical trip are shown in Figure 4-5, where significant differences in overall trip time can be observed. The main reason behind this difference is that the Google router can have only walking as the access mode to transit, whereas the RTA trip planner is able to find a PNR route which selects from a set of prespecified parking locations. On the other hand, the TDIMA* algorithm is much more flexible in the sense that it does not limit the parking locations.

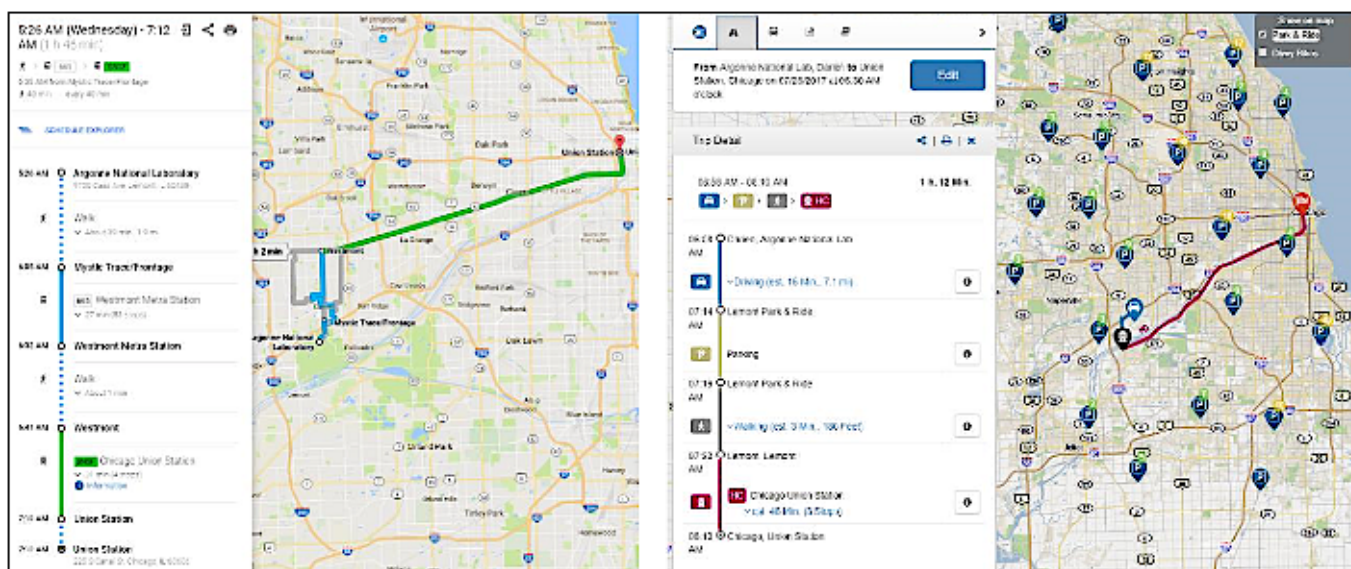


Figure 4-5 Online-routing results from (left) Google API and (right) RTA Trip Planner (Map Data © 2018 Google)

The TDIMA* algorithm used the following weights and upper bounds:

- Base transfer penalty; $x = 5$ min
- Weight of time spent waiting; $w_{\omega} = 2$
- Weight of time spent walking; $w_{\kappa} = 2$
- Weight of time spent in a transit vehicle; $w_{\lambda} = 1$
- Weight of time spent in a traffic vehicle, $w_{\mu} = 3$
- Upper bound on individual waiting time; $U_{\omega} = 60$ min
- Upper bound on total walking time; $U^{\kappa} = 60$ min; with walking speed $v_{\kappa} = 1.39$ m/s; $U^{\kappa} = 5$ km in distance
- Upper bound on total time in a traffic vehicle; $U^{\mu} = 60$ min

The results for each trip were compared in terms of total travel time, total walking/driving (non-transit) time, total waiting time (including waiting during transfers), and total in-transit-vehicle time (see Figure 4-6). Unknown are which upper bounds, weights, or transfer penalties are used by the online algorithms, and in case they are used, the values thereof. However, the Google Directions API does not return results for about 20% of the trips. Hence, it can be inferred that there are limits on walking. Overall, the new algorithm significantly outperforms the online routing engines. Although unknown are the details of the online routers in terms of upper bounds and weights, results indicate that the TDIMA* algorithm outperforms them in terms of total travel, waiting, transit, and non-transit times. Hence, there is no trade-off between the cost components across different algorithms. The TDIMA* algorithm is mostly non-dominated.

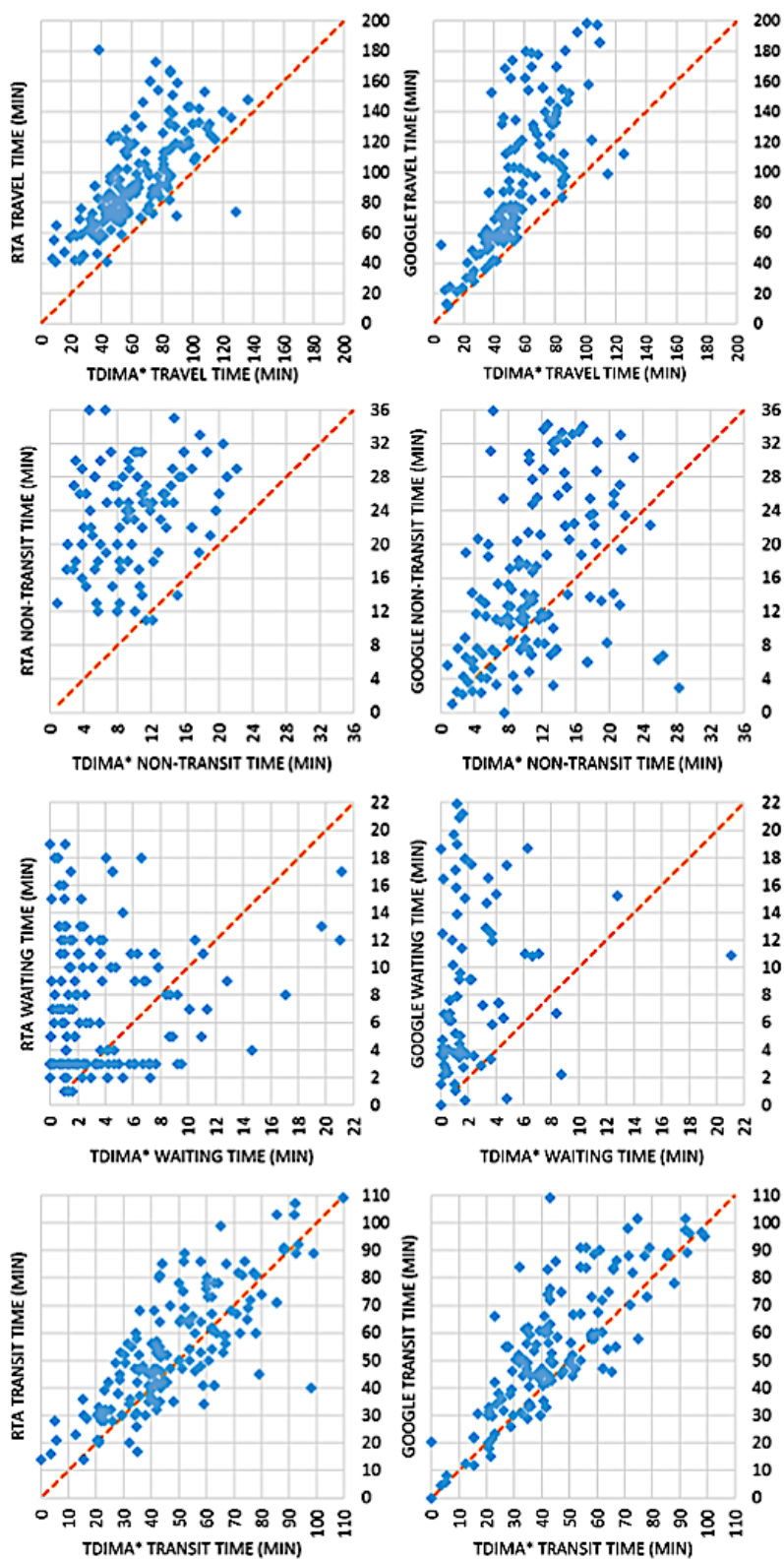


Figure 4-6 Comparison of TDIMA* results to online routers

Conclusion

A Time-Dependent Intermodal A* (TDIMA*) algorithm was introduced and described. The algorithm works on a multimodal network with transit, walking, and vehicular network links. The TDIMA* algorithm finds paths for the three major modes (transit, walking, driving) and any feasible combination thereof (e.g., PNR). For improved realism, turn penalties, progressive transfer penalties, upper bounds on waiting, walking, and driving (where necessary) are incorporated. The algorithm was validated on the large-scale Chicago regional network using real-world trips, and the results were compared with two online services (Google Directions API and RTA Trip Planner). The results provided by the TDIMA* for PNR trips are significantly better than those provided by either service.

As a next step, the algorithm will incorporate seating and standing capacity penalties, as well as monetary costs, e.g., tolls, parking fees, and transit fare. Although this algorithm can serve as a stand-alone routing tool, it is designed as an integral component of POLARIS. This integration will allow for comprehensive modeling capabilities such as supply-side interactions between different modes, abandoning the use of skims for mode choice and activity scheduling, and en-route mode switching and re-routing.

Bayesian Forecast of Transit Demand⁵

Introduction

Background

The notion of mobility was first introduced around 2009, and since then, it has gradually incorporated individual practices and lifestyles into the analysis of transport demand, which made it necessary to redefine the meaning of the term. The aim of technically optimizing the straightforward spatial movement of goods and individuals (i.e., planning, flow, traffic, vehicle technology, etc.) has been supplemented, or even replaced, by the objective of obtaining a detailed understanding of the variation in individual ability to travel (accessibility), individual experience of daily travel conditions (comfort, sustainability), and/or even the role that mobility plays in individual lifestyles in terms of both actual and possible interactions. Consequently, mobility is now studied by economists, sociologists, urban planners, geographers, and data scientists.

Traditionally, the analysis of mobility is based on travel surveys (OD surveys, household travel surveys). However, these surveys tend to be expensive and consequently are undertaken fairly infrequently, which means any current developments and the public policies that aim to influence them are not closely monitored. In recent years, there has been increased interest in using completely anonymous data from real-time smart card collection systems to better understand the behavioral habits of public transport passengers. Such use of smart card data to generate insights into passengers' travel practices and to identify or predict travel patterns becomes a very active research area. In particular, the problem of making inference on the arrival time and modeling dynamic, real-time traffic OD to estimate demand flow of a bus network based on either link count or smart card data, have been covered extensively in the literature over the last twenty years. Novel methods for modeling and analyzing the dynamic OD demand flow of a large-scale public bus network include passenger clustering with Gaussian mixture generative model using smart card data over five-year span and taking into account the continuous representation of time and the usage habits of passengers and their behavioral changes over time, Bayesian approach with Markov Chain Monte Carlo (MCMC) simulation methods, and single-level time-dependent path flow estimation model with constraints on traffic flow dynamics and updated states. Due to inherent structural features in the problems of inference about OD demand flow during disruptive events such as flooding, tornadoes, blizzards, and man-made emergencies, a Bayesian model and method are presented for effectively

⁵ Authored by Vadim Sokolov and Tuan Le, GMU. Acknowledged for their contributions are Dr. Hubert Ley, Director of TRACC at Argonne National Laboratory; James Garner, Manager of Research and Analysis Department at Pace; and Dr. Kathryn Laskey.

analyzing transit data. The objective for this project includes four goals—1) developing a statistical model incorporating prior knowledge about the historical demand and the noise of the number of on/off-boarding passengers (ON/OFF count) at each stop to estimate demand between individual (or groups of) bus stops; 2) based on estimated demand, predicting the crowded zone-level destinations of riders; 3) obtaining the estimated populations' means of traffic flows between any two zones; and 4) analyzing rider travel patterns based on two datasets (APC and Ventra) and documenting them.

Motivation and Problem Statement

Due to an increasing number of PACE bus riders annually, its managers sought to improve their fleet allocation (re-routing and re-scheduling its buses, given that it has a limited number of buses). To do this effectively, they wanted a better demand forecasting tool to predict the future traffic flows. This tool was expected to incorporate their prior knowledge on historical demand of riders and capture the uncertainty in ON/OFF counts data into its forecasting process. Since an OD matrix is the most fundamental representation of demand between bus stops (or groups of bus stops), PACE's managers sought a statistical model to estimate this matrix accurately. The estimated OD matrix would be used by PACE's managers as a fundamental input for improving POLARIS, the integrated traffic simulation model supporting PACE managers in re-routing and re-scheduling buses to meet demand of riders.

A plausible approach is using Bayes' formula to incorporate prior knowledge on historical demand and capture the uncertainty in ON/OFF counts data. With this approach, after obtaining the estimated demand as well as its distributions, crowded zone-level destinations can be predicted, and the estimated population means of traffic flows can be obtained.

Objectives, Scope, and Deliverables

To achieve a unique goal of the PACE managers, the objective of this study included four major actions:

- Develop a statistical model to estimate the OD matrix based on the two historical datasets (APC and Ventra) obtained from PACE.
- Estimate population means of traffic flows based on the estimated results by the statistical model.
- Predict the crowded “zone-level” destinations of riders based on the estimated results.
- Analyze and document rider traveling patterns based on the APC and Ventra datasets.

The scope of this study included performing data exploratory analysis on the APC dataset, which was available for 2015 and for October 2016, and the Ventra

dataset, which was available only for March 2016, and providing insights on rider travel pattern at different time variations. The Bayesian model used to estimate demand was considered only with two specific classes of distributions assigned to prior—likelihood (Normal-Normal, Poisson-Normal, Poisson-Poisson, Normal-Poisson). These were selected based on the positive results of previous research work. Second, there exists an analytical solution in one case (Normal-Normal), which is helpful for comparing against the performance of the numerical solution in the case of Normal-Normal.

Finally, the deliverables of this study include a detailed exploratory data analysis on analyzing rider travel patterns, a detailed introduction of Stan and its functionality, and simulation results of each of the four possible pairs of prior-likelihood to make a recommendation to PACE managers on the optimal pair of prior-likelihood for our Bayesian model (i.e., the pair whose estimated demand is closest to the simulated true demand over a time period of 365 days). The sensitivity analysis of the result given by the optimal pair of prior-likelihood with respect to priors and the variance parameter (represents noise in the COUNT data) of a specific distribution assigned to prior is also provided.

Model Formulation, Assumptions and Limitations

As the Bayesian model contains routing matrix in one of its parameters; a routing matrix in the context of this problem can be conveyed through a simple example—assume a bus network with only three stops, A, B and C, with exactly three routes. Assume data only on the number of people getting on at stop A and get off at stop C (see Figure 5-1). For the particular three-node network, the column labels denote all feasible routes in the order of AB , BC , AC , and the two row labels are A^{in} and C^{out} . For the first row, the (1,1) and (1,3) entries are 1 because the first row denotes all possible destinations of people getting on at stop A (so they would either get off at stop B or stop C), which corresponds to column AB and AC (BC are irrelevant in this case, since the first row A^{in} denotes only routes starting from A). Similarly, for C^{out} , the (2,2) and (3,2) are 1 because those are all possible paths for riders to get off at stop C (either they start from A or B, which corresponds to columns AC and BC). The first entry in the same row corresponds to column AB is 0, because AB is irrelevant in this case.



$$\text{In this example, } A = \begin{bmatrix} 1 & 0 & 1 \\ 0 & 1 & 1 \end{bmatrix}$$

Routing Matrix

$$A = \begin{array}{c} \text{Stop In/Out} \\ \downarrow \\ \begin{array}{c} A \\ B \\ C \\ \dots \\ Z \end{array} \end{array} \begin{array}{c} \xrightarrow{\text{Feasible Routes}} \\ \begin{array}{c} AB \quad AC \quad AD \quad \dots \quad ZY \end{array} \end{array} \left(\begin{array}{c} \\ \\ \\ \\ \\ \end{array} \right)$$

General Form of Routing Matrix

Figure 5-1 General form of routing matrix for three-stop problem

The above argument can be extended to a network with more than three nodes, the general form of the routing matrix is as follows:

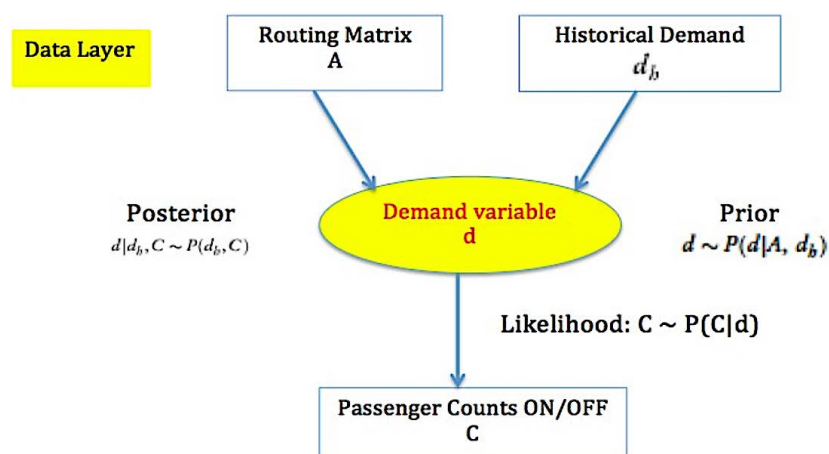


Figure 5-2 Relationship between variables d , c and data A , d_h

The probabilistic graphical model indicates the relationship between the given data (extracted from APC dataset), the demand variable d , and currently-observed ON/OFF counts (x). From the relationship between the data layer and the demand variable d (meaning, given d_h , we can make inference on possible values of d) and between the demand variable d and ON/OFF counts x (meaning, given d , we can make inference on possible values of C), denoted are the prior and likelihood distributions as $P(d|d_h, A)$ and $P(C|d)$. Now, our objective is to obtain $P(d|d_h, C)$, which is the posterior $d|d_h, C$.

Inspired by the success of the work by West and Tebaldi (1998), the fact that the ON/OFF counts data are discrete and the technical validity of Bayes' formula, the three following assumptions are made:

- Only two classes of distributions, specifically Poisson and Normal, are considered for prior and likelihood.
- Counts data (x) and demand (d_h) are conditionally independent given historical demand (d_h). The traffic flows of any two routes are independent.

Under these assumptions, by applying Bayes' formula twice, we obtain

$$P(d|d_h, x) \propto P(x|d)P(d|d_h)$$

The major difficulty for evaluating the posterior distribution $P(d|d_h, x)$ in the equation above is the non-existence of analytical formula for most pairs of prior–the likelihood (with the exception of Normal-Normal, in which case a Kalman Filter can be used to obtain a Normal distribution for the posterior, with closed-form formulas to compute mean and variance). However, if only considering Normal-Normal for prior-likelihood, we limit the flexibility and suitability of the model when taking into account the given APC dataset. Therefore, in most cases, Markov Chain Monte Carlo (MCMC) simulation is a powerful technique to obtain the posterior distribution of $d|d_h, C$, because it can deal with any distributions assigned to prior and likelihood. Now, by noting that $x = Ad$, we can model the likelihood $x|d \sim P_1(A * d, \sigma_1)$ where P_1 is either Normal or Poisson, and σ_1 is a vector accounting for the noise in the estimated demand d . Similarly, based on the methods used to collect the counts data in the APC dataset, the historical demand d_h most likely under-estimates the true demand. Therefore, the prior can be modeled as $d|d_h \sim P_2(d_h, \sigma_2)$ where P_2 is also Poisson or Normal, and σ_2 is a vector representing the difference between our historical demand d_h and true demand.

Finally, the approach using Bayes' formula and MCMC simulation as main tools has three major drawbacks. First, the assumed distributions for either prior or likelihood might not be true, which then leads to inaccurate posterior distribution if the Bayesian analysis is not robust. This also means the obtained posterior distribution is valid only with respect to specific class of distributions of prior-likelihood. Furthermore, the computational cost of MCMC is very high when working with high-dimensional data. Due to this limitation, MCMC is not scalable to very large-scaled networks with approximately one million nodes.

Exploratory Data Analysis

From PACE, the two datasets denoted as APC and Ventra were obtained, which contain data for all PACE bus rides. Together, these datasets have 71.18 million data points, with 16 common qualitative categories such as Latitude, Longitude,

Days of a Week, Route, Stop Name, ON, OFF (counts data) and Bus ID. PACE managers noted that the Counts data in the APC dataset were quite inaccurate, and sometime misleading, because there were certain days in which the sensors are malfunctional or the bus driver did not keep track of the counts correctly for cash-paid passengers. In addition, to comply with the regulatory and non-discriminatory requirements, the buses must be assigned to different routes every day.

APC Dataset

The APC dataset was collected in two different time periods—October 2016 and the entire year of 2015 (equivalent to 365 days, from 01/01/2015 to 12/31/2015). There were three major differences between these datasets—the Trip Time column was included in the one-month data but not in the whole-year; the one-month dataset recorded trips made by only 63 buses departing from the same garage of PACE in the Northwest region of Chicago, but the second dataset included all 635 buses from the 9 garages located across the state; and third, for the one-month dataset, approximately 85% of the data were collected during weekdays. However, in both datasets, the counts data are noisy.

Exploratory data analysis for the one-month dataset is as follows. Using the library packages tidyverse and ggplot2 and the groupby function in R, the average number of riders ON and OFF was computed across every hour of a day and bar plots were created to observe the trends throughout different hours (note that the dataset does not include data at 3:00 am). The result was interesting, as the highest average hourly APC ON occurred at 10:00 pm (= 0.2758), and the lowest average hourly APC ON occurred at 1:00 am (= 0.2187). However, a different pattern was observed for the highest and lowest average APC OFF, which was at 11:00 pm (= 0.2831) and 4:00 am (= 0.2333). To check whether these differences were statistically significant or just due to noises in the data, the Mann-Whitney-Wilcoxon test was conducted using the function `wilcox.test()` in R, and the p-value = 0.0685 was obtained, which is greater than 0.05, and the standard errors for average ON and OFF are 0.2251 and 0.2518, respectively. This implies that we cannot reject the null hypothesis that the two groups came from non-identical populations, so the difference between average ON and average OFF at the above hours were mainly due to noise in the counts data. We then look at the total ON count to observe the most active time of the majority of riders. We used the `ggplot()` function to create the bar plot for the total APC ON across different hours of a day (see Figure 5-3) and observed that the early morning time period (6:00–7:00 am) is the most active time of riders, with very few riders traveling between midnight and 4:00 am. However, the peak time of total hourly APC ON and OFF are both quite different from the average hourly APC ON. The reason is that at 10:00 pm when average hourly APC ON peaks, the amount of data collected is only equal to approximately

one-fifth that of data at 6:00 am, at which the total APC ON and OFF peak (= 42483). Since average hourly APC ON at time t = total APC ON at time t divided by number of ON counts data collected at time t and the ratio between counts data at 10:00 pm and 6:00 am is larger than the ratio between total hourly APC ON at 10:00 pm and 6:00 am ($5.035 > 42483/9863 = 4.307$), we conclude that the substantial difference in the amount of data collected at 6:00 am and 10:00 pm cause the difference in the peak time of total APC ON vs. average APC ON.

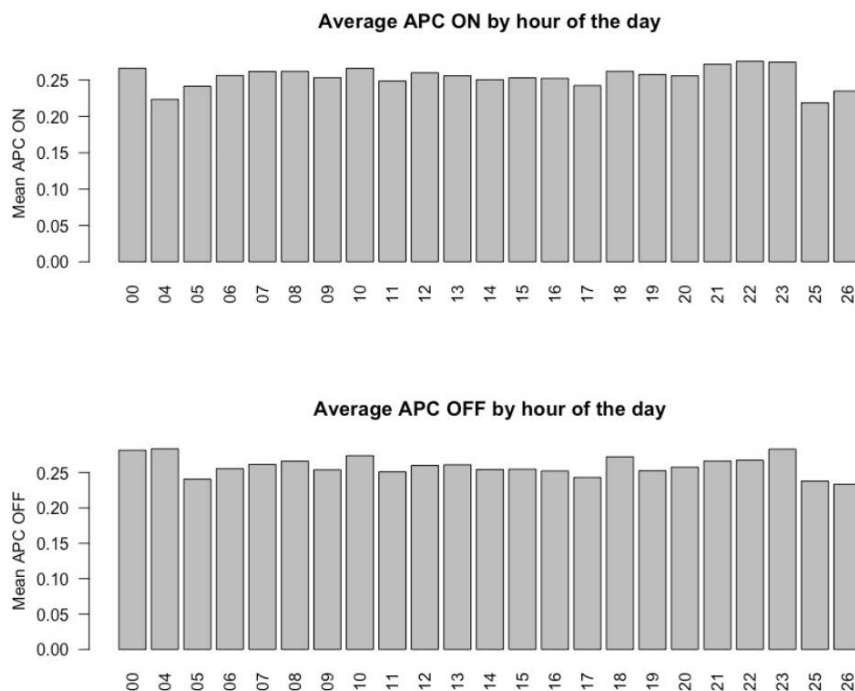


Figure 5-3 Distribution of average hourly APC ON and OFF (October 2016)

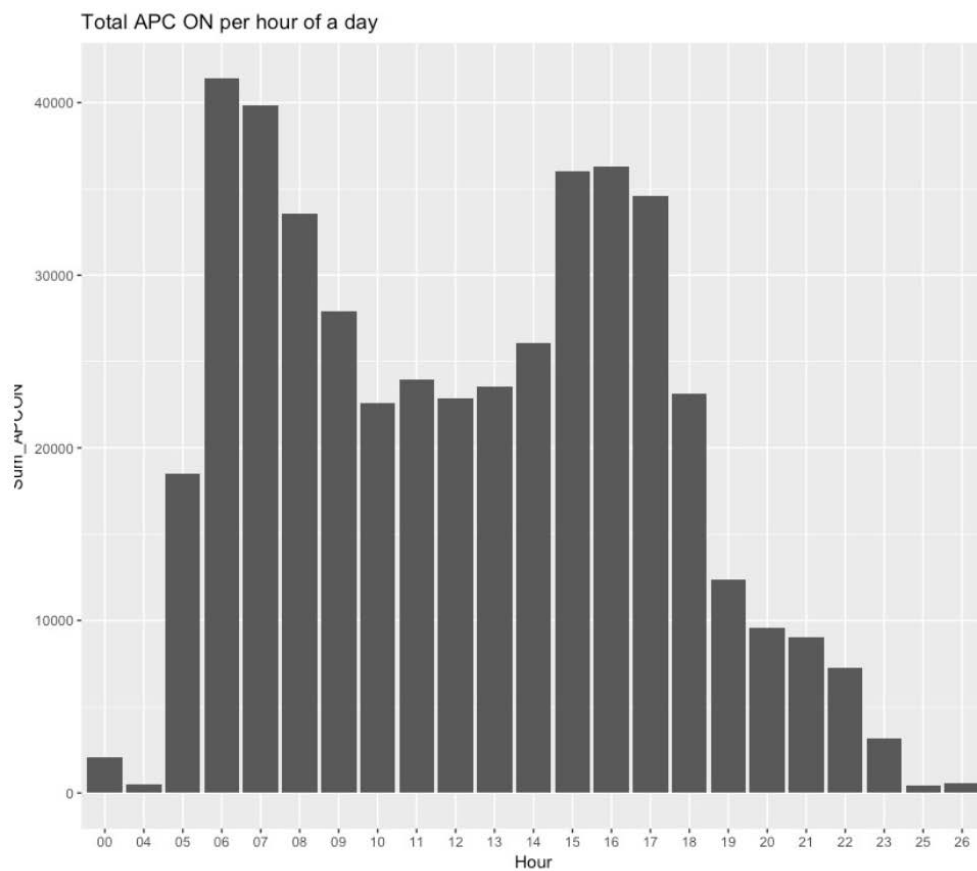


Figure 5-4 Distribution of total hourly APC ON and OFF (25 = 1:00 am, 26 = 2:00 pm, October 2016)

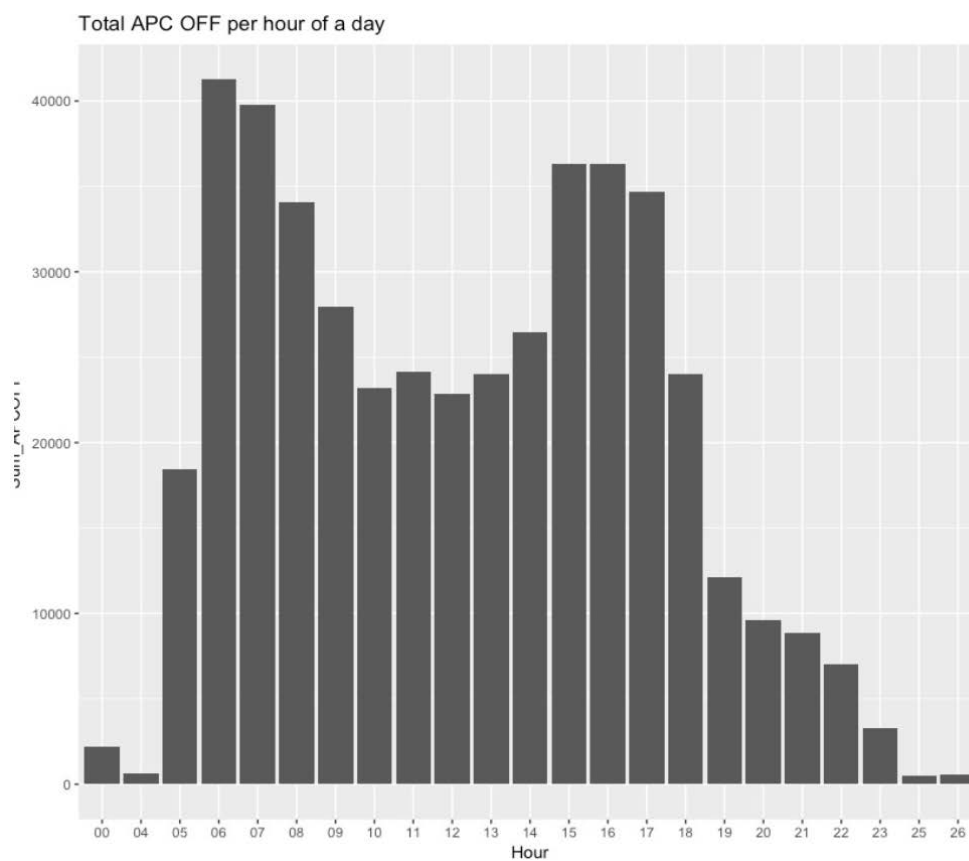


Figure 5-5 Distribution of total hourly APC ON and OFF (25 = 1:00 am, 26 = 2:00 pm, October 2016)

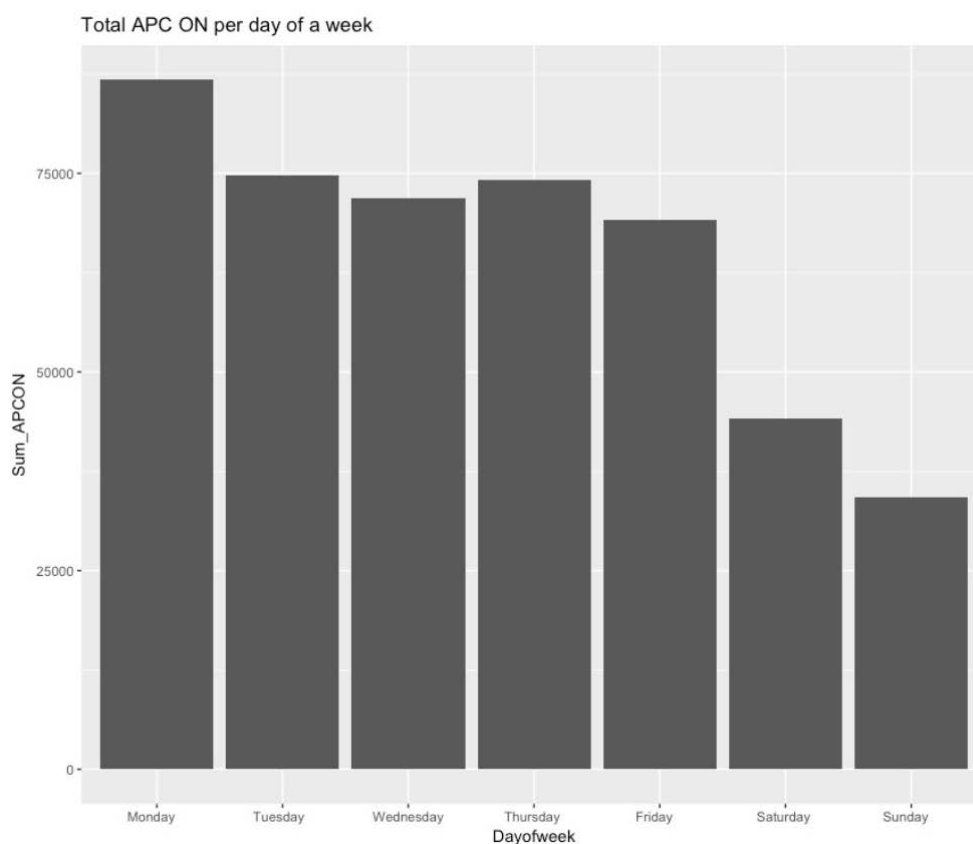


Figure 5-6 Distribution of total APC ON per weekdays (October 2016)

A similar analysis was conducted for the average APC ON and OFF per days of a week to observe the distributions of ON and OFF. The conclusion was that the same pattern holds for both average APC ON and OFF—the peak and trough days were both on Saturday and Monday, respectively. The absolute magnitudes were not substantially different—for average daily APC ON, the highest and lowest were 0.2960 and 0.2434, whereas that of APC OFF were 0.300 and 0.2457. Here, the averages were not much different because only high demand routes are served on the weekend.

The Mann-Whitney-Wilcoxon test was then conducted using the `wilcox.test()` function in R to see if the difference between average APC ON and OFF were statistically significant. The standard errors obtained for average APC ON and OFF were 0.219 and 0.232, and the p-value obtained was 0.127, which is greater than 0.05. Thus, we cannot reject the null hypothesis that the average APC ON and OFF comes from an identical data distribution, so the minor difference between the highest and lowest average APC ON and OFF was due to the noise in the data. In addition, we also computed the total number of APC ON and OFF per days of a week and observed that Monday was the most active time of riders, evidenced by the highest APC ON and OFF (86,772 and 87,610), and Sunday was the most inactive time of riders with the lowest total APC ON and

OFF (34,246 and 34,091). Once again, the Mann-Whitney-Wilcoxon test was conducted to check if there was any statistical significance in the difference between highest total APC ON and average APC ON, as well as between highest and lowest total APC OFF. For total APC ON and OFF, the standard errors were 25.3 and 28.9 and the p value for total vs. average APC ON and OFF were 0.0417 and 0.0439, respectively. Since the p -values were both less than 0.05, the differences in total APC ON and average APC ON (as well as total APC OFF and average APC OFF) per days of a week were statistically significant at the 95% confidence level. When conducting the same analysis and computing the standard error and p -value for t-test statistics with respect to the total daily APC ON and OFF, the above pattern still held, with weekday (Thursday, 10/19) at the highest number of riders and weekend (Sunday, 10/30) at the lowest number of riders (the standard errors for total daily APC ON and OFF in the month of October was 145.22 and 152.31. The p -values for total daily APC ON vs. total daily APC OFF were 0.067, which were greater than 0.05. This implies the difference in total daily APC ON and OFF were not statistically significant at the 95% confidence level, and such difference was due to noise in counts data).

To complete the analysis for this one-month APC dataset, the number of riders within a particular route per days of a week, hours of a day, and days of a year was examined. This was helpful to the managers at PACE because they could gain insight into the usage frequency of each route, which can help them in future planning if they want to eliminate certain low-usage route and re-route certain buses. First, we found that route 215 is used only two days per week (Thursday and Friday) and serves, on average, 240 riders per day. Second, route 237 was available only on Thursday, and very few people used that route (only 63 riders in October). Researching this particular route, we found that it operates for special events or serves riders taking long outbound trips to Chicago. As there was no large event occurring during October 2016 in Chicago, this explains why it manages, on average, approximately 2 riders per day in October.

The same exploratory data analysis was conducted for the one-year APC dataset, which had 69.4 millions of rows and 18 columns. First, using the library `dplyr` and `groupby` function in R, we created a bar plot for the total number of riders across different days of a week and observed that the peak of total ON was on Tuesday and Wednesday, while the trough was on Sunday (see Figure 5-7).

In addition, we examined the average APC ON across days of a week (total APC ON per particular day of a week/amount of data collected on the same day of the week in a year) to see if it had different pattern. The amount of data collected on the same day of a week in a year opposite pattern occurred: average APC ON peak on Sunday. We conducted the Mann-Whitney-Wilcoxon test to examine if the difference in the distribution between average and total APC ON across days of week was statistically significant. The standard errors

of average and total APC ON were 0.169 and 11,528, and the p -value = 0.045, which is less than 0.05, so the difference in the distribution between total and average APC ON was statistically significant at the 95% confidence level. We then observed the trends in the average and total monthly APC ON in the corresponding bar plots. The pattern was pretty much similar—both average and total monthly APC ON peaked in October, and the distribution of average and total monthly APC ON were both skewed to the left. This meant October was the most active month of riders (see Figures 5-9 and 5-10). Finally, regards to the total APC ON per days of year 2015, the peak was approximately 75,000 and occurred nearly in the middle of the year. The day-to-day variations were quite large, with the approximate range between 5,000 and 60,000 (see Figure 5-11. Note that the x-axis includes all days starting from 01/01/2015 to 12/31/2015).

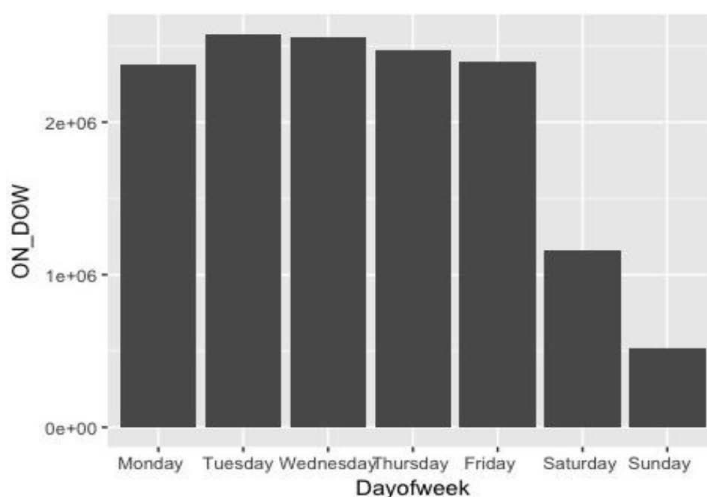


Figure 5-7 Total APC ON per day of week

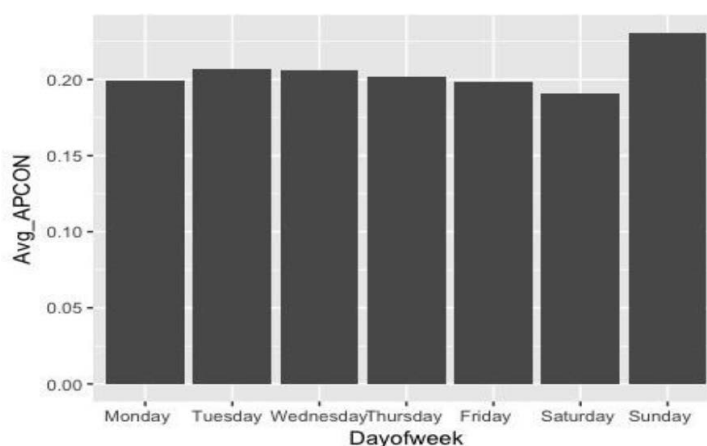


Figure 5-8 Average APC ON per day of week

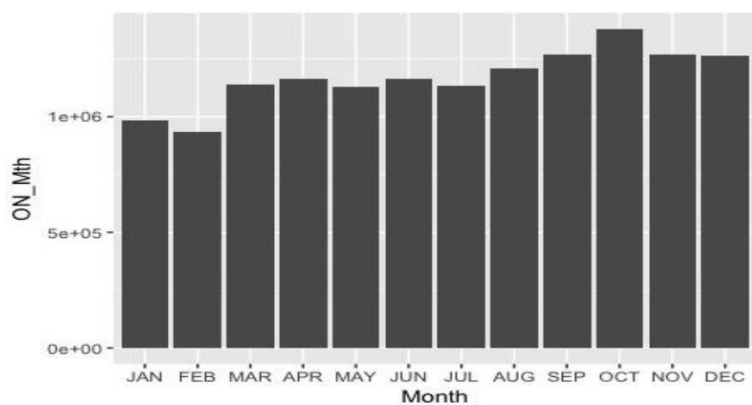


Figure 5-9 Total APC ON per each month

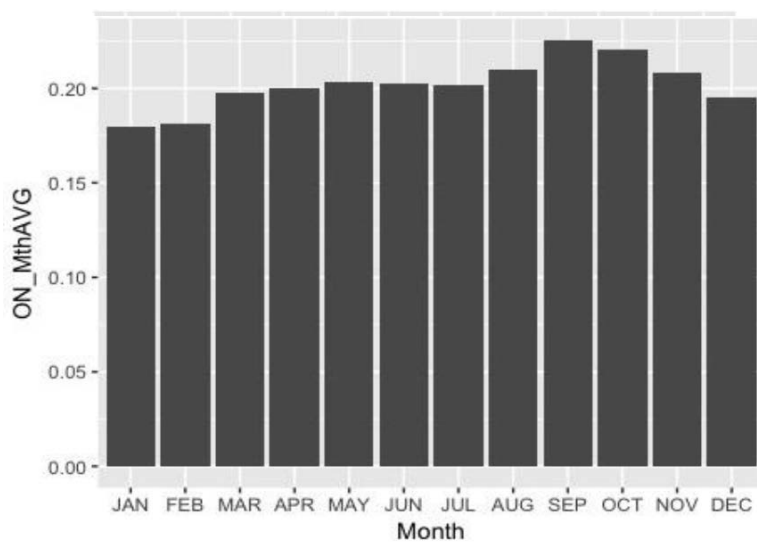


Figure 5-10 Average APC ON per each month

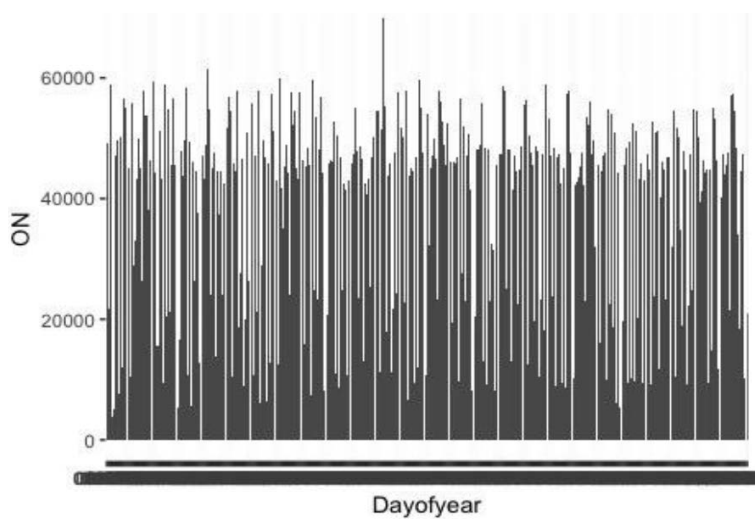


Figure 5-11 Total APC ON per day of year (2015)

VENTRA Fare Card Dataset

Technological advancements allow the transit authority in Chicago to issue a declining balance RFID-enabled card called Ventra, which allows passengers to add an unlimited number of ride passes into their card for any time period. Moreover, passengers can transfer between different transit agencies (CTA and PACE, PACE and Metra, etc.) without having to purchase a new fare, unlike the old fare payment method. These features significantly help improve user experience for frequent riders and/or commuters, which, in turn, encourages more people in the area to use public transportation for getting around the city. Note that the Ventra dataset did not have the OFF counts (unlike APC dataset). However, the Ventra dataset also contained information that was not available in the APC dataset such as passenger transaction history and transfer points and customer trip types. This information was not collected previously because the old payment methods could not obtain them without affecting the rider user experience negatively.

The Ventra dataset was available for March 2016 and included buses coming from all nine garages of PACE (unlike the one-month APC dataset, which only covered buses coming from the Northwest garage of PACE). The dataset had 88 columns for each observation, for a total number of 404,643 observations. For the purpose of data manipulation, we chose only columns that were crucial to perform the exploratory data analysis—location information, trip start time, direction of bus trips, hour, types of trips riders made, bus stop number, number of on-boarding riders, specific route a bus covers, and status of transactions recorded from the card swipe.

Repeating the same steps as with the APC datasets above, we first computed the total and average ON across different hours and created the bar plots to observe the trends in the distributions of these two quantities. For the Ventra dataset, the "COUNT" data were available for every hour of a day (unlike the APC dataset, which did not have count data at 3:00 am). Once again, the average ON count at time t was computed with the formula (total ON count at time t /total number of ON count data at time t).

After creating the bar plots for the average and total ON count across hours of a day, the following trends were observed: at time 2:00 am, the average "ON" count peaked (= 2.20822 riders) and troughed at 4:00 am (= 1.1172 riders). The total ON count peaked at 3:00 pm (= 54,859 "ON" riders) and troughed at 1:00 am (= 225 "ON" riders). To verify if the difference was statistically significant, we conducted the Mann-Whitney-Wilcoxon test using `wilcox.test()` function in R. The standard errors obtained for total and average ON counts were 358.17 and 1.451, and the p -value was 0.0317, which is less than 0.05. Thus, the difference between total and average ON count was statistically significant. Finally, we observed that the distribution of total hourly "ON" count was similar to the

combination of two Normal distributions (one for the morning–noon period and one for the afternoon–midnight period); the distribution of average hourly "ON" count looked similar to the Poisson distribution.

For the total and average "ON" count per days of a week, the trends observed from the bar plots were similar to those observed in the two APC datasets. The distribution of average ON count per days of a week peaked on Saturday (= 1.3941 riders) and troughed on weekday (= 1.3088 riders), while that of total ON counts peaked on Tuesday (= 105,647 riders) and troughed on Sunday (= 16,513 riders). The Mann-Whitney-Wilcoxon test was conducted once again and gave the standard errors for total and average as 11251.72 and p -value = 0.0415, which was less than 0.05. Thus, the difference in total and average ON counts was statistically significant. Finally, the distributions of the total ON counts per each day of March were very similar to that of the total ON counts per days of a week, as it peaked on weekday (Tuesday) and troughed on weekend (Sunday). The most active time for riders was Tuesday.

Bayesian Model

The Bayesian model was demonstrated previously to obtain the posterior distribution of $d|d_h, x$, with d_h and x as data from the APC dataset in 2015. This was equivalent to compute $P(x|d)P(d|d_h)$, where prior-likelihood are among four possible choices. The first step was recovering the historical demand d_h , which was the solution to the system of linear equations $Ad_h = x_h$, where A is the routing matrix between individual bus stops. This system of linear equations was inconsistent, so it did not have unique solution. Therefore, we employed the least-squares method with the `npls` package in R to solve for the non-negative solution d_h that minimizes $\|Ad_h - x\|_2^2$. Unfortunately, this package was unable to handle the size of matrix A . To resolve this scaling issue, a common way is to divide the maps into zones and group bus stops in the same zones together. Given the `stopzone.csv` file that contained the column ZONE, where each bus stop was mapped into an unique zone using their lat-lon pair (the region was divided into 1993 different polygon zones), we used the `leftjoin()` function in R to assign the zones to each bus stop based on their common `geonodeID`. We then aggregated the total ON counts of all stops within the same zones and reconstructed the zone-level routing matrix A . Dimensionalities of A were reduced to the size of hundreds \times hundreds. Using the same `npls` package, we recovered the non-negative zone-level solution d_h that minimized $\|Ad_h - x\|_2^2$ (by doing this, we implicitly relaxed that the constraint d_h must be integer). This d_h then was chosen to be the rate λ of the Poisson distribution when assigning to the prior or likelihood.

Stan, a Probabilistic Programming Language

To specify the data, the prior and likelihood in our Bayesian model, the parameter d , and to compute the Bayesian inference for continuous-variable

models through MCMC simulation, we extensively used Stan, a C++ program to perform Bayesian inference. A Stan program makes inference by computing directly the log-posterior density function over parameters conditioned on specified data and constants. The result is a set of posterior simulations of the parameters in the model (or a point estimate, if Stan is set to optimize). Stan differs from BUGS and JAGS in two ways: first, Stan is based on a new probabilistic programming language that is more flexible and expressive than the declarative graphical modeling languages underlying BUGS or JAGS, in ways such as declaring variables with types and supporting local variables and conditional statements. Second, Stan's MCMC simulation is based on Hamiltonian Monte Carlo (HMC), a more efficient and robust sampler than Gibbs sampling or Metropolis-Hastings for models with complex posteriors. Stan has multiple interfaces for command line shell (`cmdstan`), for Python (`pystan`), and for R (library `rstan`).

A typical Stan program includes multiple blocks, and each block serves a unique purpose. Such blocks must be specified in the same order as follows. A Stan program always starts with the data block (unless a program has a user-defined function, then those functions must be specified before the data block), which declares the data (double types) required to fit the model. From the modeling approach, this is different when comparing to BUGS and JAGS, which determines which variables are data and which are parameters at run time based on the shape of the data input to them. Thanks to these declarations, Stan compiles a much more efficient code (the underlying language supporting Stan's compiling is C++, which compiles data variables as double types much faster). The next (optional) block is transformed data block, which may be used to define new variables that can be computed based on the data. This block is executed during construction, after the data is read in (note that the transformed data variables can only be used after they are declared). Next is the parameter block, which defines the parameters we are interested in finding the posterior distribution and/or point estimate. This block is executed every time the log density is evaluated. The probability distribution defined by a Stan program works with unconstrained support (i.e., no points of zero probability), so for variables declared with constrained support, they are implicitly transformed to an unconstrained space over which the model block is defined. These unconstrained parameters are then inverse transformed back to satisfy their constraints before executing any statements in the model block. To account for this change of variables, the log absolute Jacobian determinant of the inverse transform is added to the overall log density. No validation required for this parameter block. Next is the (optional) transformed parameters block, which is executed after the parameter block. Constraints are validated after all statements defining the transformed parameters have executed. If the constraints are not satisfied, the execution of the log density function is halted. Next is the model block, which is to define the log density on the constrained

parameter space. It can contain as many sampling statements as possible, but every such statements are translated to the log density functions (e.g., if parameter 'beta ~ normal(0,1)' has the exact same effect as incrementing log density directly with the value of the log probability density function for the Normal distribution using the target += normal-lpdf(beta|0, 1)). Stan does not require proper priors, but if the posterior is improper, Stan will halt with an error message. Finally, an (optional) generated quantities block allows values that depend on parameters and data, and might be used to compute predictive inferences. Figure 5-12 is an example of a Stan model in vectorization form that contains three must-have blocks—data block, parameter block, and model block.

```

data {
  int<lower=0> N;
  vector[N] y;
  vector[N] x;
}
parameters {
  real alpha;
  real beta;
  real<lower=0> sigma;
}
model {
  alpha ~ normal(0,10);
  beta ~ normal(0,10);
  sigma ~ cauchy(0,5);
  y ~ normal(alpha + beta * x, sigma);
}

```

Figure 5-12 Stan program modeling linear regression with unknown coefficients

Finally, despite its strength in computing the log-posterior density to perform Bayesian inference, the main limitation of Stan is that it does not allow inference for discrete parameters. Stan allows discrete data and discrete-data models such as logistic regressions, but it cannot perform inference for discrete unknowns. This explains why in the approach for obtaining the posterior distribution when the prior follows Poisson distribution, we have to use Normal distribution with equal mean and approximately equal variance to approximate the original Poisson distribution.

The following four subsections contain the simulation results given by MCMC (and analytical solution given by Kalman Filter for the Normal-Normal case) for all four pairs of prior-likelihood. Each MCMC simulation contain estimated demand in 365 days. For each day, the estimated demand vector d has hundreds of parameters to sample. Notice that some pairs of prior-likelihood provide very good estimations between certain zone-level origin-destination pairs on some days, but did very poorly on other days. Other pairs consistently provide good estimated demand d over the entire 365 days, and such pairs are the ones that

should be chosen by the project sponsor. The comparison plots shown below mainly focus on the days on which certain pairs of prior-likelihood provided bad results. For the pairs that provided consistently good estimated results across all days, the comparison plots shown over certain days were chosen randomly. Note that the label on the x -axis only stands for the ordering of different zone pairs on a particular day (e.g., zone index = 100 corresponds to zone pairs 1795–1375 on day 15).

Normal-Normal (Prior-Likelihood)

The prior and likelihood follow $N(d, \sigma_2)$ and $N(Ad + \epsilon_1, \sigma_1)$ where ϵ_1 is randomly drawn from $U(0,20)$ indicates the random difference between Ad and x , vectors σ_1 and σ_2 are drawn from $U(0,10)$ (component-wise). They represent noise in each component of d and $Ad + \epsilon_1$. Since we did not have currently observed true demand d' , we simulated it as $d_h + \epsilon_2$, where $\epsilon_2 \sim U(0,10)$ is the expected difference between d_h and d' (since count data x_h were underestimated, which led to d_h underestimates d'). For this particular case, an analytical solution existed by Kalman-Filter. The posterior follows Normal distribution and explicit formula for computing mean and variance exists. The numerical solution was obtained from running MCMC simulations with 250 iterations and 3 chains. From the one-year APC dataset, we observed that each day had a different zone-level routing matrix A , and the estimated demand vector d also has dimensions change day-to-day. Computational complexity of the MCMC simulation required writing the model in Stan and the execution code written in R and data onto Amazon Web Server with the package m5.2x large (32GB RAM, 8 CPUs). With the library(rstan) and the sampling() function in R, the MCMC calculation was performed. Each figure, on average, still took more than 3896 seconds to be produced. Figure 5-13 is the comparison plot for the OD pair zones 98 and 124 over a 365-day time period.

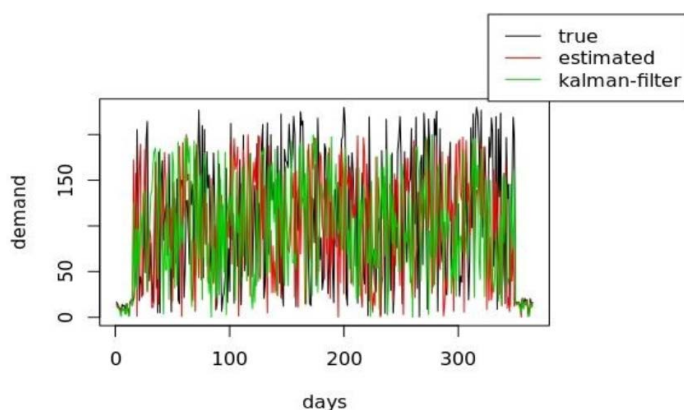


Figure 5-13 OD pair zones 98 and 124 – MCMC solution (red) and Kalman-Filter solution (green) vs. simulated true demand (black) over 365 days

From the graph above, the solution by Kalman Filter always underestimated the true demand over most days, except it matched pretty well with the true demand on low-demand days (i.e., days with demand less than 50). On the other hand, in this case, the MCMC solution also matched well with the true demand on low-demand days (e.g., days 23, 56 and 103), but it severely underestimated the days with peak in demand (e.g., days 19, 87 and 151). We then computed the mean squared error (MSE) and the mean absolute percentage error (MAPE) over 365 days of the MCMC and Kalman-Filter's solutions and obtained quite large values for both MSE and MAPE of Kalman Filter (29.77 and 31.45) and MCMC (25.33 and 26.41%). The major sources of errors in MSE and MAPE came from severe underestimation of both solutions on the high-demand days. Combining the above results, we concluded that Normal-Normal gave poor estimated demand d over high-demand days, although it did capture low demand days pretty well.

Poisson-Normal (Prior-Likelihood)

When the prior was Poisson, $d \sim \text{Pois}(d_h)$. The estimated parameter d was in the discrete unbounded space, and Stan cannot sample discrete parameters. However, by observing that most of the non-zero components of d_h were sufficiently large, we approximated Poisson distribution with rate d_h by a Normal distribution having the same mean and approximately equal variance (recall that mean and variance of $\text{Pois}d_h$ are both d_h).

Therefore, the Normal distribution approximation was of the form $N(d_h, d_h + k)$, where $k \sim U(0.02, 0.5)$ (the reason we have $d_h + k$ rather than d_h is because some components of d_h are zero, but Stan, by default, starts its MCMC simulation from the interval $[-2, 2]$. Since $\log 0$ is not well-defined, we want to avoid those cases. But we also want k to be small enough to match the second moment of $N(d_h, d_h + k)$ with that of $\text{Pois}(d_h)$). Thus, we ran the MCMC simulation with 250 simulations and 3 chains to obtain the posterior of $N(d_h, d_h + k) \times N(Ad + \epsilon_1, \sigma_1)$. Figure 5-14 is the comparison plot for OD pair zones 98 and 124 over a 365-day time period.

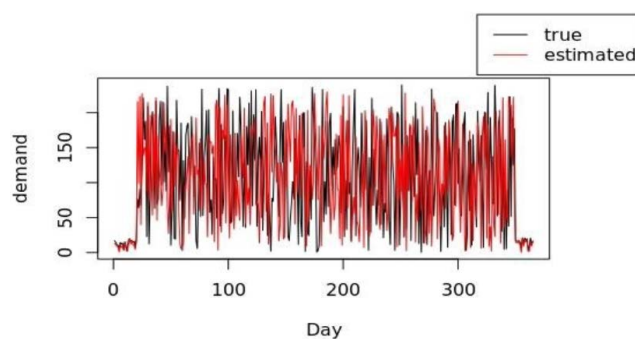


Figure 5-14 pair zones 98 and 124 – MCMC solution (red) vs. simulated true demand (black) over 365 days

From the graph above, we see that the estimated demand d given by Poisson-Normal model captured well days with moderately high demand (i.e., days with demand between 50 and 150 such as days 33, 87, 113). However, on very high/low-demand days (i.e., days with demand greater than 150 or less than 50), it underestimated with a relatively high margin (for example, days 19, 87 and 151). The MSE and MAPE computed were lower than that of the Normal-Normal case, but it still pretty high regardless—19.42 vs. 25.33, and 17.84% vs. 26.41%. The main factor to cause these relatively high MSE and MAPE were consistent underestimations of true demand on very high/low-demand days. In general, this pair of prior-likelihood was better than Normal-Normal, as it captured the moderately high days really well.

Poisson-Poisson (Prior-Likelihood)

Since the prior was still Poisson, we used the same Normal distribution $N(d_h, d_h + k)$, where $k \sim U(0.02, 0.5)$ to approximate Poisson distribution. The likelihood in this case became $\text{Pois}(Ad + \epsilon_1)$. Using MCMC simulation (250 iterations, 3 chains) to obtain the posterior distribution of $N(d_h, d_h + k) \times \text{Pois}(Ad + \epsilon_1)$, Figure 5-15 is the comparison plot for the OD pair zones 98 and 124 over 365 days.

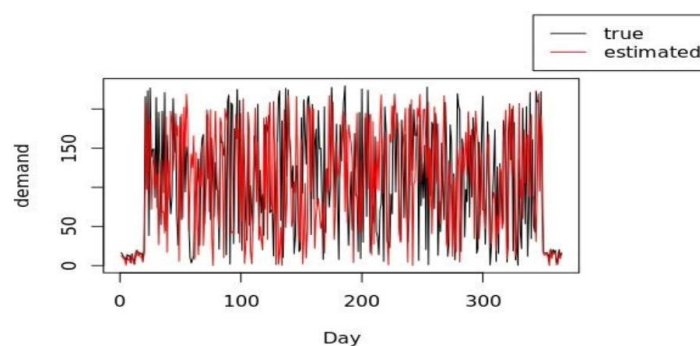


Figure 5-15 OD pair zones 98 and 124 – MCMC solution (red) vs. simulated true demand (black) over 365 days

From the comparison plot above, for the OD pair zones 98 and 124, the MCMC solution was close to the true demand on days with low and moderately high demand (i.e., days with demand < 150). However, it tended to underestimate the true demand on high-demand days (i.e., days with demand ≥ 150), such as days 37, 95 and 115. The MSE was lower than that of the Poisson-Normal case (15.26 vs. 19.42) and the MAPE was smaller (13.79% vs. 17.84%). The major source for the high MSE was because of severe underestimation of the estimated solution on the high-demand days. The MAPE was lower because the total number of low and moderately high demand days were nearly five times the number of high-demand days, and the MCMC solution matched quite well with low and moderately high demand.

Normal-Poisson (Prior-Likelihood)

As the Poisson distribution was assigned to likelihood, which Stan can sample because the parameter is not discrete anymore, we did not have to use Normal distribution to approximate it. Using MCMC simulation to obtain the posterior distribution of $N(d_h, d_h + k) \times \text{Poisson}(Ad + \epsilon_1)$, where ϵ_1 is drawn from $U(0,20)$, Figure 5-16 is a comparison plot between the estimated solution d given by MCMC vs. true simulated demand d' of a particular OD pair zones 98 and 124 over 365 days.

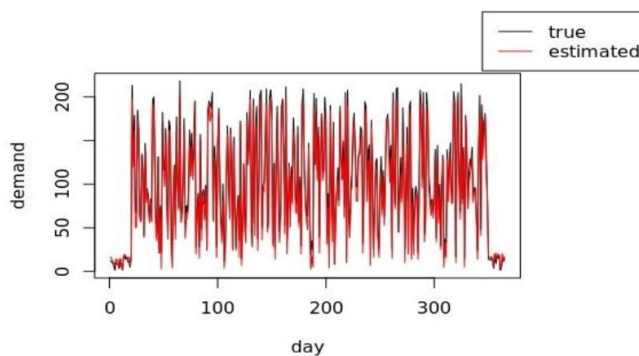


Figure 5-16 OD pair zones 98 and 124 – MCMC solution (red) vs. true demand (black) over 365 days

From the comparison plot above, the MCMC solution fit quite well to the simulated true demand for OD pair zones 98 and 124 over the period of 365 days. There were a few days that the estimated demand still underestimated the true one, such as days 62, 160 and 341. However, these underestimations were pretty small compared to the underestimation by other methods, as its range was narrower (between 4.5 and 11.4) and the mean was lower (7.61). The average MSE and MAPE across these 365 days were 10.73 and 6.35%, which are the lowest among all four cases, respectively. The reason MSE and MAPE were small is because the estimated demand given by this particular prior-likelihood did not severely overestimate or underestimate the demand between these two zone pairs (there were still days when true demand could not be matched very well by estimated demand, but the difference between the estimated and the true one was moderately small, as reflected through the low MSE. The three previous methods have a much wider margin of error for over and underestimation). Finally, for this optimal pair of prior-likelihood, we also examined the histograms of the estimated demand between other OD zone pairs such as 86 and 315, 1 and 39 over day 362. The histograms show distributions that are similar to the Normal distribution, which is the same distribution assigned to the prior.

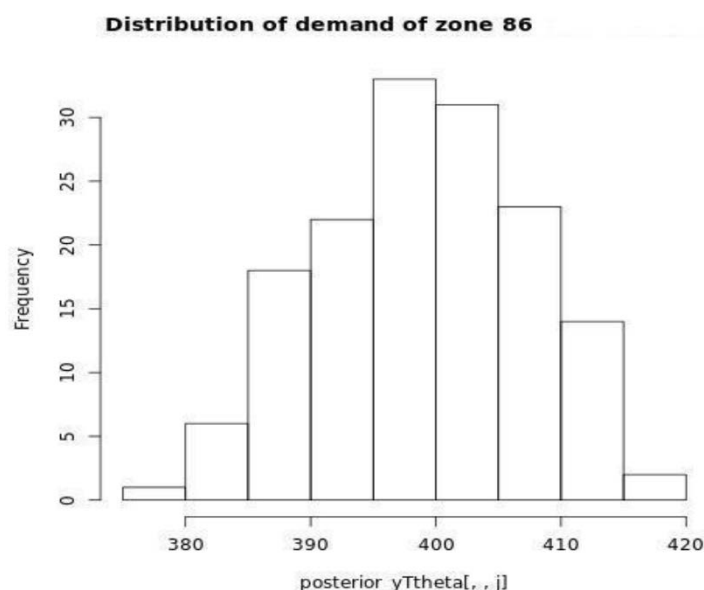


Figure 5-17 *distribution of estimated demand between OD zone pairs 86 and 315 and 1 and 39 look similar to Normal*

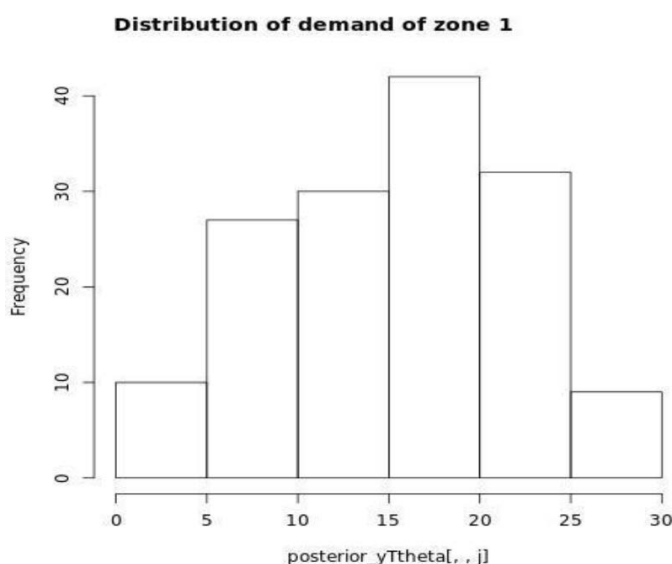


Figure 5-18 *Day 362 – distribution of estimated demand between OD zone pairs 86 and 315 and 1 and 39 look similar to Normal*

Bayesian Sensitivity Analysis

From the results above, for the OD pair zones 98 and 124, it is easy to see that when the class of distributions assigned to Prior changes (such as from Poisson to Normal), the estimated demand changes substantially. Thus, the simulation result from the best case of Normal-Poisson (prior-likelihood) is sensitive to specific distributions assigned to prior-likelihood (i.e., they cannot be generalized when Prior does not follow Normal distribution). However, when

we modified the variance parameter ϵ_1 in the Normal distribution by increasing or decreasing the range of the uniform distribution where they are drawn from, the former is $k \sim U(0.02, 0.5)$ (instead of $U(0.02, 0.9)$) and the latter is $k \sim U(0.02, 0.2)$. Running the MCMC simulation again with 250 iterations and 3 chains, the estimated demand d still matched quite closely to the true demand d , but the MAPE for those cases were approximately 7.53% and 9.74%, while MSE increased to 7.33 and 9.53, respectively. However, increasing the range of possible values for variance helped fix the underestimation problem, as Figure 5-19 shows that the estimated demand matched quite closely with the true demand on the very high-demand days (such as days 118, 183, 265), while decreasing such range did not help cure this problem, as Figure 5-20 shows the margin missed by the estimated solution on the days with peak demand (e.g., days 118, 183 or 265). Therefore, the result given by Normal-Poisson (prior-likelihood) is pretty robust with respect to the variance parameter of the Normal distribution assigned to prior.

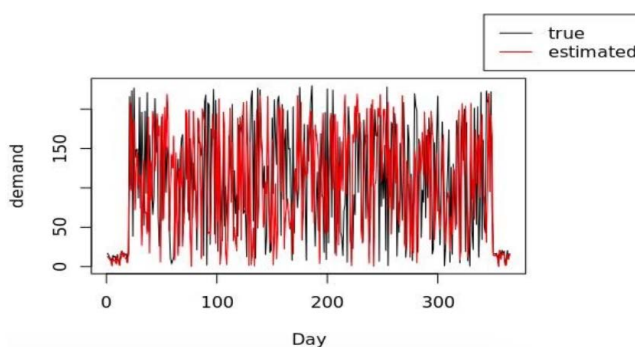


Figure 5-19 Day 362 – OD pair zones 98 and 124 – MCMC solution (red) vs. true demand (black) when $\epsilon_1 \sim U(0.02, 0.5)$

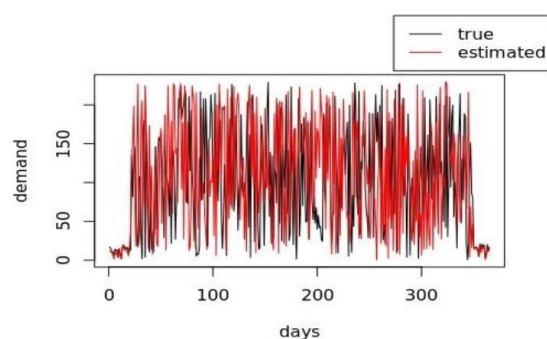


Figure 5-20 OD pair zones 98 and 124 – MCMC solution (red) vs. true demand (black) when $\epsilon_1 \sim U(0.02, 0.2)$

Summary of Results

From the results obtained and the sensitivity analysis, among four possible pairs of prior-likelihood for OD pair zones 98 and 124, the Normal-Poisson

for prior-likelihood performed consistently well across 365 days, as it had the lowest MAP and MSE errors (there are still a couple of zone pairs missed, but this is obvious because we are doing forecasting). The second-best model were either between Poisson-Normal or Poisson-Poisson, as there were trade-off between these two (the first has lower MSE but higher MAP, the second has higher MSE and lower MAP). Furthermore, based on the simulation result, we can compute the sample mean of traffic flows between any zone pairs. This sample mean, by Central Limit Theorem, would be expected to converge to the population's means. However, the result was not robust with respect to prior, so no inference can be made from the estimated demand once we relax the assumption that prior follows Normal distribution. The second-best model for this particular problem is Poisson-Normal, as it had the lower mean squared error compared to that of the Poisson-Poisson and Normal-Normal case. Finally, Normal-Normal did not work well over certain days due to its severe underestimation that results in the highest MSE and MAPE among four cases.

Table 5-1 *OD Pair Zones 98 and 124 – 365-day Average MSE and MAPE for Four Cases of Prior- Likelihood*

Error Types	Normal-Normal	Poisson-Normal	Poisson-Poisson	Normal-Poisson
MSE	25.33	19.42	15.26	10.73
MAPE	26.41%	17.84%	13.79%	6.35%

Table 5-2 *365-day Average MSE and MAPE of Every OD Pair for Four Cases of Prior-Likelihood*

Error Types	Normal-Normal	Poisson-Normal	Poisson-Poisson	Normal-Poisson
MSE	28.79	16.48	17.61	10.73
MAPE	32.62%	17.15%	14.43%	6.35%

Future Work

There are many different ways that can be built upon this model, and results for a future team that might be interested in conducting further research on this topic. First is exploring other pairs of prior and likelihood, both at the zone level and at the individual stop level. For the latter case, zero-inflated negative binomial distribution assigned to prior is the promising candidate, as the counts data has lots of zeros. Second, a future team can attempt to find the robust Bayesian model for this APC dataset, so that we do not have to depend on the choice of prior (or if such robust model does not exist, prove it). Third, a future group can either incorporate other factors, such as distance traveled, transaction types, etc., that might affect demand into the Hierarchical Bayesian model and come up with the posterior distribution for the estimated demand, or they simply can apply the model above (potentially with different choices of priors and likelihood) to other transportation systems

such as Amtrak, bikesharing and carsharing. Fourth, even with this dataset, a future group can reduce the forecasting period from one day to half a day or even one hour, assuming that the trip time information can be collected by PACE (which should be the case as people use the Ventra card now). Finally, a future team can reformulate the original problem as a two-stage non-linear stochastic optimization problem and obtain the estimated demand by solving such problem and then compare the obtained results against those with a Hierarchical Bayesian model to see which one produces the best result.

Literature Research Summary

Profile clustering has been conducted on mobility data in recent years for studying the temporal habits of passengers on their networks, and several methods have been developed to this end. The authors in McNichols (2010) proposed the use of a Gaussian mixture approach instead of a unigram mixture. The two-level generative mixture model uses non-aggregated data and fits a Gaussian mixture onto it. Specifically, the first-level model cards were partitioned into groups (card clusters) and the second took all ticketing logs of the clusters' cards to represent temporal activity profiles of these groups as a Gaussian mixture model. This choice of Gaussian mixture is reasonable because we need to preserve the continuous nature of timestamps.

Gaussians Mixture Generative Model

For modeling the cluster memberships of the cards, the authors introduced the use of latent variable $Z_i^1 \sim M(1, \pi)$ where M denotes a multinomial distribution, Z^1 denotes membership of one of the K card's clusters and Z_i^1 denotes membership of card i ($i \in \{1, \dots, M\}$) onto one of the K cards' clusters and follows a multinomial distribution of parameter $\pi = (\pi_1, \dots, \pi_K)$. Similarly, for the second level, let Z^2 denote membership of one of the H Gaussians. and Z_{ij}^2 denotes membership of trip j ($j \in \{1, \dots, N_j\}$ where N_i being the number of trips of cards i) to one of the H Gaussians to describe the temporal activity of cluster Z_{ik}^1 for the day D_{ijl} ($l \in \{1, \dots, 7\}$ being the set of the days of a week). Finally, X_{ij} denotes trip time, which the authors assumed follows a Gaussian distribution $N(\mu_{khl}, \sigma_{khl})$. Thus, mathematically, the two-level model could be written as follows:

$$Z_i^1 \sim M(1, \pi),$$

$$Z_{ij2} | Z_{ik1} D_{ijl} = 1 \sim M(1, \tau_{khl})$$

$$X_{ij} | Z_{ik1} Z_{ij2h} D_{ijl} = 1 \sim N(\mu_{khl}, \sigma_{khl})$$

The conditional density of X_{ij} is $f(X_{ij} | \{Z_{ik}^1 Z_{ij2h} D_{ijl} = 1\}) = \sum_{h=1}^H \tau_{khdij} f(x; \mu_{khdij}, \sigma_{khdij})$ where $f(\cdot; \mu, \sigma^2)$ is the density function of Gaussian distribution of mean μ and variance σ . From this, we obtained the likelihood model:

$$L(\theta) = \prod_{i=1}^M \sum_{k=1}^K \pi_k \left(\prod_{j=1}^{N_i} \prod_{h=1}^H \tau_{khdij} f(x; \mu_{khdij}, \sigma_{khdij}) \right)$$

At this step, we could estimate the likelihood parameters in the mixture models using either Expectation Maximization (EM) algorithm or a Classification Expectation Maximization (CEM) when including a classification step. Since our model consists of two levels, it is natural to adopt a two-maximization step process for this parameter estimation. We would first use a complete log-likelihood as a maximization criterion for the estimation. Then a CEM algorithm is used since it includes a classification step that assigns each observation to its most probable cluster (rather than yielding a vector of membership probabilities, as in the classic EM). Finally, this algorithm would take three key inputs: user ID (comprising anonymized card ID, card type, transaction date and time, stop location, transport line, method of validation, and type of transaction), day of the week, and hour of validation (service hours only, with no break at midnight). Then it returns the associated cluster for each user, the Gaussian mixture parameters and the complete log-likelihood.

The disadvantages of the above model is mainly due to taking into account the days of the week, which could increase the number of clusters combinatorically, and the data used in McNichols (2010) for analysis are incomplete (lost or stolen cards do not keep the same ID when they are replaced). Furthermore, a dedicated model needs to be developed if we want to better understand the motivations behind the cards' cluster changes.

Single-level Time Dependent Path Flow Estimation Model

Time-dependent OD demand matrices are fundamental inputs for dynamic traffic assignment (DTA) models to describe network flow evolution as a result of interactions of individual travelers. Intending to develop an internally consistent approach for the dynamic OD demand estimation problem, single-level path flow estimators (PFEs) have been proposed for the static OD estimation problem (e.g., the linear programming PFE by estimating deterministic UE path flows, and the nonlinear programming PFE by estimating stochastic UE path flows). Inspired by those works, the authors in Ma, Smith, and Zhou (2016) present a new path flow-based optimization model and an effective Lagrangian relaxation-based solution framework for jointly solving the complex OD demand estimation and UE DTA problems. Their model simultaneously minimizes the deviation between measured and estimated traffic states, as well as the deviation between aggregated path flows and target OD flows, subject to a dynamic user equilibrium (DUE) constraint, which is reformulated using an equivalent gap function. The proposed Lagrangian relaxation-based algorithm dualizes the gap function-based DUE constraint into the objective function and solves the single-level relaxation problem by reducing the difference between

the upper and the lower bounds. This is different from the previous research, which developed column generation algorithms to solve the VI-based single-level model.

The nonlinear program is formulated as follows, where $DNLF(r)$ denotes the given DNL function of path flows proposed based on Newell's simplified KW model (see for more details).

$$\text{Min } Z = \beta_d \sum_w \left[\sum_{\tau \in H_d} \sum_p r(w, \tau, p) - \bar{d}(w) \right]^2 + \sum_{l \in S} \sum_{\tau \in H_0} \{ \beta_q [q(l, \tau) - \bar{q}(l, \tau)]^2 + \beta_k [k(l, \tau) - \bar{k}(l, \tau)]^2 \}$$

Subject to

$$\begin{aligned} (c, q, k) &= DNLF(r), \\ g(r, \pi) &= \sum_w \sum_{\tau} \sum_p \{ r(w, \tau, p) [c(w, \tau, p) - \pi(w, \tau)] \} = 0, \\ c(w, \tau, p) - \pi(w, \tau) &\geq 0 \forall w, \tau, p \\ \pi(w, \tau) &\geq 0 \forall p \in P(w, \tau) \forall w, \tau \\ r(w, \tau, p) &\geq 0 \\ r(w, \tau, p) &\geq 0 \forall w, \tau, p \end{aligned}$$

Set

A = set of links

P = set of paths

H_d = set of discretized departure time intervals

W = set of OD pairs

List of Indices

t = index of simulation time intervals ($t = 0, \dots, T$)

τ = index of departure time intervals ($\tau \in H_d$)

w = index of OD pairs ($w \in W$)

p = index of paths for each OD pair ($p \in P$)

l = index of links ($l \in A$)

Estimation Variables

$r(w, \tau, p)$ = estimated path flow on path p of OD pair w and departure time interval τ

$c = \{c(w, \tau, p) \forall w, \tau, p\}$ = estimated path travel time on path p of OD pair w and departure time interval τ

$\pi(w, \tau)$ = estimated least path travel time of OD pair w and departure time interval τ

$q = \{q(l, t) \forall l, t\}$ = estimated number of vehicles passing through an upstream detector on link l during observation interval t

$k = \{k(l, t) \forall l, t\}$ = estimated density on link l during observation interval t

$d(w, t)$ = estimated demand of OD pair w and departure time interval τ

The final solution is a set of path flows satisfying “tolled user equilibrium” (Lawphongpanich and Hearn, 2004), where the deviation with respect to traffic measurements can be viewed as an additional penalty for over-estimated or under-estimated path flows. By incorporating heterogeneous real-world measurements in the objective function, such as link densities from video surveillance and roadside detectors, the proposed estimation model fully uses available information to reflect route choices in a congestion network.

The main advantage of such formulation is that it could directly aggregate estimated path flows to obtain final OD flow patterns and obviate explicit dynamic link-path incidences, as opposed to the majority of previous studies. Moreover, the proposed OD demand estimate model circumvents the difficulty of providing complex mapping matrices between OD demand flows and those measurements in most of the existing dynamic OD demand estimation methods. However, the authors did not explore the generalization of their modeling framework into the problems of real-time traffic state estimation and prediction. This would require further investigation into numerous issues, such as calibrating the maximum queue discharge rates that critically affect flows on downstream links, and accommodating possible modeling errors and behavioral heterogeneity in the DUE assignment.

Bayesian Modeling for Large-Scale Dynamic Network Flow

The authors used internet browser traffic flow through domains of the Fox News website to present Bayesian analyses of two linked classes of models which allow fast, scalable, and interpretable Bayesian inference. Their strategy was as follows:

- Developed a class of Bayesian dynamic flow models (BDFMs), which are (non-stationary and non-normal) state-space models, for streaming count data to adaptively characterize and quantify network dynamics effectively and efficiently in real-time.
- Developed Poisson Dynamic Models and Multinomial Dynamic models for describing network inflows and transitions between network nodes, respectively.
- Used such efficiently implemented models as emulators of time-varying gravity models to allow closer and formal dissection of network dynamics.
- Yielded interpretable inferences on traffic flow characteristics and on dynamics in interactions among network nodes.

- Developed Bayesian model assessment methodology for sequential monitoring of flow patterns with the ability to signal departures from predictions in real-time and allow informed interventions as a response

Bayesian Dynamic Flow Models (BDFMs)

Given x_t is a time series with $x_t | \phi_t \sim P(m_t \phi_t)$ conditionally independent for $t = 1, 2, \dots$. Define ϕ_t is a latent process, m_t a scaling factor known at time t . Using Markov model, ϕ_t process appears as:

$$\phi_t = \phi_{t-1}^{\delta_t} \eta_t, \eta_t \sim B(\delta_t r_t, (1 - \delta_t) r_t), \eta_t \text{ and } \eta_s, \phi_s \text{ are independent for } s < t$$

where $\delta_t \in (0, 1)$ is a discount factor, r_t is a given function of t , $x_{0:t-1}$ and independent innovations $\eta_{\delta_t}^t$ drive the ϕ_t process's evolution. Note: The beta distributions imply (1) $E(\phi_t | \phi_{t-1}) = \phi_{t-1}$, thus it is a multiplicative random walk model (i.e., “steady” evolution), and (2) a lower value of δt leads to a more diffuse distribution for $\eta_{\delta t}$, and hence increased uncertainty about ϕ_t and adaptability to changing rates over time.

The BDFM above ensures full conjugacy in the forward filtering/Bayesian sequential learning over time. x_0 is a synthetic notation for initial information.

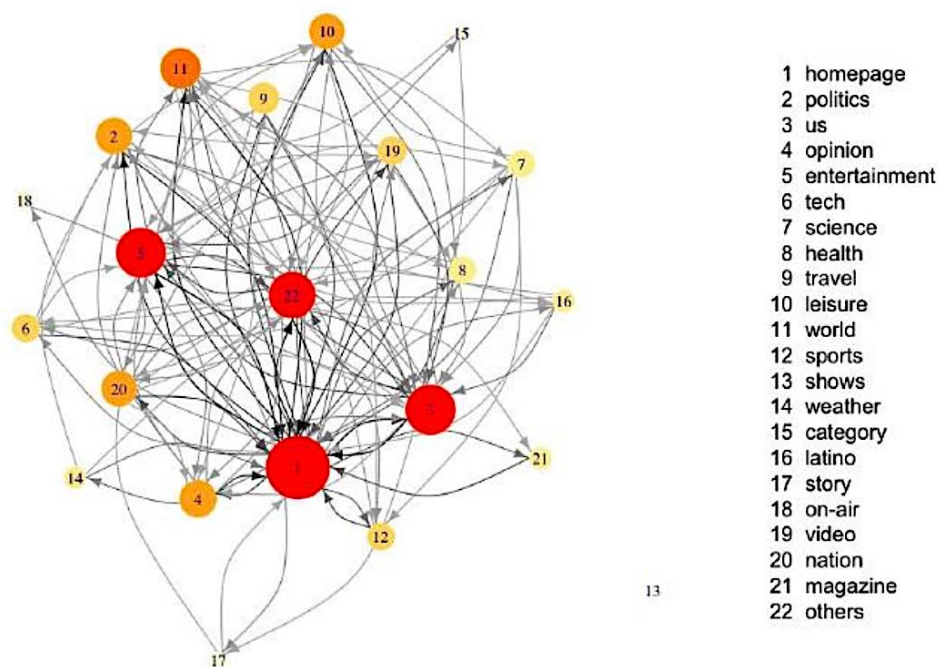


Figure 5-21 Snapshot of counts and flows on Fox News at time $t = 1$ (9:05:30 Feb 23, 2015)

- Forward Filtering (FF): At any time t , both the prior $p(\phi_t | x_{0:t-1})$ and posterior $p(\phi_t | x_{0:t})$ for “current” latent level are gamma distributions, with parameters that are updated as t evolves.

- One-Step Forecasts: The one-step ahead forecast distribution made at time $t - 1$ to predict time t is generalized negative binomial with p.d.f.

$$p(x_t | x_{0:t-1}, \delta_{t-1}) = \frac{\Gamma(\delta_{t-1}) \delta_{t-1}^{r_{t-1} + x_t}}{\Gamma(\delta_{t-1}) \Gamma(x_t + 1)} \frac{m_t^{x_t} (\delta_{t-1} c_{t-1})^{\delta_{t-1} r_{t-1}}}{(\delta_{t-1} c_{t-1} + m_t)^{\delta_{t-1} r_{t-1} + x_t}}$$

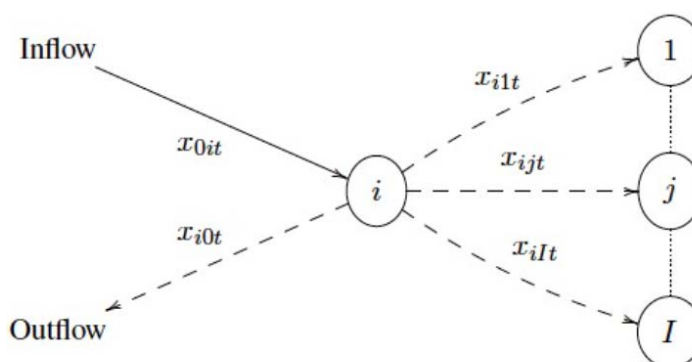


Figure 5-22 Network schematic and notation for flows at time t

The above model could be defined by any sequence of discount factors $\{\delta_t\}$. A constant value over time defines a global smoothing rate; values closer to 1 constrain the stochastic innovation and hence the change from ϕ_{t-1} to ϕ_t . Also, smaller discount factor values lead to greater random changes in these Poisson levels. Intervention to specify smaller discount factors at some time points, to reflect or anticipate higher levels of dynamic variation at those times, are sometimes relevant. In our network flow models below, we customize the specification of the sequence of discount factor to address issues that arise in cases of low flow levels. That extension of discount-based modeling defines the t as time-varying functions of an underlying base discount rate, and the latter are then evaluated using MML measures.

Network Inflows: Poisson Dynamic Models

Adding suffices i for network nodes and setting the Poisson mean scaling factors to 1, the authors customized this model via specification of discount factor sequences. At any node i , the time t inflow to node i is $x_{0it} \sim P(\phi_{it})$ independently across nodes $i = 1: I$, and the latent levels ϕ_{it} it follow node-specific gamma-beta discount models with discount factor δ_{it} at time t . The time $t \rightarrow t + 1$ update/evolve steps are as follows:

- Time t prior $\phi_{it} | x_{0i,0:t-1} \sim G(\delta_{it} r_{i,t}, \delta_{it} c_{i,t-1})$ updates to the posterior $\phi_{it} | x_{0i,0:t} \sim G(r_{it}, c_{it})$ with $r_{it} = \delta_{it} r_{i,t-1} + x_{0it}$ and $c_{it} = \delta_{it} c_{i,t-1} + 1$.
- This then evolves to the time $t + 1$ prior $\phi_{i,t+1} | x_{0i,0:t} \sim G(\delta_{i,t+1} r_{i,t}, \delta_{i,t+1} c_{it})$, and so on.

Discount factors δ_{it} relates to the information content of gamma distributions as measured by the shape parameters r_{i*} ; evolution each time point reduces this by discount factor, the latter representing a per-time-step decay of information induced by the stochastic evolution.

Node-specific MML measures that feed into model assessment to aid in selection of the baseline discount factors d_i : These measures of short-term predictive fit of the models can also be monitored sequentially over time for online tracking of model performance.

Transitions from Network Nodes: Multinomial Dynamic Models

Transitions from any node i at time t are inherently multinomial with time-varying transition probabilities. To build flexible and scalable models for dynamics and dependencies in transition probability vectors is a challenge, with computational issues for even simple models quickly dominating. The authors extended the univariate Poisson/gamma-beta random walk models to enable flexibility in modeling node-pair specific effects as they vary over time as well as scalability.

The core model is $x_{i,0:I,t} \sim Mn(n_{i,t-1}, \theta_{i,0:I,t})$, where the current node i occupancy level is $n_{i,t-1}$, and $\theta_{i,0:I,t}$ is the $(I + 1)$ -vector of transition probabilities θ_{ijt} (including the “external” node, leaving the network - at $j = 0$). The decoupled BDFMs include $x_{ijt} \sim P(m_{it}\phi_{ijt})$ and $m_{it} = n_{it}-1/n_{it}-2$ independently, with independent gamma-beta evolutions for each latent level ϕ_{ijt} .

These BDFMs for each node pair can be customized with node-pair specific discount factors, allowing greater or lesser degrees of variation by node pair. The set of models for elements of $\phi_{i,0:I,t}$ implies a dynamic model for the vector of transition probabilities $\theta_{i,0:I,t}$ having elements $\theta_{ijt} = \sum_j = \phi_{0:ij}^t \phi_{ijt}$. Independence across nodes enables scaling, as the analyses can then be decoupled and run in parallel for the ϕ_{ijt} and then recoupled to infer the θ_{ijt} .

Now, the decoupled, scaled models are not predictive of overall occupancy; rather, they are decoupled, tractable models that are relevant to tracking and short-term prediction of relative occupancy levels through the implied multinomial probabilities. In sequential analysis of transitions, the node-pair specific models generate full joint predictions one-step ahead (or more, if desired) for the theoretically exact set of multivariate flow vectors $x_{i,0:I,t}$ across all nodes.

Model Mapping for Bayesian Emulations of Dynamic Gravity Models (DGMs) by BDFMs

The DGM model is defined as within each network node $i = 1: I$ and all $j = 0: I$,

$$\phi_{ijt} = \mu_{ait}\beta_{jt}\gamma_{ijt}$$

with (i) a baseline process μ_t ; (ii) node i main effect process α_{it} , adjusting the baseline intensity of flows-origin or outflow parameter process for node i ; (iii) a node j main effect process β_{jt} ; representing the additional “attractiveness” of node j the destination or inflow parameter process for node j ; and (iv) an interaction term γ_{ijt} , representing the directional “affinity” of node i for j over time relative to the combined contributions of baseline and main effects.

The authors also commented that analysis via MCMC is computationally very demanding, and the burden increases quadratically in I , and inherently non-sequentially.

Now, the mapping to *DGM* parameters requires aliasing constraints to match dimensions, then define $h_t = \log(\mu_t)$, $a_{it} = \log(\alpha_{it})$, $b_{jt} = \log(\beta_{jt})$ and $g_{ijt} = \log(\gamma_{ijt})$. Using the $+$ notation to denote summation over the range of identified indices, constrain via $a_{+t} = b_{+t} = 0$, $g_{+jt} = g_{i+t} = 0$ for all i, j, t . We then have a bijective map between BDFM and DGM parameters; given the ϕ_{ijt} we can directly compute implied, identified DGM parameters. The emulating BDFM enforces smoothness over time in parameter process trajectories, and this acts to substantially reduce the effective model dimension.

Define $f_{ijt} = \log(\phi_{ijt})$ for each $i = 1: I$, $j = 0: I$ at each time $t = 1: T$. Then at each time t , we compute the following in order:

- Baseline level $u_t = e^{h_t}$ where $h_t = \sum_i (f_{i+}^{\pm} \pm 1^t)$
- For each $i = 1: I$, the origin node main effect $\alpha_{it} = e^{a_{it}}$ where $a_{it} = f_{i+}^{\pm} \pm 1^t - h_t$
- For each $j = 0: I$, the destination node main effect $\beta_{jt} = e^{b_{jt}}$ where $b_{jt} = f_{+j}^{\pm} \pm 1^t - h_t$
- For each $i = 1: I$ and $j = 0: I$, the affinity $\gamma_{ijt} = e^{g_{ijt}}$ where $g_{ijt} = f_{ijt} - h_t - a_{it} - b_{jt}$

The authors then apply this to all simulated ijt from the full posterior analysis under the BDFM to map to posteriors for the DGM parameter processes.

The disadvantage of this mapping approach arises in cases of sparse flows, i.e., when multiple x_{ijt} counts are zero or very small for multiple node pairs. In such cases the posterior for ϕ_{ijt} favors very small values and the log transforms are large and negative, which unduly impacts the resulting overall mean and/or origin or destination means. While one can imagine model extensions to address this, at a practical level it suffices to adjust the mapping as is typically done in related problems of log-linear models of contingency tables with structural zeros. This is implemented by simply restricting the summations in identifiability constraints to node pairs for which $x_{ijt} > d$, for some small d , and adjusting divisors to count the numbers of terms in each summation.

Bayesian Inference on Network Traffic Using Link Count Data

In Tebaldi and West (1998), the authors considered the fixed network of n nodes, arbitrarily labeled A, B, \dots , and solved the problem of estimating the actual counts of messages travelling between pairs of nodes in the network, based on observation of traffic counts on all individual directed links in the network without intervening nodes. Let r be the total number of directed links in the network, $s = (i, j)$ represent the directed link from node i to node j , and Y_s for the traffic count on this link.

Then, given an observed link counts $Y := (Y_1, \dots, Y_r)^T$, they inferred OD counts $X := (X_1, \dots, X_c)^T$. Using the relationship $Y = AX$ where $A = r \times c$ routing matrix $\{A_{s,a}\}$, $A_{s,a} = 1$ if the directed link s belongs to the directed route through the network between OD pair a , and $A_{s,a} = 0$ otherwise. From an algebraic perspective, Y imposes a set of linear constraint on X . Note that $(AA^T)_a, a$ counts the number of OD routes passing through link a , and $(AA^T)_{a,b}$ counts the number of routes that pass through both links a and b .

The authors attempted to compute the posterior distribution $p(X|Y)$ for all route counts X given the observed link counts Y . To solve this problem, they assumed X is generated from a collection of independent Poisson distributions for the elements X_a (i.e., $X_a \sim P(\lambda_a)$ independent over a). Then the prior joint model is $p(X, \Lambda) = p(\Lambda) \prod_{a=1}^c \lambda_a^{X_a} e^{-\lambda_a} / (X_a!)$. Now, to find the posterior $p(X, \Lambda | Y)$, they developed iterative MCMC simulation methods, in particular Gibbs sampling in which they iteratively resample from conditional posteriors for elements of the X and Λ variables.

Since $p(\Lambda | X, Y) \equiv p(\Lambda | X) = \prod_{a=1}^{c-1} p(\lambda_a | X^a)$ which has components of the form of prior density $p(\lambda_a)$ multiplied by the gamma form arising in the Poisson-based likelihood function. Thus, by conditioning on X , the authors simulated new Λ values as a set of independent draws from the implied univariate posteriors. For such simulation, they used embed Metropolis-Hasting step in the MCMC scheme. Finally, by fixing Λ , they deduced the posterior distribution $p(X | \Lambda, Y)$ with the constraints imposed on X by the equation $Y = AX$ using simulation in the MCMC scheme. To effectively simplify the computations for making this inference, they used the following result.

Theorem Assume A is full rank r . Then the columns of A can be reordered so that the revised routing matrix has the form $[A_1, A_2] = A$ where A_1 is a non-singular $r \times r$ matrix. Also, by reordering the elements of X vector and partition $X^T = (X_1^T, X_2^T)$, it follows $X_1 = A_1^{-1}(Y - A_2 X_2)$

Using this theorem, the conditional distribution $p(X | \Lambda, Y)$ is concentrated in a subspace of dimension $c - r$ defined by partition $[A_1, A_2] = A$ of the routing matrix A . This posterior has the form $p(X_1 | X_2, \Lambda, Y) p(X_2 | \Lambda, Y)$ where $p(X_1 | X_2, \Lambda, Y)$ is degenerate at $X_1 = A_1^{-1}(Y - A_2 X_2)$, and

$\lambda_{X_a}^{X_a}$ where with $X_2 = (X_{r+1}, \dots, X_c)^T$ defining $X_1 = (X_1, \dots, X_r)^T$ as earlier,
 $p(X_2 | \Lambda, Y) \propto \prod_{a=r+1}^c \frac{\lambda_a^{X_a}}{X_a!}$

$X_a \geq 0$ for all $a = 1, \dots, c$. This is the product of independent Poisson priors for the X_i constrained by the identity $Y = AX$ rewritten in the form $X_1 = A_1^{-1}(Y - A_2 X_2)$. Now, by considering each elements X_i of X_2 ($i = r + 1, \dots, c$) and write $X_{2,-i}$ for the remaining elements, the authors obtained the conditional distribution

$$p(X_i | X_{i-1}, \Lambda, Y) \propto \frac{\lambda_i^{X_i}}{X_i!} \prod_{a=1}^r \frac{\lambda_a^{X_a}}{X_a!}$$

where $X_i \geq 0$ and $X_a \geq 0$ for each $a = r + 1, \dots, c$ and $i = r + 1, \dots, c$.

Gibbs and Metropolis-Hastings Algorithms

Fix starting values of the route counts X and proceed as follows:

- Draw sampled values of the rates Λ from the c conditionally independent posteriors $p(\lambda_a | X_a)$.
- Conditioning on these values of Λ , simulate a new X vector by sequencing through $i = r + 1, \dots, c$ and at each step, sampling a new X_i from (14), with conditioning elements $X_{2,-i}$ set at their most recent sampled values; at each step X_i is explicitly reevaluated via $X_1 = A_1^{-1}(Y - A_2 X_2)$ as a function of the most recently sampled elements of X_2 .
- Return to step 1 and iterate.

This is a standard Gibbs sampling setup in which the scalar elements of both A and X are resampled from the relevant distribution conditional on most recently simulated values of all other uncertain quantities. Sampling steps in 1 are easy. Sampling steps in 2 require evaluation of the support of (14), and subsequent evaluation of the unnormalized posterior (14) at each step. Sampling may be performed directly, treating (14) as a simple multinomial distribution on this relevant range. But in larger, more realistic networks, the implied evaluation of (14) across what may be a very large support, at each iteration and for each element X_i , leads to a computational burden that may be excessive when compared to alternative approaches. To do this requires identifying the support of (14) which, as mentioned earlier, can become computationally very burdensome in net-works of even moderate size.

A more efficient algorithm is based on embedding Metropolis-Hastings steps within the Gibbs sampling framework. Specifically, assume a fixed proposal distribution with probability mass function $q_i(X_i)$ for each element X_i in step 2. A candidate value X_i^* is drawn from $q_i(\cdot)$ and accepted with probability

$$\min\left[1, \frac{p_i(X_i^*)q_i(X_i)}{p_i(X_i)q_i(X_i^*)}\right]$$

where X_i is the current, most recently sampled value and $p_i(\cdot)$ is the normalized conditional posterior in equation (14). From the structure of the network equations in (1), it is possible to identify bounds on each X_i so that a suitable range for proposal distribution can be computed. Then, based on the specified bounds, the implied vector X_1 in (14) is recomputed and checked for feasibility; that is, nonnegative values. If any element of X_1 is negative, then the trial value of X_a is either incremented, in searching for the lower bound on its range, or decremented, in searching for the upper bound. This process terminates and delivers the resulting bounds once the X_1 vector has r nonnegative entries.

Theoretical assurance that the MCMC algorithm so defined converges—that is, ultimately generates samples from the true joint posterior $p(X, \Lambda | Y)$ —follows if we can determine that the Markov chain is irreducible. This is equivalent to determine whether or not the current value (X, Λ) can “move” to any other point in the joint parameter space following a finite number of iterations of the scheme (1) and (2). For the elements of Λ , there is no problem, because of continuous priors with fixed support. But for the X , the support of the conditional posteriors (14) depends on resampled values of elements of X_2 and so it changes after each iteration. It can be shown, however, that in fact X_2 is free to move arbitrarily around its parameter space in consecutive iterations, despite the support constraints and complications. Thus, the resulting chain is irreducible, and convergence is assured.

Use-Case Problem

From now on, we denote the distribution for prior and likelihood as P_1 and P_2 , respectively. We then apply our Hierarchical Bayesian model demonstrated above with prior and likelihood following Normal distributions. In this particular case, we will use both Kalman-Filter (since the analytical solution exists in this case) and MCMC to obtain the posterior distribution for $d|d_h, A$. The sample network we consider comprises eight bus stops, where every two pairs are connected either directly or indirectly.

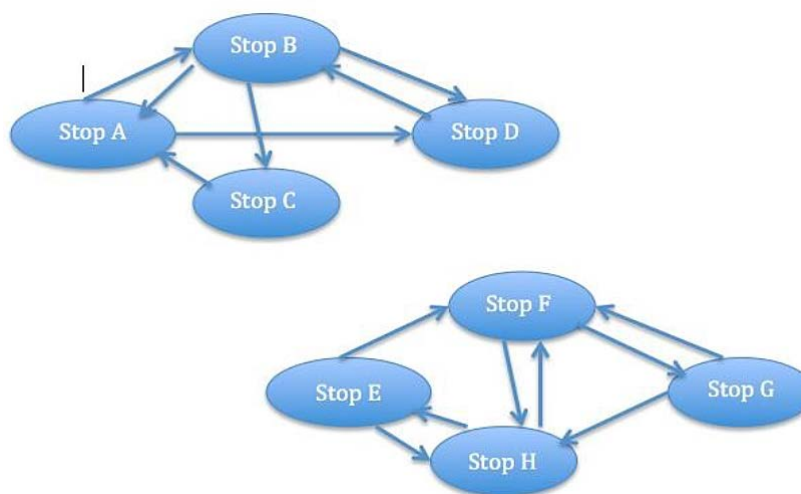


Figure 5-23 Sample network with eight bus stops

Denote set of bus stops as $I = A, B, C, D, E, F, G, H$, historical demand $d_h = (d_h)_{ij}$ where $i, j \in I$, and d_{ij} = demand from i to j . The true demand is denoted as vector $d = (d)_{ij}$. We now construct the routing matrix A using the following heuristic algorithm.

Routing Matrix Construction Heuristic Algorithm

Initialize a zero routing matrix A whose columns are labeled ij ($i \neq j$) if stops i and j are connected directly. Row i corresponds to the ON count at stop i . Set $(a_{ij})_{\text{row } i} = 1$.

Transitivity Rule 2.1. For any two columns (ij) and (jk) , add a new column ik to the end of the matrix. 2.2. If $(a_{jk})_{\text{row } i} = 1$ and $(a_{ki})_{\text{row } i} = 1$, set $(a_{ji})_{\text{row } i} = 1$.

Based on the heuristic algorithm above, and the structure of our sample network in Figure 2, we obtain the following routing matrix A .

Step 1. Fill out all entries $(a_{ij})_{\text{row } i} = 1$ for directly connected pairs of stop i and j .

$$H = \begin{matrix} (d_A)_{ON} \\ (d_B)_{ON} \\ (d_C)_{ON} \\ (d_D)_{ON} \\ (d_E)_{ON} \\ (d_F)_{ON} \\ (d_G)_{ON} \\ (d_H)_{ON} \end{matrix} \begin{bmatrix} AB & AD & BC & BD & BA & DB & CA & EF & EH & FG & FH & GF & GH & HE & HF \\ 1 & 1 & 0 & 0 & 0 & 0 & 0 & 0 & 0 & 0 & 0 & 0 & 0 & 0 & 0 \\ 0 & 0 & 1 & 1 & 1 & 0 & 0 & 0 & 0 & 0 & 0 & 0 & 0 & 0 & 0 \\ 0 & 0 & 0 & 0 & 0 & 0 & 1 & 0 & 0 & 0 & 0 & 0 & 0 & 0 & 0 \\ 0 & 0 & 0 & 0 & 0 & 0 & 0 & 1 & 1 & 0 & 0 & 0 & 0 & 0 & 0 \\ 0 & 0 & 0 & 0 & 0 & 0 & 0 & 0 & 0 & 1 & 1 & 0 & 0 & 0 & 0 \\ 0 & 0 & 0 & 0 & 1 & 1 & 0 & 0 & 0 & 0 & 0 & 1 & 1 & 0 & 0 \\ 0 & 0 & 0 & 0 & 0 & 0 & 0 & 0 & 0 & 0 & 0 & 0 & 0 & 1 & 1 \end{bmatrix}$$

Step 2. Apply Transitivity Rule to every row (note that H_i , denotes row i of matrix H).

$$A = \begin{array}{l} (d_A)_{ON} \\ (d_B)_{ON} \\ (d_C)_{ON} \\ (d_D)_{ON} \\ (d_E)_{ON} \\ (d_F)_{ON} \\ (d_G)_{ON} \\ (d_H)_{ON} \end{array} \begin{array}{l} \text{column labels of H} \\ H_1, \\ H_2, \\ H_3, \\ H_4, \\ H_5, \\ H_6, \\ H_7, \\ H_8, \end{array} \begin{array}{cccccccc} AC & DA & DC & CB & CD & EG & FE & GE & HG \\ \begin{bmatrix} 1 & 0 & 0 & 0 & 0 & 0 & 0 & 0 & 0 \\ 0 & 0 & 0 & 0 & 0 & 0 & 0 & 0 & 0 \\ 0 & 0 & 0 & 1 & 1 & 0 & 0 & 0 & 0 \\ 0 & 1 & 1 & 0 & 0 & 0 & 0 & 0 & 0 \\ 0 & 0 & 0 & 0 & 0 & 1 & 0 & 0 & 0 \\ 0 & 0 & 0 & 0 & 0 & 0 & 1 & 0 & 0 \\ 0 & 0 & 0 & 0 & 0 & 0 & 0 & 1 & 0 \\ 0 & 0 & 0 & 0 & 0 & 0 & 0 & 0 & 1 \end{bmatrix} \end{array}$$

Since the size of A is 8×16 , the size of estimated demand variable d has to be 16×1 . Each component of d must match with both the indices of column labels of A and the corresponding row of A (for example, the first three components of d must be d_{AB}, d_{AD} and d_{AC} because row 1 of A corresponds to $(d_A)_{ON}$).

Now, from our assumption, since prior and likelihood both follow Normal distributions, we have $P(x|d) \sim N(Ad, \sigma_1)$ and $P(d) \sim N(d_h, \sigma_2)$, where discrete $\sigma_1 \sim N(0,10)$, $\sigma_2 \sim N(0,5)$ (the range of these normal distributions are chosen depending on our expectation on how much deviated from the true demand is the historical demand, and how good is our estimated demand). Since this is a use-case example, we simulated discrete $x \sim U(400,600)$. Since the equation $Ad_h = x$ does not have any solution, we recovered d_h by solving for the solution d_h in the least-square sense by minimizing $\|Ad_h - x\|_2^2$. Using equation (1), we only need to compute the posterior distribution $p(x|d)p(d) = N(Ad, \sigma_1)N(d_h, \sigma_2)$. To compute this, we will show two following methods: first is Kalman-Filter and second is MCMC simulation. For the latter case, for the purpose of showing the flexibility of MCMC simulation compared to Kalman-Filter, we apply it to obtain the posterior distribution $P(d|x, d_h)$ even for the case when d_h is not available. Finally, we generate the histograms to show the distribution of each component of our estimated demand d obtained by MCMC simulation, and compare d to the simulated "true" demand d' , where $d' = d_h + \sigma_2$.

Kalman-Filter - Analytical Solution

Since we need to compute the distribution of $p(d|d_h, x) \propto p(x|d)p(d|d_h) \sim N(Ad, \sigma_1)N(d_h, \sigma_2)$, which results in another normal-distribution N , Kalman-Filter gives the following analytical formula to compute the mean d and co-variance matrix Σ , at a given time t ,

$$d_t := K(x_{t-1} - Ad_{t-1}) + (d_h)_{t-1}$$

Where,

$$= \sigma_2^2 A^T (A \sigma_2^2 A^T + \sigma_1^2)^{-1}$$

$$K \sum_{cov} := (I - KA) \sigma_2^2$$

and I is an identity matrix.

Using R to perform the matrix multiplications and subtractions to compute the term K and plugging it into the equations, we obtain the values for the mean and co-variance matrix of the posterior distribution $N(\bar{d}, \Sigma_{cov})$:

$$\bar{d} = [40.83 \quad 33.57 \quad 53.31 \quad 24.72 \quad 39.23 \quad 21.15 \quad 29.83 \quad 21.19$$

$$30.23 \quad 20.54 \quad 32.13 \quad 46.83 \quad 18.23 \quad 42.59 \quad 12.83 \quad 16.11]^T$$

$$\sum_{cov} = \begin{pmatrix} 1 & -0.79 & -0.43 & \dots & -0.10 & 0.02 \\ -0.79 & 1 & -0.60 & \dots & 0.024 & -0.016 \\ \vdots & \vdots & \vdots & \vdots & \vdots & \vdots \\ 0.023 & -0.016 & -0.05 & \dots & -1.32 & 1 \end{pmatrix}$$

MCMC Simulation – Numerical Solution

As shown above, we need to compute $p(d|d_h, x) \propto p(x|d)p(d|d_h) \sim N(Ad, \sigma_1) N(d_h, \sigma_2)$. Using Stan, which is the probabilistic modeling language for statistical inference with the simple interface with R, and "sampling()" package in R to perform MCMC simulation in two different scenarios.

Historical Demand (d_h) is Available

With this first scenario, we assume that currently observed OD flows are close to historically observed values. To simulate the values for these current OD flows, we add some noise term $\epsilon \sim N(0, 5)$ into our historical demand d_h to account for measurement errors and taking into account the historical OD flows. Using "sampling()" package in R, I perform MCMC to estimate the current OD flows with the 3 sample chains with 500 iterations for each chain in our MCMC simulation. The results obtained show a pretty close match between our estimated demand d vs. the simulated true demand, as reflected in Figure 5-24. Furthermore, we can generate the histograms for each component of the estimated demand d to observe the distribution of its components. The four histograms for the first four component of the estimated demand d is displayed in Figure 5-24.

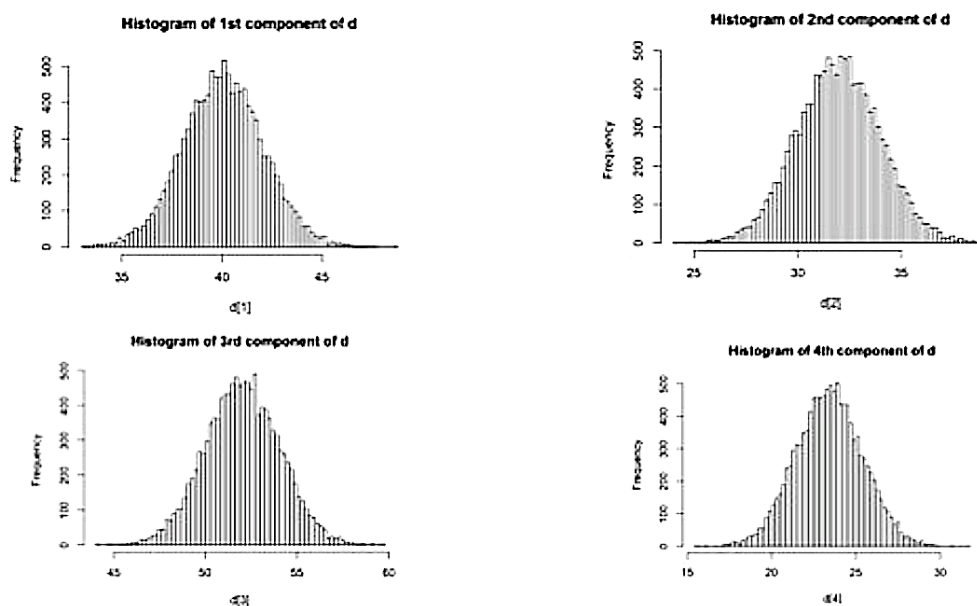


Figure 5-24 Distributions of first four components of true demand d

Finally, we compute the average of the third chains of MCMC simulation stored in a 3dimensional object in R to obtain the approximated mean value for each component of the obtained estimated demand \bar{d} :

$$\bar{d}_{MCMC} = [41.12 \ 34.22 \ 53.35 \ 24.96 \ 40.51 \ 22.75 \ 30.48 \ 22.15 \\ 31.33 \ 21.65 \ 32.09 \ 45.96 \ 19.09 \ 42.19 \ 12.93 \ 16.51]^T$$

We compare the mean \bar{d}_{MCMC} with the mean \bar{d} of Kalman-Filter by computing the L^2 norm error: $\|\bar{d}_{MCMC} - \bar{d}_{KF}\|_2^2 \approx 6.989$. This is sufficiently small because the true data d is discrete and in the order of hundreds, so the estimated demand obtained by MCMC is pretty accurate.

Historical Demand (d_h) is Unknown

With this second scenario, we assume that historical OD flows and currently observed ones are learned simultaneously (so d_h is not known anymore, but rather, we simulate $d_h \sim P(24, \lambda)$ where λ is drawn randomly 24 times from a uniform distribution $U(0,40)$). Adding some noise term $\epsilon \sim N(0, 5)$ into our historical demand \bar{d}_h to account for measurement errors and taking into account the historical OD flows, we estimate the current OD flows with MCMC (again, by using three sample chains with 500 iterations for each chain). The results obtained allowed generation of the histograms for displaying the distributions of the first four components of the estimated demand \bar{d} .

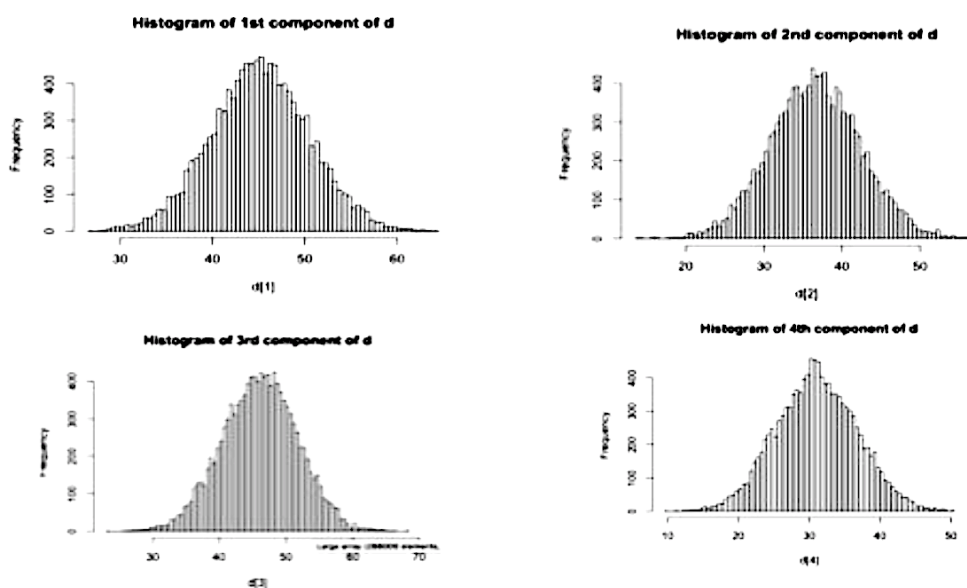


Figure 5-25 Distributions of first four components of true demand d

We then proceed exactly the same as in the first scenario and obtain the mean value of our estimated demand d :

$$\bar{d}_{MCMC} = \begin{bmatrix} 41.53 & 37.83 & 49.52 & 30.15 & 40.51 & 22.75 & 30.48 & 22.15 \\ 23.31 & 27.55 & 23.90 & 41.69 & 20.91 & 24.25 & 11.23 & 19.15 \end{bmatrix}^T$$

We then compare the mean d obtained by MCMC with the mean d_{KF} , and obtain the L^2 - norm error $\|d_{MCMC} - d_{KF}\|_2^2 \approx 9.2$. This is sufficiently small because the simulated true demand data are of the order of hundreds.

Heatmap Analysis for APC and Ventra Datasets

Using the ggmap package in R, we generated several heat maps for the average and total APC "ON" and "OFF" per hours of a day, days of a week, and days of a month to gain a better understanding about the spatial locations where people can travel with PACE buses within Northwest region of Chicago (note that the APC dataset contains only buses starting from one garage located in the Northwest region of Chicago). We observed the following results.

The heat map of average APC OFF per hours of day shows that most people, on average, get off at a few common sub-regions at each hour of the day, whereas that of average APC ON (also per hours of day) has no heat at almost every hour except at 4:00 am; the heat location at 4:00 am has longitude $\in (-87.9, -87.8)$ and latitude $\in (41.9, 42.0)$. This implies that, on average, at each hour of a day, the origins of most bus trips spread out all over the place, while the destinations of those trips concentrate on just a few sub-regions—for example, between 5:00-7:00 am, most people get off at the rectangle regions with longitude $\in (-88, -87.7)$ and latitude $\in (41.9, 42)$.

The heat map of average APC OFF per each day in the month of October also concentrates on a few sub-regions—those with longitudes $\in (-87.9, -87.7)$ and latitudes $\in (42.1, 42.2)$ or $(41.9, 42.0)$, and that of average APC ON per each day in October also concentrates on particular sub-regions with longitude $\in (-88, -87.7)$ and latitude $\in (41.9, -42)$. This means that, on average, during each day of the month, people get on at bus stops within a particular sub-region and also get off at either the same or another specific sub-region.

The heat map of average APC OFF per every days of a week except Sunday concentrates on a particular sub-regions with longitude $\in (-87.9, -87.7)$ and latitude $\in (41.9, 42.0)$, and that of average APC ON (per the corresponding days) also concentrates on that same particular regions. This means that, on average, people travel short trips most of the day and start and end the trip at the same sub-region (but the exact locations are different). On Sunday, though, the travel pattern changes, and most people start at the same sub-region as the previous days, but they mostly get off at the sub-region with longitude $\in (-87.9, -87.8)$ and latitude $\in (42.1, 42.2)$.

All three previous arguments also applied to total APC ON and OFF per day-to-day, hour-to-hour, and week-to-week variations, but the sub-regions changed.

Finally, we examined two other aspects of this October 2015 dataset: first is the heatmap of total and average APC ON and OFF (based on different time variations) to observe if there are any popular zone-level departures and destinations for the majority of bus riders. Second is the total APC ON per route per day of week to see the usage of bus riders with respect to individual routes and detect whether any route is taken much less compared to other routes (so that managers can re-route the bus to avoid this route or to assign fewer buses to cover this route due to the low demand from bus riders).

Heat map of Total APC ON per day of week

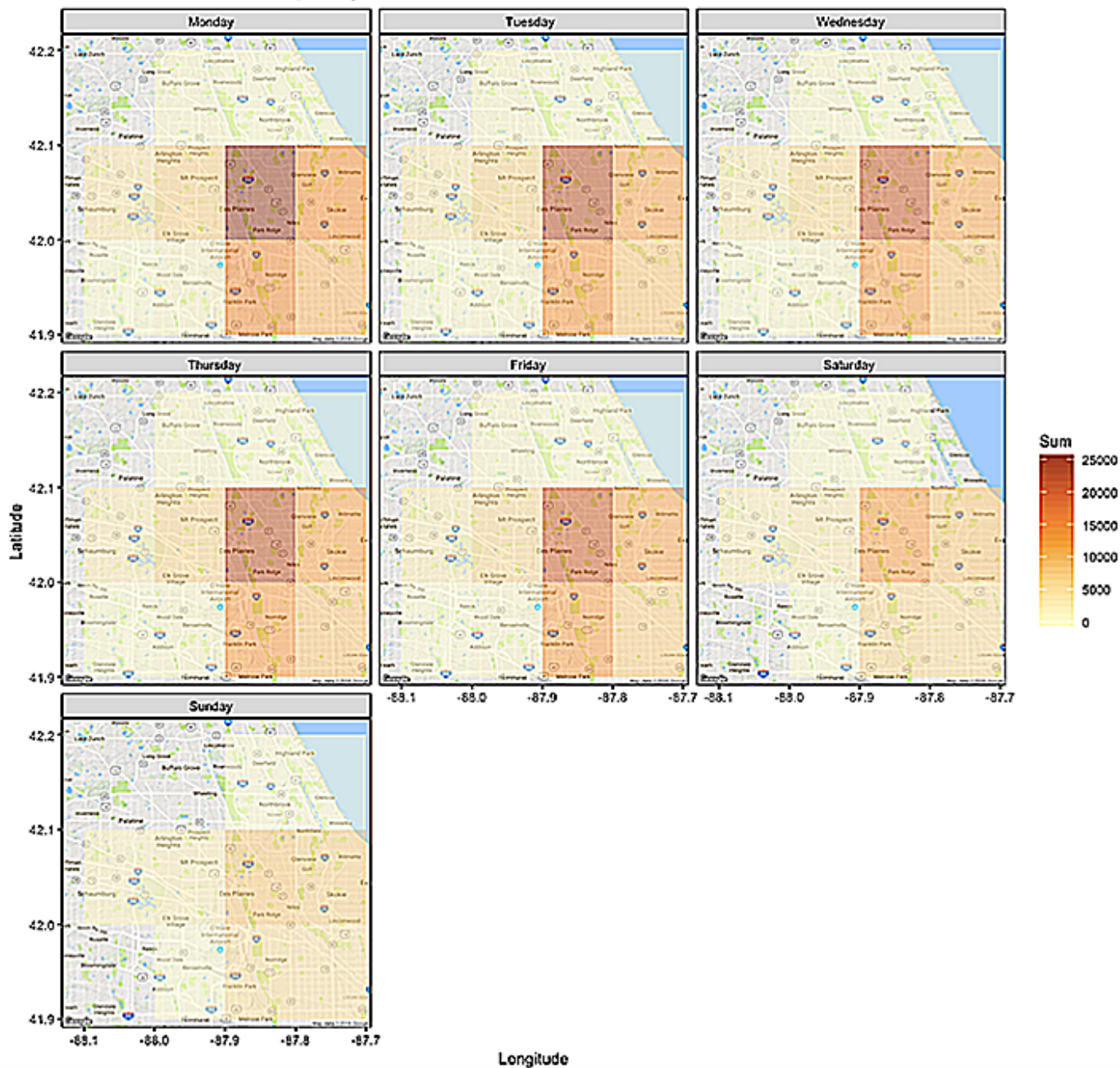


Figure 5-26 Geographical heat map of APCs for boarding PACE buses per day of week in October 2016

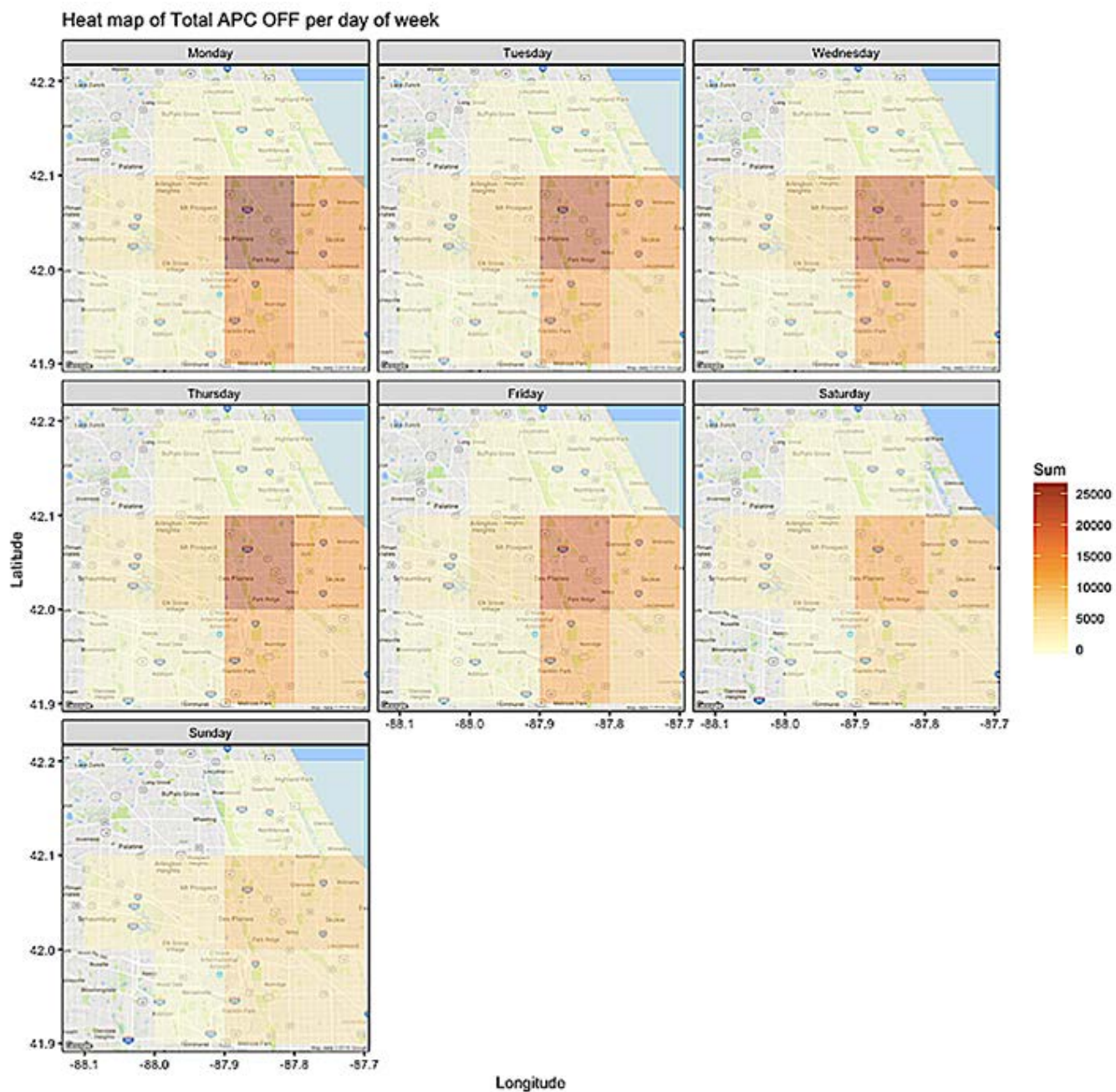


Figure 5-27 Geographical heat map of APCs for alighting from PACE buses per day of week in October 2016

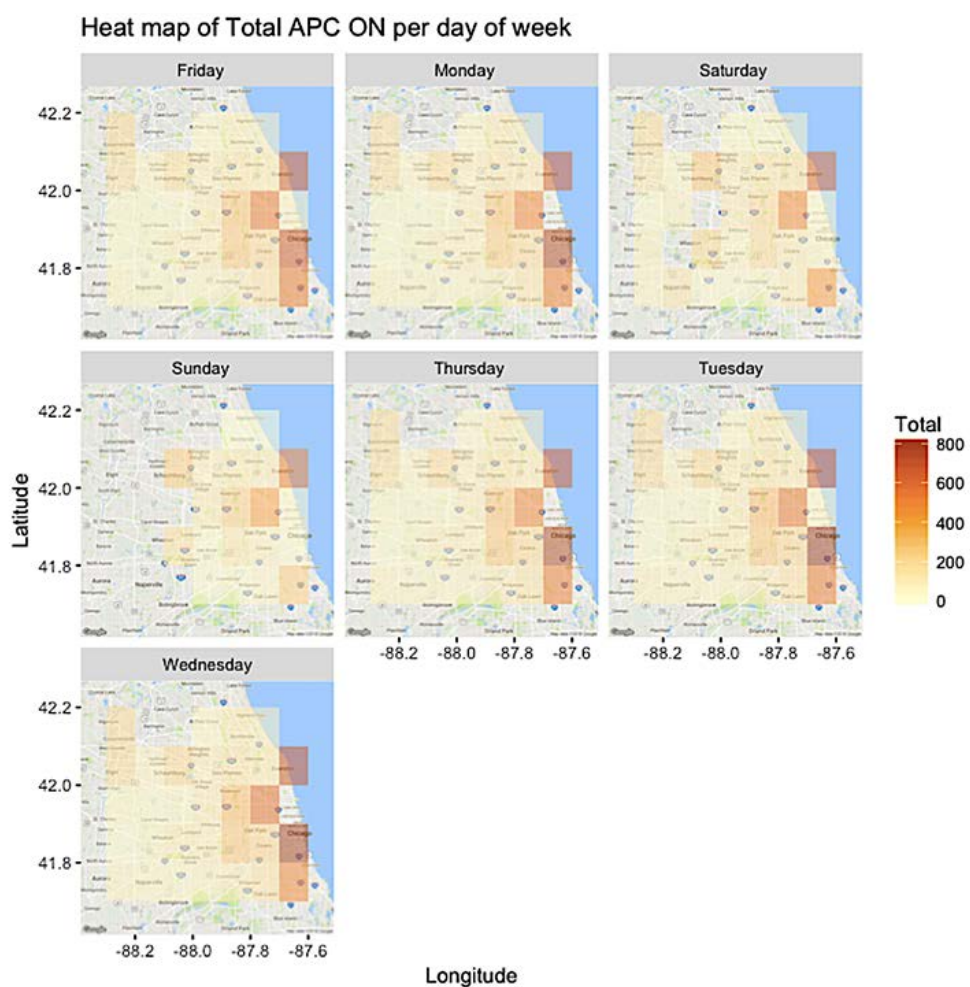


Figure 5-28 Geographical heat map of APCs for boarding PACE buses per day of week in 2015

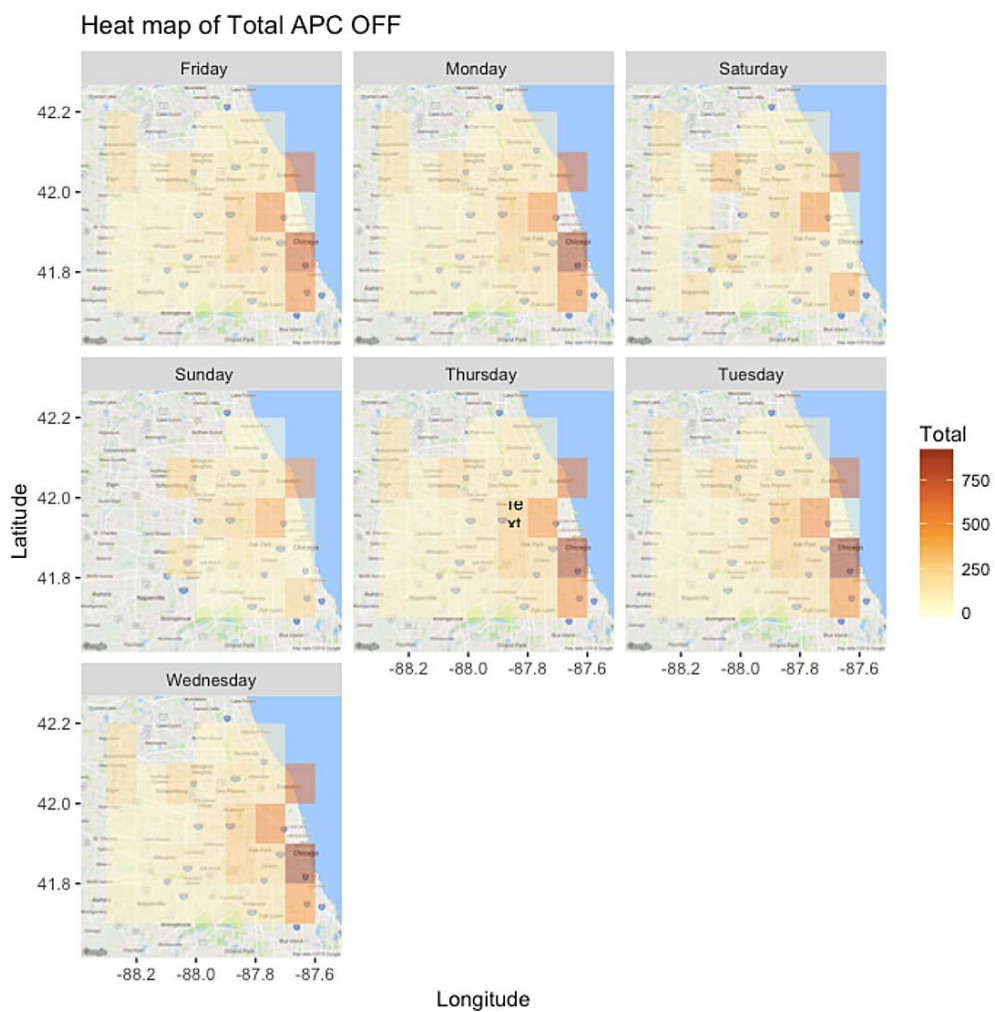


Figure 5-29 Geographical heat map of APCs for alighting from PACE buses per day of week in 2015

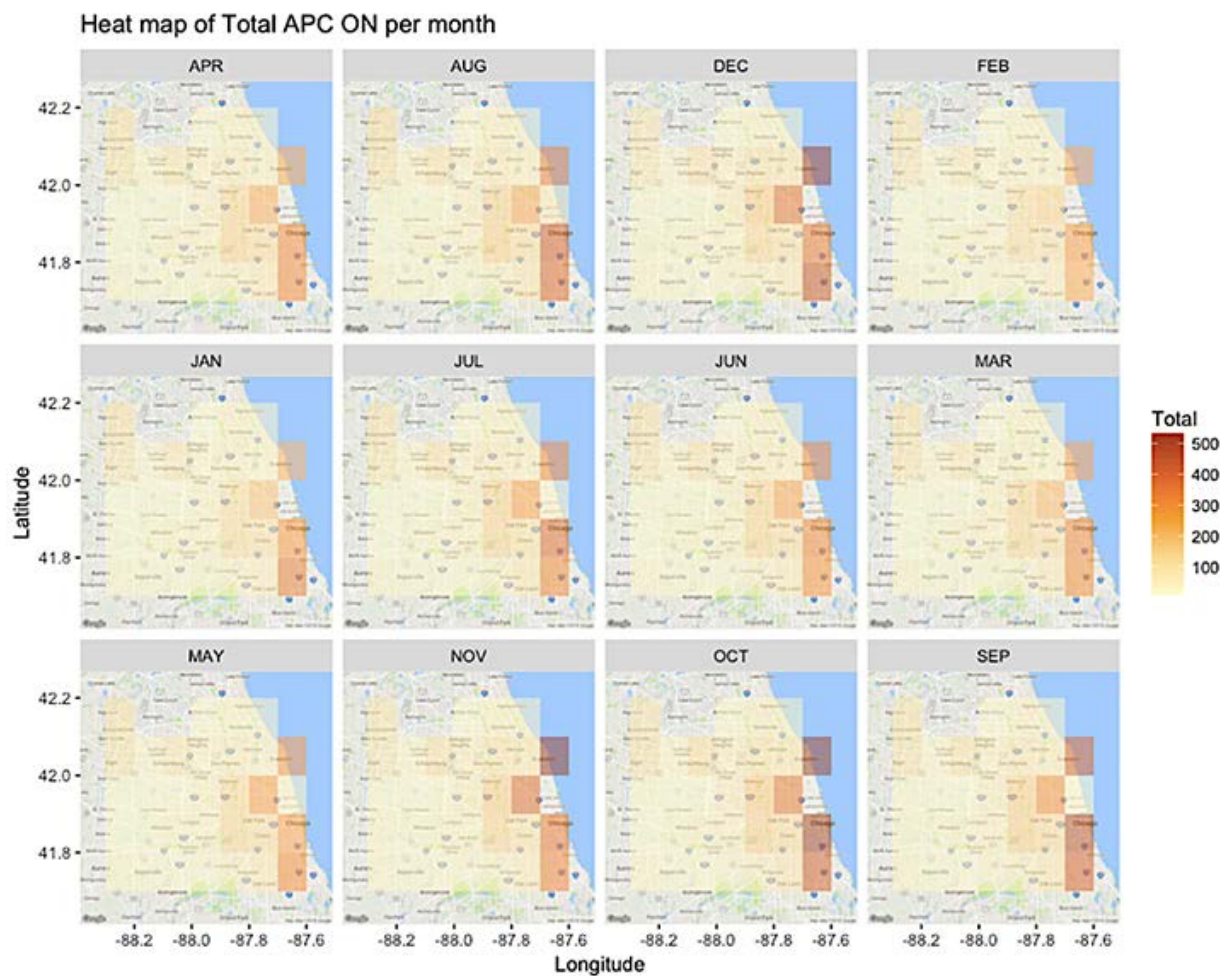


Figure 5-30 Geographical heat map of APCs for boarding PACE buses per month in October 2015

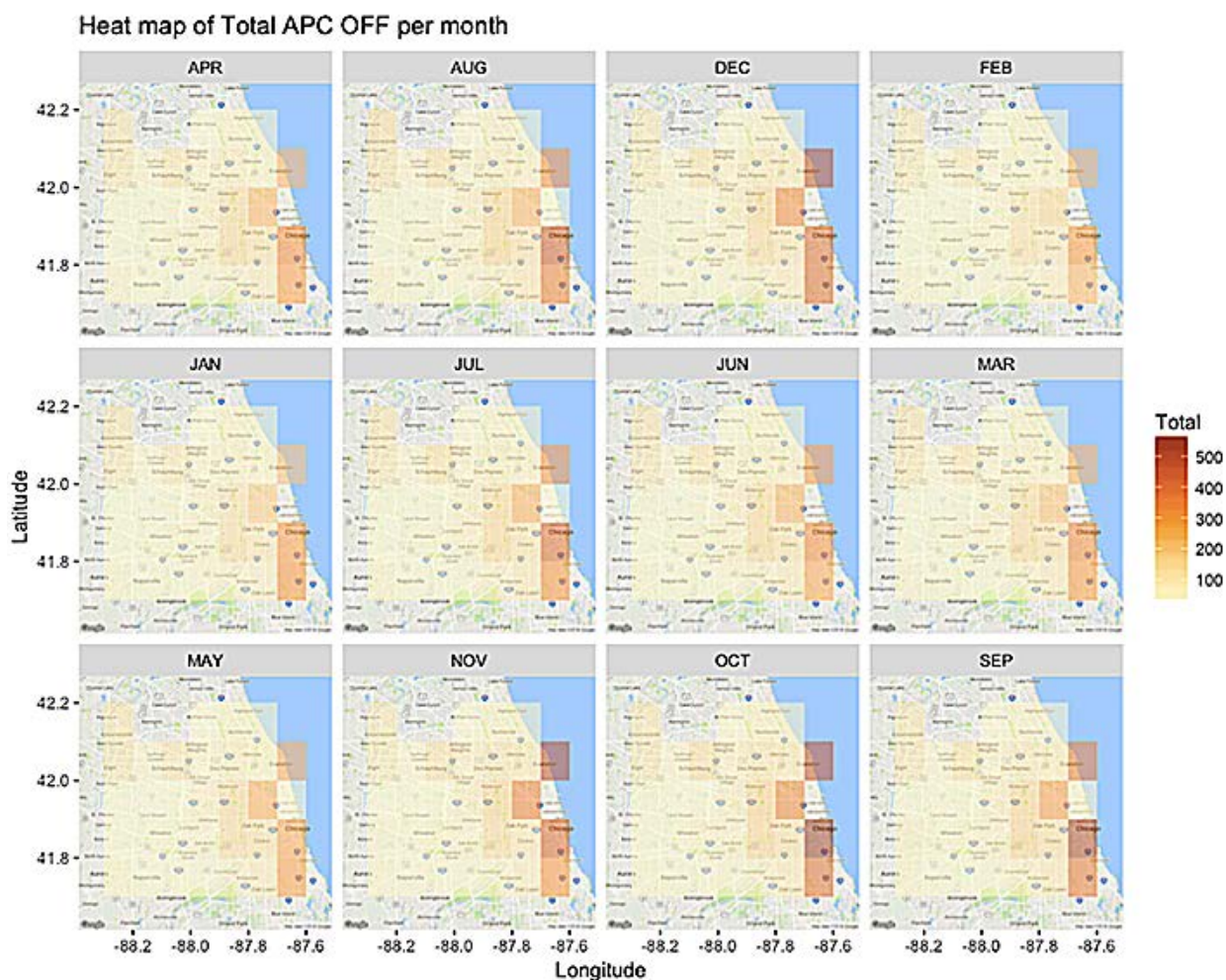


Figure 5-31 Geographical heat map of APCs for alighting from PACE buses per month in October 2015

Now, the heatmap of total APC ON and OFF (Automatic Passenger Counters for Boarding and Alighting) per days of week shows that most riders actually depart at the same regions with lat x lon in $[42.0, 42.1] \times [-87.7, -87.6]$ across the entire week. The fact that the same region has the highest number of people getting on/off the bus stops implies that bus riders departed at the same place but went to different places for arrivals and then all went back to the same location by bus. This aligns with PACE’s mission of mainly serving students, workers, and citizens to workplace, school, and public places. The total APC ON and OFF across different months also shows the same region in $[42.0, 42.1] \times [-87.7, -87.6]$, except during the January–March where another region in $[41.7, 41.8] \times [-87.7, -87.6]$ has more people get on and off. But once again, this region is the most common departure and arrival of bus riders, which confirms our observations for the total APC ON/OFF (see Figures 5-26 through 5-31). In regard to the total and average APC ON per route per days of week, route 769 was used only on Thursday and Sunday, with a total of only 170 riders using

this route compared to the most crowded route, 714, which has more than 50,000 riders per week. This is in contrast to the average APC ON per route, as the peak of average APC ON of route 769 is 17 on Thursday, compared to only 0.1 of route 714. This is mainly because the number of times riders take route 714 is more than 100 times greater than route 769, which skew the average number substantially (see Figures 5-32 through 5-35). In general, the total APC ON distributed per route across days of a week do not seem to follow a general distribution.

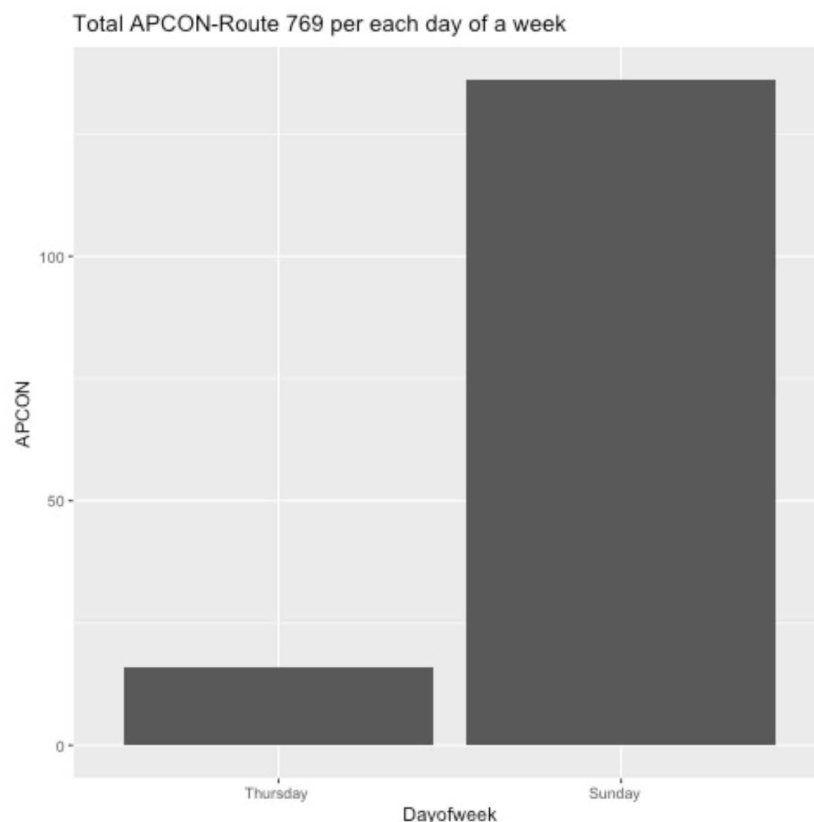


Figure 5-32 Aggregated APC values for boarding buses on Route 769 per each day of week (Tuesday and Thursday service only)

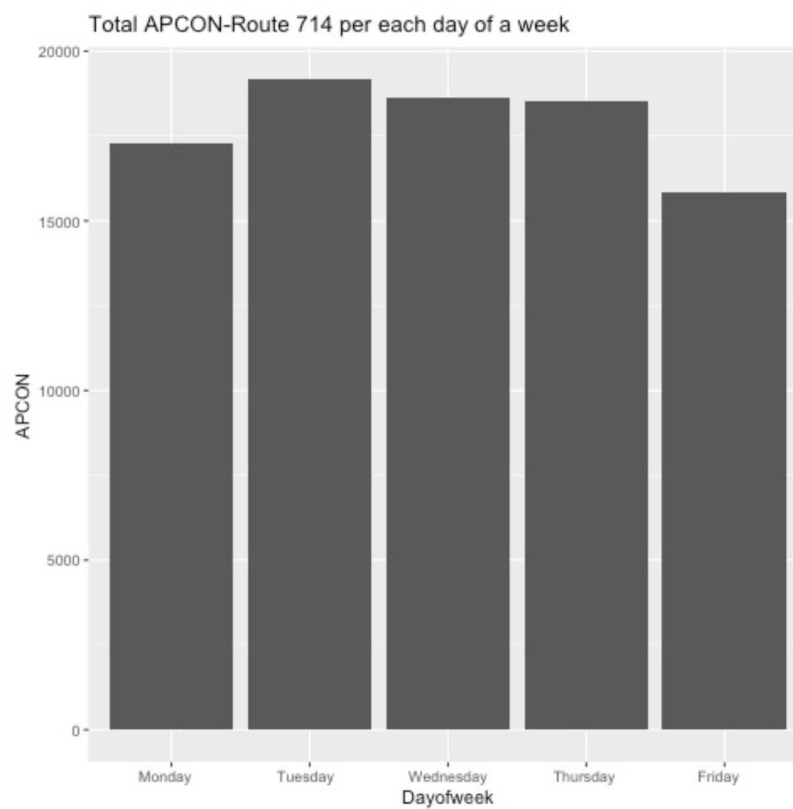


Figure 5-33 Aggregated APC values for boarding buses on Route 714 per each day of week

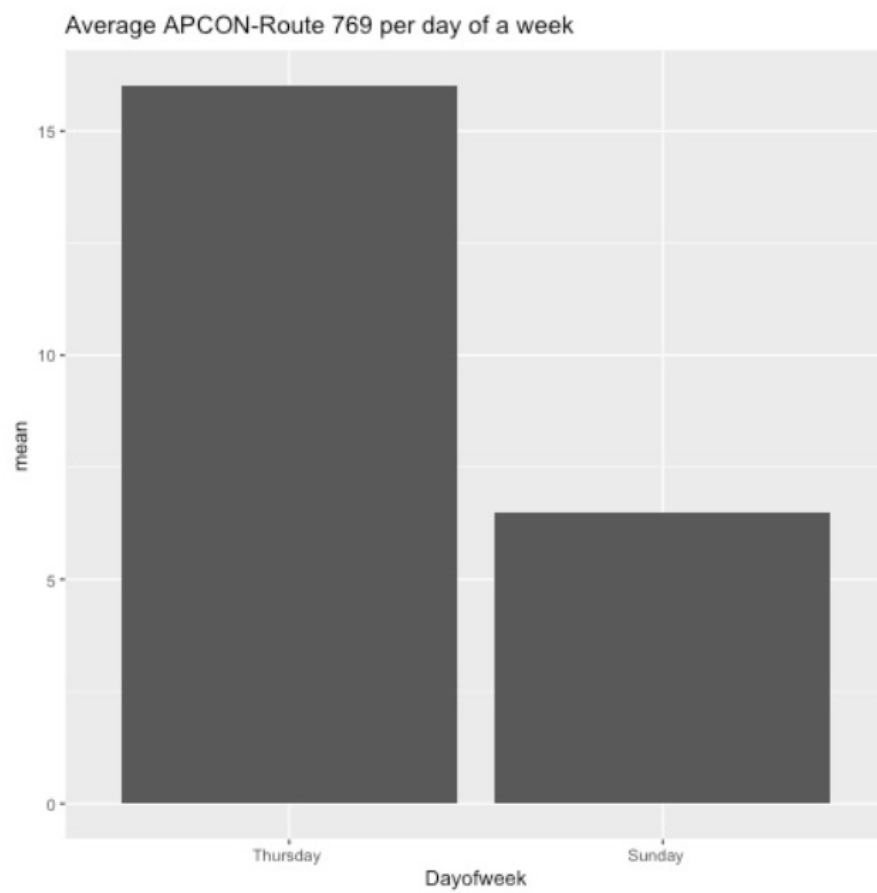


Figure 5-34 Mean APC values for boarding buses on Route 769 per each day of week (Tuesday and Thursday service only)

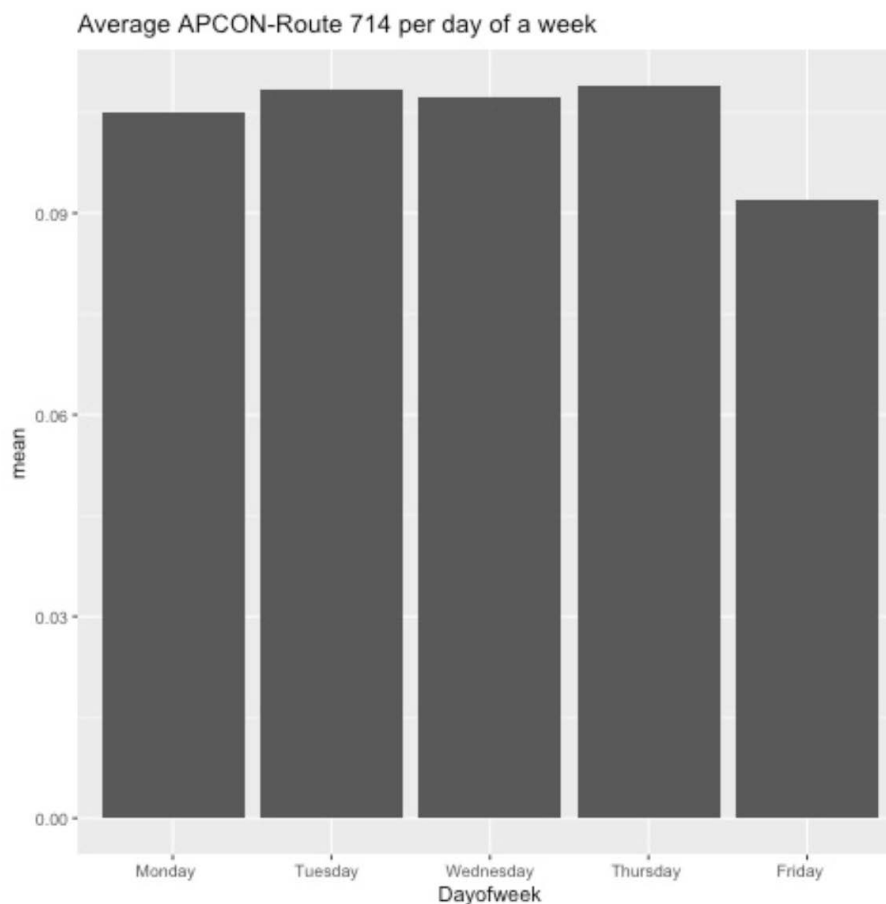


Figure 5-35 Mean APC values for boarding buses on Route 714 per each day of week

Using the bar plot function, we plotted histograms for the distributions of the aggregated number of different transaction types of riders when using the bus services across the month of March and across different hours of a day to examine when bus service is the most useful means compared to other alternative options. Counting through the list of transaction status ("Success," "Pass First Use," or "No Payment") for each transaction, we observed that in the distribution of daily trip types in March, 82% among 404,643 total riders who use Ventra's fare card in March had to re-charge the card before trying it again or paid the fare with Ventra's application on a smartphone. Such transactions were classified as "No Payment" in the "Trans-status" column. The distribution of the average number of transactions for each of the three statuses per day in March also showed a clear domination of a "No Payment" transaction, while the other two categories were equal. These results imply that a majority of riders are frequent riders, but either are too busy to care about the remaining balance on their cards or they all switch to Ventra's app on a smartphone for convenience (i.e., no need to carry Ventra card with them every time they travel). In addition, the distribution of the average number of transactions per each transaction

type per different hours of a day also show the same pattern: the majority of transaction types were classified as "No Payment" and a very small percentage of people used Ventra cards for the first time during March 2016, as evidenced through the small number of "Pass First Use" transaction status. Finally, to avoid potential biases from observing trends of only average data, we also plotted the bar plots for the distribution of total number transactions per each transaction type per each day of a month and each hour of a day to examine whether the same pattern observed from the bar plots of the average number of transactions repeated for this type of aggregated data. Indeed, the same pattern still held for the types of riders and their habits when using PACE's bus service.

We applied the same analysis to the trip types data to know how efficient PACE's bus service is in serving local commuters by examining whether a majority of riders were using PACE buses for multi-ride or single-ride trips to aid the inference on the purpose of each individual trip. To do this, we plotted the histograms for the total and average number of trips per each trip type to observe their distributions and how they vary daily and hourly. Although the average number of trips per each trip type were approximately distributed in the ratio of 2: 1 for single-ride (sum of trip type labeled "0" and "2" on the histograms) to multi-ride trip per hours of a day and per days of March, the total number of trips per each trip type showed a completely different pattern—the majority of riders opted for trip type labeled "2," which is a single-ride trip, especially at 7:00 am, which is the usual time where most people get to work, and at 5:00 pm, the time people go home. An extremely small number of riders had transfer between buses, which were labeled as "1". Gathering all the above insights, we concluded that the majority of riders opted for single-ride trips during March 2016 and very few opted for transfer-trips. This implies that riders mostly use PACE buses as a means for commuting between home and work but rarely for other activities such as grocery, laundry, shopping, etc. Finally, by using the ggmap library, we also generated a heat map for trip types and transaction types to observe more clearly their flows geographically.

Finally, using the ggmap package in R, we generated several heat maps for the average and total "ON" count per hour of a day, day of a month (i.e., March 2016), and day of a week to gain a better understanding about the spatial locations where people can travel by using PACE buses around Chicago (note that the Ventra dataset contains all buses from 9 garages across Chicago). We observed the following results.

The heat map of average "ON" count per hours of a day shows that only a few people (between 2 and 4), on average, get off at locations scattered across the region with lat x lon $\approx [41.6, 42.2] \times [-88.4, -87.5]$ at any hours between 5:00 am and 9:00 pm. Only in the very early morning (12:00– 4:00 am and 10:00–11:00 pm), the locations for those people getting off are narrower, mostly

concentrated in region with lat x lon $\approx [41.6,42.0] \times [-88.0,-87.5]$. In addition, the heat map almost shows heat scattered all over the places in the region with lat x lon $\approx [41.6,42.2] \times [-88.4,-87.5]$, and very little heat in regions with lat x lon $\approx [42.0,42.2] \times [-87.8,-87.75]$ and $[41.7,41.8] \times [-87.65,-87.7]$. We also examined the heat map of total "ON" count per hours of a day to verify if the same pattern persists. We realized that the total number of people travel during the early morning (from 12:00–5:00 am) is the smallest (between 1000 and 2000 people). Starting at 6:00 am, much greater heat appears over some separate sub-regions. The peak of the "heat" (between 4000 and 6000 people) was at 7:00 am, and it occurred at three sub-regions with lat x lon $\approx [41.7,41.8] \times [-88.2,-88.1]$, $[41.8,41.9] \times [-87.9,-87.7]$ and $\approx [42.0,42.1] \times [-88.0,-87.9]$. This implies that even though the average distribution does not show heat over those regions, there was a huge number of people traveling to particular locations at three distinct hours—7:00 am, 3:00 pm, and 4:00 pm. Since these hours tend to correspond to the time when people get to and from work/school, this might be the main reason for the source of our heat map. At other times, many fewer people travel, and they travel to many different places scattered across the Northern part of Chicago.

The heat map of average "ON" count per each day of March 2016 has the heat on different sub-regions on each day (for example, on 03/15, the heat region was lat x lon $\approx [-87.7,-87.6] \times [41.8,41.9]$ whereas on 03/28, the heat region was $\approx [-87.7,-87.6] \times [41.7,41.8]$). However, the heat map of total "ON" count per each day of March shows the heat, whose peak was around 1000, coming from a unique sub-regions with lat x lon $\approx [-87.9,-87.8] \times [42.0,42.1]$ over every days of March except on the four Sundays when there were no heat (03/06, 03/13, 03/20 and 03/27). This means there was a large number (i.e., 1000 or so) of riders getting on a fixed-route every day except Sunday, and their destinations were concentrated into a unique sub-region in the Northwest direction of Chicago.

The heat map of average "ON" count per days of a week shows a uniform distribution of the heat source over the weekday (Monday–Friday), with the heat region $\approx [-88.3,-87.8] \times [42.0,42.4]$, but different heat regions with lat x lon $\approx [-88.3,-87.8] \times [42.0,42.4]$ and $[-88.1,-88.0] \times [42.0,42.1]$ were shown on the weekend. This means that, on average, riders travel to the same location during a weekday (most likely for going to work), and only travel to other locations for other activities during weekend. The heat map of total "ON" count per days of a week show the same pattern (with different sub-regions whose lat x lon $\approx [-87.9,-87.8] \times [42.0,42.1]$) and $\approx [-87.9,-87.8] \times [42.3,42.4]$). This implies people use PACE bus mainly during the weekday, and this intuitively makes sense: on weekdays, they would need to go to work, so the locations where the heat sources were during those days are most likely that of their work office. On the weekend, they probably prefer using alternative services for better convenience and flexible in time.

Differences between APC and Ventra Datasets

Even though APC and Cubic's Ventra datasets all contain information about bus trips and number of riders on/off at each stop, they are quite different in many aspects based on how they were collected. First, since APC data were recorded from two main sources—information stored on a card swiped by each on-boarding customer and the two sensors attached to the doors of each bus for the number of passengers getting off at each bus stop. However, certain problems could arise; for example, some cash transactions might be missed, or some buses may have either the sensors or the machine might malfunction at certain time periods where the data was collected. This means the APC ON and/or OFF data are quite noisy, which explains the motivation to develop a Bayesian-based forecasting model. In addition, due to the regulation requirements on the fairness of distributing buses to everyone regardless of their gender, income, and social status, no buses were assigned the same route on two successive days. For this reason, the individual APC ON/OFF data recorded were not quite meaningful and, thus, categorizing the entire APC dataset based on different route numbers was the most reasonable choice. Finally, the number of categories of the APC dataset was quite large (81 different categories), as all buses come from all nine garages across Illinois, and the number of observations was around 69.4 million, representing the entire year of 2015, which was quite sufficient for conducting the data analysis.

On the other hand, collaborators at PACE were able to obtain Cubic's Ventra dataset by extracting the information recorded on the Ventra cards tapped by on-boarding customers. This resulted in missing a number of customers getting off at each bus stop. However, there are several advantages of this dataset compared to the APC dataset: first, the APC ON has much less noise and 100% coverage. Second, it includes buses coming from different garages across Chicago (rather than from only one garage), so many areas not covered earlier in the APC dataset were covered in this dataset. Third, it has much larger number of qualitative categories for each observation (88 total) but with only 184,318 observations. Fourth, all buses covered do not encounter the same situation that occurs in the APC dataset; that is, in the Ventra dataset the same bus could be assigned to the same route on two successive days. With these advantages, we expected to have a better data visualization on the flow of people across the entire city of Chicago (unlike the case of the APC dataset where the results were valid only in the Northwest region). However, there are two disadvantages of the Ventra dataset compared to APC dataset. First, the data were recorded only every 30 seconds, which means that riders might get on at different positions, but correspond to the same bus stops. So it was necessary to prepare the data by aggregating across the number of counts whose recorded locations, evidenced through latitude and longitude, were actually closest to the same bus stop. Second, in the column "Transaction Status," approximately 83.4% of the transaction with "No Payment" status were labeled as "Success" in another

"Transaction Status2" column and resulted in additional "ON" counts. Thus, the total "ON" count might be exaggerated by a large margin, but this means we must delete a significant amount of the current dataset to circumvent this problem. After removing all rows containing all data points with that transaction status, the total number of observations of the Ventra dataset was 67,083, an 83.4% decrease from the original size of the Ventra dataset. We then plotted the histograms to observe if there was any change to the above conclusion on the distributions of the "ON "count per hour of a day, days of a week, and days of a month in the new Ventra dataset. Fortunately, only the three histograms for the average "ON" count changed from non-uniform distribution to completely uniform distribution (which makes sense, as each successful transaction status equals to one count), while those for the total "ON" counts did not change its pattern (only the actual total counts changed, which is obvious).

Integer Programming Model for Bus Vehicle Routing Problem for Emergency Response⁶

Introduction

This section presents an integer programming (IP) model for the bus vehicle routing problem for emergency response in a transportation network. Specifically, under an emergency event, this IP model can be used to design an optimal bus systems by selecting best vehicle routes and schedules (i.e., patterns and trips) such that allowing impacted passengers (i.e., travel requests) to board and dwell at available stops along an optimized bus trip as well as to transfer between different buses to their final destination.

Definitions

To describe the problem in the section, following are the key concepts, as illustrated in Figure 6.1:

- **Route** is a set of bus stops that a bus vehicle can pickup and drop-off passengers.
- **Pattern** is a predefined sequence of bus stops for a bus vehicle to travel in the system; usually, a route can have several patterns to satisfy travel demands in the network under different scenarios.
- **Trip** is time schedule of a single journey made by a bus vehicle between two end points (i.e., stops) of a specific pattern; a trip must go through each bus stops in a route in the order defined in a specific pattern.
- **Request** is a tuple with six elements including identity (i.e., ID), number of passengers, origin and destination stops, and desired departure time window of the request; all passengers in a request should be picked up and dropped off as an unseparated group.

As each bus trip must follow a specific pattern, a bus trip may not travel from directly from a request's origin stop to its destination stop. Therefore, a travel request may need to transfer from one bus trip to another bus trip. Due to passengers not preferring to have many transfers from their origin to destination, the upper limit for the number of transfer time must be specified as a predefined number. To account for the transfer problem, we decomposed the original request into a sequence of sub-requests, as in Figure 6.2. The definition of a sub-request is as follows:

⁶ Authored by Kuilin Zhang and Qinjie Lyu, MTU.

- **Sub-request** is a tuple with four elements related to the original request. The elements include the request identity (i.e., ID) of the original request, the order index of the request in the original request, the origin and destination stops.

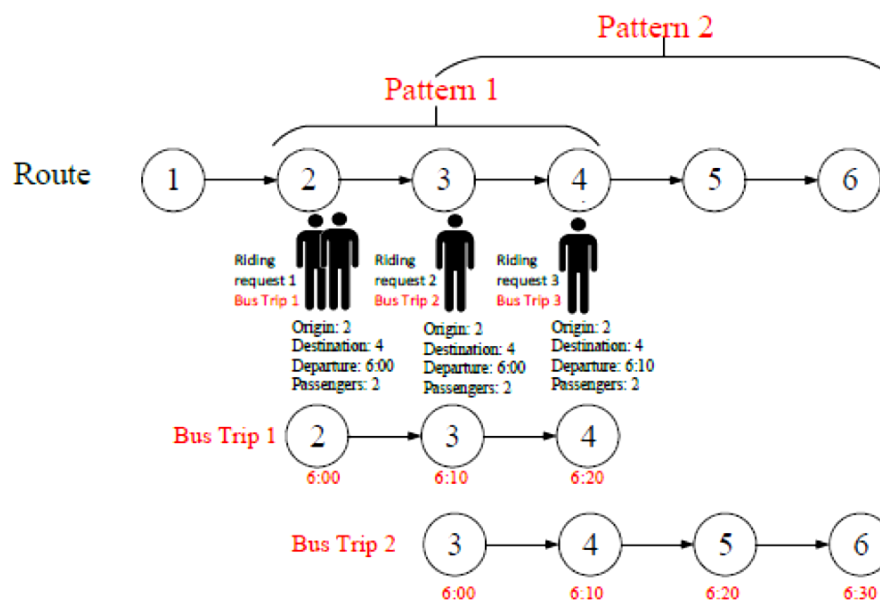


Figure 6-1 Concepts of route, pattern, trip

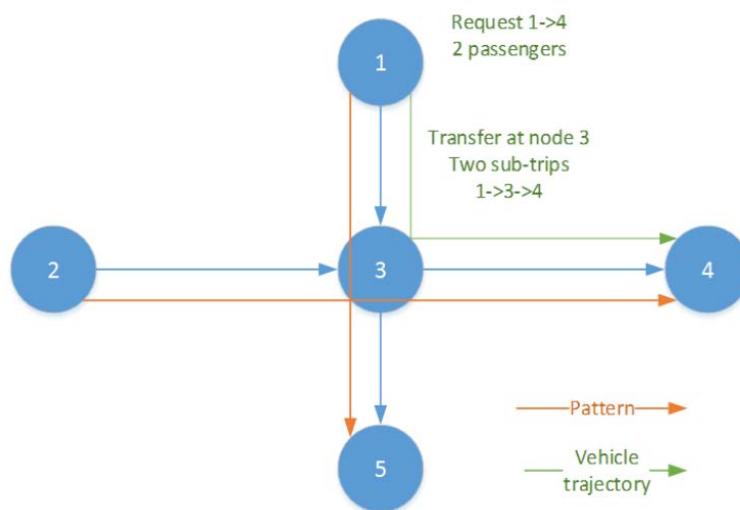


Figure 6-2 Illustration of sub-request

Notation Set

\mathcal{A} : Set of links in the transportation system

\mathcal{P} : Set of patterns in the transportation system

\mathcal{T} : Set of available bus trips in the transportation system

\mathcal{S} : Set of bus stops in the transportation system

\mathcal{Q} : Set of travel requests

Data:

S : Number of bus stops

P : Number of patterns

Q : Number of travel requests

T : Number of bus trips

V : Number of bus vehicles

L : Maximum time period

C : Capacity of a bus trip

K : Maximum number of transfers for a travel request

$l(p, i, j)$: Stops connectivity from stop i to stop j in pattern p

$p_o(p)$: Origin stop of each pattern

$p_d(p)$: Destination stop of each pattern

$q_o(q)$: Origin stop of each request

$q_d(q)$: Destination stop of each request

$q_a(q)$: The earliest time for each request q to be picked up

$q_l(q)$: The latest time for request q to be picked up

$q_n(q)$: The number of passengers in a request q

$c(i, j)$: travel cost in the network from stop i to stop j

$tt(i, j)$: travel time in the network from stop i to stop j

$d(i)$: Service time at a stop i

Decision Variables:

$x(t, p)$: Binary decision variable of trip t 's choice of pattern p

$w(t, q, k, i, j)$: Binary decision variable of whether trip t takes the k th sub-request of request q and travels from stop i to stop j .

$y(t, i)$: The time schedule for a trip t arrive stop i .

$z(t, i)$: Number of passengers on the trip t after stop i .

$r(q, k, i)$: Binary decision variable of whether the k th sub-request of request q is originated from stop i .

$v(q, k, i)$: Binary decision variable of the action (i.e., get on or get off) of the k th sub-request of request q at stop i .

$u(t, q, k)$: Binary decision variable of whether k th sub-request of request q takes bus trip t .

Problem Statement

Given a transportation network $G(\mathcal{N}, \mathcal{A})$, we consider a set of bus trips and patterns need to be selected to be used in a bus transit system to pick up and/or drop off a set of travel requests \mathcal{Q} during a time period L . Each request q in \mathcal{Q} consists of request identity (i.e., ID) q , origin bus stop $qo(q)$, destination bus stop $qd(q)$, the earliest time $qa(q)$ to be picked up, the latest time $qb(q)$ to be picked up, and the number of passenger $qn(q)$. A pattern p is a predefined sequence of stops for a vehicle to travel one stop by one stop. Each bus trip t should follow a specific pattern and can only pick up the request at the stops in the pattern p . In order to make sure all travel requests could be transferred to their final destinations, the travel requests are allowed to transfer between bus trips. To allow the transfer between one bus trip to another, each request q will be divided into several sub-requests, each sub-request (q, k) can be directly picked up from its origin to its destination by a single bus trip t . For each sub-request, the time window is the same as its original request. The number of passengers in the sub-request is the same as the original request.

When an extreme event occurs and results in several disrupted stops in the transportation network, the impacted bus trips have to be rescheduled to satisfy the impacted travel demand. The objective is to optimize the adjustment of scheduling and routing (i.e., bus trip and patterns) in the bus transit system to minimize the total cost of all bus trips while avoiding reaching the disrupted stops and satisfying all the travel requests.

Assumptions are as follows.

- Assumption 1 – The network constructed by all patterns is connected, which means there is a path between any two stops.
- Assumption 2 – A sub-request cannot be further divided to smaller requests, which means that all the passengers in the sub-request should be picked up or dropped off at the same time.
- Assumption 3 – A bus trip can pick up and drop off travel requests at each stop along its route.

Model Formulation

The objective of this model is to minimize the total travel costs of all bus trips, which is defined as in Eq. (1):

$$\mathbf{f} = \sum_{t \in \mathcal{T}} \sum_{p \in \mathcal{P}} \sum_{i \in \mathcal{S}} \sum_{j \in \mathcal{S}} \mathbf{c}(i, j) * \mathbf{x}(t, p) * \mathbf{l}(t, i, j) \quad (1)$$

Where $c(i, j)$ is the travel cost between stop i and stop j .

We have the following constraints to ensure the optimal patterns and trips can satisfy the impacted travel requests.

The first sub-request must depart from request q 's origin stop.

$$\mathbf{r}(\mathbf{q}, \mathbf{1}, \mathbf{q}_o(\mathbf{q})) = \mathbf{1}, \forall \mathbf{q} \in \mathcal{Q} \quad (2)$$

The first sub-request must depart from request q 's origin stop.

$$\mathbf{r}(\mathbf{q}, \mathbf{1}, \mathbf{i}) = \mathbf{0}, \forall \mathbf{i} \in \mathcal{S}, \mathbf{q} \in \mathcal{Q}, \mathbf{i} \neq \mathbf{q}_o(\mathbf{q}) \quad (3)$$

The last sub-request must arrive at the request q 's destination stop.

$$\sum_{\mathbf{k}=1}^{\mathbf{K}} \mathbf{r}(\mathbf{q}, \mathbf{k} + \mathbf{1}, \mathbf{q}_d(\mathbf{q})) = \mathbf{1}, \forall \mathbf{q} \in \mathcal{Q} \quad (4)$$

The sub-requests can take no more than one stop as its origin or destination stop.

$$\sum_{\mathbf{k}=1}^{\mathbf{K}+1} \mathbf{r}(\mathbf{q}, \mathbf{k}, \mathbf{i}) \leq \mathbf{1} \quad (5)$$

The previous sub-request must arrive the origin stop of the subsequent sub-request.

$$\sum_{\mathbf{i} \in \mathcal{S}} \mathbf{r}(\mathbf{q}, \mathbf{k} + \mathbf{1}, \mathbf{i}) \leq \sum_{\mathbf{i} \in \mathcal{S}} \mathbf{r}(\mathbf{q}, \mathbf{k}, \mathbf{i}) \quad (6)$$

If a sub-request arrives the request q 's destination stop, then there is no subsequent sub-request.

$$\sum_{\mathbf{i} \in \mathcal{S}} \mathbf{r}(\mathbf{q}, \mathbf{k} + \mathbf{1}, \mathbf{i}) = \mathbf{1} - \mathbf{r}(\mathbf{q}, \mathbf{k}, \mathbf{q}_d(\mathbf{q})) \quad (7)$$

If stop i is the origin stop of sub-request (q, k) , $v(q, k, i) = 1$, if stop i is the destination stop of sub-request (q, k) , $v(q, k, i) = -1$, otherwise $v(q, k, i) = 0$

$$\mathbf{v}(\mathbf{q}, \mathbf{k}, \mathbf{i}) = \mathbf{r}(\mathbf{q}, \mathbf{k}, \mathbf{i}) - \mathbf{r}(\mathbf{q}, \mathbf{k} + \mathbf{1}, \mathbf{i}), \forall \mathbf{i} \in \mathcal{S}, \mathbf{i} \neq \mathbf{q}_d(\mathbf{q}) \quad (8)$$

$$\mathbf{v}(\mathbf{q}, \mathbf{k}, \mathbf{q}_d(\mathbf{q})) = -\mathbf{r}(\mathbf{q}, \mathbf{k} + \mathbf{1}, \mathbf{q}_d(\mathbf{q})) \quad (9)$$

A trip can only use one pattern.

$$\sum_{\mathbf{p} \in \mathcal{P}} \mathbf{x}(\mathbf{t}, \mathbf{p}) \leq \mathbf{1}, \forall \mathbf{t} \in \mathcal{T} \quad (10)$$

If one trip cannot travel from stop i to stop j , then the sub-request (q, k) cannot travel from stop i to stop j .

$$\mathbf{w}(\mathbf{t}, \mathbf{q}, \mathbf{k}, \mathbf{i}, \mathbf{j}) \leq \sum_{\mathbf{p} \in \mathcal{P}} \mathbf{x}(\mathbf{t}, \mathbf{p}) * \mathbf{l}(\mathbf{p}, \mathbf{i}, \mathbf{j}) \quad (11)$$

If a sub-request depart, then it must start from a stop i except the q 's destination stop.

$$\sum_{\mathbf{t} \in \mathcal{T}} \mathbf{u}(\mathbf{t}, \mathbf{q}, \mathbf{k}) = \sum_{\substack{\mathbf{i} \in \mathcal{S}, \mathbf{i} \neq \mathbf{q}_d(\mathbf{q}) \\ \mathbf{i} \in [1, \mathbf{K}]}} \mathbf{r}(\mathbf{q}, \mathbf{k}, \mathbf{i}), \forall \mathbf{q} \in \mathcal{Q}, \mathbf{k} \in [1, \mathbf{K}] \quad (12)$$

If a sub-request (q, k) does not depart, then (q, k) will not take any trip.

$$\left(\sum_{\mathbf{i} \in \mathcal{S}} \sum_{\mathbf{j} \in \mathcal{S}} \mathbf{w}(\mathbf{t}, \mathbf{q}, \mathbf{k}, \mathbf{i}, \mathbf{j}) - \mathbf{s} \right) * \mathbf{u}(\mathbf{t}, \mathbf{q}, \mathbf{k}) \leq \mathbf{0}, \forall \mathbf{t} \in \mathcal{T}, \mathbf{q} \in \mathcal{Q}, \mathbf{k} \in [1, \mathbf{K}] \quad (13)$$

No request will go out from the stop i if it is the destination of a sub-trip,

$$\sum_{\mathbf{j} \in \mathcal{S}} \mathbf{w}(\mathbf{t}, \mathbf{q}, \mathbf{k}, \mathbf{i}, \mathbf{j}) * \mathbf{u}(\mathbf{t}, \mathbf{q}, \mathbf{k}) * \mathbf{r}(\mathbf{q}, \mathbf{k} + \mathbf{1}, \mathbf{i}) = \mathbf{0}, \forall \mathbf{t} \in \mathcal{T}, \mathbf{q} \in \mathcal{Q}, \mathbf{k} \in [1, \mathbf{K}], \mathbf{i} \in \mathcal{S} \quad (14)$$

The sub-request (q, k) will go into the link i if it is the destination of a sub-trip.

$$\sum_{\mathbf{j} \in \mathcal{S}} \mathbf{w}(\mathbf{t}, \mathbf{q}, \mathbf{k}, \mathbf{j}, \mathbf{i}) * \mathbf{u}(\mathbf{t}, \mathbf{q}, \mathbf{k}) * \mathbf{r}(\mathbf{q}, \mathbf{k} + \mathbf{1}, \mathbf{i}) = \mathbf{1}, \forall \mathbf{t} \in \mathcal{T}, \mathbf{q} \in \mathcal{Q}, \mathbf{k} \in [1, \mathbf{K}], \mathbf{i} \in \mathcal{S} \quad (15)$$

The sub-request (q, k) will not go out from link i if it is the destination of a sub-trip.

$$\left(\sum_{\mathbf{j} \in \mathcal{S}} \mathbf{w}(\mathbf{t}, \mathbf{q}, \mathbf{k}, \mathbf{i}, \mathbf{j}) - \sum_{\mathbf{j} \in \mathcal{S}} \mathbf{w}(\mathbf{t}, \mathbf{q}, \mathbf{k}, \mathbf{j}, \mathbf{i}) - \mathbf{v}(\mathbf{q}, \mathbf{k}, \mathbf{i}) \right) * \mathbf{u}(\mathbf{t}, \mathbf{q}, \mathbf{k}) = \mathbf{0}, \forall \mathbf{t} \in \mathcal{T}, \mathbf{q} \in \mathcal{Q}, \mathbf{k} \in [1, \mathbf{K}], \mathbf{i} \in \mathcal{S} \quad (16)$$

If a sub-request (q, k) could take trip t traveling from stop i to stop j , then the time when trip t arrives stop i must be before the time when trip t arrives stop j .

$$\left(\mathbf{y}(\mathbf{t}, \mathbf{i}) + \mathbf{d}(\mathbf{i}) + \mathbf{t}(\mathbf{i}, \mathbf{j}) \right) * \mathbf{w}(\mathbf{t}, \mathbf{p}, \mathbf{k}, \mathbf{i}, \mathbf{j}) \leq \mathbf{y}(\mathbf{t}, \mathbf{j}), \forall \mathbf{t} \in \mathcal{T}, \mathbf{i} \in \mathcal{S}, \mathbf{j} \in \mathcal{S}, \mathbf{i} \neq \mathbf{j}, \mathbf{p} \in \mathcal{P}, \mathbf{k} \in [1, \mathbf{K}] \quad (17)$$

If a sub-request (q, k) could take trip t traveling from stop i to stop j , the time when a trip t arrives the node i should after the lower bound of the request's desired pick-up time.

$$y(t, i) * \sum_{\substack{j \in \mathcal{S} \\ \in \mathcal{S}, q \in \mathcal{Q}, k \in [1, K]}} w(t, q, k, i, j) \geq q_a(q), \forall t \in \mathcal{T}, i \quad (18)$$

If a sub-request (q, k) could take trip t traveling from stop i to stop j , the time when a trip t arrives the node i should before the upper bound of the request's desired pick-up time.

$$y(t, i) * \sum_{\substack{j \in \mathcal{S} \\ i \in \mathcal{S}, q \in \mathcal{Q}, k \in [1, K]}} w(t, q, k, i, j) \leq q_b(q), \forall t \in \mathcal{T}, \quad (19)$$

The number of passengers on a trip t should not exceed the capacity of the trip.

$$z(t, i) \leq C(t), \forall t \in \mathcal{T}, i \in \mathcal{S} \quad (20)$$

If a trip t departs, then the number of passengers taken by this trip after the destination of the pattern chosen by this trip should be 0.

$$z(t, p_d(p)) \leq C(t) * (1 - x(t, p)), \forall t \in \mathcal{T}, p \in \mathcal{P} \quad (21)$$

The number of passengers on a trip t after arriving a stop i could be expressed by w as follows.

$$z(t, i) = \sum_q \sum_k \sum_j q_n(q) * w(t, q, k, i, j), \forall t \in \mathcal{T}, q \in \mathcal{Q}, k \in [1, K], i \in \mathcal{S}, j \in \mathcal{S} \quad (22)$$

Model Reformulation

In the model formulation, constraints (13)–(19) are nonlinear constraints. To solve the problem using existing off-the-shelf solvers, we reformulate those nonlinear constraints to linear constraints. The reformulated model is an integer linear program, which can be solved by existing solvers. This section presents all the reformulations and corresponding proofs of equivalence.

Reformulation of Constraint (13)

The constraint (13) is a classical if-else constraint, so it could be replaced by the following constraints.

$$\sum_{i \in \mathcal{S}} \sum_{j \in \mathcal{S}} \mathbf{w}(t, \mathbf{q}, \mathbf{k}, i, j) \leq S * \mathbf{u}(t, \mathbf{q}, \mathbf{k}), \forall t \in \mathcal{T}, \mathbf{q} \in \mathcal{Q}, \mathbf{k} \in [1, \mathbf{K}] \quad (23)$$

$$\sum_{i \in \mathcal{S}} \sum_{j \in \mathcal{S}} \mathbf{w}(t, \mathbf{q}, \mathbf{k}, i, j) \geq \mathbf{u}(t, \mathbf{q}, \mathbf{k}), \forall t \in \mathcal{T}, \mathbf{q} \in \mathcal{Q}, \mathbf{k} \in [1, \mathbf{K}] \quad (24)$$

Proof:

If $\text{trip}(t, \mathbf{q}, \mathbf{k}) = 1$, then $\sum_{i \in \mathcal{S}} \sum_{j \in \mathcal{S}} \mathbf{w}(t, \mathbf{q}, \mathbf{k}, i, j) \in [1, S]$

which is $\sum_{i \in \mathcal{S}} \sum_{j \in \mathcal{S}} \mathbf{w}(t, \mathbf{q}, \mathbf{k}, i, j) \leq S$

If $\text{trip}(t, \mathbf{q}, \mathbf{k}) = 0$, then $\sum_{i \in \mathcal{S}} \sum_{j \in \mathcal{S}} \mathbf{w}(t, \mathbf{q}, \mathbf{k}, i, j) \leq 0$ and $\sum_{i \in \mathcal{S}} \sum_{j \in \mathcal{S}} \mathbf{w}(t, \mathbf{q}, \mathbf{k}, i, j) \geq 0$

Therefore $\sum_{i \in \mathcal{S}} \sum_{j \in \mathcal{S}} \mathbf{w}(t, \mathbf{q}, \mathbf{k}, i, j) = 0$

So the two constraints equal to the original constraint. This ends the proof.

Reformulation of Constraint (14)

Constraint (14) regulates $\sum_{j \in \mathcal{S}} \mathbf{w}(t, \mathbf{q}, \mathbf{k}, i, j)$ must be zero if trip t takes sub-request (\mathbf{q}, \mathbf{k}) and sub-request (\mathbf{q}, \mathbf{k}) will arrive stop i . The constraint can be reformulated as constraint (24).

$$\sum_{j \in \mathcal{S}} \mathbf{w}(t, \mathbf{q}, \mathbf{k}, i, j) \leq 2 - \mathbf{u}(t, \mathbf{q}, \mathbf{k}) - \mathbf{r}(\mathbf{q}, \mathbf{k} + 1, i) \quad (25)$$

$$\forall t \in \mathcal{T}, \mathbf{q} \in \mathcal{Q}, \mathbf{k} \in [1, \mathbf{K}], i \in \mathcal{S}$$

Proof:

If $\mathbf{u}(t, \mathbf{q}, \mathbf{k}) = 1$ and $\mathbf{r}(\mathbf{q}, \mathbf{k} + 1, i) = 1$,

then $\sum_{j \in \mathcal{S}} \mathbf{w}(t, \mathbf{q}, \mathbf{k}, i, j) \leq 0$,

since $\mathbf{w}(t, \mathbf{q}, \mathbf{k}, i, j) \geq 0$, $\sum_{j \in \mathcal{S}} \mathbf{w}(t, \mathbf{q}, \mathbf{k}, i, j) \geq 0$

therefore $\sum_{j \in \mathcal{S}} \mathbf{w}(t, \mathbf{q}, \mathbf{k}, i, j) = 0$

If $\mathbf{u}(t, \mathbf{q}, \mathbf{k}) = 1$ and $\mathbf{r}(\mathbf{q}, \mathbf{k} + 1, i) = 0$ or $\mathbf{u}(t, \mathbf{q}, \mathbf{k}) = 0$ and $\mathbf{r}(\mathbf{q}, \mathbf{k} + 1, i) = 1$

Then $\sum_{j \in \mathcal{S}} \mathbf{w}(t, \mathbf{q}, \mathbf{k}, i, j) \leq 1$, which always holds.

If $\mathbf{u}(t, \mathbf{q}, \mathbf{k}) = 0$ and $\mathbf{r}(\mathbf{q}, \mathbf{k} + 1, i) = 0$,

Then $-2 \leq \sum_{j \in \mathcal{S}} \mathbf{w}(t, \mathbf{q}, \mathbf{k}, i, j) \leq 2$, which always holds.

Reformulation of Constraint (15)

Constraint (15) regulates $\sum_{j \in \mathcal{S}} w(\mathbf{t}, \mathbf{q}, \mathbf{k}, j, i)$ must be 1 if trip \mathbf{t} takes sub-request (\mathbf{q}, \mathbf{k}) and sub-request (\mathbf{q}, \mathbf{k}) will arrive stop i . The constraint can be reformulated as constraint (25).

$$\sum_{j \in \mathcal{S}} w(\mathbf{t}, \mathbf{q}, \mathbf{k}, i, j) \geq u(\mathbf{t}, \mathbf{q}, \mathbf{k}) + r(\mathbf{q}, \mathbf{k} + \mathbf{1}, i) - 1 \quad (26)$$

$$\forall \mathbf{t} \in \mathcal{T}, \mathbf{q} \in \mathcal{Q}, \mathbf{k} \in [1, \mathbf{K}], i \in \mathcal{S}$$

Proof:

If $u(\mathbf{t}, \mathbf{q}, \mathbf{k}) = 1$ and $r(\mathbf{q}, \mathbf{k} + \mathbf{1}, i) = 1$,

then $\sum_{j \in \mathcal{S}} w(\mathbf{t}, \mathbf{q}, \mathbf{k}, i, j) \geq 1$,

since $\sum_{j \in \mathcal{S}} w(\mathbf{t}, \mathbf{q}, \mathbf{k}, i, j) \leq 1$

therefore $\sum_{j \in \mathcal{S}} w(\mathbf{t}, \mathbf{q}, \mathbf{k}, i, j) = 1$

If $u(\mathbf{t}, \mathbf{q}, \mathbf{k}) = 1$ and $r(\mathbf{q}, \mathbf{k} + \mathbf{1}, i) = 0$ or $u(\mathbf{t}, \mathbf{q}, \mathbf{k}) = 0$ and $r(\mathbf{q}, \mathbf{k} + \mathbf{1}, i) = 1$

Then $\sum_{j \in \mathcal{S}} w(\mathbf{t}, \mathbf{q}, \mathbf{k}, i, j) \geq 0$, which always holds.

If $u(\mathbf{t}, \mathbf{q}, \mathbf{k}) = 0$ and $r(\mathbf{q}, \mathbf{k} + \mathbf{1}, i) = 0$,

Then $\sum_{j \in \mathcal{S}} w(\mathbf{t}, \mathbf{q}, \mathbf{k}, i, j) \geq -1$, which always holds.

Therefore, the new constraint is equivalent to the original constraint. This ends the proof.

Reformulation of Constraint (16)

Constraint (16) regulate the relationship between $w(\mathbf{t}, \mathbf{q}, \mathbf{k}, i, j)$ and $v(\mathbf{q}, \mathbf{k}, i)$. The constraint is also an if-else constraint, so it can be replaced by two linear constraints as follows.

$$\begin{aligned} \sum_{j \in \mathcal{S}} w(t, q, k, i, j) - \sum_{j \in \mathcal{S}} w(t, q, k, j, i) \\ - v(q, k, i) \leq 2 * (1 - u(t, q, k)) \quad (27) \\ \forall t \in \mathcal{T}, q \in \mathcal{Q}, k \in [1, K], i \in \mathcal{S} \end{aligned}$$

$$\begin{aligned} \sum_{j \in \mathcal{S}} w(t, q, k, i, j) - \sum_{j \in \mathcal{S}} w(t, q, k, j, i) \\ - v(q, k, i) \geq 2 * (1 - u(t, q, k)) \quad (28) \\ \forall t \in \mathcal{T}, q \in \mathcal{Q}, k \in [1, K], i \in \mathcal{S} \end{aligned}$$

Proof:

If $u(t, q, k) = 1$,

then $\sum_{j \in \mathcal{S}} w(t, q, k, i, j) - \sum_{j \in \mathcal{S}} w(t, q, k, j, i) - v(q, k, i) \geq 0$ and $\sum_{j \in \mathcal{S}} w(t, q, k, i, j) - \sum_{j \in \mathcal{S}} w(t, q, k, j, i) - v(q, k, i) \leq 0$

therefore $\sum_{j \in \mathcal{S}} w(t, q, k, i, j) - \sum_{j \in \mathcal{S}} w(t, q, k, j, i) - v(q, k, i) = 0$

If $u(t, q, k) = 0$

Then $\sum_{j \in \mathcal{S}} w(t, q, k, i, j) - \sum_{j \in \mathcal{S}} w(t, q, k, j, i) - v(q, k, i) \leq 2$ and $\sum_{j \in \mathcal{S}} w(t, q, k, i, j) - \sum_{j \in \mathcal{S}} w(t, q, k, j, i) - v(q, k, i) \geq -2$

Since $\sum_{j \in \mathcal{S}} w(t, q, k, i, j) - \sum_{j \in \mathcal{S}} w(t, q, k, j, i) \in [-1, 1]$, and $v(q, k, i) \in [0, 1]$ therefore $\sum_{j \in \mathcal{S}} w(t, q, k, i, j) - \sum_{j \in \mathcal{S}} w(t, q, k, j, i) - v(q, k, i) \in [-2, 2]$ always holds.

Therefore, the new two constraints are equivalent to the original constraint. This ends the proof.

Reformulation of Constraint (17)

Constraint (17) describes the relationship between the arriving time of trip t at two adjacent stops. The constraint is an if-else constraint, therefore, it is equivalent to the following two constraints.

$$\begin{aligned} y(t, i) + d(i) + t(i, j) * w(t, p, k, i, j) - y(t, j) \\ \leq T * (1 - w(t, p, k, i, j)) \quad (29) \\ \forall t \in \mathcal{T}, q \in \mathcal{Q}, k \in [1, K], i \in \mathcal{S} \ i \neq j, p \in \mathcal{P}, k \\ \in [1, K] \end{aligned}$$

Proof:

If $w(t, p, k, i, j) = 0$, then $y(t, i) + d(i) - y(t, j) \leq T$, which always holds.

If $w(t, p, k, i, j) = 1$, then $y(t, i) + d(i) + t(i, j) - y(t, j) \leq 0$, that is $y(t, i) + d(i) + t(i, j) \leq y(t, j)$. This ends the proof.

Reformulation of Constraints (18) and (19)

Constraint (18) and Constraint (19) regulates the time when trip t arrives the origin stop of the request q should be in the feasible time window. The two constraints can be reformulated as the two following linear constraints.

$$q_a(q) - y(t, i) \leq L * \left(1 - \sum_p \sum_k w(t, p, k, i, j) \right) \quad (30)$$

$$\forall t \in \mathcal{T}, q \in \mathcal{Q}, k \in [1, K], i \in \mathcal{S}$$

$$y(t, i) - q_b(q) \leq L * \left(1 - \sum_p \sum_k w(t, p, k, i, j) \right) \quad (31)$$

$$\forall t \in \mathcal{T}, q \in \mathcal{Q}, k \in [1, K], i \in \mathcal{S}$$

Proof:

If $w(t, p, k, i, j) = 0$, then $q_a(q) - y(t, i) \leq L$ and $y(t, i) - q_b(q) \leq L$

Since $q_a(q), q_b(q), y(t, i) \in [1, L]$, therefore the two inequality always hold.

If $w(t, p, k, i, j) = 1$, then $q_a(q) - y(t, i) \leq 0$ and $y(t, i) - q_b(q) \leq 0$

That is $y(t, i) \geq q_a(q)$ and $y(t, i) \leq q_b(q)$.

Therefore, the two new constraints are equivalent to the original constraints. This ends the proof.

Solution Algorithm

The procedures of solving the bus vehicle routing and scheduling problem is shown in Figure 6.3. The input and output files required in this algorithm are illustrated in Figure 6-4. The algorithm will take two sources of input files—network data and travel demand and scenario data. All data will be fed into the optimization model to derive the optimal solution including the optimized trips (i.e., the schedule for each vehicle to arrive each stop in the chosen pattern).

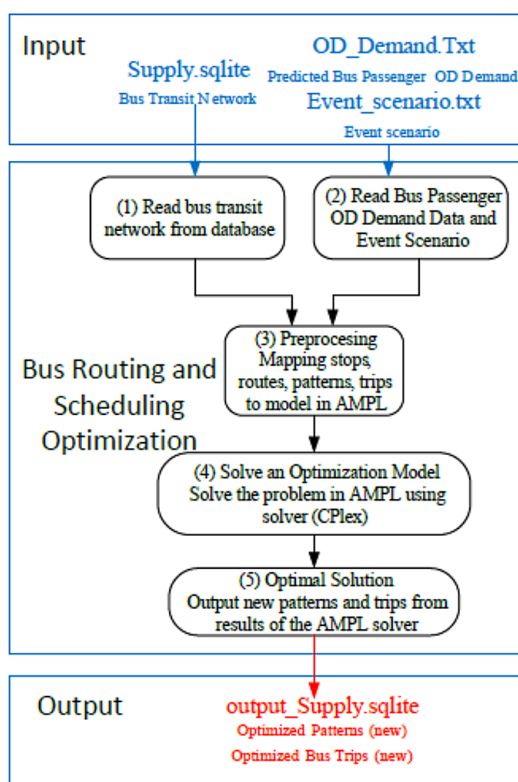


Figure 6-3 Solution procedure

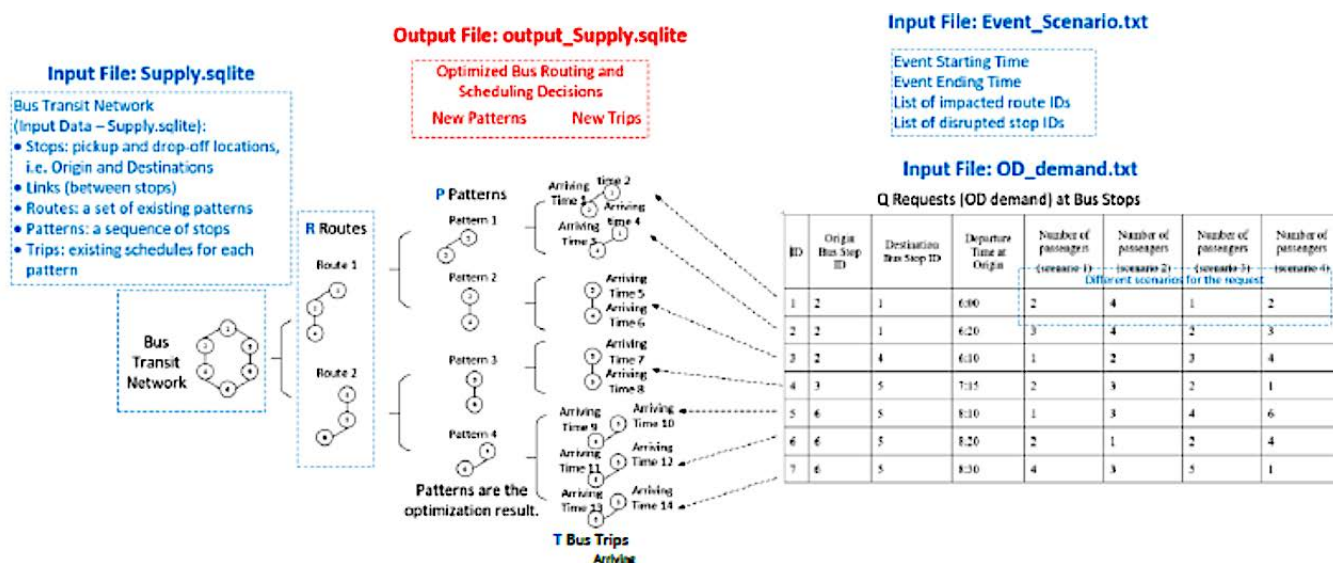


Figure 6-4 Illustration of input and output files

The implementation first requires a transportation network. The transportation network contains bus transit stops and links, the transit stops are pickup and drop-off locations, and the transit links are the connections between two bus transit stops. The travel time along a transit link will be the time constraint for guiding the arriving time of a trip at the end stop of the transit link. The travel distance will appear in the objective to regulate the cost of all trips in this problem. Transit routes are sets of transit patterns, and each pattern is a sequence of stops that regulates the order of a trip to arrive each stop.

The generated data includes two parts—a demand file, named as demand.txt and providing the request information between stops, and a scenario file, named as scenario.txt and regulating the scenario such as event information, impacted routes, and disrupted stops. Each line in the demand file defines a riding request from a specific origin stop to a specific destination stop. Four important elements are specified in each request—origin stop, destination stop, departure time, and number of passengers to reflect the time-dependent demand.

The problem tries to minimize the impact the event in the bus transit system by avoiding traveling through the impacted areas while satisfying all demand for some specific routes. The scenario file is to specify the event and the impacted area. The event information includes event start time, event end time, and a list of disrupted transit stop IDs. The list of impacted routes also needs to be specified; the stops along the impacted routes will be included in the model as impacted stops. The model will constraint the availability of these impacted stops according to the information provided in the scenario file.

Based on the transportation network, the bus transit network and the generated data will be mapped into the modeling objects (i.e., parameters, variables, constraints, objectives) in AMPL.

The non-linear integer optimization model will be reformulated as a mixed integer linear programming by a linearization method and then be implemented in AMPL. Several algorithms such as Bender's decomposition and Branch-and-Bound algorithm can be used to solve the problem. The existing solver (i.e., CPLEX) will take over the problem. The parameters are chosen carefully to make the solver solve the problem efficiently. The solutions provide the optimal trips. The result will be written into the original database file.

Numerical Results

The algorithm is implemented using the C++ programming language by calling the AMPL language and the Cplex solver. It is run on a 2.2 GHz Xeon computer with 512 GB of memory.

We selected one route named as “Warrenville-Naperville Metra” operated by Pace. The route is shown in Figure 6-5. There are X stops in the route, and 10 patterns are defined for this route. The details of the experiment are shown in Table 6-1.

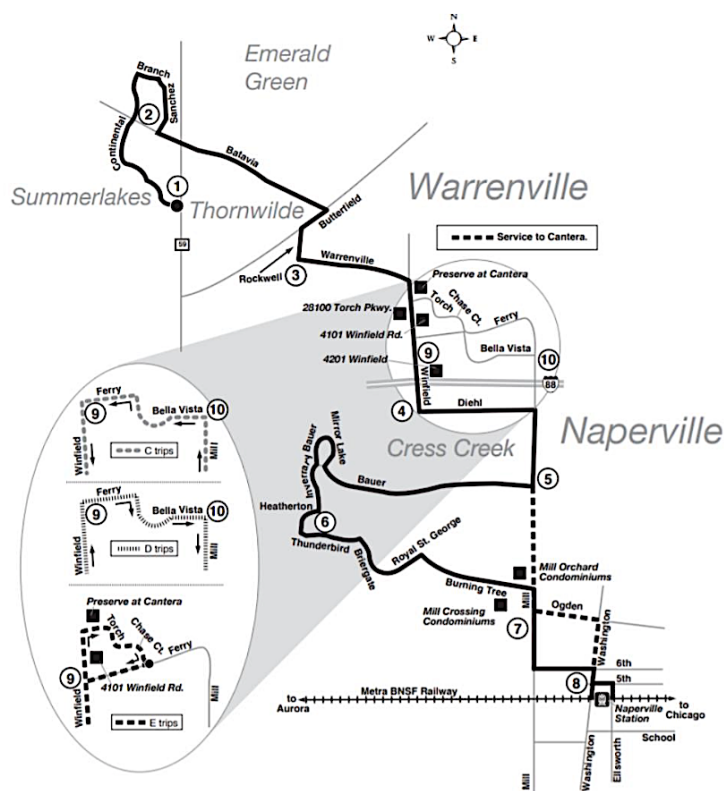


Figure 6-5 Pace 626 line

Table 6-1 Settings of Experiment

Route	Pace 262
Number of stops	222
Number of patterns	10
Maximum number of transfers	2
Maximum time period	1000
Capacity of each pattern	500
Average speed on link	50 ft/sec

To test the performance of the model in different scenarios, we generated different scenarios by changing the number of requests and number of trips in this model. To ensure each pattern was chosen by a trip, for the 2, 3, 4 scenarios, the number of trips was set as 69, the same as the number of patterns. The settings of the test scenarios are shown in Table 6.2.

Table 6-2 *Settings of Test Scenarios*

Route	Test Case Number	# of Requests	# of Requests
Warrenville-Naperville Metra	1	1	10
Warrenville-Naperville Metra	2	5	10
Warrenville-Naperville Metra	3	10	10

The linear integer programming problem was solved by Branch-and-Cut algorithm in CPLEX called by AMPL. The results for different scenarios are shown in Table 6-3. All scenarios had optimal solutions. With the increase of the size of the problem, the number of iterations, number of nodes explored in Branch-and-Cut node tree, number of variables, and number of constraints increased greatly. Therefore, the CPU time of solving the problem grows greatly.

Table 6-3 *Result of Test Scenarios*

Test Case Number	# of Constraints	# of Variables	CPU Running Time (secs)	Objective
1	47,356	14,141	39.2188	19518.5176
2	227,400	52,485	514.188	59639.0916
3	452,400	100,390	1208.58	92011.8388
4	902,460	196,200	125225	97141.1551

Conclusion

This section presented an integer programming (IP) model formulation for the bus re-routing and rescheduling problem in a disrupted transportation network. The proposed model can optimally select a set of bus trips and patterns to satisfy impacted travel requests in an emergence event for emergency response.

Section 7

Passenger Behavior in Response to Unplanned Transit Disruption⁷

Offering affordable, efficient, and green service, the public transportation infrastructure of every municipality acts as the veins of its transportation system. In the Chicago metropolitan area, the CTA provides service to over 3.5 million riders in the city of Chicago and 35 suburbs surrounding the city (Chicago Transit Authority, 2017). CTA provides the nation's second largest public transportation system which operates under a budget of \$1.64 billion in 2021 as per its web page at <https://www.transitchicago.com/finance/>. Also, the rail transportation system connects both major airports to the transit system in Chicago (Chicago Transit Authority, 2017).

However, maintaining the competing quality of transit service is challenging. Private vehicles are typically the biggest competitor to transit service. Compared to private vehicles, service reliability, privacy, convenience, availability, and travel time are among the significant dis-utilities of transit service. Further, ride-hailing and ride-sharing services have changed the game in the transportation market. Today, not only do TNCs take market share from private transportation options, but they are strong competitors of the transit system. These services provide a wide variety of affordable, door-to-door options and, thereby, encourage transit users to substitute their conventional choice (i.e., public transit) with TNCs.

This, along with the fact that transit service would not be economically viable unless adopted by enough customers (Berechman, 1993), demands shedding light on transit user satisfaction. Service disruptions, as one of the boldest dis-utilities of a transit system, could cause serious damage to the rider experience (Lin et al., 2016a). Various internal and external factors might cause transit disruption (Lo and Hall, 2006; Mattsson and Jenelius, 2015). Examples of internal factors include the staff strikes, technical failures, periodic maintenance actions such as station renovations and railway signaling changes, and strategic planning efforts such as minor or major reroutes. External issues, on the other hand, are by nature less preventable. Natural disasters such as heavy snowfalls and thunderstorms, for instance, would considerably hinder the regular operation of the fleet, imposing delays to the whole system. Terrorist attacks could be considered as an instance of such disruptions. Depending on the design of the transit system and its schedule, subtle issues on the operation might end up in huge and considerable deterioration of the user experiment (Lo and Hall, 2006; Luo et al., 2018; Saxena et al., 2019).

⁷ Authored by Nima Golshani, Ehsan Rahimi, Ramin Shabanpur, and Kouros Mohammadian, UIC; and Joshua Auld, Hubert Ley, UC, Argonne

Literature Review

The research on pre-planned or unplanned transit disruptions is a relatively new topic of research gaining growing attention in the past decade. A wide range of studies is found in the literature focusing on different aspects of transit disruption. Some scholars have focused on the effect of disruption on transportation network and transit ridership (Cadarso et al., 2013) and analyzed how transit authorities could recover the disrupted service efficaciously, while others have provided insight into the issue from the passenger point of view and analyzed how such disruptions could impact their travel behavior (Murray-Tuite et al., 2014; Saberi et al., 2018).

Two types of transit disruption are considered in the literature. First, pre-planned disruptions that may occur because of pre-planned activities such as maintenance and labor strikes (see, for instance, Pnevmatikou et al., 2015; van Exel and Rietveld, 2009; Yap et al., 2018), and second, unplanned disruptions that are mostly due to natural disaster and terrorist attacks; this study focused on the first one. As the goal of transit authorities is restoring and managing the disrupted service efficaciously, disregarding passenger behavior and perceptions could lead to adopting a management strategy that is not optimal (Currie and Muir, 2017). Therefore, a couple of studies collected data and develop behavioral models for unplanned disruptions. A comprehensive literature review on transit disruption can be found in Rahimi et al. (2019). For instance, Lin et al. (2016b) revealed that travel cost, waiting time, duration of delay, income, and type of incident could affect transit user commuting mode choice during a subway service disruption in Toronto. Yet, little is known about how the users' choices would affect the stability of the road network. This study aimed to fill the gap using activity-based simulation.

Generally, three types of survey are used in the literature of transit disruption—revealed-preference (RP), stated-preference (SP), and revealed preference-stated preference (RP-SP) survey.

As one of the first studies that conducted an RP survey to capture transit user behavior in response to unplanned transit disruption, Murray-Tuite et al. (2014) investigated the long-term impact of the deadly Metrorail collision on passenger behavior in 2009 in Washington, DC. Using a web-based survey, respondents, who had used Metrorail six months before the incident, were asked to specify what changes they made to their transit trips in terms of mode and seat location after the collision and found that 10% and 17% altered their mode of travel and their seating location in the same train, respectively.

Due to a couple of limitations of RP survey, such as insufficient variation in the RP data to investigate all variables of interest (Kroes and Sheldon, 1988) and possibly strong correlations between explanatory variables (Kroes and Sheldon, 1988), some scholars suggest an SP survey to reveal transit user behavior

during a service disruption. In an SP survey, respondents are asked to indicate their decisions when faced with hypothetical scenarios. For instance, Bachok (2008) conducted an SP survey from train passengers in Klang Valley, Malaysia to reveal the modal shift of rail users based on information of alternative modes. In this study, train passengers were asked to choose among a set of alternatives including other trains, shuttle bus, private vehicles, and wait for the restoration of the rail system in hypothetical scenarios. Fukasawa et al. (2012) investigated the effect of providing information such as estimated arrival time, arrival order, and congestion level on the modal shift in response to unplanned transit disruption using a data from an SP survey. They found that train users with access to the information had a higher frequency of shifting to other trains in comparison with passengers without access to the information. In contrast, Bai and Kattan (2014) conducted an SP survey on light rail transit riders in Calgary, Canada and revealed that respondents had more willingness to switch their transport mode if no information was provided to them regarding possible recovery period.

Because RP surveys cannot investigate a wide range of variables of interest and SP surveys may not necessarily represent transit user behavior in a real service disruption (Kroes and Sheldon, 1988), some studies suggested combining both survey methods. For instance, Lin et al. (2016a, 2017) conducted a combined RP-SP survey in Toronto to analyze transit user mode behavior in response to a subway disruption. The RP section was devoted to respondents' last experience with an unplanned service disruption and the SP section provided hypothetical disruption scenarios in which respondents were asked to either choose among alternative modes or cancel their trip. They revealed that travel cost, waiting time, duration of delay, income, and type of incident could affect transit user commuting mode choice during a subway service disruption (Lin et al., 2016a).

Survey Design

To investigate the behavior of transit riders to an unplanned service disruption, an RP-SP survey of Chicago metropolitan area transit riders was conducted. (For a complete discussion on the survey, refer to Auld et al., 2018.) In this survey, a web-based questionnaire was implemented that was accessible through a survey link and PIN. Respondents were intercepted at CTA bus and rail, Metra train, and Pace bus stations by employing a sampling plan developed considering average daily ridership as well as the information of boarding/alighting (Auld et al., 2018). Participants who agreed to participate were given a contact card with a unique PIN which identifies the service, contact time and contact stop (Auld et al., 2018). By entering the survey link and the PIN, respondents were directed to the online questionnaire to provide the details corresponded to the intercepted trip.

The survey has four primary components—person and household socio-demographic variables, transit trip characteristics such as distance, travel

time, travel cost, in-vehicle activities, access/egress to transit, etc., transit user preferences towards transit and other modes, and hypothetical scenarios for disruption based on the intercepted trip. This survey used Google Maps API to gather reliable information about the origin and destination of the transit trip, transit routes, and travel time (Figure 7-1). By employing Google Map APIs, travel times, waiting times, number of transfers, etc., were automatically saved.

This survey collected information about transit user experiences in using other mobility services in the Chicago metropolitan area, including TNCs (Uber, Lyft, etc.), taxis, car-sharing services (e.g., Car2go, Zipcar, etc.), and the city bike-sharing program (DIVVY). For each mobility service, respondents were asked to provide information regarding the frequency of usage (in the Chicago metro area as well as while traveling), the duration of usage, which service they used if multiple options existed, and in-vehicle activities.

Figure 7-1 presents an example of experience questions regarding TNC and taxi.

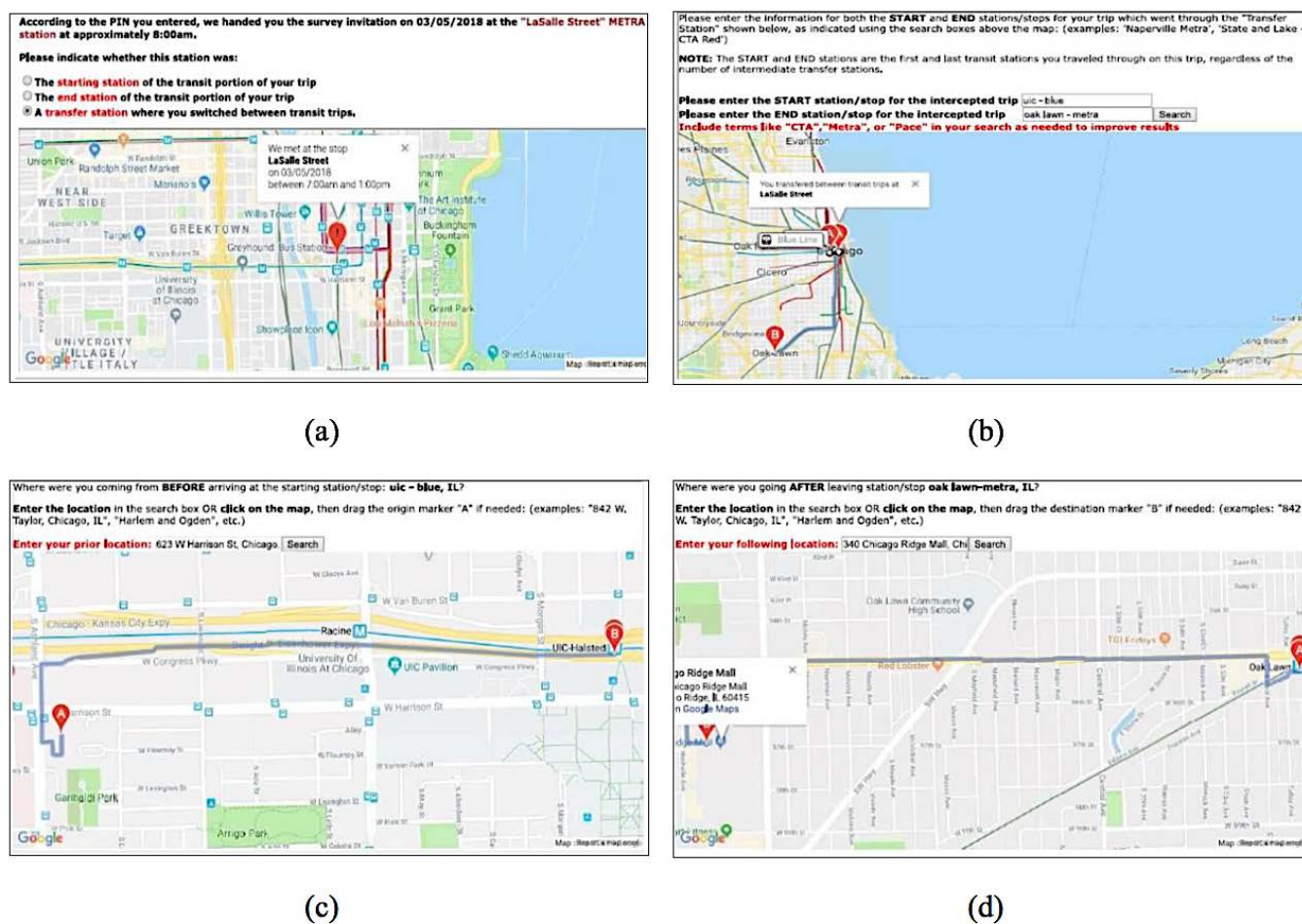


Figure 7-1 Gathering transit trip information using Google Maps API – a) Identifying location of intercepted station; b) choosing coordinates of start/stop stations; c) selecting location before arrival to station; d) selecting location following departure from station (Adapted from Auld et al., 2018) (Map Data © 2018 Google)

Design of SP Choice Sets

The SP disruption response questions were constructed by considering the characteristics of the intercepted trip as the basis for a set of SP questionnaires with the random configuration of modal characteristics according to an experimental design. (For a complete discussion on the design of the survey, refer to Auld et al., 2018.) Figure 7-2 shows an example of an SP disruption response scenario.

As noted, the real-time information of the intercepted trip such as actual time of departure, real-time traffic congestion, and current transit schedule were collected by taking advantage of Google Maps API and then considering these values as a basis for generating the scenario values (Auld et al., 2018). In this survey, each respondent was given four random transit disruption scenarios.

66. How frequently do you use Uber or Lyft-type ride-sharing services?	
While in the Chicago metro area	Frequency Once a year or less ▾
While traveling in other areas	Several times per month ▾
67. Which ridesharing/ridehailing service options do you use?	
<input checked="" type="checkbox"/> UberPool <input checked="" type="checkbox"/> UberX <input type="checkbox"/> UberBlack <input type="checkbox"/> LyftLine <input checked="" type="checkbox"/> Lyft <input type="checkbox"/> LyftLux <input type="checkbox"/> Via <input type="checkbox"/> Curb <input type="checkbox"/> Arro <input type="checkbox"/> Other _____	
68. How many years ago did you first start using ride-sharing/ride-hailing services?	
2 _____	
70. Please indicate how frequently you engage in the following activities while riding in a taxi or other ride-hailing vehicle:	
	Amount of time spent on activity
Reading a book/magazine/newspaper	All of my time ▾
Using a smartphone/tablet/laptop for entertainment (reading, videos, etc.)	Most of my time ▾
Talking on the phone	Some of my time ▾
Work related activities	Very little of my time ▾
School related activities	None ▾
Socializing or talking with others	▾
Relaxing (sleeping, resting, window gazing, doing nothing)	▾
Other	▾

Figure 7-2 Example of experience questions regarding TNC and taxi (Adapted from Auld et al., 2018)

To generate SP disruption scenarios, two sets of parameters were defined. The first group of parameters were observed using the Google Maps API includes the drive time (T_{Drive}^t), drive distance (D_{Drive}), and the transit time ($T_{Transit}^t$) based on the intercepted trip (Auld et al., 2018). The latter group of parameters, which were generated randomly for each SP scenario, includes the status of the original trip which was either canceled or delayed (S), transit travel time delay as a percentage of the original trip (D), the TNC surge pricing factor as a percent of increase in the base fare (P), taxi waiting time (W_{taxi}), TNC waiting time (W_{TNC}), and shuttle service waiting time, which is the percent of D due to waiting for the shuttle ($W_{Shuttle}$) (Auld et al., 2018).

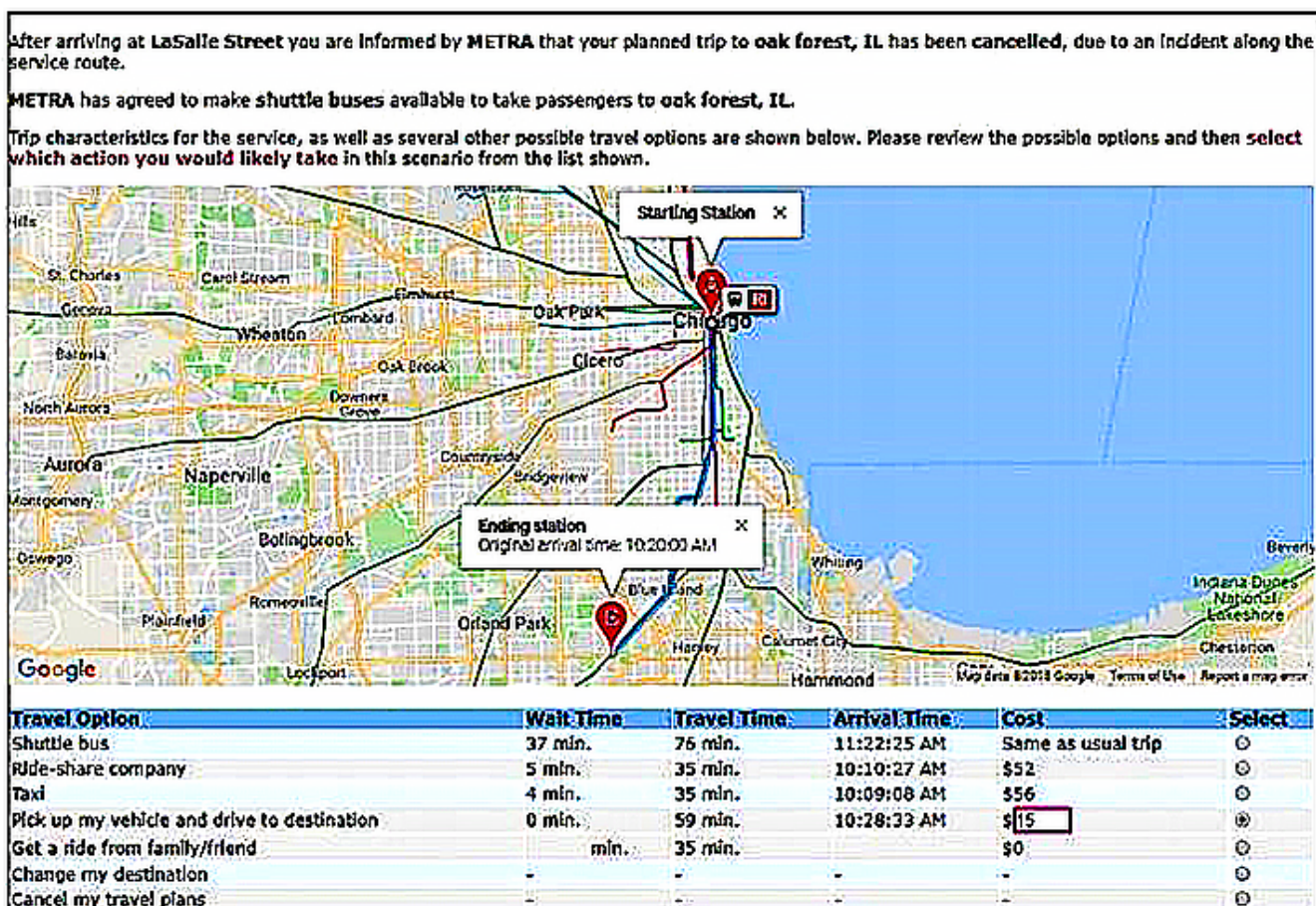


Figure 7-3 Example of SP question regarding disruption scenario (Adapted from Auld et al., 2018) (Map Data © 2018 Google)

The parameter of transit travel time delay (D) was identified based on a random value r using the following rule (Auld et al., 2018):

$$D = \begin{cases} \in (0.15, 0.3) & r \leq 0.33 \\ \in (0.5, 1) & 0.33 < r \leq 0.66 \\ \in (1.5, 3) & r \geq 0.66 \end{cases}$$

Similar to the delay parameter, the TNC surge pricing factor was identified as follows (Auld et al., 2018):

$$P = \begin{cases} \in (0.15, 0.25) & r \leq 0.33 \\ \in (0.5, 1.5) & 0.33 < r \leq 0.66 \\ \in (2.5, 4) & r \geq 0.66 \end{cases}$$

The taxi waiting time was identified as follows (Auld et al., 2018):

$$W_{\text{taxi}} = \begin{cases} \in (5, 15) & r \leq 0.50 \\ \in (30, 45) & r \geq 0.50 \end{cases}$$

The TNC waiting time was identified as follows (Auld et al., 2018):

$$W_{\text{TNC}} \in (3, 15)$$

Finally, the shuttle service waiting time was generated as follows (Auld et al., 2018):

$$W_{\text{Shuttle}} = \begin{cases} \in (0.25, 0.4) & r \leq 0.50 \\ \in (0.5, 0.75) & r > 0.50 \end{cases}$$

The values of the parameters above were then shown to the respondent. Note that both “change of destination” and “trip cancellation” as alternative options for disrupted services had no specifics (Auld et al., 2018). The “ask for ride” option used the drive time, with no additional cost. By selecting this option, the respondent was directed to enter the estimated waiting time for the pick-up (Auld et al., 2018). The “auto drive” alternative considered the drive time along with an additional travel time to pick up the vehicle based on its location, but this option was available only when the transit user indicated that there was an available vehicle (Auld et al., 2018). The rest of the parameters were estimated as follows.

The wait times for a delayed transit trip and a shuttle transit trip were (Auld et al., 2018):

$$T_{\text{transit}}^W = D * T_{\text{transit}}^t$$

$$T_{\text{Shuttle}}^W = W_{\text{Shuttle}} * T_{\text{transit}}^W$$

For the shuttle trips, the new travel times were (Auld et al., 2018):

$$T_{\text{Shuttle}}^t = T_{\text{transit}}^W + T_{\text{transit}}^t - T_{\text{Shuttle}}^W$$

The taxi and TNC fare (in dollars) were calculated considering the drive distance (D_{Drive}) as follows (Auld et al., 2018):

$$C_{taxi} = 3.25 + D_{Drive} * 2.25$$

$$C_{TNC} = (1.75 + D_{Drive} * 1) * P$$

Data Analysis

In the RP-SP survey, information for 659 individuals and 659 transit-based trips was successfully collected. The data had four primary components—person and household socio-demographic variables, intercepted transit trip characteristics such as distance, travel time, travel cost, in-vehicle activities, access/egress to transit, etc., transit user preferences towards transit and other modes, and hypothetical scenarios for disruption based on the intercepted trip. (For a complete discussion on the data, refer to Auld et al., 2018.)

With respect to the gender, 46% of male and 54% of female participants who lived in the Chicago metropolitan area completed the survey. The data included 72% full-time workers, 11% part-time workers, 3% unemployed, 3% retired, 9% students, and 2% other categories. In total, 17.87% of participant households had an annual income less than \$35k, 46.16% between \$35k and \$100k, and the other 35.93% more than \$100k per year. A full description of the sample with respect to household and individual demographic characteristics of the respondents is presented in Table 7-1 and Table 7-2, respectively.

Table 7-1 Household Demographic Characteristics

Variables	Frequency	Percentage
HH size: 1	188	28.70%
HH size: 2	315	48.09%
HH size: 3	90	13.74%
HH size: 4	39	5.95%
HH size: 5 or more	23	3.51%
HH income: < \$15,000	42	7.43%
HH income: \$15,000–\$35,000	59	10.44%
HH income: \$35,000–\$50,000	79	13.98%
HH income: \$50,000–\$75,000	85	15.04%
HH income: \$75,000–\$100,000	97	17.17%
HH income: > \$100,000	203	35.93%
Housing type: mobile/manufactured	5	0.78%
Housing type: apartment	247	38.29%
Housing type: condo	96	14.88%
Housing type: townhome/duplex	47	7.29%
Housing type: single family	238	36.90%
Housing type: other	12	1.86%
Housing tenure: own/mortgage	288	46.01%
Housing tenure: rent	322	51.44%
Housing tenure: other	16	2.56%
Housing payment: < \$500	37	6.60%
Housing payment: \$500–\$1,000	157	27.99%
Housing payment: \$1,000–\$1,500	153	27.27%
Housing payment: \$1,500–\$2,000	106	18.89%
Housing payment: \$2,000–\$3,000	69	12.30%
Housing payment: > \$3,000	39	6.95%

Table 7-2 *Individual Demographic Characteristics*

Variables	Frequency	Percentage
Gender: male	298	45.57%
Gender: female	356	54.43%
Age: < 18	1	0.15%
Age: 18–24	115	17.48%
Age: 25–34	216	32.83%
Age: 35–44	129	19.60%
Age: 45–54	99	15.05%
Age: 55–64	79	12.01%
Age: 65–74	15	2.28%
Age: > 75	4	0.61%
Race: White/Caucasian	375	57.43%
Race: African-American	109	16.69%
Race: Hispanic/Latino	69	10.57%
Race: Asian	56	8.58%
Race: 2 or more ethnicities	27	4.13%
Race: Native American	4	0.61%
Race: other	13	1.99%
Marital status: single	312	47.56%
Marital status: married/domestic partnership	275	41.92%
Marital status: widowed	4	0.61%
Marital status: separated	7	1.07%
Marital status: divorced	40	6.10%
Marital status: other	18	2.74%
Education level: no high school degree, 12 grades or less	6	0.92%
Education level: high school graduate, diploma or equivalent	35	5.36%
Education level: some college credit, no degree	92	14.09%
Education level: trade or vocational school certificate	7	1.07%
Education level: associate's degree	43	6.58%
Education level: bachelor's degree	250	38.28%
Education level: graduate or professional degree	220	33.69%
Employment status: full-time	475	72.08%
Employment status: part-time	70	10.62%
Employment status: student	57	8.65%
Employment status: homemaker	4	0.61%
Employment status: retired	22	3.34%
Employment status: unemployed or looking for work	22	3.34%
Employment status: other	9	1.37%

The survey collected detailed attributes for a randomly-intercepted transit trip in a typical day. Respondents were intercepted at a transit station (CTA bus, CTA rail, Metra, Pace) in the Chicago metropolitan area and were asked to provide information about the characteristics of transit trip as well as access and egress trips (Auld et al., 2018). Among all respondents, 53% were intercepted in CTA rail stops, 16% in CTA bus stops, 26% in Metra stops, and the remaining 5% in Pace. With respect to activity type, approximately 37% and 42% of the respondents were working or doing an in-home activity, respectively, at the origin of their intercepted trip. Also, more than 50% of the respondents had working activity at the destination of their intercepted trip. Figure 7-4 presents the distribution of activity types of both the origin and destination of the intercepted trip.

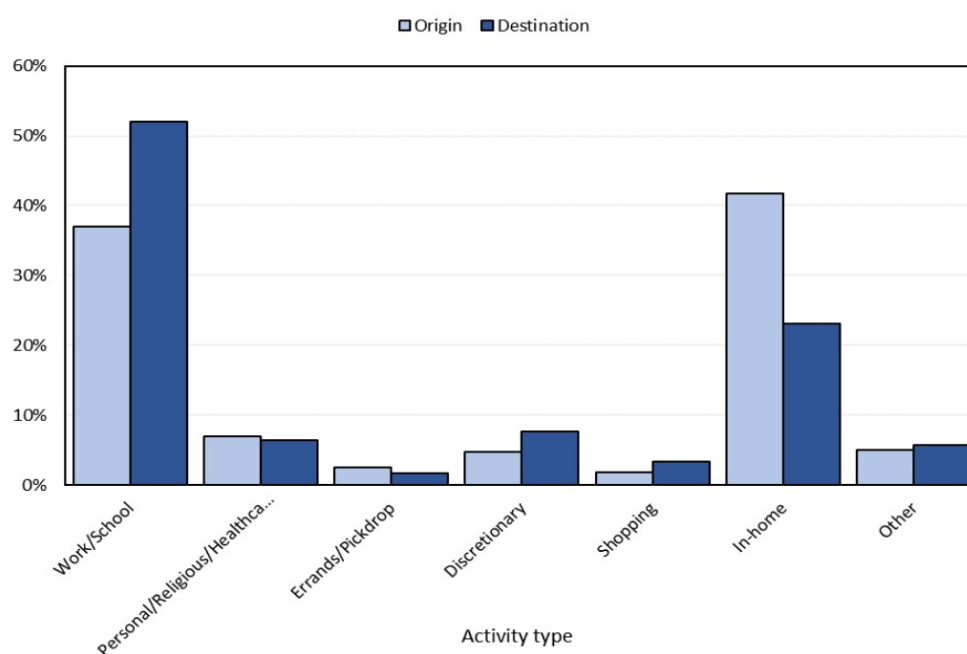


Figure 7-4 Activity types at origin and destination of intercepted trip (Adapted from Auld et al., 2018)

The survey gathered information regarding arrival/departure time flexibility of the above activities. The analysis of the sample revealed that approximately 21% and 29% of respondents had departure time flexibility from the origin and arrival time flexibility at the destination, respectively. Further, the majority of the departure times were between 6:00–9:00 am and 3:00–6:00 pm. Figure 7-5 presents the distribution of departure time in the data.

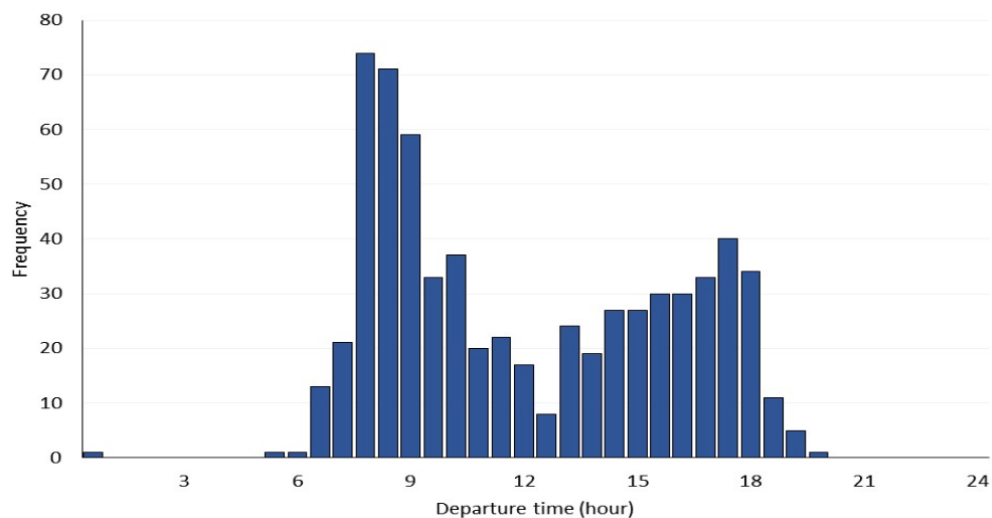


Figure 7-5 *Departure time (Adapted from Auld et al., 2018) Auld et al., 2018)*

With respect to trip characteristics, the survey also collected travel distance, travel time, and number of transfers in the respondents' transit trip. Figure 7-6 presents the distribution of the number of stops in the intercepted trip, with around 67% of respondents having no transfer in their intercepted trip. Further, Figures 7-7 and 7-8 show the distribution for travel distance and travel time in the data, respectively. According to Figure 7-7, approximately 22% of the intercepted trips were less than 5 miles and around 7% were more than 30 miles.

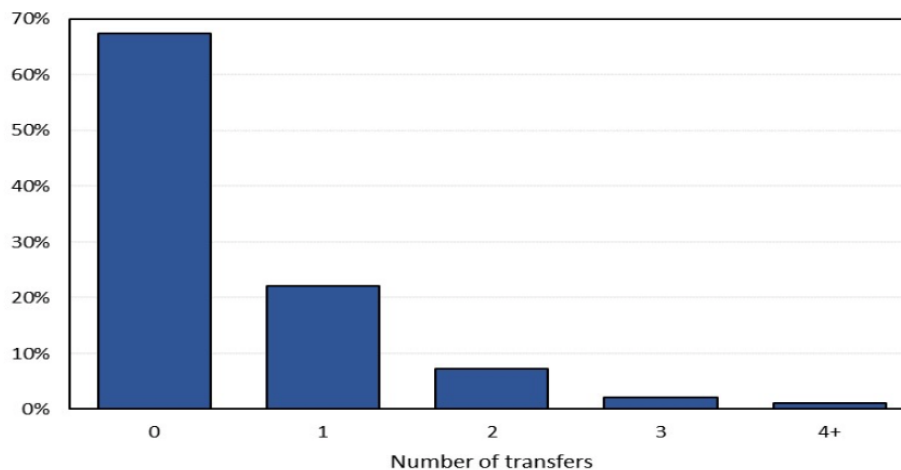


Figure 7-6 *Number of transfers during trip*

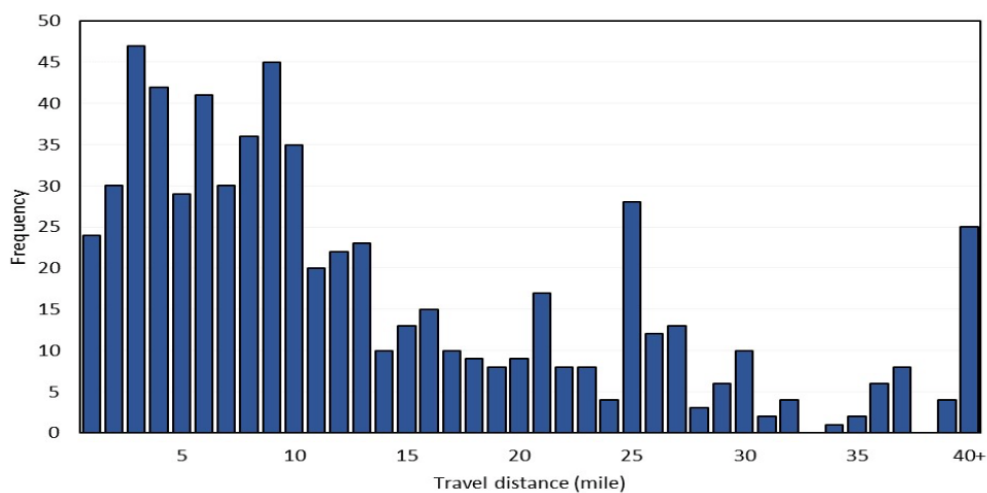


Figure 7-7 *Travel distance*

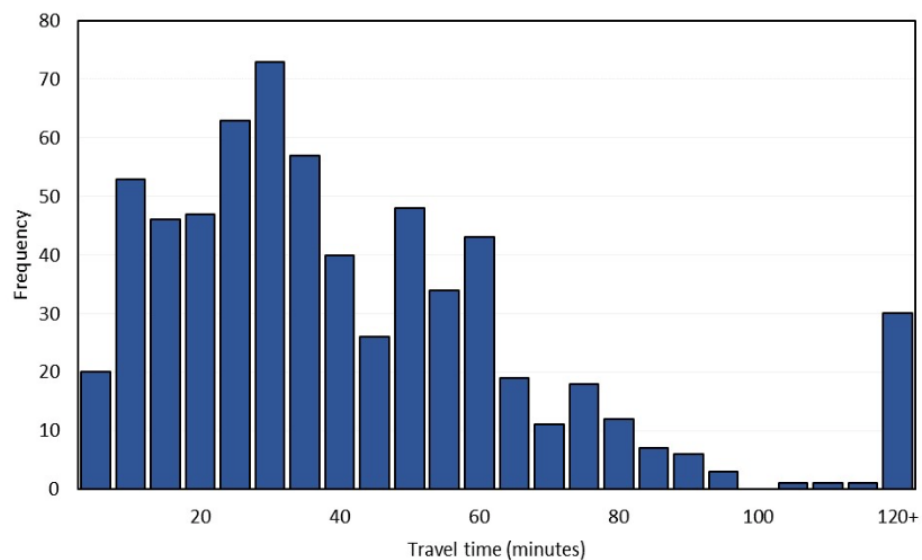


Figure 7-8 *Travel time*

Respondents were also asked about the mode they used to get from the origin to the initial transit station and from the last transit station to the destination. Walking was the prominent mode of transport (67.83% for trip to initial transit stop and 85.13% for trip from last transit stop to destination) due to the close proximity of the origin and destination to the transit stops (Figure 7-9 and Figure 7-10).

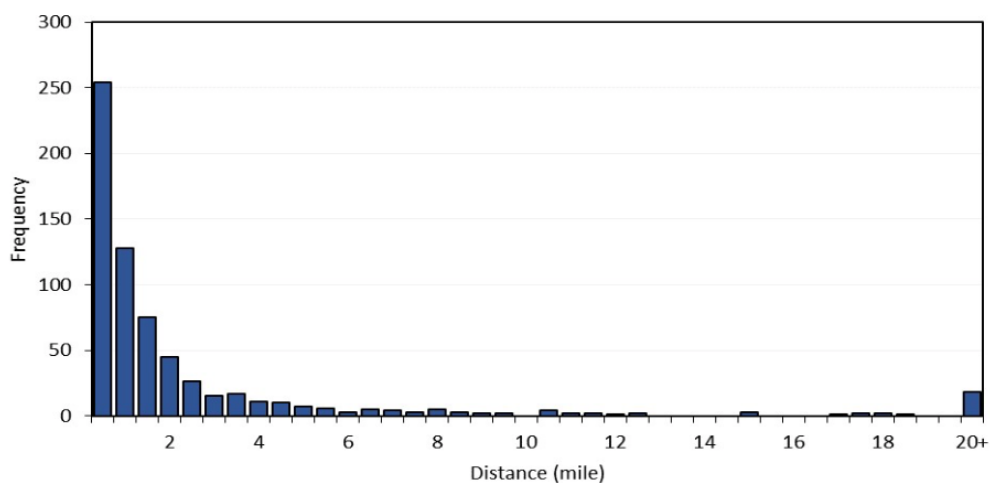


Figure 7-9 *Travel distance between origin and initial transit stop*

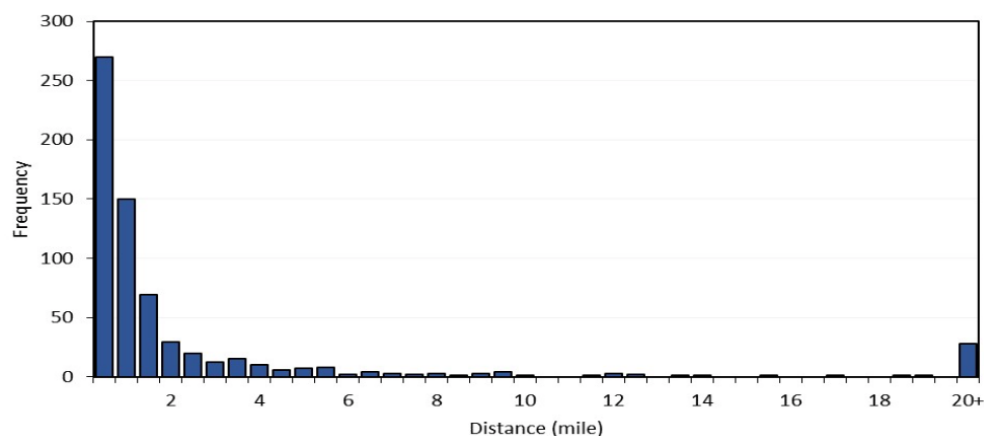


Figure 7-10 *Travel distance between last transit stop and destination*

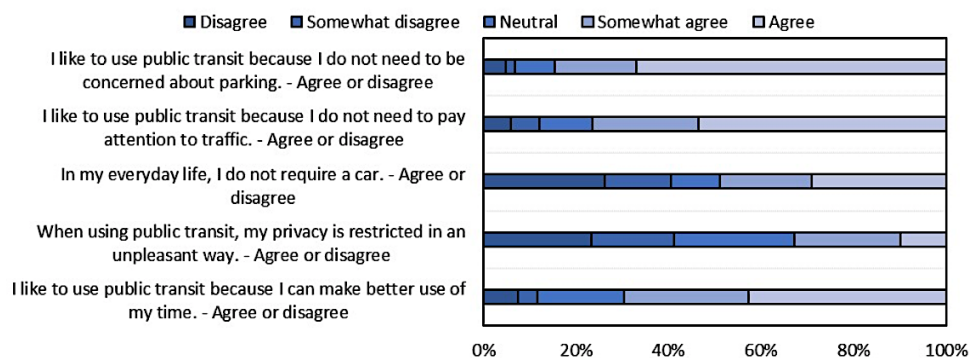
Respondents were asked to indicate the amount of time they spent on different activity types while on board the intercepted transit vehicle, including reading a book/newspaper, doing work or school-related activities, using a smartphone/tablet/laptop for entertainment, talking on the phone, socializing, and relaxing (Rahimi et al. (2019)). Table 7-3 shows the distribution of in-vehicle activity types and duration in the data. Per the analysis, using a smartphone/tablet/ laptop, reading, and relaxing were the most preferred activities.

Respondents also were asked about their reasons for selecting transit as their mode of travel. Fastest option to reach the destination, no need to worry about parking, and lower travel cost were the most influential reasons for more than half of the respondents.

Table 7-3 Duration of In-Transit Activity (Adapted from Auld et al., 2018)

Activity Type	None	Very little of the time	Some of the time	Most of the time	All of the time
Reading	68.74%	6.22%	10.17%	10.77%	4.10%
Using smartphone for entertainment	20.03%	11.53%	23.52%	28.83%	16.08%
Talking on phone	83.92%	7.28%	6.53%	1.52%	0.76%
Work-related activity	79.21%	7.13%	9.86%	2.73%	1.06%
School-related activities	91.50%	2.58%	4.25%	1.21%	0.46%
Socializing or talking with others	81.18%	5.77%	7.44%	3.49%	2.12%
Relaxing /doing nothing)	44.31%	13.66%	25.19%	10.62%	6.22%
Other	93.17%	2.12%	3.03%	0.61%	1.06%

To explore respondent opinion about transit systems, they were asked attitudinal questions about the potential benefits of and concerns of public transit and to indicate their level of agreement with a couple of statements about public transit. Figure 7-11 presents the distribution of respondent answers, indicating that less concern about parking and traffic conditions and more productive use of time while traveling were the most common opinions about transit systems. On the other hand, people had mixed opinions with regards to privacy restrictions in the transit system. According to Fig. 9, approximately 30% of respondents somewhat agree or completely agree that public transit restricts privacy and about 40% disagreed with this statement.

**Figure 7-11** General opinions on public transit

In addition to collecting information regarding the characteristics of transit-based trips, respondent attitudes during a possible disruption of the transit system were also collected. Respondents were first asked to state how long they are willing to wait for the transit system to be restored before they started to think about alternative modes in two conditions—with no information from the transit agency and if the transit agency provided information regarding the delay. Figure 7-12 presents the distribution of willingness to wait under the two

conditions, indicating that people tended to wait for higher durations when the transit agency informed them of the delay.

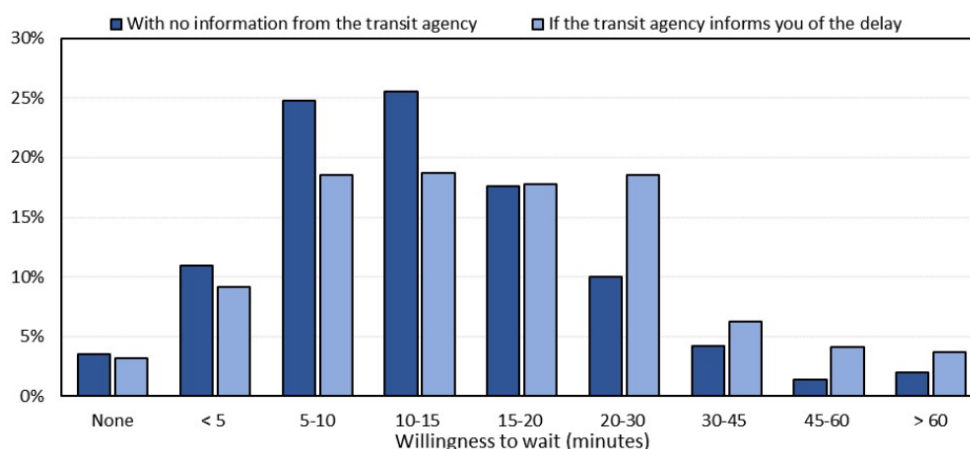


Figure 7-12 Willingness to wait for transit system to be restored

Because the respondents' source of information for receiving emergency updates was significant in their behavior at the time of possible disruption, they were asked to indicate their level of agreement with statements regarding various sources of information. Figure 7-13 illustrates the distribution of respondent level of agreement, showing that approximately 75% either somewhat or completely trust emergency updates from officials and more than 90% would somewhat or completely follow instructions from officials.

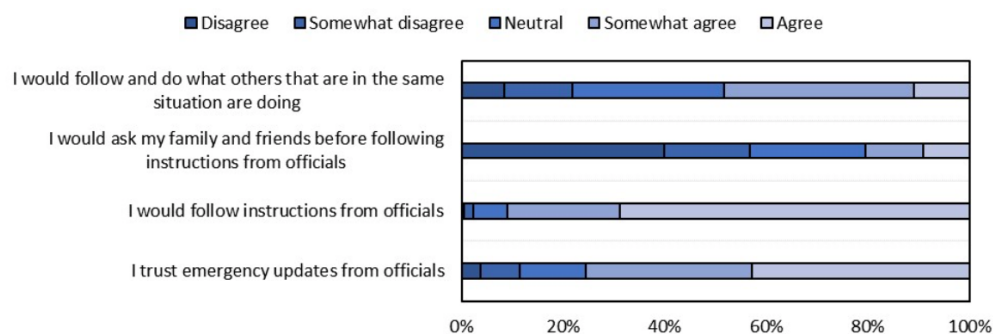


Figure 7-13 Respondent trust in various sources of information

Finally, participants were given four stated choice experiments for various hypothetical scenarios and were asked to select the most preferred choice given the designed attributes:

- Wait for the shuttle bus
- Change other trip attribute
 - Change destination
 - Cancel trip

- Change mode
 - Ask for a ride
 - Auto drive
 - Use taxi
 - Use TNC

Figure 7-14 presents the distribution of the first level alternatives and Figure 7-15 shows the distribution of different types of alternative modes in the sample.

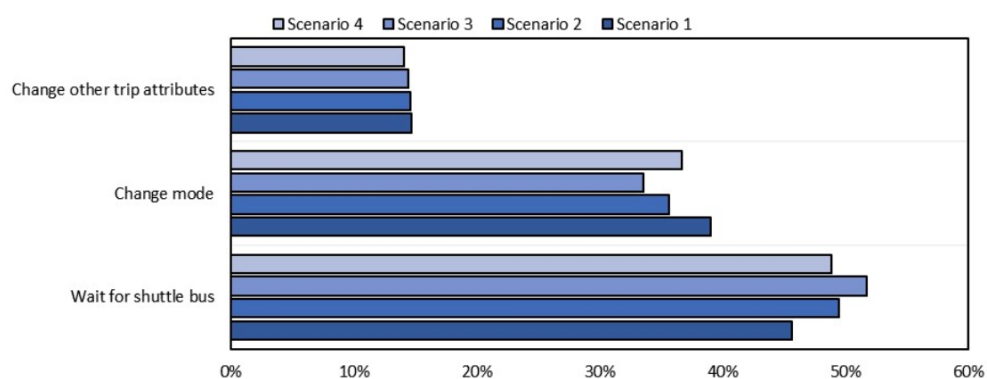


Figure 7-14 Respondent first-level alternatives

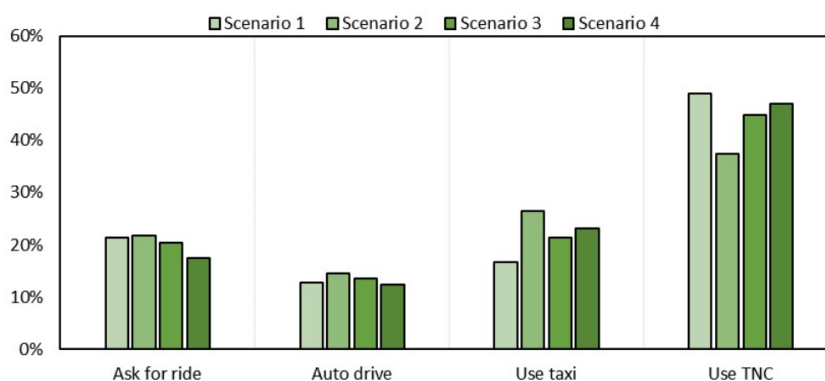


Figure 7-15 Alternative modes in case of modal shift respondent first-level

Model Estimation and Results

In this study, we were interested in predicting and simulating the transit user behavior in response to an unplanned service disruption. According to the SP scenarios provided to each respondent, we proposed a decision tree (DT) model structured in three-level. The upper level determines whether the transit user decides to cancel or perform his/her trip if the trip is disrupted, the next level determines if the user decides to change the destination provided that the trip is not canceled, and the last level estimates the alternative mode being chosen

given that the destination is not changed. The alternative modes were waiting for the shuttle bus, TNCs (e.g., Uber and Lyft), friend/family pick up, personal vehicle, and taxi.

A decision tree is a classifier that generates a tree and a couple of rules, representing the model of different classes using a given data. A typical DT structure includes three elements—each “internal node” represents a test on an attribute, each “branch” denotes an outcome of the test, and each “leaf node” represents the distribution of class(es) (Han et al., 2011). A couple of advantages are stated in the literature for DT classification models. First, because of their intuitive representation, the outcome of a DT model is easy to implement (Breiman et al., 2017). Second, it is not required for a modeler to specify any parameter and, thus, DT models are suitable for investigative knowledge discovery. Third, DT models are relatively high in terms of accuracy; also, they are fast as far as model development is concerned (Breiman et al., 2017; Han et al., 2011).

In DT models, a dataset is classified by directing it from the root of the tree down to a leaf with respect to the outcome of the tests along the path (Rokach and Maimon, 2008). A DT structure starts from the root node, and then the test is applied (i.e., a locally optimum decision about which attribute to use for subdividing the data) to the data. The appropriate branch is followed based on the outcome of the test. Gini Index, Entropy and Misclassification Error are commonly used measurements to choose an appropriate attribute (Tan, 2018). Then, the branch leads either to another internal node or a leaf node (Tan, 2018). When the leaf node is reached, the class label related to the leaf node is then assigned to the observation.

To develop a DT model, a dataset is divided into two different samples, including a training sample and a testing sample. The samples are used to generate the tree and evaluate its performance, respectively. As the training sample size and the predictive performance are positively correlated, data scientists usually prefer to use the largest possible training sample (Rokach and Maimon, 2008). However, due to some dataset limitations, especially in small ones, the training sample might be limited because the rest of the sample (i.e., testing sample) should include all available classes adequately. This study used 80% and 20% of the dataset for the training sample and the testing sample, respectively.

Bias in model development is one of the most critical issues in classification methods and usually occurs due to using an imbalanced dataset. A dataset is imbalanced if the classes are not approximately equally distributed. Our dataset was imbalanced because only around 10% of the respondents either canceled their trip or changed their destination. Then, before developing the first-level and second-level DT models, the problem should be addressed. A couple of methods are proposed in the literature to avoid the biasedness of DT models.

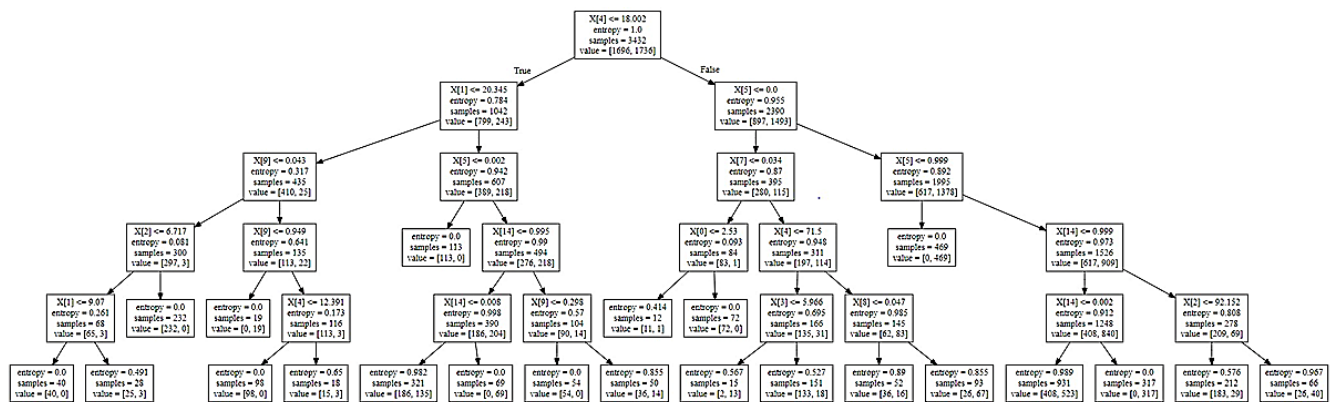


Figure 7-17 Restricted DT model for first level (performing or canceling trip)

Several performance measurements are suggested in the literature to evaluate a classification model. In this study, a couple of widely used performance measurements were estimated, including Accuracy, Precision, Recall, and F-measure to select the outstanding DT model for each level. These are calculated by employing a coincidence matrix. Table 7-5 presents a coincidence matrix corresponding to a two-class classification model.

Table 7-5 Variables Used in DT Models

Name	Definition	Mean	Std. Dev.
Demographics			
AGE_M65	1: if age of transit user is more than 65/ 0: otherwise	0.03	0.17
male	1: if gender is male/ 0: otherwise	0.45	0.50
Bachelor	1: if transit user has bachelor's degree/ 0: otherwise	0.38	0.49
M_Bachelor	1: if transit user has master's degree or more/ 0: otherwise	0.34	0.47
inc_U15	1: if household income is less than \$15K/ 0: otherwise	0.06	0.244
inc_15_35	1: if household income is between \$15K and \$35K / 0: otherwise	0.09	0.29
inc_75_100	1: if household income is between \$75K and \$100K /0 otherwise	0.18	0.38
inc_M100	1: if household income is more than \$100K/ 0: otherwise	0.33	0.47
full_emp	1: if transit user is full-time worker / 0: otherwise	0.72	0.45
Student	1: if transit user is student/ 0: otherwise	0.088	0.28
Dlicense	1: if transit user has driver license/ 0: otherwise	0.86	0.35
Trip Characteristics			
DriveDistance	Distance between trip origin and destination in miles (range between 0.39 and 59)	16.45	26.87
DriveTime	Estimated travel time between origin and destination (min)	35.92	29.12
home_a	1: if activity type at destination is in-home activity/ 0: otherwise	0.23	0.42
work_a	1: if activity type at destination is work activity/ 0: otherwise	0.47	0.50
flexible_a	1: if transit user has time flexibility for arrival at destination/ 0: otherwise	0.70	0.46
Activitydur_d	Activity duration at origin before going to transit station (in min) (range between 0 and 23 hrs)	7.17	5.06
trip_regular	1: if transit user makes this trip regularly/ 0: otherwise	0.84	0.37
trip_alone	1: if transit user traveling alone/ 0: otherwise	0.86	0.35
veh acc	1: if transit user has access to his/her car to make trip/ 0: otherwise		
SP Variables			
OptTransitWait	Wait time for delayed/replaced transit service (min)	57.35	121.66
OptTaxiCost	Taxi fare if transit user want to make trip using taxi	39.61	60.50
OptTNCCost	TNC fare if transit user wants to make trip using TNC	52.46	91.86

Table 7-6 Performance Measurements for First-Level (Performing Trip) DT Model

Performance Measurement	Alternatives	
	Perform Trip	Cancel Trip
Accuracy	85.31%	
Precision	88.65%	53.33%
Recall	95.08%	31.58%
F1-Score	91.75%	39.67%

Table 7-7 Performance Measurements for Second-Level (Changing Destination) DT

Performance Measurement	Alternatives	
	Does Not Change Destination	Changes Destination
Accuracy	98.36%	
Precision	98.63%	87.50%
Recall	99.54%	70.00%
F-1 Score	99.08%	77.78%

Table 7-8 Performance Measurements for Third-Level (Mode Choice) DT Model

Performance Measurement	Alternatives				
	Ask for Ride	Ask for Ride	Shuttle Auto-drive Bus	TNC	Taxi
Accuracy	58.27%				
Precision	37.84%	44.44%	74.59%	41.46%	27.08%
Recall	41.18%	47.06%	70.82%	38.64%	39.39%
F1-Score	39.44%	45.71%	72.65%	40.00%	32.10%

DT models provide not only good accuracy but also offer rich attribute importance information that could be used where the interpretability of the model is paramount (Kazemitabar et al., 2017). For an attribute, the importance score (or tree weight) is calculated in a DT model by summing the impurity reductions over all nodes where a split is made on the attribute with respect to the size of the node (Kazemitabar et al., 2017).

Per the results for the first-level DT model, the dummy variable of work activity at the destination was the most influential attribute on the performing the disrupted trip. According to Figure 7-18, having the arrival-time flexibility at the destination, the dummy variable of in-home activity at the destination, the distance between the origin and the destination, and the waiting time of the delayed/replaced service were ranked in second to fifth place, respectively.

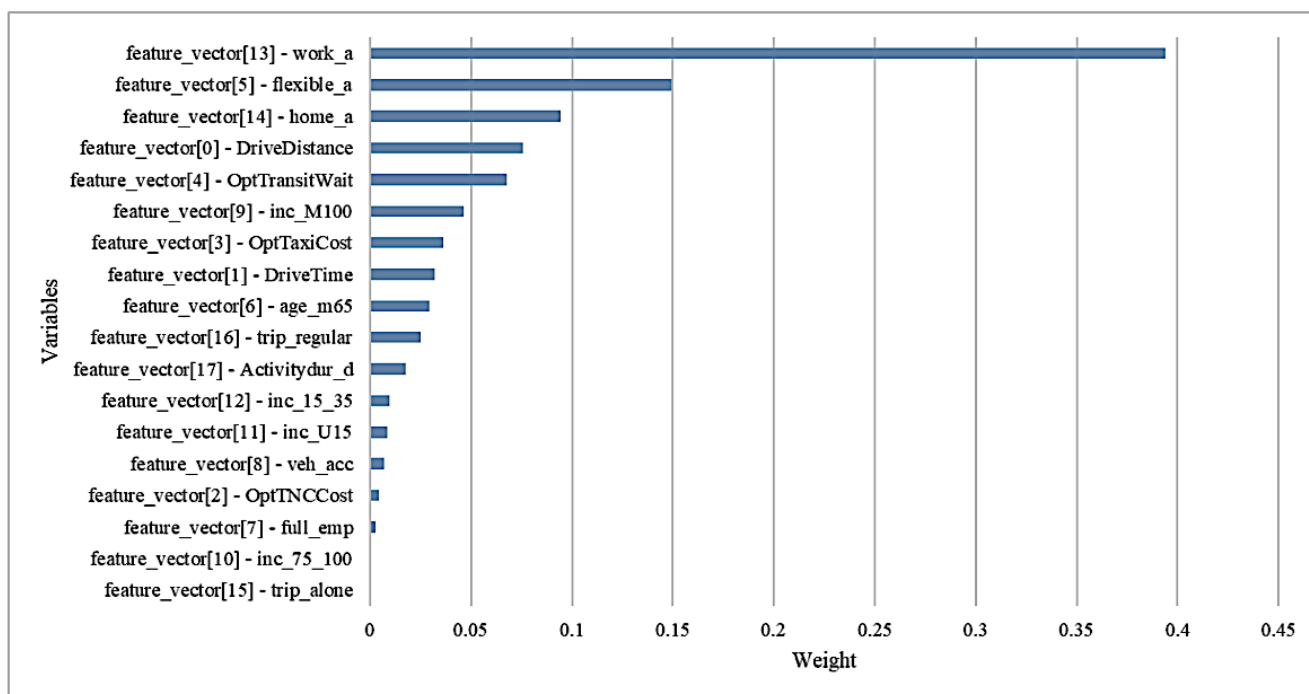


Figure 7-18 Importance of variables used in first-level DT model

The second-level DT model reveals that the waiting time of the delayed/replaced service, having the arrival-time flexibility at the destination, and the dummy variable of in-home activity at the destination are the most important attributes to develop the second-level DT model (Figure 7-19). In addition, having an income of more than \$100k, the duration of activity at the origin, the trip distance, and the TNC fare as an alternative mode for the disrupted trip play a critical role in deciding whether to change the destination of the disrupted trip or not.

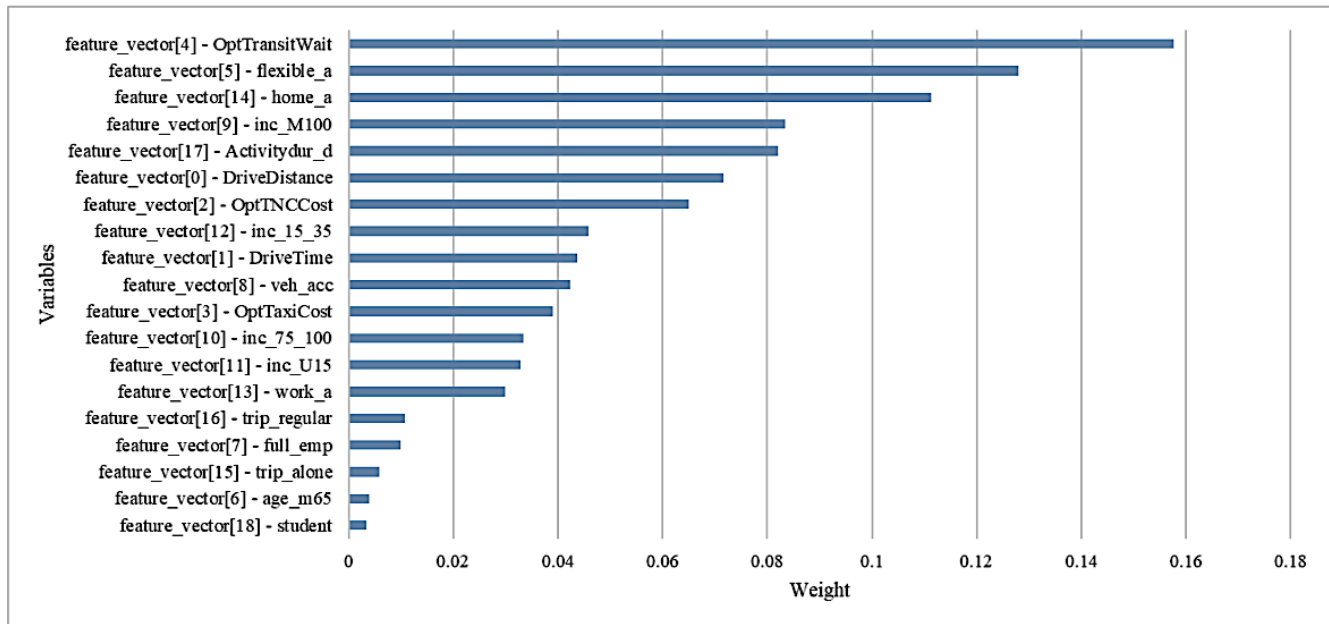


Figure 7-19 Importance of variables used in second-level DT model

Per the results of third-level DT model, the TNC fare as an alternative mode for the disrupted trip and the waiting time of the delayed/replaced service are the most influential factors on the selecting the alternative mode for the disrupted transit service (Figure 7-20). Also, the trip drive time and distance, as well as the duration of activity at the origin, are the key attributes to predict the mode behavior of the respondents.

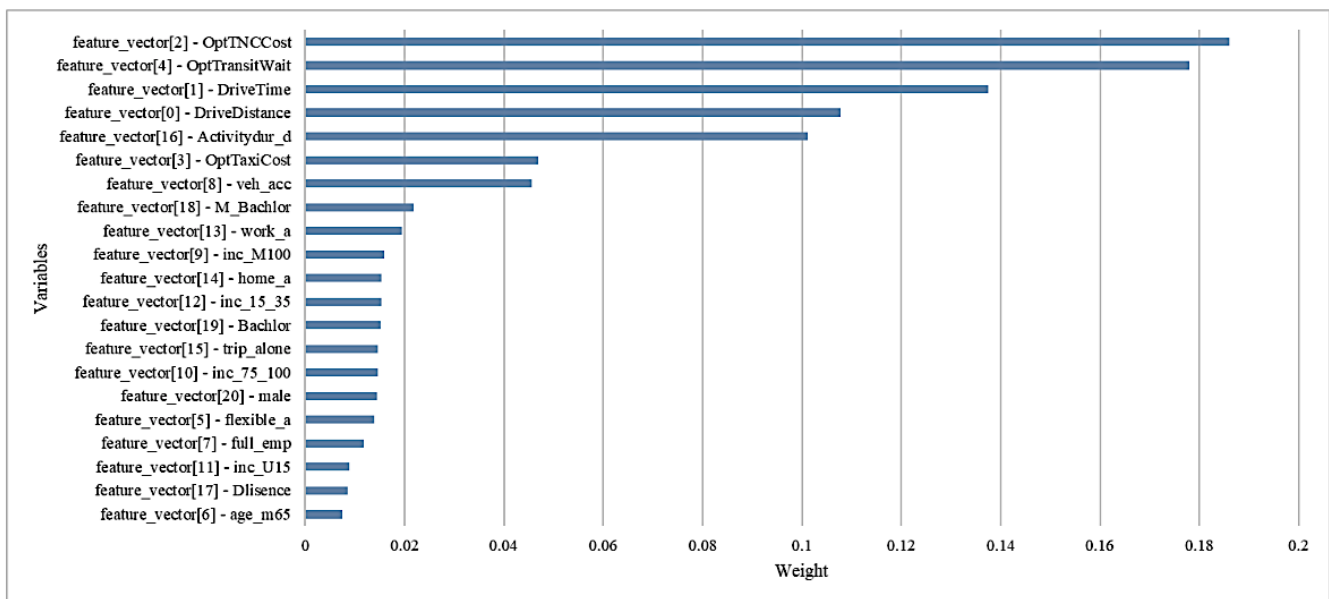


Figure 7-20 Importance of variables used in third-level DT model

Analysis of Evacuation Destination and Departure Time Choices for No-Notice Emergency Events⁸

This section presents a joint discrete-continuous model of evacuation destination and departure time choices in the context of no-notice emergency events. These two critical decisions can directly influence spatial and temporal traffic distributions in the network in case of emergency events. The joint structure is proposed to explore the interdependencies between these evacuation attributes that stem from the shared factors influencing them and/or the causal effects that they might have on each other. The proposed joint model comprises a multinomial logit model as the discrete component to estimate evacuation destination and an accelerated hazard model as the continuous component to estimate the departure time. The results indicate that socio-economic attributes of evacuees, disaster characteristics, built-environment and land use factors, and issuance of evacuation order by government are key determinants of the two decisions. The significance of the estimated copula parameters confirms the existence of unobserved shared effects between the two evacuation decisions, which entails the use of joint modeling scheme.

Introduction

A disaster is a natural or artificially-caused event or situation that disrupts normal activities and can lead to severe infrastructure damage and loss of life. It can be in the form of natural events such as tornados, hurricanes, floods, forest fires, and earthquakes or artificially-caused events such as nuclear seepages and terrorist attacks. These disasters have been increasing in frequency in recent years, resulting in sizable economic losses and casualties. For instance, 315 disastrous events occurred around the world in 2016, resulting in over \$210 billion in economic loss, compared to the 16-year average of 271 events with annual average of \$174 billion in economic loss (Benfield 2016). Due to the increased risk of these incidents over the past few decades, it is vital for the governments to develop effective evacuation strategies to alleviate the damage and fatality caused by these tragedies. Hence, a growing number of studies have focused on the emergency evacuation process to predict public responses and optimize the evacuation procedure from the affected areas. This led to development of several methodological approaches, ranging from statistical and optimization modeling to simulation-based methods to predict and simulate individual evacuation behavior.

⁸ Authored by Nima Golshani, Ramin Shabanpur, Ehsan Rahimi, and Kouros Mohammadian, Joshua Auld, Hubert Ley, University of Chicago, Argonne

In general, disasters can be categorized into two groups considering their predictability. The first group comprises predictable disasters such as hurricanes in which treatments and possible evacuation procedures can be planned from the moment they are predicted. In the case of these events, people in the affected areas are informed in advance by the officials and, if required, are guided to safe places. These events are mostly referred to as advance-notice emergency events in the literature. The second group consists of disasters that are not predictable, such as terrorist attacks, chemical spills, or earthquakes, where notifying the public prior to its occurrence is not feasible. In these situations, referred to as no-notice emergency events, it is generally considered that evacuation procedures start immediately after the occurrence of the event. Thus, pre-disaster planning is of great importance for these events.

Individual evacuation behavior during advance-notice emergency events has been extensively addressed in the literature (see, for example, Drabek and Boggs, 1968; Baker, 1991; Drabek, 1999; Hasan et al., 2013; Sadri et al., 2013). However, only a few studies have attempted to address this issue in case of no-notice emergencies mainly due to the scarcity of data. This study aims to analyze evacuee behavior in the context of no-notice emergency events using an internet-based stated preference survey conducted in the Chicago metropolitan area. In the survey, respondents were faced with multiple emergency scenarios and asked to state various aspects of their evacuation decision including the evacuation destination and departure time.

These two dimensions of evacuation behavior are of great importance because they directly affect the spatial and temporal distributions of traffic in the transportation network. Indeed, exploration of these attributes can specifically lead to preventing occurrence of gridlocks in the network and ultimately reduce economic damage and loss of life. Considering the behavioral aspects of evacuee decision behavior toward these parameters is imperative to identify the most influential factors in their evacuation planning process. From the methodological perspective, these two attributes have traditionally been modeled independently via a variety of modeling approaches. However, these decisions are closely intertwined due to the shared factors affecting them and/or the causal effects they have on each other. Hence, it is necessary to investigate these two decisions in a joint structure to be able to capture the unrestricted correlation between their unobserved influencing factors.

This study contributes to the emergency evacuation literature by presenting a discrete continuous joint structure to explore the relationship between decisions on evacuation destination choice and departure time choice. To achieve that goal, we propose a copula-based joint model that comprises a multinomial logit model as the discrete component to estimate destination choice and an accelerated hazard model as the continuous component to estimate departure time decision. The main motivation to adopt the copula

approach is that it links the stochastic error terms without imposing restrictive distribution assumptions on the dependency structures of the discrete and continuous components (Bhat and Eluru 2009).

Literature Review

This section reviews previous studies related to evacuation departure time and destination choices and highlights the need for capturing the interdependencies and underlying correlations between them. A substantial body of the evacuation-related literature has focused on evacuee behavior in terms of evacuation participation (see, for example, Dash and Gladwin, 2007; Fu and Wilmot, 2004; Hasan et al., 2011; Murray-Tuite et al., 2012) and evacuation route choice behavior (see, for example, Carnegie and Deka, 2010; Robinson and Khattak, 2010; Sadri et al., 2014; Wu et al., 2012). However, relatively little attention has been given to estimating evacuee departure time and destination choice behavior.

As one of the earliest studies on evacuation departure time, Sorensen (1991) used ordinary least square regression to uncover the relationship between evacuee departure time and other explanatory variables. He found that the time of warning receipt and the amount of time that the evacuee needs to prepare to leave (mobilization time) are the most significant factors in departure time decision. By using data collected in southwestern Louisiana after Hurricane Andrew, Fu and Wilmot (2004) developed a sequential binary logit model to estimate the probability that people evacuate at each time period before hurricane landfall. In a later study, Fu and Wilmot (2006) estimated and compared two survival analysis models, the Cox proportional model and the piecewise exponential model. Similar to their previous study, they considered discrete time intervals with a coarse aggregation of six-hour time durations and derived the evacuation probability within each time interval as a function of the household's socioeconomic characteristics, the characteristics of the hurricane, and policy decisions made by authorities.

Using the same dataset, Dixit et al. (2012) presented an evacuation departure time choice model while controlling for risk attitudes. They found that factors such as length of time spent in a region, time of day, and whether a mandatory evacuation order was issued have significant effects on the risk attitudes. In another study, Dixit et al. (2008) showed how the psychological impact of a previous hurricane can affect the evacuation decisions in a subsequent hurricane. They used the data from a survey conducted with the evacuees of Hurricane Frances, which made landfall three weeks after Hurricane Charley in 2005. In this study, the effects of the preceding hurricane were accounted for by modeling departure times simultaneously with an ordinal variable representing evacuation participation levels during Hurricane Charley.

Arguing that the risk responses are heterogeneous across the hurricane-affected individuals, Sadri et al. (2013) proposed a random parameter ordered probit model to capture underlying unobserved characteristics in the timing behavior of the evacuees. They estimated the evacuation mobilization time (time elapsed from the evacuation decision to the actual evacuation) using data from Hurricane Ivan on households from Alabama, Louisiana, Florida, and Mississippi. They reported that the variables related to household location, evacuation characteristics, and socio-economic characteristics are key determinants of the mobilization time. They also found that the effects of previous hurricane experience, source and time of evacuation notice received, work constraints, race, and income vary across the observations.

Using the same dataset, Hasan et al. (2013) proposed a continuous time approach for modeling the evacuation timing decision to overcome the limitations associated with the coarse discrete time intervals considered in the prior studies. They proposed a random-parameter hazard-based model to understand household evacuation timing behavior. It was found that the hazard-based model can reasonably estimate the end of the duration from the moment of receiving a hurricane warning to the moment of actual evacuation. They could also capture the heterogeneous risk responses in the context of departure time decision by incorporating the random parameters approach in their model. As they reported, factors such as household geographic location, type of shelter, location and time to reach the destination in normal time, time between decision and actual evacuation, whether to live in a mobile house, education status, income, type of evacuation notice (mandatory or optional) received have significant effect on departure time decision.

From a different perspective, Ng et al. (2015) investigated the departure time choice behavior in hurricane evacuations of people with special needs, referred to as the medically fragile population in their study. Using data from a large-scale phone survey conducted after Hurricane Irene, they applied the ordinal logistic regression model to uncover the differences between evacuation behavior of the medically fragile and the non-medically fragile population groups. They identified key variables that influence the evacuation departure time of these two population groups and found that fundamental differences exist between their evacuation behaviors.

Moving to evacuation destination choice models, earlier studies showed that if people decide to leave the affected area, they mostly go to public facilities or friend and relative homes. These studies have used a variety of methodological approaches that generally focus on aggregated (or zone-based) data. These methods range from trip distribution gravity models (Wilmot, Modali, and Chen 2006) to zone-based discrete choice models (Cheng, Wilmot, and Baker 2008). In this line of research, Charnkol et al. (2007) developed emergency trip destination model using the binary logistic regression and neural

network approaches. They estimated the probability of selecting evacuation destinations between public and private shelters. Two separate sets of models for permanent residents and transients are presented. They found that variables such as safety and security, medical support, comfort and convenience, communication attribute, and availability of food and beverage attribute significantly affect the shelter choice behavior of evacuees.

Cheng et al. (2008) presented two separate zonal-level multinomial logit models for friends/ relatives and hotel/motel choices. They aggregated destination zones based on the risk due to hurricane and natural geographic features and considered 28 destination alternatives in their study. They found that destination choice is affected by the trip distance and the attributes of the destination zone including risk, white population, total population, presence of a major metropolitan area, number of hotels, and presence of an interstate highway. Later, Mesa-Arango et al. (2013) developed a household-level nested logit model to identify the variables influencing destination type choice among four common alternatives—houses of friends and relatives, hotels, public shelters and churches, and other. They used data from Hurricane Ivan 2004 to calibrate the model. More recently, Parady and Hato (2016) estimated a spatially correlated logit model of evacuation destination choice and proposed an alternative allocation parameter to account for spatial correlation in the particular context of tsunami evacuation. They found that factors such as origin-destination (OD) distance, OD altitude difference, number of buildings, and number of officially designated shelters are statistically associated with evacuation destination choice. Their results suggest the existence of a high degree of correlation among unobserved attributes of zones which was suitably captured by the proposed allocation parameter. A summary of the reviewed studies is presented in Table 8-1.

Table 8-1 Summary of Studies on Evacuation Departure Time and Destination Choice

Author	Spatial Context & Data	Model	Choice Set Description
Sorensen, 1991	Hazardous materials incident (Mar 1987): 578 respondents in Atlanta	Ordinary least square regression	Continuous time
Fu and Wilmot, 2004	Hurricane Andrew (Aug 1992): 156 households in SW LA	Sequential logit model	Discrete time intervals: 12:00 am-6:00 am, 6:00 am-12:00 pm, 12:00 pm-6:00 pm, and 6:00 pm-12:00 am (for 3 consecutive days)
Fu and Wilmot, 2006	Hurricane Andrew (Aug 1992): 156 households in SW LA	Cox proportional hazard & piecewise exponential model	Discrete time intervals: 12:00 am-6:00 am, 6:00 am-12:00 pm, 12:00 pm-6:00 pm, and 6:00 pm-12:00 am (for 3 consecutive days)
Dixit et al., 2008	Hurricane Frances (Aug 2004): 454 respondents in FL	Ordered probit model	Discrete time intervals: 1 hr or less, 2-3 hr, 4-6 hr, 7-24 hr, and more than 24 hr
Dixit et al., 2012	Hurricane Andrew (Aug 1992): 157 households in SW LA	Regression model	Discrete time intervals: 12:00 am-6 am, 6 am-12 pm to noon, noon to 6 p.m., 6 p.m. to 12 am
Sadri et al., 2013	Hurricane Ivan (Sep 2004): 457 randomly selected households in FL, AL MS, LA	Random parameters ordered probit model	Discrete time intervals: 1 hr or less, 2-3 hr, 4-6 hr, 7-12 hr, 12-24 hr, and more than 24 hr
Hasan et al., 2013	Hurricane Ivan (Sep 2004): 3200 households in FL, AL, MS	Random-parameter hazard-based model	Continuous time
Ng et al., 2015	Hurricane Irene (Aug 2011): 539 households in VA and NC	Ordered logit model	Discrete time intervals: after landfall, up to 24 hr prior to landfall, 24-48 hr prior to landfall, and more than 48 hr prior to landfall
Charnkol et al., 2007	Indian Ocean earthquake & tsunami (Dec 2004): 633 individuals in Phuket, Thailand	Binary logistic regression model & Neural Network model	Public shelter vs. private shelter (two separate models for permanent residents and transients)
Cheng et al., 2008	Hurricane Floyd (1999): 1040 households in SC	Multinomial logit model	28 TAZ options (two separate models for friends/relatives & hotel/motel)
Mesa-Arango et al., 2013	Hurricane Ivan (Sep 2004): 1,419 households in FL, AL, MS, LA	Nested logit	4 options: Public shelters and churches, hotels, friends and relatives, other
Arango et al.,	Nested logit	4 options: Public shelters and churches, hotels, friends and	
Parady and Hato, 2016	Great East Japan tsunami (Mar 2011): 10,603 individuals, Kesennuma city, Japan	Spatially correlated logit model	Study area tessellated into a 1-km-sq zone mesh, used as spatial unit of analysis and constitutes universal choice set

In conclusion, while individual evacuation behavior during advance-notice emergency events has been extensively studied in the literature, only a few studies have attempted to address this matter in the case of no-notice disasters. Scarcity of available data sources is the main reason of this gap in the evacuation literature. Furthermore, although the evacuation dimensions of destination and departure time choices are closely intertwined, no study has yet investigated their correlated decisions in a joint structure. This study aimed to contribute to the literature by estimating a joint discrete-continuous model of evacuation destination and departure time choices in the context of no-notice emergency events.

Data

The data used in this study were extracted from the internet-based stated preference survey for no-notice emergency evacuations (Auld et al. 2012), conducted by the Argonne National Laboratory in 2012. The data were collected through an online platform with access to Google Maps API and consisted of two parts. The first part focused on collecting detailed demographic, location, and vehicle use information of the 500 survey participants and their household members for a typical weekday.

The sample represented participants who resided in Chicago metropolitan area and were composed of 45% men and 55% women. Moreover, 7% of the participants held high school degree or less, 19% passed some college credits, 29% held a college degree, and 45% held graduate or professional degrees. The average household size was 2.66 and the average number of adults and children in households was 2.09 and 0.57, respectively. Finally, 30% of the households had annual income below \$50,000, 40% between \$50,000 and \$100,000, and the remaining 30% more than \$100,000 per year. A full description of the survey, descriptive statistics, and validation of the data can be found in Auld et al. (2012).

In the second part of the survey, participants were presented with two random emergency scenarios. The designed scenarios varied in terms of timing, severity, risk, location, radius of the event, and government recommendation. Participants were then asked about their evacuation decision and potential trips after the occurrence of the emergency event. The collected trip information included number of stops, the reason for each stop, stop locations (e.g., pick up children from school), and the type and location of final evacuation destinations. Destination types considered were evacuation shelter, hotel/motel, stay/return home, and stay with family and friends, hereafter referred to as shelter, hotel, home, and family, respectively. Figure 8-1 presents the distribution of destination choices in the dataset, which indicates that 53.54% of the participants would travel to shelters whereas only 4.17% would select hotel as their destination. Figure 8-1 also shows that 30.42% of participants would return home and 11.88% preferred to stay with their family.

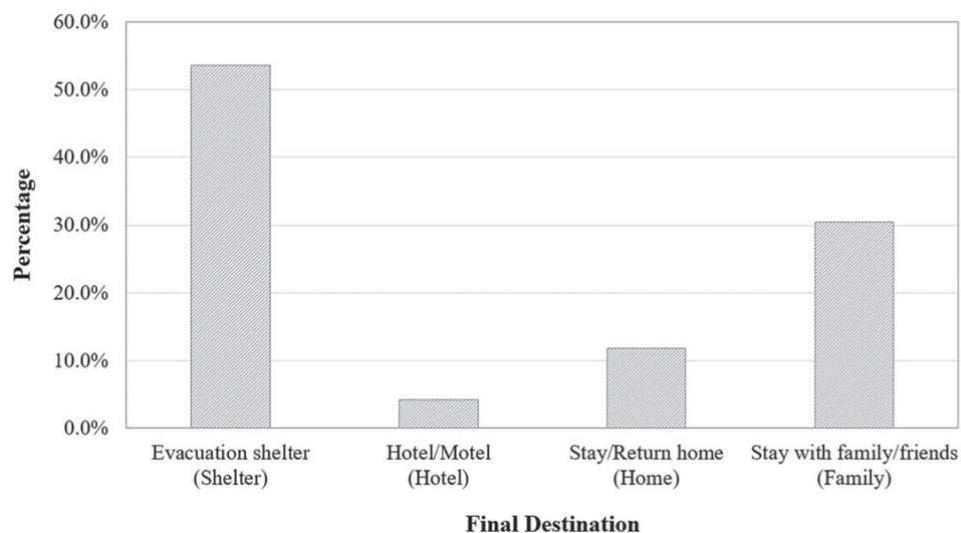


Figure 8-1 Destination choice distribution

To account for land-use and built environment characteristics, related variables such as population and housing density were extracted at the census tract level for Chicago metropolitan area and were added to the dataset. Further, we formed participants' stated tours (as illustrated in Figure 8-2 right) and extracted the corresponding tour- and trip-related variables such as total number of trips, trip travel time and distance, and total tour travel time and distance from Google Maps API. Figure 8-2 depicts the formed tours with red dots showing the final evacuation destinations.

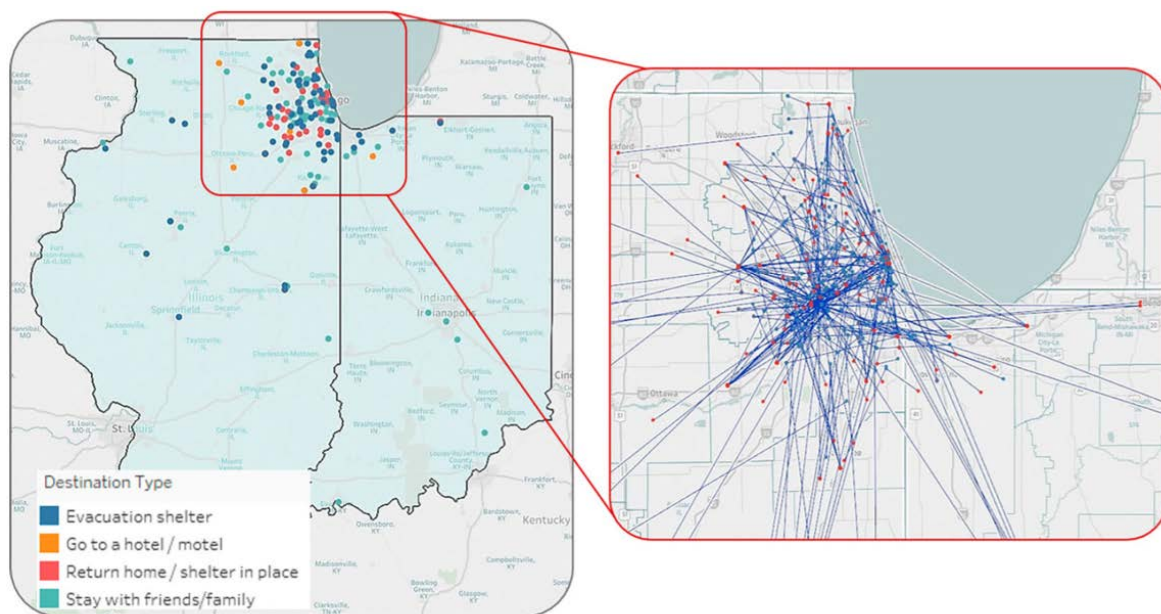


Figure 8-2 Evacuation destination type (left) and tour formation (right)

Figure 8-3 presents the distribution of total distance of evacuation tours for each type of destination. The figure reveals that participants who preferred to stay with family/friends were willing to commute longer distances compared to those who selected other destination alternatives.

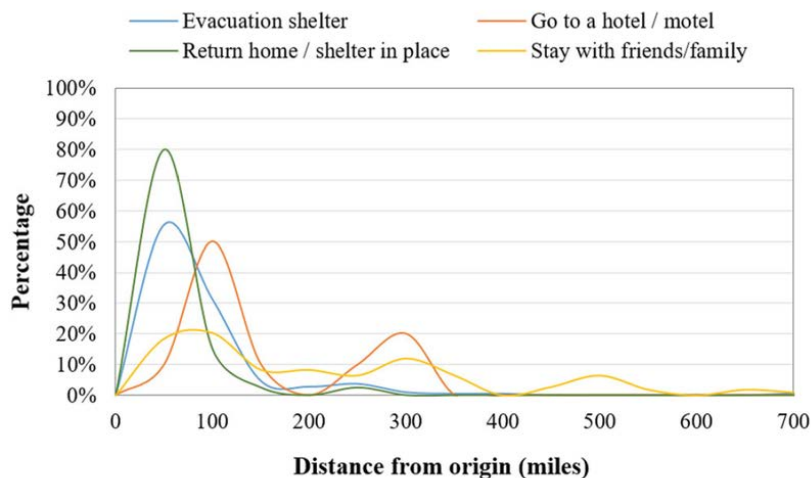


Figure 8-3 Total distances for each destination type

As previously highlighted, the second component of the proposed joint structure was evacuation departure time. Figure 8-4 presents the distribution of departure times in the dataset, which reveals that 48% of participants started their tours within the first 30 minutes after the emergency event occurrence; that is expected in the case of no-notice evacuation. Further, more than 90% of the participants stated that they would evacuate within 180 minutes after the event occurrence.

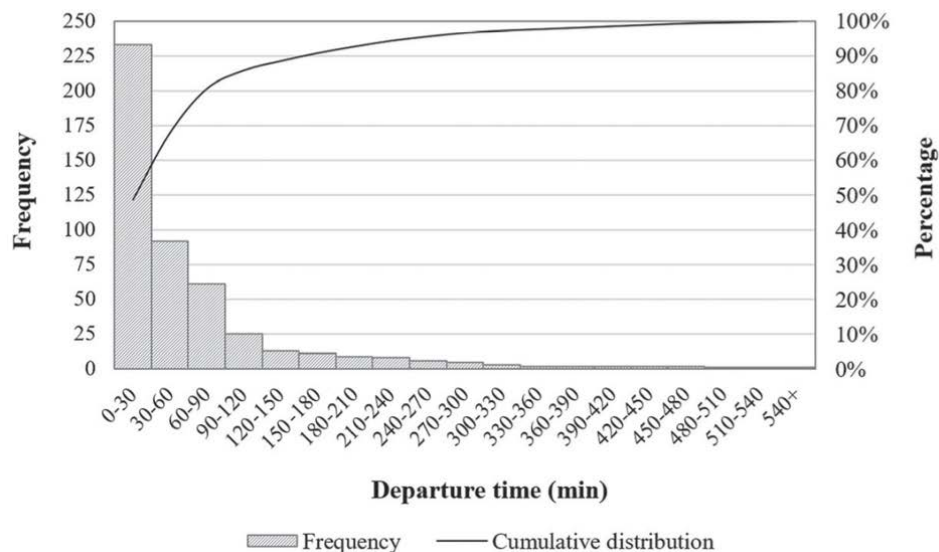


Figure 8-4 Evacuation departure time distribution

Moreover, to investigate the dependence of departure time and destination choice decisions, Figure 8-5 presents the distribution of evacuation departure time conditioned on the destination. Different patterns of departure time distributions revealed that this variable highly depends on the selected destination type, which reflects the need for a modeling approach that can account for the interdependence between the two variables.

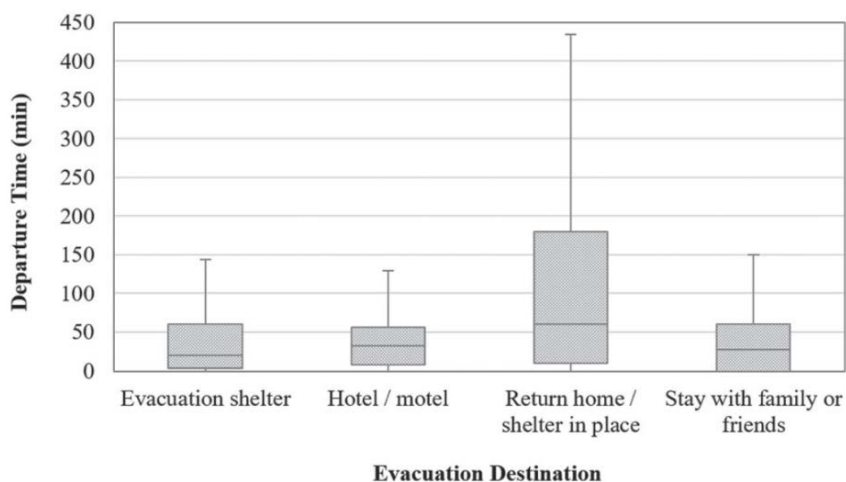


Figure 8-5 *Distribution of departure times across destination choices*

Figure 8-2 Summary Statistics of Key Variables

Variable	Description	Mean	St. Dev.
Gender_male	1: if participant is male; 0: otherwise (o/w)	0.45	0.50
Degree_low	1: if participant has high school degree or less; 0: o/w	0.07	0.25
Degree_graduate	1: if participant has graduate or professional degree; 0: o/w	0.45	0.50
Disability	1: if participant has a disability; 0: o/w	0.07	0.25
Housing_townhouse	1: if participant lives in a townhouse; 0: o/w	0.06	0.23
Housing_apartment	1: if participant lives in an apartment; 0: o/w	0.12	0.33
Housing_condo	1: if participant lives in a condo; 0: o/w	0.04	0.20
Job_retired	1: if participant is retired; 0: o/w	0.13	0.34
Job_homemaker	1: if participant is a homemaker; 0: o/w	0.04	0.19
HH_size	Number of adults in household	2.65	1.48
Government_evacuate	1: if government has issued an evacuation order; 0: o/w	0.65	0.48
Risk_high	1: if risk of event is high; 0: o/w	0.33	0.47
Risk_low	1: if risk of event is low; 0: o/w	0.31	0.47
PopulationDensity	Population density of census tract (in thousand people)	4.59	6.09
PopulationDensity_log	Log of population density of census tract (in thousand people)	0.84	1.19
PopulationDensity_10	1: if population density of participants' location during event greater than 10,000; 0: o/w	0.11	0.32
PopulationDensity_3	1: if population density of participants' location during event less than 3,000; 0: o/w	0.57	0.50
Distance	Total distance of tour (miles)	133.07	267.80
Distance_log	Log of total distance of tour	4.07	1.27
Distance_10	1: total distance of tour is greater than 10 mi; 0: o/w	0.95	0.22
Distance_30	1: total distance of tour is greater than 30 mi; 0: o/w	0.74	0.44
Distance_50	1: total distance of tour is greater than 50 mi; 0: o/w	0.54	0.50
TT_40	1: if the total travel time of tour is greater than 40 min; 0: o/w	0.58	0.49
Stops_high	1: if more than 1 stop in participants' tour; 0: o/w	0.23	0.42
Stop_pickup	1: if participant's first trip is to pick up child; 0: o/w	0.05	0.22
Mode_family	1: if participant's first trip is to meet up with family; 0: o/w	0.97	0.17

Modeling Approach

As noted, this study aimed to jointly model the evacuation destination and departure time choices in case of no-notice emergency events. To achieve this goal, we adopted the copula-based modeling approach which is able to simultaneously estimate these interrelated decisions and capture the underlying correlation between them. In the proposed joint structure, destination choice is estimated using a multinomial logit model and departure time is estimated using accelerated hazard formulation.

As the first component, evacuation destination choice is estimated using a multinomial logit model. The utility function of the choices can be written as:

$$U_{di} = \beta_d X_{di} + \varepsilon_{di} \quad (1)$$

where U_{di} is the person-specific utility of destination d for individual i , X_{di} is the set of explanatory variables, β_d corresponds to the estimable parameters, and ε_{di} is the random error term of the utility corresponding to unobserved factors, which is assumed to have standard type I extreme value distribution.

As the second component of this joint structure, continuous departure time can be suitably modeled using hazard duration approach. Hazard models focus on the elapsed time until occurrence of an event, which in this study would be equal to the time until one evacuates. In fact, hazard models estimate the conditional probability of event occurrence (i.e., evacuation action) between t and $t + dt$ given that it has not happened up to t . This conditional probability can be formulated as follows:

$$\lambda(t) = \frac{f(t)}{1 - F(t)} \quad (2)$$

where, $\lambda(t)$ is the hazard rate, $f(t)$ is the probability density function of the elapsed time, and $F(t)$ is the corresponding cumulative density function that represents the probability of event occurrence until t . From the available hazard models, accelerated hazard formulation allows the covariates to directly influence the length of the elapsed time until the event occurrence. Therefore, the effects of the estimated parameters on the elapsed time can be easily interpreted. In addition, this model assumes that the hazard rate can be accelerated/decelerated over time in direct response to changes in covariates. The accelerated time hazard model can be expressed as:

$$\lambda(t|Z) = \lambda_0[t \cdot \exp(\alpha Z)] \exp(\alpha Z) \quad (3)$$

where Z is the set of explanatory variables affecting elapsed time, α is the vector of estimable parameters, and λ_0 represents the baseline hazard function.

As Kiefer (1988) stated, assuming that the covariates exponentially influence the duration, this formulation is mathematically equivalent to the log-linear regression model as (for each individual i and destination d):

$$\ln(t_{di}) = \alpha_d Z_{di} + v_{di} \quad (4)$$

where $\ln(t_{di})$ represents the natural logarithm of elapsed time for person i and destination choice d , only if choice d is selected as the evacuation destination, α is the vector of estimable parameters, Z is the vector of explanatory variables, and v is the error term corresponding to unobserved factors.

The linkage between destination choice and evacuation timing decisions depends on the type and the extent of the dependency between the stochastic terms v_{di} and ε_{di} . To capture the dependency between these two decisions, this study applies the copula approach, which presents the joint probability distribution of random variables with pre-defined marginal distributions as follows (Sklar 1973):

$$F_{v_{di}, \varepsilon_{di}}(X_1, X_2) = C_\theta(u_1 = F_{v_{di}}(X_1), u_2 = F_{\varepsilon_{di}}(X_2)) \quad (5)$$

where, $F_{v_{di}, \varepsilon_{di}}(\cdot, \cdot)$ is the multivariate joint distribution, $C_\theta(\cdot, \cdot)$ is the copula function with θ as its corresponding copula parameter, $F_{v_{di}}(\cdot)$ and $F_{\varepsilon_{di}}(\cdot)$ are marginal distributions.

Several copula functions have been formulated in the literature including FGM copula, Gaussian copula, and the Archimedean class of copulas (i.e., Clayton, Gumbel, Frank, and Joe copulas). The Archimedean class of copula has been widely used in the literature because of their closed-form functions and their ability to cover a wide range of dependency structures (Bhat and Eluru 2009). This study adopted the Frank copula (Frank 1979) to jointly estimate the evacuation destination and departure time choices because it is the only copula function that allows for both positive and negative dependence and has no limitations in parametrizing the complete range of dependence between the two dependent variables (Bhat and Eluru 2009). The copula function for Frank model with u_1 and u_2 as marginal distributions of the stochastic error terms and θ as the copula parameter is as follows (Bhat and Eluru 2009):

$$C_\theta(u_1, u_2) = -\frac{1}{\theta} \ln \left[1 + \frac{(\exp(-\theta u_1) - 1)(\exp(-\theta u_2) - 1)}{\exp(-\theta) - 1} \right] \quad (6)$$

Using the equations (3)-(5) for estimating the joint distribution, the likelihood function of the joint model can be formulated as (Spissu et al. 2009):

$$L = \prod_{i=1}^N \left[\left\{ \prod_{d=1}^D \frac{1}{\sigma_{vdi}} \times \frac{\partial C_{\theta d}(u_{i1}^d, u_{i2}^d)}{\partial u_{i2}^d} f_{vdi} \left(\frac{\ln(t_{di}) - \alpha_d Z_{di}}{\sigma_{vdi}} \right) \right\}^{R_{di}} \right] \quad (7)$$

where, R_{di} is the binary variable indicating whether destination d is selected by individual i , f_{vdi} is

$$u_{i1}^d = F_{vdi} \left(\frac{\ln(t_{di}) - \alpha_d Z_{di}}{\sigma_{vdi}} \right) \quad (8)$$

$$u_{i2}^d = F_{\varepsilon di}(\beta_d x_{di}) \quad (9)$$

Model Estimation Results

Table 8-3 outlines the estimation results of the joint discrete-continuous destination and departure time model. A full set of possible variables and variable interactions was tested, and the statistically significant variables are presented in this table. The results indicate that a wide range of socio-demographic and land-use variables, event characteristics, and travel-related parameters affects evacuees' decisions during emergency events. The following discussion is organized to explore the role of these variables in the evacuation decision process.

Table 8-3 Estimation Results of Joint Destination and Departure Time Choice Model

Variable	Shelter		Home		Home		Family	
	Param.	t-stat	Param.	t-stat	Param.	t-stat	Param.	t-stat
Destination Choice: Constant 4.44								
Disability	-	-	-	-	1.22**	2.02	-	-
Degree_graduate	0.89**	2.48	-	-	-0.70*	-1.80	-	-
Housing_townHouse	-	-	-	-	6.38***	7.62	-	-
Housing_apartment	5.33***	9.74	-	-	-	-	-	-
Housing_condo	-	-	4.82***	8.94	-	-	-	-
Job_retired	-	-	-	-	-2.17**	-2.34	1.63***	3.84
Government_evacuate	0.61**	2.15	-	-	-1.39***	-3.19	-	-
Risk_high	1.22**	2.35	0.93*	1.72	-	-	-	-
PopulationDensity_log	0.38***	2.63	-	-	-	-	0.21***	4.19
PopulationDensity_10	-	-	-4.79***	-8.56	-	-	-	-
Distance_50	-	-	-	-	-	-	1.71***	5.35
Distance_log	-0.27**	-1.99	-	-	-0.56***	-3.18	-	-
Mode family	-	-	-	-	-	-	2.17**	2.08
Copula parameter: 0	-1.86***	-3.80	.635**	-2.07	-6.14**	-2.40	04.97***	-2.98
Timing								
Constant	4.38**	2.09	3.85*	1.82	5.18***	3.65	3.71***	2.79
Disability	2.71**	2.30	-	-	-	-	4.43***	6.21
Gender_male	-	-	1.99**	2.39	-	-	2.52**	2.05
Degree_low	2.55***	5.19	-	-	-	-	-	-
Job_retired	-	-	-	-	-	-	4.33***	4.42
HH_size	0.73**	2.03	0.64***	2.71	-	-	-	-
Government_evacuate	-0.95**	-2.26	-0.53*	-1.88	-	-	-	-
Risk_low	-	-	-	-	1.49***	2.93	1.65*	1.84
Distance_30	-1.97**	-2.39	-1.28*	-1.89	-	-	02.42*	-1.92
TT_40	-	-	-	-	-2.61***	0-2.64	-	-
Stops_high	-2.78***	-3.32	-	-	-	-	-	-
Stop_pickup	-4.01***	-3.59	-3.45***	-2.73	-	-	-	-
Scale parameter: σ	5.34***	20.87	4.28**	2.25	2.71***	4.91	5.58***	16.91
Kendall's τ	-0.20		-0.53		-0.52		-0.46	
Restricted LL	-1804.87							
LL at convergence	-1485.67							

*Significant at 90% **Significant at 95% ***Significant at 99%

The results indicate that disability significantly increases the probability of staying at/returning home during emergency events possibly because of evacuee's mobility restrictions. Furthermore, retired participants tend to stay with their family whereas they are less likely to choose home, which is not surprising because older adults typically rely on their family members for emergency evacuation. The results also suggest that housing type plays an important role in evacuation destination choice. That is participants who live in houses tend to return home or shelter in their place whereas those who live in apartment and condominium are more likely to opt for shelters or hotels as their destination. Positive sign of population density in utility functions of shelter and family indicates that these destinations in areas with higher population densities (e.g., metropolitan areas) are more attractive to evacuees. Similar findings can be found in Cheng et al. (2008) for selecting to stay with family as evacuation destination.

Moreover, variables representing the characteristics of the emergency event significantly affect the evacuation destination choice. Per results, participants are less likely to return home if an evacuation order has been issued by the government but they are more willing to opt for shelters. On the same note, participants who are experiencing events associated with high risks tend to take refuge in hotels and shelters where medical assistance is usually provided. This finding is in line with previous studies suggesting that public perceptions towards shelters are associated with the availability of food, water, and basic medical facilities (Sadri, Ukkusuri, and Murray-Tuite 2013; Smitherman and Soloway-Simon 2002).

Finally, it was found that distance significantly affects the evacuation destination choice. The results indicate that long distance evacuation tours (greater than 50 miles) are more likely to associate with selecting family as evacuation destination. Further, increasing the distance leads to reducing the probability of selecting home and shelters. Similar results are found in Mesa-Arango et al. (2013) in the context of hurricane evacuation.

Turning to the departure time decision, the results show that participants with high school degree or less tend to evacuate in later times which in line with findings of previous studies on evacuation timing (see, for example, Hasan et al. 2013). Positive signs of the variable representing participants with disability suggests that they are associated with later evacuation departure times. This can be because of their need for more preparation time, mobility restrictions, and reliance on others to evacuate. We also found that the higher the household size of the evacuees, the longer it takes for them to evacuate.

As expected, participants who have received the government evacuation order tend to depart sooner to take refuge in shelters or hotels compared to those who have received a nonmandatory seek shelter order. These findings are

similar to those from Hasan et al. (2013) in the context of hurricane evacuation where they stated that this variable may capture the severity of the event. On the same note, low risk of an emergency event leads to later departure times for trips destined to home or family.

It was also found that trip- and tour-related variables significantly influence the timing of evacuation. According to Table 8-3, participants tend to depart sooner if their final destinations are associated with travel distances longer than 30 miles and travel times greater than 40 minutes. The results also suggest that increasing the number of stops in the evacuation tour advances the departure time. Trip purpose is also confirmed to be influential. As expected, respondents who stated that they would first pick up their child and then evacuate to a shelter or a hotel tend to depart very soon. Participants who prefer to wait to be picked up by their family members tend to evacuate in later times. These variables are of great importance in the case of no-notice emergency events since household members are possibly dispersed throughout the network in daytime. The diversity of household members may result in additional trips (e.g., picking up family members) in the network, which can conflict with the evacuation procedure by adding extra trips in either the direction or the opposite direction of the expected routes (Liu, Murray-Tuite, and Schweitzer 2012; Zimmerman, Brodesky, and Karp 2007). Failing to consider these additional trips may result in underestimation of travel time that can ultimately lead to higher number of fatalities during emergencies.

Moving to the parameters of the joint modeling structure, the significance of the copula parameters confirms the existence of unobserved common factors in destination and departure time choices which, if ignored, can lead to inconsistent estimates. Furthermore, the significance of the scale parameters, which represent the variance of the error terms in continuous departure times, indicates the considerable effect of unobserved factors on departure time for each destination. To better show the dependency structure of destination and departure time choices, the Kendall's τ measure of dependency was calculated and is presented in Table 8-3. This measure of dependency (τ) transforms the copula parameter (θ) into a number between -1 and 1 (Bhat and Eluru 2009) and can be derived as follows:

$$\tau = 1 - \frac{4}{\theta} \left[1 - \frac{1}{\theta} \int_{t=0}^{\theta} \frac{t}{e^t - 1} dt \right], \quad -1 \leq \tau \leq 1 \quad (10)$$

The negative sign of the resulted Kendall's τ indicates that the unobserved factors that increase the propensity to choose a destination tend to increase the departure time. Furthermore, the magnitude of the estimated Kendall's τ for shelter is less than those for other destinations, which demonstrates that evacuees who decide to take refuge in a shelter, are more likely to start their trips sooner compared to other destinations.

Conclusions

Although behavioral analysis of people's response to advance-notice emergency events has been extensively addressed in the literature, only a few studies have focused on no-notice emergencies. Furthermore, modeling joint decisions in the context of these events to capture their interrelated decision mechanism is another potential gap in the literature. To tackle these issues, we presented a joint discrete-continuous model of destination and departure time choices during no-notice emergency events using an internet-based stated preference survey conducted in Chicago. These two decisions are of great importance because they directly impact the spatial and temporal distribution of traffic in the network in case of emergency events. Understanding evacuee behavior towards these decisions can lead to development of effective policies to manage the evacuation-induced traffic in case of these events and ultimately reduce economic damage and loss of life.

The proposed joint model consists of a multinomial logit model to estimate the destination choice and an accelerated hazard formulation to estimate the departure time of the evacuation. The results confirmed that a wide range of demographic (e.g., disability, education level, housing type, and employment status), land-use (e.g., population density), characteristics of the event (e.g., type of the government order and event's severity and risk) and travel-related variables (e.g., distance, travel time, number of intermediate stops, trip purpose) are influential in evacuee decision behavior during no-notice disasters.

The significance of copula and scale parameters in the proposed joint structure confirms that there exist unobserved factors between the two attributes which, if ignored, can lead to inconsistent estimates. Furthermore, comparison of estimated Kendall's τ measures indicates that the participants who select shelter as their final destination tend to start their trip sooner than others.

This study has several potentials for future research directions. First, the model can be expanded to account for unobserved heterogeneity in the dataset by incorporating random parameters or latent class modeling approaches. Also, the modeling framework can be expanded by developing a joint model that considers the correlation of other evacuation attributes such as mode choice with these two dimensions. Furthermore, applying other joint modeling techniques and comparing their results with the employed copula approach would be informative about their performance. Finally, all models can be used in a large-scale microsimulation model to develop a policy-sensitive framework that captures the dynamics in evacuees' responses with respect to traffic conditions of the network.

Section 9

All-Hazard Emergency Events for Transit Response Case Studies⁹

The U.S. Census Bureau confirmed that the estimated population of Chicago in 2016 was 2,704,958, ranked as the third largest city in the U.S. just behind New York (8,537,673) and Los Angeles (3,976,322). The Chicago metropolitan area, also named as Chicagoland, refer to an area that includes the city of Chicago and surrounding suburbs; the population is around 9.7 million. The Chicago Metropolitan Statistical Area (MSA) was originally designated by the U.S. Census Bureau in 1950, which covers Cook, DuPage, Kane, Lake and Will counties in Illinois and Lake County in Indiana. Later, surrounding counties that met Census criteria were then added to the MSA; now, the Chicago MSA is defined by the U.S. Office of Management and Budget (OMB) as the Chicago-Naperville-Elgin, IL-IN-WI Metropolitan Statistical Area and is the third largest MSA by population in the country.



Figure 9-1 Map of Chicago metropolitan area

Figure 9-2 shows the population distribution and guides for evacuations in emergency situations. Specifically, Figure 9-2 shows the southern and northwestern sides of Chicago with more residents, and several downtown Chicago areas with relatively high population concentration. All hazard events within these areas may cause severe consequences. Figures 9-3 through 9-7 display the distribution of “special needs” populations, including those with poor English proficiency, low median retirement income, residents age 19 and under, and residents age 65 and older. Evacuation in those areas may attract more attention. Extending to the Chicago metropolitan area, people living in the northern suburban areas along Lake Shore are relative affluent; comparatively, residents on the southern side are more likely to have lower incomes. According

⁹ Authored by Zongzhi Li, Yongdoo Lee, Yunseung Noh, Lu Wang, and Ji Zhang, ITT.

to the 2000 U.S. Census data, within Chicagoland, the poverty rate of counties from the highest to the lowest are Cook (14.5%), Kane (7.4%), Lake (6.9%), Will (6.7%), DuPage (5.9%), and McHenry (3.7%).

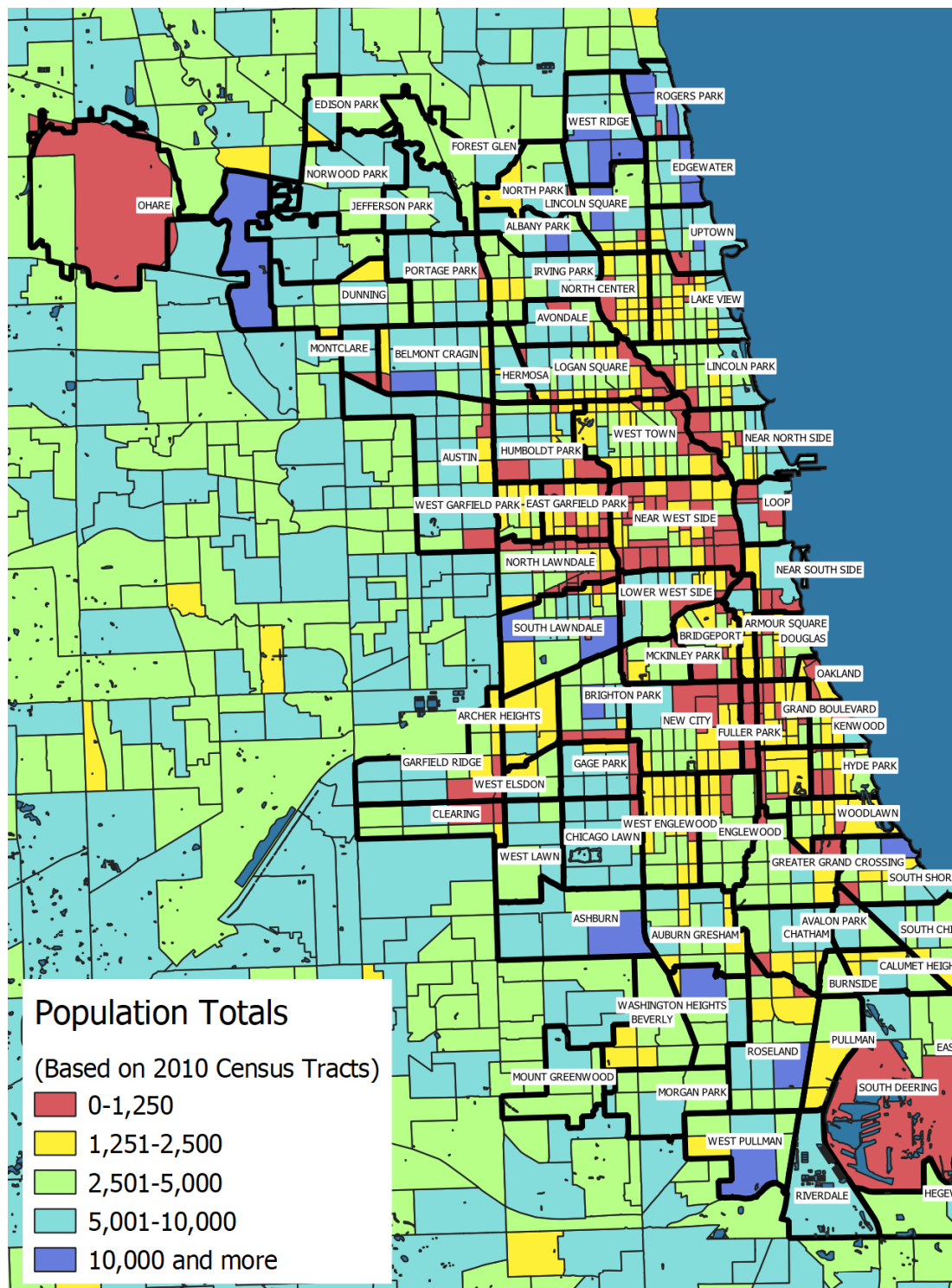


Figure 9-2 Residents across Chicago

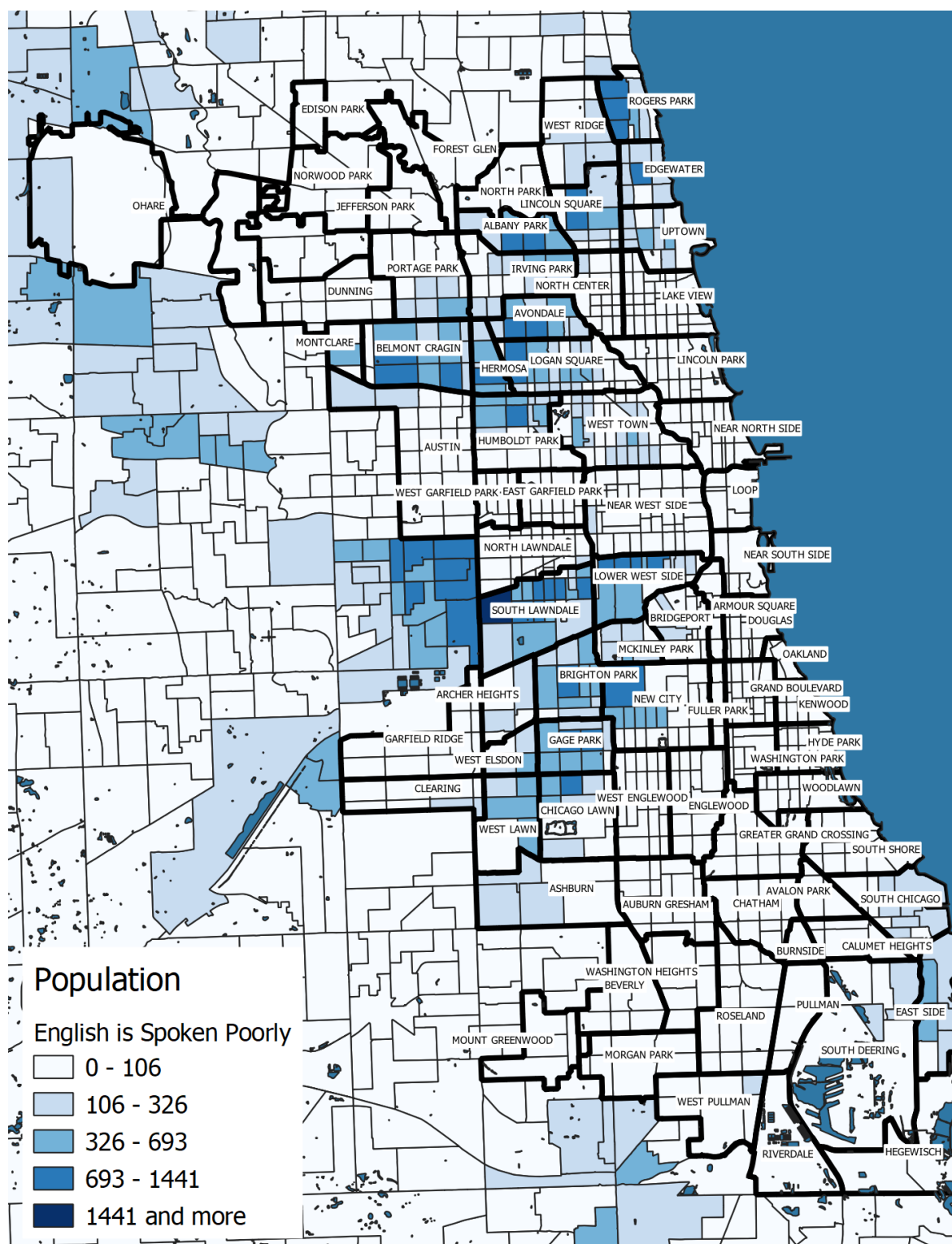


Figure 9-4 Households where English poorly spoken

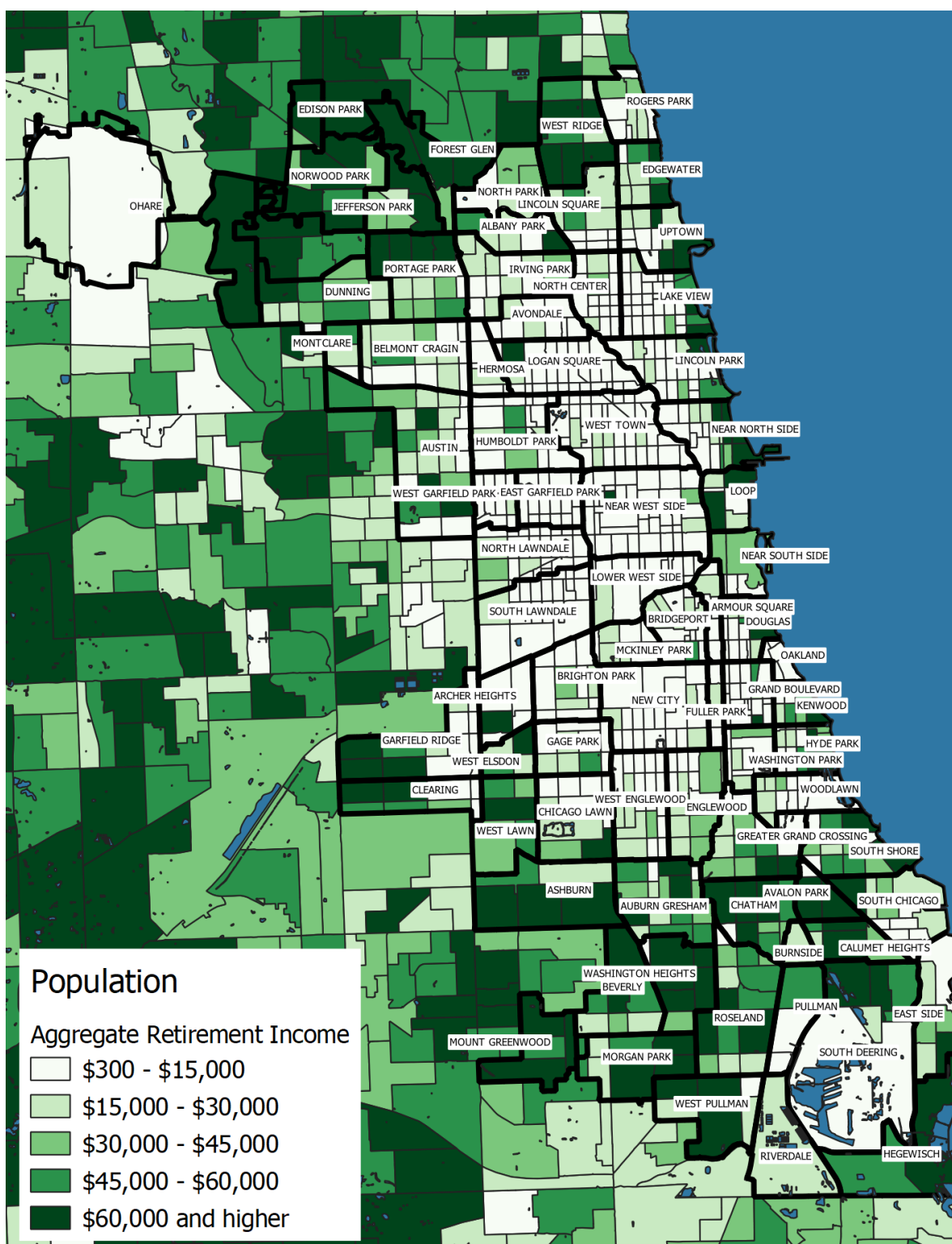


Figure 9-5 Aggregate retiree income

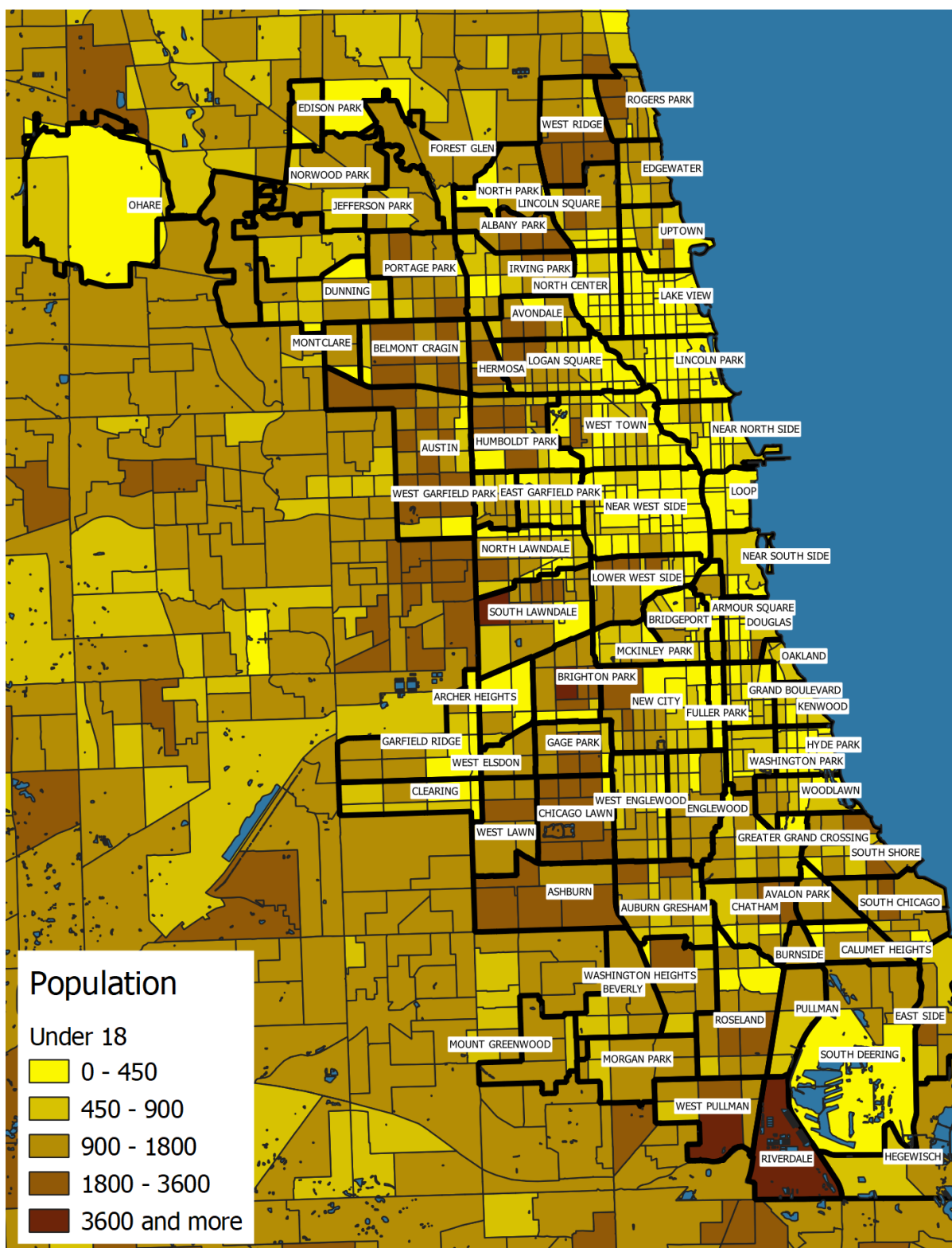


Figure 9-6 Residents age 18 and under

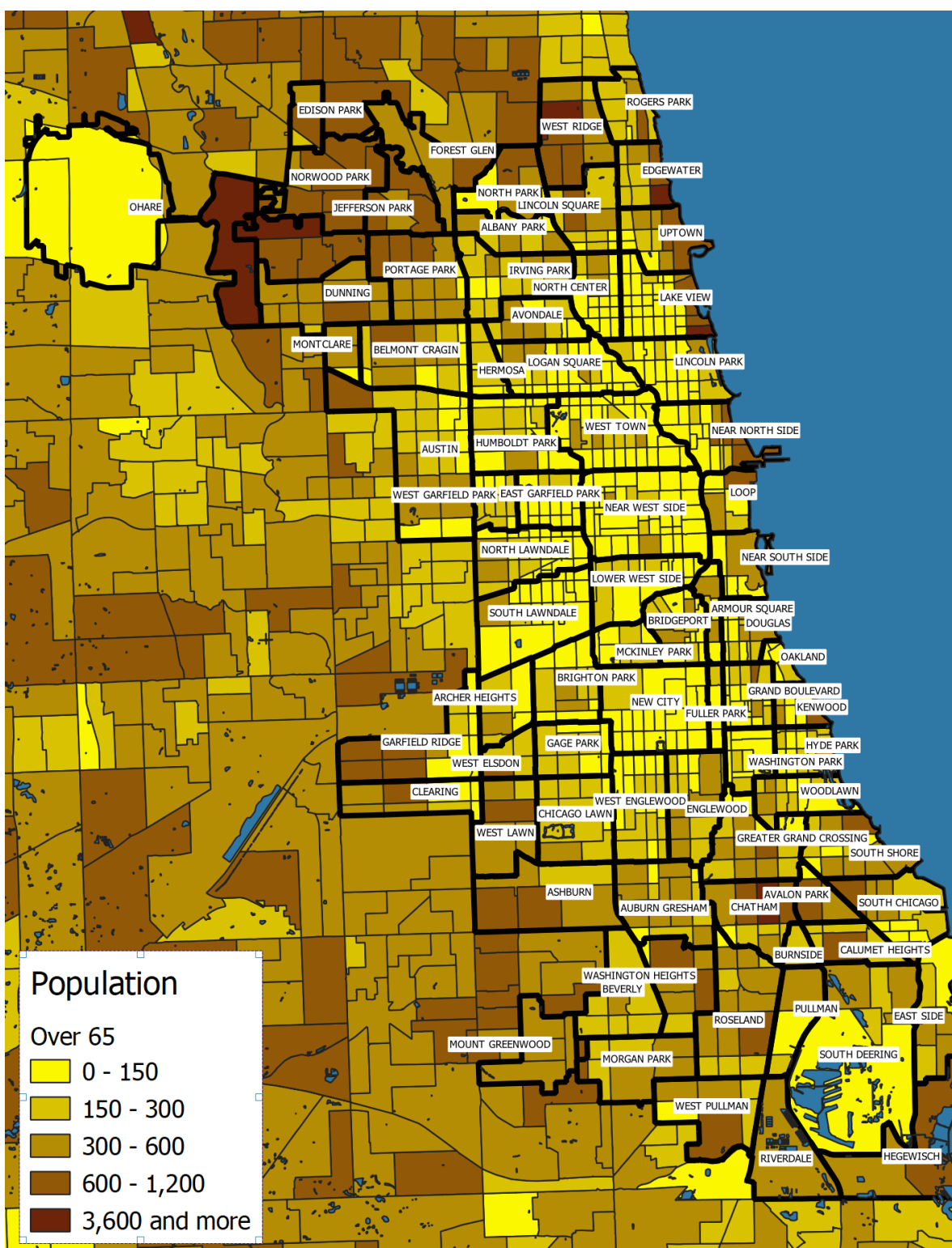


Figure 9-7 Residents age 65 and older

Case 1: PACE Bus Route Emergency from Bomb Threats

Two common forms of terrorist bomb threats for which transit systems could play an essential role for evacuation are on-board and out-board bomb threats. In the case of an on-board bomb threat, one or more terrorists might board one or multiple PACE buses and threaten to detonate bombs. The bomb explosions might be triggered simultaneously with synchronized threats or progressively with leveraged threats. On-board terrorist activities normally are a direct danger to humans, with severity levels depending on the number of on-board passengers, which vary across time-of-day commuting. It is essential to prepare for a worst-case scenario, where a perpetrator attempts to cause maximum damage. Therefore, it was assumed that the peak hours during which PACE buses are serving the maximum number of riders are the potential target hours for terrorists, and emergency evacuation plans must be prepared accordingly for passengers on the attacked buses. As such, other buses around the affected area might be used to help with evacuation if needed, or they can make a detour to minimize damages of the terrorist attack.

For out-board bomb threats, suburban recreational centers, shopping malls, or transit stations with dense population might be terrorist attack targets. Similar to an onboard threat, it could be an isolated threat or multiple threats to several locations simultaneously. Transit could play an essential role in helping in these emergency situations to evacuate victims and people in surrounding areas to mitigate damage consequences. Paratransit vehicles and smaller vans nearby might also be used to conduct evacuation in narrow spaces where large-sized PACE buses cannot access.

The specific evacuation strategy will be different depending on which of these two emergency cases occurs; however, it follows the same process. As such, once the emergency case occurs, the impact factors and severity level need to be assessed first. The countermeasure library will then be searched to retrieve an evacuation strategy accordingly. In the case where the evacuation strategy retrieved from the simulated countermeasure library does not precisely match with the real case emergency, the operative decision support tool featured on the POLARIS EvacPlan tool will enable emergency responders/transit operators to modify certain variables and adjust for the countermeasure of the real case.

It is also noted that special-needs populations require particular attention during evacuation. Populations without private vehicles or vulnerable people who cannot access private vehicles during the emergency, also known as the transportation disadvantaged population, should also be considered as a special-needs population in the evacuation plan.

Bomb Threat Activity

Bomb threats/ scares are threats designed to detonate an explosive or incendiary device to cause property damage, injuries, or deaths. These physical damages are mostly caused by bomb fragmentations, heat, and blast waves. Threats can be made when an explosive or incendiary device actually exists, but sometimes they are only verbal or written without physical device. Nevertheless, every case should be taken seriously and reacted accordingly. Due to the severe consequences caused by bombs, it is stated by law that all bomb threats are assumed to be with bad intent, and even a false threat can incur a fine up to \$5,000 and 5 years in prison. In several U.S. states, the punishment is even more strict.

In general, bombs using for bomb threats are different variations of homemade bombs. Homemade bombs refers to improvised explosive devices (IEDs) that are constructed and deployed in ways other than in conventional military actions. Due to their static nature, IEDs are commonly deployed as roadside bombs. Another variation of IEDs is vehicle-borne improvised explosive devices (VBIEDs), so-called car bombs or truck bombs. VBIEDs are actually IEDs carried by any transportation vehicle. The sizes, shapes, and materials may vary among all kinds of bombs.

Types of Bomb Threats

A bomb threat can occur with or without a prior notification. Bomb threats with prior notification normally are used when a terrorist want to stir chaos beyond the affected range, draw attention from the media, or use the bombs as a leverage tool. These threats may be received via telephone, written message, electronic device, social media, email, or in person. On the other hand, if the terrorist intent is to disrupt social and business activities and cause as much damage as possible, the threats may not be delivered prior to the bomb detonating.

Types of Bombs

Most of the physical damage from bombs is caused by bomb fragmentation, heat, and blast waves. Therefore, explosive capacity is one of the most essential attributes when comparing various bomb types. The National Counterterrorism Center published a guideline for bomb threat stand-off distances, as shown in Table 9-1. It is noted that the table should be used only as reference information; in reality, radiation from an affected area caused by certain bomb types varies greatly depending on the construction of a building or obstacles at an outdoor location.

Table 9-1 Bomb Stand-off Distances

Threat Description	Explosives Capacity ¹ (TNT equivalent, lbs)	Building Evacuation Distance (ft) ²	Outdoor Evacuation Distance (ft) ³
Pipe bomb	5	70	850
Briefcase/ suitcase bomb	50	150	1,850
Compact sedan	500	320	1,500
Sedan	1,000	400	1,750
Passenger/ cargo van	4,000	600	2,750
Small moving van/ delivery truck	10,000	860	3,750
Moving van/ water truck	30,000	1,240	6,500
Semi-trailer	60,000	1,500	7,000

¹ Based on maximum volume or weight of explosive (TNT equivalent) that could reasonably fit in a suitcase or vehicle.

² Governed by the ability of typical US commercial construction to resist severe damage or collapse following a blast. Performances can vary significantly, however, and buildings should be analyzed by qualified parties when possible.

³ Governed by the greater of fragment throw distance or glass breakage/falling glass hazard distance. Note that pipe and briefcase bombs assume cased charges that throw fragments farther than vehicle bombs.

PACE Bus Major Stops and Stations

As a division of Chicago Regional Transportation Authority (RTA), PACE has served the commuting demands of suburban residents in Chicagoland since 1983. Since then, PACE has served 40 million riders and continues to build an environment-friendly and ridership-convenient service system. All PACE buses are equipped with bike racks and are wheelchair accessible during all operation hours. The first fleet of diesel-electric hybrid buses was introduced in 2011, and the first fleet of compressed natural gas (CNG) buses was operational in 2015, which mainly serving the southern suburb residents.

The operation range of PACE buses includes six Illinois counties—Cook, Lake, Will, Kane, McHenry, and DuPage—and some areas in Indiana. On average, the routes of PACE buses are much longer than CTA bus routes due to the broader range and longer distances between stations. PACE also coordinates various dial-a-ride services, usually sponsored by various municipalities and townships, and provides the nation's largest paratransit service, with approximately 17,000 daily trips on paratransit, dial-a-ride, and ADvAntage vanpools. Since 2014, CTA and PACE have provided Ventra as a unified payment system, whereas Metra keeps its fare system separate.

Many of PACE's route terminals are located at CTA rail and bus terminals and Metra stations. During rush hours, PACE buses are allowed to use shoulder of expressways to shorten travel time. Figure 9-8 illustrates the stops of PACE

buses. Major stops are available on PACE's official website (<http://tmweb.PACEbus.com/TMWebWatch/MultiRoute>).

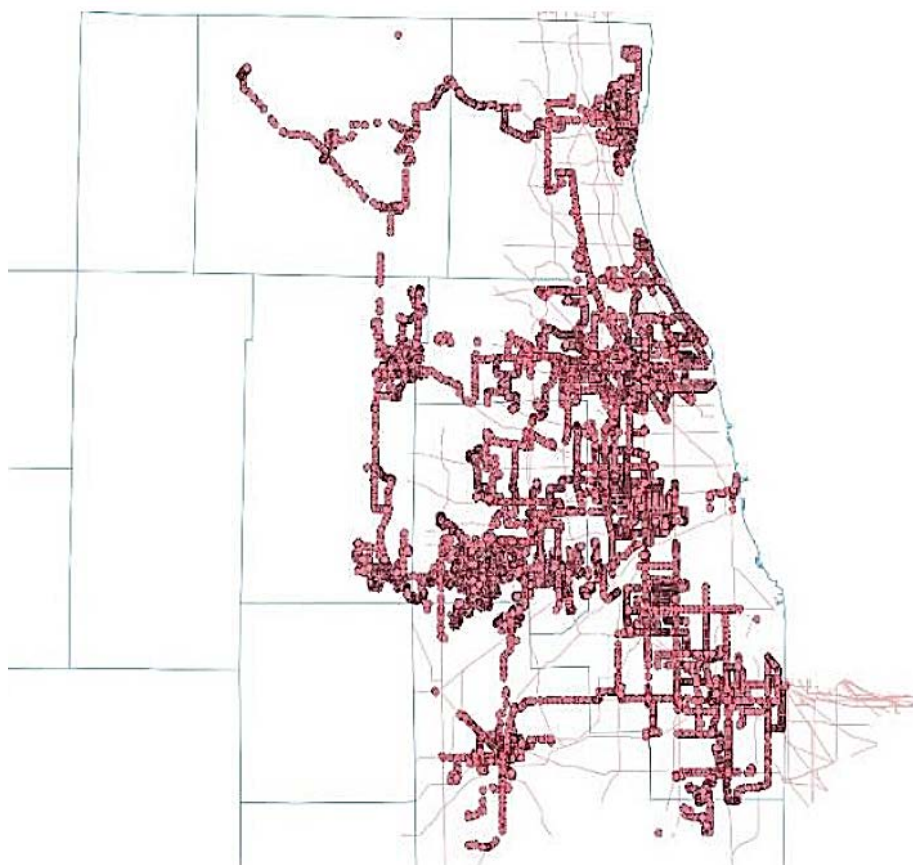


Figure 9-8 *PACE bus stops*

Concentrated Population Locations

Public Schools

Over the past 10 years, the number of terrorist activities targeting educational institutions has increased dramatically. Students and faculty studying and working in those institutions are facing unprecedented danger from terrorist activities. According to data published by the Global Terrorism Database, since 2004, a sharp uptick in terror attacks has been recorded (Figure 9-9). Figure 9-10 displays all public schools in Chicago for school year 2014/15, which could be potential targets of bomb threats to conduct the case study.

Terrorist Activities (Educational Institutions)

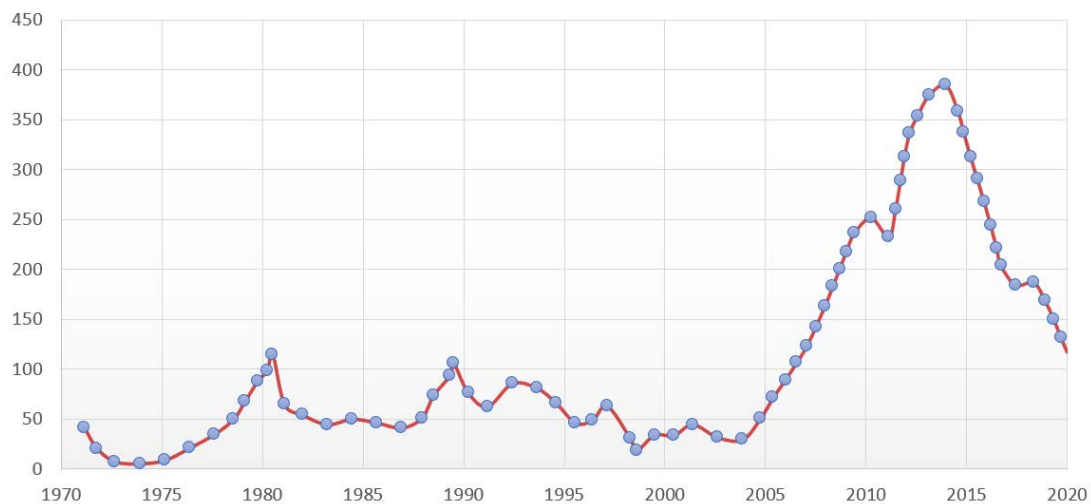


Figure 9-9 Number of terrorist activities targeting educational institutions in world (1970–2020)

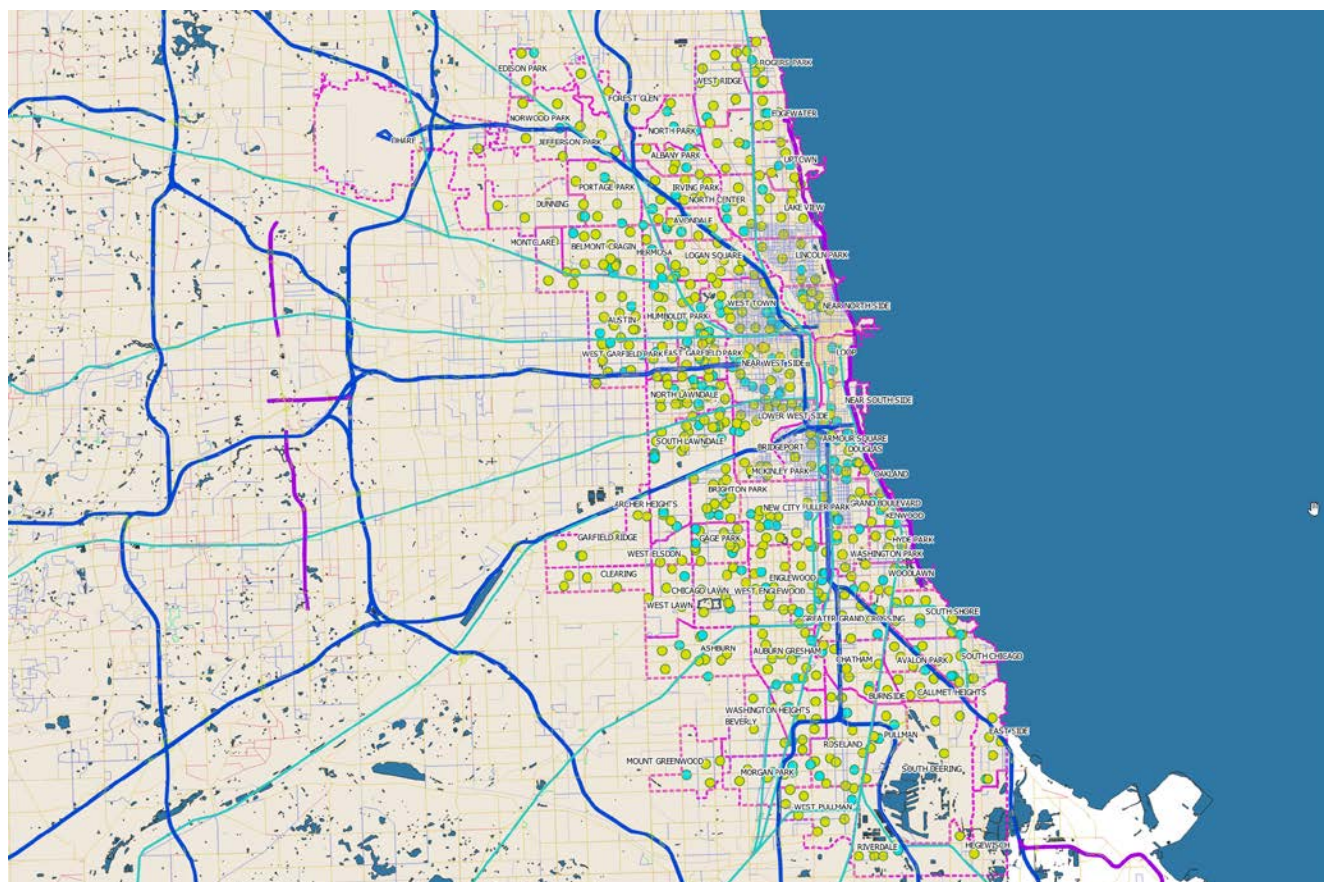


Figure 9-10 Locations of educational units in Chicago Public School District

Hospitals

Hospitals can be another target of bomb threats, and the consequences may be severe, as people being treated might have limited moving ability. A specially-prepared evacuation plan is required to improve evacuation efficiency. Figure 9-11 depicts major hospitals in Chicago.

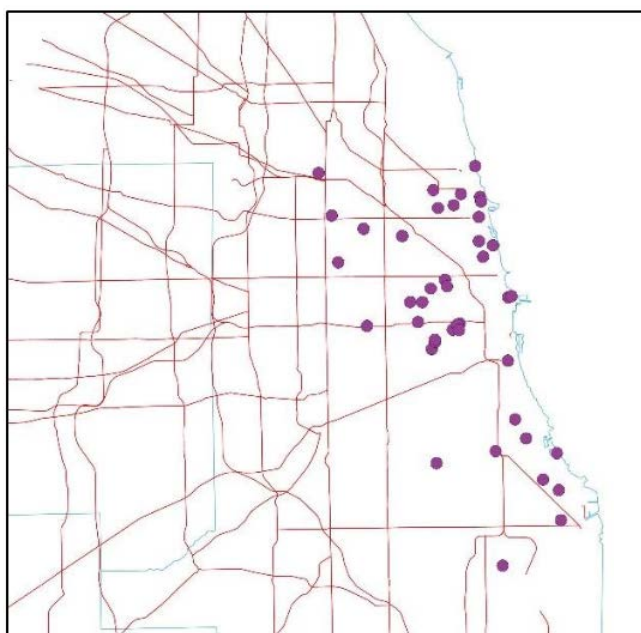


Figure 9-11 Major hospitals in Chicago

Shopping Malls

Shopping malls are another population-concentrated area that may suffer from bomb threats. The Bureau of Justice Assistance of the U.S. Department of Justice noted several types of suspicious activity prior to a terrorist activity:

- Efforts to picture or video the shopping center
- Unusual inquiries about security procedures
- Tests of security responses
- Distribution of extremist literature and graffiti
- Unattended packages, bags, or vehicles
- Thefts of official vehicles, uniforms, identification, and access cards
- Attempts to access restricted areas
- Extremist attacks on other malls
- Other loitering, vandalism, or suspicious activities around the mall

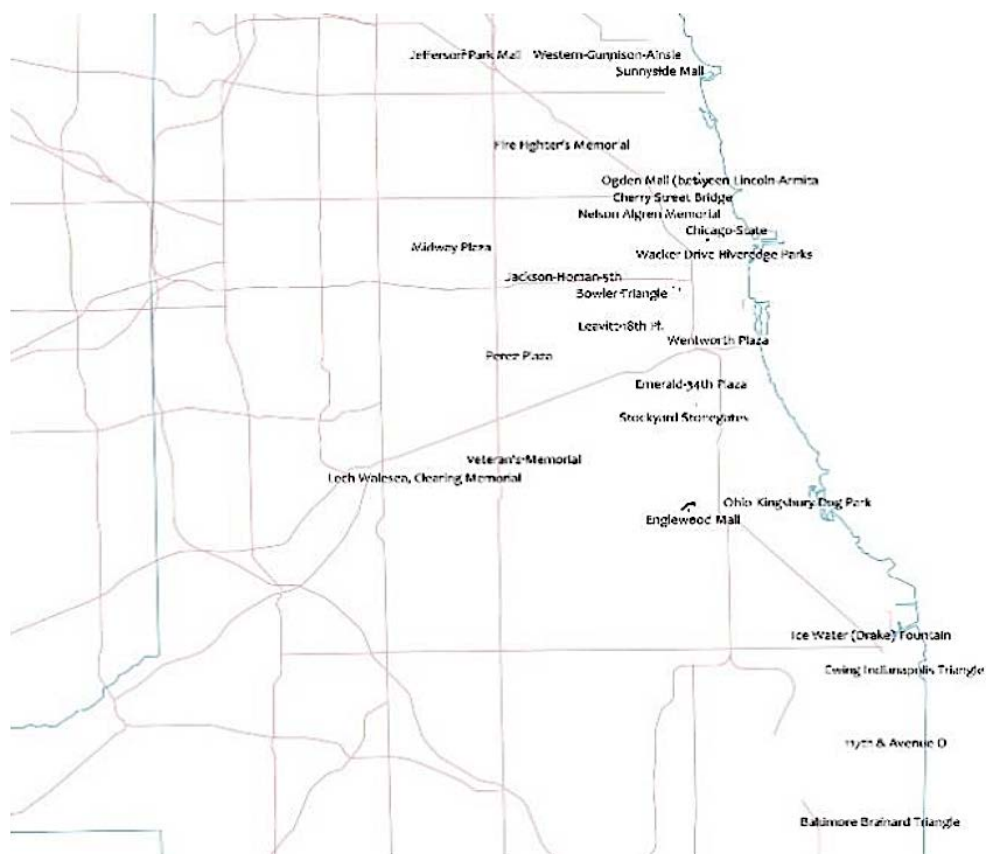


Figure 9-12 Major malls and plazas in Chicago

On-board Bomb Scenario

This scenario considers a PACE bus receiving a bomb threat on a platform during operation in transit facilities.

Selection of Bomb Attack Location and Time

In this case, the perpetrator tends to cause the maximum damage at a minimum cost. Therefore, in the development of this scenario, bus routes with relatively high ridership should be considered as potential targets. A PACE bus ridership summary revealed that route 270 along Milwaukee Avenue is the one of most ridership-concentrated routes, as shown in Figure 9-13. Route 270 serves as a CTA connector in the PACE bus service system, connecting one CTA train station (Jefferson Park of the Blue line), one Metra station (Jefferson Park of UP-NW), and 10 CTA bus routes (91, 85, 92, 88, 81, 56, 86, 85A, 68, 81W). Jefferson Park serves as the transit hub in the northwest suburban area. A large number of passengers use it to transfer among Metra and CTA train and bus services. Moreover, the CTA Blue line train connects O'Hare International Airport to the Chicago Central Business District (CBD), moving many flight passengers, especially those who fly domestically. Route 270 travels along Milwaukee

Avenue mostly in the village of Niles, which has been making extensive efforts to improve the function and aesthetics of the Milwaukee Avenue corridor from the perspective of a Transit-Oriented Development (TOD) Plan and Transit Improvement Plan since 2004. Considering the pivotal role that the PACE route 270 plays from the regional transit system, it was selected to be the case study route.

Generally, ridership on weekdays is always higher than on weekends. This is also reflected by ridership statistics. For example, in December 2018, the average weekday, Saturday, and Sunday or holiday ridership was 2,550, 1,601, and 1,003 per day, respectively. Further, on a typical weekday, transit service during peak hours always carried the highest amount of trips.

Therefore, a bomb incident occurring during the AM peak and/or PM peak was considered for this scenario.



Figure 9-13 PACE bus Route 270 area map

Scenario Development

The on-board bomb scenario can be subcategorized into two cases, depending on whether a prior notification is received or not. Terrorists may send a threat to the agency and use the on-board bomb as leverage. Conservatively, the only usable information is that the bomb is equipped on at least one bus of route 270, and any bus could be a possible target. Also, as the bomb can be detonated remotely and the time is unpredictable, the affected area can be anywhere

along the route within a certain radius. This makes the stand-off area a buffer zone along the route. From the perspective of the evacuation team, any human activity within this area should be evacuated as soon as possible to minimize damage.

Affected Transportation Supplies

A briefcase/ suitcase bomb was assumed to be used in this scenario, so a 2,000 ft stand-off distance was used, which is slightly larger than 1,850 ft. Figure 9-14 illustrates the stand-off area of PACE route 270. It covers 30 traffic analysis zones (TAZs) and will roughly affect 25,512 households with 63,975 residents. There are 16 schools, 5 hospitals/nursing centers, and 11 shopping plazas within the range. It will affect 548 transit stops/stations including 90 CTA bus stops, 1 CTA train station, 2 Metra stations, and 455 PACE bus stops. Further geographic analysis reveals the detailed transit services affected, as shown in Table 9-2. In terms of surface transportation infrastructure, the range covers 141 major intersections and intersects 150 major roads, 57 minor roads, 18 ramps, and part of I-90/94.

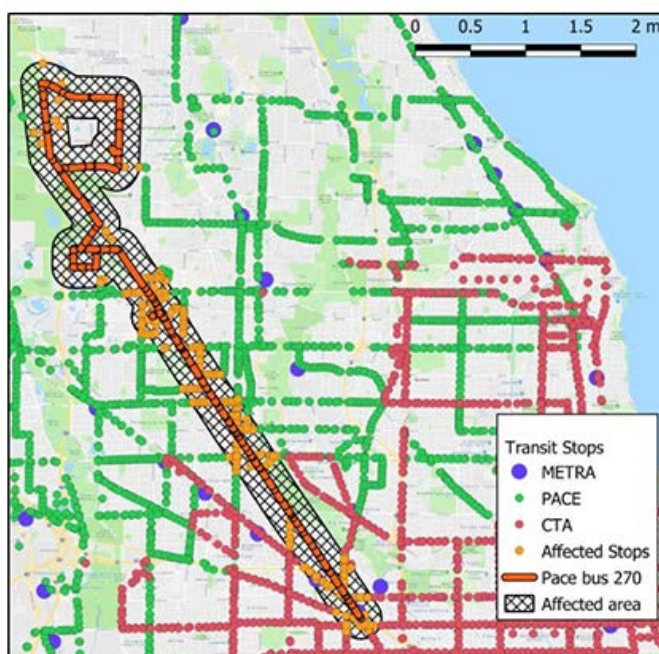


Figure 9-14 PACE bus Route 270 area map

Table 9-2 *Transit Services Expected to be Affected*

Agency	Route	Number of Patterns Affected	Number of Trips Affected
CTA	56	4	157
CTA	68	4	95
CTA	81	2	250
CTA	81W	2	80
CTA	85	2	189
CTA	85A	2	78
CTA	86	5	112
CTA	88	4	91
CTA	91	3	156
CTA	92	3	155
CTA	X98	1	1
CTA	Blue line	9	370
Metra	UP-NW	22	45
PACE	208	11	60
PACE	210	8	34
PACE	225	2	12
PACE	226	13	49
PACE	240	2	33
PACE	241	6	20
PACE	250	4	102
PACE	270	6	125
PACE	272	7	48
PACE	290	12	114
PACE	410	4	38
PACE	411	8	44
PACE	412	2	16
PACE	423	6	46
PACE	619	2	6
PACE	620	2	4
PACE	623	2	5

As long as the threat is not eliminated or narrowed down to a smaller area, all people within the affected area should be evacuated to the nearest shelter with prior notice and instructions, including shelter locations and evacuation vehicle pickup locations. In this scenario, it is assumed that 10% of the residents need to be evacuated using the transit, and the rest will drive private vehicles. The pickup locations for each community will be located properly to minimize total evacuation

time. Schools and hospitals are population-concentrated public facilities with more demand generally, each of which should have at least one pickup location. Patients in hospitals are generally travel-disadvantaged, which requires more evacuation resources. Most people go to a shopping plaza via private vehicle, so there is minimal need to dispatch buses if sharing a ride is encouraged.

At the time the threat is received, every bus serving route 270 will do a preliminary search for any suspicious package/people. In the meantime, on-board passengers need to get off the bus and be directed to the nearest pickup location for evacuation. Meanwhile, passengers waiting for transit services in the affected area will be notified to leave the area by any means. In-service buses that are about to drive into the affected area should immediately terminate service by dropping off current on-board passengers to the nearest shelter and serve as evacuation vehicles afterwards. For both Metra UP-NW line and CTA blue line train services, before knowing the bomb threat will not jeopardize operations, the service will be temporarily shut down, notifying the on-board passengers of the situation. After the affected area is narrowed down, knowing that train services can be operated safely, both the Metra UP-NW and CTA blue line can serve as a high-efficiency evacuation mode by using Jefferson Park as a major evacuation hub.

In terms of the surface transportation network, the in-range segments and intersections will be closed accordingly. Vehicles will be asked to leave the area to allow space for service vehicles including evacuation vehicles, firetrucks, ambulances, and so forth.

The scenario is complicated because of the high level of uncertainty brought by limited information. The affected area may shrink depending on how much information gathered as time passes, and the evacuation strategy may be updated accordingly.

Another case of the on-board bomb scenario is that the bomb is detonated without any prior notification. This case is a pure point event in terms of space and time. The geographic pattern is very similar to the off-board bomb scenario. Therefore, more details are revealed in the offboard scenario built.

Off-Board Bomb Scenario

This scenario is when there is a bomb threat and the transit service can be used to evacuate the immediate premises and nearby vicinity for minimal damage. A dense suburban transportation center was selected as a target location.

Selection of Bomb Attack Location and Time

The Jefferson Park Transit Center is an intermodal passenger transport center in the northwest suburbs of Chicago and serves as a CTA train and Metra station as well as a bus terminal. The Metra Jefferson Park railroad station is located on

the first-floor platform level. It is on the Union Pacific/Northwest Line and is 9.1 miles away from Ogilvie Transportation Center in Downtown Chicago, the inbound terminal of this Line. The CTA Blue line Jefferson Park station is located on the B1 platform level, roughly 25 minutes away from the Chicago loop. The ground level of the Jefferson Park Transit Center serves as a terminal for 13 PACE/CTA bus routes in total.

Bombs can be detonated at any time, but they can cause catastrophic damage during rush hours on a typical weekday when the travel demand is the highest. After detonation, it may take days or even weeks to restore affected services depending on the severity level. Therefore, this scenario was simulated to occur during morning rush hour on a weekday.

Scenario Development

The off-board bomb scenario also has two cases, depending on whether a prior notification is received or not. If a prior notification is received, the evacuation team needs to dispatch vehicles to evacuate people in that vicinity. Meanwhile, some transit services and a part of the network will be changed or even shut down accordingly. If the bomb is detonated without any notice, the evacuation team also needs to conduct the same workflow. Therefore, the two cases can follow an identical evacuation strategy in a holistic way.

Possible bomb types can be complex, as there is no space limitation for carrying a bomb in this case. For example, the bomb can be carried inside a briefcase/suitcase and dumped in a dust bin in the station, or it can be a large bomb carried by a small van parked in a parking lot. In this scenario, the bomb type was selected to be carried by a small moving van parked in the parking lot, where the outdoor stand-off distance is 3,750 ft.

Affected Transportation Supply

Figure 9-15 illustrates the stand-off area of the Jefferson Park Transit Center. It covers 4 transportation analysis zones (TAZs) and will affect 5,753 households with 14,487 residents. There are 6 schools, 1 hospitals/nursing centers, and 5 shopping plazas within this range. It affects 111 transit stops/stations, including 90 CTA bus stops, 1 CTA train station, 2 Metra stations, and 18 PACE bus stops. Table 9-3 shows details of the affected transit services. In terms of the surface transportation infrastructure, the range covers 141 major intersections and affects 28 major roads, 5 minor roads, 9 ramps, and part of I-90/94.

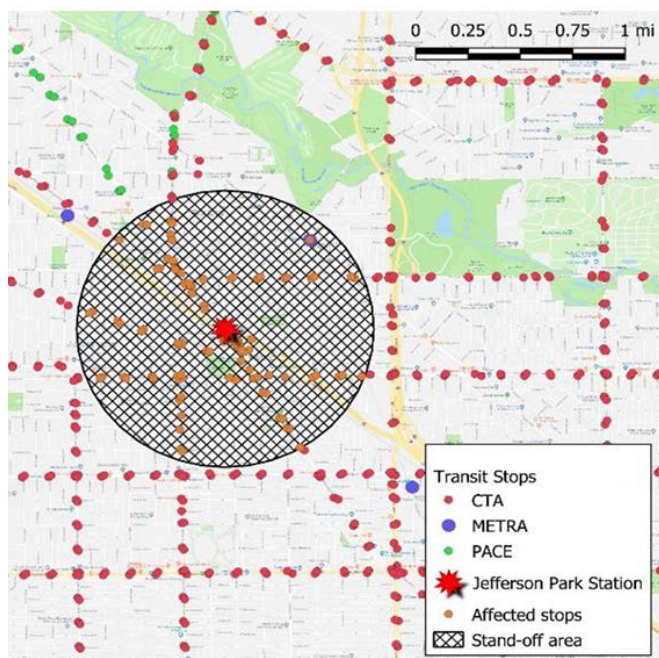


Figure 9-15 PACE bus Route 270 area map

Table 9-3 Transit Services Expected to be Affected

Agency	Route	Number of Patterns Affected	Number of Trips Affected
CTA	56	4	157
CTA	68	4	95
CTA	81	2	250
CTA	81W	2	80
CTA	85	2	189
CTA	85A	2	78
CTA	88	4	91
CTA	91	3	156
CTA	92	3	155
CTA	X98	1	1
CTA	Blue	9	370
Metra	MD-N	18	45
Metra	UP-NW	22	45
PACE	225	2	12
PACE	226	13	49
PACE	270	6	125

At the time the threat is received, the agency needs to notify the field transit operator of the emergency and guide them to search for any suspicious activity. In the meantime, the Metra and CTA Blue lines will pause service and post the information, notifying all passengers including those who want to use the service in the next few hours. Since the ground level of the Jefferson Park Transit Center is used as a terminal for multiple bus routes, it can be used as a pickup spot to evacuate on-platform passengers. The buses will transport these passengers to the nearest shelters outside the stand-off area. In-service buses heading to the affected area should drive to the nearest shelters directly and serve as evacuation vehicles afterwards.

For the surface transportation network, the in-range segments and intersections will be closed accordingly. On the highway front, all nearby segments of I-90/94 will be closed, and highway users will be directed to use arterials in the vicinity as alternatives, such as Irving Park Road.

Case 2: PACE Bus Service Shutdown by Des Plaines River Flooding

The PACE bus system will act an important role in emergency scenarios. As the Chicago metropolitan area has rich water resources, flooding records and threats exist every year. Appropriate and practical evacuation strategies and guidelines are required to be developed to ensure efficiency and effectiveness during the evacuation.

Weather data, including precipitation, catchment, and flooding records, will be analyzed for the specific region to determine the case study area. Flooding occurrence chance, impact severity level, and potential consequences are taken into consideration to conduct the case study. Moreover, to make the case study more practical, a demand-responsive transit system with the capability of evacuees and access to the specific area issues were included.

Flooding

Flooding is the overflow of water that submerges land, which is usually dry. Reasons for flooding vary; it can be the overflow of water from natural water bodies such as rivers, lakes, or oceans or artificial structures such as levees and dams. Natural disasters such as storms and hurricanes are another reason for flooding. Huge amounts of water are not the only threat to people and property; moving water with speed and debris in the water contribute to extra damages.

Floods are relative predictable, and protective actions and evacuation plans should be conducted before the estimated time. All transit evacuation routes must be above the estimated flood elevation; potential inundation must be considered. If complete evacuation is not practical, locations of high-ground shelters and safe routes should be noted to the affected population. Attention is

particularly required for recreational areas, as visitors may not be familiar with evacuation routes.

Description of Des Plaines River

As shown in Figure 9-16, the Des Plaines River is 133 miles long; the stream flows between southern Wisconsin and northern Illinois, the longest stream in the Chicago area. Merging with the Kankakee River southwest of Joliet to form the Illinois River, it is a significant tributary of the Mississippi River. The Des Plaines River originated from south of Union Grove, Wisconsin, flows in the south direction, and enters Illinois at Russell. Through Lake and Cook counties, the river turns southwest from Salt Creek, a major tributary, and joins the river from Lyons, Illinois. Between DuPage and Will counties, it runs parallel to the Chicago Sanitary and Ship Canal, which reverses the flow of the Chicago River. Until Joliet, Illinois, it flows to the confluence of Kankakee, the beginning of the Illinois River.

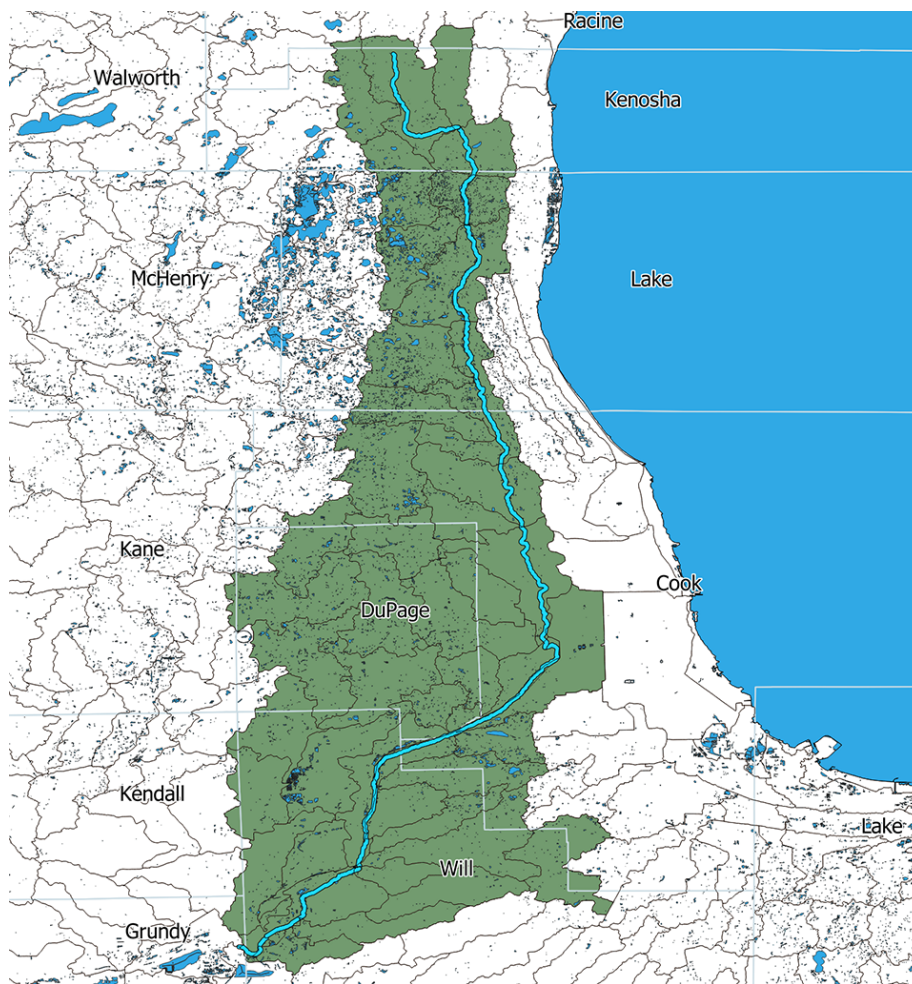


Figure 9-16 *Des Plaines River watershed area*

During wet weather, the Des Plaines River sometimes pours into Mud Lake to the Chicago River rather than to the usual westward direction. Chicago Portage is known as the wetland between the Des Plaines River and the Chicago River. The watershed covers 1,554 square miles in Illinois and 1,320 square miles in Wisconsin. Major streams include Des Plaines River, DuPage River, Chicago Sanitary and Ship Canal, Salt Creek, Mill Creek, Indian Creek, Willow Creek, Lily Cache Creek, Grant Creek, Hickory Creek, and Spring Creek (FEMA, 2014). Most of the watershed of the rural and agricultural areas is in Kenosha, Wisconsin, and Lake and Will, Illinois. The urban and industrial part belong primarily to the greater Chicago metropolitan area.

Flooding of Des Plaines River

Flooding is a major problem of the Des Plaines River; damage is estimated at \$25 million per year along the Des Plaines River in Lake and Cook counties. According to the historical record, maximum flooding occurred in September 1986, causing damage to 10,000 dwellings and 263 business and industrial sites. At least 15,000 residents needed to evacuate, and 7 people lost their lives (Figure 9-17). Total cost exceeded \$35 million, with the transportation systems in the cities along the river suffering severe damages. In the following year, rain in Cook and DuPage counties had damages of \$77.6 million. More than 100 cars, trucks, and buses were stranded on the Eden's Expressway, and 300 vehicles were trapped in intersections soaked by water. Four deaths occurred, and 3,000 homes were damaged. Over 10,000 structures were destroyed in the two years. Major flooding has occurred along the Des Plaines River 15 times in the past 60 years, and more watershed has developed, which increases the risk of potential flooding damage.

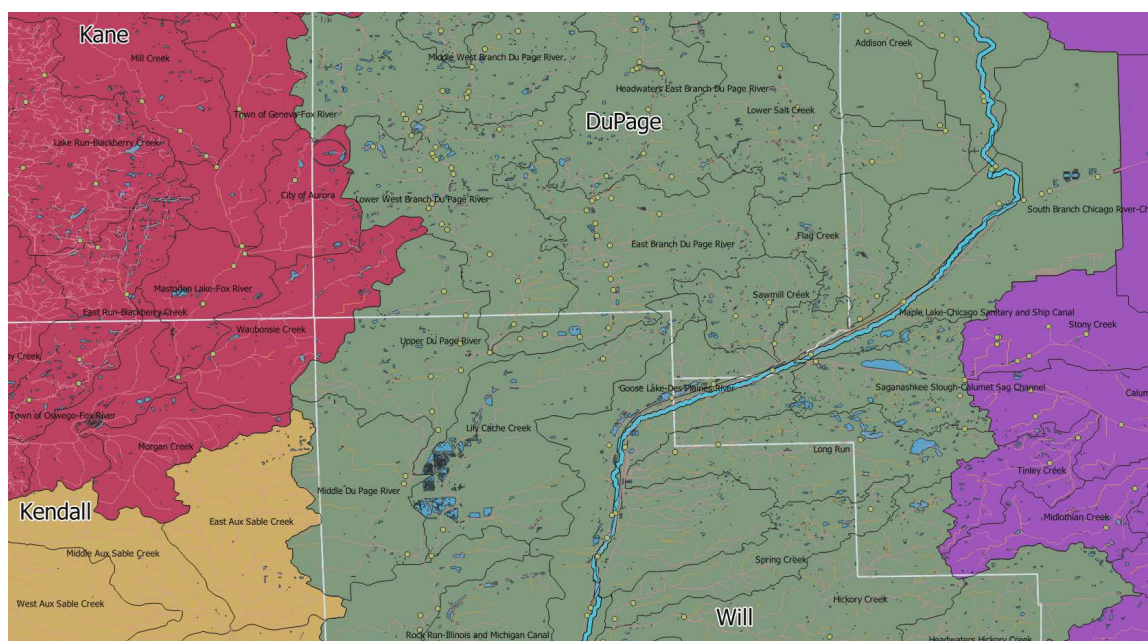


Figure 9-17 *Flooding in 1986*

Flooding Risk Analysis

Flooding is the overflow of an accumulation water that submerges land that is usually dry. Severe flooding threatens lives of humans and causes severe damage to manufactured structures such as dams and buildings. Even mild flooding can impact properties and cause economic loss.

Flooding prediction methods have improved significantly to inform people where a flooding may occur and how to mitigate damages. According to Federal Emergency Management Agency (FEMA), flooding risk refers to the vulnerability estimated by production of the probability of flooding and the consequences of flooding, as below:

$$\text{Flood Risk} = \text{Probability} \times \text{Consequences}$$

Probability is the chance of flooding in a given area. It may vary from year to year due to changes in physical, environmental, and human activity-related factors. Probability prediction accuracy is mainly influenced by the quality of historical data and modeling approaches. Consequences of flooding are the estimation of damages, especially human activities that may result during and after flooding. More residents and more structures may lead to more severe consequences.

A popular flood loss estimation tool is Hazus, developed by FEMA and originally used for earthquake risk assessment. With updating and revising, Hazus is now a powerful tool for hurricane loss estimation as well. Assisted by Hazus, emergency management can conduct flooding risk analysis and evaluate the cost-effectiveness of flooding mitigation. Hazus is refined every time additional reliable data are applied.

Flooding losses are typically expressed as currency, and losses within a particular area attracts more attention. Methodology and reliable data are major factors influencing the quality of final estimation of potential losses. Losses include but are not limit to:

- Infrastructure – Two major types of infrastructure are considered in the estimate—utility systems and transportation systems. Utility systems include electric power, communication, petrol and natural gas, and water reserve systems. Transportation systems include highway, railway, ports, and airport systems.
- Residential properties – All types of residential buildings are included—apartments, townhouses, and houses. Losses are estimated to be the costs of repairing or rebuilding.
- Commercial assets – Building types include retail, wholesale, and parking facilities; repairing and rebuilding cost are estimated to be the losses, and goods and inventory in commercial buildings are also considered.

- Other – Buildings and properties belonging to industrial, agriculture, government, and education sectors are in this category.

Des Plaines River Flooding Map

Figure 9-18 illustrates streams of concern for the northern and southern portions of the Des Plaines River watershed, and Figure 9-19 displays locations of interstate and major highways along the Des Plaines River. Both maps show that the concentrated areas lacking mitigating measures could be potential risk areas.

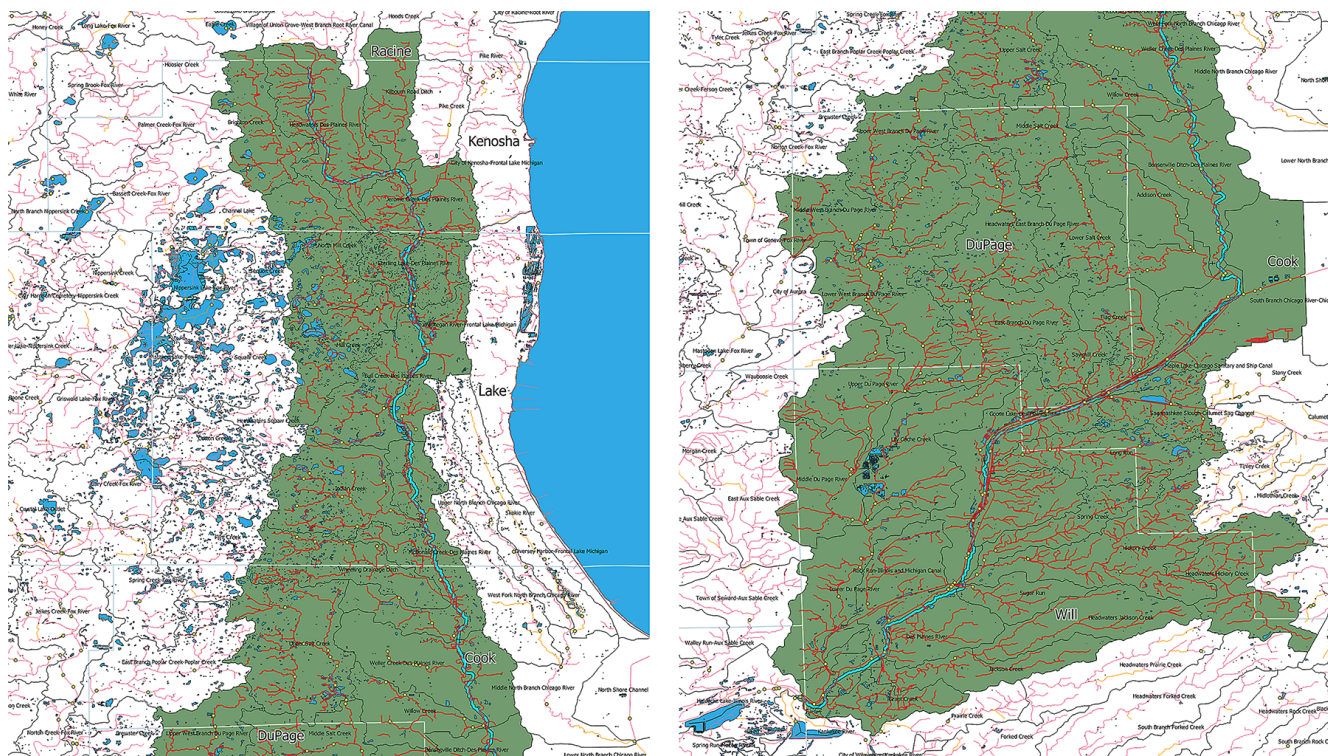


Figure 9-18 Streams of concern of Des Plaines River

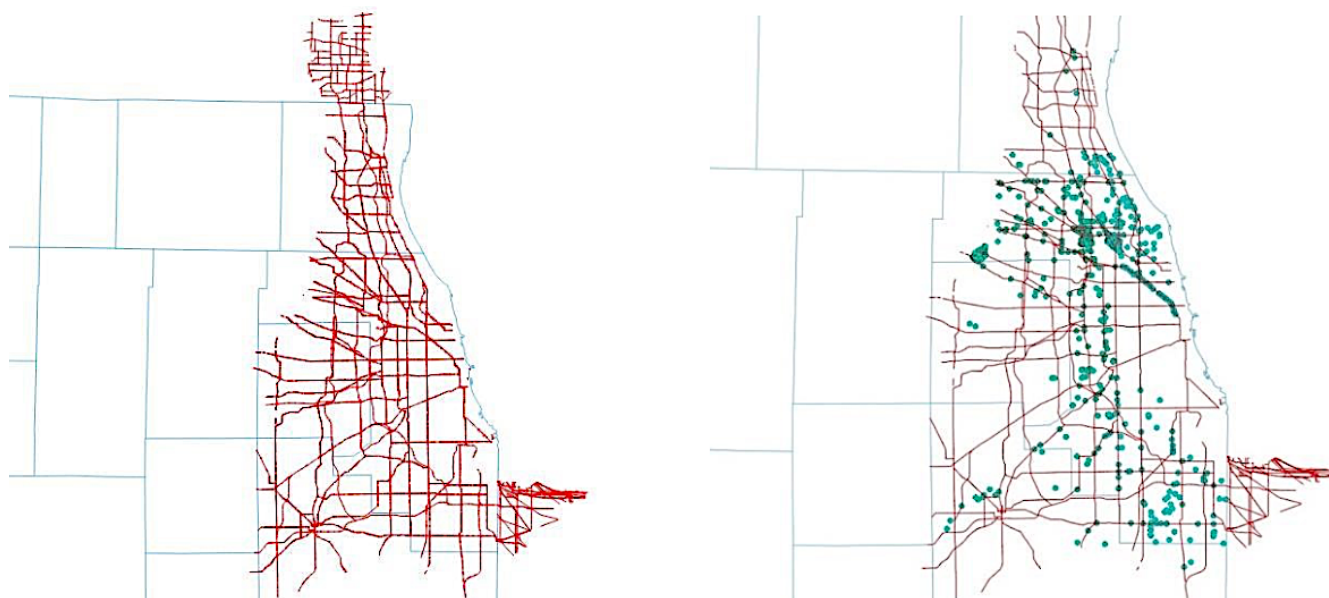


Figure 9-19 Primary road system and overtopping map along Des Plaines River watershed

Flooding Risk Locations

Figure 9-20 shows potential areas or essential facilities at risk of flooding. Any potential risk areas could be used to conduct the case study.

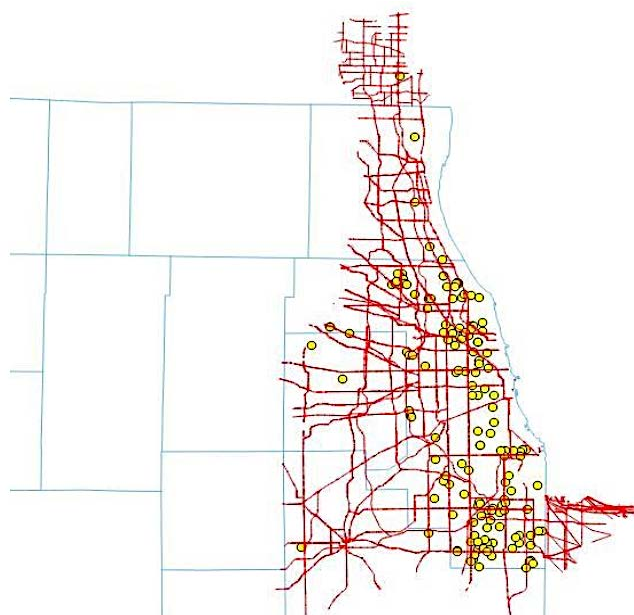


Figure 9-20 Map of risk of flooding

General Evacuation Strategies

Time durations that allow for city jurisdictions to prepare for reaction plans are different depending on the causes and distance of flooding origin. In upstream areas, intense storms might create a flood within a few hours or even minutes; downstream locations might take one day or sometimes weeks to form a flood. In addition to the common types of flooding formed by accumulation of water during rain and intense storms, an uncommon type of flooding can develop from snowmelt. Even though it might take months to develop, inspection is required. Essential considerations include:

- Understanding protective facilities in or near the jurisdiction
- Keeping in touch with monitor stations to update flooding information
- Identifying and present current and potential inundated areas
- Disseminating flood information, give suggestions to evacuees
- Recognizing the possible route for transit operators to rescue affected population
- Determining the shelter locations and stops along the route
- Assessing the loss of transit resources and use the available resources
- Estimating the number of affected population and locate their positions
- Refining and optimizing the rescue routes

Case Study of Des Plaines River Flooding and Power Outage

The Des Plaines River flows through Des Plaines, Elk Grove, Glenview, Park Ridge, and Morton Grove as well as Chicago (Figure 9-21). Historically, many flooding events have occurred near the riversides due to its low elevation. The lowest elevation at the river is 185 ft above sea level, as depicted in Figure 9-22, and nearby residential and commercial areas with the elevation of 190 to 195 ft are likely to have flooding problems.

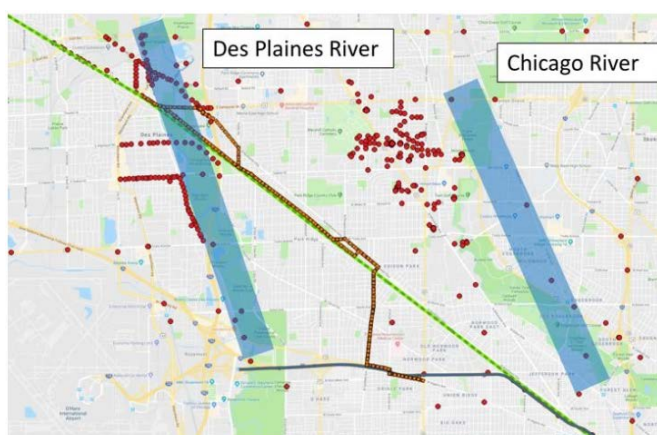


Figure 9-21 Historical flooding event map, Des Plaines area

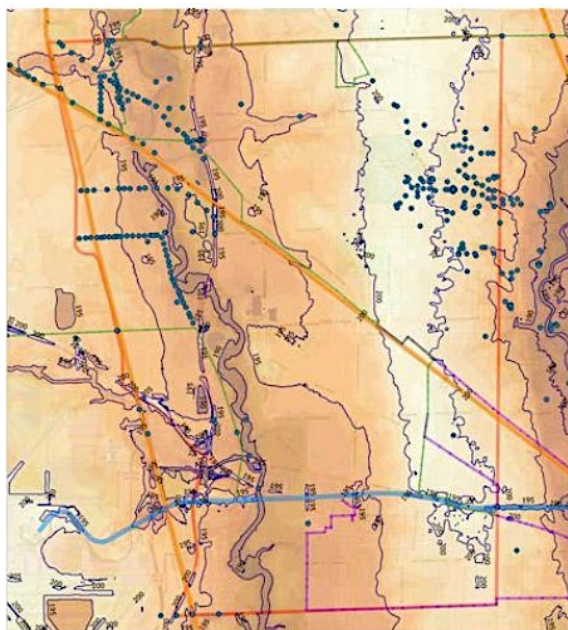


Figure 9-22 Contour map, Des Plaines area

Based on information from the historical flooding event and contour maps, the boundary of the case study area was selected as Golf Road on the north, Harlem Avenue on the east, Mannheim Road on the west, and Lawrence Avenue on the south. The geographical position of the case study area and historical flooding event locations are shown as Figures 9-23 and 9-24.



Figure 9-23 Case study area

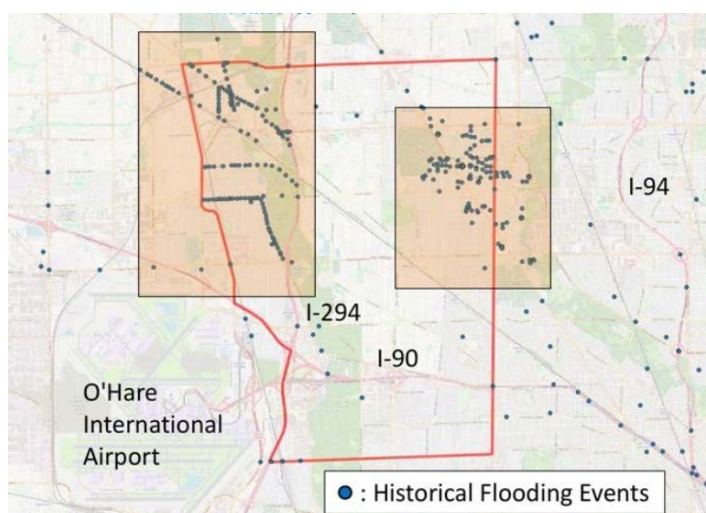


Figure 9-24 Historical flooding event map

In the case study area, two major interstate highways, I-90 and I-294, pass through it as east/west oriented and south/north oriented, respectively. According to the 2017 CTA Annual Ridership Report, the CTA BlueLine along the I-90 alignment is a main public transit route that connects O'Hare International Airport and the city of Chicago, conveying 26,833,303 passengers annually. As shown in Figure 9-25, Metra commuter rail, multiple CTA routes, and PACE bus routes also pass through it, making this traffic-intensive area an ideal place for the case study.

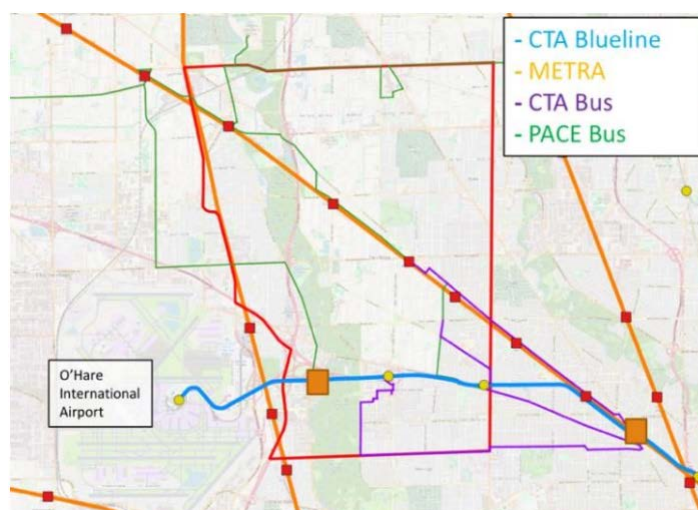


Figure 9-25 Transit routes in study area

PACE Bus and Northwest Division Garage

The Northwest division PACE bus garage is located near the boundary of the case study area. It is on the E Northwest highway, which is the extension of Miner Street passing through downtown Des Plaines, 1.2 miles from the Metra Des Plaines station. This garage was used as an initial destination for all evacuation for this case study. The Northwest Division garage operates two types of buses, as shown in Table 9-4. Typically, 20% of PACE buses are in the garage; therefore, it is assumed that 25 vehicles could be deployed for flooding events.

Table 9-4 *PACE Buses, Northwest Division Garage*

Bus Model	Bus Type	Seats	Standees	Number of Vehicles
ELDorado EZII	Short bus	27	5	17
ELDorado AXESS	Standard bus	36	9	105

Weather in Des Plaines Area

Precipitation

Based on data of national averages from the Weather Service of the National Oceanic and Atmospheric Administration (NOAA), the highest daily precipitation occurs in August and the lowest in February in the Des Plaines area. From the daily high records for July to September, over six inches of rain occurs.

Table 9-5 *Precipitation in Des Plaines Area*

Precipitation	Jan	Feb	Mar	Apr	May	Jun	Jul	Aug	Sep	Oct	Nov	Dec
Avg (in./day)	1.73	1.77	2.52	3.39	3.66	3.46	3.7	4.88	3.23	3.15	3.15	2.24
Daily (in./day)	2.76	3.34	3.2	3.83	4.12	4.64	6.86	6.49	6.64	3.94	3.34	2.66

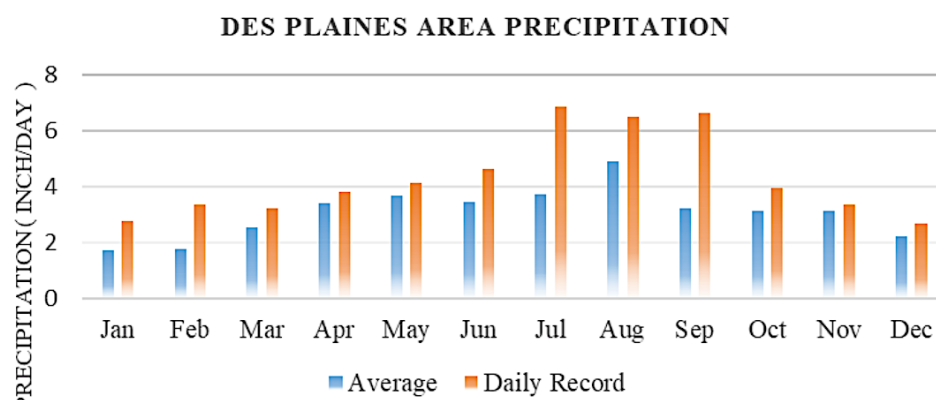


Figure 9-26 *Monthly precipitation distribution in Des Plaines area*

River Stages

The U.S. Geological Survey operates one river stream-gauge station on the Des Plaines River in cooperation with U.S. Army Corps of Engineers (USACE). The gauge is located at the Euclid Avenue Bridge with data collection since October 1, 1993. The average annual height of the Des Plaines River is 11.07 ft, and highest average gauge heights are 11.7 ft in April and May (Figure 9-27). Overall, the average monthly gauge does not show much difference by month; however, depending on precipitation, the river gauge was measured as high as 16.3 ft and as low as 7.8 ft in 2018 (Figure 9-28).

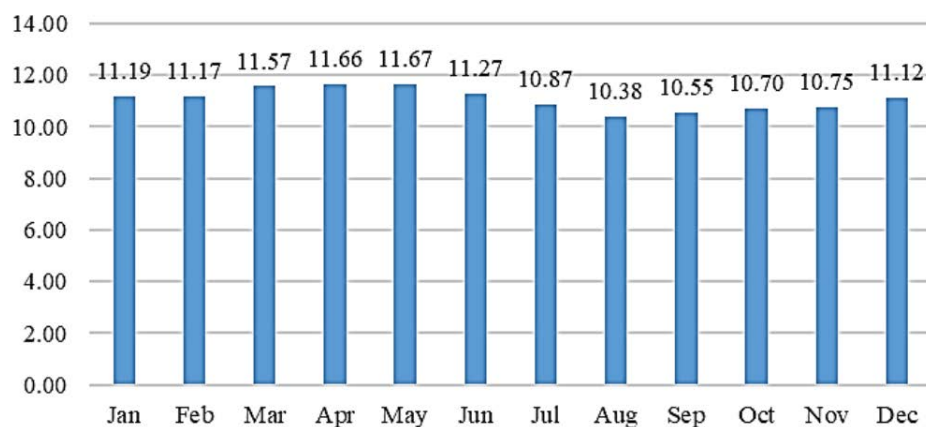


Figure 9-27 Average monthly gauge heights in Des Plaines Area

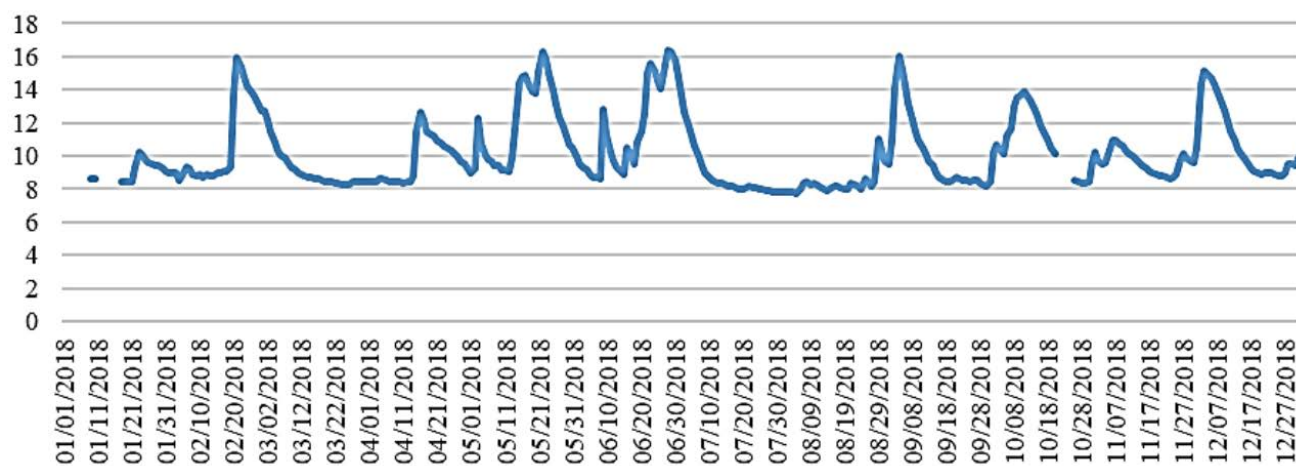


Figure 9-28 Des Plaines River gauge height changes, 2018

With extensive flooding events occurring near the Des Plaines River, FEMA set flood categories according to the river stream-gauge height. Four categories of flood stages were classified—Action Stage, Flood Stage, Moderate Flood Stage, and Major Flood Stage, as described in Figure 9-29 and Table 9-6.

Flood Categories (in feet)

Major Flood Stage:	19
Moderate Flood Stage:	18
Flood Stage:	15
Action Stage:	13.5

Figure 9-29 Categories of FEMA Flood stages for Des Plaines River

Table 9-6 Description of FEMA Flood Stages

Flood Category	River Gauge Height (ft)	Description
Major Flood Stage	19	At this stage, life-threatening flooding is expected. Significant to catastrophic. Low-lying areas completely inundated is likely. Structures may be submerged. Large-scale evacuations may be needed
Moderate Flood Stage	18	At this level, inundation of buildings begins. Roads are likely to be closed and some areas cut off, and some evacuations may be needed
Flood Stage	15	At this stage, minor flooding is expected. Slightly above flood stage. Few buildings can be inundated, and water may go under buildings on stilts or higher elevations; however, roads, parklands, and lawns may be covered with water
Action Stage	13.5	Water surface is near or slightly above the top of the river bank, but no flood damages on manmade structures. In general, any water overflowing is limited to small areas of parkland or marshland.

Historically, flooding events in Des Plaines area have occurred due to intensive precipitation or a combination of high river stage caused by continuous precipitation and a moderate amount of precipitation. For example, 6.86-in. daily precipitation was shown on September 13, 2008, and the stream-gauge Des Plaines River increased from 11.14 ft to 19 ft in 20 hours (Figure 9-30). As a result, the downtown Des Planes area was flooded. In addition, the Des Plaines River flooded with 3.54 in. of daily precipitation. The river height was 15.4 ft because of a week of rains before the downpour in 7 hours on April 18, 2014; at the end, the river flooded (Figure 9-31).

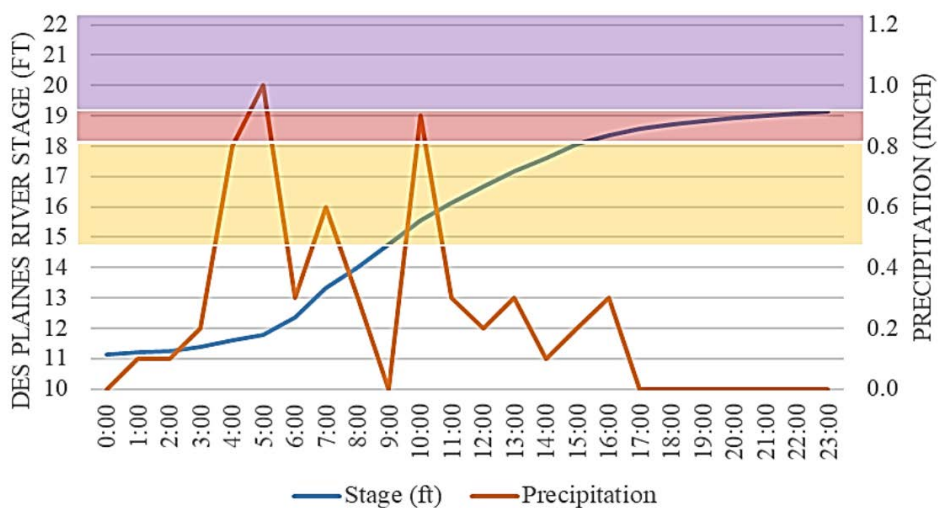


Figure 9-30 Des Plaines River flooding, September 13, 2008

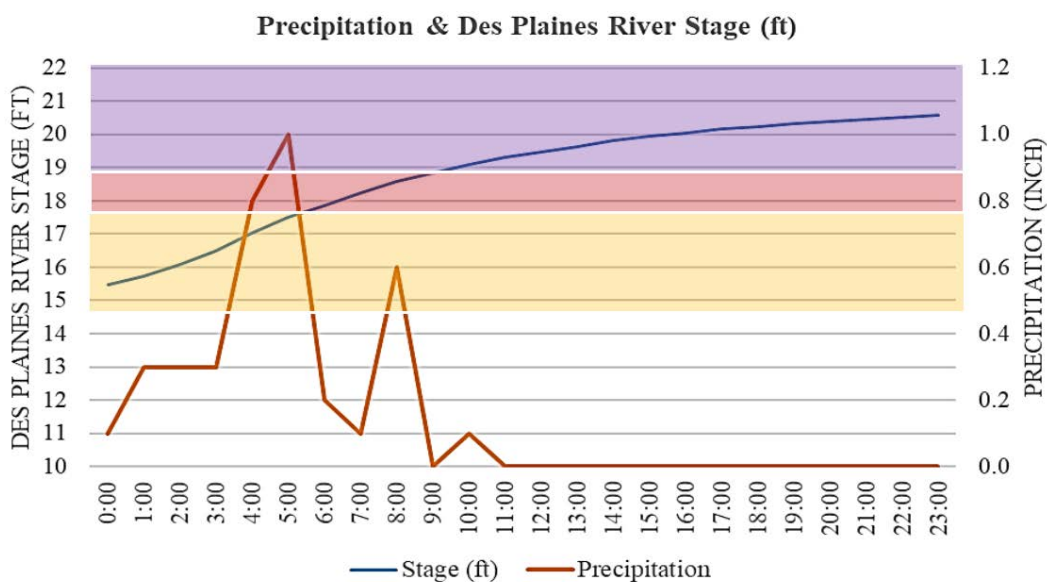


Figure 9-31 Des Plaines River flooding, April 18, 2014

Des Plaines River Flooding Scenario

Background

For the case study, it was assumed that a flooding event lasted for one full day, and the stage of the Des Plaines River was 11 ft, the annual average stage of the river before the rain. Based on Des Plaines area flooding records for September 13, 2008, 6–7 in. of precipitation were required to reach the Major Flood stage; therefore, one weekday of September was selected among the months of the daily record of precipitation over 6 in. (Figure 9-32). Precipitation and the river stage follow the same pattern of flooding as on September 13, 2008.

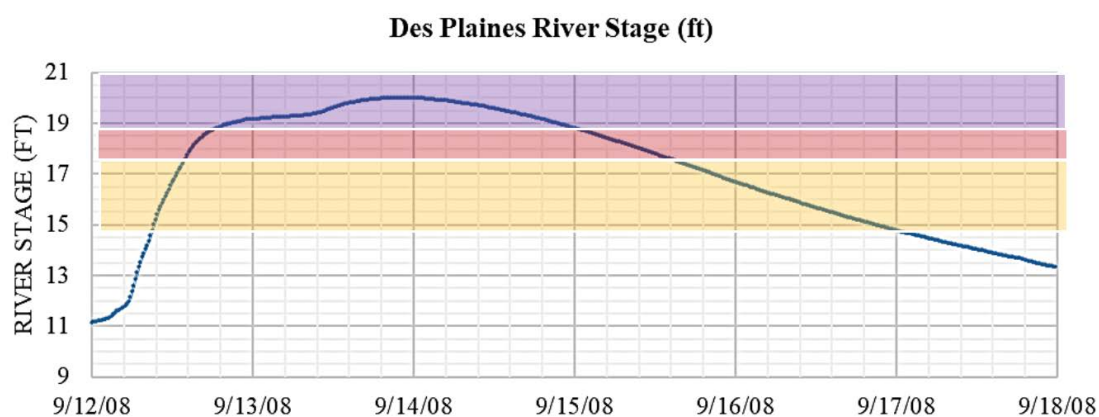


Figure 9-32 Changes in Des Plaines River flood stages after flooding event

Flood Stages

The flood stages were assumed as follows: At 10:00 am, the Des Plaines River stream-gauge reached up to 15.6 ft after hours of rain from 1:00 am. At this stage, some segments of South River Road were covered by flooded water, and parklands near the river were inundated. Due to the South River road closure, PACE bus route 230 rerouted its path from South River road to Lee Street and Oakton Street.

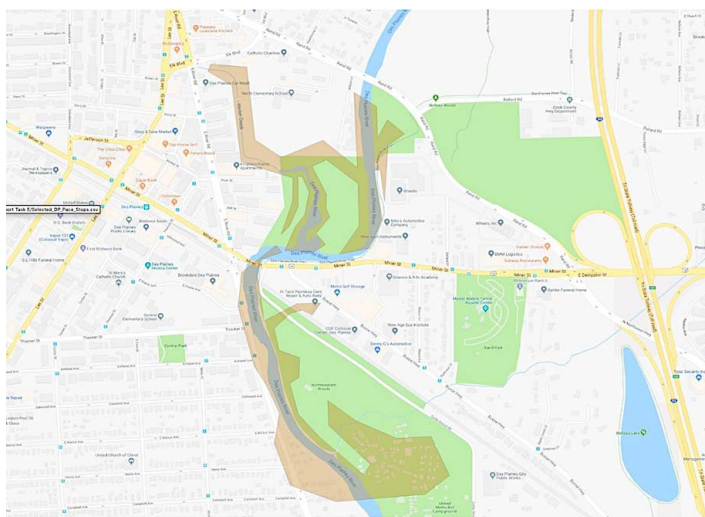


Figure 9-33 Des Plaines River flood stages

Moderate Flood Stages

At 3:00 pm, the stream-gauge of the Des Plaines River reached 18 ft, which is a Moderate Flood stage. At this level, the residential area along with South River Road was inundated, and the flooding area extended toward North Elementary School. As such, evacuation for the 523 students was required before further

inundation. For the evacuation, PACE bus routes 208, 234, and 412, which were already operating, were deployed first, and 10 PACE buses from the PACE Bus Northwest Division garage were deployed to load the remaining demand. In addition to South River Road, Busse Highway was also covered by water at this stage; as a result, additional PACE bus routes, including routes 209 and 226, were needed to bypass the flooded segments of the road using Miner Street and N Northwest Highway.

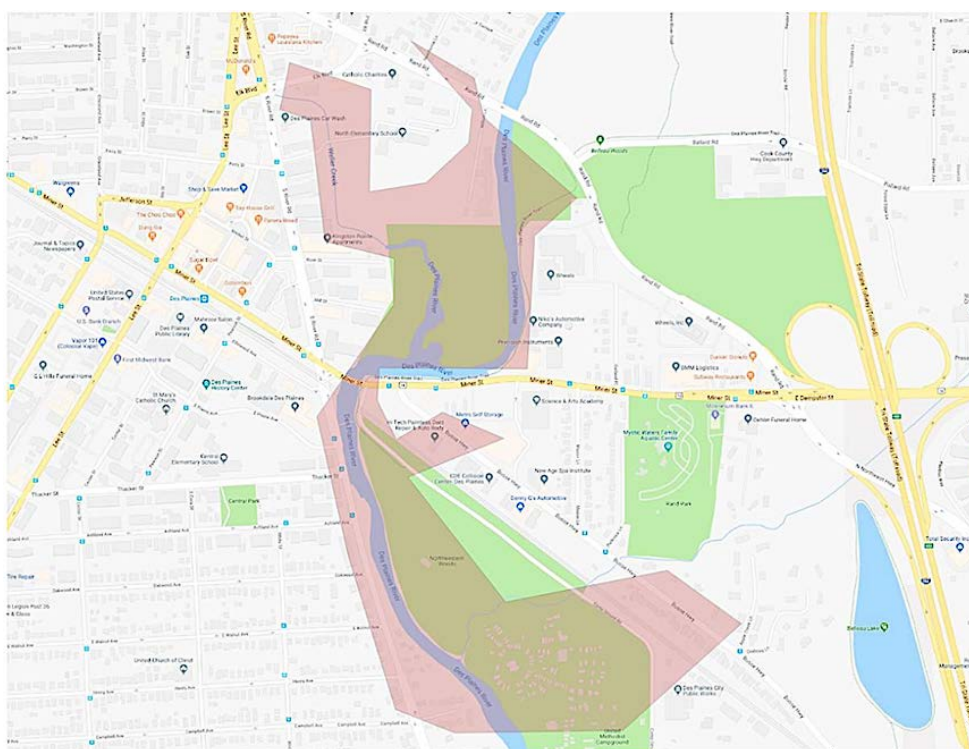


Figure 9-34 *Des Plaines River moderate flood stage*

Major Flood Stage

At 9:00 pm, the river stream-gauge height of the Des Plaines river was over 19 ft, and the downtown Des Plaines area near the Des Plaines Metra Station was inundated. The elevation of the Metra railroad was slightly higher than Miner Street where the Metra station is located, so there was no problem to operate Metra commuter rail. However, the Des Plaines Metra station was inundated, so passengers could not use the station. As a result, the 151 passengers (Table 9-7) expected to board or alight from the Metra UP-NW at Des Plaines Station in the evening period needed to use Metra Dee Road station or Metra Cumberland station. For those passengers, PACE bus routes 209, 240, and 250 extended their routes to the station to handle initial demand, then two PACE buses from the Northwest Division garage were deployed to each station to manage ridership.

Table 9-7 Des Plaines River flood stages

UP-NW	Direction	AM Peak	Midday	PM Peak	Evening	Total
Boarding	Inbound	717	112	105	38	972
	Outbound	19	25	120	6	170
Alighting	Inbound	100	28	13	16	157
	Outbound	123	105	725	91	1,044

"AM Peak" refers to from Start of service to 9:15 am. "Midday" refers to from 9:16 am to 3:29 pm. "PM Peak" refers to from 3:30 am to 6:45 pm. "Evening" refers to from 6:46 pm to End of Service.

At this stage, Miner Street, E Rand Street, and Busse Highway near the Des Plaines area were closed because of inundation. These roads are main access roads of the area, so PACE bus routes 209, 220, 230, and 250 passing through downtown Des Plaines could not be operated. E Golf Road, I-294, and E Dempster Road were used as evacuation roads.

There are 58,364 residents in the city of Des Plaines, and from the flooding event, 3.6% of land was submerged; however, this submerged residential area is located downtown, and there are many multi-floor condos; As a result, it was assumed that 10% of residents (5,836) were living in the flooded area as evacuees. In addition, it was assumed that 10% of these 5,836 people would use transit service for evacuation rather than using personal vehicles. In sum, about 600 residents in the submerged area needed to be evacuated using PACE buses. For the evacuation, 20 PACE buses from the Northwest Division garage were deployed at the border of flooding area to the nearest shelters.

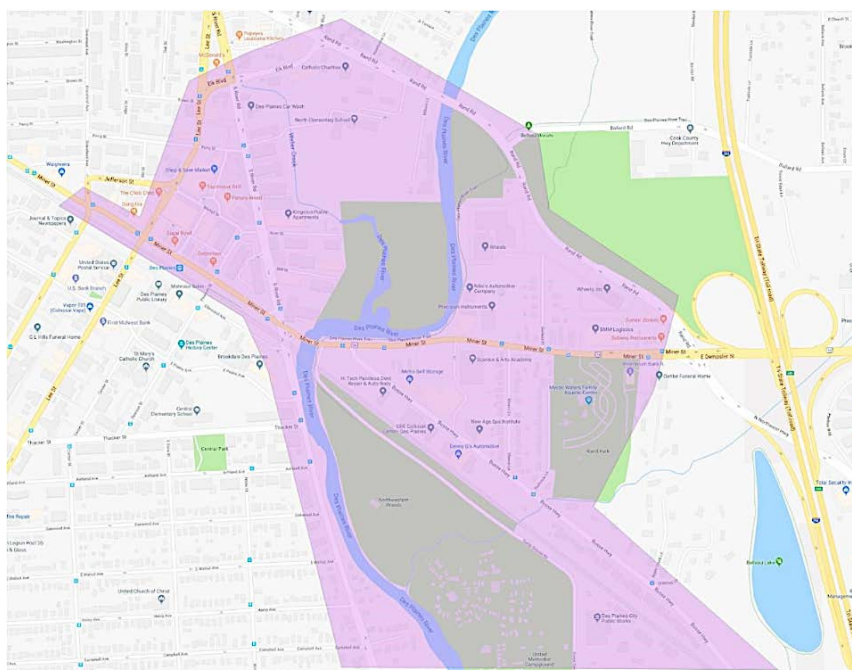
**Figure 9-35** Des Plaines River major flood stage

Table 9-8 *Flooding Event by Flooding Stage and Countermeasures in Des Plaines Area*

Time	FEMA Flood Category	Event	Demand	Transit Service	Countermeasure	Supply	
10:00 AM	Flood stage (river stream gauge: 15.4 ft)	South River Rd closure		PACE bus route 230	Re-routing: Lee St and Oakton St		
3:00 PM	Moderate flood stage (river stream gauge: 18 ft)	Busy Hwy		PACE bus routes 209, 226	Re-routing: Miner St and N Northwest Hwy		
		Elk Blvd		PACE bus routes 208, 234	Re-routing: Rand Rd		
		NW Elementary School evacuation	523			Emergency dispatch: PACE bus routes 208, 234, 412	135
						10 extra pace buses from NW Division Garage	450
9:00 PM	Major flood stage (river stream gauge: 19ft)	Miner St closure		PACE bus routes 208, 226, 230, 250	Transit service closure		
		Des Plaines Metra station shutdown	151		Metra UP-NW	Dispatch and operate 2 extra PACE buses from NW Division Garage to Dee Rd Station	90
						Dispatch and operate 2extra PACE buses from NW Division Garage to Cumberland Station	90
		Downtown Des Plaines evacuation	600		Dispatch 15 extra PACE buses to transport residents to nearest shelters	Dispatch 15 extra PACE buses to transport residents to nearest shelters	675

Power Outages

Usually, an emergency event does not occur alone—it comes with multiple problems triggered by the event. In this case study, it was assumed that a predictable event and an unpredictable event occurred at the same time in the study area; as a result, it would be required to set a multi-dimensional plan that could be helpful to handle real-world events. For the case study, it was assumed that the predictable event, Des Plaines River flooding, was forecasted before the event, and a power outage occurred on the first day of downpour because of the flooding sites in the Des Plaines area.

CTA Blue Line Loss of Power Records

On June 6, 2016, CTA Blue Line trains stopped after a loss of power. Two southbound trains lost power just after 9:00 am, and trains were single-tracking for four hours on the northbound tracks. A total of 200 CTA Blue Line passengers were evacuated outside the Clinton Station with the assistance of the Chicago Fire Department after the two trains lost power. At first, they were escorted along the tracks to the platform and then rerouted to their destinations using CTA buses.

On November 1, 2017, after a power outage at the Jefferson Park Station on the northwest side, CTA Blue Line trains bound for Forest Park were delayed from Wednesday night to early Thursday. Trains were standing at Jefferson Park, and service was suspended between Rosemont and Jefferson Park. CTA asked people to use alternate transit while crews work to restore power; as a result, CTA buses operate between O'Hare and Jefferson Park and Harlem and Jefferson Park. At the O'Hare and Jefferson Park route, 20 buses are operated, and 56 buses provide alternate service between Harlem and Jefferson Park route. Normal service restarts one hour later.

CTA Blue Line Loss of Power Scenario

At 11:00 pm, because major flooding occurred in the Des Plaines area and nearby riverside area at 9:00 pm, a power outage occurred at CTA Blue Line between Cumberland station and Rosemont Station. This caused outbound trains toward O'Hare International Airport to be stopped at Cumberland Station, leading to service suspension between Cumberland and O'Hare.

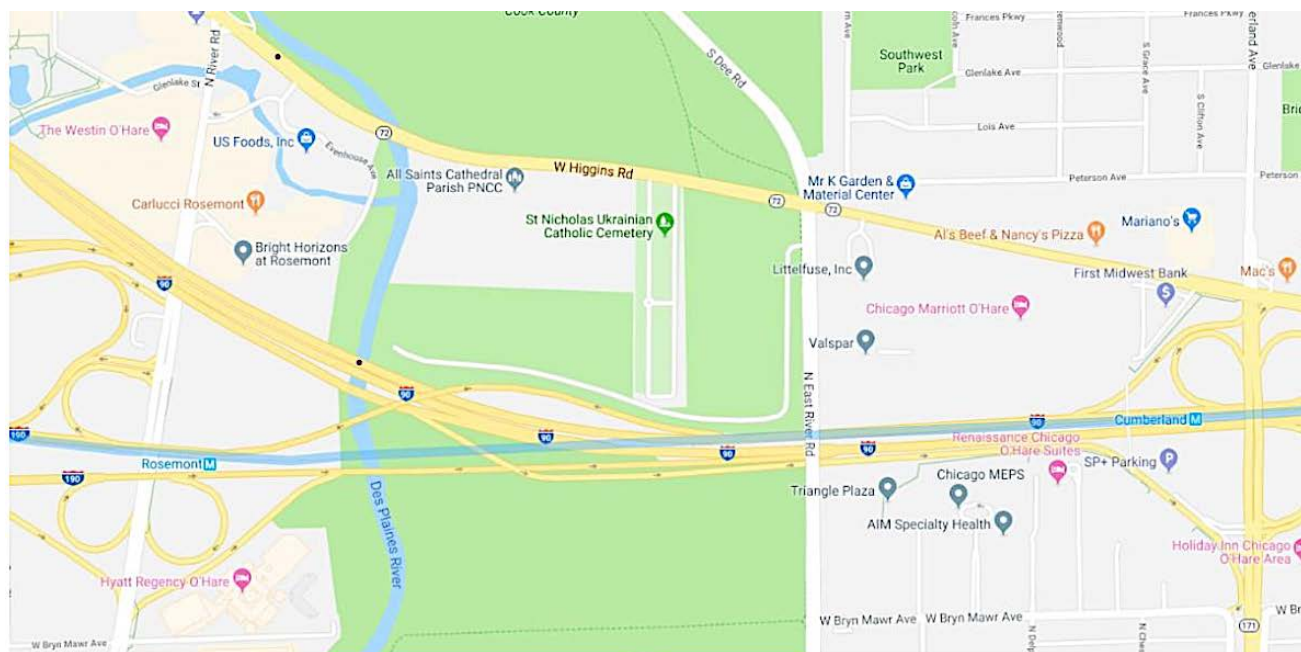


Figure 9-36 CTA Blue Line Station at Cumberland and Rosemont

The CTA Blue Line operates normally between Cumberland and Harlem stations, and from Cumberland Station, passengers were asked to transfer to PACE buses for travel to the Rosemont and O'Hare stations. From 11:00 pm, many PACE bus routes were not in service. As a result, 4–10 buses could be deployed from the PACE Northwest Division garage for both inbound and outbound travel between the O'Hare and Cumberland stations, depending on demand (Table 9-9).

Table 9-9 CTA Blue Line Demand, Rosemont and O'Hare International Airport

		Time	23	0	1	2	3	4
Inbound	Headway (min)		15	15	10	15	15	10
	Frequency (per hr)		4	3	6	4	4	8
	Demand (passengers per hr)		209	157	314	209	209	419
Outbound	Headway (min)		10	15	60	15	15	10
	Frequency (per hr)		6	4	1	4	4	7
	Demand (passengers per hr)		314	209	52	209	209	366

Advocate Lutheran General Hospital Power Outage Scenario

At 11:00 pm, a power outage event occurred at the Advocate Lutheran General Hospital. The hospitalized patients and employees of the hospital needed to be evacuated to the nearest shelters or to the Presence Resurrection Medical Center for patients who needed intensive care. Advocate Hospital has 625 beds for hospitalization; for demand estimation, it was assumed that 70% of beds were occupied and 100 employees were in the hospital for the night shift. As a result, 600 people would need to be evacuated, including guests of patients. The PACE Northwest Division garage is located 5.2 miles from the hospital if buses are bypassing the flooding area using Golf Road, and it takes 12 minutes from the hospital. A total of 15 PACE buses from the garage would be deployed to the hospital for evacuation.

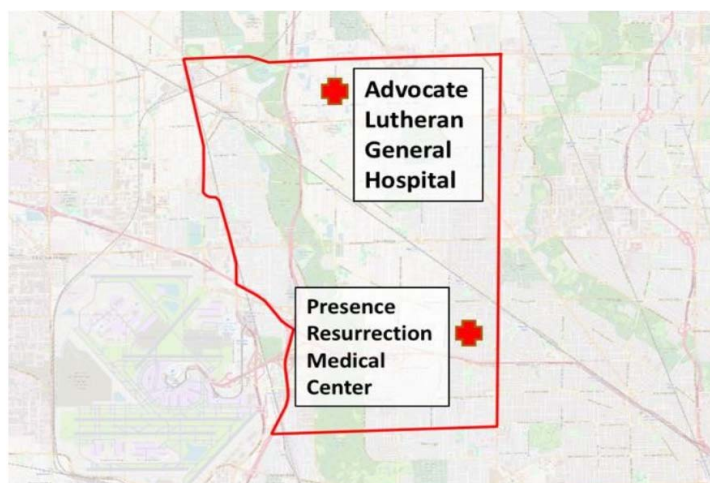


Figure 9-37 Two major hospitals in case study area

Table 9-10 Power Outage Scenario and Countermeasures by Hour

Event Counter Measure		Time	Demand (Passenger)		Supply (Bus)	
			Inbound	Outbound	Inbound	Outbound
Outbound CTA	Extra PACE buses from Northwest Division Garage, transport passengers from Cumberland to O' Hare	11:00 pm	209	314	5	7
		12:00 am	157	209	4	5
		1:00 am	314	52	7	2
		2:00 am	209	209	5	5
		3:00 am	209	209	5	5
		4:00 am	419	366	10	9
Evacuation of Advocate Lutheran	Dispatch extra PACE buses from Northwest General Hospital Division Garage to transport patients to nearest shelters or Presence Resurrection Medical Center	11:00 pm	600		15	

Case 3: Metra BNSF Line/Cass Avenue Grade Crossing Failure from Hazmat Truck Crashes

The case study first analyzed when the event occurred and the vicinity required to be evacuated and the impacts assessed. Nearby PACE buses would be re-routed to the event location and aid the process of evacuation. After the event, if the emergency causes a complete service failure at a local point, the case study will be analyzed. In case when the highway-rail grade crossing is damaged, there will be some time required for complete service restoration, and alternate routing is needed for bus routes using the service as well the normal traffic using the route. Rail service, which uses the track, requires substitution by alternate services by means of shuttles service along the track to ensure service and accessibility to train riders. In this situation, PACE buses can be used to provide shuttle services without causing major service inadequacies to original patrons on the original routing network and to the new riders who are using the service as an alternate to rail until the service is restored.

BNSF Background Information

The BNSF Railway Line is a Metra commuter rail line operated by the BNSF Railway and serves one of the busiest origin-destination areas, Chicago and Aurora. Timetables show that 31 of 47 trains leaving Chicago headed to Aurora in July 2017. Comparably, 47 trains arrived in Chicago, of which 29 started from Aurora. In 2010, the BNSF Railway Line continued to have the highest weekday ridership of the 11 Metra lines—64,600, on average, per day.

The first rail service from Aurora to Chicago began in 1850, a 12-mile railroad in length from Aurora east to Chicago via UP west (Galena and Chicago Union tracks). In 1855, it became a part of the Chicago Burlington and Quincy. The service line become congested, and in 1864, Chicago, Burlington and Quincy built their own direct line and started to serve passengers. The name changed to BNSF, from Burlington Northern to Burlington Northern Santa Fe. To improve the service level, this line was the first to use bi-level coaches. Now, BNSF is operated under an agreement called a “purchase of service agreement” between BNSF Railway and Metra. Metra owns the equipment and BNSF is responsible for management and employment. Metra plans to study the feasibility of extending the service line to Plano, Illinois, which beyond the current terminal, Aurora.

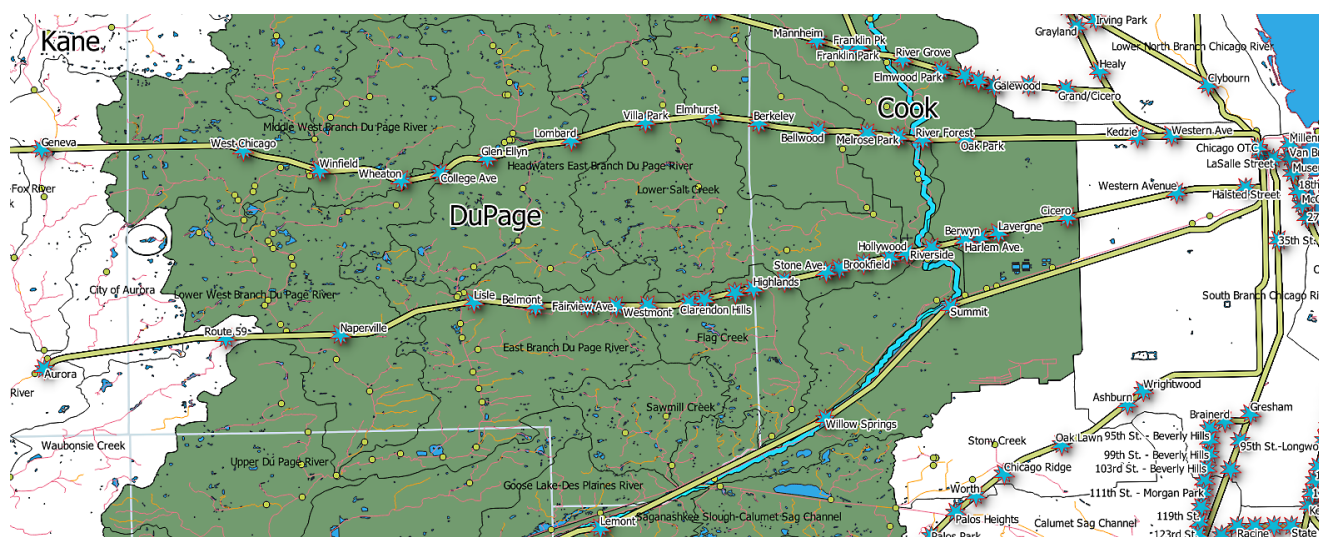


Figure 9-38 BNSF route map

Hazmat

Hazmat is the abbreviation for “hazardous materials” that may pose a risk to human health, public property, or the environment. Many subcategories are included, such as toxic materials, chemical materials, fuels, nuclear products, and biological and radiological products. The forms of hazmat vary, which may be shown as liquids, solids gases, dust, smoke, gas, mist, vapor, or combinations of them.

Hazmat spills may cause severe health problems, injuries, or even death to surrounding residents and animals and also poses damage to private or public buildings and properties and the environment. Even if the hazmat is dangerous, it is essential in daily life, meaning that the risk is close, as related materials need to be shipped from one place to another via the nation's highways, railroads, waterways, and pipelines. Every year, thousands of hazmat accidents occur; according to the *Houston Chronicle*, more than 1,000 heavy

truck accidents occurred in 2017, and 10% of local large truck accidents involved hazmat incidents.



Figure 9-39 *Hazmat example*

All truck companies and carriers that transport hazardous materials are required to have a federal hazardous materials safety permit. The Federal Motor Carrier Safety Administration (FMCSA) classifies hazardous materials into the nine categories listed below; if one truck transports a particular type of hazardous material, the truck must be categorized and marked properly, and every type of hazardous material in the nine categories poses a unique risk if an emergency occurs:

- Explosives
- Gases, including flammable and toxic gases
- Flammable liquid and combustible liquid
- Flammable solid, spontaneously combustible and dangerous when wet
- Oxidizer and organic peroxide
- Poison (toxic) and poison inhalation hazard
- Radioactive
- Corrosive
- Miscellaneous

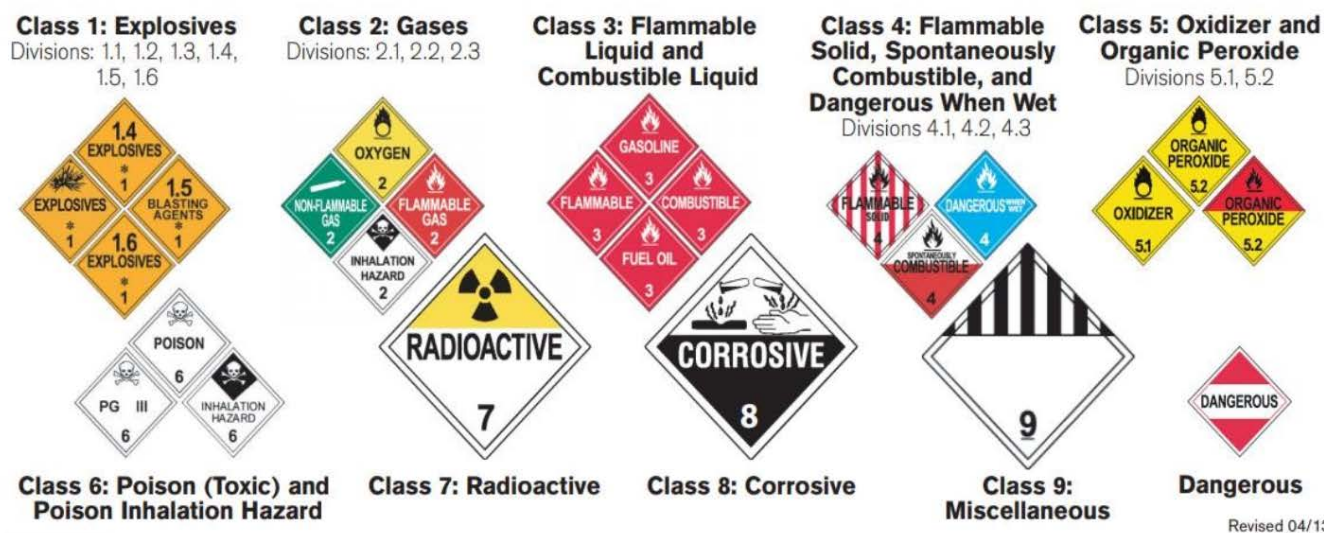


Figure 9-40 Hazardous materials signs (Source: fmcsa.dot.gov)

In general, the consequences of hazardous materials include thermal burn injuries, explosions resulting in burn injuries, amputation injuries, loss of hearing, chemical burns, poisoning, exposure to cancer causing chemicals, and others. Many factors affect the estimation of consequences. U.S. Department of Defense (USDOD) provides a method called CARVER to evaluate the consequences to people and environmental damages. CARVER is an acronym for Criticality, Accessibility, Recuperability, Vulnerability, Effect, and Recognizability. It assigns a relative value to illustrate severity, ranging from 1 to 5, with consequences becoming more severe.

Table 9-11 Hazmat Accident Consequence Levels

Consequence Value	People	Environment
1	No deaths or serious injuries; only relatively minor injuries	Less than \$1 million
2	1 to 10 deaths or serious injuries	\$1 million to \$10 million
3	11 to 100 deaths or serious injuries	Over \$10 million to \$100 million
4	101 to 1,000 deaths or serious injuries	Over \$100 million to \$1 billion
5	More than 1,000 deaths or serious injuries	Over \$1 billion

Potential consequences of hazardous materials truck accidents depend on the type and quantity of materials, location of accidents, surrounding environment, and weather condition. To accurately estimate the hazard and risk of consequences, the chemical and physical properties of the material should be understood, how much of the material is released, and how fast the damage will spread under the certain environmental and weather conditions. The affected population related to population density in the given location, the number of

special-needs populations, social-economic conditions, and transit evacuation resource supply should also be assessed. Environmental damages depend on the specific environmental features, the presence of waterways, parks or preserves, and how fast and how far the hazardous materials would spread, including wind speed, humidity, temperature, and so on.

Human-Health Consequences

The focus is to estimate number of people suffering from a hazardous material accident. Before estimating the number of affected population, it should first identify the affected area. Estimation of the affected area depends on the type of hazardous materials, the chemical and physical attributes, and environmental conditions. Previous work provides useful methods. For instance, the ERG and the Argonne report (Kawprasert and Barkan 2010) provides specific protection actions for responders. Several modeling tools in ERG could help determine more details of the affected area for different hazardous materials.

The Non-Radioactive Hazardous Material Routing Guidelines (NRHM 1996) present a simpler method to estimate the hazard distance, as shown in Table 9-12. It provides a guide to hazard distance, typically 0.5 miles (800 meters) for non-radioactive hazardous materials, infectious substances, or radioactive materials. In addition, weather conditions such as wind speed and direction should be considered. In this respect, the affected circle is a dynamic circle by both the location and radius.

Table 9-12 *Hazard Distances used in NRHM Routing Guidelines*

Hazardous Materials	Hazard Distances (mi)
Explosives	1
Flammable gas	0.5
Toxic gases	5
Flammable/combustible liquid	0.5
Flammable solid, spontaneously combustible, dangerous when wet	0.5
Oxidizer/organic peroxide	0.5
Poisonous (not gas)	5
Corrosive	0.5

To estimate the number of people within the impacted area, census data can be used with the help of Geographic Information System (GIS) software and counting the residents. However, the number will be different for daytime vs. nighttime; in daytime, there will be fewer residents but more transit people, and the situation is reversed at night. On average, the estimated population is

$$\text{population density} \times \text{people miles}^2 \times \text{affected area}(\text{miles}^2)$$

Note that the area can be a circle or rectangle depending on different hazmat accidents.

Environmental Consequences

A similar approach can be adopted to estimate environmental consequences. Usually, consideration includes property damages and land/aquatic contamination. Property damages can be assessed based on the total damaged area or structure, multiplying the unit price to arrive at total property damages. Fire and explosives always cause more property damage than hazardous fluid or gas. The circular area specified by this radius is the suggested area to be used to estimate damages to nearby structures. Alternatively, the dispersion code in the Areal Location of Hazardous Atmospheres model (ALOHA 2007) has an option to estimate the damage radius from fires and BLEVEs. The user only needs to specify the material and quantity present.

For land/aquatic contamination, the concern is how many plants and trees are killed by the hazmat accident immediately and potential future damages. Land/aquatic contamination is sensitive to the type of hazmat; for example, ammonia does much damage on wetlands because of its aquatic toxicity but little damage to solids. NRHM (2007) may be used to estimate the potential affected area.

Table 9-13 shows representative values for different types of land use to estimate economic losses on a per-acre basis. However, the number maybe not valid for all regions; each region should develop its own value table to estimate losses. If the property is not totally destroyed, a specific percentage of the value may be used to replace the original value, such as 10% or 20%.

Table 9-13 *Estimated Unit Values for Damages to Structures*

Type	Structure		
	<i>Residential</i>	<i>Commercial</i>	<i>Industrial</i>
Rural	\$ 150,000	\$ 1.2 million	\$ 2.4 million
Suburban	\$ 1.2 million	\$ 12 million	\$ 24 million
Urban	\$ 8 million	\$ 50 million	\$ 80 million

Table 9-14 *Estimated Unit Values for Damages to Environment*

Land Use	Environment	
	<i>Farm Land</i>	<i>Wetland</i>
Fallow	\$ 200	\$ 50,000
Low-value crop	\$ 1,000	\$ 100,000
High-value crop	\$ 400,000	\$ 400,000

Case Study

The case study location is the Metra BNSF Line and Cass Avenue rail-highway crossing intersection. The intersection is close to BNSF Westmont station in Westmont, Illinois. Distance to Union Station is 19.4 miles. The station house is diagonally across from the Village Hall at W Quincy and S Lincoln streets. Bus connections including PACE bus routes 661, 662, 665 and 715.

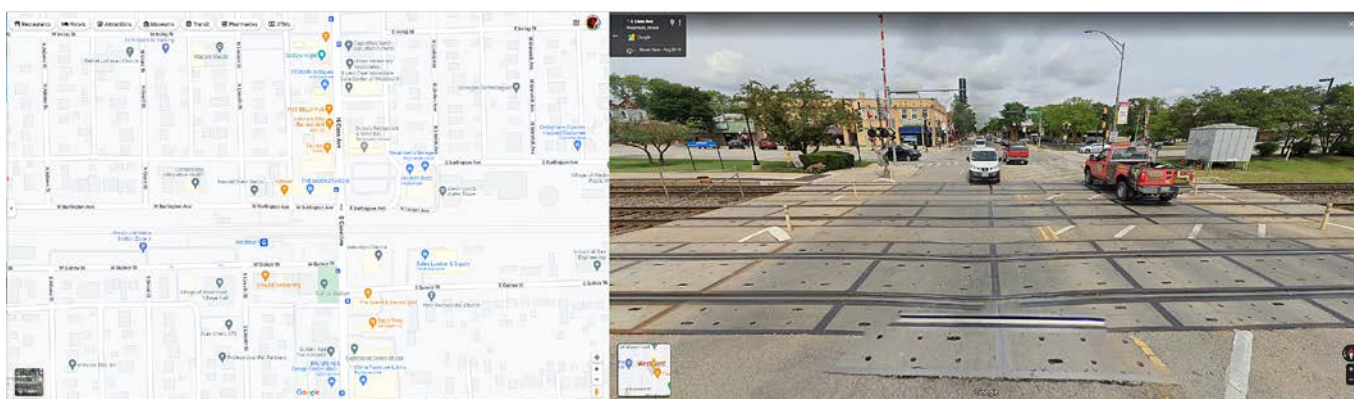


Figure 9-41 Metra BNSF line and Cass Avenue rail-highway crossing intersection (Source: Google Maps)

Demand

Census Data

The studied rail-highway crossing intersection is the cross of the Metra BNSF Line and Cass Avenue, which is close to the BNSF Westmont station. As shown in Table 9-14, the hazard distance depends on the type and characteristics of materials. For example, radioactive or nonradioactive may range from a few hundred meters to one mile, without considering extreme weather conditions. For this case study, we assumed a severe vehicle crash involving a hazmat truck, and the hazard distance is more than 1 mile. Therefore, all residents in the emergency area need to be evacuated. The case study intersection is located in the middle of Westmont, Illinois, which means the worst case is that all residents living in Westmont are under the threat of hazardous materials. Table 9-15 summarizes the basic census information of Westmont.

Table 9-15 *Census Data, Village of Westmont, IL*

Data	#/%
Population	24,576
Age and Gender	
Under 5	6.8%
Under 18	21.7%
65 and over	16.8%
Female	52.6%
Race	
White only	74.8%
Black or African American only	6.9%
American Indian and Alaskan native only	0.0%
Asian only	12.0%
Native Hawaii and other Pacific Islanders only	0.0%
Two or more races	2.5%
Hispanic or Latino	13.9%
White alone, not Hispanic or Latino	65.2%
Health	
With a disability, under age 65	6.6%
Without health insurance, under age 65	11.0%
Income and Poverty	
Median household income (2017 \$)	\$60,437
Per capita income in past 12 months (in 2017 %)	\$36,458
Persons in poverty	12.1%

According to the census and social economic data, 12.1% of residents in Westmont are below the poverty line. This portion would be the transit-dependent population during evacuations. Moreover, children, older adults, persons with disabilities, and non-English speaking residents are all assumed to be special-needs populations. Emergency responders should assign proper assistants with special skills for these special-need populations to be involved to help with evacuation.

BNSF Ridership

If an emergency event occurs in the case study location, people who are using the related transit will be impacted directly. The Metra BNSF line runs east-west between two terminals, Chicago downtown area and Aurora. Metra Reports provided station level boarding and alighting ridership to help estimate the affected population, as shown in Tables 9-16 and 9-17.

Table 9-16 BNSF Station-Level Ridership (AM)

Route	Station	AM Peak (Start of Service 9:15 am)				Midday (9:16 AM–3:29 pm)			
		Inbound		Outbound		Inbound		Outbound	
		On	Off	On	Off	On	Off	On	Off
BNSF	Aurora	1547	0	0	73	156	0	0	314
BNSF	Route 59	5376	7	1	93	206	3	5	489
BNSF	Naperville	3550	15	11	137	256	5	14	379
BNSF	Lisle	1444	9	7	132	96	6	9	182
BNSF	Belmont	1265	4	1	73	71	1	1	148
BNSF	Main Street	1957	8	9	96	182	8	12	304
BNSF	Fairview	347	3	5	7	42	2	10	37
BNSF	Westmont	867	6	8	40	98	10	5	112
BNSF	Clarendon Hills	701	2	2	8	51	0	5	92
BNSF	West Hinsdale	366	0	0	0	9	0	0	19
BNSF	Hinsdale	912	6	8	70	107	6	6	165
BNSF	Highlands	197	0	0	2	0	0	0	23
BNSF	West Springs	1011	4	7	14	70	3	3	141
BNSF	Stone Ave.	923	4	1	6	83	6	2	113
BNSF	LaGrange	1075	7	11	23	118	16	27	151
BNSF	Congress Park	286	1	0	0	0	0	0	28
BNSF	Brookfield	463	9	13	9	51	12	7	46
BNSF	Hollywood	92	1	0	0	21	4	4	77
BNSF	Riverside	400	21	4	4	50	3	16	77
BNSF	Harlem	341	7	6	0	34	15	17	36
BNSF	Berwyn	429	8	18	16	54	8	73	57
BNSF	La Vergne	184	4	0	0	0	0	1	13
BNSF	Cicero	80	10	35	1	5	23	23	10
BNSF	Western Ave.	3	13	24	1	1	18	15	0
BNSF	Halsted	21	55	4	0	0	9	65	3
BNSF	Union	0	23633	630	0	0	1606	2696	0

Table 9-17 BNSF Station-Level Ridership (PM)

Route	Station	PM Peak (3:30 PM–6:45 pm)				Evening (End of Service 6:46 pm)			
		Inbound		Outbound		Inbound		Outbound	
		On	Off	On	Off	On	Off	On	Off
BNSF	Aurora	167	0	0	1297	66	0	0	236
BNSF	Route 59	144	6	8	44117	38	3	3	529
BNSF	Naperville	198	21	8	3253	57	4	10	395
BNSF	Lisle	175	7	28	1382	29	4	1	186
BNSF	Belmont	91	3	32	1006	9	2	2	129
BNSF	Main Street	136	9	32	1837	40	7	8	249
BNSF	Fairview	34	8	12	321	6	2	2	52
BNSF	Westmont	55	12	5	800	16	3	4	113
BNSF	Clarendon Hills	36	7	0	608	10	4	1	108
BNSF	West Hinsdale	0	0	1	264	0	0	0	21
BNSF	Hinsdale	90	10	21	743	11	2	5	108
BNSF	Highlands	5	0	0	167	0	0	1	15
BNSF	West Springs	33	5	5	797	2	3	2	151
BNSF	Stone Ave.	31	3	1	617	2	0	3	115
BNSF	LaGrange	61	45	12	1035	26	4	10	171
BNSF	Congress Park	0	0	4	218	0	0	0	22
BNSF	Brookfield	19	9	10	442	4	0	5	97
BNSF	Hollywood	2	3	1	97	0	0	0	9
BNSF	Riverside	15	8	7	382	6	7	1	72
BNSF	Harlem	12	11	7	243	0	6	4	59
BNSF	Berwyn	21	16	26	497	8	7	3	73
BNSF	La Vergne	0	0	1	165	0	0	1	21
BNSF	Cicero	1	37	18	113	1	28	22	13
BNSF	Western Ave.	0	23	25	6	0	16	1	0
BNSF	Halsted	3	12	27	18	0	0	0	0
BNSF	Union	0	1074	20434	0	0	229	2855	0

PACE Ridership

GTFS data provide public transportation schedules and associated geographic information in detail. With the help of GTFS, stops/stations in the affected area can be determined and ridership estimated that need to be evacuated or shifted to other transit routes. In this study area, most riders tend to choose park-and-ride or driving alone to the work place directly. PACE ridership is relatively low in Westmont, and the schedule is pretty flexible. Therefore, PACE passengers will not cause pressure on evacuation, but PACE buses could help with evacuation under the emergency circumstance.

Supply

All available transit can be involved in the evacuation during emergency. For complete preparation, the capacity of each transit means, including CTA, PACE bus, and Metra's BNSF line services, needs to be analyzed. Figure 9-42 shows possible alternative bus routes in an extended area.

Table 9-18 PACE Bus Supply

Route	Available Buses	Capacity
661	2	~ 35 seats, 9 standees
662	2	~ 35 seats, 9 standees
665	1	~ 35 seats, 9 standees
715	4	~ 35 seats, 9 standees

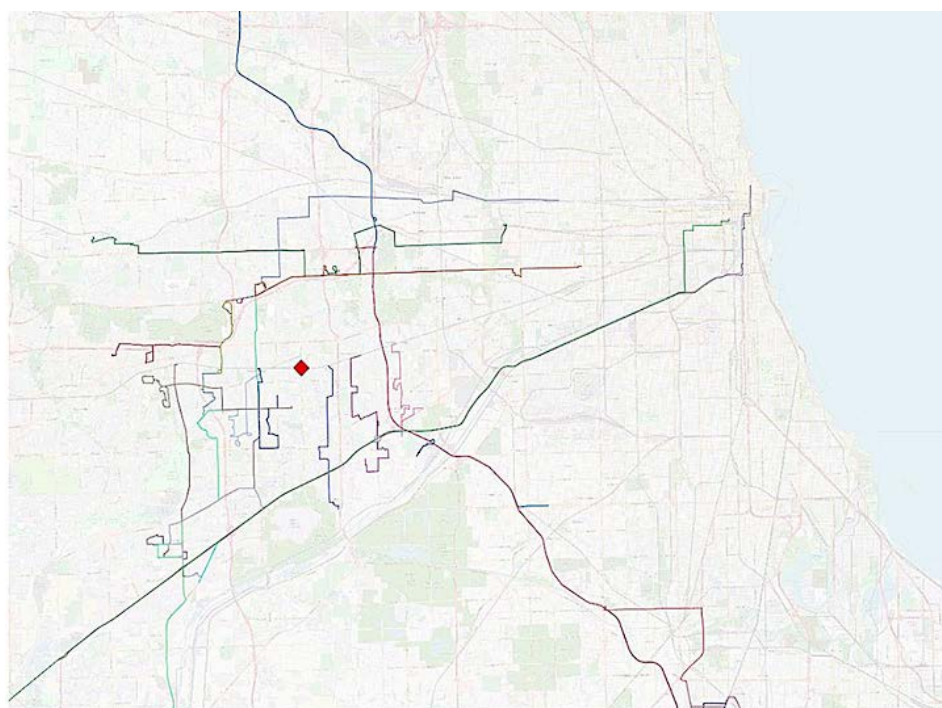


Figure 9-42 Alternative PACE bus routes

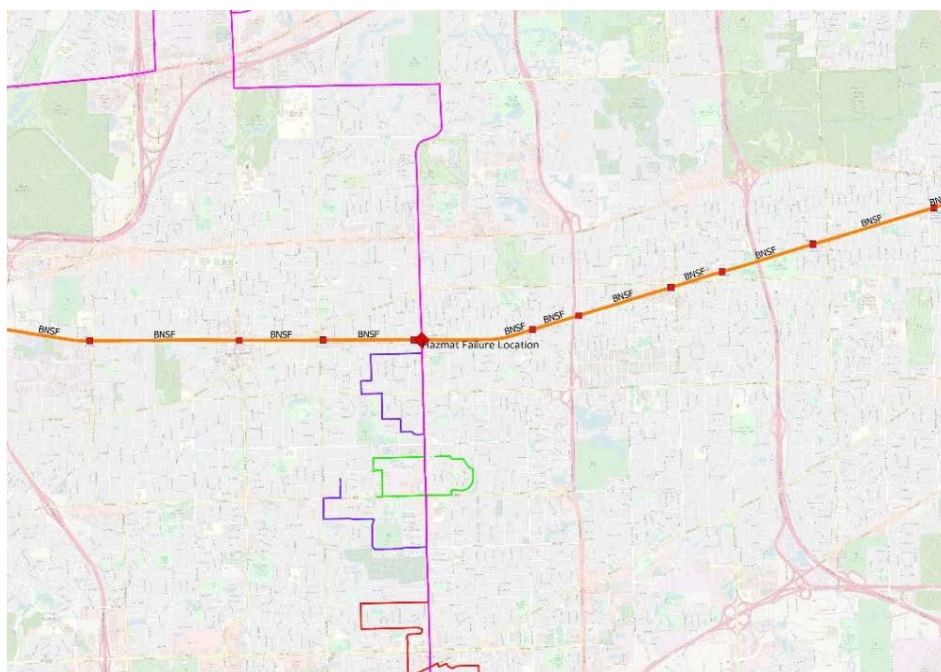
Wind Data

The Illinois State Water Survey, a research team supported by the University of Illinois Board of Trustees, published a study of average wind speed in Illinois. The highest average wind speed is in Spring, about April, which is 9.2 mph. Table 9-19 summarizes the average wind speed in Illinois. However, according to the field data collected in recent years, wind speed can reach 30 mph occasionally and 20 mph frequently. The wind speed was assumed to be 20 mph towards the northern direction in this case study.

Table 9-19 *Historical Data on Wind Speed in Illinois*

Month/Season	Wind Speed
January	8.7
February	8.6
March	9.1
April	9.2
May	7.6
June	6.3
July	5.6
August	5.0
September	5.6
October	7.0
November	8.4
December	7.9
Winter	8.4
Spring	8.7
Summer	5.7
Fall	7.0
Annual	7.4

Case Study Consideration

**Figure 9-43** *Hazmat failure location*

Phase 1. Reporting of a Hazmat Emergency Event

The case study assumes that a hazmat-related emergency event occurs in the busiest time period of a day, the AM peak. The emergency communication center receives calls reporting a truck crash at the Cass Avenue and Metra BNSF crossing intersection with hazard gas leakage. 911 dispatches the initial responders, including police, firefighters, and ambulances, to the accident location.

Phase 2. Initial Response

The emergency team roughly recognizes the color, odor, and type of the gas and establishes the initial clearance zone. Adjacent intersections will be blocked by police vehicles. Even though the initial buffer is relatively small, the operation of BNSF and PACE route 715 is interrupted. According to Metra ridership data, in the AM period, a majority of passengers are moving from the west to Union Station; therefore, almost all passengers on BNSF commuting rails need to choose alternative transit such as PACE buses. The number of passengers from the west is estimated to be 16,353, with 583 from the east in AM peak period. With PACE route 715 affected, multiple PACE routes as shown in Table 9-20 are available as alternatives.

Table 9-20 *Alternative Transit Options*

N-S Oriented PACE Route	E-W Oriented PACE Route
462	301
463	313
465	322
661	755
662	826
664	850
665	851
668	855
669	
715	
821	
825	
834	
877	
888	
890	
895	
BNSF	

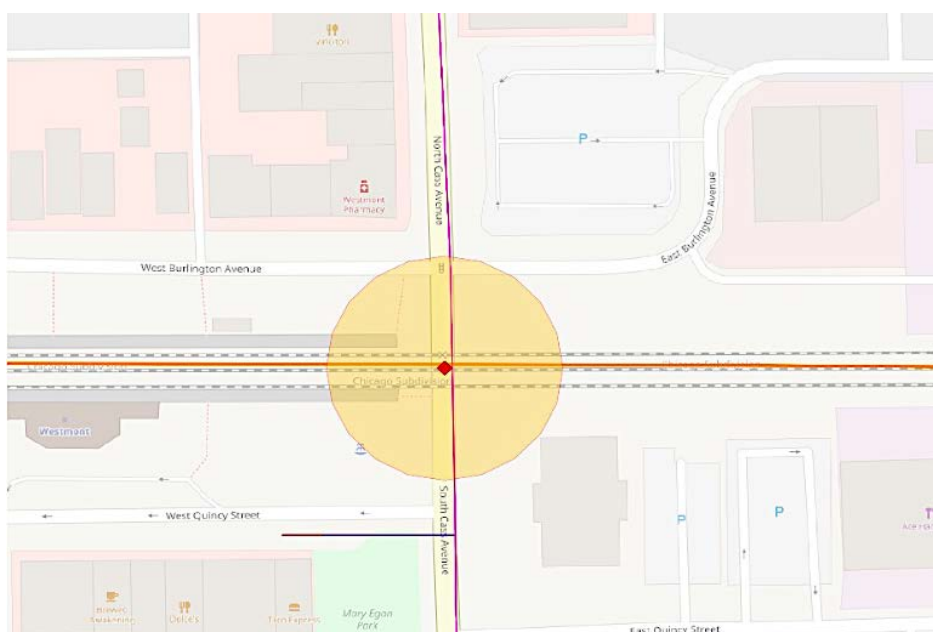


Figure 9-44 Initial clearance

Phase 3 Hazmat Spreading

Additional traffic control is executed, and the hazardous materials start to spread to the residential area. This affects Metra train passengers as well as local residents in need of evacuation. At this time, the area is at risk and the number of impacted population need to be re-estimated. According to the new assessment, the emergency management team revises and implements a new evacuation strategy and considers if State or federal assistance is required. Residents affected in this phase are estimated to be 4,000, including 12.1% of populations in poverty.

Table 9-21 *Affected Transit Pattern in Phase 3*

Route	Pattern	# of Trips
M-BNSF	M-46f5dde94d610c28a64135c90f995da7	1
M-BNSF	M-ad6e46c45599e833a42ccacf81202fc1	1
M-BNSF	M-cc21bd70b91f2356278c8d196288566c	1
M-BNSF	M-cc9350807394baf960f26d853b6e30d1	1
M-BNSF	M-2472b7c521a15eee6719e54b82854bb5	1
M-BNSF	M-901ec95959b7658792fcacccf25b46a1	2
M-BNSF	M-bee454d3fe1aecb96980622ba3a3200e	1
M-BNSF	M-f50d83684e564f492afed9df8eb1865f	1
M-BNSF	M-f630c95184d3a6df4758366021aeb53f	2
M-BNSF	M-70ab64c658b70a41f5d781c581d8cfec	3
M-BNSF	M-7f99a2b89b3e56bede59e29a1c243a90	1
M-BNSF	M-efbe3c637a501f20ac8f8be31d1852a8	2
P-661-200	P-16ba63c010fdb6951f5d35e8ec9fa36c	1
P-661-200	P-0addec4fb336c9cba8c03b7bb24e8719	1
P-662-200	P-860ab2eaf34fb72dcfb95d6388e1f717	2
P-662-200	P-e71da395ff8a4ef54c68160155d65be9	1
P-665-200	P-4fffba5c861e248e13de37c399ecee08	2
P-715-0	P-55de2ff6b193f418947ec7cfacd4b8b7	2
P-715-0	P-e3ba1f47a7698e3b37ac8a3515421114	2
P-715-0	P-8bc44f1fdf832930ff2fa1a68178fe2e	4
P-715-0	P-43e44ee82f7fc1f60aee4b19ec41e86e	3

**Figure 9-45** *Hazmat emergency affected area in Phase 3*

Phase 4. Final Impact

In this phase, hazardous materials spread to the largest area possible. Out of the area, the density of the hazmat is too low to adversely affect human health and the environment. However, the emergency response team should closely monitor the weather condition and air quality to prepare for any unexpected secondary emergency. The affected area is estimated to be up to 2 square miles, and residents within the area are about 9,000, with around 1,100 below the poverty level. In the end, the reentry process of BNSF is planned, and media updates on the emergency evacuation progress need to be prepared and disseminated.

Table 9-22 *Affected Transit Pattern in Phase 4*

Route	Pattern	# of Trips
M-BNSF	M-46f5dde94d610c28a64135c90f995da7	1
M-BNSF	M-ad6e46c45599e833a42ccacf81202fc1	1
M-BNSF	M-cc21bd70b91f2356278c8d196288566c	1
M-BNSF	M-cc9350807394baf960f26d853b6e30d1	1
M-BNSF	M-8ae18881035e88223e354adcb91cc489	1
M-BNSF	M-2472b7c521a15eee6719e54b82854bb5	1
M-BNSF	M-901ec95959b7658792fcacccf25b46a1	2
M-BNSF	M-bee454d3fe1aecb96980622ba3a3200e	1
M-BNSF	M-f50d83684e564f492afed9df8eb1865f	1
M-BNSF	M-f630c95184d3a6df4758366021aeb53f	2
M-BNSF	M-70ab64c658b70a41f5d781c581d8cfec	3
M-BNSF	M-7f99a2b89b3e56bede59e29a1c243a90	1
M-BNSF	M-efbe3c637a501f20ac8f8be31d1852a8	2
P-661-200	P-16ba63c010fdb6951f5d35e8ec9fa36c	1
P-661-200	P-0addec4fb336c9cba8c03b7bb24e8719	1
P-662-200	P-860ab2eaf34fb72dcfb95d6388e1f717	2
P-662-200	P-e71da395ff8a4ef54c68160155d65be9	1
P-665-200	P-4fffba5c861e248e13de37c399ecee08	2
P-715-0	P-55de2ff6b193f418947ec7cfacd4b8b7	2
P-715-0	P-e3ba1f47a7698e3b37ac8a3515421114	2
P-715-0	P-8bc44f1fd832930ff2fa1a68178fe2e	4
P-715-0	P-43e44ee82f7fc1f60aee4b19ec41e86e	3

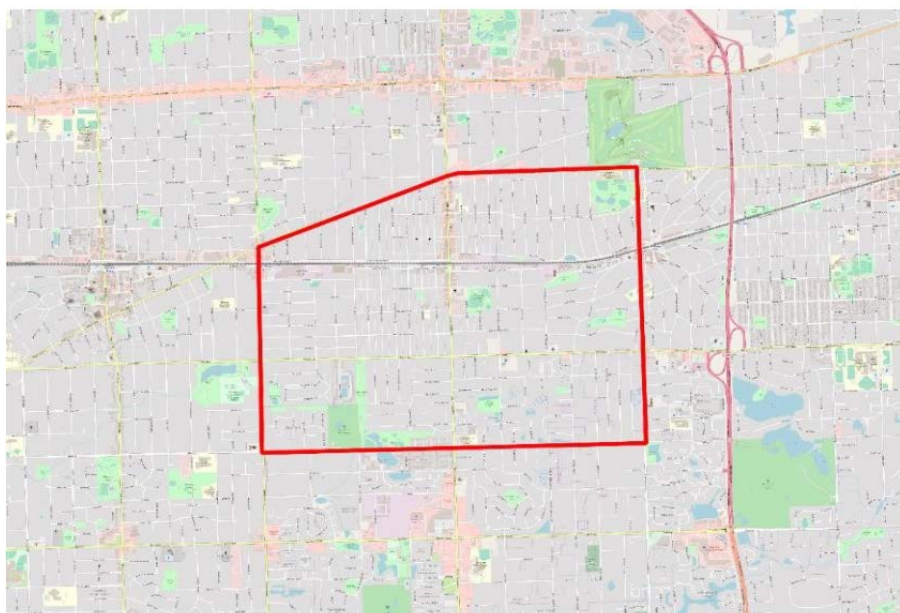


Figure 9-46 Hazmat emergency affected area in Phase 4

Table 9-23 Summary of Four-Phase Hazmat Emergency Response Process

Phase	Demand		Supply	Countermeasure (Bus Rerouting)			
	Residents	Passengers		East-West		North-South	
				Origin	Destination	Origin	Destination
1	-	-	~ 10 buses in operation, 30 buses in garages nearby	-	-	-	-
2	-	W-E 720		Fairview	Clarendon Hills	Cass/ Irving	Cass/ Richmond
		E-W 195					
		N-S <100					
		S-N <50					
3	500	W-E 1,136		Fairview	Clarendon Hills	Cass/ Norfolk	Cass/ 56th
		E-W 173					
		N-S <100					
		S-N <50					
4	550	W-E 1,568		Main	W Hinsdale	Cass/ Melrose	Cass/ 60th
		E-W 162					
		N-S <100					
		S-N <50					

Review of Hazards Classification, Detection, Communication, and Mitigation Methods and Technologies¹⁰

Hazard Classification and System Resilience

Hazard Characteristics

Cities and urban areas generally maintain extensive architectural structures, interconnected infrastructure systems, a high density of population, and concentrations of human activities. This makes them livable and attractive. However, it also puts them at high risk to all kinds of hazards such as floods, hurricanes, earthquakes, terrorist attacks, and so forth. As illustrated in Figure 10 1, hazards can be largely classified into with-notice and no-notice categories. With-notice hazards refer to those that can be predicted based on data collected on a real-time basis; consequently, some counteractions can be prepared in advance. This type of hazard contains weather-related natural disasters. No-notice hazards refers to those that cannot be well predicted. This kind of hazards includes fires, power supply failures, nuclear events, and so forth.

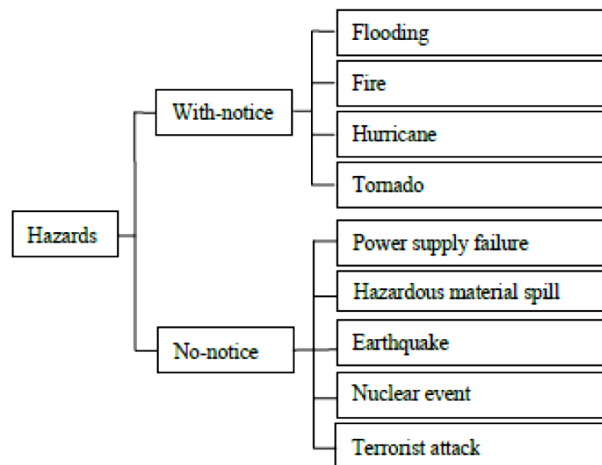


Figure 10-1 Typical hazard classifications

¹⁰ Authored by Zongzhi Li, Yongdoo Lee, Yunseung Noh, Lu Wang, and Ji Zhang, IIT.

With-Notice Hazards

Flooding

As cities and urban areas expand outwards to accommodate modern urbanization, ever-increasing population and inefficient decision-making often bring unexpected results in the form of unplanned development in floodplains and flood-prone areas. Global climate change is another critical fact perceived to have a significant impact on flood risk increases. The meteorological patterns movement associated with a warmer climate is also likely to increase risk.

Climate change can contribute to flood risk increases in multiple ways. For example, global warming augments the rate of sea-level rise that will lead to more flood damage in coastal areas. It also changes local rainfall patterns that may cause more frequent and higher levels of flash floods from local rivers and other water bodies. Climate change may alter the frequency and duration of drought events that lead to groundwater extraction and land subsidence compounding the impact of sea-level rise. Further, climate change could result in more extreme weather conditions such as storms causing more frequent sea surges. The intensity of a flood event is measured by flood category.

Table 10-1 *Flood Categories*

Flood Category	Description
Minor	Minimal or no property damage, but possibly some public threat.
Moderate	Some inundation of structures and roads near stream. Some evacuations of people and/or transfer of property to higher elevations
Major	Extensive inundation of structures and roads. Significant evacuations of people and/or transfer of property to higher elevations
Record	Flooding that equals or exceeds the highest stage or discharge at a given site during the period of record keeping

Fire

Fires are one of the most severe hazards to anything flammable. Fire hazards can be classified into three types in terms of the location of occurrences—Indoor, Urban, and Wildfire. The first two are discussed in this section. Indoor fires are mainly caused by overloaded electrical outlets or overworked extension cords. Nowadays, installations of indoor smoke detectors and fire alarms are mandatory. This minimizes indoor fire risk and stops an indoor fire from expanding to a large-scale urban fire hazard. Urban fire hazards are largely related to architectural buildings and transportation infrastructure.

In recent decades, the rapid expansion of urban transportation systems and increases in shipping of hazardous materials such as flammable, spontaneously combustible, and poisonous materials have raised concerns about fires. This

type of fire hazard is primarily caused by crashing of vehicles and burning of gasoline. Gasoline fires, referred to as hydrocarbon fires, are likely to be more severe than building fires due to a fast heating rate and a higher peak temperature. Currently, there is no well-known standard to measure fire hazard intensity. Normally, the location, time duration, property loss, and number of fatalities and injuries associated with a fire are factors used to describe fire hazards and analyze their impacts.

Hurricane and Tornado

Hurricanes are one of the costliest natural hazards in the southeast coastal area of the U.S., mostly near the Caribbean Sea. This kind of hazard occurs near the tropical zone and over warm waters in the Atlantic and Pacific. A hurricane always lasts for days and occurs around 10–15 times per year in the U.S. It always brings heavy wind, flooding, storm surge, rain, and tornadoes. Spatial coverage could have a diameter of hundreds of kilometers. Hurricanes are classified by the Saffir-Simpson Wind Scale into five categories.

Table 10-2 *Saffir-Simpson Wind Scale for Hurricane Hazard Measurement*

Category	Wind Speed (mph)	Types of Damages
1	74–95	Very dangerous winds causing some damages to well-constructed homes on roofs, shingles, vinyl siding, and gutters; snapping large tree branches and topping shallowly rooted trees; and extensive damage to power lines and poles with multi-day power outages
	96–110	Extremely dangerous winds causing extensive damage to well-constructed homes on roofs and sidings; snapping or uprooting many shallowly rooted trees with road blockage; near-total power loss with outages lasting several days or weeks
3	111–129	Devastating damage severely damaging well-built homes or removing roof decking and gable ends; snapping or uprooting many trees with road blockage; loss of electricity and water for days or weeks after storms
4	130–156	Catastrophic damages to well-built framed homes with loss of most of the roof structure and/or some exterior walls; snapping or uprooting most trees and downing power poles with residential areas isolated; power outages lasting weeks to possibly months with most areas uninhabitable
5	≥157	Catastrophic damages to destroy a high percentage of framed homes with total roof failure and wall collapse; fallen trees and power poles isolating residential areas; power outages lasting for weeks to possibly months with most areas uninhabitable

Similar to a hurricane, a tornado brings very strong cyclonic winds, heavy rain, large hail, and strong cloud-to-ground lightning. However, the time duration of a tornado is always less than one hour. One tornado can have a diameter of hundreds of meters. The U.S. records about 1,200 tornadoes per year, which commonly occur in Spring and Fall when cold and warm fronts converge and can occur anywhere. The scale used for rating the strength of tornadoes is the Fujita (F) scale, developed in 1971. The Enhanced Fujita (EF) scale was unveiled by the U.S. National Weather Service on February 2, 2006. The EF Tornado Scale was put into use in the U.S. effective on February 1, 2007.

Table 10-3 *Enhanced Fujita Scale for Tornado Hazard Measurement*

Scale	Wind Speed (mph)	Frequency (%)	Potential Damages
EF0	65–85	56.88	No reported damage in open fields or minor damages to homes with some roofs peeled off or some damage to gutters or siding; branches broken off trees; shallow-rooted trees pushed over
EF1	86–110	31.07	Weak to moderate damage with roofs severely stripped; mobile homes overturned or badly damaged; loss of exterior doors; windows and other glass broken
EF2	111–135	8.80	Considerable damage to well-constructed houses with roofs torn off; foundations of frame homes shifted; mobile homes completely destroyed; large trees snapped or uprooted; light-object missiles generated; cars lifted off ground
EF3	136–165	2.51	Severe damage to entire stories of well-constructed houses and large buildings such as shopping malls; trains overturned; trees debarked; heavy cars lifted off the ground and thrown; structures with weak foundations badly damaged
EF4	166–200	0.66	Devastating or extreme damage to well-constructed and whole frame houses; cars and other large objects thrown and small missiles generated
EF5	> 200	0.08	Total destruction of buildings; level of strong-framed, well-built houses; sweeping of foundations; critical damages to or severe deformations of steel-reinforced concrete structures; collapse of tall buildings; blowing away cars, trucks, and train cars

No-Notice Hazards

Power Supply Failure

The U.S. electric power grid is an interconnected network for electricity delivery from suppliers to end-use customers. Driven by changes in federal law, regulatory changes, and electric power infrastructure modernization, the grid is continuously evolving from a mainly patchwork system to a national interconnected system, transferring electrical power in the country. Although the U.S. electric grid has operated with a high degree of reliability in the history, many components of the electric grid system are vulnerable due to natural, operational, or manmade blackout events. It is possible power supply failure event comes any time. The intensity of a blackout event is measure using the time duration and spatial coverage along with the economic loss caused by the power outage.

Hazardous Material Spills

Hazardous material spills can be categorized into two types by the spill location—on site and during transportation. This review focuses on the second type because it is more likely to affect the transportation system and the traveling public. Hazardous material spills during transportation could be mainly caused by vehicular crashes, pipe failures, and container failures.

According to USDOT, a hazardous material is defined as any substance or material capable of causing harm to people, property, and the environment. Dependence on hazardous materials is the basis of running industrialized societies. At present, tens of thousands of hazardous materials are used in daily life. The United Nations sorts hazardous materials into nine classes based on their physical, chemical, and nuclear properties: explosives and pyrotechnics; gases; flammable and combustible liquids; flammable, combustible, and dangerous-when-wet solids; oxidizers and organic peroxides; poisonous and infectious materials; radioactive materials; acidic or basic corrosive materials; and miscellaneous dangerous goods, such as hazardous waste.

Earthquake

An earthquake is a natural phenomenon bringing fault rupture, ground shaking, ground displacement, liquefaction, and induced-landslide. Consequently, it could trigger more hazards such as flooding, tsunami, and nuclear events. The combined impact would be far more complicated. There are four different types of earthquakes—tectonic, volcanic, collapse, and explosion. A tectonic earthquake is one that occurs when the earth's crust breaks due to geological forces on rocks and adjoining plates that cause physical and chemical changes. A volcanic earthquake is any earthquake that results from tectonic forces that occur in conjunction with a volcanic activity. A collapse earthquake is a small earthquake in underground caverns and mines caused by seismic waves

produced from the explosion of rock on the surface. An explosion earthquake is resulted from detonation of a nuclear and/or chemical device.

An earthquake is recorded and measured by recording seismic waves, which are the vibrations from the earthquake that travel through the earth. The influenced area varies from place to place. One large earthquake could destroy a small village in a short period, and a small earthquake will not affect anything. In general, the larger the earthquake, the more intense the shaking and the duration of the shaking. The instrument used to record seismic waves is called a seismograph and could greatly magnify and record these ground motions as a function of time. They could also catch the time, locations, and magnitude of an earthquake typically at periods of between 0.1 and 100 seconds. The Richter scale was developed in 1935 and is a mathematical tool to compare the size of earthquakes.

Table 10-4 *Richter Scale for Earthquake Hazard Measurement*

Richter Scale	Frequency	Effects
2.5 or less	900,000	Usually not felt, but can be recorded by seismograph
2.5–5.4	30,000	Often felt, but only causes minor damage
5.5–6.0	500	Slight damage to buildings and other structures
6.1–6.9	100	May cause a lot of damage in very populated areas
7.0–7.9	20	Major earthquake. Serious damage
≥ 8.0	0.3	Great earthquake. Can totally destroy communities near the epicenter

Nuclear Event

Nuclear accidents generally contain two types of hazards. One is radioactivity leakage in a nuclear power plant caused by equipment failure, human error committed during field operations, and other reasons. The direct consequences are radioactive emissions into atmosphere, soil contamination, and water effluence. Further, food and drinking water will be affected from a nuclear accident.

The other type is nuclear attack using nuclear weapons. Compared to conventional chemical explosives such as gunpowder and TNT, nuclear weapons are significantly more compelling and capable of creating devastating effects that other common chemical explosives cannot create. Effects of a nuclear weapon attack are more complicated, which generally contain thermal pulse, blast, prompt radiation, electromagnetic effects, mass fire, and residual radiation.

A severe nuclear event can devastate an area with a diameter of at least 10 miles. Apart from instant massive destruction made by a nuclear event, the radioactive material contamination may last for years or even decades. The intensity of a nuclear event is measured using the International Nuclear Event

Scale (INES) classified on a seven-level scale. An event classified from level 1 to level 3 is considered an incident, and it becomes an accident when the level is greater than 3. Each one-level increase on the INES represents a 10-time increase in severity.

Table 10-5 *INES Scale for Nuclear Hazard Measurement*

INES Level	Description
Level 1: Anomaly	Public exposure in excess of annual limits, caused by stolen radioactive source, device, or transportation package
Level 2: Incident	Public exposure in excess of 10 mSv, worker's exposure in excess of the statutory annual limits
Level 3: Serious incident	Near-accident at a nuclear power plant without safety provisions
Level 4: Accident with local consequences	Minor release of radioactive material with at least one death from radiation
Level 5: Accident with wider consequences	Limited release of radioactive material with at least several deaths from radiation
Level 6: Serious accident	Significant release of radioactive material
Level 7: Major accident	Major release of radiative material with widespread health effects

Terrorist Attack

Terrorism is not like natural or even other manmade hazards. To the extent that terrorist incidents might even resemble natural or technological disasters, the response could be very similar. A bridge or a building collapse, a dirty bomb detonation, a fire, an explosion, a power outage, and even a flood might result from terrorist actions.

Because a terrorist attack could cause other types of hazard, there is no specific standard to measure the intensity of the general terrorist attack. Time duration, spatial coverage, intensity, casualty, and economic loss are general measures for all hazards triggered by terrorist attacks.

Impact on Transportation System and Resilience

Infrastructure

Flooding

Flooding with long-duration will deteriorate structural components of transportation infrastructure, including roads, bridges, and tunnels with high recovery cost. Depending on the form of reconstruction and characteristics of flooding, much infrastructure may survive a flood but will be damaged extensively by the corrosive effect of salinity and damping and be in need of substantial repairs and refurbishment. The infrastructure will be out of service

as long as it is located in the flood area. Indirect impacts in terms of loss of transportation network-wide mobility are significant, especially when the spatial coverage is large.

Like roadway system, rail tracks and stations would be partially out of service after flooding. The impacts of flooding on underground subway systems can be devastating. Entire platforms, stations, and tracks and tunnels can be soaked for a long time. The time costs and labor needed for recovery are extremely high. The resilience of the transit system depends on the intensity of the flooding event. If the spatial coverage is small, the unimpacted transit service near the event area could be used as an alternative for travel if available.

Signs, pavement markings, and crash cushions will not be affected much in terms of their quality loss caused by flooding. They will temporarily lose function in a roadway that is no longer usable. Signals and lighting are different from other traffic control and safety hardware because their functions rely on electricity power supply, which is extremely vulnerable in the flood hazard.

Fire

Building fire hazards will not directly have any impact on infrastructure. However, transportation infrastructure fires may cause damage in different ways. Transportation infrastructure fires can lead to significant economic and public losses. Traffic damaged by fire is usually difficult to detour and affects the traffic mobility in the local area, especially on a highway. A severe fire may lead to permanent damage or even collapse of a bridge or tunnel.

Generally, the spatial coverage of a fire is relatively small, but the impacted area varies from site to site. Rail service would be shut down if a track or station is on fire. If the fire hazard location is on a roadway network, bus transit service could detour if possible. If the fire hazard occurs on a major bridge or in a tunnel, system resilience will come to the minimum due to the lack of alternative bypasses. In an urban network, closing fire-affected roadway segments and using temporary traffic control measures could mitigate impacts. In this case, the unimpacted transit service near the event area could be used as an alternative mode to evacuate affected people and keep the transportation system running.

Hurricane and Tornado

Primary hurricane phenomena of concern are storm surge, extreme rainfall, extreme winds, tornadoes, and wind driven waves. The interaction of these phenomena with natural and built environments generates additional hazards, including coastal surge, inland rainfall, flooding, erosion, scour, rain-induced landslides, and flood borne and windborne debris.

In the short term, bridges, especially suspension bridges, can be easily damaged and even destroyed by high winds. The components made from steels suffer rust in the long run. The entire structure will deteriorate remarkably under a long time of erosion. The situation is slightly better in terms of roads and tunnels. For most of traffic signs, lighting poles, and signal heads, they might be blown away by winds instantly. Similarly, the erosion is another critical issue for all kinds of traffic control and safety hardware.

Power Supply Failure

If a power failure occurs in an urban area especially the densely populated central business district, the local street network quickly becomes full of vehicles and people. On the transportation supply side, one of the most immediate impacts is the instant failure of traffic signals that will reduce the system capacity. The increase in vehicular and passenger demand, coupled with system capacity reduction, will inevitably lead to severe traffic congestion and even deadlock of the urban street network. Roads and bridges will not be affected, but the loss of lighting supply inside tunnels will potentially reduce efficiency of evacuation. At nighttime or in rural areas, the impacts of power supply failures are minor. All electricity-driven equipment in transit system is out of service instantly. However, nowadays, transit systems are equipped with backup power sources. Therefore, the resilience of transit systems in this case is very high.

Hazardous Material Spill

The damages caused by hazardous material spill depends on the material type. Explosive, flammable, or combustible materials are harmful to transportation infrastructure if ignited. The effects could be as same as by fire or explosive hazards. Corrosive materials may directly corrode pavements, bridges, and rail tracks. Effects brought by other types of materials are minor.

Earthquake

The first main effect of a severe earthquake hazard is the ground shaking. Bridges, tunnels, and rail tracks can be damaged and even destroyed by the shaking itself or by the ground beneath them settling to a different level than it was before the earthquake. Generally, concrete and masonry structures are brittle and more susceptible to damages. Wood and steel structures are more flexible and less susceptible to damages. Likewise, transit stations and platforms can be damaged and even sink into the ground if soil liquefaction occurs. These facilities can also be damaged by strong surface waves making the ground heave and lurch. Any facilities in the path of these surface waves can lean or tip over from all movements. Traffic control and safety hardware may not be influenced directly from the moving ground, but they might be damaged by ground shaking and falling elements from buildings failure. In most cases,

the affected infrastructure needs to be rebuilt, and traffic has to re-route during the rebuilding process.

Nuclear Event

Normal nuclear material leakage will not bring damage to the transportation infrastructure directly. As for a nuclear attack, the damage to the infrastructure is catastrophic. The thermal pulse will melt everything near the center of explosion, and the blast created by the explosive could instantly inflict a city-wide infrastructure failure.

Vehicles

Flooding

Floods with a high depth can have devastating impacts on automobiles. Direct impacts are physical damages to vehicles. When cars encounter flooding, they may stay inside water for days or weeks while water saturates everything. This can severely compromise a vehicle's interior, electronics, and powertrain. Salt water flooding, even light flooding, does the worst damage to cars. If the engine of a vehicle is soaked by water for a certain period, the vehicle is not capable of moving at that moment. After the flooding event, the repair cost is as high as the cost to rebuild a car in the worst case. Situations in terms of trucks and buses are slightly better because of their relative high profiles.

Fire

Any vehicle would be extremely vulnerable if it is on a fire unless a fire extinguish is used in the beginning to stop the fire. The most evident impacts on most vehicles involved are mobility losses due to the fire hazard ahead. Without an in-time response, the influenced area may be expanded over time and more vehicles will be involved, leading to traffic congestion.

Hurricane and Tornado

Operating vehicles in all kinds of travel modes are extremely dangerous in heavy winds. Passenger cars may be blown away even if they are not running. From this perspective, the transportation system has literally failed to function properly. The ground transportation system is mainly influenced by winds and the underground transportation system is constrained by flood. Trains, buses, and trucks are relatively heavier than passenger cars and are more likely to keep steady in strong winds. However, driving them as usual is still impossible.

Power Supply Failure

Power supply failures pose a minor effect on passenger cars. Some power-driven cars may not be able to charge during the blackout. However, most of the vehicles could still function properly. The same is true for buses and trucks. Although

some trains need electricity as power sources, temporary blackout is unlikely to bring any significant difference with available backup power. Conversely, a power outage with a long duration could cause failure of a train system.

Hazardous Material Spill

Damage to vehicles caused by hazardous material spills also depends on material type. Explosive, flammable, and combustible materials could explode or burn vehicles nearby, similar to fire hazards or explosive hazards. Corrosive materials could directly corrode vehicles if any contact occurs.

Earthquake

There is a possibility that some vehicles may sink into ground because of soil liquefaction. Vehicles are relatively safe in a clear space such as a suburban or rural area. In an urban area, the dense building layout could potentially damage or even bury vehicles with falling construction materials.

Nuclear Event

Normal radioactivity leakage does not affect vehicles directly. In a nuclear attack, damage to vehicles is catastrophic; the thermal pulse and blast created by the explosive could instantly destroy all vehicles nearby.

Users/Non-users

Flooding

Floods worldwide pose a range of threats to human life, health, and well-being. On average, reported flood disasters directly kill over 8,000 people in each year. The amount and seriousness of impacts on the affected population will vary and can involve physical fatalities, injuries, or other health effects. The mental trauma of flooding, caused by witnessing deaths, injuries, and destruction of homes, can result in severe psychological effects in some individuals. Grief and material losses, as well as physical health problems, can lead to depression or anxiety. The most vulnerable members of the community can also be those worse affected—the poor, older adults, and the youngest members of the community who often require special assistance. Research has found that children and older adults are more likely to die, particularly from drowning, than are adults.

Fire

Transportation infrastructure fire hazards are generally caused by crashing of vehicles and burning of gasoline. The impacts on drivers and passengers directly involved in this kind of hazard are devastating. Pedestrians and cyclists near crashes could be hurt by the explosion after the occurrences. Like flooding, mental trauma caused by witnessing the hazards also exists.

Hurricane and Tornado

Any exposure to a hurricane and tornado is dangerous, even in an area where the hazard is not severe. People should stay in a hurricane shelter until the hazard severity level reduces to a safe level. Public awareness about general needs for evacuation and how to deal with a hazard is essential for efficient evacuation. Without this, public panic will become another impact brought by hurricane and tornado.

Power Supply Failure

Power supply failures place no threat to people's health. However, a large-scale outage could create public panic.

Hazardous Material Spill

Hazardous materials could injure and kill people. The severity level of damages to human beings caused by hazardous materials also depends on material type. Explosive, flammable, and combustible materials could lead to fire hazards or explosive hazards. Corrosive material could directly corrode people if any contact occurs. The consequence of releasing poisonous and radioactive materials can have health concern (death, injury, or long-term effects due to exposure). Environment effects including soil contamination and water contamination could also influence human health in the long run.

Earthquake

Similar to vehicles, earthquakes pose little direct danger to people. However, the shaking caused by the seismic waves of an earthquake could damage buildings and cause them to collapse, and the collapse buildings could bury and kill people.

Nuclear Event

Human beings are vulnerable in nuclear events. A nuclear attack in populated areas would inflict massive loss of lives, and the residual radiation will affect human health in multiple ways. For instance, people could be affected through ingestion of contaminated food and water. Children and pregnant women are particularly sensitive to radioactive iodine, which can harm the thyroid. Tens of thousands of people could be unable or unwilling to return to their homes because of fears of contamination in the area. Public panic is another critical effect brought by nuclear events. Public confidence in government could be significantly lost if the effectiveness of government responds to the events is perceived to be low.

Summary

To summarize the impact on transportation system brought by hazards and system resilience in general, Table 10-6 shows the hazard impact level and transportation system resilience level using scales of high (H), moderate (M), and low (L), respectively.

Table 10-6 Summary of Hazard Impact and System Resilience Levels

Hazards	Infrastructure					Vehicles	Users
	Roads	Bridges	Tunnels	Traffic control and safety hardware	Transit		
Flooding	H/L	H/M	H/L	M/L	H/L	H/L	H/L
Fire	H/L	HM	H/L	L/L	M/M	H/L	H/M
Hurricane	M/M	H/L	H/L	H/L	H/L	H/L	H/L
Tornado	M/M	H/L	H/L	H/L	H/L	H/L	H/L
Power failure	L/H	L/H	L/H	L/H	L/H	L/H	L/H
Hazardous material spill	M/M	L/H	M/M	L/H	L/L	M/L	H/L
Earthquake	H/M	H/L	H/L	M/M	H/M	M/H	M/L
Nuclear release	L/H	L/H	L/H	L/H	L/H	L/H	H/L
Nuclear attack	H/L	H/L	H/L	H/L	H/L	H/L	H/L

Hazard Detection Technologies

Advanced hazard detection technologies can prevent and ameliorate negative impacts of hazards. Hazard detection technologies include radar, satellite, camera surveillance, hazard material sensors, radioactive particle sensors, and electrical sensor, etc. The technologies can be divided into intrusive and non-intrusive detection depending on their method of installation. Intrusive methods collect data by embedding sensors in the infrastructure; non-intrusive methods use external equipment and primarily active detection technologies.

Table 10-7 *Classification of Hazard Detection Technologies*

Hazard Type	Detection Technologies	
	<i>Intrusive</i>	<i>Non-Intrusive</i>
Flooding	Rain gauge	Radar, satellite
Fire	Smoke detector, heat detector, flame detector, fire gas detector	Vision sensor detector
Hurricane		Satellite, ocean temperature detector, airborne
Power grid failure	Passive detection	Active detection
Hazardous material		Active monitoring, passive monitoring
Earthquake	Seismograph, electromagnetic measurements	Fluid pressure changes
Nuclear material		Gamma ray detector, neutron detector

Flood Detection

Flooding is water is flowing excessively onto land and then dry land is inundated, which is one of the most common natural disasters in both urban and rural areas. Flooding generally occurs when heavy rainfall causes a rapid rise of water in a short period of time. In addition, flooding can occur when ocean waves come on shore, dams or levees break, or snow melts quickly. Recently, the frequency and intensity of heavy rainstorms have been increasing because of global climate change. Type of storm, ground topography, and rainfall amount over an area as well as urban features and topography have an impact on flooding occurrence and its severity. Flooding can yield extensive damage to a highly-populated city and areas near rivers. Therefore, urban flooding modeling to detect inundation is necessary to set up measures and ameliorate risk. Radar, satellite, and rain gauges are used to detect heavy rainfalls.

Radar

Radar sensors are often used to graphically detect precipitation on a map because of their day-night capability regarding weather, as well as establishing flood relief management and improved urban flood inundation modeling. Radar provides sufficient resolution to show the location of heavy rainfall cores. The images and animations extracted from radar technology can be used for estimation of flooding extents and duration of rainfalls and for tracking movement and development of storms over time. In other words, radar technology provides specific information to help forecasters observe the intensity of an existing storm, predict how the storm begins to develop and where the location of flooding potentials over urban or rural areas is, and assess total rainfall accumulations for the duration of the event. For instance, the U.S. National Weather Service, which provides weather forecasting

and warnings for the protection of lives, uses Weather Surveillance Radar (WSR)-88D radar to estimate the amount of precipitation and assess rainfall intensities for flooding warnings. However, a difficulty with using radar for urban flood detection includes that radar cannot reveal several ground areas visually because of radar layover or shadow caused by buildings and taller vegetation.

Rain Gauge

A rain gauge is a helpful tool to detect how much rain has fallen at a single geographic point and to warn timing of flash flooding. This method is the most accurate equipment for measuring rainfall. Therefore, a rain gauge is used as the most useful method for flooding detection in case of requiring accurate rainfall observation. Rain gauges are installed as automated reporting networks, which provide real-time data. A rain gauge is also used to determine the accuracy of a radar system by comparing the value estimated by radar technology to the actual rain gauge amount. The accuracy of estimation can decrease in an area where there are obstructions over them such as leaves, trees, or building roofs. There are two types of rain gauge—analogue rain gauges, which typically consist of a clear acrylic or glass cylinder, and digital rain gauges, which are using a rain sensor for estimating and analyzing precipitation data.

Satellite

The use of satellites is a less direct and less accurate method for detecting flooding than radar or gauge technologies. However, this method shows high resolution and can be used over oceans, mountainous regions, or sparsely-populated areas where other sources of rainfall data are not available. Therefore, satellites can be useful for detecting hazards in the area where heavy rainfall originates from smaller-scale rainfalls or is not detected from other technologies.

Table 10-8 *Advantages and Disadvantages of Flooding Detection Technologies*

Technology	Advantages	Disadvantages
Radar	Shows high resolution, can be used in both day and night	Cannot be used in the shadow area
Rain gauge	Most accurate rainfall observation	Accuracy is affected by obstructions such as trees and building roofs
Satellite	Can be used in the area where other rainfall detectors cannot be used	Indirect technology, less accurate

Fire Detection

Technologies for fire detection can be categorized depending on detected sources. Particles produced by combustion, visible colors monitored by cameras, thermal energy, and visible light emitted by flames can be used as indicators to detect fires.

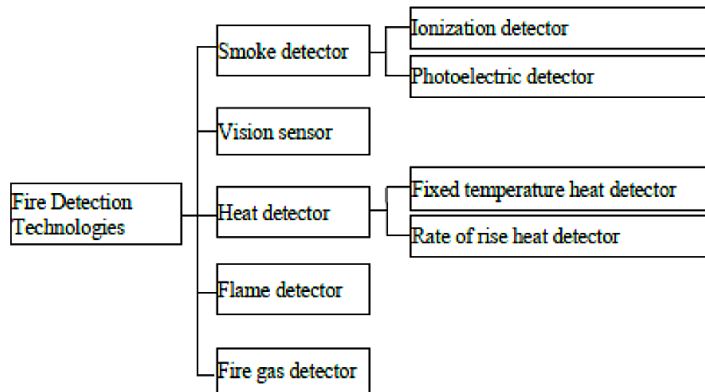


Figure 10-2 Classification of fire detection technologies

Smoke Detector

A smoke detector, which typically is used in large commercial, industrial, and residential buildings as an indicator of fires, is a fire alarm device that responds to visible or invisible smoke particles produced by combustion. Methods of smoke detection are photoelectric (optical process) detection and ionization (physical process) detection.

A photoelectric detector, also called an optical smoke detector, uses a light sensor and a light source containing infrared, visible, or ultraviolet light. When smoke particles enter the light path, some of the light is scattered and redirected into the light sensor, which triggers an alarm. This detector responds quickly to visible smoke particles from a smoldering fire while it is less sensitive at detecting particles generated in the flaming stage of fires or very hot fires.

An ionization smoke detector uses a radioactive source that generally emits alpha particles to ionize air and charges the air inside a small chamber. An electric current passes through the chamber because of a potential difference of voltage, and electrical circuit is completed by the charged air. When any smoke particles enter the chamber, they shield the radiation, which stops the electronic current from flowing and then an alarm is activated. Ionization detector is sensitive to small smoke associated with flaming or very hot fires because it can detect very small smoke particles and respond to them quickly. However, it reacts very slowly to the smoke associated with smoldering or low-temperature fires.

Vision Sensor Detector

A vision sensor detector uses fire color pixels and movement of a fire. A luminance map is made based on characteristics that the shape of a fire can be constantly changed by wind or burning material, and fire regions generally have a higher luminance contrast than neighboring regions, which can be used to identify a fire. When a camera obtains the information on occurrence of a fire, subtle differences between consecutive frames can be analyzed and the fire can be detected.

Heat Detector

A heat detector is a device that detects the thermal energy of a fire. The technology is normally used in dirty environments or where dense smoke is produced. The thermal mass and conductivity of the element regulate the flow rate of heat into the element. The detector has a fixed temperature heat detector and rates rising heat. Heat detectors use thermistors that reduce resistance as the temperature rises. One thermistor is sealed and protected from the surrounding temperature, whereas the other is exposed. When temperature increases, the resistance in the revealed thermistor would be reduced, large current happens, and then alarm is generated.

Flame Detector

A flame detector is a device designed to respond to specific types of light such as ultraviolet (UV), infrared light, and visible light emitted by flames during combustion. If light is detected by a sensor, it triggers an alarm sound. Flame detectors can often detect smoke particles more quickly and accurately than a smoke or heat detector because of the technical method it uses to respond to the specific flame.

Fire Gas Detector

A fire gas detector uses the presence of carbon monoxide (CO) gas to detect fire particles. CO is a colorless, tasteless, and odorless compound generated by incomplete combustion of carbon-containing materials. Unlike smoke detectors, which detect the smoke particles produced by a flaming or smoldering fire, a fire gas detector measures CO levels by using a fuel-burning device and sends a signal to activate alarm.

Hurricane Detection

Satellite

Satellites are used to detect hurricanes. This method enables to obtain visible images of clouds and the developing patterns of hurricanes. There are two major types of satellites for detecting hurricanes—geostationary operational environmental satellites, which observe weather above the same spot, and

polar-orbiting operational environmental satellites, which orbit the planet in above the poles.

Ocean Temperature Detector

The temperature of ocean surface waters is measured to monitor the occurrence of a hurricane and its potential intensity. For the measurement, rainfall-measuring microwave imagers and microwave scanning radiometers are used by a floating buoy which senses water temperature and radios and sends the information to detectors.

Airborne Detector

Airplanes could fly into hurricanes to measure wind speeds and intensity. Radar and microwave technologies are used in aircraft to visually scan the water surface and forecast hurricanes by gathering snapshots about the potential hazard area.

Power Grid Failure Detection

Synchronization, the process of matching the voltage, frequency, and phase angle of a generator to a grid supply, is a method used to monitor power grid failure. In an alternating current electric power system, a generator should be synchronized with the grid prior to connection. If a generator is not with the same frequency as the network, power cannot be delivered to an electrical grid. Therefore, the technique of synchronization can be implemented to detect the failure of electronic supply. Active and passive methods are used for power grid failure detection.

Active Detection

Active detection uses the technique of sending a signal between a distributed generator and a grid to prove electrical supply in the grid network. The method is relatively effective and easy to implement. Methods include impedance measurement, active frequency drift (AFD), reactive power export error detection, slip mode frequency shift algorithm (SMS), active frequency drift with positive feedback (AFDPF), automatic phase-shift (APS), and adaptive logic phase shift (ALPS).

Passive Detection

Passive detection is a method to use transient events in the electrical grid for detection of a power grid failure. The method continuously monitors the system factors such as frequency, voltage, and harmonic distortion. Passive detection methods are rate of change of frequency, voltage unbalance, harmonic distortion, and rate of change of output power of a distributed generator (DG).

Hazardous Material Detection

Once hazardous material spills out, it is difficult and takes a long time to restore to its former state, which also has a substantial impact on human in urban and rural areas and the environment. Therefore, timely detection of harmful material is important to ensure adequate functioning of the infrastructure and reduce damage. The detection methods of hazardous material spilled out have passive and active monitoring technologies. The major difference between active and passive monitoring techniques is whether illuminating sources are used. In other words, while active monitoring methods are using illuminating sources, passive monitoring methods do not use them.

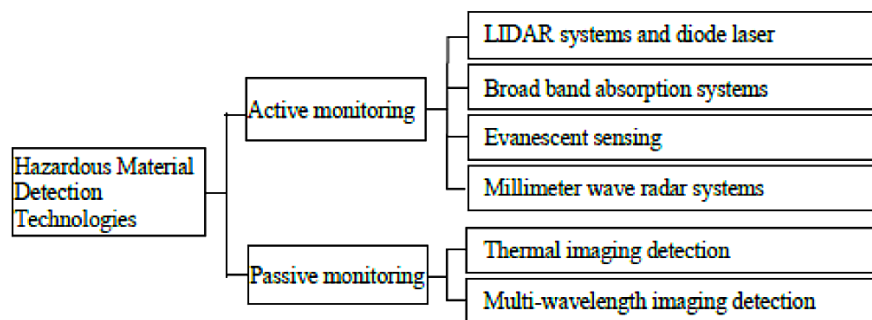


Figure 10-3 Classification of hazardous material detection technologies

Active Monitoring

Active monitoring uses a laser or broad band source as illuminating sources above hazard materials. The sources are illuminated, and the presence of detrimental sources is determined by detecting the absorption or scattering images caused by molecules over the potential danger surface. Methods for active monitoring include LIDAR systems and diode laser absorption, broad band absorption systems, evanescent sensing, and millimeter wave radar systems based on a used illuminating source.

Table 10-9 *Characteristics of Active Monitoring Detection*

Active Monitoring	Illumination Source	Description
LIDAR systems and diode laser absorption	Pulsed laser, diode laser	Detector monitors scattered energy; laser can be affected by dust particles, which yields false alarms
Broad band absorption systems	Lamp	Uses low cost lamps as source; multiple wavelengths are needed to reduce false alarms
Evanescent sensing	Optical fiber	An optical fiber is buried along with pipe; change in pressure when hazardous material escapes causing a change in transmission character of optical fiber, which can be used as an indicator of leak
Millimeter wave radar systems	Millimeter wave radar (carbon dioxide laser)	Can be used for monitoring materials containing methane; density difference between methane and air can be monitored to detect leakage

Passive Monitoring

Passive monitoring uses radiation produced by hazardous materials or background radiation as a source of detection instead of illuminating sources. The technology requires sensitive detectors and imagers to respond to a relatively weak radiation source. Passive monitoring methods include thermal imaging detection and multi-wavelength imaging detection.

Table 10-10 *Advantages and Disadvantages of Hazardous Material Detection Technologies*

Type	Advantage	Disadvantage
Active monitoring	Can be used on moving vehicles, aircraft or on location; able to monitor over an extended range and without temperature differences; high spatial resolution and sensitivity	High incidences of false alarm; skilled operators are required; cannot be used for unsupervised monitoring because of safety issues of using powerful lasers
Passive monitoring	Long sections can be monitored; can be used from ground, vehicle, aircraft, and satellite platforms; remote monitoring is possible	Infrared arrays are very expensive; requires very sensitive and expensive imagers and detectors

Earthquake Detection

Earthquakes generate significant damage in a short time and can result in considerable loss of lives. Earthquake detection covers a wide range of time spans—long-term (tens to hundreds of years), mid-term (years to months), and short-term (days to hours). Earthquakes occur in certain regions intensively, which can be a milestone to identify the area where earthquakes are most likely to happen. They tend to recur along the same fault line in separate event

and have not regular cycle. Moreover, an earthquake can yield a series of other earthquakes along a fault line.

Seismograph

A seismograph is an instrument commonly used to detect ground vibration generated by earthquakes. It can determine where an earthquake has happened (location), the amount of energy released (magnitude), and how deep the earthquake is (depth) by recording seismic wave. A seismograph consists of a frame and a mass. If a seismic activity occurs, the frame vibrates and the difference between the frame and mass is recorded on a seismograph, which can be used to calculate ground motion. It is deployed at the solid surface and used on land. However, they are not effective for fault measurements in marine areas.

Electromagnetic Measurement

Radiation is emitted prior to the occurrence of an earthquake, and when a deformation in the crust occurs because of ground motion, the electrical and magnetic properties of rock can be changed. Therefore, magnetometers deployed in rocks are used to detect and measure the changes in the electromagnetic field. Moreover, satellites can be used to detect electromagnetic radiation field change and infrared radiation emitted prior to earthquakes.

Fluid Pressure Changes

When crusts are deformed in a short time period due to an earthquake, the height of the groundwater table can be changed. Therefore, changes in ground water levels can be used as an indicator to detect an earthquake.

Nuclear Event Detection

Nuclear materials such as dirty bombs or radioactive materials contain highly-enriched uranium and plutonium. They emit many radiation, especially gamma rays (high-energy photons) and neutrons. Therefore, they are used as the main detected radioactive materials to sense nuclear materials because of a feature that they can readily penetrate most materials. When gamma rays or x-rays can be beamed into nuclear materials, fission can be generated and causes emission of neutrons and gamma rays, which can be sensed to distinguish the nuclear materials.

Gamma Ray Detector

A gamma-ray detector uses electrical energy to measure nuclear materials. Therefore, specialized electronics are needed to turn a gamma ray emitted from the nuclear material into electrical energy. There are two methods to convert to electrical energy—scintillator material such as PVT and use of a semiconductor material such as HPGe. When a gamma ray interacts with these materials,

it generates an electrical signal, which can be used as an indicator to detect nuclear materials.

Neutron Detector

This technology uses charged particle converted from neutron energy. The most common detector is a gas-filled proportional counter (tube of helium-3 gas). When fission neutrons pass through the tube, energetic charged particles are generated and identify nuclear materials. The detector has a high detection probability and efficiency. Other types of neutron detectors are high thermal-neutron reaction detector and bubble detector.

Table 10-11 *Advantages and Disadvantages of Hazardous Material Detection Technologies*

Sensor	Advantage	Disadvantage
Gamma ray detector	Relatively low cost units for survey; less time-consuming process; portable detector for field use	High rates of false alarms; less sensitive to nuclear material; low detector efficiency
Neutron detector	More effective for isolating Plutonium and highly Enriched Uranium materials; lower false alarm rates; can be made in any size and shape	More expensive to use than gamma ray technology; requires nuclear reactor

Summary

Data on hazard detection can be collected by sensors deployed in infrastructure or non-intrusive technologies can be used to detect hazards. Major detection technologies include radar, satellite, advanced camera surveillance, hazard material sensors, radioactive particle sensors, and electrical sensor, and so forth.

Rain gauges, radar, and satellites are typically employed to collect data that could be used to forecast flooding. Satellites and airborne or temperature sensor technologies are used to detect hurricanes in advance. Seismographs on land or magnetometers in rocks are deployed to detect seismic activities. Technologies detecting thermal energy, smoke, flame, and gas particles emitted from combustion or vision sensor are used for fire detection, and gamma rays or neutrons are detected to sense nuclear materials which can be a risk of dirty bombs or radioactive terror. The methods of synchronization and detection technologies for illuminating sources or radiation are used for detecting power grid supply failures and hazardous materials, respectively. Improved detection technologies help ameliorate adverse impacts of hazards and prevent severe damages. Since these technologies have their advantages and disadvantages, it is required to select appropriate technologies for hazard detection.

Communication Technologies

Efficient communication technologies are important for evacuation from hazards, such as flooding, fires, and other events with notice. Shadow phenomena occur if ineffective communication for the disaster events is made. Shadow evacuees, people who do not have appropriate information about a disaster event and decide to evacuate without instruction, can cause traffic congestion and make the entire process of evacuation from the hazard area more complicated. As a result, overall evacuation can be delayed and people can be killed or injured unnecessarily.

Variable Message Signs

Variable message signs (VMS) are large electronic signs used to display traveler information. Their use has been increasing, as roadway users want more information about traffic conditions, and transportation agencies know how important this information is. Hence, it is possible to see the growing trend of VMS installation. In the past, VMS were used for displaying travel times and posting safety messages around holidays or other events; now, VMS continuously inform about travel times, safety messages, and events that can influence traffic conditions. Normally, public service announcements (PSAs) and safety messages are from the state level, whereas information on travel time, crashes, and construction activities is from the local level.

VMS are also used for contraflow operations and are deployed just before a key decisionmaking point outside of event area. They help drivers use appropriate travel lanes for expected trips. When roadway closure or route diversion is required for an evacuation, VMS and portable variable message signs (PVMS) provide information to users. During the disaster event, VMS display evacuation traffic, route, shelter, and fuel availability.

VMS and PVMS can be used not only for emergency travel information but also for future evacuation situations. Four different information stages exist where drivers may desire different types of information to make them feel comfortable with their travel decisions—all noticeable disasters such as flooding; a threatened area determined before a formal evacuation order being called; after the issuance of a formal evacuation order; and no longer safe to start to evacuate, such as within a few hours of expected landfall within the area.

Highway Advisory Radio

Highway advisory radio (HAR) stations are licensed low-power amplitude modulation (AM) radio stations. They are managed and operated by DOTs, airports, local governments, colleges, parks, events, and destinations. Information about travel and situations of imminent danger and emergencies are broadcasted. In emergency evacuation situations, such as an accident

near chemical and nuclear facilities, these radio stations have permission to exceed normal power levels for emergency operations. To prevent music from being played on a low power AM station, the audio of this radio station needs to pass through an audio low-pass filter that rolls off frequencies above 3 kHz. The content of the station is defined as non-commercial voice information and offers information about traffic hazards and travel advisories, traffic and road conditions, directions, availability of lodging, rest stops and service stations, and descriptions of local points. It is not allowed to identify the commercial name of any business whose service may be available within or outside the coverage area of a travelers' information station. HAR units are used when there is a need to provide extensive roadway information to motorists, such as chain control or adverse weather conditions.

Smartphone Applications

By using mobile smartphones, more successful evacuation of people in a disaster event area can be made and an easier evacuation process can be expected because users can be informed and updated where and how to reach a shelter or appropriate locations. These applications use interactive maps for the evacuation plan and monitor people in the affected area. During an emergency situation, it is possible to send personalized messages and information on evacuation routes.

USDOE's Lantern Live

Smartphone applications for emergency preparedness have become more useful. From this platform, it is possible keeping emergency preparedness notification alerts readily available to the users. The U.S. Department of Energy (DOE) released a new smartphone preparedness app called Lantern Live that can guide users to quickly find and share critical information about nearby gas stations and power outages during energy emergencies. This app allows consumers to report operational status of local gas stations, find fuel, look up local utility power outage maps, and access useful disaster tips. The USDOE plans to adopt standardized social media hashtags for updating the apps likely to use the crowd-source information on the status of gas stations.

FEMA

A smartphone app from FEMA helps get alerts from the National Weather Service. By using this app, it is possible to receive severe weather information for up to five locations across the U.S. and can provide information about how to stay safe. In addition, a disaster reporter allows uploading of photos and sharing information on damage and recovery efforts. Another function of this app is maps of disaster resources that locate and receive driving directions to open shelters and disaster recovery centers. Users also can apply for federal disaster assistance through this smartphone app and can save a custom list

of items in personal emergency kits and shelters in case of an emergency and can have information to learn how to stay safe before, during, and after various types of hazards.

Ready NYC and Ready TN

The Ready NYC app encourages the public to set an emergency plan before a disaster based on the Ready New York City campaign. A main function of this smartphone app contains tips and information about what to do during emergencies and alerts feed from New York City's official source for information about emergency events and important city services. Ready TN serves situational awareness before, during, and after emergencies in Tennessee and individual preparedness at the community level.

Vehicle-to-Vehicle Communication

The application of vehicle-to-vehicle (V2V) communication is a system designed to transmit basic safety information between vehicles to facilitate warnings to drivers regarding impending events. USDOT and National Highway Traffic Safety Administration (NHTSA) have been conducting research on this technology for more than a decade. V2V communications can warn users about impending danger. Messages about speed of a vehicle, heading, brake status, and other information are transmitted through on-board short-range radio communication devices. Different from sensors, cameras, or radar, V2V has longer detection distance and the ability to sense around corners or through other vehicles helping V2V-equipped vehicles perceive. As a result, V2V equipped vehicles can detect threats sooner than another device can and warn their drivers accordingly. NHTSA has researched how various levels of vehicle automation will play an important role in reducing crashes and how on-board systems may someday work cooperatively with V2V technology.

Web/Social Media

This strategy involves using Web sites and information kiosks in public areas to disseminate information about incidents.

Notify NYC

New York City informs about emergency events and important city services to the public through Notify NYC. One of the purposes of this website is to make the public aware of emergencies and other planned incidents in New York City by attempting to provide accurate and timely information under emergency circumstances with high reliability. To use this service, users are required to register with a valid New York City address and can select the types of notification, such as short message service (SMS) and phone through a registered phone number.

Notification is provided 24 hours per day and 7 days per week, and emergency activities in the city are monitored by the Watch Command team operated by the Office of Emergency Management. Radio, computer, 911 dispatches, and federal, state, and local agencies monitors for incidents that affect the city. Once an emergency is identified as an event that can affect many New Yorkers, Watch Command provides information to the public through Notify NYC. Messages can be received related to emergency alerts, significant events, major mass transit disruptions, major traffic disruptions, public health, school notification, waterbody advisories, emergency parking suspension, and missing person notifications.

Virtual Joint Planning Office

A Virtual Joint Planning Office (V-JPO) is a crucial joint information system. From this office, public information officers in various locations can post and access information that is trustable and current from online. It can share information before a physical joint information center (JIC) has been established. Through a V-JPO, interaction among incident sites can be made, and consistent and timely information can be sent for those who need information. A V-JPO collects information from many different channels, and assembles them as one after verification. Many state, county, and city agencies are involved and contribute information through this system. Authorities can deliver critical information from the affected areas to JPO staff for assessment and potential message development and distribution during an emergency or disaster. The Emergency Management Office of the Communications Director or delegated authority may then place selected information from a V-JPO to an external Website for the public to complement information disseminated through media.

Summary

As part of the hazard emergency management decision process, data collected on hazard detection needs to be transmitted and processed for analysis and effective means developed for impacts mitigation. Communication is key to the success implementation of impacts mitigation measures. This section provides a thorough of various communication technologies, as summarized in Table 10-12.

Table 10-12 Summary of Communication Technologies and Characteristics

Communication Technologies	Description	Advantages	Disadvantages
Variable message sign (VMS)	Permanent or portable variable message signs to provide information about incidents to users	<ul style="list-style-type: none"> • Provision of traveler information to road users • Information provided to affected drivers • Widely used with Transportation Management Plans (TMP) 	<ul style="list-style-type: none"> • Limitation of message length • Cannot inform complicated messages • Cannot reach travelers outside immediate vicinity of sign
Advisory radio	Low-powered AM or frequency modulation (FM) radio system to provide users with incident information	<ul style="list-style-type: none"> • Information providers can provide more detailed messages • Wider coverage to inform travelers in area 	<ul style="list-style-type: none"> • Users must tune to radio station • Signing needed for users to get a message available
Smartphone app	Incident alerts distributed through SMS or email	<ul style="list-style-type: none"> • Possible to send to travelers widely • Easy to deploy • Many urban areas have systems already in place 	<ul style="list-style-type: none"> • Users required to subscribe to service • Requires staff to manage system
Vehicle-to-vehicle (V2V) communication	Network between vehicles and roadside units through dedicated short range communication	<ul style="list-style-type: none"> • More intuitive and direct communication • Faster notification 	<ul style="list-style-type: none"> • Hard to apply to old vehicles • Hacking and privacy issues • Technical difficulties to handle many vehicles in metropolitan area
Website	Websites or social media to disseminate incident information	<ul style="list-style-type: none"> • Potential to reach travelers before departing trip • Can influence mode choice, routing, and departure time choices 	<ul style="list-style-type: none"> • Cannot reach drivers already in area of hazard • Requires integration with other systems
Virtual Joint Planning Office	Help for responding public officers to post and access latest collaboration	<ul style="list-style-type: none"> • Faster decision-making • Possible to process information faster • Standard of verified information required 	<ul style="list-style-type: none"> • Bypass normal command channels • Information overload

Evacuation Strategies

Identification

Hazard Categorization

Once there is a potential hazard, the first urgent action is to identify the hazard category and the potential severity. Hazards are generally divided into with-notice and no-notice, depending on if they are predictable. With-notice and no-notice hazards have different evacuation strategies. No-notice emergency evacuation is much more difficult than with-notice incident evacuation because of the pressure of time or no time for action. For this reason, emergency plans are always prepared by emergency management agencies, with evacuation

routes and shelter locations predesigned. If the designated transportation network and emergency shelters are not destroyed during the disaster, they will be used for evacuation purposes. That is why a well-established evacuation planning is crucial for emergency management. Advance planning is required to be updated and modified according to tabletop drill outcomes and changes in real-world conditions. A reliable communication system is another essential component to ensure the plan can be implemented timely.

Impact Assessment

For different types of hazards, impacts vary considerably. Even for the same type of hazards, the range, time duration, and intensity will be different. This will lead to varying consequences. How the hazard will impact the transportation infrastructure, vehicles, and users/non-users requires careful evaluation.

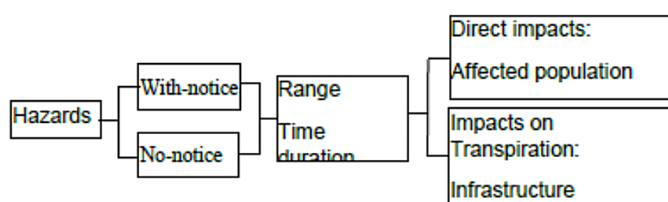


Figure 10-4 Hazard impacts assessment process

The objective of impacts assessment is help an agency know the hazards better. Historical events analysis, scientific analysis report, and expert experiences can provide critical information. For example, the Security Advisory System used by the U.S. Department of Homeland Security (DHS) is a color-coded terrorism threat advisory scale. Different colors represent different level of threats and will trigger different levels specific actions by local governments and federal agencies. Another example is a color-coded warning system used by the U.S. Forest Service to inform the public about the level of wildfire hazards.

In the context of transit-based evacuation, hazard and risk assessment identifies the most vulnerable components and how they impact passengers and the transit system. Optimal operating conditions ensure better service during an evacuation. For instance, a transit threat condition model was developed by FTA to supplement the existing Homeland Security Advisory System (HSAS) Threat Condition model. It uses five colors from green to red to indicate the level of hazard from low to severe. Black indicates an attack is underway against a specific transit agency or within the agency’s immediate geographic area. Purple indicates the recovery of transit service after an attack. For each level of emergency management agency, FTA provides a guide to adopt corresponding measures, recommends transit protective measures, including refining and exercising preplanned protective measures to ensure personnel receive proper

training on the HSAS, and develops and implements hardware, software, and communications security for computer-based emergency operations.

Response

Agency Coordination

Prior to the painful lessons of Hurricane Katrina, a transit authority was considered as the first responding entity for a transit-based evacuation. However, thousands of transit-dependent people were not able to be moved out of the affected area effectively. Post-event evaluation revealed that transit is highly depended upon by traditional first responder organizations to help with emergency response planning and implementation. The connection between transit agencies and first responders is essential to improve evacuation efficiency.

Further, it is common that a disaster caused by a hazard affects a specific area with multiple jurisdictions involved. Coordination and corporation are highly needed as part of evacuation planning and implementation to protect lives and properties. Poor coordination across jurisdictions will slow the response and deem the evacuation plan to be inefficient, so available resources cannot be used efficiently. Mutual aid agreements ensure that jurisdictions provide or support each other during the emergency. Therefore, essential resources for public transportation evacuation, such as buses, commuters, or skilled drivers, can be shared to save lives and properties.

Transportation Supply Strategies

Emergency Traffic Signal Timing Plans

Traffic signal timing is a technique to determine optimal right-of-way (ROW) plans by selecting appropriate values for traffic signal timing parameters. Essential parameters include but are not limited to cycle length, number of phases, green splits, and offsets between adjacent intersections. Optimized and effective signal timing plans ensure the flexibility of traffic flow and are consistent with traffic needs for all approaches and minimization of total delays, fuel consumption, and intersection-related vehicle stop-and-go conditions. In case of an evacuation, time is of essence—reducing time will save more lives.

Central to evacuation is sending more evacuees to safe places as quickly as possible. Transit vehicles can play a key role owing to high passenger capacities. For efficient transit operations, bus signal priority (BSP) or transit signal priority (TSP) techniques can be effective means of evacuation to transport more people out of an affected area, helping to reduce or eliminate dwell time at a signalized intersections by extending the green interval or shortening the red interval of the phase designated to alternative movements. As such, transit travel time is reduced and corresponding efficiency is improved. Transportation agencies,

evacuation planners, and emergency responders should carefully assess the impacts and benefits of BSP or TSP to support efficient evacuation in a holistic manner.

Traffic-Crossing Conflict Minimization

Conflict points refer to the points that roadway users may cross, diverge or merge with other roadway users at an intersection. Drivers are likely to make mistakes due to misperception, and sometimes vehicle crashes may be triggered by movement conflicts. Figure 10-5 shows conflicts at a normal intersection. Without signalized control, there are 32 conflict points at an intersection, including 16 crossing points, 8 merging points, and 8 diverging points. If bicycles and pedestrians are considered, the number will raise to 48.

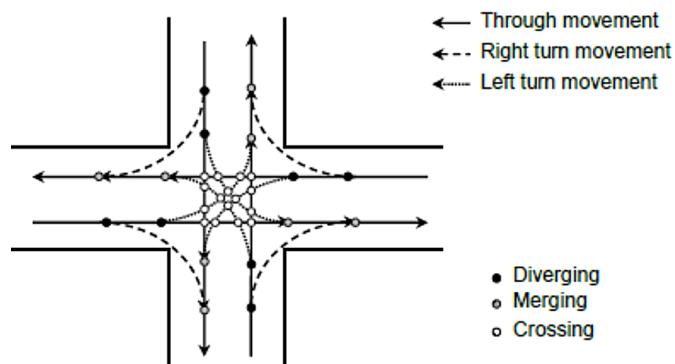


Figure 10-5 Conflict points at intersection

There are several ways to reduce conflict points. Common strategies include improving driveway geometrical design, relocating, consolidating, and eliminating driveways, adopting protected left-turn signals, using left-turn prohibition, and so on. During the evacuation process, normal signalized control is not enough. Additional traffic control measures are required to minimize the conflict points. Typical methods are shown in Figure 10-6.

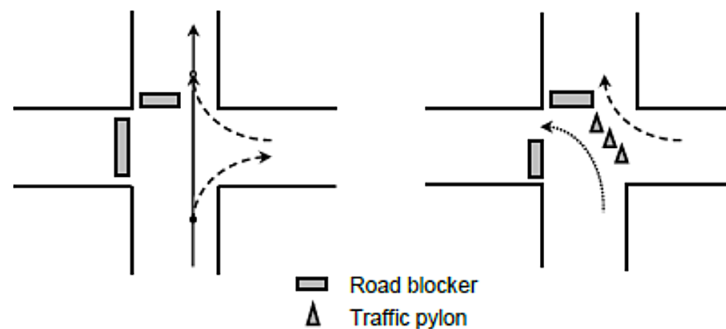


Figure 10-6 Conflict-point reduction strategy

Traffic Condition Monitoring

Modern technologies such as intelligent transportation systems (ITS) are crucial supplemental aids. ITS installations are advanced applications to enable users to be better informed and understand the real-time traffic situation to make a trip faster and safer. During evacuation, ITS will help emergency evacuation managers monitor traffic conditions, make coordination between the supply and demand sides, disseminate traffic condition information to evacuees and other road users to guide them choosing the optimal ways out of the affected area.

Contraflow

Contraflow is a practical strategy to make full use of available capacity. During an evacuation, inbound and outbound traffic needs are significantly imbalanced. The majority of or all inbound traffic lanes can be converted to outbound lanes. Sometimes, one or two inbound lanes are required for emergency responding vehicles to reach evacuation site for traffic management. If a contraflow strategy is implemented, outbound capacities for arterials and freeways will be significantly increased. Freeway contraflow is more recommended because of high design standards with limited access points and signalized control.

The most essential element of a contraflow plan is to identify the appropriate start/end points and corresponding traffic control strategies since congestion is very likely to happen at these points, which will reduce the effectiveness of contraflow strategy. Therefore, it is highly recommended that contraflow should be considered at the planning, programming, and design stages, and special consideration is suggested for potential start and end points of contraflow. Additional signs and traffic control plans should be prepared, which include “Evacuation Route” signs, median-crossovers, access control gates/ railroad crossing barriers, and start/ end points strategies.

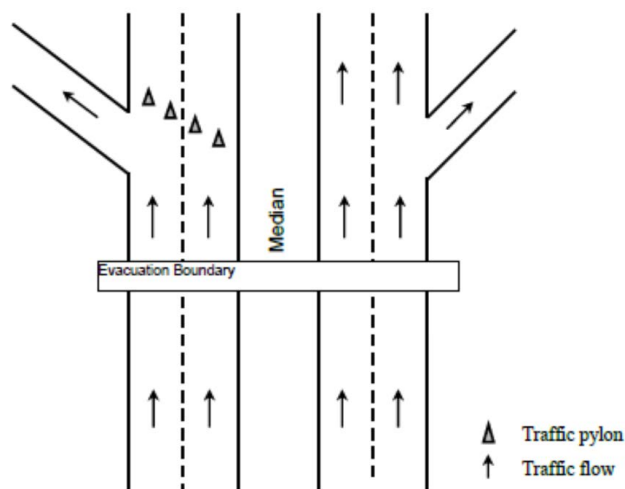


Figure 10-7 *Contraflow Alternative 1*

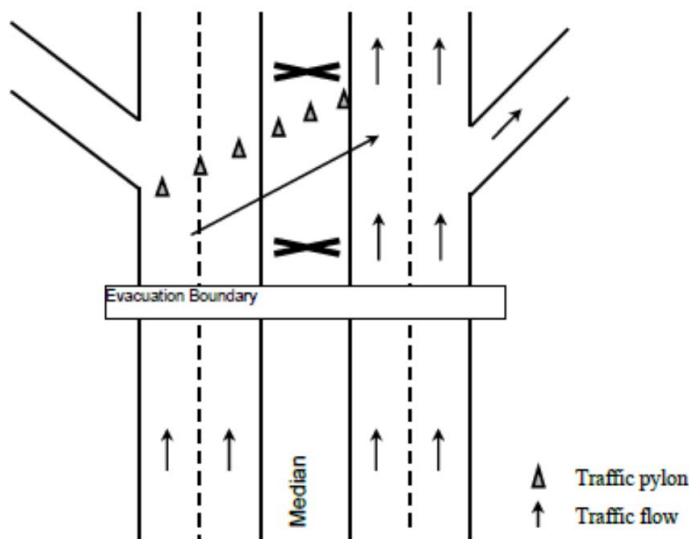


Figure 10-8 *Contraflow Alternative 2*

Work Zone Removal

For traffic safety, work zones should be removed during evacuation if possible to maximize roadway capacity. Without considering legal issues with contractors, careful assessment of traffic safety is required. If an unfinished work zone is removed, there is potential to endanger traffic. Drivers willing to go through a work zone or change lanes or routes may be affected.

Shoulder Use

Temporary shoulder use, also referred to as hard shoulder running, is considered if traffic volume is relatively high. By allowing vehicles to use paved shoulders, it is possible to improve the roadway level of service. In Netherlands, Germany, Great Britain, and other European countries, temporary shoulder use is applied as a management strategy to ease traffic congestion. For paved shoulder users, the speed limit may not be the same as normal lane users for safety reasons. Shoulder lanes can provide extra capacity during times of evacuation and congestion. The essential problem for an agency is to determine the location of start and end points. Special traffic facilities and signs are required to indicate the evacuees that the paved shoulders are temporarily permitted.

Travel Demand Management Strategies

If an emergency situation occurs, travel demand will increase expeditiously and could quickly exceed the design capacity of road network. Demand reduction becomes an effective strategy that is desirable to be considered.

Phased Evacuation Plan

Phased evacuation is a systematic evacuation process in different affected areas that is guided or suggested to be separated as a controlled sequence of evacuation phases. The priority can be the level of risk, and parts under greatest risk should be evacuated firstly. Therefore, evacuation is implemented as a series of successive, geographically smaller evacuations. In this way, affected people are suggested to evacuate at different time ranges at different locations so the traffic pressure and “peak hour” scenario from the demand side is mitigated. The major challenge of a phased evacuation plan is whether the affected people are willing to follow the agency’s recommendations, especially under the pressure of time during evacuation. Also, from the perspective of human nature, phased evacuation should be voluntary; mandatory is not recommended. Therefore, disseminating accurate disaster information, making an acceptable phased evacuation plan, and avoiding panic evacuation are crucial tasks for evacuation management.

Special-Needs Populations

The U.S. GAO conducted a study focusing on the issue of preparedness of evacuation for special-needs populations, specifically transportation-disadvantaged populations. These populations vary widely in definition, not only populations with mobility issues but also potential users of transit in an emergency evacuation, such as populations without private vehicles and vulnerable populations that cannot access private vehicles during the emergency. A special plan should be prepared for the transportation-disadvantaged population, and corresponding training and exercises are required as well. Although challenging, several measures are proposed to make it operational to serve special-needs populations in an emergency evacuation. Here we list several practical strategies based on National Consortium on the Coordination of Human Services.

Identification and Location of Special-Needs Populations

- Historical demographic profile
- Transportation-disadvantaged population voluntary registration
- Special-needs population service organization records

In-Advance Planning

- Pre-designed transit evacuation routes for special-need populations
- Provision of information about evacuation routes, shelter locations, and stops
- Human service agencies and volunteers to assist special-need populations
- Specially-designed training and drill exercises for special-need populations

Communication

- Establishing accessible communication devices and formats for special-need populations
- Providing communications to special-needs populations that service agencies can provide assistance
- Special warning messages and guidance for special-needs populations

Transportation Assistance

- Matching potential evacuation needs with available transit resources
- Encouraging carpools to help special-need populations
- Equipping transit with appropriate facilities for special-needs populations
- Cooperation among transit providers

Evacuation Information Dissemination

Timely and accurate information on a disaster triggered by a hazard is valuable during evacuation. Information dissemination can be provided by internet, message, email, or broadcast radio. Recommended evacuation routes should be provided as well as road condition, weather information, and suggested evacuation timing for specific areas should also be included.

Long-Term Response Strategies

Effective and close coordination among multiple departments and jurisdictions is required to achieve success during an emergency evacuation. Training and preparation in advance will shorten the response time for agencies and help evacuees take actions effectively. Recommended preparation activities are as follows:

- Regular training
- Mutual aid coordination agreements
- Advance data collection
- Weekly input and push of information to emergency managers
- Establishing evacuation response coordinating team
- Continued deployment of infrastructure to support evacuation
- Developing jurisdictional-specific evacuation plans

Accurate advance data guarantees developing a comprehensive and practical evacuation plan for an emergency situation. Related data should be collected, analyzed, and updated routinely. Useful data include those related to socioeconomic characteristics, census surveys, transit-dependent populations, and transit system resources. A short list of typical data for evacuation plan development includes the following:

- Census data
 - Size of population
 - Population density in specific area
 - Transit-dependent and potential transit-dependent population
- Socioeconomic data
 - Special-needs people (persons with disabilities, older adults)
 - Low-income people (potential transit-dependent population)
 - Private vehicles per capita for each income level
- Geographic and political data
 - Jurisdictional boundaries
 - Size and capacity of transportation network
 - Potential factors to reduce capacity
 - Principal jurisdictions
- Transit system data
 - Size of transit system
 - Service coverage
 - Transit mode composition
 - Capacity of transits
 - Available transit resource during evacuation
 - Transportation and transit control techniques and devices

These data are typically required but maybe not sufficient. A useful tool to capture, store, manipulate, analyze, manage, and present large datasets is a Geographic Information System (GIS), which makes it easy to observe the disaster area and shelter locations and plan for transit evacuation routes.

Prevention/Mitigation

Response activities comprise the immediate actions to save life, protect property and the environment, and provide services to meet basic human needs. Execution of emergency plans and related actions are essential elements of phased response.

Prevention/mitigation is typically the first response of emergency management. The objective of prevention is to minimize the possibility of the occurrence of emergency incidents. Mitigation aims to eliminate or reduce the loss of lives and properties if the incident is inevitable. Since different hazards maintain diverse characteristics, agencies need to conduct hazards identification and risk assessment and develop mitigation strategies. Typically, prevention/mitigation activities have a long-term and sustained effect. In many cases, mitigation activities are elements of evacuation at the recovery stage. Take flooding incidents as an example, prevention/mitigation actions may include:

- Developing strategies for specific levels of flooding
- Protective and restrictive constructions in floodplains
- Rebuilding damaged structures with more resilient materials
- Flood mapping to identify low lying areas and relocating homes and structures located in floodplains and flood prone areas

For transit agencies, the following strategies are recommended:

- Involve staff in identification of hazards and threats
- Involve staff in creating strategies to prevent or mitigate emergency incidents
- Raises staff awareness and conduct training across all departments for specific incidents
- Assess and improve emergency response plan
- Train staff in use of emergency equipment and communication technologies properly

Maintenance of Available Resources

Vehicle Inspection

As a safety control measure, careful bus or transit vehicle inspection should be conducted before each trip. This is especially needed for buses or transit vehicles participating in evacuation. Pre-trip inspection ensures the safe operating of transit vehicles. Typical inspection items are:

- Fuel quantity and unusual indicators
- Low-beam/high-beam headlight, turning lights and other light systems
- Suspicious persons or objectives in the transit
- Security equipment and emergency supplies
- Suspicious objectives under the bonnet and transit
- Mechanical conditions

A checklist should be created to make sure every item inspection has been covered. If security risks are found, inform agencies immediately.

Vehicle Maintenance

Transit maintenance is required to remove potential risk to the transit drivers and passengers. It is crucial to keep the transit operation functional. Typical maintenance includes:

- Daily servicing maintenance on consumables such as fuel, water, and oil and tire pressure
- Periodic maintenance on potential damage items such as belts, electrical cables, and tires

- Interval maintenance on preventive repair or replacement of parts are loss or deterioration from use
- Failure maintenance on repair or replacement of parts that fail in-service

Emergency Planning

A formal developed and organized Safety, Security, and Emergency Preparedness Plan (SSEPP) should be prepared across all potential involved agencies. The plan should outline the corresponding responsibilities of agencies, such as the process of preparedness, mitigation, response, and recovery for specific emergency incidents. Further, the plan should clearly illustrate the potential hazards and corresponding evacuation routes and strategies as well. It is desirable to post the plan template online.

Regular Training

Adequate and proper training is necessary to make clear the roles and responsibilities during evacuation. Tabletop exercises to discuss a simulated emergency scenario should be regularly conducted to test the evacuation plan in a relatively low-stress situation; the target is to clarify roles and responsibilities, improve the jurisdictional coordination, point out weaknesses of the current plan, and propose remedies to improve it. Ideally, all potentially affected people should participate in the training to fully understand the emergency evacuation plan, including but not limit to potential types of emergency situations or disasters, evacuation procedures, and responsibilities. For certain areas, people should focus on the potential type of emergency with the greatest possibility to occur. General and regular training should address the following:

- Individual roles and responsibilities
- Types of potential emergencies and disasters
- Essential protective actions
- Warning, communication, and information dissemination system
- Emergency response procedures
- Location of shelters and surrounding routes
- Timing to help family member and others
- First-aid knowledge and procedures
- Necessary tools and equipment should be prepared

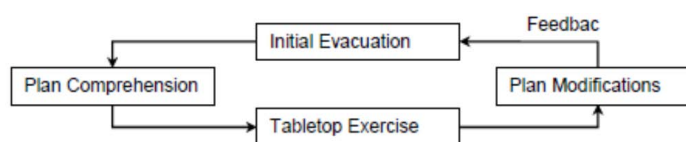


Figure 10-9 *Evacuation plan feedback process*

Recovery

Recovery activities are intended to assess the current status of service facilities and restore available essential services. Repair and improvement are also included.

Recovery Period

In the early recovery period, the main task for agencies is to provide basic necessities for affected populations such as food and clean water supply, shelters can prevent secondary hazards. The early recovery process may last for a few weeks or months, depending on the severity of disaster. According to initial vulnerability, severity of disaster, and other considerations, a reasonable timeline should be developed. During medium and long-term recovery periods, the primary task is to rebuild the physical infrastructure per the new standards and experiences to make them more stable for disasters in the future. Schools for children should take extra care as they are always vulnerable and lack awareness about emergencies.

Transit Recovery

Continuity of Operations

After a disaster, transit agencies need to assess the current transit system status to make sure it can still operate and proper measurements are required to remove the potential risk. A certain amount of funds is recommended to be reserved for the recovery of transit system in emergency after disasters.

Operating Restoration

Transit systems usually suffer destructive damage, and service must be suspended until essential parts are recovered. Under the condition of safety, transit agencies are recommended to sustain identified essential functions for up to 30 days.

Long -Term Recovery

The objective of long term recovery strategies is improved the service condition and try to improve the performance during the evacuation. Here are typical steps:

- According to disaster or emergency reports, develop long-term recovery strategies and a corresponding schedule
- Estimate the loss caused and budget for recovery
- Assess the performance of transit during evacuation to attract more people to take transit; if performance is not satisfied, strategies are required to improve the situation and rebuild the confidence for transit users
- Strengthen coordination with other agencies or first responders

Example Disaster Mitigation Strategies

Flooding

Flooding is the overflow of water that submerges land which is usually dry. Reasons for flooding vary; it can be the overflow of water from a natural water body, such as rivers, lakes, or oceans or from artificial structures such as levees and dams. Natural disasters such as storms and hurricanes are another reason for flooding. A huge amount of water is not the only threat to people and property; moving water with speed, debris in the water all contribute to extra damage.

Floods are relatively predictable, protective actions and evacuation plans should be conducted before the estimated time. All transit evacuation routes must be above the estimated flood elevation; potential inundation must be considered. If complete evacuation is not practical, locations of high-ground shelters and safe routes should be noted to impacted populations. Particular attention is required for recreational areas as visitors may not be familiar with evacuation routes.

Different causes and the distance of flooding origin may give jurisdictions varying time to prepare. Intense storms may produce a flood for upstream locations in a few hours or even minutes; downstream area may have one day or weeks to prepare. Floods may also destroy protective measures such as dams in a short time. Another uncommon type of flood is from snow melt; even though it may take months to develop, inspection is required.

Essential considerations include the following:

- Understanding protective facilities in or near the jurisdiction
- Keeping in touch with monitor stations to update flooding information
- Identifying and present current and potential inundated areas
- Disseminating flood information, giving suggestions to evacuees
- Recognizing the possible route for transit operators to rescue affected population
- Determining shelter locations and stops along the route

- Assessing loss of transit resources and using available resources
- Estimating the number of affected population and locate their positions
- Refining and optimizing rescue routes

Hurricane

Hurricanes are a type of severe tropical cyclone that forms over tropical or subtropical waters, with sustained strong winds spiraling inward and upward at speed of 75–200 mph. Hurricanes usually last around one week with speed of 10–20 miles per hour over the ocean. They rotate in a counter-clockwise direction with an “eye” as the center, which is the calmest part of a hurricane. Hurricanes bring heavy rains and strong winds and cause damages to trees and buildings. They are also potential contributors to secondary hazards such as flooding, tornados, and power outages.

Assessments about affected population, facilities, and properties should be prepared and updated during hurricane disasters. An assessment is essential for agencies to determine the hurricane category and develop an evacuation plan. It should be compatible with the general evacuation plan and strategies. Typically, it is possible to predict the time duration and wind levels. According to previous research, 60–72 hours before the arrival is the awareness time phase, 48–60 hours before the arrival is standby, and 48 hours before arrival is response phase. Corresponding strategies should be developed, and the following considerations should be included:

- Recognizing agencies that should be involved for hurricane evacuation strategy
- Identifying affected and potentially affected populations
- Determining timing to publish information and take actions
- Collecting information of available and damaged resources
- Determining priority of evacuation
- Identifying evacuation zones based on collected information
- Identifying location of evacuation shelters
- Designing evacuation routes for specific zones
- Estimating the number of transit-dependent populations
- Recommending a phased evacuation plan

Earthquake

An earthquake is a sudden, violent shaking or movement of the earth surface resulting from the sudden release of energy in the Earth's lithosphere that creates seismic waves and displacement of rock masses. Harmful consequences include:

- Ground motion damage to buildings, structures or roads, etc.
- Ground surface rupture
- Rock fall and landslide in mountainous area
- Undersea earthquake causing tsunamis
- Secondary hazards such as flooding and fires

For emergency response agencies, it is urgent to gather earthquake damage assessment information, which is essential to estimate the severity of the damage and plan the evacuation routes. It is also essential for rescue teams to re-enter the affected area to conduct Urban Search and Rescue (USR) activities, inspection, searching, and rescue:

- Determining severity and scope of damage
- Rescuing trapped population
- Emergency personals re-entry
- Checking current status of buildings and roads to avoid secondary hazards
- Restoring electrical power, natural gas, and water
- Emergency information dissemination and evacuation suggestions

Nuclear Events

Typically, the possibility of nuclear accidents is extremely low. A possible way of nuclear accidents can be an operational accident or a terrorist attack. Civil nuclear facilities have higher productivity than traditional energy; however, if accidents occur, harmful effects may be as severe as nuclear weapons. Nuclear radiation is the major effect. Nuclear energy is from nuclear fission, a process that produces radioactive substances. If a nuclear power plant experiences an explosive accident, the debris produced by the explosion becomes radioactive. The debris is carried high into the air and falls back when it cools down in the form of particles called fallout. Radiation emitted from these particles is called gamma radiation, which is bad for human health. Consequences include radiation sickness such fatigue, vomiting, diarrhea, hemorrhage, infections, or even death.

Once a nuclear accident occurs, it is crucial for emergency agencies to determine the location and amount of radiation materials. Coordination with involved jurisdictions is essential. Experienced persons in dealing with hazards associated with nuclear accidents should be assigned as emergency responders.

Evacuation of the affected population is required. An evacuation plan should be developed based on a nuclear accident assessment. If a phased evacuation plan is implemented, details of evacuation timing, route, location of shelters, available transit resources, and stops along routes are required. All evacuation work must be done before the radiation moves into a specific jurisdiction.

Since nuclear accidents are always no-notice, advance evacuation should be prepared. Predesigned shelters and evacuation routes are significant. If a nuclear accident occurs, responders should focus on:

- Identifying location of accidents and corresponding quantity of radiation materials
- Determining levels of radiation exposure
- Using available protective equipment to mitigate situation
- Determining number of evacuees dependent on transit
- Distributing available radiological detection and decontamination equipment
- Searching and treating the population affected by radiation
- Preparing recovery strategies after the nuclear accidents

Summary

Generally, emergency management consists of four phases—identification, response, mitigation, and recovery. Actions and activities in each phase are not completely independent but often overlap. For instance, transit system rebuilding is an element of recovery; however, measures to prevent or mitigate a similar emergency should be considered. Phases of response and recovery overlap with each other. Lessons learned from emergencies in other cities, urban areas, or metropolitan areas should be referenced to be prepared for incidents in the future. As funding and jurisdictions are obstacles to building a complete and collaborative four-phase emergency management system, local and state governments may focus on different tasks in each phase. For this reason, inter- and intra-agency agreements are required among to make them work as integrated teams.

Implementation of Emergency Response Technologies¹¹

Signal Timing Prioritization without Power Failure

Signal timing prioritization plays an important role in emergency management. During an evacuation, aggravation of traffic flow or increase of evacuation time are primarily generated at intersections with signals. The method of signal timing optimization/prioritization can be applied to an urban street network with extensive signals, which can decrease delay at an intersection significantly. In congested metropolitan areas, evacuation routes consist of freeways and urban street segments. In the case of freeways without signals, one direction or shoulders can be used for preemption to emergency vehicles. On the other hand, in emergency situations, optimizing traffic signal coordination could potentially help automobiles and transit vehicles traversing through an urban street network without experiencing extensive delays at intersections, which reduces evacuation time and improves the safety, stability, and regularity of evacuation traffic flow. According to several studies based on traffic simulation modeling (Chen et al., 2007; Jahangiri et al., 2011), it is shown that varied traffic signal coordination in an urban network has a significant impact on reducing clearance time and delay for cross-street traffic in evacuation circumstances.

Under emergency situations, traffic signals have a significant influence on the progression of evacuation traffic flow. Therefore, optimizing signal timing and coordinating the system can substantially improve the performance of the evacuation traffic networks. Also, it is needed to offer signal time prioritization to respond vehicles and transits for effective evacuation in an emergency situation. There are several factors that affect signal timing prioritization—traffic volume, capacity, magnitude of incidents, population of evacuees, transit, special event traffic, and weather.

When an urgent circumstance occurs, it is common that chaotic traffic conditions or traffic fluctuation exist. For signal timing prioritization under an evacuation situations, traffic conditions can be separated into evacuation traffic delivering a population of evacuees (vehicles and transit), background traffic that affects capacity, and emergency response vehicles (ambulances, police, fire/rescue, and law enforcement). All need a different set of strategies for signal timing prioritization and coordination. For example, an important action is to transfer the population of evacuees in the affected area to safe places as quickly as possible, and it is crucial to stop background traffic from

¹¹ Authored by Zongzhi Li, Yongdoo Lee, Yunseung Noh, Lu Wang, and Ji Zhang, IIT

entering the influence area and move them out of the area. Also, it is necessary to allow emergency vehicles to enter quickly without concern for traffic signals in the emergency situation. In addition, when signal timing prioritization is implemented, traffic regarding multiple directions of major intersections should be considered. Figure 11-1 shows the process of signal timing prioritization.

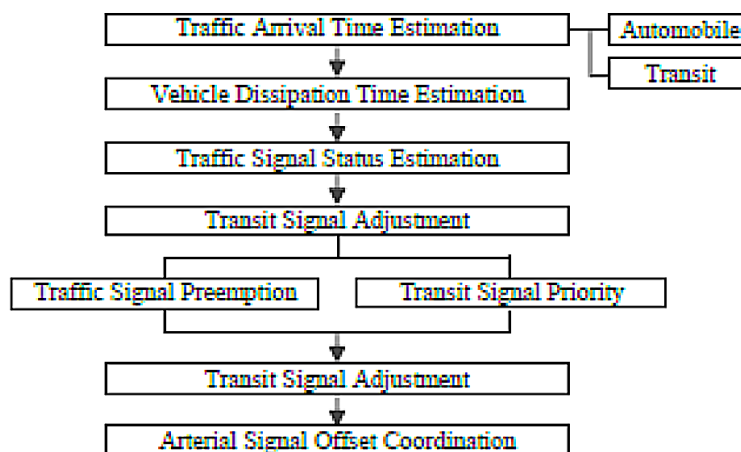


Figure 11-1 Signal timing prioritization

Conventional Traffic Signal Operations

Signalized intersections provide the safe and efficient movement of vehicles and pedestrian traffic. In general, conventional traffic signal operations are coordinated to optimize the movement of vehicles and pedestrians on intersections. Each vehicle and pedestrian has sufficient time to move through the intersection safely and to minimize delay. In other words, along the arterial, traffic signal timing is coordinated to assign the right-of-way for alternating traffic movement to decrease the probability of crashes by reducing conflict and to minimize the average delay to a group of vehicles and pedestrians. The normal concept of conventional traffic signal operations is to minimize the number of phases, as the amount of lost time caused by starting delays and clearance intervals on intersection can be increased by additional phase.

Traffic Signal Preemption for Emergency Vehicles

Traffic signal preemption (SP) is to give the right-of-way to emergency response vehicles passing through signalized intersections. Generally, it uses special preempt control tools on authorized vehicles to enable to pass through signalized intersections in a safe and timely manner. In an evacuation situation, an SP system can be used for emergency vehicles as well as transit passing through major intersections by coordinating normal signal operation, including police, firefighter, rescue, ambulance law enforcement, and transit operators.

To initiate SP, there are several technologies to detect the approaching vehicles including light and infrared-based system, sound-based system, radio-based emitter/detector system. Table 11-1 describes the features of the TSP technology (Paniati et al., 2006).

Table 11-1 *Signal Preemption Technology Features*

Technology Consideration	Light and Infrared-Based System	Sound-Based System	Radio-Based System
<i>Emitter System</i>	<i>Light/Optical Unit, Power Supply</i>	<i>Siren Microphone</i>	<i>Radio Pulse, Omni-directional Antenna</i>
Dedicated vehicle emitter required	Yes	No	Yes
Susceptible to electronic noise interference	No	No	Yes
Clear line of sight required	Yes	Yes	No
Affected by weather	Yes	Yes	No
Possible preemption of other approaches	No	Yes	Yes

When initiated, traffic signal preemption yields several negative impacts on traffic flow since it puts the traffic in other direction in stagnation. In other words, SP interrupts normal signal operation by truncating or omitting the normal vehicles and pedestrian phase on other approaches, which causes an increase in delay time at intersections. In addition, once preemption is made, it also takes time to recover to the normal signal cycle. Therefore, it is crucial to set signal preemption in a collaborative and coordinated manner with stakeholder groups to ensure their need. Major coordination considerations are cycle length, signal timing interval and split, and offset.

Cycle Length

The cycle length of a traffic signal is the total time for one complete sequence of signalization at an intersection. In general, cycle length is predetermined based on traffic volume of each direction on an intersection. The cycle length has an impact on the amount of lost time taken by the change and clearance intervals and adjacent signalized locations, and it determines intersection capacity. Once preemption is implemented, intersections are saturated with stagnant vehicles, which can increase in delay time. Therefore, change to optimum cycle length is important both to operate preemption efficiently for emergency vehicles in multiple directions of a major intersection and to reduce evacuation time under an emergency situation.

Signal Phases

The cycle length includes segments of individual phase splits, which is typically defined as the sum of the green, yellow, and red intervals. If emergency vehicles

will be crossing within a phase, enough crossing time has to be provided with the minimum phase length. At the same time, a phase should have proper time to avoid over-saturating other approaches. Therefore, signal timing intervals and splits should be properly input to efficiently balance the movement of evacuees and emergency vehicles.

Offset

The offset is the time lapse between the beginning of a green phase at an intersection and the beginning of a corresponding green phase at the coordinated intersection. During emergency situations, properly designed offsets provide the efficient movement of emergency vehicles passing through multiple intersections, substantially reduce delay time on the intersection, and then yield decrease in clear time of evacuation in the network.

Transit Signal Priority

Transit signal priority (TSP) is to assign right-of-way to transit vehicles passing through intersections by traffic signal coordination to improve service of traffic capacity and reduce delay in an urban network. TSP is commonly used for buses but can be also used for streetcars, trams, or light rail lines. Under an evacuation circumstance, typical evacuees and special-needs populations such as injured victims or older adults use transit. Moreover, as the transit resource is an essential mode to evacuate carless population and it can move many evacuees out of the influence area at a time in emergency situations, TSP techniques substantially decrease evacuation time and improve the safety and stability of evacuation traffic flow by using traffic signal coordination along evacuation routes.

To implement TSP, the existing signal timing along the arterial is modified without interrupting coordination. Several methods can be used for signal timing modifications, including changing phase sequences, extending or initiating early green time on the intended phase, and devising special phases to facilitate transit operations through the intersection.

As TSP needs communications between the transit vehicle and traffic signal, the systems to detect the presence of approaching transit vehicles are required to implement priority in the traffic signal controller. TSP should also be conducted by considering transits and evacuation vehicles in major corridors in terms of network. TSP techniques can generally be classified as passive and active transit signal priority.

Passive Transit Signal Priority

Passive TSP operates signal timing by creating a green wave for traffic based on knowledge of transit route and ridership pattern along the transit line's route, which may improve traffic flow and reduce transit travel time. An operation

of passive transit signal priority does not require special transit detectors and specialized traffic signal controller. The passive technique is applied when transit operation is predictable with routes, passenger load, schedule, and dwell time.

Active Transit Signal Priority

Active TSP is a strategy to provide a specific transit vehicle with priority treatment by detecting transit vehicles. Unlike passive TSP, active transit signal priority needs detector which is a transmitter on the transit vehicle and the signal controller. The techniques detect transit vehicles approaching an intersection and adjust the signal timing dynamically to enhance the transit vehicle service. Various types of active transit signal priority strategies can be used. Table 11-2 shows the strategies to apply active transit signal priority.

Table 11-2 Strategies of Active Transit Signal Priority

Strategy	Description
Green extension	Extends green time for TSP movement if a transit vehicle is approaching. Applied only when signal is green for transit. Green extension is one of the most effective applications, as additional clearance intervals not required
Early green	Shortens green time of preceding phases to expedite return to green whenever transit vehicle arrives at a red light. Used only when signal is red; green time shortened by predetermined time.
Actuated transit phase	Displayed only when a transit vehicle detected at intersection; enables transit vehicle to enter mainstream lane before general traffic given green phase to move forward. Can be used in location of near-side bus bay, streetcar lines, or on dedicated bus lanes
Early red	Ends green interval early and returns to red interval sooner. If a transit vehicle is approaching during a green interval, it is estimated whether vehicle is far enough away that light would change to red by time it arrives. If transit vehicle would arrive at intersection during red light time, signal changes to red light early before vehicle approaches.
Phase rotation	Changes order of phases so transit vehicles arrive at intersection during phase they need.
Phase escape/insertion	Returns phase that transit vehicles need in same cycle by using signal controller.

Intermodal Transit Signal Optimization

Intermodal Transit Signal Optimization (ITSO) is to deploy traffic signal timing plan that takes all transit modes into consideration. Transit operating characteristics ranging from travel speeds to acceleration/deceleration are considered to design for timing plans. Also, ITSO enables to sustain coordinated travel along the arterial for vehicles by optimizing timing at individual

intersections to minimize vehicle delay. It allows transit to move not-stop by traveling between stations alongside other vehicles using the normal coordinated timing along the arterial. For example, when a bus is approaching a station, the traffic signal system detects the vehicles and determines to either hold the bus at the station or discharge it so it will reach the next intersection during the green phase for other traffic. ITSO can be useful for two-way bus operations, relatively short headways, and short distances between stations. Furthermore, it can be used in arterial with exclusive transit lanes where other traffic has not an impact on the operation performance.

Bus and Train Bridging for Efficient Transit Resource Use

Role of Transit in Emergency Evacuation

In an urban area, transit systems in terms of buses, BRT, trains, and alternative rail lines play an important role in an emergency evacuation situation, as demonstrated in the terrorist attack of September 11, 2001, and Hurricane Katrina in 2005. The population of evacuees might exceed the evacuation capacity due to congestion on urban networks, in which case transit assets can be used to transfer evacuees to shelters or other destinations outside the affected area. Also, transit services can be useful means of evacuation for those who lack access to private vehicles or vulnerable people (e.g., persons with disabilities, older adults, special-needs populations) during an emergency. In addition, in an aspect of supply side, transit systems can play a crucial role in transporting emergency workers and equipment to incident sites. Therefore, it is necessary to optimize the use of available transit resources in a time- and cost-effective manner under various emergency responses scenarios.

Factors Affecting Efficient Transit Resource Use in Emergency Evacuations

Use of transit resources under emergency evacuation depends strongly on several characteristics in affected area, including the characteristics of urban area and emergency and transit system and technology. These factors have an impact on the plan of efficient transit assets allocation to respond to an emergency. Specific factors are shown in Figure 11-2.

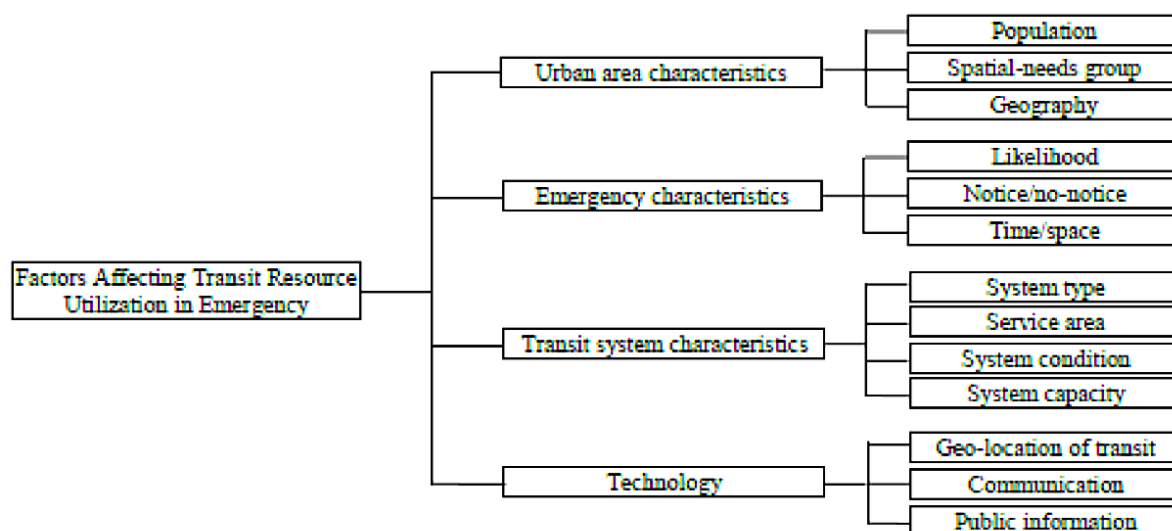


Figure 11-2 Factors affecting efficient transit resource use

In evacuation plans, need for public transit resources is considered on the basis of the number of self-evacuating individuals, medically fragile individuals, and transit-dependent evacuees. Also, the plans for transit systems use depend on event strength, which has an influence on the number of evacuees and evacuation destinations.

Transit Evacuation

In general, people are more likely to use either transit or other modes for their daily commute in congested metropolitan areas. Therefore, when emergency situations occur, they may not have access to their private vehicles to respond immediately to an incident. When an incident occurs, responsible agencies ranging from city transportation administrations to emergency units should quickly devise and execute a plan to allocate available public transit resources to evacuate carless population. For transit-supported evacuation, it is important to consider how to determine available transit and drivers, how to identify potential pick-up locations, how to provide transit routes/schedule to dispatch public transit resources efficiently, and how to determine a timetable for the drivers.

Pick-up Locations

During evacuations, it is needed first to guide and coordinate evacuees to nearby convening points and to schedule the transit vehicles at these pick-up points in accordance with time-dependent arrival pattern of the evacuees. When pick-up locations are set, they should cover all evacuees such as persons with disabilities, older adults, or the carless and minimize their total walking distance and time.

Transit Schedule/Route

As the purpose of transit resource use for evacuation is to transport evacuees quickly by minimizing the transport time from pickup locations to shelters, it is important to optimize transit schedules and routes in the minimal amount of time. In other words, transit can be used as an efficient mode having flexible routes by servicing different pick-up locations at various runs based on actual need. During evacuations, for example, buses would be run on more relatively flexible routes than BRT operated on fixed route by being dispatching to the most needed pick-up location and serving adjustable routes and schedule.

Boarding/Alighting Time

Loading/unloading time is based on the actual boarding/alighting time. The actual boarding/ alighting time should be significant to generate transit routes and scheduling timetables. Neglecting this will overestimate the transport efficiency.

Transit/Destination Capacity

Capacity constraints regarding both transit and destination should be considered. If such constraints are not assessed properly, evacuees can be sent to the same places, which can result in overcrowding problems.

One-Way Roadway and Urban Street Operations

A well-designed road network will help the evacuation. Traffic control and operations management can make significant contributions to effective evacuation as well. During an evacuation, the main target is to move evacuees out and take emergency personals and vehicles into the affected areas as soon as possible. In this case, inbound and outbound demand will be unbalanced, and efficient traffic management strategy is required to deal with the problem. Coordinated signal timing prioritization, contraflow strategies, and demand/ capacity control strategies are all possible ways to make emergency evacuation more efficient.

Traffic Control Devices

Traffic control devices are traffic signs, signals, or markers to inform, guide, and control road users. Typically, they are placed along the highway or urban streets, intersections, and other places that require traffic control. For emergency evacuation, more temporary emergency traffic control devices are required to ensure the evacuation process clearly and efficiently.

Signs

Functions of traffic signs including guiding, restricting, or controlling traffic operations to limit access of vehicles, give prior right-of-way to emergency vehicles, and provide emergency information. The location and use of signs should strictly follow the judgment and research of traffic engineers, in which the physical conditions and traffic factors should be considered to give the road users necessary warning guidance and other importation information. Specific signs such as contraflow signs and shelter locations signs are specially designed for emergency evacuation.

Regulatory and warning signs should be used conservatively, as excess use of these signs will diminish effectiveness. Traffic signs for route guidance should be used frequently to help drivers perceive their real-time locations. This will be helpful if electronic systems are damaged during an emergency situation. To maintain the effectiveness of traffic signs, regular assessment or management methods should be used, including:

- Visual nighttime inspection (retro-reflectivity satisfied the minimum levels)
- Measured sign retro-reflectivity
- Expected sign life (signs cannot older than expected design life)
- Blanket replacement
- Control signs
- Other methods.

State and local highway agencies have the rights and obligations to develop special word message signs for emergency situations if it is necessary to provide road users with additional regulatory, warning, or guidance information. For instance, for the contraflow strategy, signs along the reverse direction lanes are particularly important and differ to the regular signs. Drivers must always be aware of the start and end point of contraflow, especially if the freeway or the urban street is separated by medians, as they cannot see the traffic signs in the opposite direction.

Pavement Markings

Pavement markings are another way to convey messages to road users. Pavement markings can provide information on road conditions ahead, guide the route, and indicate the passing area. Typically, pavement markings include solid yellow lines, dashed yellow lines, solid white lines, and dashed white lines. Yellow lines are used to separate traffic flowing in the opposite direction and white lines are used to separate traffic flowing in the same direction. Dashed lines allow passing or lane change and the solid lines prohibit these actions. Following are factors that may have an impact on the performance of pavement markings:

- Environmental conditions (temperature, humidity, etc.)
- Roadway surface type
- Traffic volume
- Pavement marking materials
- Pavement surface cleaning moisture

Note that as pavement markings may be destroyed by the emergency situation, it is crucial to prepare emergency markings to avoid panic during an evacuation.

Traffic Signals

Traffic is defined as road users, including pedestrians, bicyclists, and vehicles using the roadway for the purpose of travel. Traffic signals are designed to control the right-of-way of traffic by giving signals directed to stop and permitted to proceed. Essentially, deciding parameters should include cycle length, number of phases, green splits, and offsets between adjacent intersections. The prerequisites to design the traffic signal are efficiency and safety. However, in reality, with an increase in demand, especially during an evacuation, it could be difficult to balance the two essential factors. Purposes of signal time designs are:

- Maximize movement volume at intersections
- Provide orderly and efficient movement for road users
- Minimize frequency and severity of safety issues
- Consider requirements of special-needs people

Emergency signal time will significantly improve the efficiency of evacuation. To send more people out of the affected areas, transit vehicles can play a key role because of the large capacity. Bus signal priority (BSP) or transit signal priority (TSP) techniques are two advanced methods during an evacuation; time delay of transit vehicles is significantly reduced or even eliminated by either extending the green interval or shortening the red interval of the phase. Then, the efficiency gets improved.

Shoulder Use

Temporary shoulder use during an emergency evacuation means allowing specific types of vehicles to run on shoulder lanes temporarily if traffic demand exceeds available road capacity. It is possible to improve the road level of service by implementing shoulder use strategy. By allowing shoulder use, the speed limit may differ to normal lane use for safety. A major challenge that should be considered about shoulder use is how to give a way to the emergency vehicles, especially if the traffic volume is extremely high. Moreover, it is essential to determine the start-end point. Special traffic facilities and signs are required to indicate to evacuees if shoulder lane use is temporarily permitted or

where the start and end points are. Several European countries take temporary shoulder use as a management strategy to ease traffic congestion.

Contraflow

A practical strategy to make full use of available roadway capacity is contraflow. Inbound and outbound traffic demand will be significantly imbalanced during an emergency evacuation. Therefore, extra inbound traffic lanes are suggested to be converted to outbound lanes. Contraflow is a form of reversible traffic operation in which one or more travel lanes of a divided highway are used for the movement of traffic in the opposing direction. Contraflow has become one of the most typical evacuation traffic management strategies since Hurricane Floyd in 1999 and has been developed for use in coastal states from New Jersey to Florida on the Atlantic seaboard and from Florida west through Texas along the Gulf of Mexico. Transportation agencies play the leading role in the process. Contraflow is highly effective because it can significantly increase the directional capacity of a roadway almost without time and cost required. What is more, it is easy to understand for the public during an evacuation.

Contraflow traffic management strategy is usually used on freeways as they have larger capacity and higher-speed operation. Moreover, freeway routes do not incorporate at-grade intersections so that the traffic flow will not be interrupted or restricted if access to the reversed segment. Freeway contraflow can be implemented and controlled with fewer human resources and facilities than typical urban streets. Also, shoulders in both direction can be considered as a temporary lane in an emergency to maximize the road capacity. The effectiveness of contraflow during a live operation was quantified by Wolshon (2008) based on traffic counts recorded during the Hurricane Katrina evacuation of south Louisiana in 2005. The flow rates measured during this event were about 75% of the adjacent normally flowing lanes. Although no firm explanation for these lower rates has been determined, this reduced flow is consistent with modeling predictions and simulation studies.

Design Issues

It is still complex to implement and operate in practice even though the basic concept of contraflow is simple. Drivers can be confused about the contraflow segments without clear and careful design and management. To ensure safety, improper access and egress movements are strictly prohibited at all the times during its operation. Opposing traffic should be fully cleared before initiating contraflow operations. Reversible roadways have a number of physical and operational attributes that are common among all applications. The principal physical attributes are related to spatial characteristics of the design, including its overall length, number of lanes, and the configuration and length of the inbound and outbound transition areas. The primary operational attributes are associated with the way in which the segment will be used and include the temporal control

of traffic movements. The temporal components of all reversible lane segments include the frequency and duration of a particular configuration and the time required to transition traffic from one direction to another.

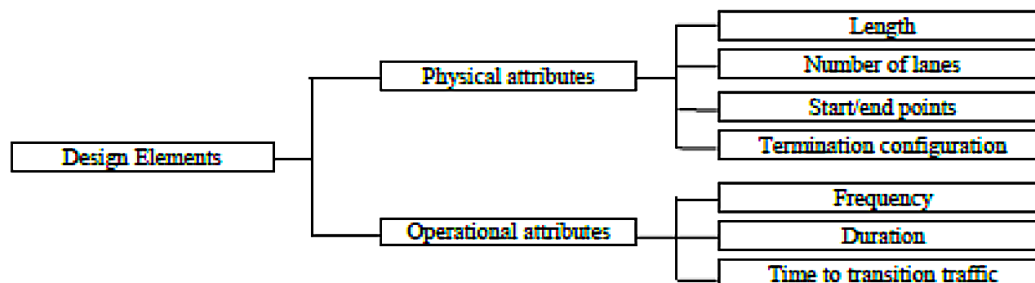


Figure 11-3 Design elements for use of contraflow

Contraflow Design

The essential element of a contraflow plan is to identify the appropriate start/end points and corresponding traffic control strategies since congestion is very likely to occur at these points, which will reduce the effectiveness of contraflow strategy.

According to the reviewed contraflow segments, the termination configurations are typically classified into two groups, split designs and merge designs. Split designs refer to the normal traffic and contra-flowing traffic will be routed to separate roadways at the terminus or the end of contraflow section. However, merge designs will merge two traffic flows and route to the normal direction. Traffic volume, road configuration, and availability of routing options at the end of the segment are typical significant factors to decide whether split designs or merge designs are to be implemented by traffic agencies. Generally, split designs offer higher levels of operational efficiency than merge designs. It is obvious that split designs reduce the potential bottleneck of traffic so possible congestion and crashes will be reduced or even avoided. However, it requires two groups of traffic flow to exit to different routes, and road network resources need to be satisfied and experienced traffic staffs are required. In some older designs, the contraflow traffic flow stream was routed onto an intersecting arterial roadway. This type of split design requires adequate capacity on the receiving roadway.

Similarly, merge termination designs also have pros and cons. The costs and benefits are almost the exact opposite of split designs in their end effect. For example, merge designs do not need to design a route for vehicles running in opposite direction lanes, which save road capacity and staff resources. However, merge designs have a greater potential to cause congestion and crashes because multiple lanes tend to merge into fewer lanes. During an evacuation, how to merge two high-volume roadways into one effectively and safely will be a main task for traffic agencies to consider.

Lane-Based Routing

Typically, intersections are a bottleneck problem that keep the traffic operating smoothly in urban areas, especially during an emergency evacuation. As shown in Figure 11-4, for a normal signalized intersection, there are 32 conflict points, including 16 crossing points, 8 merging points, and 8 diverging points. The number will be increased to 48 if bicycles and pedestrians are considered.

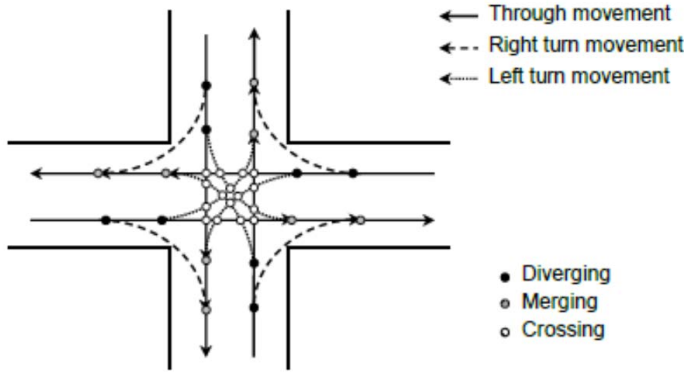


Figure 11-4 Conflict points at intersection

One effective method to reduce the number of conflict points is signal timing, but the lane-based route method is much more useful during an evacuation, as it not only reduces conflict points but also transfers traffic flow into a continuous flow and guides evacuees in the primary outbound direction away from a hazard area to the shelters and the safe locations. A lane-based routing plan selects turning options at intersections to improve the efficiency of traffic flow. Both police control and traffic barricades can be used in intersections. Figure 11-5 is an example.

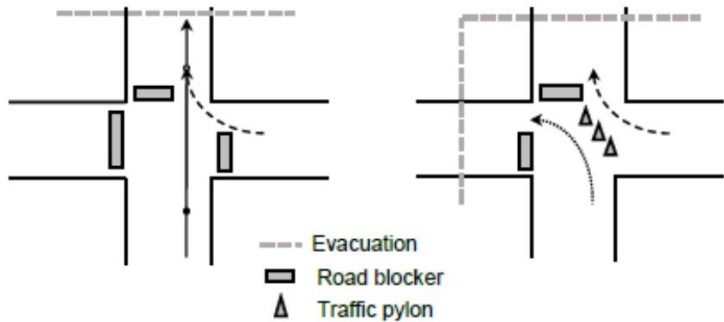


Figure 11-5 Lane-based routing strategy

Street Parking Restrictions

The primary function of streets is providing movement conditions for traffic. To preserve the primary function of a street, street parking needs proper control and management to make traffic operate smoothly. Street parking is permitted to engage people in social activities, however; street parking may be a potential factor of accidents and traffic delay. A parked vehicle can induce the delay of hundreds of vehicles; especially for the following cases, safety and delay problems are more severe:

- Vehicles parked close to traffic lanes
- Process of vehicle parking and leaving
- Driver/passenger boarding or getting off
- Parking area near intersections

During emergency evacuations, street parking may be a constraint to conduct evacuations. Evacuees may have escaped the affected area by other transportation modes but left cars along the street, thus reducing the capacity of road segments and dragging the efficiency of evacuations. All illegally parked vehicles should be towed. Therefore, flexible and reasonable street parking policies are required to safeguard the evacuation proceed smoothly.

Demand Responsive Emergency Response and Emergency Fleet Management

Demand for Emergency Response

Evacuation demand refers to the forecasted amount of travel demand during an evacuation; the basic principle is behavioral analysis. Emergency management departments need to determine the total number of evacuees to be moved to shelters or safety places and how many of them are willing to take transit and private vehicles. The analytical process typically follows the four-step method but special considerations are required. Transportation evacuation zones are divided based on the affected population and the severity of the affected areas. It will be a worst case if more people need to evacuate and emergency situations take place without notice. There is limited time for agencies to conduct and manage the evacuation.

Demand management is an alternative effective way to deal with surging demand in an emergency evacuation. Typical methods including phased evacuation, background traffic management, transit evacuation encouragement, and shelter location selection. Phased evacuation is a systematic and controlled sequence of the evacuation process in different part of affected areas. The priority is typically defined by the level of risk or the severity of the emergency situation. Areas under the greatest risk or that suffered from the most severity should be evacuated as the first priority. Phased

evacuation is implemented as a series of successive, geographically smaller evacuations. Therefore, if affected people in different locations are guided to evacuate at different time periods, the surging traffic demand problem is mitigated or eliminated. The major challenge of phased evacuations is whether evacuees are willing to follow the guidance of agencies under great time pressure and the sense of fear of emergency. Therefore, although phased evacuation is voluntary, accurate disaster information and recommendations should be disseminated. Background traffic minimization refers to the cancellation of unnecessary trips and makes full use of vehicle space. However, several unnecessary trips are not likely to be canceled due to work and family responsibilities. Special consideration is required. Shelter location selection is another major task for agencies that will greatly impact the evacuation route choice and corresponding road capacity.

EMS Fleet Management

A comprehensive emergency management system (EMS) is a concept that ensures the effectiveness of emergency management by minimizing risks, preparing for emergency situations, and helping in recovering from an emergency.

Special Considerations for EMS Management

Since Hurricane Katrina, planning for evacuations for special care facilities such as hospitals gained significantly increased attention. In most locations, responsibility for the movement of individuals who reside in care facilities fell to the manager of that facility. For example, contracts were signed between care facilities traffic providers such as ambulance and bus companies. Care centers, hospitals, and older adult residential areas cooperated to prepare for potential disasters. Special facilities and other suppliers include hospitals and healthcare facilities, gas stations, delivery and distribution of fuel, water, food and wrecker services, and schools.

Evacuation Groups with Special Needs

Special-needs populations such as transit-dependent individuals refer to persons with disabilities and older people with walking or cognitive problems. Individuals with physical or cognitive limitations are not easy to evacuate by transit or private vehicle since further assistance could be required for walking, dressing, communicating, or recognizing directions correctly. All conditions limit the affected special-needs population to communicate with agencies or other people and it could be difficult to gather in the pick-up location by themselves. Agencies should pay special attention to special-needs populations to help them understand the situation and make arrangement as soon as possible; door-to-door pick up may be required for resource allocation and minimization lost during an emergency.

People with lower income or who live in low-income residential areas are more likely to be transit-dependent evacuees. They may have little knowledge about evacuation and lack regular exercise. Agencies should identify these groups ahead of a disaster and provide necessary training to them to optimize evacuation efficiency. It is also necessary to estimate the number of these people for agencies to prepare enough daily supplies.

Older people and children are particularly vulnerable groups during an emergency. Older adults are more likely to have medical problems. Chronic health problems or limited mobility are threats to conducting a successful evacuation. Sight, hearing, or cognitive abilities can make things worse, which limits their capacity to follow instructions. Older people with lower incomes, living in isolation, or without communication facilities need more help as they have limited resources. Young children have yet to develop the resources, knowledge, or understanding to effectively cope with disaster and are more likely to be injured or disease during a risk. Young children also are more vulnerable when they are separated from their parents or guardians, for example, at school or in daycare.

Special-needs populations include people with cognitive, physical, or sensory impairment that limits daily life activities. Physical impairments might include sight, hearing, or mobility limitations. Also, people depending on electricity to stay alive are considered part of the special-need population. Individuals with access and functional needs are categorized as special-needs as well. Assistants and assistant facilities are required to disseminate accurate information to this population group.

Providing Medical Services during an Evacuation

Medicine and treatment for injured people should be prepared during an evacuation. Medical and support staff in affected and adjacent areas must be properly licensed to permit their use. Ambulances and emergency supplies must be acquired. Administrative support must also be provided to account for and track the injured. Since roadway system will likely to be the primary means of transporting injured populations, agencies should consider priority for ambulances and vehicles with injured people. Additional assistance should be offered if required.

Demand Uncertainty of Transit Evacuees

The numbers of transit-dependent evacuees mainly depends on residential locations. Locations with higher-income residential areas may have a lower transit-dependent population. However, transit will be recommended during an evacuation. Therefore, the number of transit-dependent evacuees remains uncertain. The number of transit-dependent evacuees is usually represented as a random variable within a range, and stochastic programming approaches are

applied. But the result may be not satisfactory since it is difficult to define the range of random variables based on limited information during an evacuation. A more recent method to optimize decisions under uncertainty is robust optimization, which considers the worst case to apply in the model. Experience and supplementary algorithms are required to avoid being overly conservative.

Transit System Protection and Recovery

Transit system conditions need to be assessed after an emergency to determine proper working conditions or that potential risks should be removed. Specific funding is recommended to be reserved for the recovery of the transit system so it can be functional in a short time and used as an evacuation mode. If transit systems suffer destructive damage and service must be suspended, restoration operation is required for recovery. Transit agencies are recommended to sustain identified essential functions for up to 30 days.

For long-term recovery, transit service conditions and performance should be improved in either a regular or evacuation situation. Typical steps include developing long-term recovery strategies and corresponding schedule according to the disaster or emergency reports, estimating the budget and loss for recovery, improving or rebuild the transit system to attract more users during evacuations, and strengthening coordination with other agencies or first responders.

To ensure the transit system has good performance, vehicle inspection and maintenance are necessary. Theoretically, before each trip, transit inspection is required to be conducted carefully, especially for evacuations, to optimize safety performance. Typically inspecting items include fuel quantity and indicators inspection, headlight beam and light system inspection, clearing suspicious persons or objectives, security equipment and emergency supplies check, and mechanical conditions.

A form for checking items should be created to make sure every item for inspection has been covered. If security risks are found, inform agencies immediately. Transit maintenance is required to remove potential risks to the transit drivers and passengers. It is crucial to keep the transit operating functionally. Typical maintenance includes daily servicing maintenance (fuel, water, oil and tire pressure), periodic maintenance (potential damage of belts, electrical cables and tires), interval-related maintenance (preventive repair or replacement of parts are loss or deterioration from use), and failure maintenance (repair or replacement of parts that fail in-service and cannot be used anymore).

Improved Sensor, Detection, and Probe Technologies

During evacuations, it is needed to provide timely and accurate traffic information to effectively guide evacuees. Improved technologies for detecting information to access traffic flow rates and speeds, lane closures, hazard conditions, incident severity, and the availability of alternative routes are crucial for the effective management of evacuation processes.

Intelligent Transportation Systems

ITS technologies are advanced applications used to collect data and communicate and coordinate with travelers, agencies, and emergency vehicles by incorporating existing and developing technologies into their response plans for emergency situations. During evacuations, ITS enables transportation agencies to respond to the need for up-to-date evacuee information. The technology consists of both intelligent infrastructure systems and intelligent vehicle systems. ITS is commonly applied for real-time monitoring of travel condition such as traffic volume and speed and monitored information can be used to help not only agencies to make emergency plans and reroute traffic, but also evacuee determine when they start and end an evacuation. ITS technologies are capable of insights into the existence of flow-impeding incidents.

Closed-Circuit Television Cameras

CCTV cameras are a surveillance method to remotely monitor traffic condition. These cameras provide direct visual confirmation of traffic conditions at remote locations, which means incidents and their removal can be visually detected for evacuation management. Also, CCTV can be used as a security tool for linking the special spots in operation including public safety, hospital, and shelters during an evacuation. However, CCTV typically requires direct power and hardwired communication connections, which makes it difficult to achieve in remote locations along evacuation routes.

Real-Time System Management Information Programs

Real-time system management information programs are designed to monitor traffic and travel conditions in real time on major highways. The program is used to provide real-time highway and transit information needs and address the system to meet those needs. Additionally, the information can be used with ITS by updating the technology.

Advanced Traveler Information Systems

ATIS has been developed to enhance personal mobility, safety, and productivity of transportation. The systems monitor traffic and road conditions and provide

en-route traveler information including route-specific traffic, route guidance, and other pertinent information, which especially leads to reducing traffic congestion during evacuations. ATIS varies from highway advisory radio (HAR) with limited broadcast ranges to speech-activated automated phone services that enable users to obtain useful information about available transit service and expected travel times and evacuation duration.

In-Vehicle Systems

In-vehicle information systems use a video display inside a vehicle to detect a wide array of information and provide evacuees with information about route guidance and emergency situation. The systems are linked to national emergency organizations such as NOAA or the hazard radio system; they play an active role as a channel to provide information received from official governments to travelers. They also connect with satellite radio providers to spread information quickly to a broad area and provide information to travelers carrying crucial recovery materials about any temporary changes to commercial vehicle restriction and offer emergency alert notifications such as evacuation text or audio messaging. Furthermore, in-vehicle information systems enable publicly-sponsored systems to monitor and disseminate information more accurately in emergency circumstances.

Responder Communication and Coordination, Public and Traveler Information Dissemination Technologies

When an emergency alarm occurs, it is essential for evacuees to know whether they need to evacuate, when they should leave, and where they could go. Therefore, authorities should offer this information and suggest safe routes by providing evacuees with timely, accurate, and useful information for an effective evacuation. Also, communication between public agencies and evacuees (vehicles and passengers) and coordination between emergency responders are critical components of an effective evacuation. Communication requires remote-sensing for information acquisition and dissemination technologies. The communication should treat information regarding before, during, and after an evacuation:

- (Before) To enable potential evacuees to be aware of a code of behavior and prepare for emergency situation, and develop strategies to ensure their personal safety
- (During) To provide evacuees with available transit information, location of shelter, and route guidance
- (After) To offer information about when they should return and where they may not be able to access

Responder Communication Guidance

Timely and accurate communication to evacuation responders plays a crucial role in emergency situations, as evacuations are dynamic events. Especially at the initial level, it is useful to have the capacity to communicate to evacuees for effective evacuation. Plans and procedures to communicate with responders must be developed by both emergency management and transportation agencies long before emergency situations occur, which helps potential evacuees to anticipate their needs and plan accordingly and know when they should take action. Also, evacuation route maps and tip sheets should be disseminated in newspapers, stores, phone books, and even utility bills; emergency management and transportation agencies should use local media to provide information about the beginning of a hazard or use public/traveler information technologies including emergency alarm systems, message signs, and radio to communicate with responders during evacuation.

Coordination

The coordination strategy for emergency response should be established by transportation agencies and emergency management together. For example, when an emergency happens, emergency management agencies should evaluate the situation accurately and announce both public response and transit agencies, and each agency should provide timely and accurate information. However, lack of coordination can yield duplication of efforts or gaps in response.

Emergency Operations Center

An emergency operation center (EOC) is a coordination hub designed to provide technical assistance to emergency responders and increase coordination capabilities to transportation agencies, emergency or safety agencies, and regional travelers at the scene of an emergency. It plays a role as a control center to coordinate response and recovery actions and resources. The center is a physical facility to collect and analyze data, establish strategies to protect life and property, make a decision about resource allocation, and disseminate decisions to all concerned responders. The EOC helps emergency responders to know the needs of transit resources, to coordinate transit resources use to provide emergency transportation requests and to disseminate information to transit evacuees. An EOC should have the capability of serving as the central coordination point for all emergency operations, information gathering and dissemination, and coordination with concerned governments and organizations.

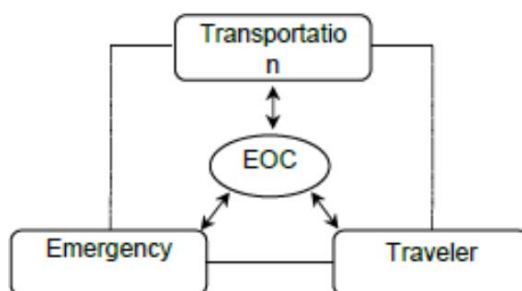


Figure 11-6 Role of EOC for coordination of emergency management

Effective Coordination

An effective practice to enhance coordination is that an agency representative is sent to the EOC during emergencies to interact with other transportation representatives directly as dictated by local plans and policies. Also, transportation providers can join a unified command to address emergency transportation needs and coordinate with the EOC.

Public and Traveler Information Dissemination Technologies

Emergency Alert Systems

An emergency alert system (EAS) is a national public warning system that uses an alert-and warning network on traditional TV and radio to alert the occurrence of an emergency. The system requires cable-television system, broadcasters, digital audio radio service providers, wireless cable systems, or direct broadcast satellite providers to provide the communications capability to concerned responders including local, state, and federal authorities to inform them of emergency situation. An EAS is regarded as one of the most efficient national alert systems since the system offers one message over more media to more people before, during, and after an emergency.

Variable Message Signs

VMS are traffic control devices called changeable message signs (CMS) or dynamic message signs (DMS) that can be pre-programmed or programmed in real time to offer information to travelers. The signs are commonly installed along major roadways in urban areas and designed to improve traffic flow and operations controlled from a remote centralized location or locally at the site. The information on VMS is generated as a result of a planned or unplanned event, which enables emergency responders to obtain real-time information such as travel times, locations of incidents, and the location of shelters, to avoid an incident and prepare for unavoidable conditions.

Web Alert

Web alerts are an information dissemination technology used primarily before evacuation due to the limited availability of the wireless Internet along evacuation routes. However, today, it can be used before, during, and after evacuation with smartphone application or social media technologies. Web alerts help evacuees obtain information about emergency situations, traffic, and road conditions in real time and offer evacuation routes and shelter availability.

Text Messaging

Text messaging is an information dissemination technology to alert about an emergency. As nearly everyone has a cellphone, it is a useful tool to send emergency notification to the public easily within a second. Also, in times of emergency, text messaging can help recipients have additional information. However, a disadvantage is that only registered individuals receive the service.

Highway Advisory Radio

Highway advisory radio (HAR) is a form of emergency notification system to broadcast information to the public in a localized area. During emergency periods, HAR is used to disseminate incident information, evacuation routes, shelter locations, and locations of emergency services such as gas stations, hospitals, and rest areas while offering general travel information in non-emergency situations. HAR uses AM radio band and requires a transmitter and radio station to send information. In emergency evacuation situations, it enables transportation and emergency managers to send information quickly to travelers.

References

Section 1

Blumenthal, R., 2005. Miles of Traffic as Texans Heed Order to Leave. Article in the New York Times, Sep 22, 2005. <https://www.nytimes.com/2005/09/23/us/nationalspecial/miles-of-traffic-as-texans-heed-order-to-leave.html>.

Section 3

Bachok, S., 2008. Estimating, calibrating and validating demand for feeder services during incident detections. Presented at 30th Conference of Australian Institutes of Transport Research, Perth, Australia, 16.

Bai, Y., Kattan, L., 2014. Modeling riders' behavioral responses to real-time information at light rail transit stations. *Transportation Research Record*, 2412, 82–92.

Barnett, A., 1974. On controlling randomness in transit operations. *Transportation Science*, 8, 102–116.

Bender, M., Büttner, S., Krumke, S.O., 2013. Online delay management on a single train line: Beyond competitive analysis. *Public Transportation*, 5, 243–266.

Cacchiani, V., Huisman, D., Kidd, M., Kroon, L., Toth, P., Veelenturf, L., Wagenaar, J., 2014. An overview of recovery models and algorithms for real-time railway rescheduling. *Transportation Research Part B, Methodology*, 63, 15–37. <https://doi.org/10.1016/j.trb.2014.01.009>

Cadarso, L., Marín, Á., Maróti, G., 2013. Recovery of disruptions in rapid transit networks. *Transportation Research Part E, Logistics*, 53, 15–33.

Candelieri, A., Galuzzi, B.G., Giordani, I., Archetti, F., 2019. Vulnerability of public transportation networks against directed attacks and cascading failure. *Public Transportation*, 11, 27–49.

Carosi, S., Gualandi, S., Malucelli, F., Tresoldi, E., 2015. Delay management in public transportation: Service regularity issues and crew re-scheduling. *Transportation Research Procedia*, 18.

Euro Working Group on Transportation (EWGT) 2015, July 14–16, 2015, Delft, The Netherlands 10, 483–492.

CMAP, n.d. Travel Tracker Survey, CMAP. www.cmap.illinois.gov/data/transportation/travel-tracker-survey.

Currie, G., Muir, C., 2017. Understanding passenger perceptions and behaviors during unplanned rail disruptions. *Transportation Research Procedia*. Presented at World Conference on Transport Research, Shanghai, China, 4392–4402.

Eberlein, X.J., Wilson, N.H.M., Barnhart, C., Bernstein, D., 1998. The real-time deadheading problem in transit operations control. *Transportation Research Part B, Methodology*, 32, 77–100.

Eberlein, X.J., Wilson, N.H.M., Bernstein, D., 2001. The holding problem with real-time information available. *Transportation Science*, 35, 1–18.

Fukasawa, N., Yamauchi, K., Murakoshi, A., Fujinami, K., Tatsui, D., 2012. Provision of forecast train information and consequential impact on decision making for train-choice. *Q. Rep. Railway Technology Research Institute*, 53, 141–147.

Ghaemi, N., Cats, O., Goverde, R.M.P., 2017. Railway disruption management challenges and possible solution directions. *Public Transportation*, 9, 343–364.

- Hua, W., Ong, G.P., 2018. Effect of information contagion during train service disruption for an integrated rail-bus transit system. *Public Transportation*, 10, 571–594.
- Jin, J.G., Tang, L.C., Sun, L., Lee, D.-H., 2014. Enhancing metro network resilience via localized integration with bus services. *Transportation Research Part E, Logistics*, 63, 17–30.
- Kepaptsoglou, K., Karlaftis, M.G., 2009. The bus bridging problem in metro operations: Conceptual framework, models and algorithms. *Public Transportation*, 1, 275–297.
- Kiefer, A., Kritzing, S., Doerner, K.F., 2016. Disruption management for the Viennese public transport provider. *Public Transportation*, 8, 161–183.
- Krueger, R., Rashidi, T.H., Auld, J., 2019. Preferences for travel-based multitasking: Evidence from a survey among public transit users in the Chicago metropolitan area. Presented at 98th Annual Meeting of the Transportation Research Board.
- Lin, T., Shalaby, A., Miller, E., 2016. Transit user behaviour in response to service disruption: State of knowledge. Presented at Canadian Transportation Research Forum 51st Annual Conference, North American Transport Challenges in an Era of Change, Toronto, Ontario, May 1-4, 2016.
- Lin, T., Srikukenthiran, S., Miller, E.J., Shalaby, A., 2018. Econometric analysis of subway user mode choice in response to unplanned subway disruptions. Presented at Transportation Research Board 97th Annual Meeting.
- Malucelli, F., Tresoldi, E., 2019. Delay and disruption management in local public transportation via real-time vehicle and crew re-scheduling: a case study. *Public Transportation*, 11, 1–25.
- Murray-Tuite, P., Wernstedt, K., Yin, W., 2014. Behavioral shifts after a fatal rapid transit accident: A multinomial logit model. *Transportation Research Part F, Traffic Psychologic Behavior*, 24, 218–230.
- Pnevmatikou, A.M., Karlaftis, M.G., Kepaptsoglou, K., 2015. Metro service disruptions: How do people choose to travel? *Transportation*, 42, 933–949.
- Rubin, G.J., Brewin, C.R., Greenberg, N., Hughes, J.H., Simpson, J., Wessely, S., 2007. Enduring consequences of terrorism: 7-month follow-up survey of reactions to the bombings in London on 7 July 2005. *British Journal of Psychiatry, Journal of Mental Sciences*, 190, 350–356.
- Saxena, N., Rashidi, T.H., Auld, J.A., 2019. Comparing commuters' willingness to pay under transit disruptions: Delayed vs. canceled services. Presented at 98th Annual Meeting of the Transportation Research Board.
- Shen, S., Wilson, N.H.M., 2001. An optimal integrated real-time disruption control model for rail transit systems, in Voß, S., Daduna, J.R. (eds.), *Computer-Aided Scheduling of Public Transport, Lecture Notes in Economics and Mathematical Systems*. Springer Berlin Heidelberg, Berlin, 335–363.
- Teng, J., Liu, W.-R., 2015. Development of a behavior-based passenger flow assignment model for urban rail transit in section interruption circumstance. *Urban Rail Transit*, 1, 35–46.
- Tsuchiya, R., Sugiyama, Y., Arisawa, R., 2007. A route choice support system for use during disrupted train operation. *Japanese Railway Engineering*, 47.
- van Exel, N.J.A., Rietveld, P., 2009. When strike comes to town: Anticipated and actual behavioural reactions to a one-day, pre-announced, complete rail strike in the Netherlands. *Transportation Research Part C, Policy and Practice*, 43, 526–535.

- Xing, Y., Lu, J., Chen, S., Dissanayake, S., 2017. Vulnerability analysis of urban rail transit based on complex network theory: A case study of Shanghai Metro. *Public Transportation*, 9, 501–525.
- Yap, M., Nijenstein, S., van Oort, N., 2018. Improving predictions of public transport usage during disturbances based on smart card data. *Transportation Policy*, 61, 84–95.

Section 4

- Abdelghany, K. F., and Mahmassani, H.S., 2001. Dynamic trip assignment-simulation model for intermodal transportation networks. *Transportation Research Record*, 2001, 52–60.
- Abdelghany, K. F., Mahmassani, H.S., and Abdelghany, A.F. 2007. A modeling framework for bus rapid transit operations evaluation and service planning. *Transportation Planning and Technology*, 30, 571–591.
- Auld, J., Hope, M., Ley, H., Sokolov, V., Xu, B., and Zhang, K., 2016. POLARIS: Agent-based modeling framework development and implementation for integrated travel demand and network and operations simulations. *Transportation Research Part C: Emerging Technologies*, 64, 101–116.
- Bander, J.L., and White, C.C., 1991. A new route optimization algorithm for rapid decision support, 2, 709–728.
- Bellman, R., 1958. On a routing problem. *Quarterly of Applied Mathematics*, 16(1), 87–90.
- Chriqui, C., and Robillard P., 1975. Common bus lines. *Transportation Science*, 9, 115–121.
- Cominetti, R., and Correa, J., 2001. Common-lines and passenger assignment in congested transit networks. *Transportation Science*, 35, 250–267.
- Cooke, K.L., and Halsey, E., 1966. The shortest route through a network with time dependent internodal transit times. *Journal of Mathematical Analysis and Applications*, 14, 493–498.
- Chabini, I., and Lan, S., 2002. Adaptations of the A* algorithm for the computation of fastest paths in deterministic discrete-time dynamic networks. *IEEE Transactions on Intelligent Transportation Systems*, 3(1), 60–74.
- Dijkstra, E.W., 1959. A note on two problems in connexion with graphs. *Numerische Mathematik*, 1(1), 269–271.
- Ford, L R., Jr., 1956. *Network Flow Theory* (DTIC Document).
- Friedrich, M., Hofsaess, I., and Wekeck, S., 2001. Timetable-based transit assignment using branch and bound techniques. *Transportation Research Record*, 1752, 100–107.
- Furth, P.G., 1985. Alternating deadheading in bus route operations. *Transportation Science*, 19, 13–28.
- Furth, P.G., 1986. Zonal route design for transit corridors. *Transportation Science*, 20, 1–12.
- Furth, P.G., and Day, F.B., 1985. Transit routing and scheduling strategies for heavy demand corridors. *Transportation Research Record*, 23–26.
- Glover, F., Klingman, D., and Phillips, N., 1985. A new polynomially bounded shortest path algorithm. *Operations Research*, 33, 65–73.
- Google. General Transit Feed Specification (GTFS) Static Overview, <https://developers.google.com/transit/gtfs/>. Accessed May 1, 2017.

- Hamdouch, Y., Ho, H.W., Sumalee, A., and Wang, G., 2011. Schedule-based transit assignment model with vehicle capacity and seat availability. *Transportation Research Part B: Methodological*, 45, 1805–1830.
- Hamdouch, Y., and Lawphongpanich, S., 2008. Schedule-based transit assignment model with travel strategies and capacity constraints. *Transportation Research Part B: Methodological*, 42, 663–684.
- Hamdouch, Y., and Lawphongpanich, S., 2010. Congestion pricing for schedule-based transit networks. *Transportation Science*, 44, 350–366.
- Hart, P.E., Nilsson, N.J., and Raphael, B., 1968. A formal basis for the heuristic determination of minimum cost paths. *IEEE Transactions on Systems Science and Cybernetics*, 4(2), 100–107.
- Khani, A., Hickman, M., and Noh, H., 2015. Trip-based path algorithms using the transit network hierarchy. *Networks and Spatial Economics*, 15(3), 635–653.
- Lu, C.-C., and Mahmassani, H.S., 2008. Modeling user responses to pricing: Simultaneous route and departure time network equilibrium with heterogeneous users. *Transportation Research Record*, 2008, 124–135.
- Lu, C.-C., and Mahmassani, H.S., 2009. Dynamic pricing with heterogeneous users: Gap driven solution approach for bicriterion dynamic user equilibrium problem. *Transportation Research Record*, 75–85.
- Lu, C.-C., and Mahmassani, H.S., 2011. Modeling heterogeneous network user route and departure time responses to dynamic pricing. *Transportation Research Part C: Emerging Technologies*, 19, 320–337.
- Lu, C.-C., Mahmassani, H.S., and Zhou, X. 2008. A bi-criterion dynamic user equilibrium traffic assignment model and solution algorithm for evaluating dynamic road pricing strategies. *Transportation Research Part C: Emerging Technologies*, 16, 371–389.
- Lu, C.-C., Mahmassani, H.S., DeCea, J., and Fernández, E., 1993. Transit assignment for congested public transport systems: An equilibrium model. *Transportation Science*, 27, 133–147.
- Mahmassani, H.S., and Abdelghany, K., Dynasmart-IP: Dynamic traffic assignment meso-simulator for intermodal networks. In *Advanced Modeling for Transit Operations and Service Planning*, Pergamon, 201–229.
- Noh, H., 2013. *Capacitated Schedule-Based Transit Assignment Using a Capacity Penalty Cost*. University of Arizona.
- Noh, H., Hickman, M., and Khani, A., 2012. Hyperpaths in network based on transit schedules. *Transportation Research Record*, 29–39.
- Nguyen, S., and Pallottino, S., 1988. Equilibrium traffic assignment for large scale transit networks. *European Journal of Operational Research*, 37, 176–186.
- Nguyen, S., and Pallottino, S. Hyperpaths and shortest hyperpaths. In *Combinatorial Optimization*, B. Simeone, ed., Springer Berlin Heidelberg, 258–271.
- Regional Transit Authority. RTA Trip Planner, <http://www.rtachicago.org/plan-your-trip>. Accessed Jul. 1, 2017.
- Schmöcker, J.-D., Bell, M.G.H., and Kurauchi, F., 2008. A quasi-dynamic capacity constrained frequency-based transit assignment model. *Transportation Research Part B: Methodological*, 42, 925–945.
- Schmöcker, J.-D., Fonzone, A., Shimamoto, H., Kurauchi, F., and Bell, M.G.H., 2011. Frequency-based transit assignment considering seat capacities. *Transportation Research Part B: Methodological*, 45, 392–408.

- Spieß, H., and Florian, M., 1989. Optimal strategies: A new assignment model for transit networks. *Transportation Research Part B*, 23, 83–102.
- Verbas, Ö. *Transit Network Assignment, Simulation and Frequency Setting: Integrated Approaches and Large Scale Application*. Northwestern University, 2014.
- Verbas, İ.Ö., and Mahmassani, H.S., 2015. Finding least cost hyperpaths in multimodal transit networks. *Transportation Research Record*, 2497, 95–105.
- Zhao, L., Ohshima, T., and Nagamochi, H., 2008. A* algorithm for the time-dependent shortest path problem.
- Ziliaskopoulos, A.K., 1994. *Optimum Path Algorithms on Multidimensional Networks: Analysis, Design, Implementation and Computational Experience*. University of Texas at Austin.
- Ziliaskopoulos, A.K., and Mahmassani, H.S., 1993. Time-dependent, shortest path algorithm for real-time intelligent vehicle highway systems applications. *Transportation Research Record*, 94–100.
- Ziliaskopoulos, A.K., and Mahmassani, H.S., 2000. A note on least time path computation
- Ziliaskopoulos, A. K., and W. Wardell, 2000. An intermodal optimum path algorithm for multimodal networks with dynamic arc travel times and switching delays. *European Journal of Operational Research*, 125, 486–502.

Section 5

- Tebaldi, C., West, M., 1998. Bayesian inference on network traffic using link count data. *Journal of the American Statistical Association*, 1998.
- McNicholas, P. D., 2010. Model-based classification using latent Gaussian mixture models. *Journal of Statistical Planning and Inference*.
- Ma, J., Smith, B.L., Zhou, X., 2016. Personalized real-time traffic information provision: Agent-based optimization model and solution framework. *Transportation Research Part C: Emerging Technologies*.

Section 7

- Auld, J., Ley, H., Verbas, O., Golshani, N., and Fontes, A., 2018. A stated-preference intercept survey of transit-rider response to service disruptions.
- Bachok, S., 2008. Estimating, calibrating and validating demand for feeder services during incident detections. 30th Conference of Australian Institutes.
- Bai, Y., and Kattan, L., 2014. Modeling riders' behavioral responses to real-time information at light rail transit stations. *Transportation Research Record*, 2412, 82–92.
- Berechman, J., 1993. *Public Transit Economics and Deregulation Policy*. Elsevier.
- Breiman, L., Friedman, J.H., Olshen, R.A., and Stone, C.J., 2017. *Classification and Regression Trees*. Routledge, New York.
- Cadarso, L., Marín, Á., and Maróti, G., 2013. Recovery of disruptions in rapid transit networks. *Transportation Research Part E, Logistics*, 53, 15–33.
- Chawla, N. V., Bowyer, K.W., Hall, L.O., and Kegelmeyer, W.P., 2002. SMOTE: Synthetic Minority Over-sampling Technique. *Journal of Artificial Intelligence Research*, 16, 321–357.

- Chicago Transit Authority, 2017. CTA Facts at a Glance.
<https://www.transitchicago.com/facts/>. Accessed 1/28/19.
- Currie, G., and Muir, C., 2017. Understanding passenger perceptions and behaviors during unplanned rail disruptions. *Transportation Research Procedia*, 25, 4392–4402.
- Fukasawa, N., Yamauchi, K., Murakoshi, A., Fujinami, K., and Tatsui, D., 2012. Provision of forecast train information and consequential impact on decision making for train-choice. *Q. Rep. RTRI*, 53, 141–147.
- Han, J., Kamber, M., and Pei, J., 2011. *Data Mining: Concepts and Techniques*, 3rd Ed. Elsevier Science.
- Kazemitabar, J., Amini, A., Bloniarz, A., and Talwalkar, A., 2017. Variable importance using decision trees. 31st Conference on Neural Information Processing Systems (NIPS 2017), Long Beach, CA.
- Kroes, E.P., and Sheldon, R.J., 1988. Stated preference methods: An introduction. *Journal of Transportation Economic Policy*.
- Kubat, M., and Matwin, S., 1997. Addressing the curse of imbalanced training sets: One-sided selection. *ICML*, 97, 179–186.
- Lin, T., 2017. Transit user mode choice behaviour in response to TTC rapid transit service disruption. University of Toronto.
- Lin, T., Shalaby, A., and Miller, E., 2016a. Transit user behaviour in response to service disruption: State of knowledge. Canadian Transportation Research Forum 51st Annual Conference-North American Transport Challenges in an Era of Change, Toronto, Ontario.
- Lin, T., Shalaby, A., and Miller, E., 2016b. Transit user behaviour in response to subway service disruption. Canadian Society for Civil Engineering. London, Ontario, Canada.
- Lo, S.-C., and Hall, R.W., 2006. Effects of the Los Angeles transit strike on highway congestion. *Transportation Research Part A, Policy and Practice* 40, 903–917.
- Luo, Y., Wang, Y., Cao, F., Su, S., Yin, J., Zhang, M., Tang, T., and Ning, B., 2018. Train rescheduling and circulation planning in case of complete blockade for an urban rail transit line. Transportation Research Board 97th Annual Meeting.
- Mattsson, L.-G., and Jenelius, E., 2015. Vulnerability and resilience of transport systems – A discussion of recent research. *Transportation Research Part A, Policy and Practice*, 81, 16–34.
- Murray-Tuite, P., Wernstedt, K., Yin, W., 2014. Behavioral shifts after a fatal rapid transit accident: A multinomial logit model. *Transportation Research Part F, Traffic Psychology and Behavior*, 24, 218–230.
- Olson, D., and Delen, D., 2008. *Advanced Data Mining Techniques*. Springer Berlin Heidelberg, Berlin, Heidelberg.
- Pazzani, M., Merz, C., Murphy, P., Ali, K., Hume, T., and Brunk, C., 1994. Reducing misclassification costs. *Mach. Learn. Proc.*, 217–225.
- Pedregosa, F., Varoquaux, G., Gramfort, A., Michel, V., Thirion, B., Grisel, O., Blondel, M., Prettenhofer, P., Weiss, R., Dubourg, V., Vanderplas, J., Passos, A., Cournapeau, D., Brucher, M., Perrot, M., and Duchesnay, É., 2011. Scikit-learn: Machine learning in Python. *Journal of Machine Learning Research*, 12, 2825–2830.
- Pnevmatikou, A.M., Karlaftis, M.G., and Kepaptsoglou, K., 2015. Metro service disruptions: How do people choose to travel? *Transportation (Amst)*, 42, 933–949.

- Rahimi, E., Shamshiripour, A., Shabanpour, R. Mohammadian, A. Auld, J., 2019. Analysis of transit users' waiting tolerance in response to unplanned service disruptions. *Transportation Research Part D: Transport and Environment*, 77, 639-653.
- Rokach, L., and Maimon, O., 2008. *Data Mining with Decision Trees: Theory and Applications*, 2nd ed. World Scientific.
- Saberi, M., Ghamami, M., Gu, Y., Shojaei, M.H., and Fishman, E., 2018. Understanding the impacts of a public transit disruption on bicycle sharing mobility patterns: A case of Tube strike in London. *J. Transportation Geogr.*, 66, 154-166.
- Saxena, N., Rashidi, T.H., and Auld, J., 2019. Comparing commuters willingness to pay under transit disruptions: Delayed vs. canceled services. Transportation Research Board 98th Annual Meeting.
- Tan, P., 2018. *Introduction to Data Mining*. Pearson Education India.
- van Exel, N.J.A., and Rietveld, P., 2009. When strike comes to town: Anticipated and actual behavioural reactions to a one-day, pre-announced, complete rail strike in the Netherlands. *Transportation Research Part A, Policy and Practice*, 43, 526-535.
- Yap, M.D., Nijënstein, S., and van Oort, N., 2018. Improving predictions of public transport usage during disturbances based on smart card data. *Transportation Policy*, 61, 84-95.

Section 8

- Auld, J., Sokolov, V., Fontes, A., and Bautista, R., 2012. Internet-Based Stated Response Survey for No-Notice Emergency Evacuations. *Transportation Letters*, 4(1), 41-53.
- Baker, E.J., 1991. Hurricane evacuation behaviour. *International Journal of Mass Emergencies and Disasters*.
- Benfield, A. 2016. 2016 Annual Global Climate and Catastrophe Report, http://thoughtleadership.aonbenfield.com/Documents/20150113_ab_if_annual_climate_catastrophe_report.pdf.
- Bhat, C.R., and Eluru, N., 2009. A copula-based approach to accommodate residential self-selection effects in travel behaviour modeling. *Transportation Research Part B: Methodological*, 43 (7), 749-765.
- Carnegie, J., and Deka, D., 2010. Using hypothetical disaster scenarios to predict evacuation behavioural response. Transportation Research Board 89th Annual Meeting.
- Charnkol, T., Hanaoka, S., and Tanaboriboon, Y., 2007. Emergency trip destination of evacuation as shelter analysis for tsunami disaster. *Journal of the Eastern Asia Society for Transportation Studies*, 7, 853-868.
- Cheng, G., Wilmot, C.G., and Baker, E.J., 2008. Destination choice model for hurricane evacuation. Transportation Research Board.
- Dash, N., and Gladwin, H., 2007. Evacuation decision making and behavioural responses: Individual and household. *Natural Hazards Review*, 8(3), 69-77.
- Dixit, V., Pande, A., Radwan, E., and Abdel-Aty, M., 2008. Understanding the impact of a recent hurricane on mobilization time during a subsequent hurricane. *Transportation Research Record*, 2041, 49-57.
- Dixit, V., Wilmot, C., and Wolshon, B., 2012. Modeling risk attitudes in evacuation departure choices. *Transportation Research Record*, 2312, 159-163.
- Drabek, T.E., 1999. Understanding disaster warning responses. *The Social Science Journal*, 36(3), 515-523.

- Drabek, T.E., and Boggs, K.S., 1968. Families in disaster: Reactions and relatives. *Journal of Marriage and Family*, 30(3), 443–451.
- Frank, M.J., 1979. On the simultaneous associativity of $F(x, Y)$ and $X + Y - F(x, Y)$. *Aequationes Mathematicae*, 19, 194–226.
- Fu, H., and Wilmot, C., 2004. Sequential logit dynamic travel demand model for hurricane evacuation. *Transportation Research Record*, 1882, 19–26.
- Fu, H., and Wilmot, C., 2006. Survival analysis-based dynamic travel demand models for hurricane evacuation. *Transportation Research Record*, 1964, 211–218.
- Hasan, S., Mesa-Arango, R., and Ukkusuri, S., 2013. A random-parameter hazard-based model to understand household evacuation timing behaviour. *Transportation Research Part C, Emerging Technologies*, 27: 108–116.
- Hasan, S., Ukkusuri, S., Gladwin, H., and Murray-Tuite, P., 2011. Behavioural model to understand household-level hurricane evacuation decision making. *Journal of Transportation Engineering*, 137(5), 341–348.
- Kiefer, N.M., 1988. Economic duration data and hazard functions. *Journal of Economic Literature*, 26(2): 646–679.
- Liu, S., Murray-Tuite, P., and Schweitzer, L., 2012. Analysis of Child pick-up during daily routines and for daytime no-notice evacuations. *Transportation Research Part A, Policy and Practice*, 46 (1).
- Mesa-Arango, R., Hasan, S., Ukkusuri, S.V., Asce, A.M., and Murray-Tuite, P., 2013. Household-level model for hurricane evacuation destination type choice using Hurricane Ivan data. *Natural Hazards Review*, 14, 11–20.
- Murray-Tuite, P., Yin, W., Ukkusuri, S., and Gladwin, H., 2012. Changes in evacuation decisions between hurricanes Ivan and Katrina. *Transportation Research Record*, 2312, 98–107.
- Ng, M., Diaz, R., and Behr, J., 2015. Departure time choice behaviour for hurricane evacuation planning: The case of the understudied medically fragile population. *Transportation Research Part E*, 77, 215–226.
- Parady, G.T., and Hato, E., 2016. Accounting for spatial correlation in tsunami evacuation destination choice: A case study of the Great East Japan earthquake. *Natural Hazards*, 84(2), 797–807.
- Robinson, R., and Khattak, A., 2010. Route change decision making by hurricane evacuees facing congestion. *Transportation Research Record*, 2196, 168–175.
- Sadri, A.M., Ukkusuri, S.V., and Murray-Tuite, P., 2013. A random parameter ordered probit model to understand the mobilization time during hurricane evacuation. *Transportation Research Part C, Emerging Technologies*, 32, 21–30.
- Sadri, A.M., Ukkusuri, S.V., and Murray-Tuite, P., 2014. How to evacuate: Model for understanding the routing strategies during hurricane evacuation. *Journal of Transportation Engineering*, 140(1), 61–69.
- Sklar, A., 1973. Random Variables, Joint distribution functions, and copulas. *Kybernetika*, 9(6), 449–460.
- Smitherman, H., and Soloway-Simon, D., 2002. Special needs of children following a disaster. *Clinical Pediatric Emergency Medicine*, 3(4), 262–267.

- Sorensen, J.H., 1991. When shall we leave? Factors affecting the timing of evacuation departures. *International Journal of Mass Emergencies*.
- Spissu, E., Pinjari, A.R., Pendyala, R.M., and Bhat, C.R., 2009. A copula-based joint multinomial discrete-continuous model of vehicle type choice and miles of travel. *Transportation*, 36(4), 403–422.
- Wilmot, C.G., Modali, N., and Chen, B., 2006. Modeling hurricane evacuation traffic: testing the gravity and intervening opportunity models as models of destination choice in hurricane evacuation.
- Wu, H-C., Lindell, M.K., and Prater, C.S., 2012. Logistics of hurricane evacuation in hurricanes Katrina and Rita. *Transportation Research Part F, Traffic Psychology and Behaviour*, 15(4), 445–461.
- Zimmerman, C., Brodesky, R., and Karp, J., 2007. *Using Highways for No-Notice Evacuations: Routes to Effective Evacuation Planning Primer Series*.
https://ops.fhwa.dot.gov/publications/evac_primer_nn/primer.pdf.

Section 9

- Chicago Population, 2018. Retrieved from
<http://worldpopulationreview.com/uscities/chicago/>.
- Des Plaines - Home. Retrieved from <http://www.desplaines.org/civicax/filebank/blobdload.aspx?Blob-ID=24238>.
- Eltagouri, M., 2015. Chicago area sees greatest population loss of any major U.S. city, region in 2015. *Chicago Tribune*.
- Encyclopedia of Chicago. Des Plaines River.
<http://www.encyclopedia.chicago-history.org/pages/375.html>.
- Federal Motor Carrier Safety Administration, 2018. Nine classes of hazardous materials, https://www.fmcsa.dot.gov/sites/fmcsa.dot.gov/files/docs/Nine_Classes_of_Hazardous_Materials-4-2013_508CLN.pdf.
- FEMA, 2006. *Hazardous Materials Tabletop Exercises Manual*. Archived from the original, July 2006.
- FEMA, 2014. Discovery report, Des Plaines River Watershed, HUC #07120004.
- Gilsinan, K., 2014. Terrorist attacks on schools have soared in the past 10 years. <https://www.theatlantic.com/international/archive/2014/12/terrorist-attacks-on-schools-have-soared-in-the-past-10-years/383825/>.
- Hazardous Materials Cooperative Research Program, United States, Pipeline, Hazardous Materials Safety Administration, & Battelle Memorial Institute, 2011. A guide for assessing community emergency response needs and capabilities for hazardous materials releases (No. 5). Transportation Research Board.
- Illinois Floodmaps, Des Plaines Watershed. <http://www.illinoisfloodmaps.org/desplaines-discovery.aspx>.
- Kawprasert, A., Barkan, C., 2010. Effect of train speed on risk analysis of transporting hazardous materials by rail. *Transportation Research Record*, 2010.
- Metra, 2010. Ridership reports System facts. Archived from original, January 2, 2010. Retrieved July 17, 2012.
- Metrarail.com., 2018. BNSF history. <https://metrarail.com/aboutmetra/our-history/bnsf-history>.

- NHRM, National Highway Institute, 1996. Highway routing of hazardous materials. Publication Number FHWA-HI-97-003. Guidelines for Applying Criteria.
- Northeast Illinois Regional Commuter Railroad Corp, 2016. BNSF railway full timetable. Retrieved 2017-07-04.
- Oswego Ledger-Sentinel, 2009. A step closer on local Metra station. Archived from original, December 28, 2010. Retrieved November 14, 2010.
- PACEbus.com., 2018. PACE bus. http://www.PACEbus.com/sub/vanpool/traditional_van-pool.asp.
- PACEbus.com, 2018. PACE bus. http://www.PACEbus.com/sub/paratransit/sd_dial_a_ride.asp.
- PACEbus.com. PACE bus. http://www.PACEbus.com/sub/about/history_facts.asp.
- Start.umd.edu, 2016. GTD search results. <https://www.start.umd.edu/gtd/search/-Results.aspx?chart=overtime&search=educational>.
- U.S. Census, 2016. Combined statistical area population and estimated components of change, April 1, 2010 to July 1, 2016 (CSA-EST2016-alldata).
- U.S. Department of Commerce, Oceanservice.noaa.gov, 2018. What does HAZMAT stand for? <https://oceanservice.noaa.gov/facts/hazmat.html>.
- U.S. Department of Justice, Bureau of Justice Assistance. Communities against terrorism. http://assets.lapdonline.org/assets/pdf/shopping_malls.pdf.

Section 10

- Aedo, I., Yu, S., Díaz, P., Acuña, P., and Onorati, T., 2012. Personalized alert notifications and evacuation routes in indoor environments. *Sensors*, 12(6), 7804-7827.
- Al-Deek, H., Sandt, A., Alomari, A., Rogers, J., and Muhaisen, N., 2016. Evaluating the impact and usefulness of Highway Advisory Radio (HAR) and Citizens' Band Radio Advisory Systems (CBRAS) in providing traveler information and improving the user experience on the Florida Turnpike Enterprise's Toll road network and the Florida Interstate Highway System.
- Baird, M.E., 2010. The "phases" of emergency management. Background paper. Prepared for Intermodal Freight Transportation Institute, University of Memphis. Vanderbilt Center for Transportation Research, Nashville, TN.
- Balog, J.N., Boyd, A., and Caton, J.E., 2003. *Public Transportation System Security and Emergency Preparedness Planning Guide*. Report No. DOT-VNTSC-FTA03-01, Federal Transit Administration, U.S. Department of Transportation.
- Birenbaum, I., 2009. Information sharing for traffic incident management. Report No. FHWA-HOP-08-059, Federal Highway Administration, U.S. Department of Transportation.
- Boyle, L., Cordahi, G., Grabenstein, K., Madi, M., Miller, E., and Silberman, P., 2014. Effectiveness of safety and public service announcement messages on dynamic message signs. Report No. FHWA-HOP-14-015, Federal Highway Administration, U.S. Department of Transportation.
- CALTRANS, 2007. Transit emergency planning guidance. Division of Mass Transportation, California Department of Transportation, Sacramento.

- CALTRANS, 2007. Transit emergency planning guidance technical appendices. Division of Mass Transportation, California Department of Transportation, Sacramento.
- Colliers International, 2013. Emergency procedures and evacuation plan. Cambridge, MA.
- Cova, T.J., Dennison, P.E., Li, D., Drews, F.A., Siebeneck, L.K., and Lindell, M.K., 2016. Warning triggers in environmental hazards: Who should be warned to do what and when? *Risk Analysis*, doi: 10.1111/risa.12651.
- Emergency Plans Fact Sheet, 2012. <http://www.safeworkaustralia.gov.au/sites/swa/about/publications/pages/emergencyplans-fact-sheet>. Retrieved February 1, 2017.
- Erkut, E., Tjandra, S.A., and Verter, V., 2007. Hazardous materials transportation. *Handbooks in Operations Research and Management Science*, 14.
- Fox, G. J., 2004. Virtual collaboration: Advantages and disadvantages in the planning and execution of operations in the information age. Naval War Coll Newport RI Joint Military Operations Department, Newport, RI.
- FTA, 2006. Transit threat level response recommendation. Federal Transit Administration, U.S. Department of Transportation.
- Garlock, M., Paya-Zaforteza, I., Kodur, V., and Gu, L., 2012. Fire hazard in bridges: Review, assessment and repair strategies. *Engineering Structures*, 35, 89-98.
- Goss, K.C. (ed), 1998. *Guide for All-Hazard Emergency Operations Planning*. DIANE Publishing.
- Gupta, K., Gupta, S., Verma, K., Singh, A., and Sharma, A., 2016. Detecting power grid synchronization failure on sensing bad voltage or frequency documentation. *International Journal of Engineering Research and General Science*, 4(2), 721-725.
- Harding, J., Powell, G., Yoon, R., Fikentscher, J., Doyle, C., Sade, D., and Wang, J., 2014. Vehicle-to-vehicle communications: Readiness of V2V technology for application. Report No. DOT HS 812 014, U.S. Department of Transportation.
- Higgins, L., Carlson, P., Miles, J., Rozyckie, S., Averso, M., Graham, D., and Jenssen, G., 2015. Emergency exit signs and marking systems for highway tunnels. Report No. NCHRP Project 20-59 (47). National Cooperative Highway Research Program, National Research Council, Washington, DC.
- INES, 2008. *The International Nuclear and Radiological Event Scale User's Manual*, 2008 ed. IAEA and OECD/NEA.
- IAOGP, 2016. Country evacuation planning guidelines. International Association of Oil and Gas Producers, London, UK.
- Jha, A.K., Bloch, R., and Lamond, J., 2012. Cities and flooding: A guide to integrated urban flood risk management for the 21st century. World Bank Publications, Washington, DC.
- Kasamura, Y., 2004. UrEDAS, urgent earthquake detection and alarm system, now and future. 13th World Conference on Earthquake Engineering, Vancouver, Canada.
- Ko, B.C., Cheong, K.H., and Nam, J.Y., 2009. Fire detection based on vision sensor and support vector machines. *Fire Safety Journal*, 44(3), 322-329.
- Kuhn, B., 2010. Efficient use of highway capacity summary. Report No. FHWA-HOP10-023, Federal Highway Administration, U.S. Department of Transportation.

- Lamb, S., Walton, D., Mora, K., and Thomas, J., 2011. Effect of authoritative information and message characteristics on evacuation and shadow evacuation in a simulated flood event. *Natural Hazards Review*, 13(4), 272-282.
- Lindsay, B.R., 2012. Federal emergency management: A brief introduction. Congressional Research Service, Library of Congress, Washington, DC.
- Mason, DC., Davenport, I.J., Neal, J.C., Schumann, G.J.P., and Bates, P.D., 2012. Near real-time flood detection in urban and rural areas using high-resolution synthetic aperture radar images. *IEEE Transactions on Geoscience and Remote Sensing*, 50(8), 3041-3052.
- Ma, X., and Yates, J., 2014. Optimizing social media message dissemination problem for emergency communication. *Computers and Industrial Engineering*, 78, 107-126.
- McCarthy, D., 2007. The Enhanced Fujita Scale. 35th Conference on Broadcast Meteorology, San Antonio, TX.
- Medalia, J., 2010. Detection of nuclear weapons and materials: science, technologies, observation. Congressional Research Service (CRS) Report for Congress, Washington, DC.
- NFPA, 2014. Guidelines to developing emergency action plans for all-hazard emergencies in high-rise office buildings. National Fire Protection Association, Quincy, MA.
- NSSL, 2017. National Severe Storms Laboratory, Norman, OK. <http://www.nssl.noaa.gov/>. Accessed February 2017.
- OSHA, 2001. How to plan for workplace emergencies and evacuations. Occupational Safety and Health Administration, U.S. Department of Labor.
- Paniati, J.F., 2003. Use of Changeable Message Sign (CMS) for emergency security messages. Memorandum. Federal Highway Administration, U.S. Department of Transportation.
- Peeta, S., and Hsu, Y.T., 2009. Integrating supply and demand aspects of transportation for mass evacuation under disasters. NEXTRANS Project No. 019PY01, Purdue University, West Lafayette, IN.
- Phillips, G.W., Nagel, D.J., and Coffey, T., 2005. A Primer on the detection of nuclear and radiological weapons. National Defense University Center for Technology and National Security Policy, Washington, DC.
- Qiu, K.F., and Jin, W.L., 2008. Studies of emergency evacuation strategies based on kinematic wave models of network vehicular traffic. 11th International IEEE Conference on Intelligent Transportation Systems, 222-227.
- Roelofs, T., and Brookes, C., 2014. Synthesis of intelligent work zone practices. Report No. ENT-2014-1. Lansing, MI.
- Rosen, A. (2012). Effects of the Fukushima nuclear meltdowns on environment and health. University Clinic Dusseldorf, Dusseldorf, Germany.
- Ronchi, E., and Nilsson, D., 2014. Traffic information signs, color scheme of emergency exit portals and acoustic systems for road tunnel emergency evacuations. Technical Report 3173, Department of Fire Safety Engineering and Systems Safety, Lund University, Lund, Sweden.
- Roy, C., 2008. Furnace of creation, cradle of destruction: A journey to the birthplace of earthquakes, volcanoes, and tsunamis. AMACOM, New York, NY.

- SOES, 2008. City of Sacramento evacuation plan for floods and other emergencies. Sacramento Office of Emergency Services, Sacramento, CA.
- Schott, T., Landsea, C., Hafele, G., Lorens, J., Taylor, A., Thurm, H., and Zaleski, W., 2012. The Saffir-Simpson hurricane wind scale. National Weather Services, National Hurricane Centre, National Oceanic and Atmospheric Administration, U.S. Department of Commerce, Washington, DC.
- Spence, W., Sipkin, S.A., and Choy, G.L., 1989. Measuring the size of an earthquake. *Earthquake Information Bulletin*, 21(1), 58-63.
- Tung, T.X., and Kim, J.M., 2011. An effective four-stage smoke-detection algorithm using video images for early fire-alarm systems. *Fire Safety Journal*, 46(5), 276-282.
- Tyshchuk, Y., Hui, C., Grabowski, M., and Wallace, W.A., 2012. Social media and warning response impacts in extreme events: Results from a naturally occurring experiment. 45th Hawaii International Conference on System Science (HICSS), 818827.
- USDHS, 2014. National Emergency Communications Plan. US Department of Homeland Security, Washington, DC.
- USDOT, 2004. Hazmat summary by mode/cause: Calendar year 2003 serious incidents. Office of Hazardous Materials Safety, U.S. Department of Transportation.
- Vasconez, K.C., and Kehrl, M., 2010. Highway evacuations in selected metropolitan areas: Assessment of impediments. Report No. FHWA-HOP-10-059, Federal Highway Administration, U.S. Department of Transportation.
- Wang, J.H., Collyer, C.E., and Yang, C.M., 2006. Enhancing motorist understanding of variable message signs. Research and Technology Development, Rhode Island Department of Transportation, Providence, RI.
- White, R.A., Blumenberg, E., Brown, K.A., Contestabile, J.M., Haghani, A., Howitt, A.M., and Velásquez III, A., 2008. *The Role of Transit in Emergency Evacuation*. Transportation Research Board, National Research Council, Washington, DC.
- Wolshon, B., Urbina, E., Wilmot, C., and Levitan, M., 2005. Review of policies and practices for hurricane evacuation. I: Transportation planning, preparedness, and response. *Natural Hazards Review*, 6(3), 129-142.
- Woo, G., 2008. Probabilistic criteria for volcano evacuation decisions. *Natural Hazards*, 45(1), 87-97.
- Zeigler, D.J., Brunn, S.D., and Johnson Jr, J.H., 1981. Evacuation from a nuclear technological disaster. *Geographical Review*, 1-16.

Section 11

- Boyd, M. A., 2013. *Paratransit Emergency Preparedness and Operations Handbook*. Transportation Research Board, National Academies Press, Washington, DC.
- CALTRANS, 2017. Traffic Signal Operations Manual. California Department of Transportation, Sacramento, CA.

- Campos, V., Bandeira, R., and Bandeira, A., 2012. A method for evacuation route planning in disaster situations. *Procedia-Social and Behavioral Sciences*, 54, 503-512.
- Chen, M., Chen, L., and Miller-Hooks, E., 2007. Traffic signal timing for urban evacuation. *Journal of Urban Planning and Development*, 133(1), 30-42.
- Cova, T. J., and Johnson, J. P., 2003. A network flow model for lane-based evacuation routing. *Transportation Research Part A: Policy and Practice*, 37(7), 579604.
- Elmitiny, N., Ramasamy, S., and Radwan, E., 2007. Emergency evacuation planning and preparedness of transit facilities: Traffic Simulation modeling. *Transportation Research Record*, 1992, 121-126.
- FHWA, 2002. United States Pavement Markings. *Manual on Uniform Traffic Control Devices*. Federal Highway Administration, U.S. Department of Transportation.
- Hausknecht, M., Au, T. C., Stone, P., Fajardo, D., and Waller, T., 2011. Dynamic lane reversal in traffic management. *Intelligent Transportation Systems (ITSC), 14th International IEEE Conference.*, 1929-1934.
- Houston, N., 2006. Using highways during evacuation operations for events with advance notice: Routes to effective evacuation planning primer series. Report No. FHWA-HOP-06-109, Federal Highway Administration, U.S. Department of Transportation.
- ILDOT, 2015. Pavement Marking Selection, *Installation and Inspection Manual*. Illinois Department of Transportation, Springfield, IL.
- Jahangiri, A., Afandizadeh, S., and Kalantari, N., 2011. The optimization of traffic signal timing for emergency evacuation using the simulated annealing algorithm. *Journal of Transport*, 26(2), 133-140.
- Kulshrestha, A., Lou, Y., and Yin, Y., 2014. Pick-up locations and bus allocation for transit-based evacuation planning with demand uncertainty. *Journal of Advanced Transportation*, 48(7), 721-733.
- Lin, C., and Gong, B., 2016. Transit-based emergency evacuation with transit signal priority in sudden-onset disaster. *Journal of Discrete Dynamics in Nature and Society*, 2016, 13-14
- Liu, Y., Chang, G. L., Liu, Y., and Lai, X., 2008. Corridor-based emergency evacuation system for Washington, DC: system development and case study. *Transportation Research Record*, 2041, 58-67.
- Murray-Tuite, P., and Wolshon, B., 2013. Evacuation transportation modeling: An overview of research, development, and practice. *Transportation Research Part C, Emerging Technologies*, 27, 25-45.
- Paniati, J. F., and Amoni, M. (2006). Traffic signal preemption for emergency vehicles. Research and Innovative Technology Administration, U.S. Department of Transportation.
- SCOOT, 2016. *SCOOT User Manual*. Siemens Mobility, Traffic Solutions UTC System, Munich, Germany.
- Urbanik, T., Tanaka, A., Lozner, B., Lindstrom, E., Lee, K., Quayle, S., and Sunkari, S., 2015. *Signal Timing Manual*. NCHRP Report 812, National Cooperative Highway Research Program, Transportation Research Board. National Academies Press, Washington, DC.
- Wang, Y., Corey, J., Lao, Y., Henrickson, K., and Xin, X., 2013. Criteria for the selection and application of advanced traffic signal systems. Report No. FHWA-ORRD-14-08, Federal Highway Administration, U.S. Department of Transportation.
- White, R. A., Blumenberg, E., Brown, K. A., Contestabile, J. M., Haghani, A., Howitt, A. M., and Velásquez III, A., 2008. The Role of transit in emergency evacuation. Transportation Research Board, Washington, DC.

- Wisconsin DOT, 2012. *Emergency Traffic Control and Scene Management Guidelines*. Statewide Traffic Operations Center, Wisconsin Department of Transportation, Madison, WI.
- Wolshon, P. B., 2009. Transportation's role in emergency evacuation and reentry. NCHRP Synthesis 392. National Cooperative Highway Research Program, Transportation Research Board. National Academies Press, Washington, DC.
- Zhang, X., and Chang, G.L., 2014. A transit-based evacuation model for metropolitan areas. *Journal of Public Transportation*, 17(3), 129-147.



U.S. Department of Transportation
Federal Transit Administration

U.S. Department of Transportation
Federal Transit Administration
East Building
1200 New Jersey Avenue, SE
Washington, DC 20590
<https://www.transit.dot.gov/about/research-innovation>